

FINAL REPORT

Tin Whisker Testing and Modeling

SERDP Project WP-1753

NOVEMBER 2015

Stephan J. Meschter
Polina Snugovsky
BAE Systems

Distribution Statement A
This document has been cleared for public release



Page Intentionally Left Blank

This report was prepared under contract to the Department of Defense Strategic Environmental Research and Development Program (SERDP). The publication of this report does not indicate endorsement by the Department of Defense, nor should the contents be construed as reflecting the official policy or position of the Department of Defense. Reference herein to any specific commercial product, process, or service by trade name, trademark, manufacturer, or otherwise, does not necessarily constitute or imply its endorsement, recommendation, or favoring by the Department of Defense.

Page Intentionally Left Blank

REPORT DOCUMENTATION PAGE

*Form Approved
OMB No. 0704-0188*

Public reporting burden for this collection of information is estimated to average 1 hour per response, including the time for reviewing instructions, searching existing data sources, gathering and maintaining the data needed, and completing and reviewing this collection of information. Send comments regarding this burden estimate or any other aspect of this collection of information, including suggestions for reducing this burden to Department of Defense, Washington Headquarters Services, Directorate for Information Operations and Reports (0704-0188), 1215 Jefferson Davis Highway, Suite 1204, Arlington, VA 22202-4302. Respondents should be aware that notwithstanding any other provision of law, no person shall be subject to any penalty for failing to comply with a collection of information if it does not display a currently valid OMB control number. **PLEASE DO NOT RETURN YOUR FORM TO THE ABOVE ADDRESS.**

1. REPORT DATE (DD-MM-YYYY) 30/11/2015			2. REPORT TYPE Final Report			3. DATES COVERED (From - To) Jan. 2012 to Oct. 2015		
4. TITLE AND SUBTITLE Tin Whisker Testing and Modeling			5a. CONTRACT NUMBER W912HQ-10-C-0052					
			5b. GRANT NUMBER					
			5c. PROGRAM ELEMENT NUMBER					
6. AUTHOR(S) Meschter, Stephan J. and Snugovsky, Polina			5d. PROJECT NUMBER — W74RDV13124767					
			5e. TASK NUMBER A006					
			5f. WORK UNIT NUMBER					
7. PERFORMING ORGANIZATION NAME(S) AND ADDRESS(ES) BAE Systems Controls 1098 Clark Street Endicott, NY 13760			8. PERFORMING ORGANIZATION REPORT NUMBER PM-LF-2015-11					
			9. SPONSORING / MONITORING AGENCY NAME(S) AND ADDRESS(ES) SERDP/ESTCP PROGRAM OFFICE ROBIN NISSAN 4800 Mark Center Drive, Suite 17D08 Alexandria, VA 22350-3605					
10. SPONSOR/MONITOR'S ACRONYM(S) SERDP/ESTCP			11. SPONSOR/MONITOR'S REPORT NUMBER(S)					
			12. DISTRIBUTION / AVAILABILITY STATEMENT Approved for public release; distribution is unlimited					
13. SUPPLEMENTARY NOTES								
14. ABSTRACT Driven by legislation resulting from two European Union directives (RoHS and WEEE), most commercial electronics manufacturers began delivering lead-free electronic components, assemblies, and equipment beginning in 2006. One aspect of the global movement away from using lead (Pb) is that component manufacturers have primarily switched to tin-rich finishes and solder alloys in commercial-off-the-shelf products. Unfortunately, this creates an increased risk of tin whisker formation that can result in undesirable electrical failures unless military and aerospace electronic systems failure effects are understood and appropriate risk mitigations are implemented. This report describes the multi-year testing and modeling program to analyze tin whisker growth on lead-free manufactured assemblies and utilizes whisker short circuit statistical modeling to enable improved reliability assessments. This series of tests includes COTS parts assembled using standard high reliability manufacturing processes. Testing to date has found that thin (less than approximately 25 microns) tin-3.0silver-0.5copper alloy (SAC305) assembly solder can grow relatively long whiskers (greater than 100 microns) that can short								
15. SUBJECT TERMS Tin Whiskers, Short Circuits, Lead-Free Solder, Electronic Assembly, Humidity Exposure, Thermal Cycling, Corrosion, Contamination, Whisker Length Statistics								
16. SECURITY CLASSIFICATION OF:			17. LIMITATION OF ABSTRACT SAR	18. NUMBER OF PAGES 302	19a. NAME OF RESPONSIBLE PERSON Stephan Meschter			
a. REPORT U	b. ABSTRACT U	c. THIS PAGE U					19b. TELEPHONE NUMBER (include area code) 607-770-2332	

Page Intentionally Left Blank

Abstract:

Driven by legislation resulting from two European Union directives, Reduction of Hazardous Substances (RoHS) and Waste Electrical and Electronic Equipment Regulation (WEEE), most commercial electronics manufacturers began delivering lead-free electronic components, assemblies, and equipment beginning in 2006. The DoD must now include lead-free materials considerations in the evaluation of commercial-off-the-shelf parts and assemblies intended for use in DoD systems. In particular, lead-free tin rich finishes and solder alloys are susceptible to tin whisker growth that can cause electrical short circuits and reduced reliability. This report describes the multi-year testing and modeling program to analyze tin whisker growth on lead-free manufactured assemblies and utilizes whisker short circuit statistical modeling to enable improved reliability assessments. This series of tests includes COTS parts assembled using standard high reliability manufacturing processes with and without conformal coating. Various contamination levels, contamination types were evaluated. The materials included in the evaluation were: Cu and alloy-42 (Fe42Ni) alloy part leads, various SnAgCu lead-free assembly solders (including some with Y, L, and Ce rare earth element additions, rework fluxes, and immersion Sn finished Cu circuit board pads. The assemblies were exposed to various thermal cycling and isothermal high humidity and whisker growth was evaluated. In total, over 120,000 whiskers were observed on uncoated assemblies. Conformal coated assemblies exhibited significantly reduced whisker growth. Thin lead-free solder (less than approximately 25 microns of Sn3.0Ag0.5Cu alloy) can grow whiskers greater than 100 microns long that can short circuit fine pitch parts or board pads. It was found that the entire solder joint material system must be considered. Contamination induced corrosion promoted whisker growth in high humidity environments, which is important because it has not been thoroughly tested by the consumer electronics community. Coefficient of expansion stresses associated with low coefficient of expansion alloy-42 resulted in increased whisker growth in thermal cycling. Whisker growth was particularly pronounced with rare earth element (REE) additions to lead-free solder and improperly cleaned rework fluxes. In these cases, the whiskers were not limited to the thin solder regions. The alloying of Sn with Ag and Cu in the solder and melting (reflow) of the tin finished COTS parts were not sufficient to mitigate whisker growth in the environments tested. It is recommended that additional tin whisker mitigations, such as validated whisker resistant conformal coating materials and processes, be used for DoD equipment in harsh environments or with long service life.

Key words: tin whiskers, lead-free, assembly, contamination, risk modeling, Monte Carlo, SAC305 solder, tin plating, intermetallics, rare earth elements, high humidity, thermal cycling, corrosion, copper, alloy-42, conformal coating

Table of Contents

1. Objective	1
2. Approach.....	1
3. Project summary and conclusions	2
3.1 Background	2
3.2 Summary of whisker growth experiment methods and materials	5
3.3 Characterization of parts before and after assembly	8
3.3.1 As-received parts	8
3.3.2 Assembly characterization	9
3.4 PCTC +50 to 85°C results.....	10
3.5 TC 55 to +85°C results.....	11
3.6 HTHH 85°C/85%RH results	12
3.7 LTHH 25°C/85%RH results.....	14
3.8 Whisker growth location observations	15
3.9 Solder microstructure and whisker growth observations	15
3.9.1 Recrystallization and grain change	15
3.9.2 IMC	17
3.9.3 Oxidation/corrosion	17
3.9.4 Broken whiskers	18
3.9.5 Thin whiskers	19
3.9.6 Non-whisker stress relaxation	20
3.9.7 Test considerations	22
3.9.8 REE Oxidation	22
3.10 Conformal coating observations.....	23
3.10.1 Thermal cycling	23
3.10.2 High humidity	23
3.11 Whisker risk modeling	25
3.11.1 Whisker risk modeling method	25
3.11.2 Gull wing lead modeling results	27
3.12 Project summary.....	29
3.12.1 Experimental results summary	29
3.12.2 Whisker short circuit risk modeling summary	31
3.13 Conclusions and implications for future research/implementation	31
4. Whisker growth literature review	33

4.1	Environment and whisker growth	35
4.1.1	Room temperature	35
4.1.2	Isothermal high humidity	35
4.1.3	Thermal cycling	35
4.1.4	Corrosion	36
4.1.5	Effect of circuit electrical bias	37
5.	Screening experiment 1: SAC305 assembly ionic contamination induced whisker growth.....	38
5.1	Approach	38
5.2	Methods and materials.....	38
5.2.1	Test vehicle, components and assembly	38
5.2.2	Cleaning, component contamination, and post-assembly contamination methods	40
5.2.3	Environmental exposure, whisker measurements and metallurgical analysis	42
5.3	Results and discussion.....	43
5.3.2	Results of Testing at 85°C/85%RH	44
5.4	Summary	57
6.	Screening experiment 2: Microstructure and whisker growth of SAC solder alloys with rare earth additions in different environments.....	59
6.1	Approach	59
6.2	Methods and materials.....	59
6.3	Results and discussion.....	59
6.3.1	Microstructure formed during solidification	60
6.3.2	Interaction of phases present with atmosphere	61
6.3.3	Growth of whiskers	62
6.3.4	REE in SAC whisker formation theory	66
6.4	Summary	67
7.	Primary experiments: Methods, materials, experiment design and assembly	68
7.1	Approach	68
7.2	Design and environment variables	68
7.2.1	SOT, QFP, and BGA board test vehicle design	70
7.2.2	Environments	77
7.3	Design of experiments (DOE)	78
7.3.1	Inspection plan	80
7.4	Inspection methodology and measurement approach.....	81
7.4.1	Whisker inspection	81
7.4.2	Metallurgical analysis	84
7.4.3	Conformal coating inspection	85

7.5	Part and assembly methods and materials.....	85
7.5.1	As-received part characterization	86
7.5.2	Cleaning and contamination method	87
7.5.3	Assembly soldering	88
7.5.4	Conformal coating	88
7.5.5	Initial SOT, QFP, and BGA assembly characterization	89
7.6	Whisker density calculation areas	92
8.	Primary experiment 1 results and discussion: PCTC +50 to 85°C cycling.....	97
8.1	Experimental conditions.....	97
8.2	Whisker growth results.....	98
8.2.1	SOT board first inspection: 250 cycles	98
8.2.2	SOT board second inspection: 730 (250+480) cycles	98
8.2.3	SOT board third inspection: 1,797 (250 + 480 + 1067) cycles	99
8.3	Metallographic evaluation.....	104
8.3.1	SOT metallographic observations	104
8.3.2	BGA ball whisker examination	108
8.4	Conformal coating.....	109
8.5	Summary	110
9.	Primary experiment 2 results and discussion: TC -55 to +85°C cycling.....	111
9.1	Experimental conditions.....	111
9.2	Whisker growth results.....	111
9.2.1	First inspection: 500 cycles	111
9.2.2	Second Inspection: 2,110 (500+1,610) Cycles	112
9.3	Metallographic evaluation.....	119
9.4	Conformal Coat Observations	127
9.5	Summary	130
9.5.1	Whisker length	130
9.5.2	Metallurgical observations	131
9.5.3	Conformal coating	131
9.6	Conclusions	131
10.	Primary experiment 3 results and discussion: HTHH 85°C/85%RH	132
10.1	Environmental conditions.....	132
10.2	Whisker growth results.....	132
10.2.1	First inspection: 1,000 h SOT Board	132
10.2.2	Final inspection: 4,000 h SOT board	138
10.3	Metallurgical observations	148

10.3.1	SOT board	148
10.3.2	QFP board	151
10.3.3	BGA board	152
10.4	Conformal coating.....	154
10.5	Summary	156
10.5.1	As-Received part factors	156
10.5.2	Whisker length of SOT and QFP terminations	156
10.5.3	Metallurgical observations	157
11.	Primary experiment 4 results and discussion: LTHH 25°C/85%RH.....	158
11.1	Experimental conditions.....	158
11.2	Whisker growth results.....	158
11.2.1	First inspection: 1,037 h SOT and QFP boards	159
11.2.2	Second Whisker Inspection: 4,398 h SOT Boards	159
11.2.3	Second inspection: 4,398 h QFP Boards	162
11.2.4	Final Inspection: 16,910 h SOT board	169
11.2.5	Comparison between second (4,398 h) and final (16,910 h) LTHH inspection	180
11.3	Metallurgical Observations	181
11.3.1	First inspection metallurgy: 1,037 h LTHH	181
11.3.2	Second inspection SOT metallurgical observations: 4,398 h LTHH	182
11.3.3	Second inspection QFP metallurgical observations: 4,398 h LTHH	184
11.3.4	Final Inspection Metallurgical Observations: 16,910 h	191
11.4	Conformal coating.....	197
11.5	Summary	200
11.5.1	Whisker Length	200
11.5.2	Metallurgical Observations	200
12.	Whisker risk modeling.....	202
12.1	Approach	202
12.2	Gull wing model development	203
12.2.1	Motivating cases	204
12.2.2	Bridging risk geometric modeling	207
12.2.3	Lead geometry modeling	207
12.2.4	Whisker risk data subset	210
12.2.5	Simplified model development	211
12.2.6	Whisker spacing distribution	215
12.2.7	Whisker length distributions	220
12.2.8	Whisker density	222

12.2.9	Whisker bridging probability	223
12.2.10	Bridges per lead pair	224
12.2.11	Shorts per lead pair	224
12.2.12	Overall roll-up	225
12.2.13	Whisker risk Spreadsheet	225
12.2.14	Gull wing lead modeling	225
12.2.15	Gull wing lead risk calculation example	226
12.3	Basic geometry risk modeling	233
12.3.1	Whisker mirror	233
12.3.2	Whisker risk data subset	234
12.3.3	Basic geometry model development	237
12.3.4	Special case of parallel large and small plates	242
12.3.5	Basic geometry whisker risk model spreadsheet snapshot	245
12.4	Whisker modeling assumptions.....	252
12.5	Discussion of assumptions	253
12.6	Summary	254
13.	Transfer of knowledge	255
13.1	Presentations and papers	255
13.2	SAC solder whisker growth in IPC-PERM GEIA-STD-0005-2	255
13.3	REE element specification in IPC J-STD-006	255
14.	Literature cited.....	256
Appendix A – List of Scientific/Technical Publications		263
Appendix B – Initial test vehicle characterization.....		272

List of Figures

Figure 1: Compressive stresses from intermetallic growth, thermal cycling, corrosion, and mechanical loads contribute to whisker growth.....	3
Figure 2: Potential whisker growth regions and roughness features on SAC soldered assemblies.....	4
Figure 3: SOT, QFP and BGA assemblies.	5
Figure 4: Contamination level definition.....	6
Figure 5: Whisker test environments.....	6
Figure 6: Typical whisker growth observed in the primary experiments; (A) PCTC +50 to 85°C, (B) TC -55 to 85°C thermal shock cycling, (C) HTHH 85°C/85% RH, and (D) LTHH 25°C/85% RH long duration storage.....	7
Figure 7: As-received part lead conditions contributing to whisker growth; (A) SOT6 overall part optical view, (B) SOT5 lead SEM image showing exposed Cu on lead near package body, (C) SOT6 lead SEM image showing exposed alloy-42 base metal near package, (D) SOT6 overall lead optical cross-section view showing thin tin plating caused by lead forming. SEM images of tin plating cross sections show (E) a void within the tin plating, (F) voids and a rough surface, and (g) rough surface with deep grooves.	9
Figure 8: Alloy-42 leaded SOT solder joint cross-section SEM images after assembly; (A) SOT3 overall, (B) SOT6 overall, (C) (Cu, Ni) ₆ Sn ₅ IMC on board, and (D) Cl contamination trapped in solder joint.....	10
Figure 9: SOT3 maximum whisker length results after a total of 1,750 PCTC cycles.	11
Figure 10: SEM images showing whisker growth on alloy-42 lead solder joint after a total of 1,750 PCTC cycles; (A) overall view highlighting whisker growth where the lead exits the top of the solder joint with (B) and (C) showing higher magnification whisker growth images.....	11
Figure 11: Top 10 longest whiskers after 2,110 TC cycles.	12
Figure 12: SEM images showing whiskers growing from alloy-42 lead after 2,110 TC cycles; (A) overall of lead with (B) and (C) showing whisker region at increasing magnifications.	12
Figure 13: Comparison of top 10 longest whiskers after 1,000 and 4,000 h HTHH.	13
Figure 14: SEM image showing whisker growth from TQFP64 board pads after 4,000 h HTHH. Arrow shows a broken whisker between the pads long enough to bridge the gap. The solder bulge wrapping around the two ounce thick board pad reduced the typical 100 micron clearance between pads to 60 microns.	13
Figure 15: Top ten whisker densities at location-2 from the SOT board inspection after 4,000 h HTHH.....	14
Figure 16: Ten longest whiskers of the QFP board parts from the second inspection at 4,398 h LTHH.....	14
Figure 17: Ten longest whiskers on the SOT board parts from the final inspection at 16,910 h LTHH.....	15
Figure 18: Primary whisker growth locations after PCTC, TC, HTHH and LTHH environments. PCTC resulted in growth on the alloy-42 leads where the thin solder at the transition area between the main solder fillet (region B) and the upper part of lead (region A). The thin solder in region A exhibited the majority of the whisker growth after TC on alloy-42 lead terminations and after LTHH on Cu lead terminations. The thin solder over the copper board pad in region C produced the most whisker growth after HTHH. The thick solder in region B displayed little or no whisker growth.	15
Figure 19: SEM image showing whisker growth near recrystallized grains and dendritic grain boundaries on the SAC solder fillets after (A) 1,750 PCTC cycles and (B) 2,110 TC cycles.	16
Figure 20: Subsurface grain recrystallization: (A) from subgrain region after 1,750 PCTC cycles, (B) from primary tin dendrite triple junction after 1,750 PCTC cycles, and (C) a whisker on top of an underlying recrystallized grain after 2,110 TC cycles.	16

Figure 21: SEM image showing whisker diameter change during TC exposure on alloy-42 SOT6 with 1-0 contamination; (A) increasing, (B) and C) decreasing whisker diameters.....	16
Figure 22: SEM image showing whisker on alloy-42 lead adjacent to Ag_3Sn IMC plate; (A) after 1,750 PCTC cycles, (B) after 500 TC cycles, and (C) continued growth of whisker in (B) and new whisker growth near intermetallic after 2,110 TC cycles.	17
Figure 23: Cross section showing uneven Sn oxidation into the IMC region between the primary Sn grain boundaries; (A) secondary electron SEM image highlighting the IMC with (B) and (C) backscatter SEM images emphasizing the Sn oxide penetration into the solder. Image (C) is a higher magnification view of the circled area in (B).....	17
Figure 24: Cross section showing partial oxidation of SAC solder with Cu leaded part (SOT5) and 1-1 contamination after 4,000 h LTHH; (A) SEM image of oxide near 98-microns long whisker, (B) SEM image of oxide in a thicker region of the SAC solder, (C) optical image of oxidation near solder wetting line, and (d) SEM image of region shown in (C).	18
Figure 25: SEM image showing alloy-42 leads attached to Cu board pads after; (A) 1,000 h and (B) 4,000 h of HTHH.....	18
Figure 26: SEM image showing voids and cracks observed in the whisker base after 4,000 HTHH h. Inset shows a high magnification image of the whisker root crack.....	19
Figure 27: Thin whiskers growing from La_3Sn IMC in a bulk SAC105+0.5La cross-section held at room ambient conditions for 3,050 h.	20
Figure 28: An 81 micron long 0.3 micron diameter whisker observed during the LTHH test at 16,910 h on a Cu alloy SOT5 lead with a 1-1 contamination level; (A) Overall SEM image, 100x, (B) increased magnification of whisker, 1,000x, (C) close-up of the whisker base, 10,000x and (D) close-up of the whisker tip, 10,000x.20	20
Figure 29: SEM image showing faceted grains on alloy-42 SOT3 with a 1-1 contamination level after 1,750 PCTC cycles; (A) overall view and B) high magnification view of circled region.	21
Figure 30: SEM image showing an alloy-42 termination solder joint with massive cracking after 2,110 TC cycles.	21
Figure 31: SEM images showing whisker growth interruption by the inspection process during HTHH testing. Red arrows indicate whiskers that stopped growing and yellow arrows indicate new whisker growth: (A) SOT5 1-0, U26, lead 1, 1,000 h; (B) SOT5 1-0, U26, lead 1, 4,000 h; (C) SOT5 1-1, U37, lead 5, 1,000 h; (D) SOT5 1-1, U37, lead 5, 4,000 h; (E) SOT5 1-1, U38, lead 2, 1,000 h; and (F) SOT5 1-1, U38, lead 2, 4,000 h.....	22
Figure 32: SEM images comparing SAC105 (A) with SAC105 + 0.01Ce (B–F) solder balls attached to BGA board pads with SAC305 solder paste after 4,000 HTHH h (A, D–F) and after 1,750 PCTC cycles (B and C) at a 0-0 contamination level; (A) highlights no whisker growth on a SAC105 ball. Image (E) shows whisker highlighted by arrow in (D).....	23
Figure 33: Conformal coating on QFP 44, with 1-1 contamination level after 16,910 h LTHH; (A) overall, 40x and (B) lead tip, 150x and (C) top of lead, 150x. No cracks or coating degradation observed.	24
Figure 34: Conformal coated SOT3 alloy-42 lead with 1-1 contamination level after 2,110 cycles, 100X. Arrows indicate coating crack locations.	24
Figure 35: Coated and un-conformal coated alloy-42 SOT6 after 2,110 cycles -55°C to 85°C, (500+1,610); (A) Coated, 0-0 contamination level, 1,500x, and (B) no conformal coating, 0-1 contamination level, 1,500x....	25
Figure 36: Influence of voltage bias on corrosion on coated SOT5 parts with 1-1 contamination level after 4,000 h HTHH; (A) electrical schematic, (B) corrosion on lead 2 at 5V.....	25
Figure 37: Conformal coating on SAC105+Ce BGA ball after 16,910 h LTHH.....	25

Figure 38: (A) schematic of gull wing leads with bridging and non-bridging whiskers (B) equal parallel plate, (C) unequal parallel plates, (D) equal perpendicular plates, and (E) parallel cylinders.....	26
Figure 39: Determination of lead-to-lead spacing distance for a bridging whisker.	26
Figure 40: (A) Part drawing nomenclature, (B) lead dimension nomenclature, (C) side view of modeled lead and pad, and (D) top view of modeled lead and pad.....	27
Figure 41: (A) Whisker growth locations, (B) probability plot of whisker lengths (microns) from the HTHH testing for Cu leads after 4,000 h at 85°C/85%RH; broken down by location (from Figure 283) and (C) conversion of lognormal mean parameters from ln(microns) to ln(mm) by subtracting ln(1000) from the ln(mm) location parameter.....	28
Figure 42: Summary of computed TQFP128 short circuits for three levels of coating mitigation.	29
Figure 43: Schematic diagram illustrating the conditions leading to cyclic dynamic recrystallization and whisker growth.	33
Figure 44: Some of the factors influencing whisker growth.	34
Figure 45: Contamination screening test assembly.	39
Figure 46: Loose piece part contamination schematic.	40
Figure 47: Assembly and post assembly contamination schematic.....	40
Figure 48: Test vehicle (A) and loose components and (B) placement in environment chamber.....	42
Figure 49: Main areas of contamination segregation; (A) grain boundaries, (B) gaps between leads and plastic body (C) surface roughness grooves, and (D) open voids and crack defects in plating.....	44
Figure 50: Maximum assembly whisker lengths after 500 h at 85°C/85%RH as a function of assembly cleanliness.	45
Figure 51: Micrographs of PIDP14T (A) and PLCC44 (B) after 500 h at 85°C/85%RH with 280 microns and 277 microns whiskers, respectively.	45
Figure 52: Maximum assembly whisker lengths after 500 h at 85°C/85%RH as a function of assembly cleanliness; (A) The effect of component contamination and flux residues on whisker formation and (B) showing no significant difference in whisker length as a function of component contamination type.....	47
Figure 53: Loose and assembled components whisker lengths comparison after 500 h at 85°C/85%RH	48
Figure 54: Maximum assembly whisker lengths after 1,500 h at 85°C/85%RH as a function of assembly cleanliness.	49
Figure 55: Assembly whisker images (A, C, E) after 500 h, and (B, D, F) 1,500 h at 85°C/85%RH. Circled whiskers appeared after 500 hr and did not continue growing after additional 1,000 hr. New whiskers formed during additional exposure are shown with arrows.	50
Figure 56: Maximum assembly whisker length comparison after 500 h and after additional 1,000 h at 85°C/85%RH for (A) as-received and (B) contaminated components in no-clean assemblies.....	51
Figure 57: Whisker assembly density comparison after 500 h and additional 1,000 h at 85°C/85%RH	52
Figure 58: Assembly whisker thickness/diameter distribution; (A) thickness distribution after 1,000 h, and (B) thickness distribution for long whiskers (greater than 40 microns) after 1,000 h with flux.	53
Figure 59: Maximum assembly whisker lengths after 1,500 h at 85°C/85%RH showing no significant difference in whisker length as a function of component contamination type.....	54
Figure 60: Maximum assembly whisker lengths after 1,500 h at 85°C/85%RH showing longer whiskers in assemblies with no-clean ROL0 resin flux residue compare to ROL1 rosin flux.....	54

Figure 61: TTSOP20 (A, B) loose and (C, D, E) assembled component tin or solder coverage. Cross-sections after 500 at 85°C/85%RH were used as an example.....	55
Figure 62: TTSOP20 assembly images illustrated whisker growth from solder fillet on (A) toe area and (B, C, D) from the top and sides of leads.....	56
Figure 63: Typical locations of long whiskers on low and high stand-off height components, PTH, and discrete components; red arrows – longest whiskers, green arrows – shorter whiskers, yellow circles – hillocks; (A) SOT, (B) QFP, (C) PLCC, (D) PDIP, and (E) chip resistor.....	57
Figure 64: REE-Sn phase diagrams; (A) Ce-Sn, (B) Y-Sn and (C) La-Sn (Note: Sn rich side of the phase diagrams are shown.)	60
Figure 65: CeSn ₃ particles in SAC105 solder; (A) fresh after polishing and (B) exposed to air for several days... ..	60
Figure 66: Microstructure of SAC105 +0.5Y.....	61
Figure 67: Examples of morphology of eutectic intermetallics; (A) Ag ₃ Sn and B Cu ₆ Sn ₅ . Note that the IMC images were obtained by etching the Sn away.....	61
Figure 68: Microstructure and composition of LaSn ₃ in SAC105 +0.5La after ambient atmosphere exposure.	62
Figure 69: Segregation of RESn intermetallic particles on solder surface. Black arrows show the RESn IMC regions and the red arrow indicates a whisker.....	63
Figure 70: Whisker growing from cross-section of a solder joint of SAC105 +0.5La; (A) Overall and (B) high magnification SEM image. The blue arrow shows a whisker growing from the tin between the La ₃ Sn IMC above and the Cu ₆ Sn ₅ on the substrate below. The red arrow shows a whisker growing from the LaSn ₃ IMC. The dark material in (A) is debris on the section.....	64
Figure 71: Thin whiskers growing from La ₃ Sn IMC in a bulk SAC105+0.5La cross-section held at room ambient conditions for 3,050 h.	64
Figure 72: Whiskers growing from a cross-section of bulk SAC105+0.5La after 2,690 h of nitrogen cabinet storage; (A and B) Re-crystallization: Whisker growth from tin dendrite grain boundaries which indicates new grain nucleation (C and D) Entire grain growing: Typical hillock-whisker growth.	65
Figure 73: Whisker length after different environmental exposure.....	65
Figure 74: Schematic illustrating whisker growth of SAC with REE. For example, the oxidation of surface CeSn ₃ IMC edges formed CeO ₂ . The CeO ₂ causes compressive stress due an increase in volume. In addition, Sn is liberated and becomes available for whisker growth. The whiskers can grow inside the CeSn ₃ IMC and in the adjacent solder.....	66
Figure 75: Primary experiment factors.....	69
Figure 76: Typical view of test vehicles installed in an environmental chamber.....	69
Figure 77: Test vehicle panel	70
Figure 78: SOT Board	71
Figure 79: SOT board voltage bias; (A) bias voltage on the overall board, with (B)(C) and (D) showing the device connections to the SOT3 (SOT23-2), SOT5(SOT23-5) and the SOT6 parts respectively.....	72
Figure 80: QFP Board.	73
Figure 81: J-lead tin whisker conformal coating mitigation challenges. Underside of the part is difficult to conformal coat and the sheared lead tips enhance corrosion whisker stresses.....	74
Figure 82: QFP board electrical schematic; (A) QFP44 (B) TQFP64 and (C) interconnects to 5V.	75
Figure 83: BGA board.....	76
Figure 84: Board contamination levels.....	79

Figure 85: Whisker length definition.....	82
Figure 86: Whisker length error versus tilt angle.....	83
Figure 87: Whisker location definition. The hatched region 2 indicates the thick solder region on the lead and includes the thinner solder that wet onto the board pad. Areas 1, 3, 4 and 5 represent the thin solder or tin region above the thick solder area.....	83
Figure 88: Whisker angle measurement definition.....	84
Figure 89: Whisker diameter or thickness measurement.....	84
Figure 90: Cross-section, SEM and optical images of typical as-received part lead conditions that could contribute to whisker growth.....	86
Figure 91: Typical contamination regions on intentionally contaminated (SOT6 shown).....	88
Figure 92: SOT3 soldered assembly cross-section.....	89
Figure 93: SOT6 soldered assembly cross-section.....	90
Figure 94: SOT5 soldered assembly cross-section.....	90
Figure 95: Board pad intermetallic on the alloy 42 SOT6 termination.	91
Figure 96: Cross-section of coated SOT3; (A) overall and (B) higher magnification view of the top of the lead showing thin coating.	91
Figure 97: SEM images that were analyzed for the SOT 3. Top left: <i>Cross section side view for regions 1, 2a and 2b</i> Top Right: <i>Cross section front view for regions 4 and 2a</i> Bottom left: <i>Region 5</i> Bottom right: <i>Region 3</i> .92	92
Figure 98: SEM images that were analyzed for the SOT 5. Top left: <i>Cross section side view for regions 1, 2a and 2b</i> Top Right: <i>Cross section front view for regions 4 and 2a</i> Bottom left: <i>Region 5</i> Bottom right: <i>Region 3</i> .93	93
Figure 99: SEM images that were analyzed for the SOT 5. Top left: <i>Cross section side view for regions 1, 2a and 2b</i> Top Right: <i>Cross section front view for regions 4 and 2a</i> Bottom left: <i>Region 5</i> Bottom right: <i>Region 3</i> .93	93
Figure 100: The SOT 3 coordinates graphed overtop the SEM image; (A) regions 1, 2a and 2b, (B) region 3, (C) region 4 and 2b, and (D) region 5.	94
Figure 101: The SOT 5 coordinates graphed overtop the SEM image; (A) regions 1, 2a and 2b, (B) region 3, (C) region 4 and 2b, and (D) region 5.	94
Figure 102: The SOT 6 coordinates graphed overtop the SEM image.....	95
Figure 103: Summary of whisker growth location areas for the SOT3, SOT5 and SOT6 part terminations.....	95
Figure 104: Simulated power cycling temperature cycling chamber.	97
Figure 105: Temperature and humidity during simulated power cycling temperature cycling.....	98
Figure 106: Whiskers observed after 730 PCTC cycles on alloy 42 parts with a 1-1 board (part contamination and assembly contamination).....	99
Figure 107: Percentages of SOT3 parts that grew whiskers between the second (730 cycles) and the third (1,797 cycles) PCTC inspection interval.....	100
Figure 108: Maximum whisker lengths of SOT3 parts between the second (730 cycles) and the third (1,797 cycles) PCTC inspection interval.	100
Figure 109: Box plot comparing whisker length (microns) for lead alloy, part contamination and board contamination combinations after 1,797 PCTC cycles where no flux was applied.	103
Figure 110: Whisker length (microns) probability plot for the alloy-42 leads with no flux after 1,797 PCTC cycles for various board contamination combinations.	103

Figure 111: Whisker length (microns) probability plot from the alloy-42 lead set with flux applied after 1,797 PCTC cycles for various board contamination levels.....	104
Figure 112: Whiskers observed on the SOT3 part with 1-1 contamination without flux after 1,797 PCTC cycles.	105
Figure 113: Whiskers observed on the SOT6 part with 1-1 contamination with flux applied after 1,797 PCTC cycles.	105
Figure 114: Competing mechanisms of stress relaxation (SOT3, 0- 0 contamination level) after 1,797 PCTC cycles.	106
Figure 115: Micro-cracks (red arrows) in SAC305 fillets observed after 1,797 PCTC cycles; (A) SOT3 0-0 contamination level, (B) SOT3 1-1 contamination level with whisker adjacent to Ag ₃ Sn IMC and (C) SOT3 1-0 contamination level with whisker growing from primary tin dendrite triple junction Micro-cracks.....	106
Figure 116: Cross-sections of a whisker growing from solder on a SOT6 alloy-42 lead with 1-1 contamination without flux showing evidence of corrosion after 1,797 PCTC cycles.....	107
Figure 117: Cross-sections of a whisker growing from solder on a SOT6 alloy-42 lead with 1-1 contamination with flux applied after 1,797 PCTC cycles.	108
Figure 118: Cross-sections of a whisker growing from solder on a SOT6 alloy-42 lead with 1-1 contamination with flux applied after 1,797 PCTC cycles.	108
Figure 119: SEM images of tin whisker growth on SAC105+0.01Ce alloy balls soldered with SAC305 paste on a cleaned board with no contamination at the second simulated power cycling inspection point after 730 PCTC cycles; (A) overall ball, and (B-D) higher magnification images of whiskers.....	109
Figure 120: Conformal coating on SOT3 alloy-42 part after 1,797 PCTC cycles; (A) SOT6, 45x (B) SOT6, 100x, and (C) SOT6, 400X. No cracks observed.....	110
Figure 121: Sample set-up; (A) Thermal shock cycling chamber, (B) bias power supplies and (C) sample orientation in the chamber.	111
Figure 122: Individual value plot of whisker lengths (microns) after 2,110 TC cycles broken down by lead alloy, part contamination, and board contamination levels (Note: Bias2=0).	112
Figure 123: Ten longest whiskers after 2,110 TC cycles.	113
Figure 124: SEM images of whiskers on an alloy-42 lead frame SOT6 part termination with a 1-1 contamination level after 2,110 TC cycles; (A) Overall, (B) 350x close-up, and (C) 700x close-up.....	114
Figure 125: Massive recrystallization and solder fatigue cracks on a SOT6 after 2,110 TC cycles.	114
Figure 126: SEM images of whiskers on the board pad on a copper lead frame SOT5 part joint with a 1-1 contamination level after 2,110 TC cycles. (B) 1,800X close-up.	115
Figure 127: Average and maximum whisker count for the total whisker 24,879 count broken down by part and location after 2,110 TC cycles. Note: minimum whisker count is zero and is not plotted.....	115
Figure 128: Number of instances where the lead location had no whiskers after 2,110 TC cycles. The SOT5 had many leads with no whiskers.	116
Figure 129: Whisker location histogram for SOT3, SOT5 and SOT6 termination whiskers longer than ten microns after 2,110 TC cycles.	116
Figure 130: Probability plot of whisker length (microns) for SOT3, SOT5 and SOT6 part terminations with bias=0 after 2,110 TC cycles.	116
Figure 131: Probability plot of tin whisker lengths (microns) from SOT6 alloy-42 part lead terminations after 2,110 TC cycles.....	117

Figure 132: Probability plot of tin whisker lengths (microns) from SOT3 alloy-42 part lead terminations after 2,110 TC cycles with bias2=0 (top) and bias2=5 (bottom).....	117
Figure 133: Box plot of average whisker diameter (microns) for the SOT6 part lead terminations after 2,110 TC cycles.....	118
Figure 134: Probability plot of SOT6 average whisker diameter (microns) after 2,110 TC cycles.....	118
Figure 135: Scatter plot of whisker length (microns) versus diameter (microns) for copper and alloy-42 leads after 2,110 TC cycles; linear diameter (top) and natural log diameter (bottom)	119
Figure 136: Histogram of whisker growth angle after 2,110 TC cycles.....	119
Figure 137: Cross-section of 115 micron long whisker on SOT6 alloy-42 lead with a 1-1 contamination level after 2,110 TC cycles; (A) Overall SEM, (B) overall cross-section optical image, (C) close-up optical image, and (D) SEM image of whisker base.	120
Figure 138: Comparison of whisker growth locations between (A) -55 to 85°C TC cycles and milder +50 to 85°C PCTC cycles with alloy-42 lead terminations dominating whisker growth and (B) 85°C/85%RH HTHH with copper lead terminations having the greatest whisker growth.	121
Figure 139: Whisker retraction (black arrow) and whisker growth termination (red arrows) between the (A) 500 and (B) 2,110 TC cycle inspections. SOT3, 0-1 contamination level, U36, lead 3 shown.....	121
Figure 140: Whisker growth angle and diameter change on alloy-42 lead termination between the (A) 500 and (B) 2,110 TC cycle inspections. SOT3, 1-1 contamination level, U24, lead 1.	122
Figure 141: Comparison recrystallized grains after (A) +50 to 85°C PCTC, 1,797 cycles, one cycle per hour, 15 minute dwells, and (B) -55 to 85°C TC, 2,110 cycles, three cycles per hour, 10 minute dwells.....	123
Figure 142: Recrystallized grains are not always visible; (A and B) +50 to 85°C PCTC, 1,797 cycles, one cycle per hour, 15 minute dwells, and (C) -55 to 85°C TC, 2,110 cycles, three cycles per hour, 10 minute dwells.	124
Figure 143: Large step like non-whisker growth between the (A) 500 and (B) 2,110 TC cycle inspections. SOT3, 1-1 contamination level, U24, lead two shown.....	125
Figure 144: Massive eruptions of non-whisker growth and the resumption of whisker growth between the (A) 500 and (B) 2,110 TC cycle inspections. SOT6, 0-1 contamination level U73, lead six shown.	125
Figure 145: Extensive recrystallization on alloy-42 lead termination after 2,110 TC cycles; (A) First cross-section, (B) second cross-section with ion beam milling, and (C) close-up rotated image of (B). SOT6 at a 0-0 contamination level shown.....	126
Figure 146: Whiskers compete with other relaxation mechanisms; (A) SOT3 with 1-1 contamination level in relatively mild +50 to 85°C PCTC, after 1,797 cycles, one cycle per hour, 15 minute dwells, and (B) SOT6 with 0-0 contamination level in -55 to 85°C TC, after 2,110 cycles, three cycles per hour, 10 minute dwells.	127
Figure 147: Conformal coated alloy-42 leads after 2,110 TC cycles (A) SOT3, 1-1 contamination level, 100X, and (B) SOT6, 0-0 contamination level, 100X. Arrows indicate coating crack locations.....	128
Figure 148: Conformal coated alloy-42 leads after 2,110 TC cycles (A) overall of the lead top, 200x, (B) whisker appears to be pushing the edge of the coating away from the lead, 1,000x, (C) whisker growth in a coating crack, 1,000x, and (D) whisker growth in a coating crack, 1,000x.....	128
Figure 149: Part variables influencing coating fillets; (A) Large fillets on thinner finer lead pitch package: (A1) large fillet between leads, (A2) small gap behind the lead, and (A3) large coating fillet in section between leads. (B) Small fillets on thicker larger lead pitch package: (B1) small fillet between leads, (B2) coating does not fill large gap behind the lead, and (B3) small coating fillet in section between leads.	129
Figure 150: Coated and un-conformal coated alloy-42 SOT6 after 2,110 TC cycles; (A) Coated, 0-0 contamination level, 1,500x, and (B) no conformal coating, 0-1 contamination level, 1,500x.....	130

Figure 151: Temperature/humidity test set-up; (A) chamber and (B) sample orientation in the test chamber.....	132
Figure 152: Box plot of whisker lengths after 1,000 h HTHH broken down by lead alloy, part contamination, and board contamination levels (Note: Bias2 = 0 e.g. leads tied to ground)	133
Figure 153: SEM images of copper lead frame SOT5 part with a 1-0 contamination level after 1,000 h HTHH; (A) toe, (B) side, and (C) heel region of a typical solder joint. In (B), an arrow indicates the location of a lone straight whisker along the edge. (Note that the large dark piece on the top of the joint in A and C are not whiskers.)	134
Figure 154: Whisker locations after 1,000 h HTHH with Bias2 = 0; histogram (left) and location definition (right). Note that for the 85°C/85%RH environment the majority of the whisker growth occurs along the very bottom of region 2 along the board pad edge.....	134
Figure 155: Whiskers per lead termination after 1,000 h HTHH for various contamination levels. The SOT5 device has copper leads and the SOT3 and SOT6 devices have alloy-42 leads.....	135
Figure 156: Probability plot of whisker lengths of terminations with copper leads after 1,000 h HTHH; bias2 = 0 (left) and bias2 = 5 (right) levels broken down by part contamination and board contamination level.....	135
Figure 157: Probability plot of whisker lengths of terminations with alloy-42 leads after 1,000 h HTHH; lead bias2 = 0 (left) and lead bias2 = 5 (right) levels broken down by part contamination and board contamination level.....	136
Figure 158: Box plot of whisker lengths of terminations with copper leads after 1,000 h HTHH showing the effect of board contamination and bais1 with no part contamination.....	136
Figure 159: Box plot of whisker lengths of terminations with alloy-42 (SOT3 device) leads after 1,000 h HTHH showing the effect of board contamination and bais1 with no part contamination.....	136
Figure 160: Dot plot of whisker length of terminations with copper (SOT5) leads at a 1-1 contamination level after 1,000 HTHH; ground leads (left) and 5V leads (right) with and without 5V part bias applied (e.g. bias1 = 0 and 5)	137
Figure 161: Dot plot of whisker length for terminations with alloy-42 (SOT3) leads at a 1-1 contamination level after 1,000 h HTHH; ground leads (left) and 5V leads (right) with and without 5V part bias applied (e.g. bias1 = 0 and 5)	137
Figure 162: Dot plot of whisker diameter after 1,000 h HTHH broken down by lead material, part contamination, and board contamination.....	137
Figure 163: Scatterplot of (A) whisker length (microns) versus average diameter (microns) and (B) ln(length) versus ln(average diameter) for terminations with copper and alloy-42 leads after 1,000 HTHH.....	138
Figure 164: Whiskers longer than 100 microns after 4,000 h HTHH	139
Figure 165: Dot plot of whisker length showing the difference between 1,000 and 4,000 h HTHH. Only whiskers longer than 30 to 40 microns were measured in the 4,000 hour data set.....	140
Figure 166: Box plot of whiskers per lead termination after 4,000 h HTHH broken down by lead alloy, part contamination, and board contamination (Bias1=0, Bias2 = 0).....	141
Figure 167: SEM images of an alloy-42 SOT6 at a 0-0 contamination level, part reference designator U65, lead 4 (A) 1,000 h and (B) 4,000 h HTHH. Whisker growth was shorter than the copper leaded SOT5.....	141
Figure 168: Probability plot of whisker lengths after 4,000 h HTHH; broken down by lead alloy for measured whiskers longer than 30 to 40 microns.....	142
Figure 169: Probability plot of whisker lengths for Cu leads after 4,000 h HTHH; broken down by contamination level for measured whiskers longer than 30 to 40 microns.....	142

Figure 170: Probability plot of whisker lengths for Cu leads after 4,000 h HTHH; broken down by location for measured whiskers longer than 30 to 40 microns.....	143
Figure 171: Probability plot of whisker lengths for alloy-42 leads after 4,000 h HTHH; broken down by contamination level for measured whiskers longer than 30 to 40 microns.....	143
Figure 172: Histogram of whisker density (whiskers/mm ²) at location-1 and -2 after 4,000 h HTHH for all contamination levels of Cu and alloy-42.....	144
Figure 173: Histogram of whisker density (whiskers/mm ²) at location-3 and -4 after 4,000 h HTHH for all contamination levels of Cu and alloy-42.....	145
Figure 174: Histogram of whisker density (whiskers/mm ²) at location-5 after 4,000 h HTHH for all contamination levels of Cu and alloy-42.....	146
Figure 175: Top ten whisker densities at location-2 after 4000 h HTHH.....	146
Figure 176: Box plots of whisker density (whiskers/mm ²) comparing lead alloy and contamination after 4000 h HTHH for location-1, and -2, which grow directly toward the opposite lead.....	147
Figure 177: Box plots of whisker density (whiskers/mm ²) comparing lead alloy and contamination after 4000 h HTHH for location-3, -4 and 5, growing from the front surfaces.....	147
Figure 178: SEM images of a copper (SOT5) leaded part with a 1-1 contamination level after 1,000 h HTHH. Increasing magnification views shown from (A) to (B).....	148
Figure 179: SEM images of an alloy-42 (SOT6) leaded part with a 1-1 contamination level after 1,000 h HTHH. Increasing magnification views shown from (A) to (C).....	149
Figure 180: Partial oxidation of SAC solder with copper leaded part (SOT5) and 1-1 contamination; (A) SEM image of oxide near whisker, (B) SEM image of oxide in a thicker region of the SAC solder, (C) optical image of oxidation of solder near the base metal wetting line, and (D) SEM image of region shown in (C)	150
Figure 181: SEM image of voids and cracks observed in the whisker base. The crack is highlighted by an arrow. A large number of voids were observed in the root of the whisker.....	150
Figure 182: SEM images of vertical striations observed on smaller diameter whiskers. SEM images (A), (B) and (C) show increasing magnification views of typical striations.....	151
Figure 183: SEM images of vertical and horizontal striations observed on thicker whiskers. SEM images (A) and (B) show increasing magnification views of typical striations.....	151
Figure 184: SEM images of a copper alloy lead 64 pin quad-flat-pack (QFP64 U08, lead 28) with a 0-0 contamination level after (A) 1,000 h and (B) 4,000 h HTHH. Arrow indicates a broken whisker that has nearly bridged between the printed wiring board pads. The TQFP lead alloy is C7025, which contains Ni, which is different from the SOT5 C194 alloy which does not.....	152
Figure 185: No whisker growth was observed on SAC105 alloy balls soldered with SAC305 solder after 4,000 h of 85°C/85%RH.....	152
Figure 186: SEM images of tin whisker growth on a SAC105+0.01%Ce alloy ball soldered with SAC305 paste on a cleaned board with no contamination after 4,000 h of 85°C/85%RH.....	153
Figure 187: SEM images of a thicker whisker growing from a SAC105+0.01%Ce alloy ball soldered with SAC305 paste on a cleaned board with no contamination after 4,000 h of 85°C/85%RH.....	153
Figure 188: Additional SEM images showing varied density, morphology and length of tin whisker growth on SAC105+0.01%Ce alloy balls soldered with SAC305 paste on a cleaned board with no contamination after 4,000 h of 85°C/85%RH.....	154
Figure 189: Influence of voltage bias on corrosion on coated SOT5 parts after 4,000 h HTHH; (A) electrical schematic, (B) 0-0 contamination level assembly, (C and D) 1-1 contamination level assembly.....	155

Figure 190: Detailed images of coated SOT5 lead 5 with a 0-0 contamination level after 4,000 h HTHH: (A) overall, 250x, (B) side of lead, 500x, (C) detailed image of nodule rupturing thin coating, 1,000x, (D) increasing magnification, 2,500x.....	155
Figure 191: Corrosion on conformal coated SAC105+0.01%Ce (SAC+REE) solder balls after 4,000 h HTHH.	156
Figure 192: Five longest whiskers of the SOT parts from the second inspection after 4,398 h LTHH.	161
Figure 193: Corresponding average whisker diameters for SOT board from second inspection after 4,398 h LTHH (Note: some whisker diameters were not measured).....	162
Figure 194: SOT board whisker length probability plot for the second inspection after 4,398 h LTHH.....	162
Figure 195: SOT5 whisker length probability plot by location for the second inspection after 4,398 h LTHH....	162
Figure 196: Ten longest whiskers of the QFP board parts from the second inspection after 4,398 h LTHH.	163
Figure 197: QFP board probability plot of whisker length for the PLCC, QFP44 and TQFP64 parts from the second inspection after 4,398 h LTHH.	164
Figure 198: Corresponding average whisker diameters for the 10 longest whiskers of the QFP board parts from the second inspection after 4,398 h LTHH (Note: some whisker diameters were not measured).	164
Figure 199: PLCC histogram of whisker location from the second inspection after 4,398 h LTHH.....	164
Figure 200: QFP44 histogram of whisker location from the second inspection after 4,398 h LTHH.....	165
Figure 201: TQFP64 histogram of whisker location from the second inspection after 4,398 h LTHH.	165
Figure 202: QFP individual value plot of whisker length for various contamination levels from the second inspection after 4,398 h LTHH.....	167
Figure 203: QFP box plot of whisker lengths for various contamination levels from the second inspection after 4,398 h LTHH.	167
Figure 204: QFP board probability plot of whisker length for the PLCC, QFP44 and TQFP64 parts combined for various contamination levels from the second inspection after 4,398 h LTHH.	167
Figure 205: QFP board individual value plot of whisker length for Bias2, location and part type from the second inspection after 4,398 h LTHH.	168
Figure 206: QFP board probability plot of whisker length for the PLCC, QFP44 and TQFP64 parts (combined) for various locations from the second inspection after 4,398 h LTHH.....	168
Figure 207: QFP board probability plot of whisker length for the PLCC part for various locations from the second inspection after 4,398 h LTHH.	168
Figure 208: Whisker length versus diameter data from the second inspection after 4,398 h LTHH; (A) average diameter in microns and (B) ln (average diameter).....	169
Figure 209: Ten longest whiskers on the SOT board parts from the final inspection after 16,910 h LTHH.	172
Figure 210: Corresponding average whisker diameters for the 10 longest whiskers of the SOT board parts from the final inspection after 16,910 h LTHH.	172
Figure 211: Final inspection whisker length individual value plot by part lead alloy and contamination level after 16,910 h LTHH. Note no whiskers longer than 10 microns were observed for the assemblies without board level contamination.	174
Figure 212: Final inspection whisker length probability plot for the SOT3, SOT5 and SOT6 part types after 16,910 h LTHH.	174
Figure 213: Final inspection whisker length probabiltiy plot for the SOT5 part leads for various contamination levels after 16,910 h LTHH (all bias levels combined).....	174

Figure 214: Final inspection whisker length probability plot for the SOT5 part leads with Bias2=0 for various contamination levels after 16,910 h LTHH.....	175
Figure 215: Whisker length versus diameter data from the final inspection after 16,910 h LTHH; (A) average diameter in microns and (B) ln (average diameter).....	175
Figure 216: Final inspection whisker angle histogram for the SOT5 parts after 16,910 h LTHH.....	176
Figure 217: Location of whiskers longer than 10 microns from the final inspection after 16,910 h LTHH.....	176
Figure 218: Final inspection whisker length probability plot for the SOT5 part lead terminations with board contamination level = 1 for various locations on the lead after 16,910 h LTHH.....	176
Figure 219: Final inspection whisker density box plot by part and location after 16,910 h LTHH.....	177
Figure 220: Final inspection whisker density probability plot for various locations on the SOT5 part termination after 16,910 h LTHH.....	177
Figure 221: Final inspection whisker density probability plot for various locations on the SOT6 part termination after 16,910 h LTHH.....	177
Figure 222: Final inspection whisker density probability plot for various locations on the SOT3 part termination after 16,910 h LTHH.....	178
Figure 223: Final inspection whisker length box plot for various bias conditions, part contamination and lead alloy after 16,910 h LTHH.....	178
Figure 224: Final inspection whisker length probability plot for the SOT5 part lead terminations with board contamination level = 1 for various bias conditions after 16,910 h LTHH.....	178
Figure 225: Final inspection whisker length box plot for copper lead terminations for various bias conditions and lead number. Under 5V Bias1 conditions, leads two and five have a 5V bias2 condition and leads one, three and four are grounded after 16,910 h LTHH.....	179
Figure 226: Final inspection whisker density probability plot comparing part bias for location-1 on the SOT5 part termination after 16,910 h LTHH.	179
Figure 227: Final inspection whisker density probability plot comparing part bias for location-3 on the SOT5 part termination after 16,910 h LTHH.	179
Figure 228: Final inspection whisker density probability plot comparing part bias for location-4 on the SOT5 part termination after 16,910 h LTHH.	180
Figure 229: LTHH whisker length probability distribution comparison between the second (4,398 h) and the final inspection (16,910 h) of the SOT5 copper lead terminations.....	180
Figure 230: LTHH whisker length probability distribution comparison between the second (4,398 h) and the final (16,910 h) inspection of the SOT3 and SOT6 alloy-42 lead terminations.....	181
Figure 231: Hollow whiskers observed during the first inspection after 1,037 h LTHH on QFP44 termination board pad with a 0-1 contamination level observed.....	181
Figure 232: Hollow whisker observed during the first inspection after 1,037 h LTHH on QFP44 lead with a 1-1 contamination level during the first inspection; (A) overall image of lead and (B) close-up of whisker.	182
Figure 233: Elemental analysis of a hollow whisker.....	182
Figure 234: Whisker observed on SOT5 termination during the second inspection after 4,398 h LTHH, U29, lead 2, 3,500x.....	183
Figure 235: Thin whisker observed on SOT3 termination during second inspection after 4,398 h LTHH, U10, lead 3, 3,000x.....	183

Figure 236: Hollow whiskers observed on SOT5 terminations during the second inspection after 4,398 h LTHH; (A) 0-1 contamination level U29, lead 5, 3,500x, and (B) 1-1 contamination level, U40, lead 2, 1,500x.....	184
Figure 237: SEM images of whisker growth on a Cu lead frame PLCC part with a 0-1 contamination level from the second inspection after 4,398 h LTHH; (A) 100x, (B) 1800x, and (C) 2000x (A-QFP-LT-0-1-ncc-2, PLCC, U13, lead 13).....	185
Figure 238: SEM images of thin whisker growth on a Cu lead frame PLCC part with a 1-1 contamination level from the second inspection after 4,398 h LTHH, 2000x (A-QFP-LT-1-1-ncc-3, PLCC, U12, lead 18).....	186
Figure 239: SEM images of decreasing diameter whisker on Cu lead frame PLCC part termination with a 1-1 contamination level from the second inspection after 4,398 h LTHH, 2500x (A-QFP-LT-1-1-ncc-3, PLCC, U12, lead 1).....	186
Figure 240: SEM images of nodule and whisker growth on a Cu lead frame QFP44 part termination with a 0-1 contamination level from the second inspection after 4,398 h LTHH; (A) 100x and (B) 800x (A-QFP-LT-0-1-ncc-2, PLCC, U13, lead 12).....	187
Figure 241: SEM images of whisker growth from the side of the lead on a Cu lead frame QFP44 part termination with a 1-1 contamination level from the second inspection after 4,398 h LTHH; (A)100x, (B) 1200x (A-QFP-LT-1-1-ncc-3, QFP44, U05, lead 11).....	188
Figure 242: SEM images of decreasing diameter whisker with corrosion at whisker base terminating growth on Cu lead frame QFP44 part termination with a 1-1 contamination level from the second inspection after 4,398 h LTHH; (A) 1200x and (B) 3,000x (A-QFP-LT-1-1-ncc-3, QFP44, U05, lead 11).....	189
Figure 243: SEM images of increasing diameter whiskers/nodules on Cu lead frame QFP44 part termination with a 1-1 contamination level from the second inspection after 4,398 h LTHH, 1,500x (A-QFP-LT-1-1-ncc-3, QFP44, U05, lead 11).....	189
Figure 244: SEM images of whiskers observed during the second inspection on Cu lead frame TQFP64 part termination with a 0-1 contamination level from the second inspection after 4,398 h LTHH; (A) 100x, (B) 400x, (C) left whisker 2,000x, and (D) right whisker, 2,000x (A-QFP-LT-0-1-ncc-2, QFP64, U9, lead 10).	190
Figure 245: SEM images of hollow whisker on Cu lead frame PLCC part termination with a 0-1 contamination level from the second inspection after 4,398 h LTHH; (A) overall image of lead and (B) close up of long whisker, 100x (A-QFP-LT-0-1-ncc-2, PLCC, U12, lead 9).	191
Figure 246: Comparison of clean Cu lead surfaces at a 0-0 contamination level at 4,398 h (A and C) and 16,910 h (B and D) LTHH. Images A and B show lead 3, 2000x (A-SOT-LT-0-0-ncc-1, SOT5, U23, lead 3). Images C and D show lead 2, 3,000x (A-SOT-LT-0-0-ncc-1 SOT5, U26, lead 2). Arrow in D highlights additional tin growth around the original whisker.	192
Figure 247: Comparison of corrosion/oxidation and whisker growth of SOT6 alloy-42 lead terminations at a 0-1 contamination level at (A) 4,398 h and (B) 16,910 h LTHH, 200x (A-SOT-LT-0-1-ncc-1, U75, lead 3,). Arrows in A and B indicate a typical corrosion/oxidation increase.....	192
Figure 248: Comparison of corrosion/oxidation and whisker growth of SOT5 Cu lead terminations at a 0-1 contamination level at (A) 4,398 h and (B) 16,910 h LTHH, 3,500x (A-SOT-LT-0-1-ncc-1, U29, lead 2). Arrows show new whisker growth.....	193
Figure 249: Thin and hollow whiskers observed on a SOT 5 lead with a 1-1 contamination level at 16,910 h LTHH (A-SOT5-LT-1-1-ncc3, SOT5, U30, lead 2); (A) overall 250x, (B) extremely thin whisker at location-2, 3,000x, (C) thin whisker at location-1, 1,800x, (D) hollow whiskers at location-3, 1,500x. Note that the thin whiskers were not visible at 250-300x magnification.....	193
Figure 250: Thin whiskers straight and kinked whiskers observed on a SOT5 lead with a 1-1 contamination level at 16,910 h LTHH; (A) overall lead, 100x, (B) thin straight whisker, 800x, (C) close-up of B, 2500x, and (D) thin highly kinked whisker, 2500x (A-SOT5-LT-1-1-ncc3, SOT5, U40, lead 2).....	194

Figure 251: Extremely thin whiskers shaped similar to hollow whiskers observed at 16,910 h LTHH on a Cu alloy lead with a 0-1 contamination level (A-SOT-LT-0-1-ncc1, SOT5, U5, lead 2); (A) Overall SEM, 600x, (B) whisker tip, 20,000x, (C) whisker base, 8,000x, and (D) whisker base close-up 20,000x.....	194
Figure 252: Recrystallized grains and oxidation (darker areas) around IMC particles observed at 16,910 h LTHH on a Cu alloy lead with a 1-0 contamination level (A-SOT5-LT-1-0-ncc1, SOT5, U7, lead 5 and 4); (A) Overall, 100x, (B) oxidation and whisker inception, 500x, (C) recrystallization, oxidation and whisker inception, 2,000x, and (D) oxidation and recrystallization, 1,500x.....	195
Figure 253: Almost no oxidation, some recrystallization but no whiskers were observed at 16,910 h LTHH on Cu alloy leads on clean parts and assemblies with a 0-0 contamination level (A-SOT5-LT-0-0-ncc1, SOT5, U23, lead 3); (A) overall SEM, 100x, and (B) close-up, 2,000x.	195
Figure 254: Very little oxidation and no whiskers observed at 16,910 h LTHH on SOT6 alloy-42 leads on clean assemblies, 100x; (A) 1-0 contamination (A-SOT-LT-1-0-ncc2, SOT6, U70), (B) 0-0 contamination level (A-SOT-LT-0-0-ncc1, SOT6, U69) (C) 1-0 contamination level (A-SOT-LT-1-0-ncc2, SOT6, U76).	196
Figure 255: Optical image of a whisker cross-section showing oxidation around whisker after 16,910 h LTHH on a SOT5 Cu lead with a 1-1 contamination level (A-SOT-LT-1-1-ncc3, SOT5, U4, lead 1).	196
Figure 256: SEM image of a whisker cross-section showing oxidation (darker regions) around and on whisker after 16,910 h LTHH on a SOT5 Cu lead with a 1-1 contamination level (A-SOT-LT-1-1-ncc3, SOT5, U4, lead 1); (A) overall, 100x, (B) whisker, 3,000x, (C) whisker close-up showing a crack near the whisker base, 9,000x, and (D) second ion beam polish of whisker showing cracks in the oxide, 3,000x.....	197
Figure 257: Heel fillet cross-section SEM image showing solder roughness and oxidation/corrosion after 16,910 h LTHH on a SOT5 Cu lead with a 0-1 contamination level (A-SOT-LT-0-1-ncc2, SOT5, U29, lead 4); (A) overall, 100x, (B) close-up showing oxidation (darker areas) propagation along the interdendritic boundaries, 1,500x.....	197
Figure 258: Conformal coating on SOT5, with 1-1 contamination level after 16,910 h LTHH; (A) overall, 50x, (B) top of lead, 100x, and (C) top of lead, 150x.....	198
Figure 259: Conformal coating on QFP 44, with 1-1 contamination level after 16,910 h LTHH; (A) overall, 40x and (B) lead tip, 150x and (C) top of lead, 150x. No cracks or coating degradation observed.	198
Figure 260: Conformal coating on SAC105+REE BGA ball after 16,910 h LTHH.....	199
Figure 261: Cross-section of SAC105+REE BGA ball with conformal coating after 16,910 h LTHH; (A) overall ball, 100x, (B) overall ball with contrast enhanced to show coating, 100x, (C) close up of top left side, 4,500x, and (D) close-up of top right side, 4,500x. Light lines in the images is the gold sputtering applied to the top of the coating prior to cross-sectioning to enhance the demarcation between the coating and potting.....	199
Figure 262: (A) schematic of gull wing leads with bridging and non-bridging whiskers (B) equal parallel plate, (C) unequal parallel plates, (D) equal perpendicular plates, and (E) parallel cylinders.	202
Figure 263: Overall whisker risk mitigation assessment approach.	203
Figure 264: Computational approach to compute used to determine the overall bridging risk for an assembly. ..	203
Figure 265: Short circuit risk model inputs and modeling analysis step details for a given part.	204
Figure 266: Part spacing demographic for a typical digital board.....	205
Figure 267: Conformal coating coverage assessment of low VOC 100 percent solids spray coatings; (A) Optical image, (B) isometric SEM [52], and (C) top SEM view of AR/UR Manufacturer-1 and (D) top SEM view of UV40-250 used in the present work. The light color in the SEM images indicates that the coating thickness was less than three microns.....	206
Figure 268: TQFP128 soldered to a board with tin-lead solder. The nominal lead-to-lead gap spacing is 220 microns. The coating was a 100 percent solids low VOC AR/UR coating [90]; (A) overall view and (B) higher	

magnification view with package removed and ultraviolet light illumination. The UV light causes the coating to fluoresce.....	206
Figure 269: Determination of lead-to-lead spacing distance for a bridging whisker.	207
Figure 270: Simplified lead geometry	208
Figure 271: Gap spacing reduction at the board copper pad by board fabrication etch tolerances and a slightly bulbous solder joint at lead on the TQFP64 board pads (Note SEM image obtained after 4,000 h exposure at 85°C/85%RH).	209
Figure 272: Modifications to the original whisker risk model.	210
Figure 273: Example of a QFP lead view factor and whisker spacing distribution calculation flow.....	212
Figure 274: Lead whisker view factor correlation.....	213
Figure 275: Solder whisker view factor correlation	213
Figure 276: Pad whisker view factor correlation.....	214
Figure 277: Conformal coating coverage assessment of low VOC 100 percent solids AR/UR UV cure spray coatings; (A) Typical optical image, and (B), (C) and (D) showing typical isometric SEM images of different packages and coating manufacturers. The light color in the SEM images indicates that the coating thickness was less than three microns.....	214
Figure 278: Partially-coated versus uncoated view factors	215
Figure 279: Description of whisker spacing to nominal spacing ratio (SR).....	215
Figure 280: Non-dimensional spacing distribution for lead whiskers.....	217
Figure 281: Non-dimensional spacing distribution for solder whiskers.....	218
Figure 282: Non-dimensional spacing distribution for pad whiskers.....	218
Figure 283: (A) Whisker growth locations, (B) Probability plot of whisker lengths (microns) from the HTHH testing for Cu leads after 4,000 h at 85°C/85%RH; broken down by location (from Figure 170) and (C) conversion of lognormal mean parameters from microns to mm.	222
Figure 284: Hypothetical example of lead, solder and pad spacing/whisker length distribution and bridge interference plots.....	224
Figure 285: Probability of a bridge shorting (from Courey [98]).....	225
Figure 286: (A) Part drawing nomenclature, (B) lead dimension nomenclature, (C) side view of modeled lead and pad, and (D) top view of modeled lead and pad.....	226
Figure 287: TQFP128 spacing, whisker length and bridging interference plots.....	232
Figure 288: Summary of computed TQFP128 short circuits for three levels of coating mitigation.	233
Figure 289: Perpendicular plate spacing.	236
Figure 290: Parallel plate and round lead shape factor correlation.	238
Figure 291: Correlation for 95% spacing prediction	239
Figure 292: Non-dimensional spacing distribution for parallel flat plates.....	240
Figure 293: Non-dimensional spacing distribution for perpendicular flat plates.	241
Figure 294: Non-dimensional spacing distribution for parallel round leads.	241
Figure 295: Small and large plate approximation.	243
Figure 296: Comparison of whisker length distributions for plate to QFP lead and solder.	245

Figure 297: Comparison of whisker length distribution for plate to 0603 terminal and solder.....	245
Figure 298: <i>Roll Up</i> tab.....	246
Figure 299: Upper portion of <i>Model</i> tab.....	247
Figure 300: Lower portion of <i>Model</i> tab.....	248
Figure 301: <i>Whisker</i> tab.....	249
Figure 302: Numerical whisker length distribution.....	250
Figure 303: Distribution plots	251
Figure 304: Shorting probability tab	252
Figure 305: Location of whisker growth from SAC305 solder; (A) whiskers growing from the region where the lead exits the solder joint on a SOT alloy-42 lead after simulated power cycling thermal cycling from +50 to 85 °C and (B) whiskers growing from the edge of the board pad where solder has flowed around the edge on a SOT5 C194 lead at a 0-0 contamination level after 4,000 h of exposure to high temperature high humidity at 85°C/85%RH.....	253

List of Tables

Table 1: Primary experiment whisker measurement summary on the SOT boards	8
Table 2: TQFP128 lead and pad dimensions (mm)	28
Table 3: Shorting results for TQFP128 with no coating (ref . Table 78)	29
Table 4: Contamination screening test assembly component lead-frame and surface finish materials.....	39
Table 5: Flux composition.....	41
Table 6: Flux contamination on solder joints	41
Table 7: Relationship between the as-received component contamination level and assembly whisker formation.	46
Table 8: Experimental summary and results on first set of REE samples.....	62
Table 9: Experimental results on second set of samples with shorter exposure time.....	63
Table 10: SOT board parts under test.....	72
Table 11: SOT board lead material composition.....	72
Table 12: QFP board parts under test	73
Table 13: QFP board lead material composition	73
Table 14: BGA component solder pad patterns.....	76
Table 15: Primary experiment environments	78
Table 16: Non-coated SOT board set	79
Table 17: Primary WP1753 experiment DOE samples	80
Table 18: Number of experimental replicates planned.....	81
Table 19: Part contamination levels after cleaning.	87
Table 20: Part contamination levels after intentional Cl contamination.	87
Table 21: Computed areas for the SOT3 whisker growth locations (mm ²).....	95
Table 22: Computed areas for the SOT5 whisker growth locations (mm ²).....	96
Table 23: Computed areas for the SOT6 whisker growth locations (mm ²).....	96
Table 24: Alloy-42 SOT3 results from second inspection after 730 PCTC cycles	98
Table 25: Alloy-42 SOT6 results from second inspection after 730 PCTC cycles	99
Table 26: Alloy-42 SOT3 with no flux results from third inspection after 1,797 PCTC cycles	101
Table 27: Alloy-42 SOT3 with flux results from third inspection after 1,797 PCTC cycles	101
Table 28: Alloy-42 SOT6 with no flux results from third inspection after 1,797 PCTC cycles	102
Table 29: Alloy-42 SOT6 with flux results from third inspection after 1,797 PCTC cycles	102
Table 30: Copper SOT5 results from third inspection after 1,797 PCTC cycles	103
Table 31: Whisker measurement summary after 500 TC cycles.....	112
Table 32: Whisker measurement summary after 2,110 TC cycles.....	112
Table 33: Whisker measurement summary after 1,000 h HTHH.....	132

Table 34: SOT5 (copper leads) whisker distribution after 1,000 h HTHH.....	133
Table 35: SOT3 (alloy-42 leads) whisker distribution after 1,000 h HTHH.....	133
Table 36: SOT6 (alloy-42 leads) whisker distribution after 1,000 h HTHH.....	133
Table 37: Whisker measurement summary after 4,000 h HTHH.....	139
Table 38: Whiskers longer than 100 microns after 4,000 h HTHH.....	140
Table 39: Whisker density of whiskers growing from the solder at the board pad (location-2) for the SOT5 at a 0-0 cleanliness level after 4,000 h HTHH.....	147
Table 40: Long term high humidity exposure and inspection points over nearly three years.....	158
Table 41: LTHH Whisker inspection summary	158
Table 42: Whisker observations from the first inspection after 1,037 h LTHH.....	159
Table 43: Whisker measurement summary from the SOT board second inspection after 4,398 h LTHH.....	159
Table 44: SOT5 component and lead whiskering summary from the second inspection after 4,398 h LTHH.....	160
Table 45: SOT6 component and lead whiskering summary from the second inspection after 4,398 h LTHH.....	160
Table 46: SOT3 component and lead whiskering summary from the second inspection after 4,398 h LTHH.....	160
Table 47: SOT5 whisker length summary from the second inspection after 4,398 h LTHH.....	161
Table 48: SOT6 whisker length summary from the second inspection after 4,398 h LTHH.....	161
Table 49: SOT3 whisker length summary from the second inspection after 4,398 h LTHH.....	161
Table 50: Whisker measurement summary from the QFP board second inspection after 4,398 h LTHH.....	163
Table 51: PLCC20 whisker summary from the second inspection after 4,398 h LTHH.	165
Table 52: QFP44 whisker summary from the second inspection after 4,398 h LTHH.	166
Table 53: TQFP64 whisker summary from the second inspection after 4,398 h LTHH.	166
Table 54: Whisker measurement summary from the final inspection after 16,910 h LTHH.	170
Table 55: SOT5 component lead whisker growth summary from the final inspection after 16,910 h LTHH.	170
Table 56: SOT6 component lead whisker growth summary from the final inspection after 16,910 h LTHH.	170
Table 57: SOT3 component lead whisker growth summary from the final inspection after 16,910 h LTHH.	171
Table 58: SOT5 whisker growth summary from the final inspection after 16,910 h LTHH.	171
Table 59: SOT6 whisker growth summary from the final inspection after 16,910 h LTHH.	171
Table 60: SOT3 whisker growth summary from the final inspection after 16,910 h LTHH.	172
Table 61: SOT5 Total whisker count by lead for various contamination levels from the final inspection after 16,910 h LTHH.	173
Table 62: SOT5 Total whisker count by location for various contamination levels from the final inspection after 16,910 h LTHH.	173
Table 63: Number of lead gaps for various circuit boards from a control system	205
Table 64: Parts and dimensions considered for risk modeling (dimensions in mm).	211
Table 65: Coefficients to calculate minimum spacing.	216
Table 66: Coefficients to calculate maximum lead spacing	216
Table 67: Non-dimensional whisker distribution	219

Table 68: Lognormal parameters for the Dunn whisker measurements.....	221
Table 69: Whisker density of whiskers growing from the solder at the board pad (location-2) for the SOT5 at a 0-0 cleanliness level after 4,000 h at 85°C/85%RH HTHH (repeated from Table 39).	223
Table 70: Model default parameters used to determine the simplified lead geometry	227
Table 71: TQFP128 Part Drawing Dimensions (mm).....	227
Table 72: TQFP128 manual over-ride option for lead and board pad dimensions (mm).....	228
Table 73: TQFP128 Calculated parameters.....	228
Table 74: Lead whisker input sheet.....	229
Table 75: Solder whisker input sheet	230
Table 76: Pad whisker input sheet.....	231
Table 77: TQFP128 material summary.	231
Table 78: Shorting results for TQFP128 with no coating.....	232
Table 79: Shorting results for TQFP128 with a 40 percent coating effectiveness.	232
Table 80: Shorting results for the TQFP128 with added coating or tin-lead mitigation at the board (board pad whisker density set to zero).....	233
Table 81: Dimensions considered for the parallel flat plate model.	234
Table 82: Dimensions considered for the parallel round lead model.	235
Table 83: Dimensions considered for the perpendicular flat plate model.	235
Table 84: Coefficients for Length, Width, and Max./Min. Spacing for 95% Spacing	239
Table 85: Non-dimensional whisker distribution	242
Table 86: Comparison of approximate (closed-form) and Monte Carlo view factor	244

Acronyms

Acronym	Definition
A	First Bend Distance
Alloy-42	Fe42Ni composition lead material (composition is in weight percent)
AR/UR	Acrylic/Urethane
BGA	Ball Grid Array
CALCE	Center for Advanced Life Cycle Engineering, University of Maryland
CTE	Coefficient of Thermal Expansion
DAU	Defense Acquisition University
DI	Deionized
DRX	Dynamic Recrystallization
DSC	Differential Scanning Calorimeter
EDX	Energy Dispersive X-ray Spectroscopy
ENEPiG	Electroless Nickel Electroless Palladium Immersion Gold
ENIG	Electroless Nickel Immersion Gold
ER	Epoxy resin
f	Lead Foot Length
h	hours
H	First Bend Height
HT/HH	High Temperature/High Humidity
IC	Ion Chromatography
IMC	Intermetallic
iNEMI	International Electronics Manufacturing Initiative
IPA	Isopropanol
IPC	IPC Association Connecting Electronics Industries
JEDEC	Joint Electron Devices Engineering Council
JEITA	Japan Electronics and Information Technologies Association
L	Lead Span Length
LT/HH	Low Temperature/High Humidity
MSA	Methane Sulfonic Acid
ORH1	Organic water soluble flux with halide content below 2.0%
PCB	Printed Circuit Board synonymous with PWB
PWB	Printed Wiring Board synonymous with PCB
PCTC	Simulated power cycling thermal cycling
PDIP	Plastic Dual In Line Electronic Package
PLCC	Plastic Leaded Chip Carrier Electronic Package
ppm	Parts per million
PTH	Pin-Through-Hole
QFP	Quad-flat-pack Electronic Packages
QPL	Qualified Providers List
REE	Rare Earth Element (Note only RE is used in a chemical formula)
RESn	Rare Earth Sn intermetallic compound
RH	Relative Humidity
RMA	Mildly activated rosin fluxes
RoHS	Reduction of Hazardous Substances
ROL0	Low activity rosin based flux with halide content below 0.05%

Acronym	Definition
ROL0	Low activity rosin based flux with halide content below 0.05%
ROL1	Low activity rosin based flux with halide content below 0.5%
ORLO	Low activity organic acid flux with halide content below 0.05%
ORH1	High activity organic acid flux with halide content below 2.0%
ROSE	Resistance of Solvent Extraction
SAC	Sn-Ag-Cu alloy lead free solder
SAC105	Sn1.0Ag0.5Cu (composition is in weight percent)
SAC305	Sn3Ag0.5Cu alloy lead free solder (composition is in weight percent)
SAC405	Sn3.8Ag0.7Cu (composition is in weight percent)
SEM	Scanning Electron Microscopy
SMT	Surface Mount Assembly
SMTA	Surface Mount Technologies Association
SN100C	99.3Sn0.7Cu0.05Ni+Ge Lead-free alloy (composition is in weight percent)
SOIC	Small outline integrated circuit package
SOT	Small Outline Transistor Electronic Packages
SR	Silicon Rubber
S _R	Spacing ratio
t	Lead Thickness
TC	Thermal Cycling
TQFP	Thin Quad-flat-pack Electronic Packages
WEEE	Waste Electrical and Electronic Equipment Directive
XRF	X-Ray Fluorescence
um	Micrometers or microns
UV	Ultraviolet light
XY	Designation for para-xylylene conformal coating (Parylene™ is an XY coating material)
V	Volt
VOC	Volatile organic compound
wt%	Weight percent

Acknowledgements

The principle investigators would like to acknowledge the following individuals for their contributions:

David Kayser, NAVAIR project DoD technical point of contact, for his military electronics systems perspective on the tin whisker research

Jeff Kennedy, Celestica, for his help with the white papers and reports, project engineering and technical guidance.

Zorheh Bagheri, Celestica, for her patient SEM examination during the collection of whisker characteristics and her precise whisker cross-sectioning.

Marianne Romansky, Celestica, for her technical assistance, help with the original white paper creation and continuing financial oversight.

Leonid Snugovsky, University of Toronto for his contributions to understanding the microstructural impact of rare earth element additions to SAC solder

Andre Delhaise, University of Toronto, for help with the data analysis.

Jie Qian, Celestica, for her cross-section sample preparation and part contamination.

Eva Kosiba, Celestica, for her help manufacturing the test vehicles, developing the part and assembly contamination techniques and painstakingly contaminating hundreds of SOT devices and placing them back in their reels. In addition, we are thankful for her program management of the activity in the lab and the environmental testing.

Prakash Kapadia and Andrea Rawana, Celestica, for the piece part and assembly ionic contamination measurements.

Russell Brush, Celestica, for his review of the test vehicle and environmental chamber test harness design.

Stephen McKeown, BAE Systems, for his extensive efforts developing the tin whisker risk modeling framework

Clive Morris and Craig Sabin, BAE Systems, for their help with the experimental design

Don Hewett, BAE Systems, for the test vehicle board artwork design.

Sharon Cronk, BAE System, for her program management oversight.

Evan Ekstrom, BAE Systems, for his help with data analysis

David Pinsky, Raytheon, for this thoughtful review of the present manuscript.

John Dion, BAE Systems, for technical support on materials interactions and tin whisker growth mechanisms.

Paul Vianco, Sandia National Labs, for his discussions on dynamic recrystallization factors pertaining to whisker nucleation and growth

Henning Leidecker, Jay Brusse, and Lyudmyla Panashchenko (NASA Goddard), Michael Osterman, (University of Maryland CALCE), Eric Chason (Brown University), Dave Pinsky and William Rollins (Raytheon), and Dave Hillman (Rockwell Collins) for their thoughts on whisker nucleation and growth

1. Objective

The use of “commercial-off-the-shelf” (COTS) lead-free electronics assemblies in DoD systems has resulted in increased tin whisker short circuit failure risk. The objective of this effort is to evaluate the whisker risk and coating whisker mitigation on lead-free soldered assemblies to ensure reliable low cost systems with the most current technology for the warfighter. Tin whisker testing was targeted to evaluate key part, manufacturing, and environmental variable combinations hypothesized to contribute to whisker growth, with particular emphasis on areas unique to the DoD such as corrosion, rework, and long term storage. In order to utilize lead-free solders in diverse military and aerospace systems environments, the whisker risk factors posed by these material combinations must be understood and mitigated. By understanding the interaction of these variables and how conformal coating behaves in the long term it will be possible to put appropriate controls in place to manage the whisker phenomena.

2. Approach

Systematic tin whisker testing was performed on lead-free soldered assemblies over a range of environments applicable to military systems. Whisker growth from high stress short term test environments were compared to longer term lower stress environments. Two thermal cycle ranges and two isothermal high humidity conditions were evaluated. The longest test was a low temperature/high humidity storage test performed over three years. In the testing, several key design (lead materials, bias voltage and part types), manufacturing (solder alloy, flux, cleanliness level) and environmental (temperature and humidity) variable combinations are analyzed with a focus on the combination of factors that result in significant whisker growth. Particular attention was paid to the cleanliness and metallurgical details before and after environmental exposure in an effort to gain insight on the stress relaxation mechanisms associated with whisker nucleation and growth. In addition, a tin whisker risk model was created to statistically evaluate electronic assembly short circuits. A unique modeling approach was developed to rapidly evaluate different whisker length distributions for a given set of parts. The model also considers conformal coating mitigation and circuit voltage to determine the probability of a short circuit on a single part or group of parts. The short circuit failure risk of any system functional group could be obtained by combining the whisker statistics, the part geometry spacing distribution, and circuit details.

Structure of the document:

A project summary and conclusion are provided first summarizing experimental and modeling efforts. Following the summary, detailed sections are provided for whisker growth theory, the screening experiments, the primary experiments and the short circuit risk modeling efforts. The citations highlighted in bold refer to the papers generated from the WP1753 research.

3. Project summary and conclusions

A high level background section, along with a summary of the whisker growth experiments and the whisker short circuit risk modeling framework are presented next. The results from two screening experiments are presented first to establish some key parameters for the more extensive set of primary experiments used to obtain the whisker growth statistics. The primary environmental tests were designed to obtain whisker growth on Sn3Ag0.5Cu (SAC305) soldered assemblies with respect to contamination level, lead material, voltage bias, rare earth alloying, and conformal coating.

The tin whisker short circuit modeling portion of the project leveraged the experimental whisker growth results and published literature. A unique modeling approach was developed to rapidly evaluate different whisker length distributions for a given set of parts. Monte Carlo analysis was used to determine whisker bridging spacing distributions for various piece parts. The spacing distributions were then convolved with whisker length probability data and electrical conduction probabilities to determine the short circuit risk. The model also considers conformal coating mitigation and circuit voltage to determine the probability of a short circuit on a single part or group of parts.

Note that all alloy compositions are given in weight percent and that the whisker lengths and diameters are reported in microns.

3.1 Background

With the advent of lead-free electronics resulting from the European Union RoHS (Reduction of Hazardous Substances) legislation, new lead-free materials and processes have replaced heritage tin-lead materials and processes. The warfighter benefits by having the most current technology by the adaptation of low cost COTS electronics to weapon systems as long as reliability is maintained. The lead-free materials have changed piece parts, printed wiring board materials, component and printed wiring board (PWB) finishes, solder alloys, solder processes, solder flux chemistries, and cleaning chemistries. Regardless of the how the materials and processes have changed, DoD assemblies are still expected to perform in a diverse set of environments and mechanical loading conditions. These environments range from the high humidity of the jungle, the extreme cold of the arctic, the heat of the desert and the corrosive conditions of the oceans while being subjected to an equally diverse set of mechanical loading conditions, which in the most extreme cases includes gun/cannon fire, aircraft carrier landings, parachute drops, depth charges, rocket launches, and jet engine vibration.

Progress is being made towards DoD focused tin whisker risk assessments and whisker growth mechanisms (long term testing, corrosion/oxidation in humidity, and thermal cycling). The current research is addressing several priority knowledge gaps from the *Lead-free Manhattan Project's* [1] whisker mitigation topic. The Strategic Environmental Research and Development Program (SERDP) sponsorship continues to help the DoD advance toward closure of the Lead-free Manhattan Project's tin whisker knowledge gaps.

The aerospace and defense industries have introduced tin whisker risk mitigations [2] based primarily on the technical data generated by the commercial electronics manufacturers. However, there is a need to further understand the combinations of factors in DoD systems that promote whisker growth on assemblies in an effort to improve whisker mitigation practices.

Metal whisker induced electronic failures have been the subject of intensive research since 1946 [3]. Recently, almost all of the research on tin whiskers has been concentrated on components [4]-[9]; Sn plating composition and thickness, grain size, grain orientations, and Ni under-layer factors have been intensively studied, producing a great deal of knowledge. However, this approach does not consider the very real situation in which components are assembled on circuit boards using lead-free solder alloys and fluxes. Many important factors were not taken into consideration and have not been properly addressed yet, including questions such as: (1) Does the level of contamination of piece-parts and boards before assembly, and flux residue after assembly, affect whisker formation? (2) What cleanliness criteria and requirements for assembly materials and parameters may reduce the risk of whisker formation? (3) Does external contamination augment the risk of corrosion and whisker growth in harsh environments such as salt fog or sulfur-rich atmospheres?

In a previous study [10], the authors found that in lead-free solder joints to alloy-42 base material, leads can form long Sn whiskers under certain conditions. The tin whiskers grew from both bulk SAC405 (Sn3.8Ag0.7Cu) and SAC305 solder due to the following factors: solder microstructure and its modification during oxidation and corrosion, alloy-42 base material, base material underplating quality and contamination, overall piece-part contamination, and rework flux residue on solder. It is suspected that the origin of whisker growth was related to corrosion. Corrosion of the SAC solder was observed to have propagated through the eutectic regions in the interdendritic spaces of the solder and was accompanied by intensive diffusion in the bulk solder. The driving force for whisker nucleation and growth was suspected to involve local compressive stresses in solder regions with chemically modified microstructure and composition. These local zones are surrounded by non-modified solder and are under high stress because its volume is changed. Highly stressed pure tin regions generally undergo stress relaxation via hillock and whisker formation.

Compressive stress in tin or tin rich alloys thinner than approximately 25 microns are generally believed to contribute to tin whisker growth. Military equipment experiences many different stresses throughout its service life (Figure 1).

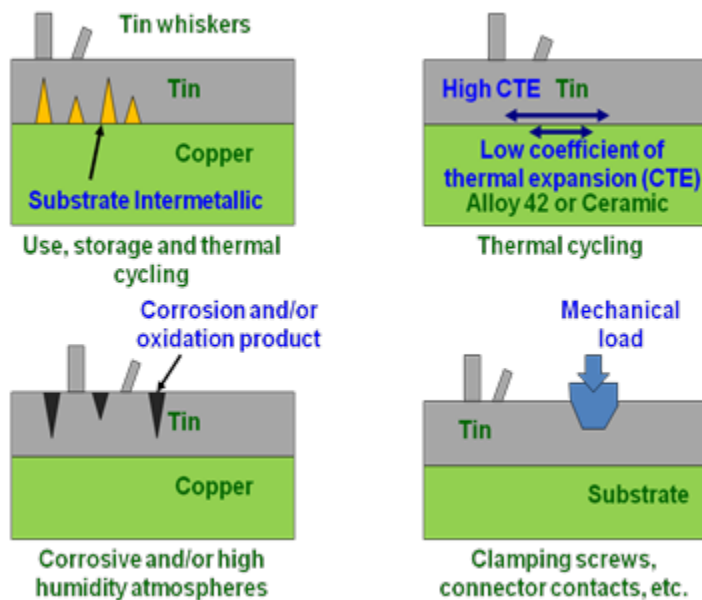


Figure 1: Compressive stresses from intermetallic growth, thermal cycling, corrosion, and mechanical loads contribute to whisker growth.

Several recently published studies support the important role of fluxes and other sources of ionic contamination and reflow atmosphere in whisker growth from solder joints [11]–[16]. However, there is still a lack of knowledge on component contamination before assembly, Sn plating integrity and other plating defects, assembly materials such as solder pastes and both wave and rework fluxes, as well as assembly cleanliness.

It has been observed that lead-free high tin solder alloys, including the widely used solder alloys SAC305, SAC405 and SN100C (99.3Sn0.7Cu0.05Ni+Ge), can create whiskers under certain circumstances. Whiskers can grow from plated or dipped lead-free high tin surface finishes as well as from bulk solder given the appropriate combination of factors. As shown in Figure 2, component and board termination finishes in lead-free assemblies are often plated pure tin having a propensity for whisker formation. Electroplated tin and lead-free solder exhibit poorer wetting than heritage tin-lead alloys which results in more thin tin plated finish when lead-free solder is used. In addition, in an effort to improve wetting, more aggressive fluxes are used which increases the ionic contamination risk. Furthermore, the solidification kinetics of lead-free alloys, (e.g. Sn-Ag-Cu), result in a rough surface that tends to accumulate contamination and is difficult to clean.

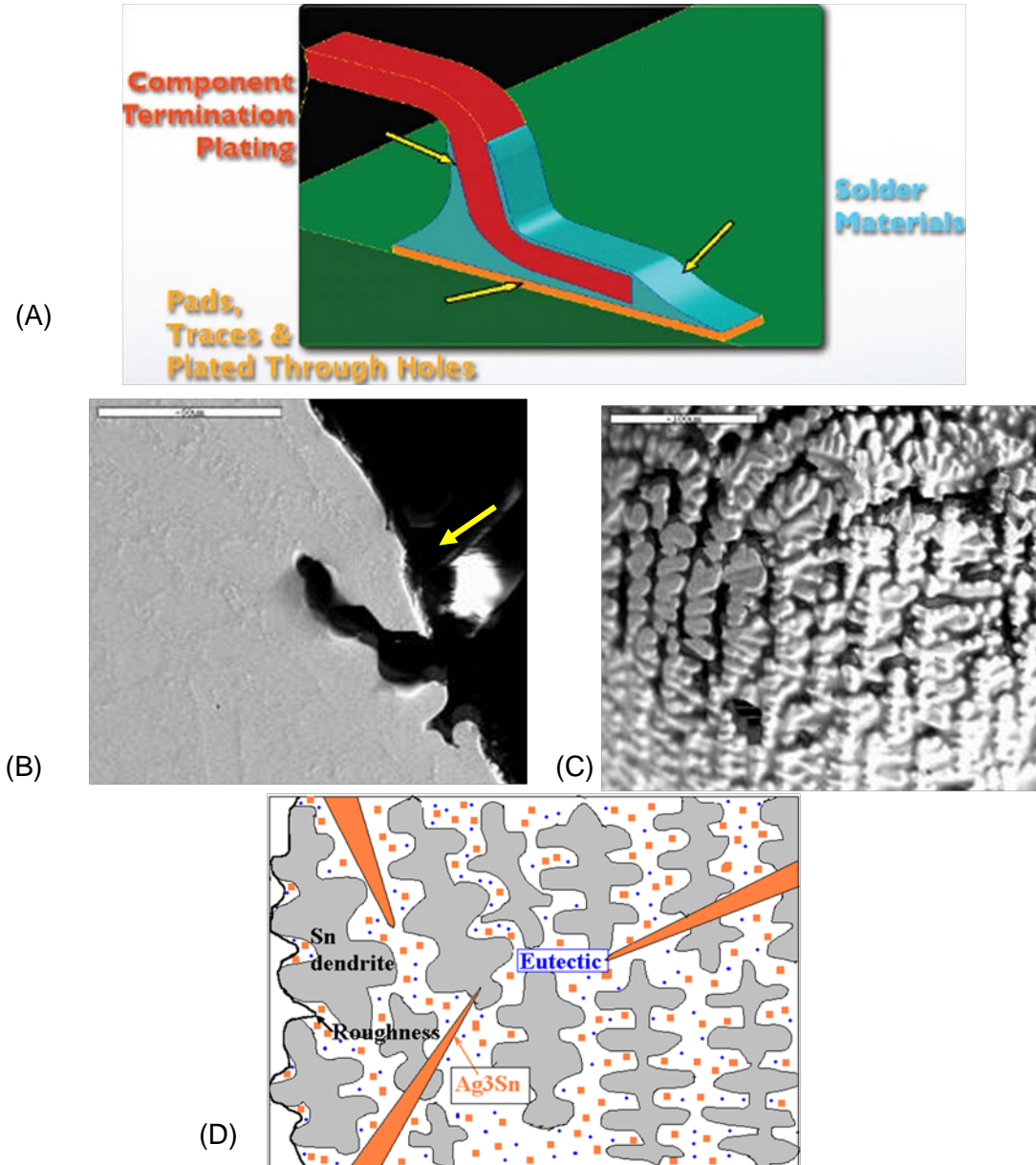


Figure 2: Potential whisker growth regions and roughness features on SAC soldered assemblies.
 (A) Schematic of a lead soldered to a printed circuit board pad, (B) cross-section of shrinkage void in Sn-Ag-Cu solder, (C) surface of shrinkage void in Sn-Ag-Cu solder imaged with a scanning electron microscope and (D) schematic showing Sn dendrites, Ag₃Sn intermetallic and eutectic in the interdendritic spaces. The eutectic in the interdendritic spaces solidifies last and shrinks with respect to the Sn dendrites forming voids. The voids tend to trap contaminants that can promote corrosion and induce whisker growth.

3.2 Summary of whisker growth experiment methods and materials

Highlights of the primary whisker environmental test results from a set of custom designed test boards with commercial parts assembled with SAC305 solder are presented next. The experiment design variables included lead material, rare earth element addition to solder, electrical bias, conformal coating and contamination. Three assembly types were evaluated (Figure 3). The boards are each 6 cm x 6 cm x 0.236 cm thick with immersion tin finished copper on glass epoxy laminate.

Low profile leaded parts were included on the small outline transistor (SOT) board, typical leaded parts were included on the quad-flat-pack (QFP) board and SAC305 soldered SAC105 solder balls with and without Ce were evaluated on the ball grid array (BGA) board. Note that the assembly solder completely wicked up the low profile part leaded in most cases, allowing the evaluation of the SAC solder's tin plating mitigation characteristics. The SOT5, QFP44, TQFP64 and PLCC part leads were all Cu alloy material and the SOT3 and SOT6 were alloy-42. The coated assemblies were spray coated with an AR/UR coating to a nominal thickness of 75 microns. All processes and materials were in accordance with J-STD-001 Class 3 [17] requirements typical of DoD electronics.

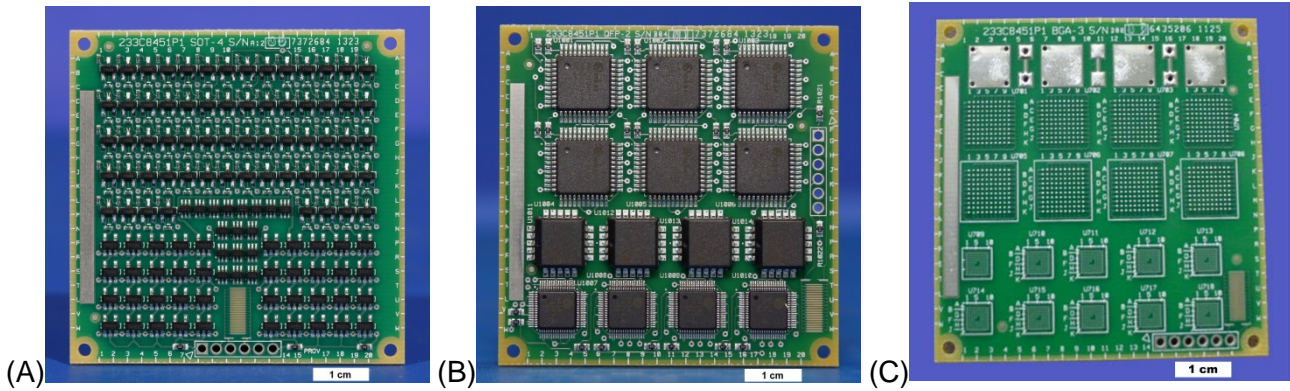


Figure 3: SOT, QFP and BGA assemblies.

A combination of part and assembly level contamination was evaluated (Figure 4). Controlled contamination levels were obtained on the parts and assemblies by immersing them in aqueous Cl solutions and then drying them. Part contamination levels were chosen to be consistent with normal industrial part practices and assembly contamination levels were chosen to be at the upper level of the J-STD-001 class 3 manufacturing standard for a newly manufactured assembly. The cleaning achieved ionic contamination levels that were about 10 times below industrial acceptance levels.

The screening experiments [18] – [20] were performed which determined the following parameters for the primary experiments:

- (1) Cl is a representative the ionic contaminant for corrosion induced whisker growth experiments
- (2) Increasing time intervals between whisker inspections should be used rather than fixed intervals when the same assembly is examined multiple times during environmental exposure
- (3) Ce is a representative the rare earth element to evaluate whisker growth in the SAC solder

The whisker growth model proposed by Vianco and Rejent [21] [22] suggests that whisker growth would occur in a certain stress range for a given Sn grain size and temperature. If the Sn stresses are too high or too low, whiskers would not form. A 4X thermal cycling stress range was evaluated by comparing the JESD-201 piece part whisker testing [23] thermal shock cycling and a lower stress representative of high temperature power cycle environments were used. Previous investigators found 85°C/85% RH to be effective for SAC solder whisker growth [25] [26] [27] and 85%RH was optimal for room temperature whisker growth [28]. The following whisker test environments were selected to generate a range of whisker growth stresses (Figure 5):

- (1) Simulated power cycling thermal cycling (PCTC) +50 to 85 °C for 1,797 cycles [29]
- (2) Thermal shock cycling (TC) -55 to +85 °C for 2,110 cycles [30]
- (3) Isothermal high temperature/high humidity (HTHH) 85°C/85% relative humidity (RH) for 4,000 h [31]
- (4) Isothermal low temperature/high humidity (LTHH) 25°C/85%RH for 16,910 h over three years [32]

The majority of whisker measurements were done on uncoated SOT boards because they were populated with similar packages having both Cu and low thermal coefficient of expansion (CTE) alloy-42 lead materials to evaluate the impact of CTE stresses during thermal cycling. Due to resource limitations, reduced inspections were performed on the QFP and BGA boards and the coated boards.

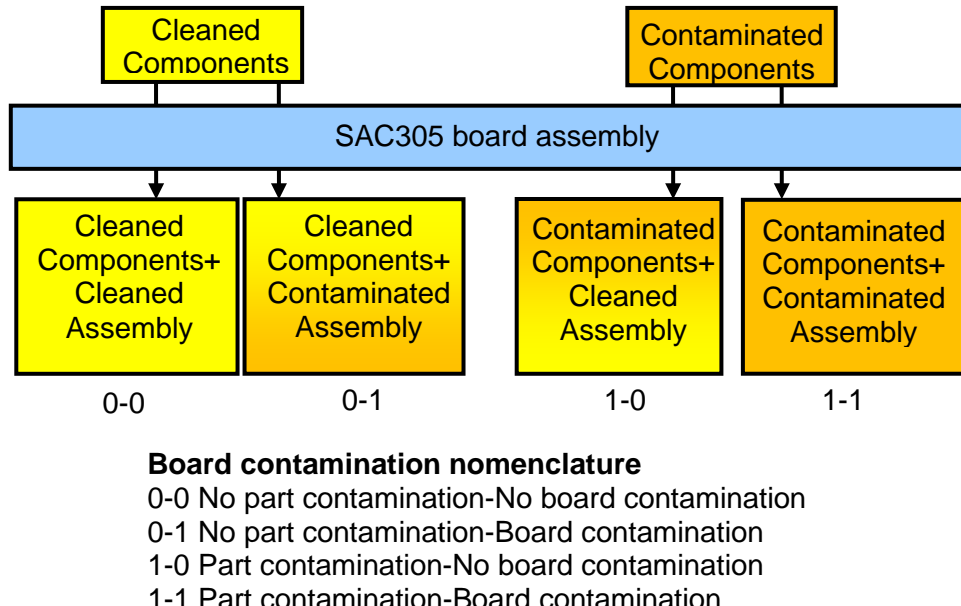


Figure 4: Contamination level definition.

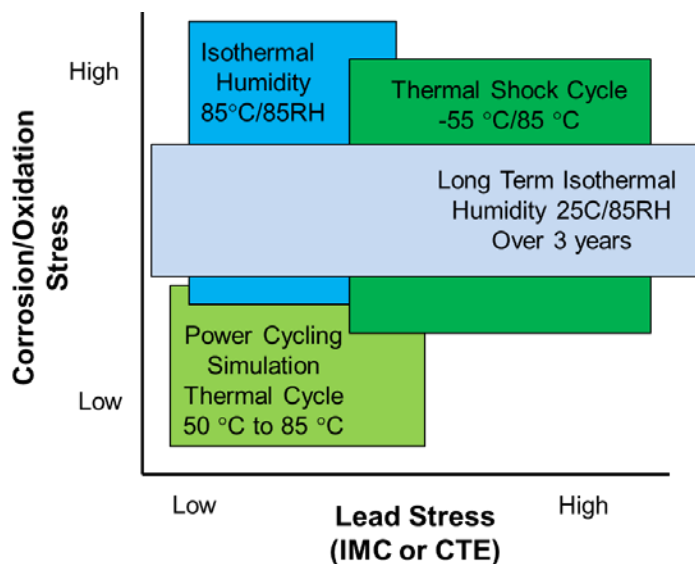


Figure 5: Whisker test environments.

Typical whisker growth images after environmental exposure are shown in Figure 6. An enormous number of whiskers grew. On the SOT boards, 120,946 whiskers were counted and 8,461 whiskers were measured (Table 1).

Generally it was found that the lead – board pad material couple was important and that lead material – environment pair was also important.

The thermal cycling environments promoted whisker growth on the alloy-42 lead terminations, whereas the high-humidity environments caused greater whisker growth on Cu-leaded terminations, especially when contamination was present. In addition, when the alloy-42 leads were soldered to the Cu board pads, the Ni in the alloy-42 formed a Cu-Ni-Sn intermetallic that retarded corrosion on the board pads during high humidity testing [31] [33]. Inspection of powered SOT devices indicated that bias did not have a significant impact on whisker growth, but the voltage was relatively low and sample size was small.

Examining the coated assemblies showed that the coating generally reduced whisker growth as compared to the non-coated assemblies. The TC thermal shock environment was found to be too harsh for assembly testing. TC cycling cracked the coating while the PCTC did not. In the LTHH testing, the coated leads with 5V applied exhibited greater corrosion and short whisker growth.

Further details from the initial parts characterization before and after assembly, experimental results, metallurgical observations, testing considerations, conformal coating and whisker risk modeling are presented next.

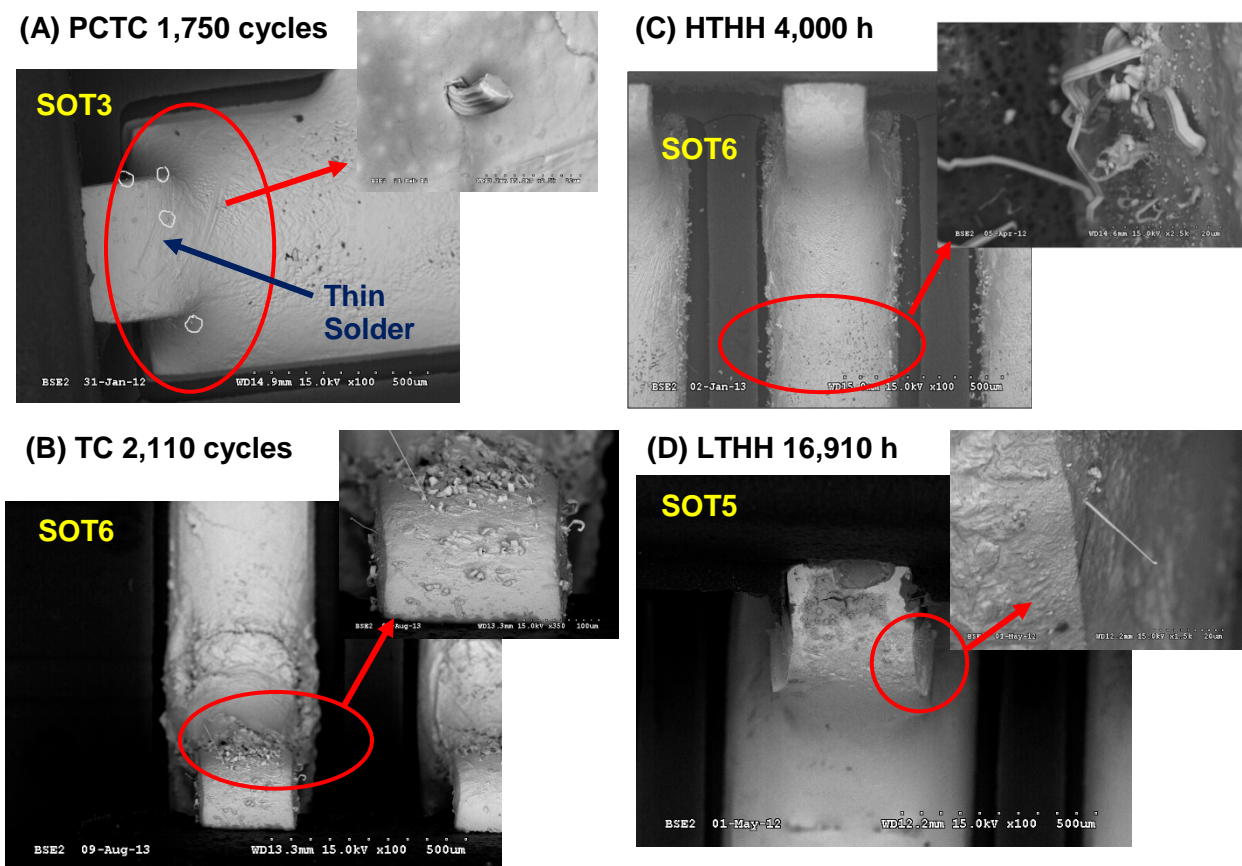


Figure 6: Typical whisker growth observed in the primary experiments; (A) PCTC +50 to 85°C, (B) TC -55 to 85°C thermal shock cycling, (C) HTHH 85°C/85%RH, and (D) LTHH 25°C/85%RH long duration storage.

Table 1: Primary experiment whisker measurement summary on the SOT boards.

Component	Counted	Measured	Component	Counted	Measured
PCTC 1,750 cycles (1)			HTHH 1,000 h (3)		
SOT3	216	216	SOT3	2,438	867
SOT6	179	179	SOT6	1,106	486
SOT5	7	7 (2)	SOT5	12,020	3,388
Total	395	395	Total	15564	4741
TC 2,110 cycles (3)			HTHH 4,000 h (4)		
SOT3	9,130	691	SOT3	24,639	197
SOT6	9,866	1,606	SOT6	37,641	185
SOT5	5,883	63	SOT5	13,106	107
Total	24,879	2360	Total	75,386	489
LTHH 16,910 h (3)					
			SOT3	134	8
			SOT6	160	11
			SOT5	4,228	457
			Total	4722	476
Notes: (1) All whiskers measured, (2) Only whisker longer than approximately 10 microns measured, (3) No whiskers were longer than 10 microns, (4) Only whiskers longer than approximately 30 to 40 microns measured.					

3.3 Characterization of parts before and after assembly

Initial metallurgical characterization was performed to examine attributes important for whisker propensity. SOT and QFP board parts were analyzed before assembly in the as-received condition, after cleaning and after intentional contamination. The assembled boards were cross sectioned to study the solder microstructure, part lead solder coverage, intermetallic (IMC) characteristics, and contamination distribution.

3.3.1 As-received parts

There were no significant anomalies in the plating of the part leads relating to solderability. Some defects important for whiskering that are not commonly reported (Figure 7) such as exposed base metal, thin plating from lead forming, voids, roughness, and deep surface grooves and some ionic contamination such as Cl, S, Si, Na, and Br were detected. The QFP44, QFP64, and PLCC20 leads exhibited some instances of plating cracks. The SOT3 part was also noted to have some silicon contamination present before cleaning. The distribution of the contamination on the cleaned and re-contaminated part was distributed into the plating grooves and valleys similar to the parts before cleaning [18]. Cross sectioning of the PLCC demonstrated that the Sn plating of the leads is extremely uneven. The XRF measurements reported Sn thicknesses of 8–10 microns; however, the actual thicknesses observed during cross sectioning varied from one to 38 microns. Because thin Sn plating is more prone to whisker growth, an eight micron minimum tin plating thickness is recommended for whisker mitigation [2].

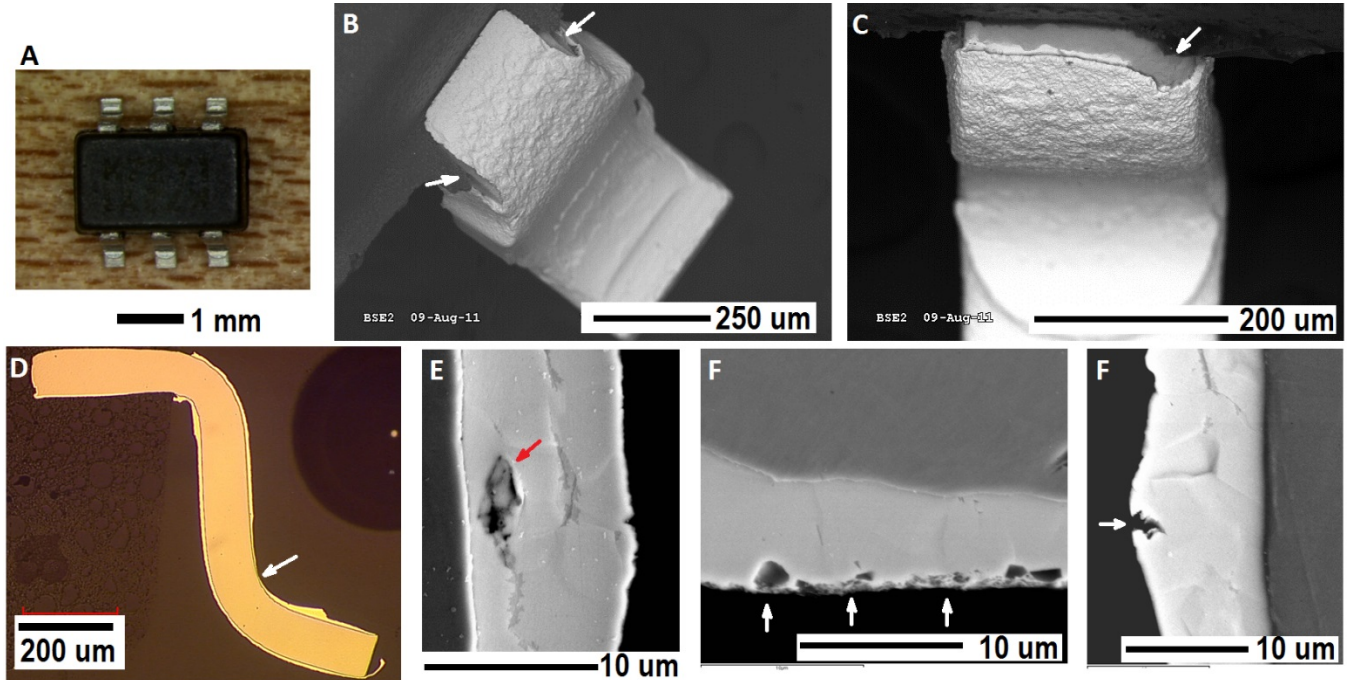


Figure 7: As-received part lead conditions contributing to whisker growth; (A) SOT6 overall part optical view, (B) SOT5 lead SEM image showing exposed Cu on lead near package body, (C) SOT6 lead SEM image showing exposed alloy-42 base metal near package, (D) SOT6 overall lead optical cross-section view showing thin tin plating caused by lead forming. SEM images of tin plating cross sections show (E) a void within the tin plating, (F) voids and a rough surface, and (g) rough surface with deep grooves.

3.3.2 Assembly characterization

After soldering, the solder coverage and IMCs were characterized using cross sectioning. A typical cross-section evaluation is shown in Figure 8. If the component contamination is high, some contamination can become trapped in the solder. The SOT3 and SOT6 and QFP64 leads were fully covered in solder, but the solder did not always extend to the top of the leads on the SOT5. The QFP44 and PLCC leads were partially covered with solder. The reflowed Sn lead finish beyond the solder no longer exhibited the fine-grain structure of the initial plating. The reflowed Sn and solder grain sizes were typically more than 25 microns. The thinnest IMC was observed on the alloy-42 leads (0.3 microns). With the alloy-42 lead parts, the board ($\text{Cu}, \text{Ni}_6\text{Sn}_5$) IMC was thicker (2.6 microns) than the lead side intermetallic. The SOT3 part was found to have Cl trapped at the thinnest part of the solder joint between the lead and Cu pad.

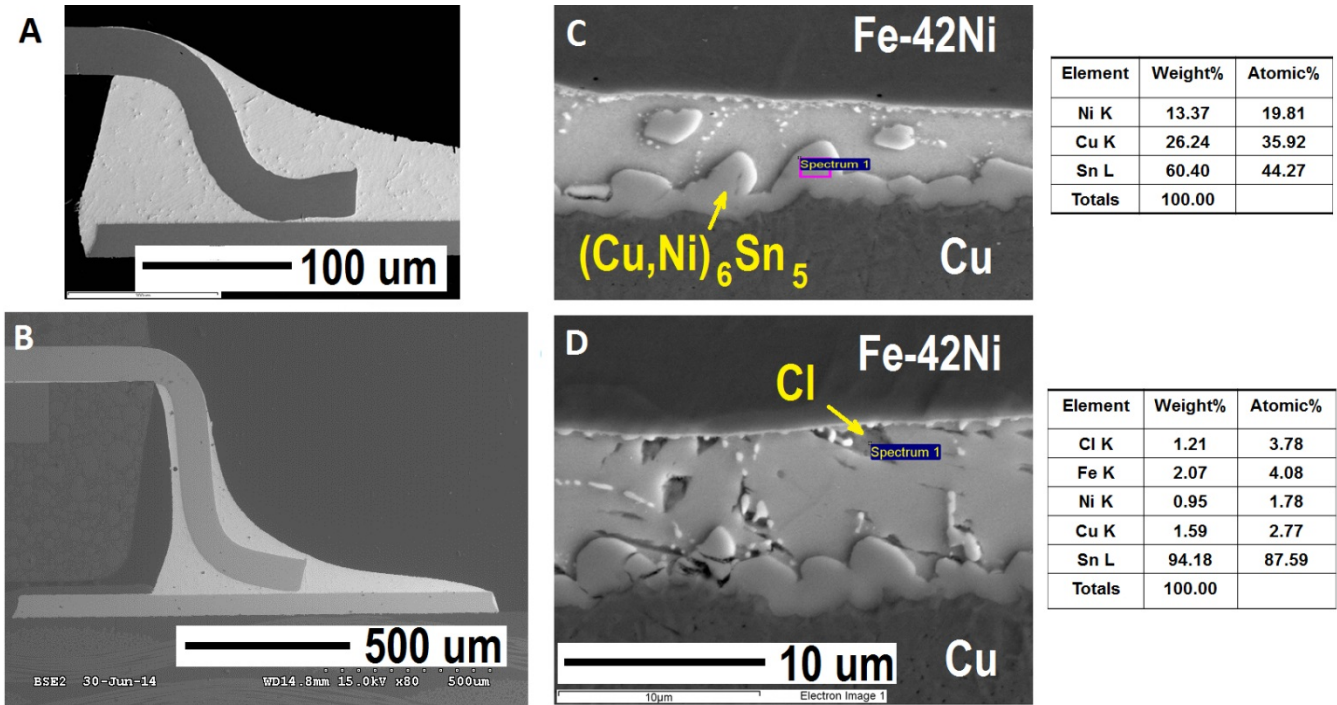


Figure 8: Alloy-42 leaded SOT solder joint cross-section SEM images after assembly; (A) SOT3 overall, (B) SOT6 overall, (C) $(\text{Cu}, \text{Ni})_6\text{Sn}_5$ IMC on board, and (D) Cl contamination trapped in solder joint.

3.4 PCTC +50 to 85°C results

Whisker inspections were performed after 250, 750 (250 + 500), and 1,750 (250 + 500 + 1,000) cycles from +50 to 85°C with a one hour cycle with 15 minute ramps and dwells. No whiskers were observed at the 250 cycle inspection. At the 750 and 1,750 cycle inspections, whisker nucleation and growth were observed. The maximum whisker length was 19.4 microns after 1,750 cycles on the SOT3 part with the 1-1 contamination level (Figure 9). Contamination level had a slight impact on whisker length and density. The whiskers grew in the region where the lead exits the solder fillet and the solder is thin (Figure 10). Between the second and the third inspection some ROL0 flux, was added to parts on board replicate three to simulate rework without cleaning [10]. Examining all other factors combined, the flux contamination resulted in the longest whisker growth. The incomplete thermal activation of the flux contributed whisker growth even though the moisture levels were very low. The promotion of whisker growth from flux has also been observed by Snugovsky [10] [18] and Ueshima [34]. Although the whiskers in the PCTC group were the shortest of all the experiments, it is believed that nucleation and growth would continue with more cycles.

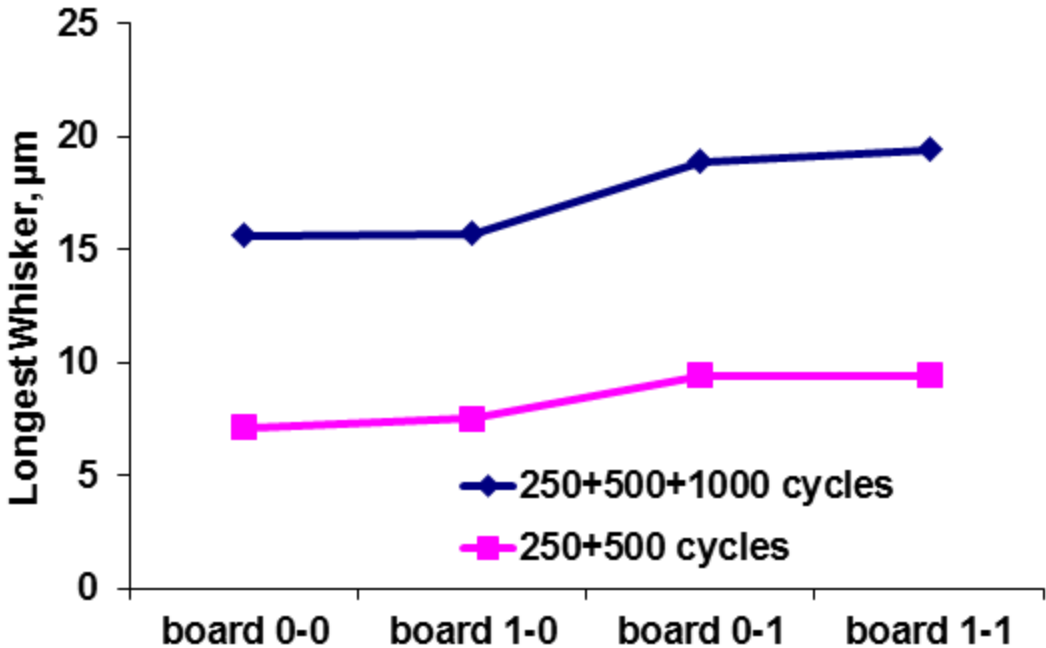


Figure 9: SOT3 maximum whisker length results after a total of 1,750 PCTC cycles.

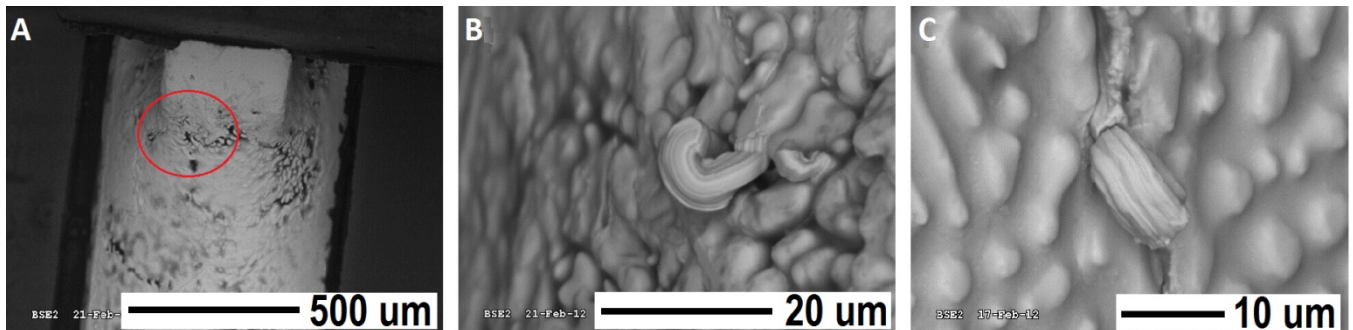


Figure 10: SEM images showing whisker growth on alloy-42 lead solder joint after a total of 1,750 PCTC cycles; (A) overall view highlighting whisker growth where the lead exits the top of the solder joint with (B) and (C) showing higher magnification whisker growth images.

3.5 TC 55 to +85°C results

Whisker inspections were performed at 500 and 2,110 (500 + 1,610) thermal shock cycles from -55 to +85°C with three cycles per hour and 10 minute dwells. The greatest whisker nucleation and growth occurred from the alloy-42 leads. During thermal shock cycling, the whisker growth was driven by the CTE differences between the low CTE alloy-42 and the higher CTE solder. The longest whiskers were on the SOT6 termination; 32 microns after 500 cycles and 115 microns after 2,110 (500 + 1,610) (Figure 11). The whiskers on the alloy-42 lead terminations predominantly grew from regions where the solder was thin near the top of the main solder fillet; however, there were also massive tin eruptions indicating a significant amount of non-whisker stress relaxation (Figure 12).

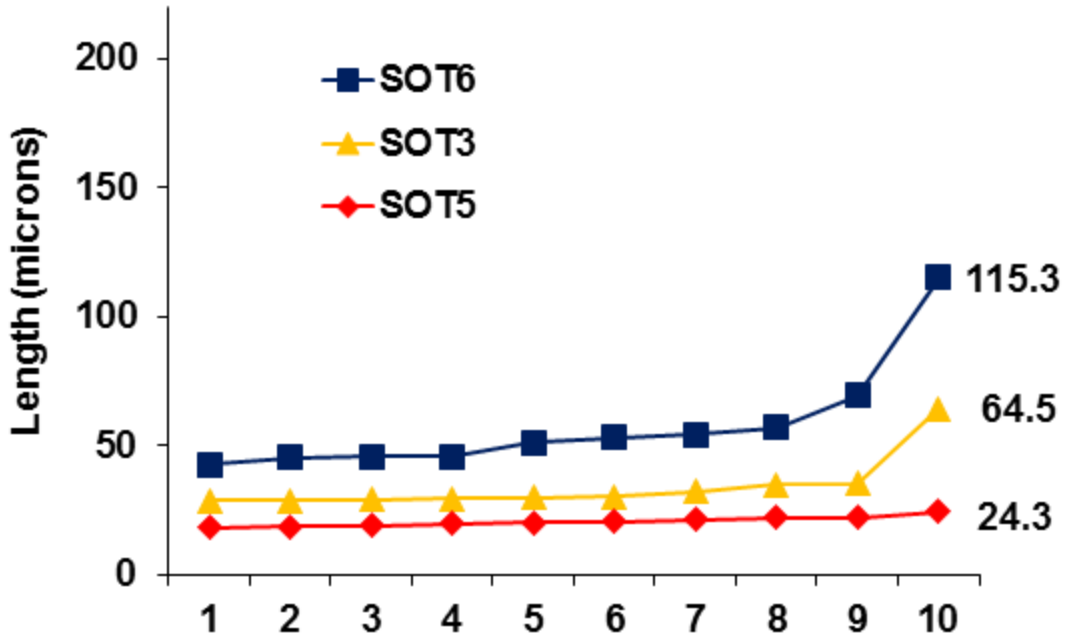


Figure 11: Top 10 longest whiskers after 2,110 TC cycles.

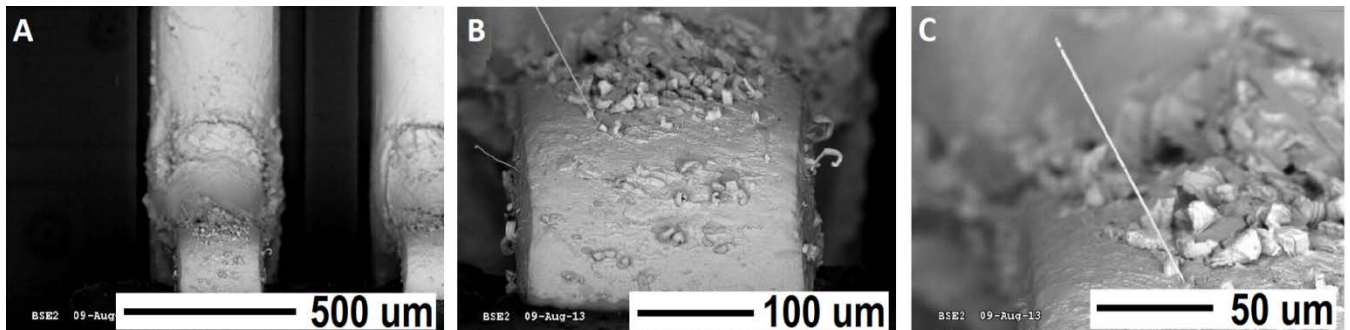


Figure 12: SEM images showing whiskers growing from alloy-42 lead after 2,110 TC cycles; (A) overall of lead with (B) and (C) showing whisker region at increasing magnifications.

3.6 HTHH 85°C/85%RH results

Whisker inspections were performed at 1,000 h and 4,000 (1,000 + 3,000) h exposure to 85°C/85% RH. The HTHH environment yielded the longest whisker growth (Figure 13) as compared with the PCTC, TC and LTHH environments. The HTHH assembly 1,000 h exposure resulted in whisker lengths up to 186 microns, more than three times longer than the 45 microns JESD201 piece part test limit for 4,000 h (55°C/85% RH). After 4,000 h, the longest whisker was 214 microns on the SOT5 termination. While not part of the main measurement set, the QFP64 terminations also exhibited long tin whisker growth (Figure 14). The intermediate contamination levels (0-1 and 1-0) exhibited the longest mean whisker length, but the 1-1 contamination grew the longest whiskers. The Cu-Cu (lead-pad) couple exhibited the greatest whisker nucleation and growth at 1,000 h. The alloy-42/Cu couple exhibited significantly less nucleation and growth at 1,000 h. However, as the exposure time increased to 4,000 h, the whisker length difference between the two material couple types the alloy-42 termination pad whisker growth was similar to the Cu lead termination pads. During HTHH, the whisker growth was driven by oxidation and corrosion. Although it is possible that additional contamination accumulated near the board contributed to the board pad whisker growth, the cleaned assembly also exhibited significant whisker growth along the board pad.

The majority of whiskers were between one micron and five microns in diameter regardless of alloy or contamination level. After 4,000 h, the whisker count varied from 50 to 500 whiskers per termination across the lead material and contamination levels. The maximum whisker densities after 4,000 h HTHH (Figure 15) were 2,027 whiskers/mm² for the alloy-42 terminations and 1,580 whiskers/mm² for the Cu SOT5 lead terminations.

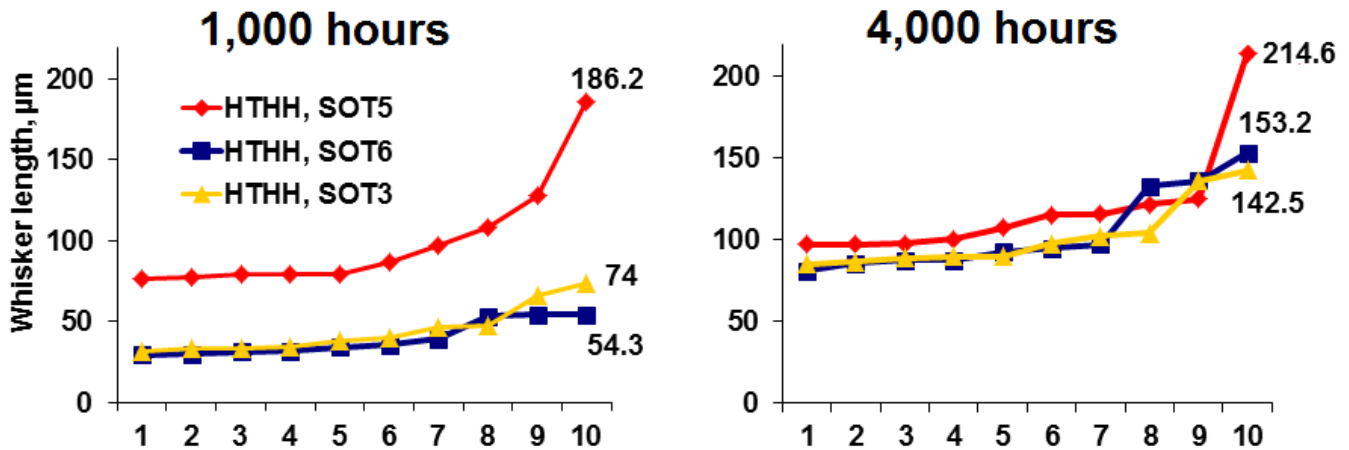


Figure 13: Comparison of top 10 longest whiskers after 1,000 and 4,000 h HTHH.

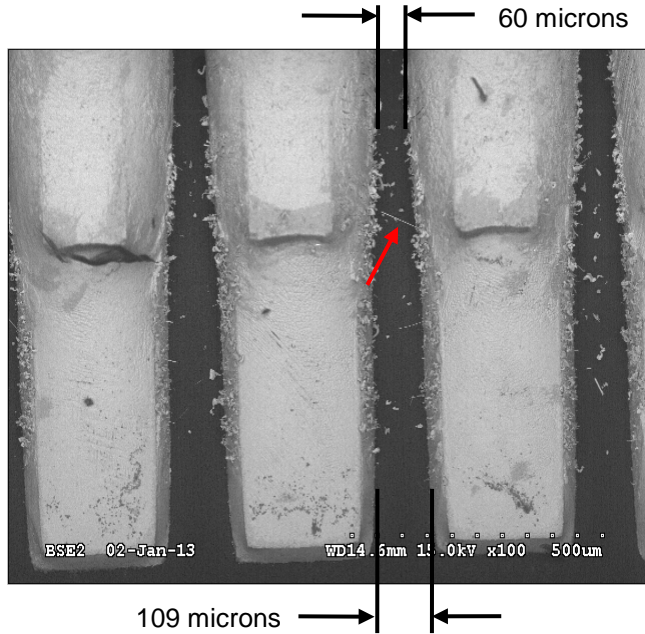


Figure 14: SEM image showing whisker growth from TQFP64 board pads after 4,000 h HTHH. Arrow shows a broken whisker between the pads long enough to bridge the gap. The solder bulge wrapping around the two ounce thick board pad reduced the typical 100 micron clearance between pads to 60 microns.

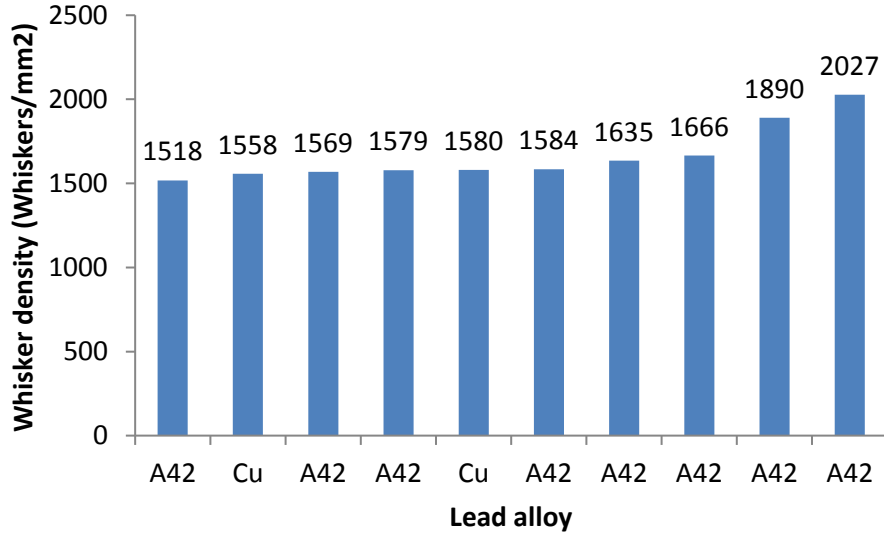


Figure 15: Top ten whisker densities at location-2 from the SOT board inspection after 4,000 h HTHH.

3.7 LTHH 25°C/85%RH results

Whisker inspections were performed at 1,037, 4,398 (1,037+3,361) and 16,910 (1,037+3,361+12,512) h exposure to 25°C/85% RH. The greatest whisker nucleation and growth occurred on the Cu alloy lead terminations. During high humidity isothermal exposure, corrosion and oxidation were the driving force for the whisker growth. The longest whisker grew from the PLCC20 termination (Figure 16); 145 microns after 4,398 h (Note: the QFP boards were not measured during final inspection). The SOT5 termination exhibited the longest whisker growth at the final inspection (Figure 17); 92 microns after 16,910 h. **No whiskers** longer than 10 microns were observed for the 0-0 and 1-0 contamination level assemblies (e.g. without board level contamination). Whiskers grew predominantly from the thin solder or tin between the top of the main solder fillet and the package body. In contrast to the other primary experiments, the LTHH environment produced many small diameter whiskers (0.1 to 0.3 microns).

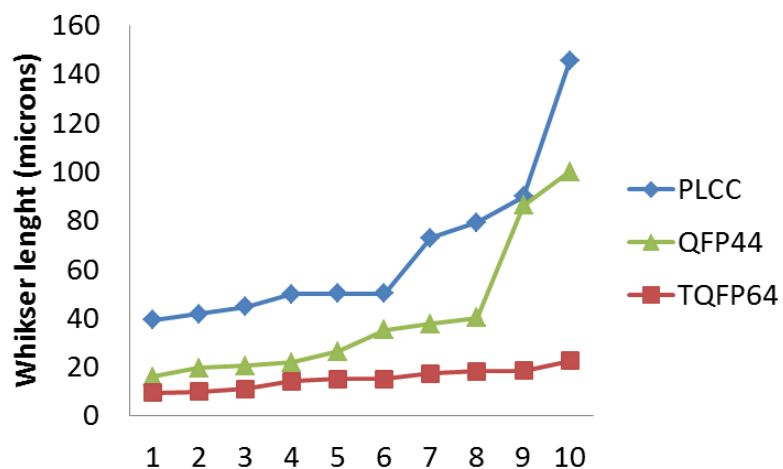


Figure 16: Ten longest whiskers of the QFP board parts from the second inspection at 4,398 h LTHH.

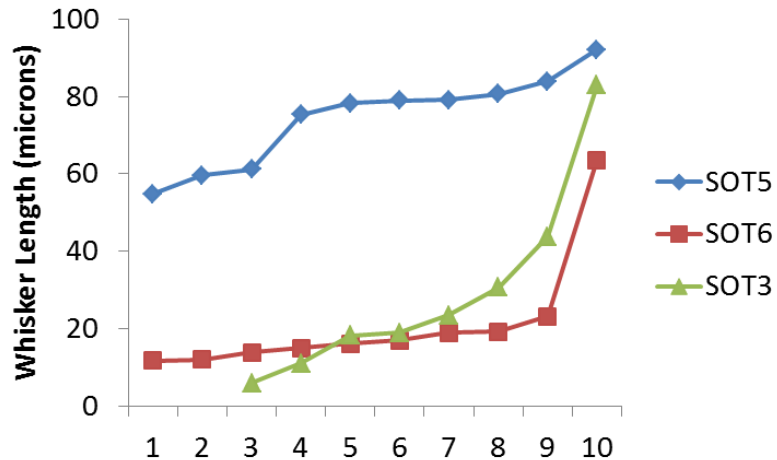


Figure 17: Ten longest whiskers on the SOT board parts from the final inspection at 16,910 h LTHH.

3.8 Whisker growth location observations

There was a marked difference in whisker growth location between the thermal cycling and HTHH. In PCTC, whisker growth was at the top of the solder fillet. In TC and LTHH, the whiskers grew from the thin solder and tin on the top of the lead. During HTHH, the majority of whiskers grew from the thin solder regions on the Cu board pad edge (Figure 18).

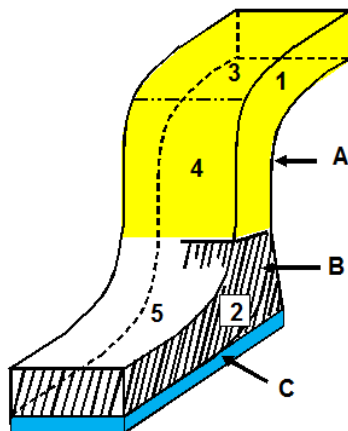


Figure 18: Primary whisker growth locations after PCTC, TC, HTHH and LTHH environments. PCTC resulted in growth on the alloy-42 leads where the thin solder at the transition area between the main solder fillet (region B) and the upper part of lead (region A). The thin solder in region A exhibited the majority of the whisker growth after TC on alloy-42 lead terminations and after LTHH on Cu lead terminations. The thin solder over the copper board pad in region C produced the most whisker growth after HTHH. The thick solder in region B displayed little or no whisker growth.

3.9 Solder microstructure and whisker growth observations

3.9.1 Recrystallization and grain change

The dynamic recrystallization theory proposed by Vianco and Rejent [21][22] suggests that there is an optimal stress for whisker growth, above which other non-whisker growth stress relaxation mechanisms occur. In the current study, varying degrees of recrystallization and stress relaxation were observed. Recrystallized grains adjacent to

whiskers have been observed after PCTC and TC (Figure 19). In some cases, the recrystallization was below the surface (Figure 20). Possible evidence of recrystallization and/or grain growth was found on the increasing or decreasing whisker diameters observed on the TC samples (Figure 21). Note that whisker growth angle changes were also observed, which could be due to tin mass transport changes at the whisker base [35] or grain rotation during cycling. In contrast to observations by Susan et al. [36], sometimes substantial whisker growth occurred after the whisker base diameter increased. The reflowed SAC alloy generally has relatively large tin grains after reflow so recrystallization processes transforming large grains to small grains was necessary for the observed whisker nucleation to occur.

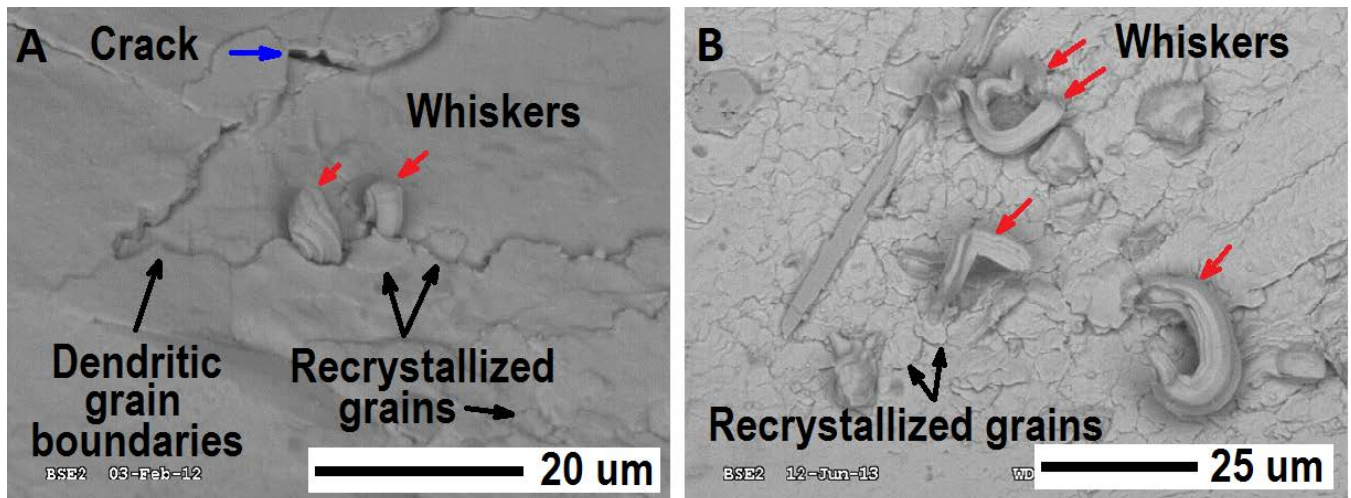


Figure 19: SEM image showing whisker growth near recrystallized grains and dendritic grain boundaries on the SAC solder fillets after (A) 1,750 PCTC cycles and (B) 2,110 TC cycles.

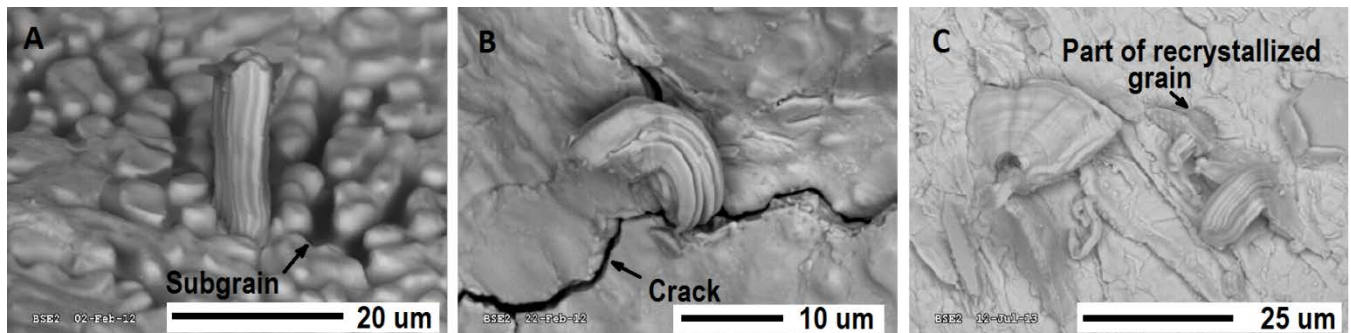


Figure 20: Subsurface grain recrystallization: (A) from subgrain region after 1,750 PCTC cycles, (B) from primary tin dendrite triple junction after 1,750 PCTC cycles, and (C) a whisker on top of an underlying recrystallized grain after 2,110 TC cycles.

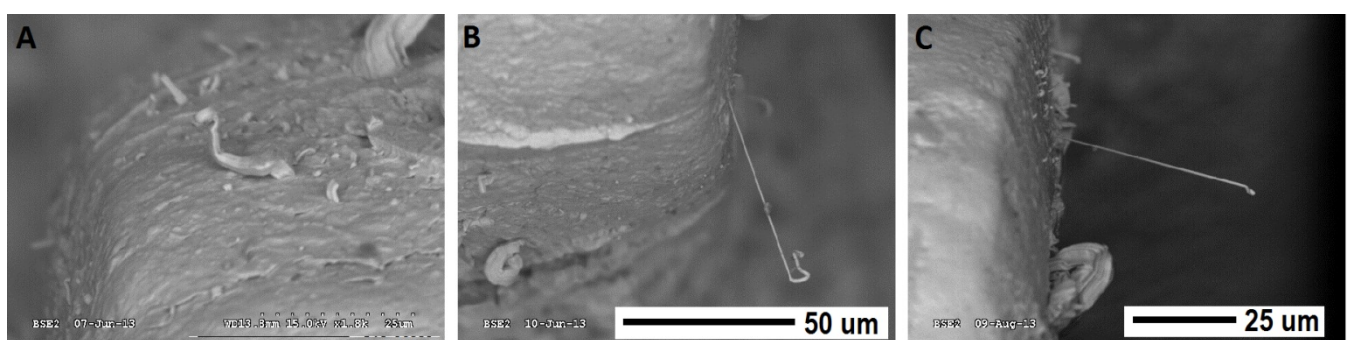


Figure 21: SEM image showing whisker diameter change during TC exposure on alloy-42 SOT6 with 1-0 contamination; (A) increasing, (B) and C) decreasing whisker diameters.

3.9.2 IMC

SAC solder joints have dispersed primary Ag_3Sn and Cu_6Sn_5 IMCs and interfacial IMC between the solder and the lead or board pad. Primary IMC Ag_3Sn and Cu_6Sn_5 particles, Ag_3Sn plates, and Cu_6Sn_5 rods promote whisker nucleation by increasing local stress in temperature cycling through differences in CTE, shear bands, and misoriented deformation zones around hard particles (Figure 22). The growth of interfacial CuSn or CuNiSn IMC between the substrate and solder can also drive whisker growth. During PCTC, the interfacial IMC on lead was observed to grow much faster than expected. The SOT3 interfacial IMC before cycling was 0.3 microns and after 1,750 PCTC cycles was 1.6 microns—more than a five times increase in thickness. In contrast, the interfacial IMC on board pads before cycling was 2.6 microns and after cycling was 3.0 microns. In addition, large CuNiSn IMCs were observed in the solder fillets next to whiskers. It is postulated that enhanced Cu diffusion from the board pad to component during cycling promotes IMC formation that increases whisker growth. As will be discussed next, IMCs also contribute to oxidation and corrosion.

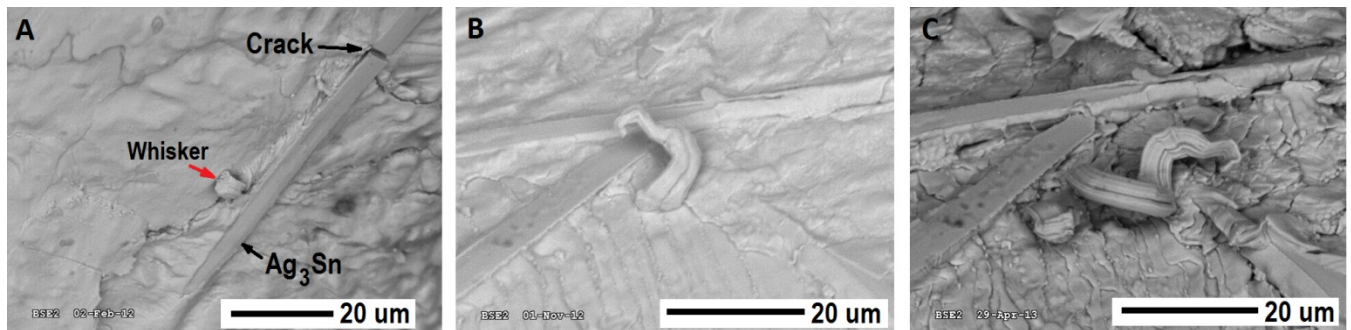


Figure 22: SEM image showing whisker on alloy-42 lead adjacent to Ag_3Sn IMC plate; (A) after 1,750 PCTC cycles, (B) after 500 TC cycles, and (C) continued growth of whisker in (B) and new whisker growth near intermetallic after 2,110 TC cycles.

3.9.3 Oxidation/corrosion

IMC particles contribute to uneven oxidation along the primary Sn grain boundaries, which creates local stress and promotes whisker formation (Figure 23). The oxidation/corrosion often begins in the Sn interdendritic spaces and can penetrate deeply into the solder. The solder fillet region was observed to be partially oxidized during the HTTH exposure with some oxide/corrosion regions traversing the entire solder fillet thickness to the substrate (Figure 24). When all the tin around the whisker base becomes oxidized/corroded the whisker will stop growing. In addition, as oxidation/corrosion proceeds, whisker ductility is reduced and it is easier for the whiskers to become detached from the substrate. Corrosion was also observed adjacent to a whisker after the very low-humidity PCTC environment. The compressive stress caused by the 29–34% volume increase of the Sn oxides compared with the β -Sn promotes whisker growth. These findings are consistent with other investigators assessing the role of humidity on tin whisker growth on electronic component leads [13][37] [41] and on lead-free assemblies [9].

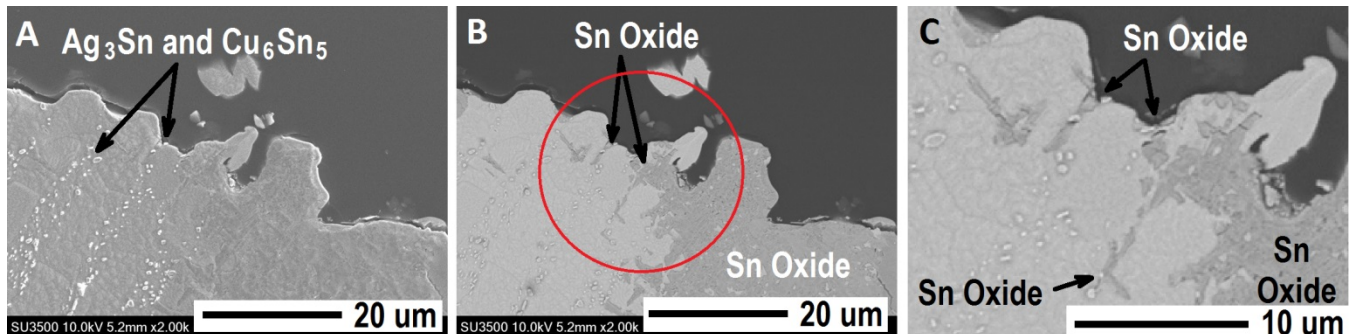


Figure 23: Cross section showing uneven Sn oxidation into the IMC region between the primary Sn grain boundaries; (A) secondary electron SEM image highlighting the IMC with (B) and (C) backscatter SEM images

emphasizing the Sn oxide penetration into the solder. Image (C) is a higher magnification view of the circled area in (B).

It is important when studying whisker growth of solder joints that all the material interaction be considered. The whisker nucleation on the Cu pads with alloy-42 leads attached (Figure 25) was reduced as compared to the Cu board pads with Cu leads (Figure 14). The Ni in the alloy-42 promoted the formation of the $(\text{Cu}, \text{Ni})_6\text{Sn}_5$ ternary IMC on the board Cu pad during reflow soldering (Figure 8). In alloy-42 solder joints, the Cu_6Sn_5 IMCs layer at the board pads and solder particles contain Ni, which reduces the galvanic potential between the IMCs and the Sn, slowing the oxidation rate and retarding whisker nucleation.

Surface roughness of the solder also contributes to corrosion-induced whiskering. The roughness is partly a result of the shrinkage of the liquid between the primary tin dendrites. The roughness tends to trap contamination, which is difficult to clean (Figure 2 and Figure 20A).

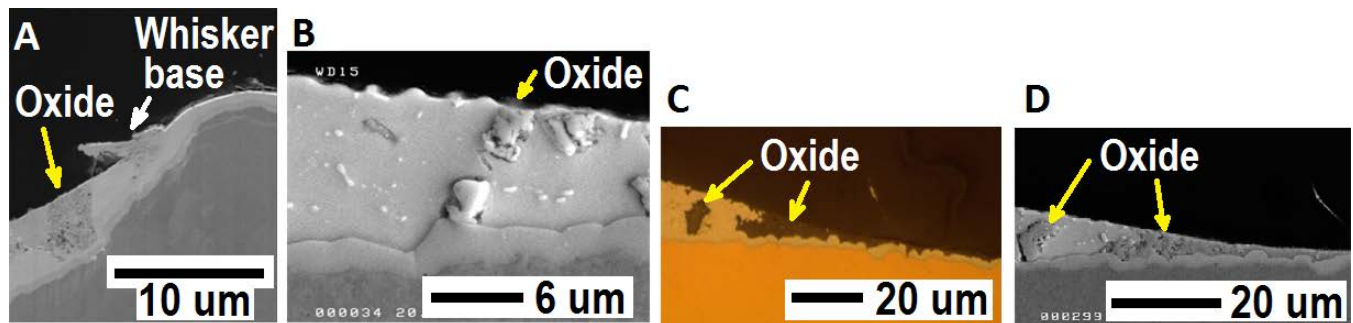


Figure 24: Cross section showing partial oxidation of SAC solder with Cu leaded part (SOT5) and 1-1 contamination after 4,000 h HTHH; (A) SEM image of oxide near 98-microns long whisker, (B) SEM image of oxide in a thicker region of the SAC solder, (C) optical image of oxidation near solder wetting line, and (d) SEM image of region shown in (C).

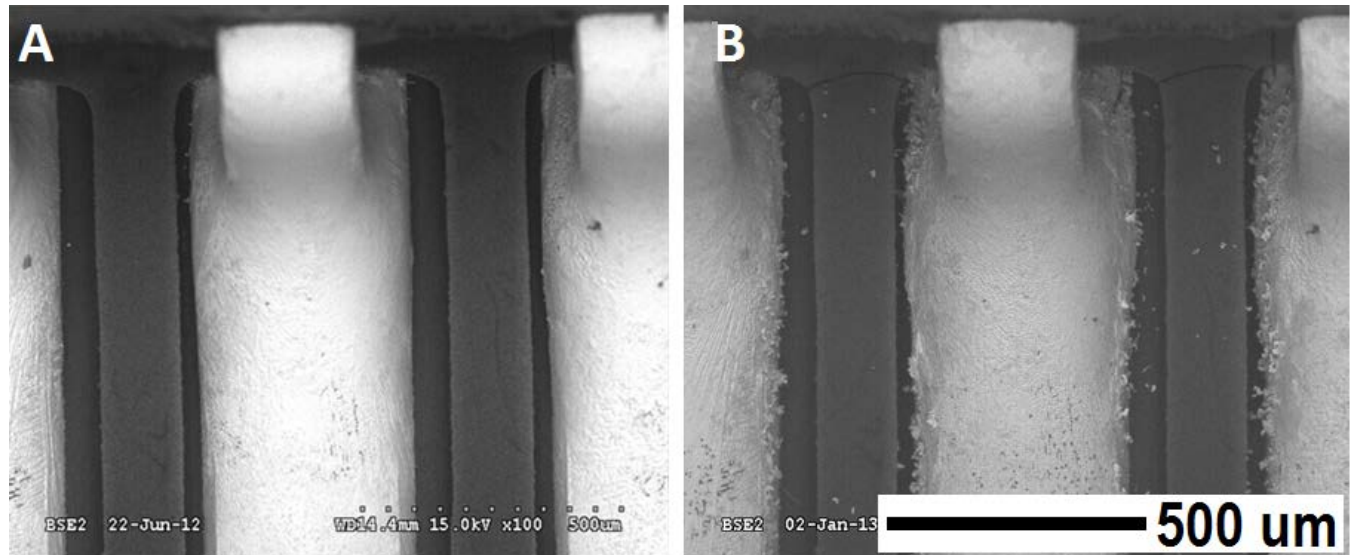


Figure 25: SEM image showing alloy-42 leads attached to Cu board pads after; (A) 1,000 h and (B) 4,000 h of HTHH.

3.9.4 Broken whiskers

There are two possible explanations for the large number of broken whiskers found during the examination at 4,000 HTHH h. Some of the thin regions of solder were completely oxidized and had no whiskers on the surface (Figure

24). This finding suggests that oxidation/corrosion propagating under a whisker can make the whisker attachment more brittle. In another cross-section of a whisker through its base, voids and a crack were observed (Figure 26).

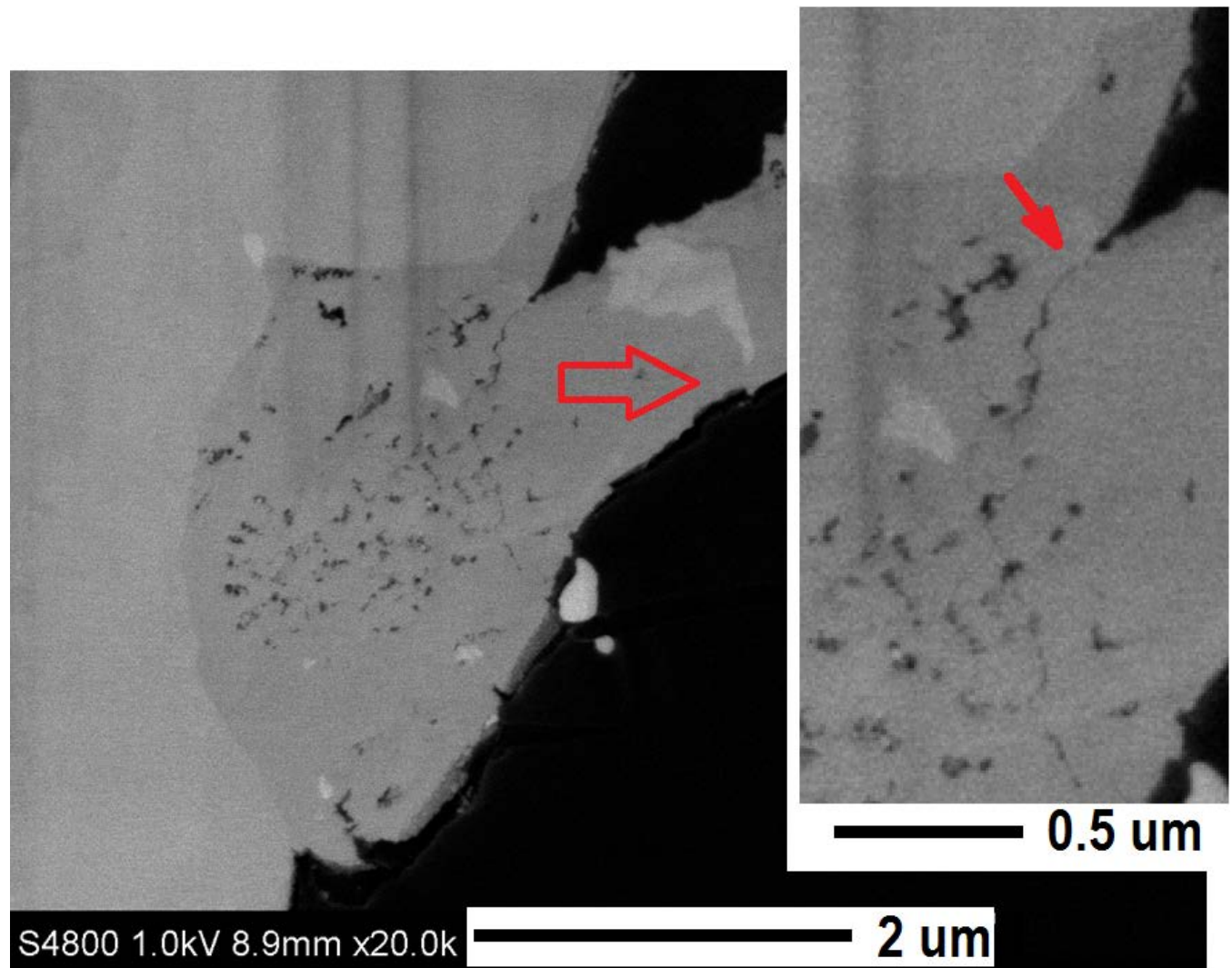


Figure 26: SEM image showing voids and cracks observed in the whisker base after 4,000 HTHH h. Inset shows a high magnification image of the whisker root crack.

3.9.5 Thin whiskers

Thin submicron diameter tin whiskers were especially evident under conditions of slow oxidation/corrosion. The SAC+Ce cross-section samples in room temperature air storage for over four months exhibited thin whisker growth from the CeSn₃ IMCs (Figure 27). In addition, the LTHH testing resulted in the formation of many sub-micron whiskers (Figure 28). The submicron whiskers were also observed on sputtered tin in high humidity [28], during vibration induced whisker growth testing [42] and, on vapor-deposited tin at 180°C [43].

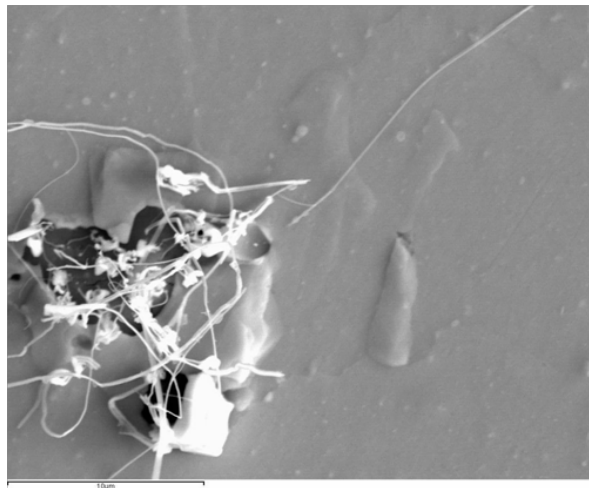


Figure 27: Thin whiskers growing from La_3Sn IMC in a bulk SAC105+0.5La cross-section held at room ambient conditions for 3,050 h.

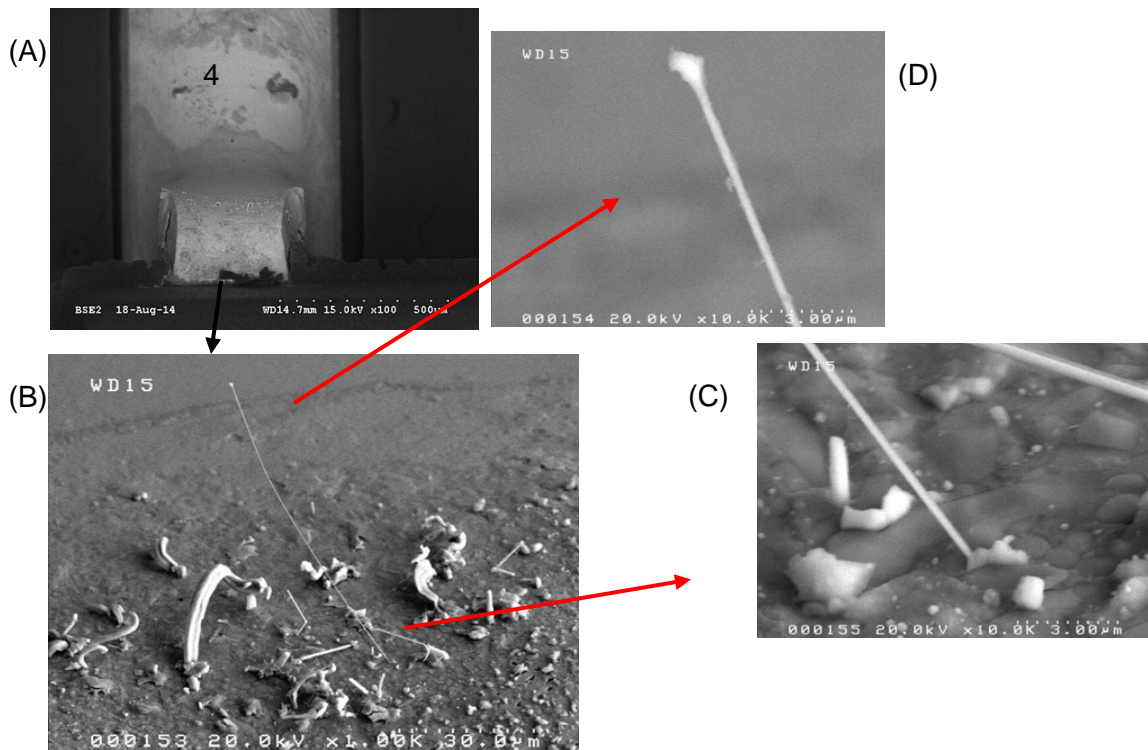


Figure 28: An 81 micron long 0.3 micron diameter whisker observed during the LTHH test at 16,910 h on a Cu alloy SOT5 lead with a 1-1 contamination level; (A) Overall SEM image, 100x, (B) increased magnification of whisker, 1,000x, (C) close-up of the whisker base, 10,000x and (D) close-up of the whisker tip, 10,000x.

3.9.6 Non-whisker stress relaxation

In some cases, non-whisker growth stress relaxation occurred. During PCTC in the thicker solder region, faceted crystal growth was observed (Figure 29). Under the higher stress conditions of TC, the alloy-42 solder joints exhibited massive cracking (Figure 30) and massive eruptions consisting of many recrystallized grains (Figure 6B) after 2,110 cycles.

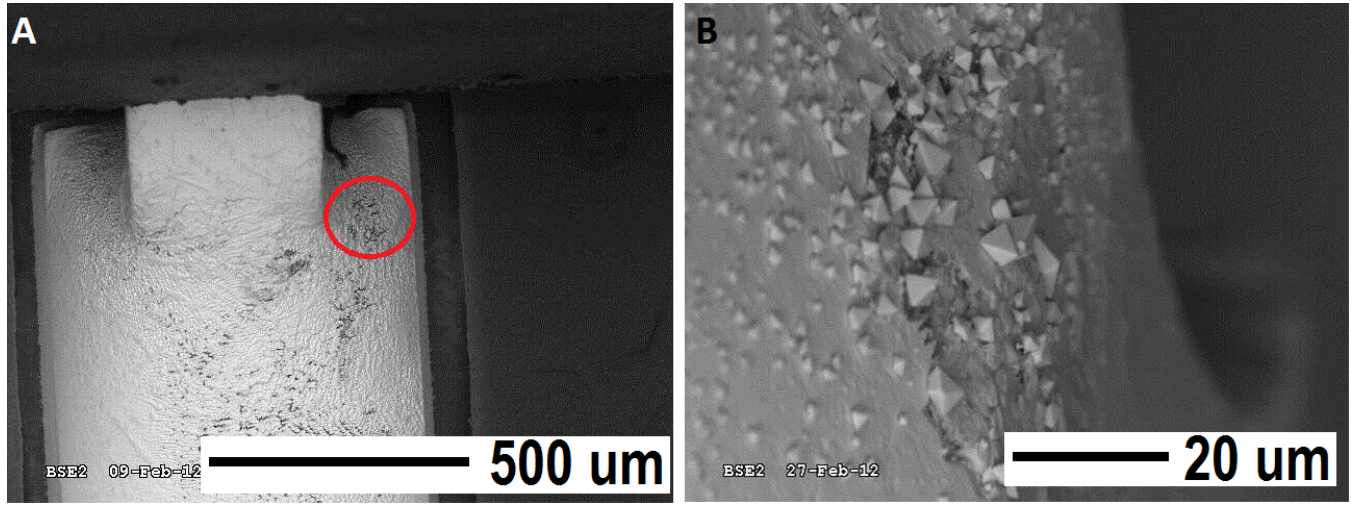


Figure 29: SEM image showing faceted grains on alloy-42 SOT3 with a 1-1 contamination level after 1,750 PCTC cycles; (A) overall view and B) high magnification view of circled region.

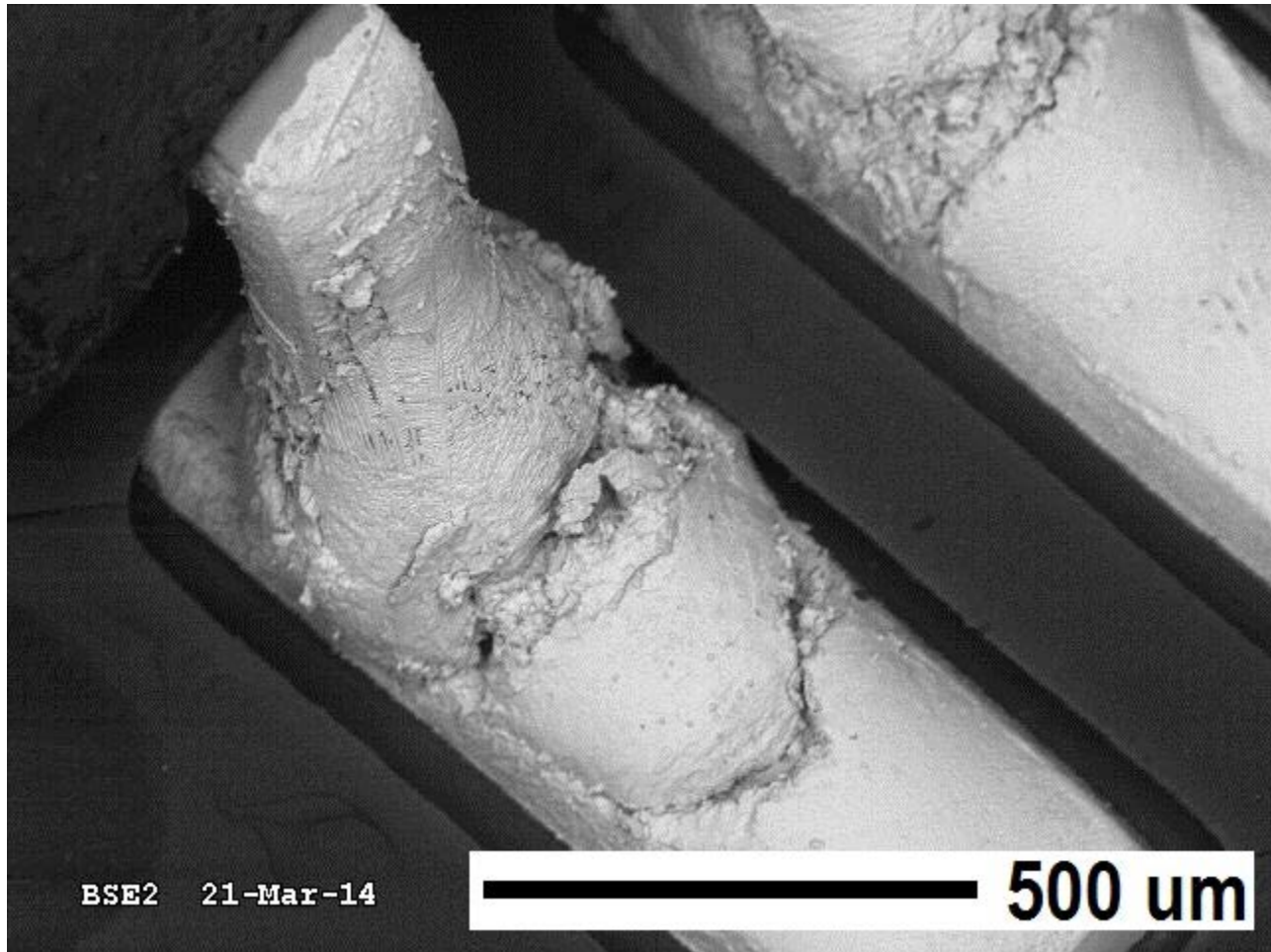


Figure 30: SEM image showing an alloy-42 termination solder joint with massive cracking after 2,110 TC cycles.

3.9.7 Test considerations

An important test observation was that the intermediate SEM inspections stopped some whiskers from further growth after resuming environmental exposure. This condition was most pronounced on the HTHH samples where the majority of whiskers inspected at 1,000 h stopped growing further when inspected at 4,000 h, but new whiskers formed (Figure 31). The interruption of whisker growth by inspection during thermal cycling (TC or PCTC) was less pronounced and sometimes existing whiskers continued to grow (Figure 22C). Thus, periodic inspection will cause an underreporting of whisker length. By progressively increasing time intervals or having longer uninterrupted tests, longer whisker growth would be obtained.

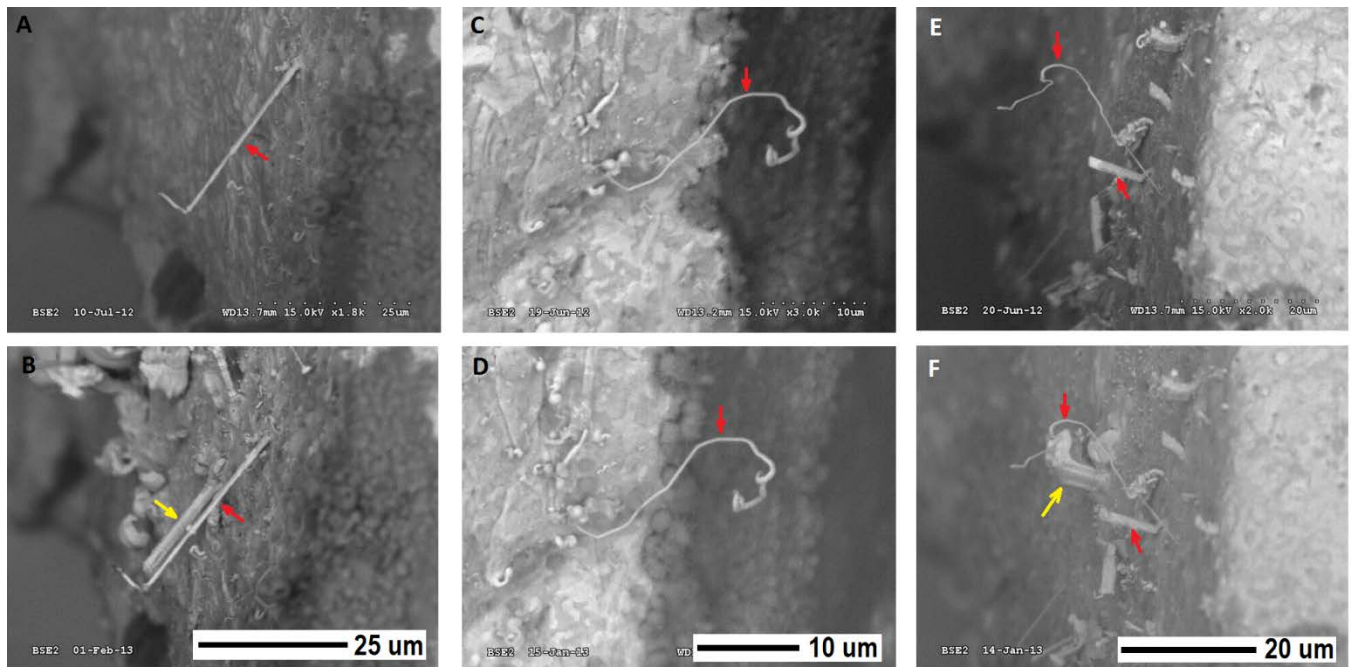


Figure 31: SEM images showing whisker growth interruption by the inspection process during HTHH testing. Red arrows indicate whiskers that stopped growing and yellow arrows indicate new whisker growth: (A) SOT5 1-0, U26, lead 1, 1,000 h; (B) SOT5 1-0, U26, lead 1, 4,000 h; (C) SOT5 1-1, U37, lead 5, 1,000 h; (D) SOT5 1-1, U37, lead 5, 4,000 h; (E) SOT5 1-1, U38, lead 2, 1,000 h; and (F) SOT5 1-1, U38, lead 2, 4,000 h.

3.9.8 REE Oxidation

The SAC solder with REE was included in the test matrix because REE additions, which can improve drop shock performance, also exhibit increased the SAC solder whisker propensity [44] – [47]. Ce was initially chosen over La and Y because results had been published indicating that Ce has better oxidation resistance, which would be promising for incorporation in lead-free solder. The screening experiment in the current work [19][20] had a different result; Ce was at least as effective as Y and La in whisker formation. The current primary experiment results should discourage industry from ever considering Ce additions to electronic solder. Whisker growth was observed on the BGA board (Figure 32), which used Ce at a concentration much lower than the 2% being considered for improving drop shock performance. The manner in which RESn compound oxidation contributes to whisker growth is (I) liberation of Sn and (II) development of compressive stress by the RE oxide. Since REEs are less noble than Sn, the REE in CeSn_3 is more prone to oxidation, which results in rapid oxidation of CeSn_3 (or YSn_3 and LaSn_3). In addition, the surface active nature of REEs results in a RESn IMCs tendency to segregate to the surface giving it improved access to oxygen. RESn IMCs can also be exposed to air when cracks form during mechanical or thermal cycling.

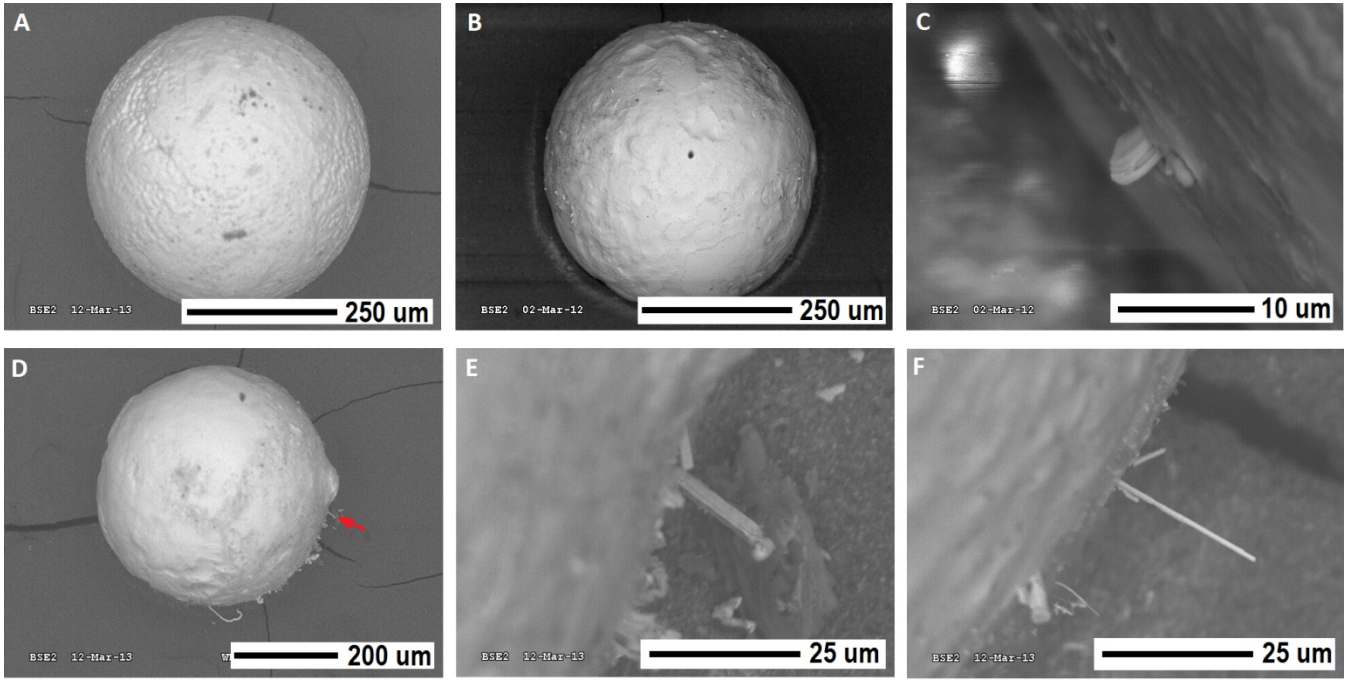


Figure 32: SEM images comparing SAC105 (A) with SAC105 + 0.01Ce (B–F) solder balls attached to BGA board pads with SAC305 solder paste after 4,000 HTHH h (A, D–F) and after 1,750 PCTC cycles (B and C) at a 0-0 contamination level; (A) highlights no whisker growth on a SAC105 ball. Image (E) shows whisker highlighted by arrow in (D).

3.10 Conformal coating observations

Conformal coating is a primary mitigation against the detrimental effects of whisker growth. Liquid polymer conformal coatings applied by dipping, spraying or brushing for humidity protection are common in DoD systems intended for harsh environments. However, obtaining uniform coating thickness on all the metal features for whisker mitigation can be challenging [48] and coating coverage improvements for whisker mitigation are possible [50]. Liquid coating surface tension causes coating thinning over corners and gravity forces result in coating thinning on vertical surfaces (Figure 33). Thinner coating areas are evidenced in the SEM images by the “lighter” areas over the leads [52]. When the coating is thinner than approximately three microns, the electron beam can penetrate the coating to the base metal making a “light image”. Where the coating is thicker, the image is darker. Historically, conformal coatings have been used for moisture protection and some thickness variations are often acceptable if the circuit impedance change is not adversely impacted.

3.10.1 Thermal cycling

The coated PCTC samples had minimal nodule growth but did not exhibit corrosion after 1,750 cycles. For the coated TC samples after 2,110 thermal shock cycles, pronounced cracks formed near the thicker coating regions (Figure 34). Thermal shock cycles such as those used in the JESD-201 [23] piece part whisker test result in assembly coating over-stress which caused cracking normally not observed under typical service environments. Even with the coating cracks and thin areas, the coating provided substantial whisker mitigation (Figure 35).

3.10.2 High humidity

After 4,000 h HTHH, corrosion and whiskers were observed on coated SOT parts (Figure 36). The coated HTHH SAC105 + 0.01%Ce BGA balls exhibited corrosion but no whiskers were observed. The coated SOT or QFP samples in the LTHH environment did not exhibit corrosion or whisker growth (Figure 33). However, the coated LTHH SAC105 + 0.01%Ce BGA balls exhibited some short whiskers where the coating was thin (Figure 37). These

were shorter than the whiskers observed after 4,000 h on the non-coated assemblies indicating that even when thin the coating retarded corrosion of the RESn IMC.

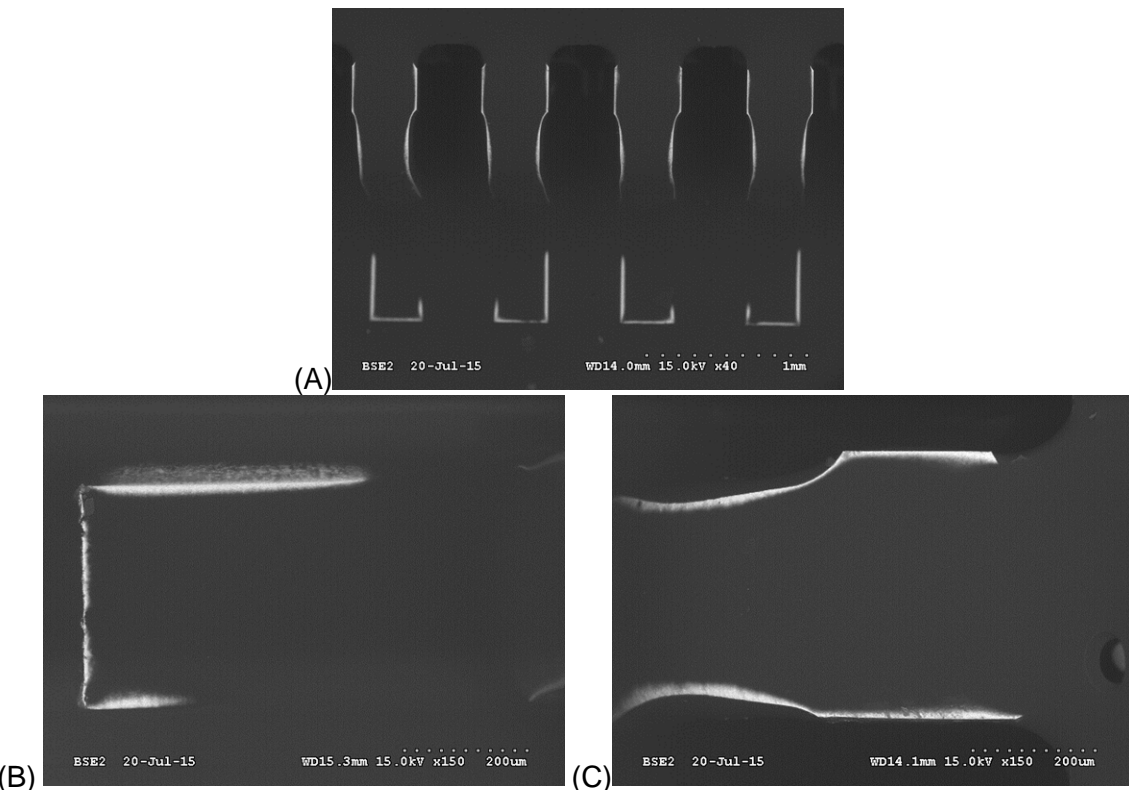


Figure 33: Conformal coating on QFP 44, with 1-1 contamination level after 16,910 h LTHH; (A) overall, 40x and (B) lead tip, 150x and (C) top of lead, 150x. No cracks or coating degradation observed.

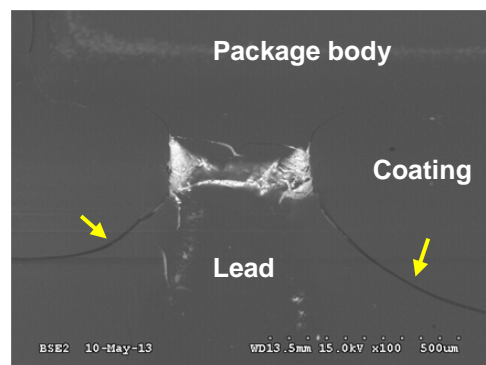


Figure 34: Conformal coated SOT3 alloy-42 lead with 1-1 contamination level after 2,110 cycles, 100X. Arrows indicate coating crack locations.

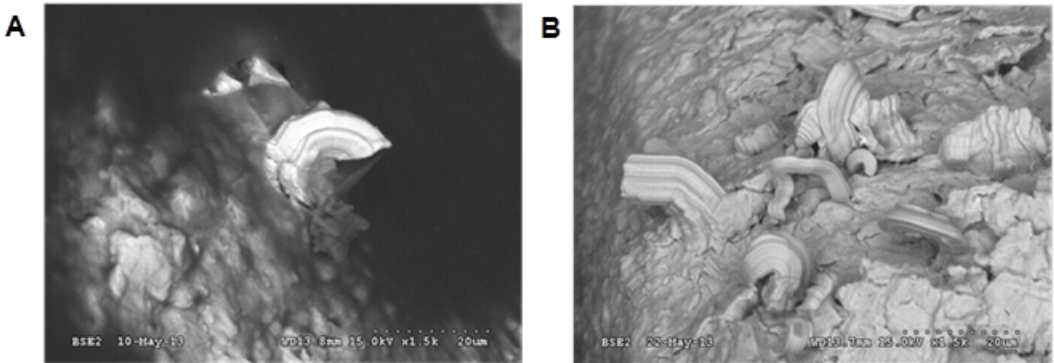


Figure 35: Coated and un-conformal coated alloy-42 SOT6 after 2,110 cycles -55°C to 85°C, (500+1,610); (A) Coated, 0-0 contamination level, 1,500x, and (B) no conformal coating, 0-1 contamination level, 1,500x.

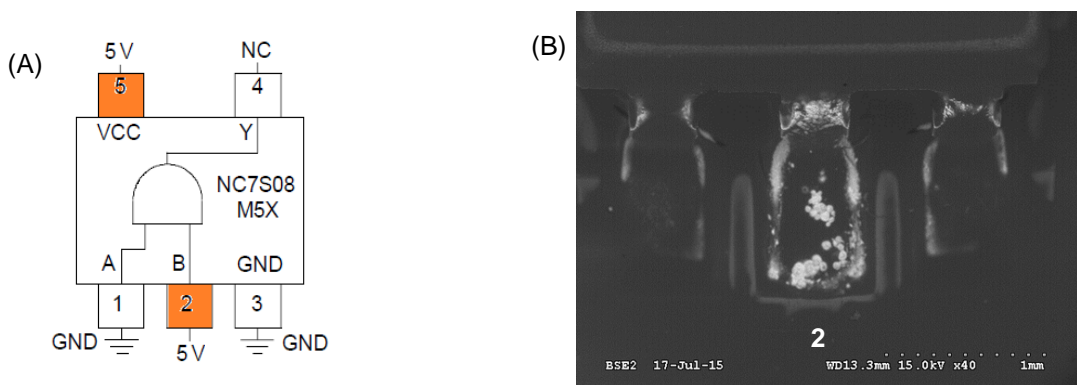


Figure 36: Influence of voltage bias on corrosion on coated SOT5 parts with 1-1 contamination level after 4,000 h HTHH; (A) electrical schematic, (B) corrosion on lead 2 at 5V.

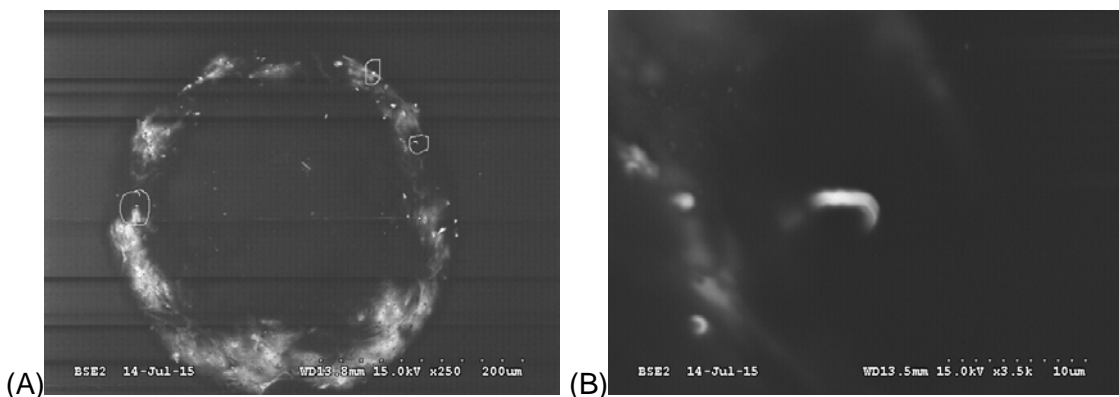


Figure 37: Conformal coating on SAC105+Ce BGA ball after 16,910 h LTHH.

3.11 Whisker risk modeling

3.11.1 Whisker risk modeling method

In addition to the testing, whisker short circuit risk modeling was performed to assist in the quantification of the overall electronic system risk. The system risk assessment enables the designer or systems engineer to make a relative assessment of mitigation effectiveness or obtain quantitative short circuit risks if a whisker incident has occurred and whisker characteristics such as length, density, etc. are available.

The whisker short circuit probability is dependent upon the probability that a whisker will grow at a location with an angle and length to form a bridge and the voltage dependent electrical conduction probability. Tin whisker short circuit risk models have been developed for (1) pairs of gull wing lead connections and (2) several basic conductor geometries for whisker prone shielding plates and leads under connector bodies which are often not conformal coated (Figure 38).

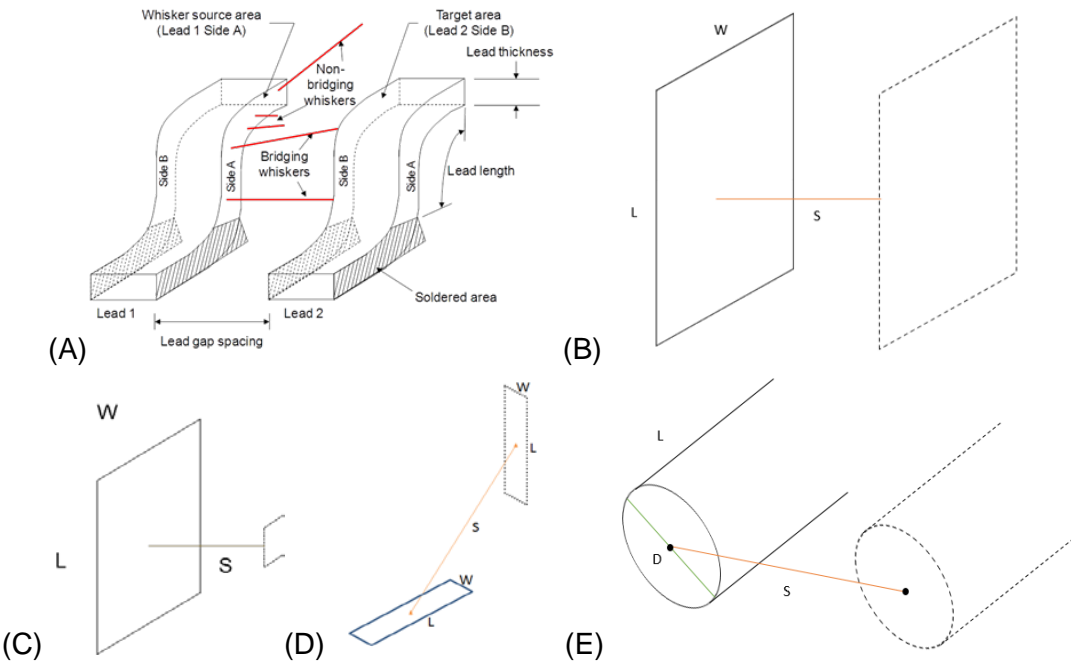


Figure 38: (A) schematic of gull wing leads with bridging and non-bridging whiskers (B) equal parallel plate, (C) unequal parallel plates, (D) equal perpendicular plates, and (E) parallel cylinders.

A key innovation was to perform a Monte Carlo analysis to create a probabilistic description of the lead-to-lead spacing distribution of whisker lengths that could bridge between conductors. As shown in Figure 39, each lead configuration had a specific “distribution of spaces” that a hypothetical whisker could bridge across. The benefit of separating the geometric modeling from the whisker length distribution was a reduced number of Monte Carlo simulations and increased modeling speed when new whisker length distributions become available.

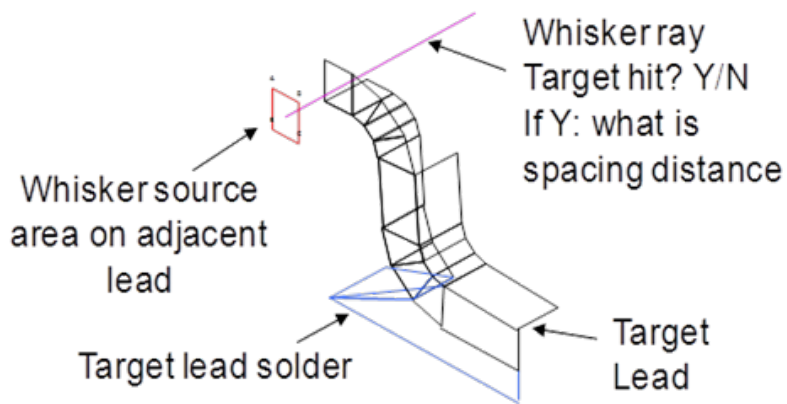


Figure 39: Determination of lead-to-lead spacing distance for a bridging whisker.

3.11.2 Gull wing lead modeling results

The spread-sheet risk model implementation has been developed to facilitate broad use in the design community. The package geometry typically available on the part manufacturers data sheet is inputted and the lead geometry is computed (Figure 40). Typically board pads are designed to be larger than the lead foot. The user inputs the pad creation rules and the pad geometry is determined. The user then can review the geometry computations and can adjust them.

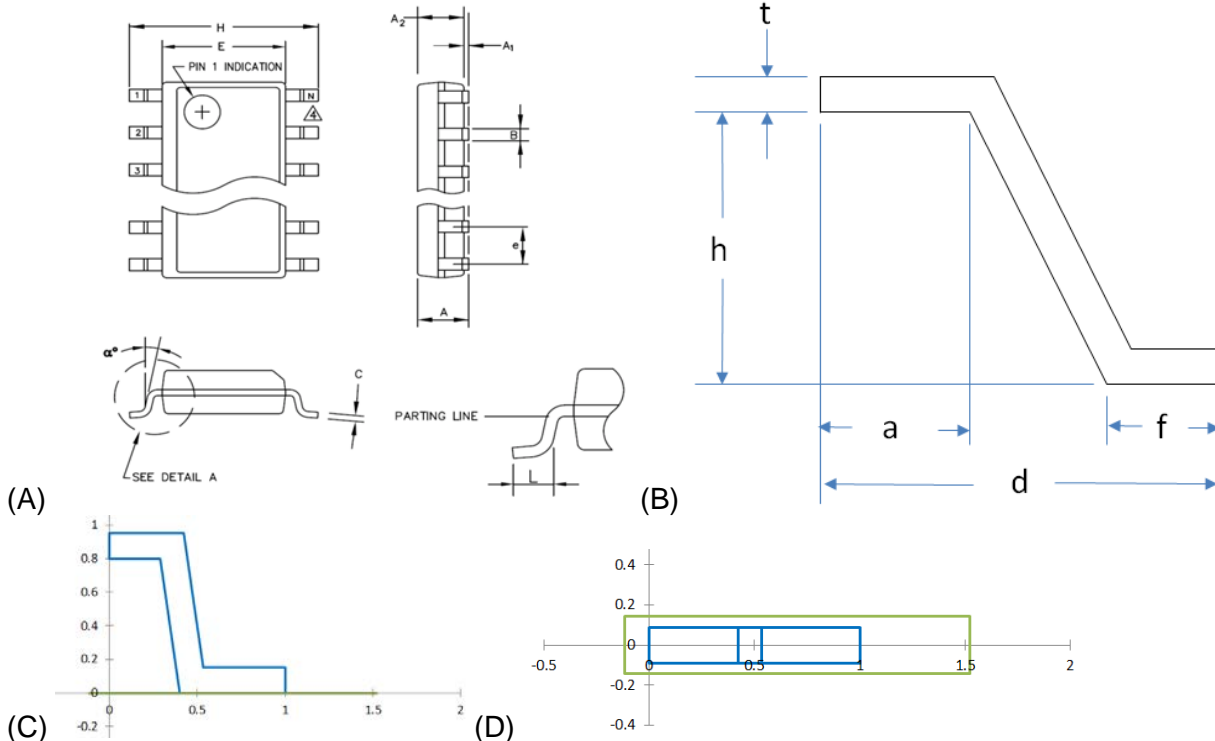


Figure 40: (A) Part drawing nomenclature, (B) lead dimension nomenclature, (C) side view of modeled lead and pad, and (D) top view of modeled lead and pad.

3.11.2.1 Gull wing lead risk calculation example

The risk model was used to compare the whisker mitigation associated with different amounts of conformal coating on a TQFP128 part. The HTHH 4,000 h data for tin finished copper leads soldered with SAC305 to immersion tin copper board pads was used and the part operating voltage was 3.3 V.

The following cases were evaluated:

1. No coating
2. 40 percent effective conformal coating coverage (50 percent side lead coverage, 90 percent front lead coverage and no coating behind the leads or on the pads behind the leads)
3. 40 percent effective conformal coating coverage with added mitigation eliminating the board pad whiskers (e.g. tin-lead board plating with tin-lead solder or sufficiently thick and strong urethane coating coverage).

The TQFP128 is a 0.4 mm pitch with leads on four sides and there are 124 spaces between adjacent leads. The computed lead dimensions are in Table 2.

The whisker length and density statistics entered into the spreadsheet for the lead, solder and pad were:

- HTHH 4,000 from Figure 41
 - Lead: Location-1 $\mu = -2.8988 \ln(\text{mm})$ and $\sigma = 0.1944$, 400 whiskers/mm²
 - Pad: Location-2 (region C) $\mu = -2.9228 \ln(\text{mm})$ and $\sigma = 0.2860$, 400 whiskers/mm²
 - 400 whiskers/mm² was used to represent a moderately high whisker density

- Solder: Estimated lognormal distribution for short whiskers: 1.7 percentile length = 1 micron, 99.8 percentile whisker = 25 microns, 10 whiskers/mm².

The tabular results for the “no coating” case (Table 3) shows that the most shorts were at the board pad. Figure 42 shows decreased short circuit risk with increased coating mitigation. The addition of supplemental conformal coating mitigation over the board pads resulted in the greatest reduction in short circuit risk.

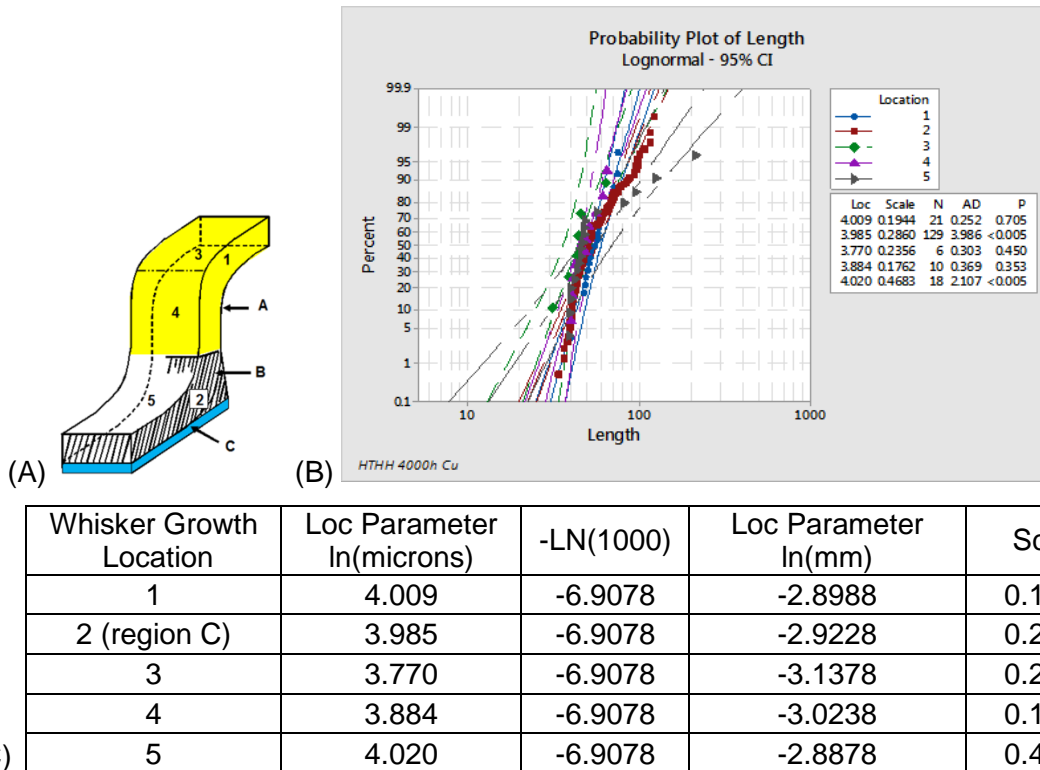


Figure 41: (A) Whisker growth locations, (B) probability plot of whisker lengths (microns) from the HTHH testing for Cu leads after 4,000 h at 85°C/85%RH; broken down by location (from Figure 283) and (C) conversion of lognormal mean parameters from ln(microns) to ln(mm) by subtracting ln(1000) from the ln(mm) location parameter.

Table 2: TQFP128 lead and pad dimensions (mm).

Lead Span Length (d, 1) =	1.0
First Bend Distance (a, 0.2876) =	.2876
First Bend Height (h, 0.8) =	0.8
Lead Foot Length (f, 0.6) =	0.6
Lead Thickness (t, 0.1524) =	0.1524
Lead Width (0.18) =	0.18
Lead Pitch (0.4) =	0.4
Total Lead Spaces (124) =	124
PWB Pad Length (1.64) =	1.64
PWB Pad Width (0.291) =	0.291
PWB Pad Thickness =	0.063
Overall Coating Effectiveness =	0%

Table 3: Shorting results for TQFP128 with no coating (ref . Table 78)

WHISKER SHORTING RESULTS:			
Coating Effectiveness =	0		
Total lead spaces =	124		
Applied Voltage =	3.3	V	
Shorting Probability =	0.225548		
Whisker Type:	Lead	Solder	Pad
Bridges per lead:	8.663E-10	4.719E-09	0.0858
Bridges per part:	1.074E-07	5.852E-07	10.6372
Shorts per part:	2.423E-08	1.320E-07	2.3992
TOTAL SHORTS (this part only) =	2.399		

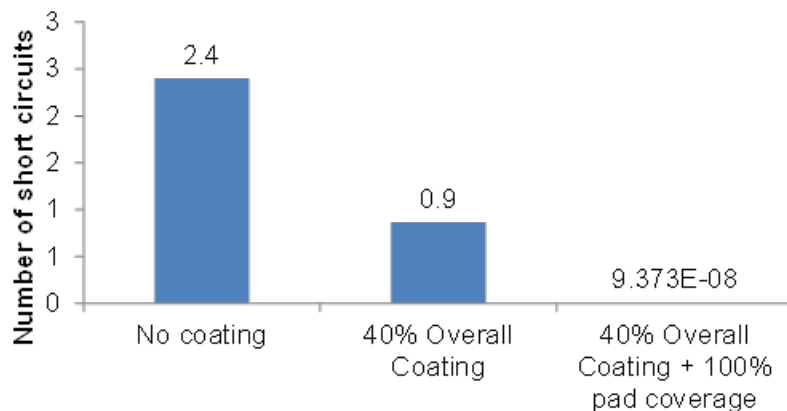


Figure 42: Summary of computed TQFP128 short circuits for three levels of coating mitigation.

3.12 Project summary

3.12.1 Experimental results summary

Based on a systematic study of electronic assemblies with component leads covered with SAC305 assembly solder, the following overall conclusions can be made:

- Whisker risks on SAC soldered assemblies must be considered for high-reliability equipment
 - Neither reflow or Ag and Cu alloy additions to Sn prevented whisker growth
 - Many whiskers grew from SAC305 solder joints where solder was thin (less than 25 microns).
 - Some whiskers were long enough to create short circuits between fine pitch parts
 - Fine pitch board spacing was typically 100 microns but was reduced to 60 microns where the SAC solder joint bulged outward
- The assembly level testing yielded whisker lengths that would fail the JESD-201 piece part test, even though the assembly level test durations were shorter than those used in JESD-201.
- The presence of conformal coating reduced whisker growth

The factor details that the electronic design and manufacturing team need to be aware of are:

Long whiskers in lead-free solder alloys

- *Corrosion effect:* Ionic contaminants from parts, manufacturing process, or environment can provide an accelerant for whisker nucleation and growth due to the formation of corrosion product that preferentially attacks the grain boundaries
- *Rare earth element in solder effect:* Rare earth element additions in solder used to improve mechanical fatigue performance significantly increases the whisker propensity
 - From a practical perspective, during electronic assembly service environments of thermal cycling, shock and vibration solder fatigue cracks would eventually form, which would expose interior RESn IMC regions creating new whisker prone areas with time
- *Manufacturing process effect:* Rework flux, such as ROL0 organic acid rework flux that does not go through the full heat cycle or halide activated fluxes, can leave behind ionic residues that increase whisker growth if not thoroughly removed

Test considerations

- Periodic inspection intervals should be avoided in high temperature/high humidity testing because the interruption of whisker growth during inspection results in an under-reporting of whisker length as a function of time; Progressively increasing the inspection interval is preferred (e.g. 500, 1,500, 3,500)
- Thermal cycling promotes whisker growth when low coefficient of expansion materials such as alloy-42 are part of the termination
- High temperature/high humidity promotes whisker growth due to corrosion and oxidation of SAC alloys
- Thermal shock cycling (-55 to 85°C, 10 minute dwells, three cycles per hour per JESD-201) is too severe for assembly testing

Environmental effects

- Thermal cycling promotes whisker growth when tin is on low CTE base materials such as alloy-42.
 - The stresses in the mild +50 to 85°C PCTC cycle were sufficient to initiate recrystallization of the lead-free solder and nucleation of whiskers.
 - Even though the -55 to 85°C thermal shock cycling from JESD201 does not create optimal stress conditions for whisker growth from alloy-42 terminations in SAC305 assembly, the alloy-42 leads still exhibited whisker lengths longer than the JESD201 piece part test limits.
- High humidity promotes whisker growth when thin SAC is on Cu.
 - The 85°C/85 RH 1,000 h exposure on an assembly resulted in whisker lengths longer than the JESD201 piece part test limits for 4,000 h.

Metallurgical factors

- SAC alloy whisker growth was observed from thin (less than 25 micron) lead-free solder regions
 - SAC dipping of leads is not a good whisker mitigation
- All the solder joint materials are important for ascertaining whisker growth.
 - Although Ni tended to retard nucleation on Cu pads in HTHH, it tended to promote whisker growth by forming thick CuNiSn IMC on alloy-42 leads during PCTC.
- Several stress relaxation mechanisms were observed other than tin whisker growth
- Rare earth element additions to lead-free solder tend to segregate to the surface
- SAC with REE grew whiskers from solder regardless of solder thickness in room air, nitrogen storage, simulated power cycling and high temperature/high humidity environments
- SAC305 with ROL0 and ZnCl rework flux residue resulted in significant whisker growth
- Solder surface roughness with contamination entrapment promoted whisker growth
- Corrosion was present between AgSn₃ plates and tin dendrites
- Preferential corrosion was present between tin dendrites
- Lower stress environmental conditions tended to form many sub-micron diameter whiskers that were not observable using the current JESD22-A121A [24] inspection methods

As-received part factors

- Tin finish voids, grooves, exposed base metal (mold flash areas and lead shear areas), and contamination that could contribute to corrosion enhanced whisker growth were observed
- Lead nodules and forming deformation result in tin regions less than eight microns thick that can have increased whisker propensity

Conformal coating

- The AR/UR blend conformal coating tested provides significant whisker mitigation especially where it was thicker
- Coating thickness was as thin as ~0.3 microns over the lead corners.
- Coating cracking was observed after thermal shock cycling, particularly where the coating was thick
 - Thick coating fillets (~450 microns thick) formed between the SOT5 and SOT6 leads and the package body

3.12.2 Whisker short circuit risk modeling summary

The quantification of whisker short circuit risk improves mitigation decision making. The analysis showed that conformal coating mitigation provides a significant reduction in short circuit risk for lead-free assemblies. It should be noted that large area tin surfaces should be avoided (e.g. tin plated shields, connector bodies, hardware, heat sinks, etc.).

3.13 Conclusions and implications for future research/implementation

The WP1753 experiments have demonstrated that reflowed SAC305 lead-free solder, particularly when it is less than 25 microns thick, grows whiskers. This whisker growth presents a statistically significant short circuit risk to fine pitch parts on non-conformal coated assemblies. The present work generated over 120,000 whiskers on low profile SOT part assemblies alone. While increasing contamination tended to increase whisker growth, the contamination levels tested were not abnormal and were within the J-STD-001 Class 3 acceptance limits. Conformal coating or other mitigation means [2] should be used to reduce whisker short circuit risks. The assembly level testing yielded whisker lengths that would cause short circuits and fail the commercial industry JESD-201 piece part test, even though the assembly level test durations were shorter than those used in JESD-201. Lead-free material mitigations in DoD electronic systems will help ensure that equipment using COTS electronics will be reliable and availability for the warfighter.

The present work highlighted that the combination of materials in the joint was important. The experiments only evaluated a small subset of the interconnect materials used in DoD electronics and resource limitations prevented inspection of all the assemblies tested. Testing has been completed on:

- Lead finish: Sn plating
- Underplating: None
- Lead/substrate material: Copper alloys C194, C7025, C151 and alloy-42
- Solder: SAC305 including BGA ball solder alloys: SAC105, SAC105+Ce
- Board finish: immersion Sn over Cu on glass epoxy laminate with solder mask
- Conformal coat: MIL-I-46058 AR/UR dual cure UV and moisture
- Environments: PCTC, TC, HTHH, LTHH

There are many more finish, lead, solder, board materials, conformal coatings, electromagnetic shielding materials, and environments that are used in DoD systems such as:

- Lead finish: Sn, SnBi, various dipped lead-free alloys, PdAu, Electrolytic Au
- Underplating: Cu, electrolytic Ni, electroless Ni
- Lead/substrate materials: BeCu, phosphor bronze, brass, ceramic, steel, silicon
- Board finishes: nickel electroless immersion gold (ENIG), electroless nickel electroless palladium immersion gold (ENEPIG), electrolytic nickel electrolytic gold, organic preservative coatings over copper

- Solder alloys: SnAgCuBi, SnAgBi, SnAgCuSb, SnAgCuSbBi, SnCuNiGe
- Coatings:
 - There are five types (AR, SR, ER, UR and XY) and many coatings qualified to MIL-I-46058
 - IPC-CC-830 total number of coatings is not available since there is no qualified providers list (QPL)

The DoD would benefit from having assembly level whisker mitigation verification qualification tests and conformal coating materials qualified to minimum strength and coverage levels for whisker mitigation.

4. Whisker growth literature review

The whisker growth process may be characterized by three distinct stages: incubation (or nucleation), period of growth at a fairly constant rate, followed by transition to growth at a much-reduced rate (or apparent cessation of growth) [8]. A consensus is lacking for a single accepted explanation of the mechanism(s) of whisker growth. However, there is agreement that whisker growth occurs from the base of the whiskers and not the tip (see discussion in [3]) and that a form of long range diffusion of tin atoms supports the growth [56]. Also, most investigators agree that a process of stress relief within the tin layer contributes to whisker nucleation and growth. Recent analysis has shown that electrostatic forces could also play a role in the formation of the unique filamentary whisker shape [38] [39].

The dynamic recrystallization (DRX) model provides a recent useful means to describe whisker growth [21][22]. In this model, whisker growth is dependent upon tin grain size, temperature, and compressive stress (Figure 43). It has been shown that whisker growth can also start from pre-existing grains [40]. An interesting aspect of the dynamic recrystallization model is that there is a compressive stress “sweet spot” that promotes whisker growth for a given temperature and grain size. If the compressive stress in the tin is either too low or too high, whisker growth would not occur.

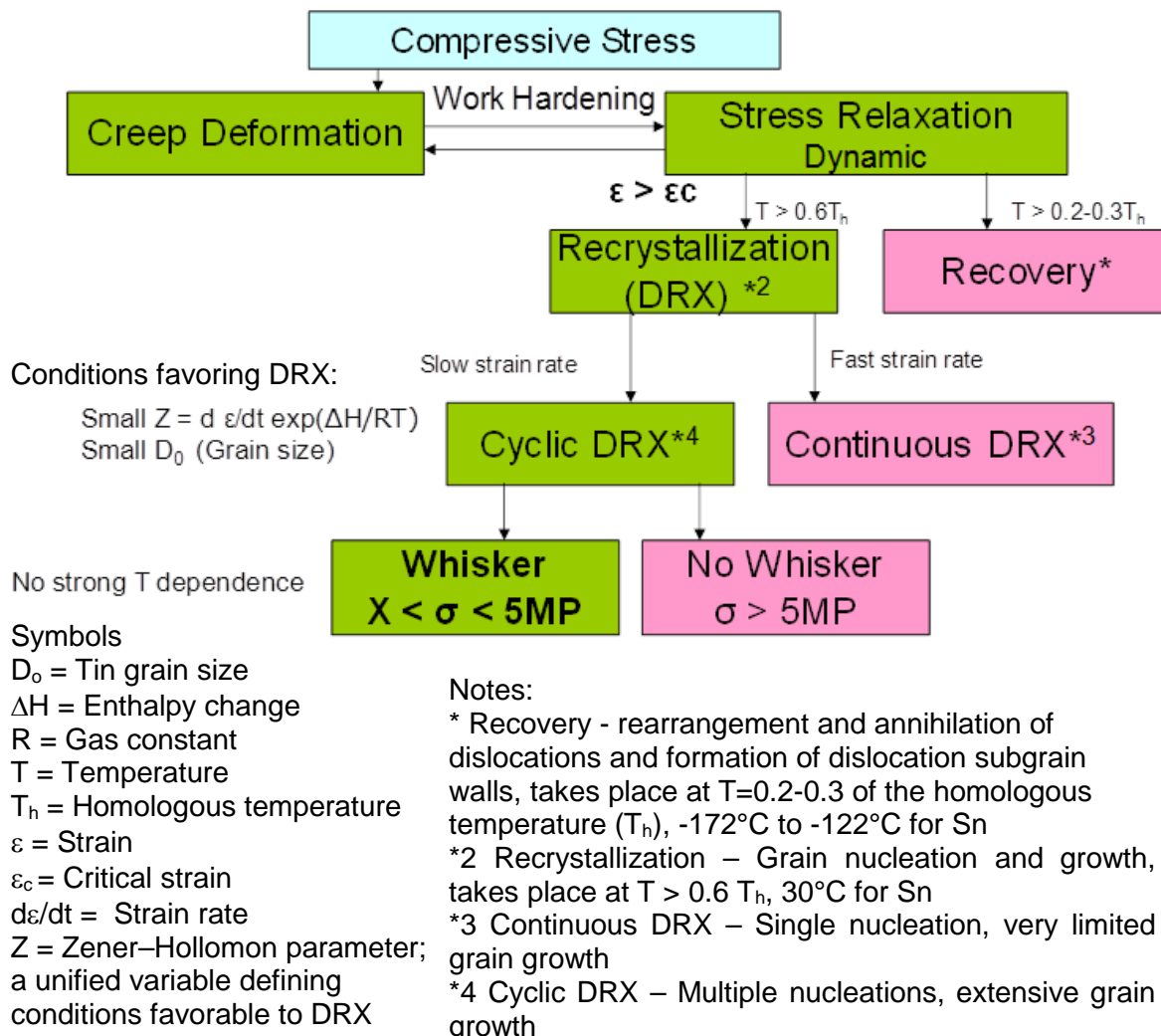


Figure 43: Schematic diagram illustrating the conditions leading to cyclic dynamic recrystallization and whisker growth.

As shown in Figure 44, there are many sources of compressive stress in a typical lead and solder joint. High humidity and corrosive environments are especially prevalent in many DoD systems. This can result in corrosion product formation and grain boundary oxidation which can increase the tendency of tin to whisker [10][12][34]. Long term storage IMC formation at the substrate interface [53] [54] [55] can also promote whisker formation. In addition, thermal cycling coupled with expansion differences between the substrate and the tin can cause whisker growth [59][60][61]. Mechanical loading (not studied in the present experiments) can cause very rapid whisker growth [62] and is of particular concern for tin finished press-in pin connector systems and tin plated connector contacts.

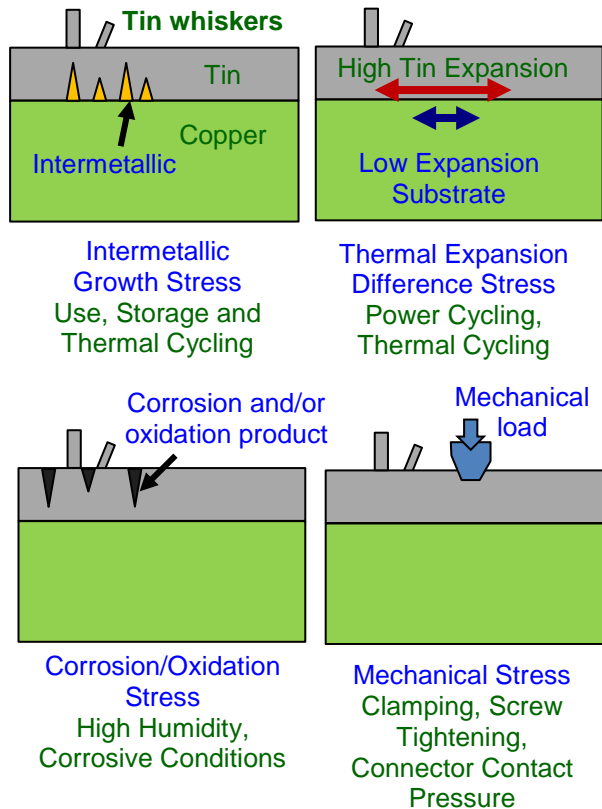


Figure 44: Some of the factors influencing whisker growth.

Recently Sarabol et.al. [35], Chason [63], and Susan et. al. [36] have examined the role of grain boundaries and grain orientation in whisker growth from tin plating. Of interest to the present work, Sarabol proposed that the preferred whisker nucleation site depends upon tin grain orientations and the tin grain mis-orientations in the plating structure as well as the elastic anisotropy of tin and suggests that shallow angled tin grains favor whisker growth. Chason has proposed a mechanism for the creation of surface grains by strain induced grain boundary migration. With this mechanism, the initially vertically oriented boundaries of the columnar plated tin grains move toward each other resulting in an hourglass shaped grain. If the hourglass grain boundaries pinch the grain in middle, two new grains are formed with the upper grain potentially being a shallow angled grain suitable for whisker growth. Susan examined the manner in which tin whiskers develop change in diameter, kinks and bends. In Susan's observations there was no simple correlation between growth angles and lengths for whiskers observed over an approximate 2-year period. In addition, the distribution of lengths was broad. The broad distribution may be due to differences in the incubation periods and growth periods of individual whiskers, in addition to the actual spread in individual growth rates.

While many two dimensional schematics and images are used to describe whisker growth mechanisms, there must be a realization that the three dimensional aspects of grain boundary orientation, tin mass flux and stresses are important [64][65]. In the absence of surface transport due to native oxide, the Sn accumulation is localized to oblique grain faces near, but under, the free surface that forces the grain upward. A curved whisker occurs when there is non-uniform accretion of Sn at the whisker base.

4.1 Environment and whisker growth

4.1.1 Room temperature

Significant whisker growth has often been observed after relatively long time periods at room temperature. If no corrosion is occurring, copper-tin intermetallic (IMC) growth is the source of stress [53] [54][55] [66] – [76]. Cu₆Sn₅ is a common IMC, which forms at a Sn-Cu boundary at ambient room temperature. It is the dominant IMC between Cu and Sn and is known to grow faster with increasing temperature. The intermetallic layer is formed by Cu diffusion into the Sn film through grain boundaries. One of the reasons why Cu-Sn intermetallic generates stress in the tin film is that Cu diffuses into Sn much more rapidly than Sn diffuses into Cu. As a result, the intermetallic growth proceeds into the tin layer increasing compressive stress in the film [4].

One of the longest duration controlled environment room temperature whisker growth studies was performed by Dunn [71] – [73]. In the aforementioned assessment that began in the 80s, growth over a 32 year period was reported for bright-tin plating over copper plated steel C-ring specimens that were maintained in a desiccated environment. Several samples with tin over copper underplating exhibited whisker growth between the 15.5 year and the 32 year inspection times.

NASA has observed long term room temperature whisker growth on the space shuttle card guides [74][75] and from tin plated brass in a conformal coating test [76]. The card guide whiskers grew from pure tin plating employed for corrosion protection of the beryllium-copper alloy retainers. After approximately 20 years of storage, eight mm long whiskers were reported in 2006. The coating test samples grew a substantial number of whiskers after 11 years (~50 whiskers/mm²) with some whiskers exceeding one mm in length in the uncoated control areas.

4.1.2 Isothermal high humidity

Isothermal high temperature with high humidity is an environment that often results in increased short term whisker growth. The 85°C/85%RH condition was selected for the present testing because it was found to be the best for growing whiskers in lead-free solder [25] [26] [27]. Crandall and co-workers found optimal whisker growth for room temperature sputtered tin to occur when the relative humidity was between 70 and 85 percent [28].

A relatively broad range of humidity and temperature conditions have been used to grow whiskers on tin finished parts. An extensive review of tin whisker growth during elevated temperature and humidity exposure is provided by Panshechenko [77]. Commercial electronic part whisker test standards use 30°C/60% RH and 55°C/85% RH ([23] [24] [78]). Oberendorff [37] and Osenbach [13][79] used 60°C/93%RH while Woodrow and coworkers [80] used 50°C/50% RH and Panshechenko [77] used 55°C/85%RH for 3,000 h, and 60°C/85% RH for 12 months.

4.1.3 Thermal cycling

Thermal cycling conditions augment tin whisker growth when tin or tin rich alloys are applied over materials with low coefficient of thermal expansion. Whisker growth has been observed during thermal cycling on ceramic capacitors [59][60] and alloy-42 lead-frames [61]. The temperature range during the whisker evaluations generally matches the extremes associated with electronic equipment storage or service. For instance, JESD 201 [23] calls out -55 to +85 °C and -40 to +85 °C ranges. Dittes [61] used a -40 to +85 °C range while Brusse [59] had a slightly higher upper temperature limit (-40°C to +90 °C) and Suganuma [60] used an even higher upper temperature limit (-40 to +125 °C). While Brusse and Dittes performed testing in an air atmosphere, Suganuma found that vacuum conditions promoted longer and straighter whisker growth, which is particularly important for space environments and hermetically sealed and dried electronic packages.

4.1.4 Corrosion

Corrosion has been identified as a compressive stress source driver for tin whisker growth. Corrosive conditions differentiate much of the harsh service DoD electronic equipment from consumer electronics [81]. Most avionics applications use conformal coating to improve corrosion resistance, however, there are many DoD ground based applications that do not utilize conformal coating. In addition, coatings can be ruptured by whisker and nodule growth [80].

Snugovsky [10] performed detailed metallurgical analyses on whiskers growing from solder joints formed on leaded components. The whiskers appeared after life testing for 10 days at 60°C at 20 to 30%RH with on-off voltage cycling to the assembly that induced a temperature increase to approximately 85°C when the voltage was applied. The lead-frame material on components with the high whisker propensity was alloy-42 with electroplated matte Sn finish. A high amount of chloride, sulfate, and ammonia was detected on the assembled devices. Whiskers over 150 microns long grew from solder contaminated with rework flux residue.

Munson [11] reported the first failure related to long whisker growth from SAC405 solder in 2007. The whisker grew from a solder fillet of a metal oxide field effect transistor (MOSFET) device. The device had an alloy-42 lead frame with matte Sn finish and was assembled using no-clean SAC405 solder paste. The assemblies were subjected to 20 days of life testing of 65°C at 25%RH with blowing air. A possible root cause of long whisker formation was attributed to flux residue that may promote corrosion.

Hillman [12] performed tests on purposely contaminated bright tin plated copper etched and bent to simulate the leads of a small outline integrated circuit (SOIC) device. The samples were immersed for 72 h in various concentrations of sodium chloride aqueous solutions and rinsed with deionized water. The samples were then exposed to 4,000 h at 85°C/85%RH. It was found that the samples immersed in the saturated NaCl solution exhibited the greatest whisker density and average whisker length. While maximum whisker length was not reported, a photograph of a whisker with a length of more than 200 microns was shown.

Osenbach [13] tested matte tin plated copper lead-frames devices and observed corrosion products around dissimilar metal regions after intentional water contamination and subsequent exposure for 2,500 h at 60°C/93%RH high humidity testing. The devices used in the study were 176-lead thin quad flats pack (176TQFP) devices. Two lead frame alloys, CDA7025 and EFTEC-64T, were used in this study. In the corroded regions, the entire thickness of the tin plating was transformed to SnO_2 . Adjacent to the corroded regions, the tin oxide thickness varied from less than five to 19 microns. An unusual whisker was observed that had a total length of 282 microns, where approximately 108 microns of its length grew under the plating and an additional 174 microns of growth occurred in free space.

Baated [14] evaluated the effects of reflow atmosphere and flux on whisker growth of Sn plated QFPs soldered with $\text{Sn}3.0\text{Ag}0.5\text{Cu}$ solder after exposure to 85°C/85%RH conditions up to 1,000 h. Reflow in air was compared with nitrogen (less than 500 ppm O_2) for RMA (rosin mildly activated) flux with (1) no activator, (2) 0.4%HBr based activator added and (3) 0.8%HBr based activator added. Both copper and alloy-42 tin plated lead frames were evaluated. The flux residue was not cleaned after assembly. No whiskers were observed on the RMA flux having no activator in either reflow atmosphere and no whiskers were observed on the samples reflowed nitrogen. With increasing halogen activator concentration in the flux, the propensity of whisker formation increased.

Kurtz [15] evaluated chloride and sulfate contamination on tin plated copper leads. A strong influence of tramp ion contamination on corrosion was observed. The maximum whisker length was dramatically increased in the presence of ion contamination. In addition, it was found that the corrosion effect was significantly accelerated if exposed copper was present immediately adjacent to the tin, as is the case in integrated circuits produced using the trim-and-form procedure or for connectors, manufactured from tin-coated strip material.

Sweatman [16] evaluated the whisker propensity of soldered printed circuit board traces with various soldering processes and fluxes exposed to different temperature/humidity environments. The extent of corrosion increased with increasing temperature and humidity. Significant whisker growth occurred only under the conditions of 60°C/90%RH and 85°C/85%RH and increased corrosion resulted in greater maximum whisker length. The first

whisker was observed after 5,000 h at 40°C/95%RH, after 1,000 to 2,000 h at 60°C/90%RH and after approximately 500 h at 85°C/85%RH.

Oberndorff [37] evaluated quad-flat-pack (QFP) samples of commonly used lead frame materials (C19400, C70250, C18040, and Fe-Ni42) that were plated, using automated production lines, with commercially available matte Sn. After 4,000 h of exposure to 60°C/93%RH, whisker lengths of 200 microns were commonly found on single components, and most of the components in test grew whiskers. Corrosion was accelerated near the areas where a galvanic couple was formed between the Sn plating and exposed lead frame material, such as the tie-bar and the toe shear areas.

Osenbach [79] evaluated tin plated Cu alloy 7025, 132 pin package QFPs during 60°C/93%RH exposure with and without reflow. In addition to the typical whisker growth observations, a unique tin whisker flower was also observed during this test. Under conditions with condensing moisture drops and sulfur (from the plating in this case), flower clusters of tin whiskers having a plate-like structure were observed after 672 h of 60°C/93%RH exposure. No whisker flowers were observed when the solder process melted the tin. It was postulated that when melted, the sulfur contamination either vaporizes or is redistributed in the bulk of the film such that it was no longer available to react with the condensed water.

4.1.5 Effect of circuit electrical bias

Whiskers grow spontaneously without requiring an applied electric field to encourage their growth [8], however, a strong electric field may promote whisker growth [39]. (Note that the typical IPC-2221 circuit board design voltages gradients (~ 400 V/cm) are considerably less than those used by Karpov [39] to promote whisker growth.) The extent and impact of bias is yet to be fully understood. Osenbach [82] studied 3.3 and 5V voltage bias on 15 micron thick tin plated lead-frame parts mounted in test sockets exposed to 60°C/95%RH. No whisker growth was observed on the socketed samples or the non-socketed controls so it was surmised that neither electrical bias nor leads bending from the socket influenced whisker growth of the tin plated leads. Hilty [83] tested tin plated coupons with in a fixture over a range of voltage stresses and also found that voltage bias did not influence whisker growth.

5. Screening experiment 1: SAC305 assembly ionic contamination induced whisker growth

5.1 Approach

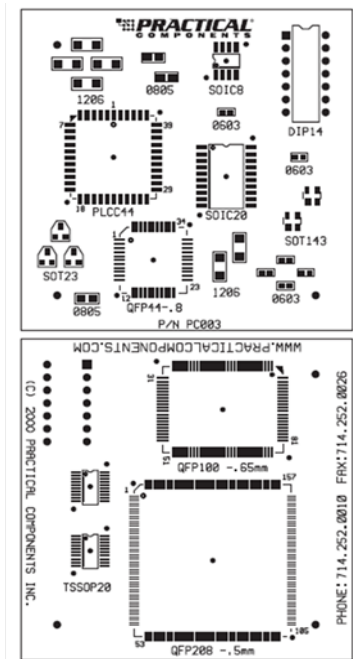
The main goal of the ionic contamination screening experiment [18] was to choose the contaminant that yields the best whisker propensity for the primary experiments. Prior work by Snugovsky [10] showed that high levels of flux residue, chloride, sulfate and ammonia contamination on SAC soldered devices could have contributed to significant whisker growth on alloy-42 lead frame parts during a 10 day 60°C/(20–30% RH) test with on-off power cycling. In contrast to the prior work at high mean temperature cycling with low humidity, this screening experiment sought to determine if similar whisker propensity with contamination existed in an isothermal high-temperature/high humidity (85°C/85% RH) environment. The assemblies were soldered with SAC305 using a no-clean process. Component contamination before soldering and assembly contamination after soldering were both evaluated. The contaminate types were chloride, sulfate, and a chloride+sulfate mixture, as well as different types of flux residues. Various part types having different lead materials were included. In addition, the whisker propensity of loose non-soldered components was compared to the same components after SAC305 solder attachment to the boards. The analysis was primarily focused on solder joint microstructure and its relationship with whisker formation.

5.2 Methods and materials

5.2.1 Test vehicle, components and assembly

The test vehicle used for the study was the Practical Components Inc. PC003 double sided rework test board shown in Figure 45. It incorporates a variety of components: both low and high stand-off SMT parts, pin-through-hole (PTH) connector and discrete chip parts. The package type, part numbers, lead finish and lead frame materials are summarized in Table 4. The dimensions of the board are 63 mm x 63 mm and the surface finish is immersion Ag over Cu.

As shown in Figure 46, the components were divided into three groups. The first group was used “as-received”. The level of contamination was analyzed using ion chromatography (IC). The second group was cleaned to achieve cleanliness about 10 times below industrial acceptance levels. The third group was intentionally contaminated to an above-average ionic content level.



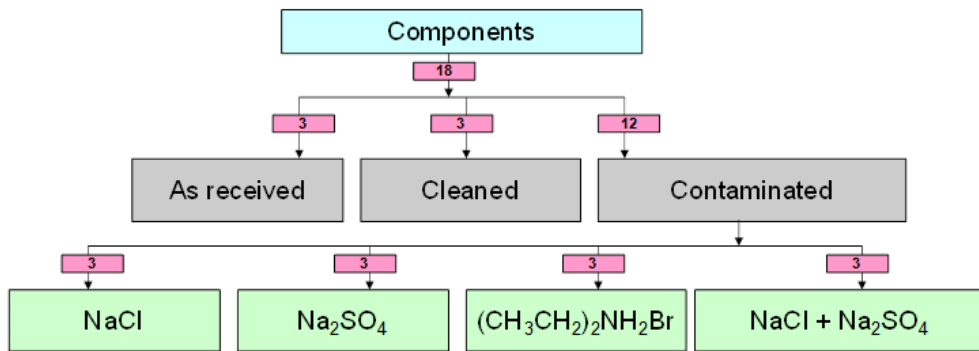
PC003 Solder Practice Board Kit (Tin-Lead and Lead-Free components available)	
Part Description	Quantity Per Kit
PCB003 Board (customer to specify finish)	1
QFP208-28mm-.5mm-2.6mm	1
QFP44-10mm-.8mm-3.2mm	1
QFP100-14x20mm-.65mm-3.2mm	1
PLCC44	1
SO8GT-3.8mm	1
SO20GT-7.6mm	1
SOT23	3
SOT143	2
TSSOP20-4.4mm	2
0603SMR	6
0805SMR	3
1206SMR	6
DIP14T	1
Kit Order Number: (Tin-Lead)	PC003
Kit Order Number: (Lead-Free)	PC003-LF

Figure 45: Contamination screening test assembly.

Table 4: Contamination screening test assembly component lead-frame and surface finish materials.

Package Type	Part Description	Lead finish / Plating	Lead Frame / Substrate	Lead Frame / Alloy
QFP	A-QFP208-28mm-.5mm-2.6-DC-Sn	Matte Sn	C7025	Cu2.2-4.2Ni0.25-1.2Si0.05-0.3Mg
QFP	A-QFP44-10mm-.8-3.2-DC-Sn	Matte Sn	C7025	Cu2.2-4.2Ni0.25-1.2Si0.05-0.3Mg
QFP	A-QFP100-14x20-.65-3.9-LF-DC-T	Matte Sn	C7025	Cu2.2-4.2Ni0.25-1.2Si0.05-0.3Mg
PDIP	A-PDIP14T-300mil-DC-Sn	Matte Sn	C194	Cu2.1-2.6Fe0.015-0.15P0.05-0.2Zn
PLCC	A-PLCC44T-DC-Sn	Matte Sn	C151	Cu0.1Zr
SO	A-SO8GT-3.8mm-DC-Sn	Matte Sn*	C194	Cu2.1-2.6Fe0.015-0.15P0.05-0.2Zn
SO	SO20GTR-7.6mm-Sn	Matte Sn*	C194	Cu2.1-2.6Fe0.015-0.15P0.05-0.2Zn
SOT	SOT23-TR-Sn	Matte Sn	Alloy-42	Fe39-41Ni0.6Mn0.05Cr0.02Si0.05C
SOT	SOT143-TR-Sn	Matte Sn	Alloy-42	Fe39-41Ni0.6Mn0.05Cr0.02Si0.05C
TSSOP	A-TSSOP20T-4.4mm-Sn	Matte Sn	C7025	Cu2.2-4.2Ni0.25-1.2Si0.05-0.3Mg
Discrete	0805SMR-PA-5K-Sn-0	Matte Sn	Ni	Ceramic
Discrete	1206SMR-PA-5K-Sn-0	Matte Sn	Ni	Ceramic
Discrete	0603SMR-PA-5K-Sn-0	Matte Sn	Ni	Ceramic

To compare whisker formation on loose components and solder joints after assembly, some samples from each of the three groups (as-received, cleaned, and contaminated) of all 13 component types, were separated from the components used for assembly. The rest of the components were assembled using SAC305 alloy and no-clean surface-mount assembly (SMT). The PTH connectors were manually attached using a solder fountain process. The schematic of the build matrix is shown in Figure 47. After building, the assemblies were cleaned, left as is, or additionally contaminated.



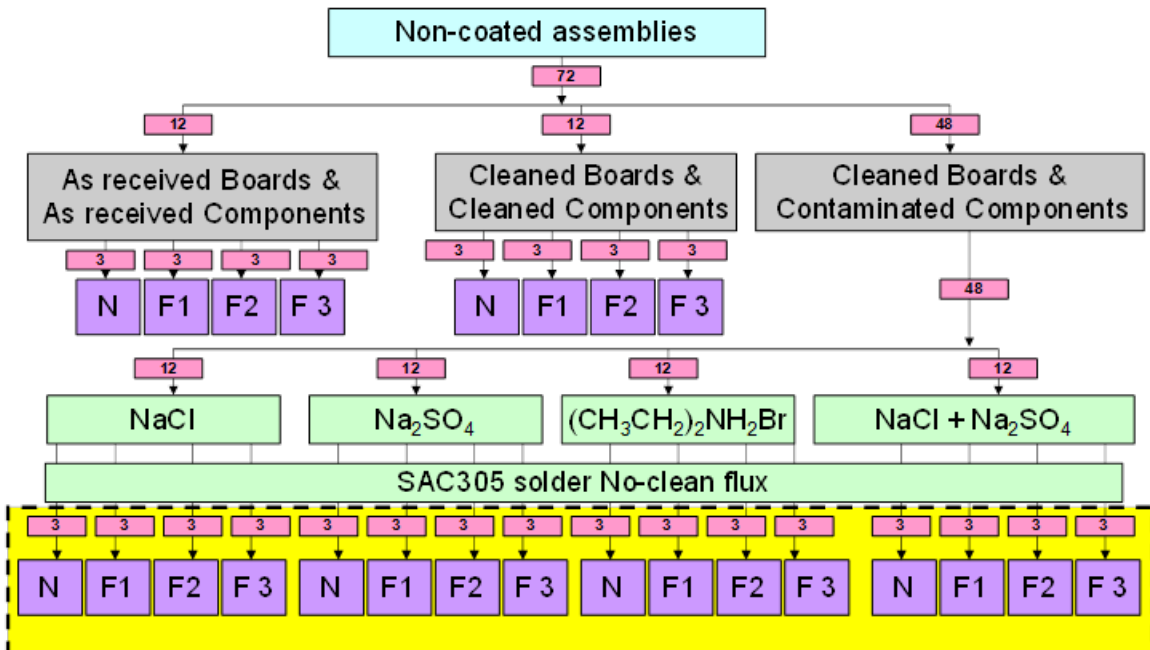
NaCl: 2.844 mM NaCl (166 ppm NaCl = 100 ppm Cl⁻)

Na₂SO₄: 2.844 mM Na₂SO₄ (404 ppm Na₂SO₄ = 243 ppm SO₄⁻²)

NaCl + Na₂SO₄: (2.844 mM NaCl + 2.844 mM Na₂SO₄)

(CH₃CH₂)₂NH₂Br: 2 wt% (CH₃CH₂)₂NH₂Br in (25% Rosin + 75% IPA)

Figure 46: Loose piece part contamination schematic.



N – No post assembly contamination

F1 – Lonco 3355-11 (ORH1)

F2 - Alpha 615-25 (ROL1)

F3 - Alpha EF8000 (ROLO)

Figure 47: Assembly and post assembly contamination schematic.

5.2.2 Cleaning, component contamination, and post-assembly contamination methods

Cleaning

Components and boards were placed into K Pak™ bags with cleaning solution of 10 percent isopropanol (IPA)/90% deionized water. The K Pak™ bags were sealed and placed in a water bath at 80 °C for 40 min. After that the bags were removed from the water bath and placed on a vibration table for solution agitation for 40 minutes. Parts were then dried in an oven at 60 °C for 10 minutes. The process was repeated for a total of two wash cycles. Ion

chromatography (IC) was performed on each type of component; the typical level of contamination was 10 times below acceptable level (or $0.009 \mu\text{g}/\text{cm}^2$ to $0.017 \mu\text{g}/\text{cm}^2 \text{Cl}^-$ and $0.069 \mu\text{g}/\text{cm}^2$ to $0.17 \mu\text{g}/\text{cm}^2$ total inorganic).

Component contamination

The basis for the method used was Kurtz's Atotech study [15] that showed accelerated whisker growth on Sn-plated components contaminated with 2 mM NaCl and 2 mM Na₂SO₄. In this study, the level of contamination was increased to 2.844 mM to obtain a component contamination level above industry acceptance [84].

To examine how NaCl and Na₂SO₄ might interact and double the overall level of contamination, a mixture of 2 mM NaCl and 2 mM Na₂SO₄ was used. (CH₃CH₂)₂NH₂Br flux (2 wt%) was chosen as a fourth contaminant based on the results of the JEITA work on creating whiskers [34].

Contamination solutions (166 ppm NaCl in deionized (DI) water, 404 ppm Na₂SO₄ in DI water, 166 ppm NaCl + 404 ppm Na₂SO₄ in DI water, and 2 wt.% (CH₃CH₂)₂NH₂Br in 25% rosin + 75% IPA) were placed in a bath until it reached 35 °C. Then components were then placed into jars containing contamination solutions. The jars were agitated and placed in a bath for four minutes. The solution and components were poured onto a stainless-steel mesh. The remaining components were placed in an oven to dry at 60 °C for 10 minutes. Components were then transferred to a clean tray. The parts were then stored in a nitrogen chamber. All components were baked at 125°C for four hours before assembly.

Assembly contamination method

Three fluxes widely employed in high-reliability electronics were used to imitate rework or hand attachment situations where flux may flood under components and through via holes to the bottom side of the board. In this case, the flux may not be properly activated and the flux residue may not be fully removed. The fluxes were low-rosin halide-free with halide content below 0.05% (ROL0), rosin based with halide content below 0.5% (ROL1), and organic water soluble with halide content below 2.0% (ORH1) (the acronyms ROL0, ROL1, and ORH1 are flux designators according to the IPC J-STD-004 standard [85]. The ORH1 flux was diluted 20x with DI water to imitate flux residue after cleaning. Syringes were used to measure a specified volume of flux for each component. Flux was slowly dispensed along the tips and tops of the leads and was allowed to dry. The flux compositions and the level of solder joint contamination are presented in Table 5 and Table 6, respectively. As will be shown in the results section, the main areas of contamination segregation on the surface were (a) grain boundaries, (b) defects in plating (open voids and cracks), and (c) surface roughness grooves.

Table 5: Flux composition

Flux	Adipate (%)	Chloride (%)	Bromide (%)
ORH1, water soluble	–	3.5	–
ROL1, rosin-based	–	–	0.1
ROL0, low-rosin halide-free	2.3	0.0032	0.0083

Table 6: Flux contamination on solder joints

Flux	Adipate (%)	Chloride (%)	Bromide (%)
ORH1, water soluble diluted 20x with DI water	–	3.5	–
ROL1, rosin-based	–	–	4.65–10.86

ROL0, low-rosin halide-free	186	0.31	0.78
-----------------------------	-----	------	------

5.2.3 Environmental exposure, whisker measurements and metallurgical analysis

5.2.3.1 Environmental exposure

The environmental whisker growth test was done per JEDEC JESD201 standard [23] except an 85°C/85%RH environment was used. The modified environment was chosen based on the data of the JEITA project [34] that demonstrated whisker formation on contaminated coupons after 500 h, which is faster than after a lower temperature treatment. Nihon Superior [16] reported much longer whisker formation on solder at 85 °C/85% RH compared with 40 °C/60% RH and 60 °C/90% RH. Loose components (13 types x 18 cleanliness variations x 3 component per point = 702 components) and assembled boards (72 cleanliness variations x 3 per point = 216 boards) were placed into the chamber as shown in Figure 48. The chamber was set up to reach 85 °C/85% RH in four hours. Then, samples were subjected to 500 h exposure. After the exposure, the chamber was slowly brought down to room temperature and humidity. The process was established to prevent water droplet formation. The samples were removed from the chamber and placed into the nitrogen chamber for two weeks during the whisker analysis. Several boards and components were cross-sectioned for microstructure analysis. After the whisker inspection, the majority of loose components and boards were returned to the high-temperature/high-humidity chamber for a second round of testing. The duration of the second test exposure was two times longer than the first one, i.e., 1,000 h. The reason for the time increase is discussed later in this report. The final whisker inspection was performed after 1,500 h (500 h + 1,000 h).

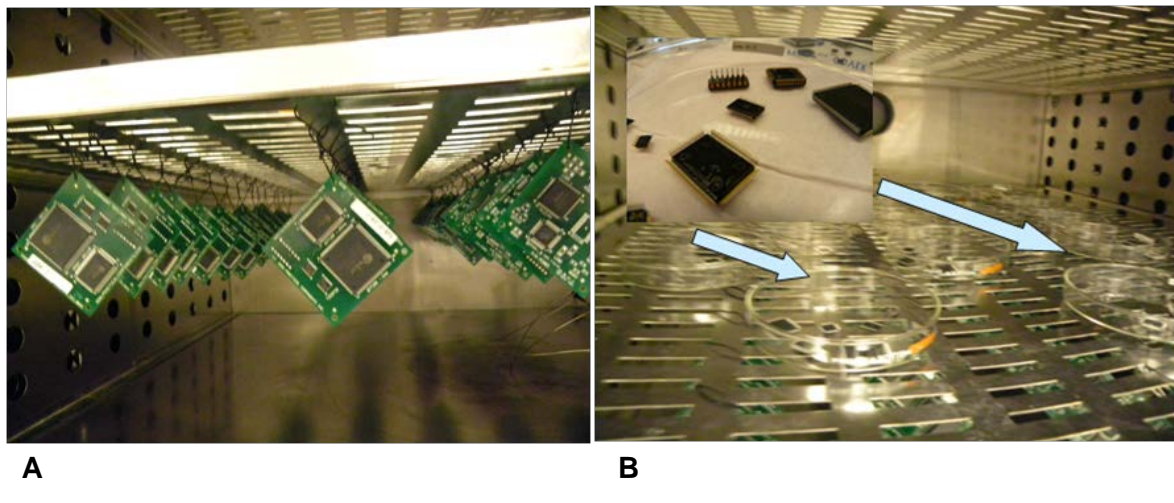


Figure 48: Test vehicle (A) and loose components and (B) placement in environment chamber.

5.2.3.2 Whisker inspection

The whisker inspection was predominantly carried out using scanning electron microscopy (SEM). The size of the board was suitable for placement into a variable-pressure Hitachi S-3000N microscope chamber. Loose components were placed with leads upward, in “dead bug” position. If whiskers were detected in the first of three boards, the remaining two were checked using optical microscopy to ensure the boards were identical to the first one and also contained whiskers. All three boards were analyzed using SEM if no whiskers were found in the first or second boards. Optical microscopy was also used for samples contaminated with 2 wt% $(\text{CH}_3\text{CH}_2)_2\text{NH}_2\text{Br}$ and ROL1 (rosin-based) flux after 500 h at 85°C/85%RH because of extreme charging and as a precaution against possible

damage of flux residue in the scanning SEM. The final inspection after 1,500 h exposure was carried out using scanning electron microscopy.

Images were taken at 40x and 90x using an optical stereoscope and at 100x, 500x, and 1,000x using SEM at typical locations and at the locations with the longest whiskers for the sample. To show whisker details, 2,000x and higher magnification was used. The whisker length, diameter, density, and distribution were measured.

5.2.3.3 Metallurgical analysis

To examine contamination levels and distributions, as-received, cleaned, and contaminated components were analyzed using ion chromatography (IC), SEM (SEM; Hitachi S-4500 and Hitachi S-3000N), and energy-dispersive x-ray spectroscopy (EDX; Oxford EDX). Loose components and assemblies were cross sectioned before and after high-temperature/high humidity exposure to analyze Sn plating quality, solder coverage and microstructure, intermetallic thickness, oxidation, and corrosion product morphology and distribution.

5.3 Results and discussion

5.3.1.1 Component contamination and plating quality

Two samples for each of 13 as-received components were analyzed for cation and anion levels using IC. Some components were contaminated above acceptable levels. Foresite recommended levels for typical ionic residue species and Celestica customers' requirements for total inorganic ions were used as criteria. For instance, after 40 minutes extraction at 80°C, the levels of chloride on PDIP14T ($0.50 \mu\text{g}/\text{cm}^2$) and sulfate on QFP44 ($1.61 \mu\text{g}/\text{cm}^2$) exceeded the Foresite requirements by 3.29x and 3.59x, respectively. The cation content was also much higher in these samples, with sodium being more than 39x the level of the Foresite recommendation. Considering the total level of anions and cations, PDIP14T and QFP44 were 2.29x more contaminated than Celestica customers' requirements: $3.69 \mu\text{g}/\text{cm}^2$, $3.41 \mu\text{g}/\text{cm}^2$, and $1.74 \mu\text{g}/\text{cm}^2$, respectively. The level of contamination of as-received components was comparable to the component contamination level in production assemblies with long whiskers from prior work [10]. Some of the as-received components were close to the industry accepted assembly contamination limit of $1.67 \mu\text{g}/\text{cm}^2$ ($10.8 \mu\text{g}/\text{in}^2$).

The components after cleaning had a typical level of contamination 10x below the acceptable level (or $0.009 \mu\text{g}/\text{cm}^2$ to $0.017 \mu\text{g}/\text{cm}^2$ Cl⁻ and $0.069 \mu\text{g}/\text{cm}^2$ to $0.17 \mu\text{g}/\text{cm}^2$ total inorganic).

The ionic level of the intentionally contaminated leaded components exceeded the level of as-received components and was above industry recommendations by factors of 2.9 to 5.3. This level was comparable to or even below the level of contamination of the components in production assemblies with long whiskers from prior work [10].

SEM/EDX analysis identified the contamination segregation locations and confirmed the presence of Cl, Br, S, and Na (Figure 49). The main areas where the contaminant segregated to were the grain boundaries (Figure 49A), the gaps between leads and plastic body (Figure 49B), the valleys in the surface roughness (Figure 49C), and the plating defects such as open voids and cracks (Figure 49D). These defects in Sn plating with exposed Cu are susceptible to galvanic corrosion. Defective Sn plating with voids and exposed Cu was detected on PIDIP14 and PLCC44.

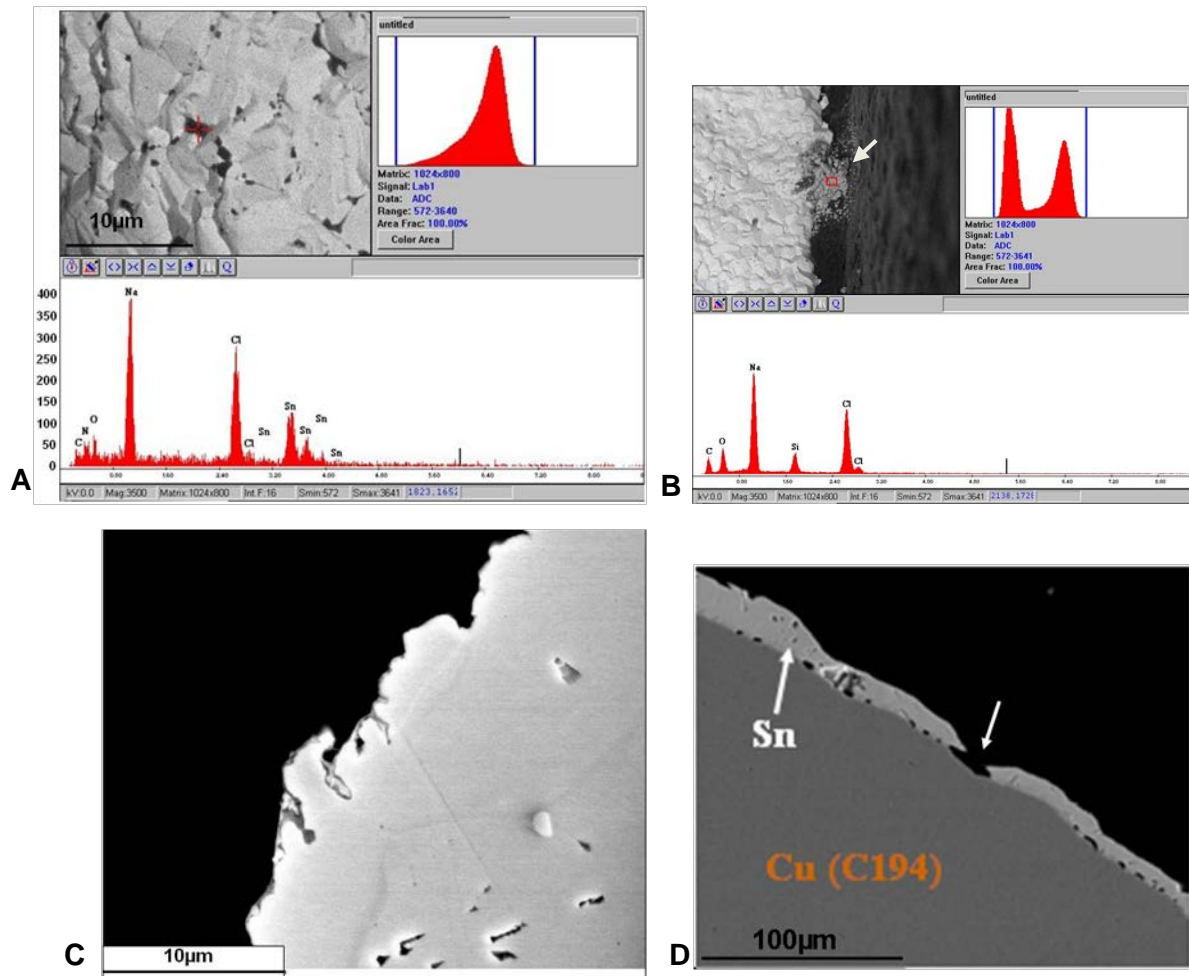


Figure 49: Main areas of contamination segregation; (A) grain boundaries, (B) gaps between leads and plastic body (C) surface roughness grooves, and (D) open voids and crack defects in plating.

5.3.2 Results of Testing at 85°C/85%RH

5.3.2.1 500 h inspection

There were no whiskers detected on the boards built using components cleaned prior to assembly and with a post assembly cleaning procedure typical for high-reliability products. Whiskers were detected in both as-received and contaminated assemblies. The longest whisker detected in assemblies with as-received parts grew on PIDP14T and PLCC44. The whisker lengths were 280 microns and 277 microns, respectively (Figure 50 and Figure 51).

Figure 50 demonstrates the importance of cleanliness for whisker growth mitigation in soldered assemblies. Out of 13 components, five components as-received and 11 in purposely contaminated assemblies showed significant whisker growth. Table 7 presents the relationship between the level of contamination of as-received components and whisker formation. If either the individual species or the total inorganic ions acceptance criteria were exceeded (bold values in Table 7), whiskers or hillocks grew.

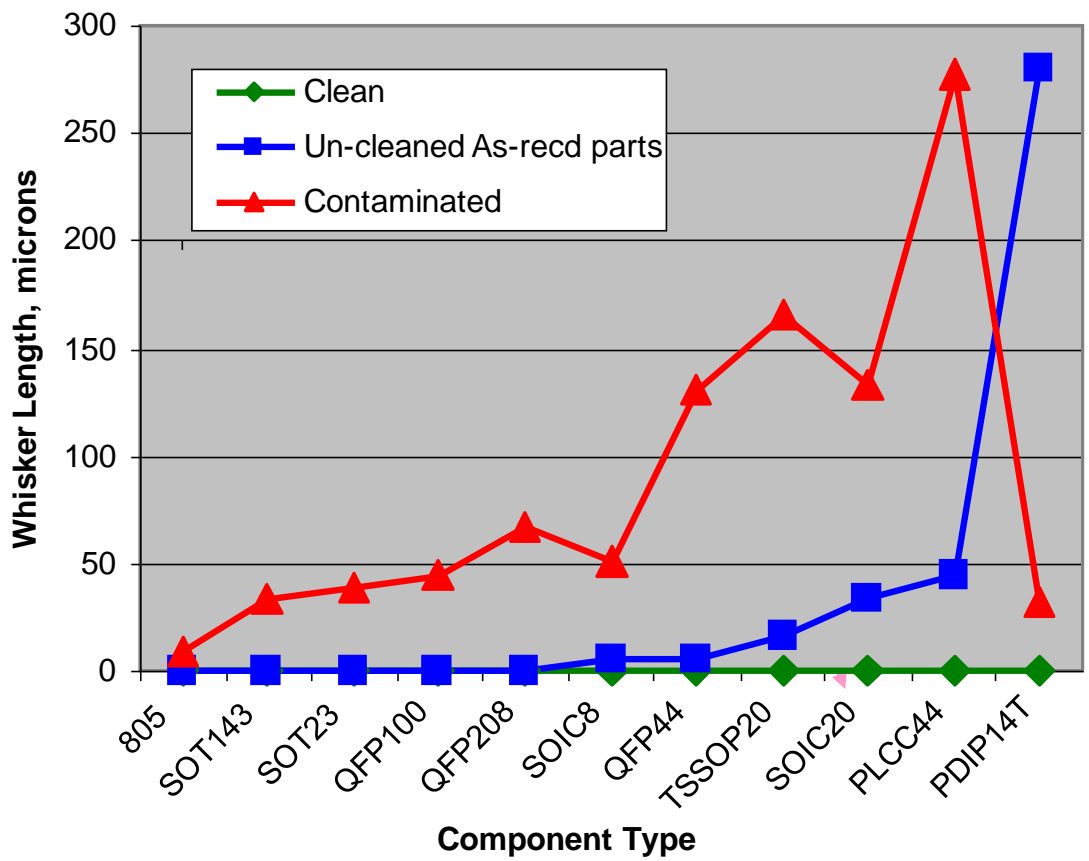


Figure 50: Maximum assembly whisker lengths after 500 h at 85°C/85%RH as a function of assembly cleanliness.

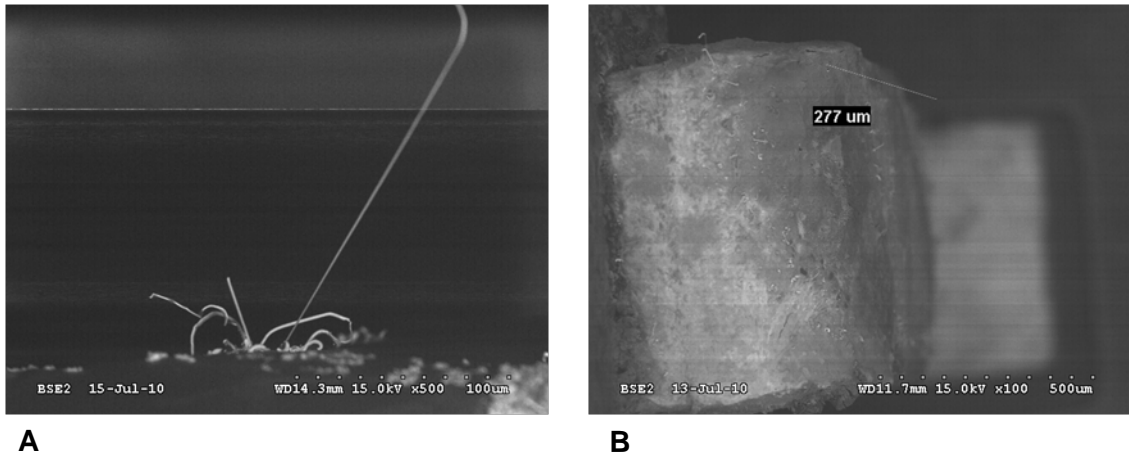


Figure 51: Micrographs of PIDP14T (A) and PLCC44 (B) after 500 h at 85°C/85%RH with 280 microns and 277 microns whiskers, respectively.

Table 7: Relationship between the as-received component contamination level and assembly whisker formation.

Sample ID	Total Inorganic anions ($\mu\text{g}/\text{cm}^2$)	Total Inorganic cations ($\mu\text{g}/\text{cm}^2$)	Total Inorganic Ions ($\mu\text{g}/\text{cm}^2$)	Whisker after 500 h 85C/85%RH
QFP208	0.95 (0.54 Cl ⁻)	0.40	1.35	Yes (Hillocks)
QFP44	1.81 (1.61 S O4 ²⁻)	1.86 (0.29 Na ⁺)	3.69	Yes (Whiskers)
QFP100	1.55 (1.27 NO ⁻³)	1.88 (0.51 Na ⁺)	3.22	Yes (Hillocks)
PLCC	0.23	1.27 (0.68 Na ⁺)	1.50	Yes (Whiskers)
SOIC8	3.61 (3.55 NO ⁻³)	0.70	4.31	Yes (Whiskers)
SOIC20	0.36	1.32 (0.68 Na ⁺)	1.67	Yes (Whiskers)
SOT23	0.53	0.31	0.84	No
SOT143	0.29	0.65	0.95	No
TSSOP20	0.26	0.25	0.51	No
0603	0.36	1.58 (0.53 Na ⁺)	1.95	No
0805	0.70	0.28	0.96	No
1206	0.14	1.16	1.32	No
PDIP14	1.38 (0.50 Cl ⁻ ; 0.39 SO4 ²⁻)	2.09 (0.85 Na ⁺)	3.63	Yes (Whiskers)

Whiskers were about five times longer in assemblies with additional contamination. The only exception was PDIP14T. The defects in Sn plating in this component were not repeatable from part to part. A trend of whisker length depending on component type was visible; QFP44, TSSOP20, SOIC20, and PLCC44 created longer whiskers than low-standoff SOT23 and SOT143 and discrete chip parts (0603, 0805, and 1206). There was no significant difference between components with similar standoff for alloy-42 (SOT23) and Cu-based alloy C7025 (SOT143) in terms of whisker formation.

Figure 52A separates the effect of component contamination and flux residues on whisker formation. Whiskers grew longer on intentionally contaminated components than on as-received components with a lower level of contamination in the assemblies without additional flux residue. Additional flux residue promoted whisker length up to 280 microns. Only data on no-clean ROL0 fluxes were included in Figure 52A.

There was no significant difference in whisker length with component ionic contamination type. Figure 52B demonstrated that 2 mM NaCl or 2 mM Na₂SO₄ promoted whisker growth to approximately the same length in a no-clean solder process.

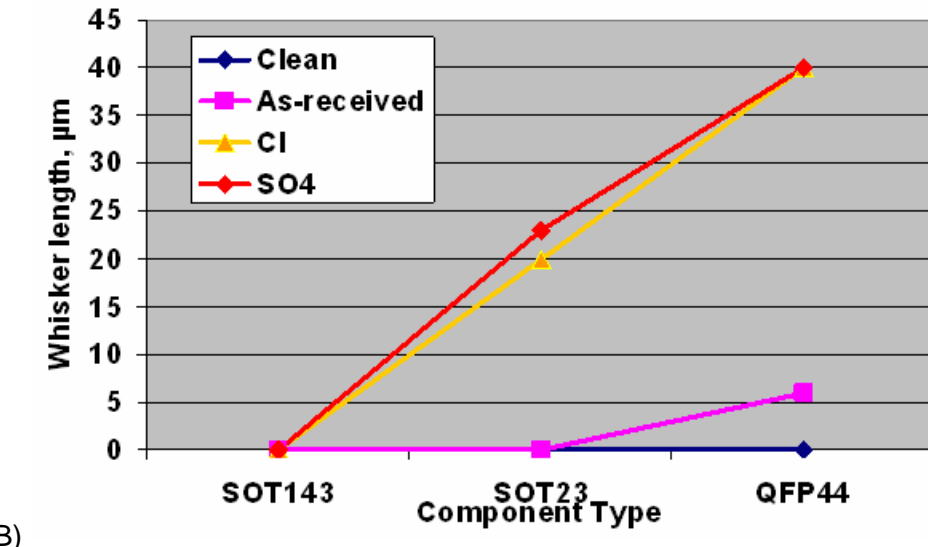
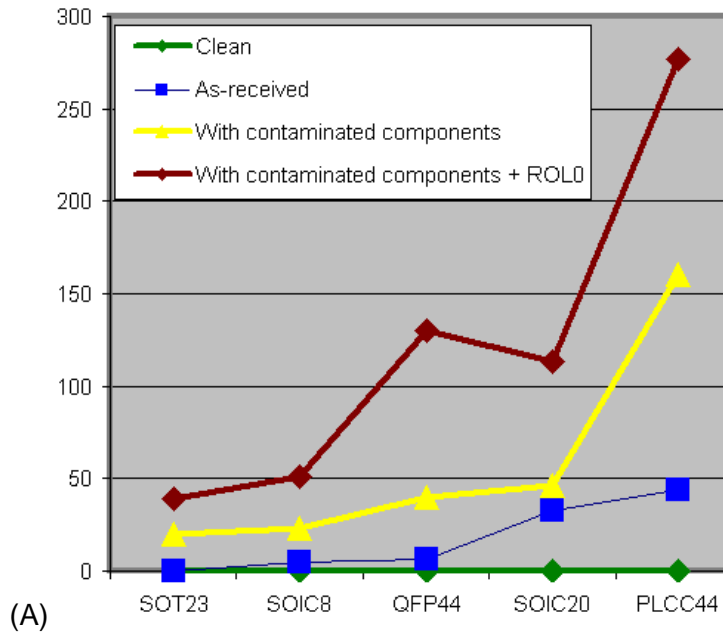


Figure 52: Maximum assembly whisker lengths after 500 h at 85°C/85%RH as a function of assembly cleanliness; (A) The effect of component contamination and flux residues on whisker formation and (B) showing no significant difference in whisker length between Cl and SO₄ ionic contamination.

Compared to assembled components, loose parts have a much lower propensity for whisker growth. Not only did clean loose components not form whiskers, but even contaminated components grew very short whiskers after 500 h at 85°C/85%RH (Figure 53). The longest whiskers were about 15 to 17 micron on components with Cu alloy lead frame materials and 23 micron on components with alloy-42. In the contaminated set of parts, five components out of 13 did not create whiskers, and hillocks shorter than 10 microns were found on two contaminated components after 500 h at 85°C/85%RH.

It has been historically assumed that the soldering reduces the whisker propensity of the Sn plated components. For Sn-Pb assemblies, it was confirmed experimentally [37] that fewer shorter whiskers grew on assembled components than on loose ones in high humidity conditions. This study showed that the situation is different for lead-free Sn-Ag-Cu solder alloys; SAC305 assemblies have a higher propensity for whisker formation than loose non-soldered components. Reflow using SAC305 solder does not mitigate whisker formation in a high temperature/high relative humidity environment. There are several possible explanations for this phenomenon. First of all, SAC alloys do not

contain Pb, which provides the strongest whisker mitigation capability. In contrast to Sn-Pb solder, SAC alloys may have a high ability to form whiskers because of microstructural characteristics that may trigger whisker formation in high humidity environments.

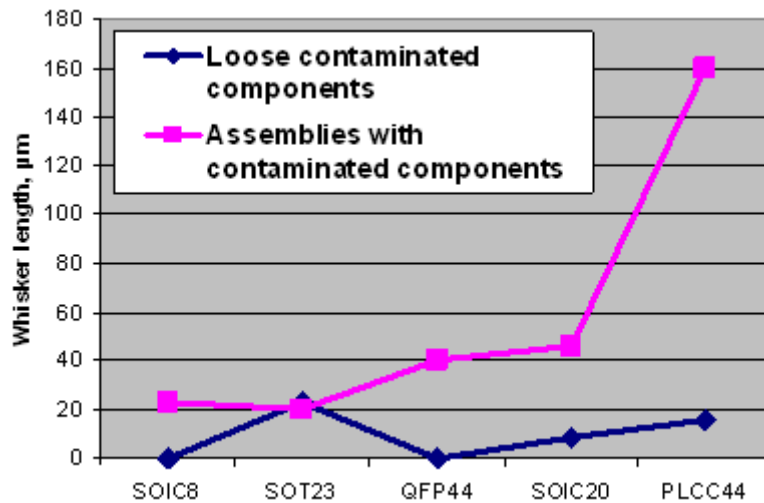


Figure 53: Loose and assembled components whisker lengths comparison after 500 h at 85°C/85%RH

5.3.2.2 1,500 h (500 + 1,000 h) inspection

The next whisker inspection was done after an additional 1,000 h of 85°C/85%RH exposure. A decision was made to increase the interval between inspections instead of using equal period of times, as it recommended by the JEDEC JESD201 standard. This was based on a previous Celestica study [86]. Martin Huehne found that the longest whiskers measured and photographed after the first 1,000 h inspection, stopped growing during the next 1,000 h interval and during subsequent inspections. Instead, new whiskers appeared. The new whiskers grew approximately as long as those previously observed after the same exposure interval (e.g. the whisker length observed after the zero to the 1,000 h interval was approximately the same as the 1,000 to 2,000 and the 2,000 to 3,000 h intervals).

Figure 54 shows a comparison of the longest whisker length between assemblies built using cleaned components and post assembly cleaning, assemblies with as-received components after a conventional no clean assembly process, and assemblies with contaminated components and additional flux residue. Whiskers longer than 10 microns, but shorter than 40 microns were detected on cleaned assemblies, except for the whiskers longer than 50 microns (64.6 microns) that were found only on highly defective PDIP14T joints. Longer whiskers were observed on assemblies with as-received components. The longest whiskers (up to 450 microns on PLCC and 300 microns on QFP208) were found on assemblies with contaminated components with the additional no clean ROL0 flux residue.

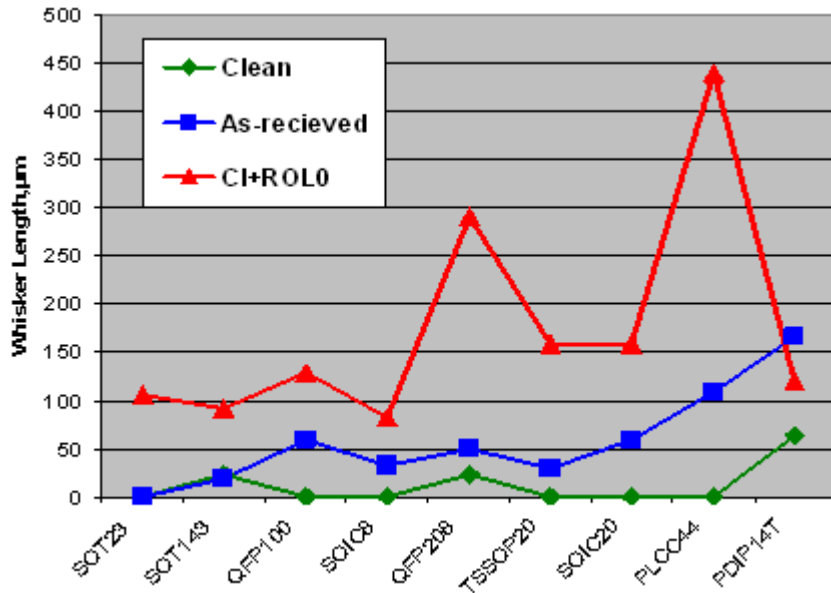


Figure 54: Maximum assembly whisker lengths after 1,500 h at 85°C/85%RH as a function of assembly cleanliness.

Detailed analysis showed that whiskers observed at 500 h did not grow further when examined at 1,500 h (500+1,000 h). In Figure 55, whiskers that appeared at 500 h are circled in pictures taken after 500 h and after an additional 1,000 h. The whiskers in the circles did not continue growing when the samples were placed in the chamber again. New whiskers grew (see arrows) when the samples were re-introduced into the high temperature/high humidity environment and inspected at 1,500 h. Thus, the whisker length depends on the time in chamber without interruption (Figure 56). This confirms the previous finding [86] and concludes that periodic removal and inspection of samples can result in under-reported whisker length as a function of time. An example of a whisker density increase with longer testing interval is shown in Figure 57. To report a proper whisker length dependence on high temperature/high humidity exposure time, one needs to increase intervals between successive examinations. Another alternative is to have enough samples and a means to remove them at each inspection point with a negligible change in environment (especially avoiding the SEM inspection vacuum exposure).

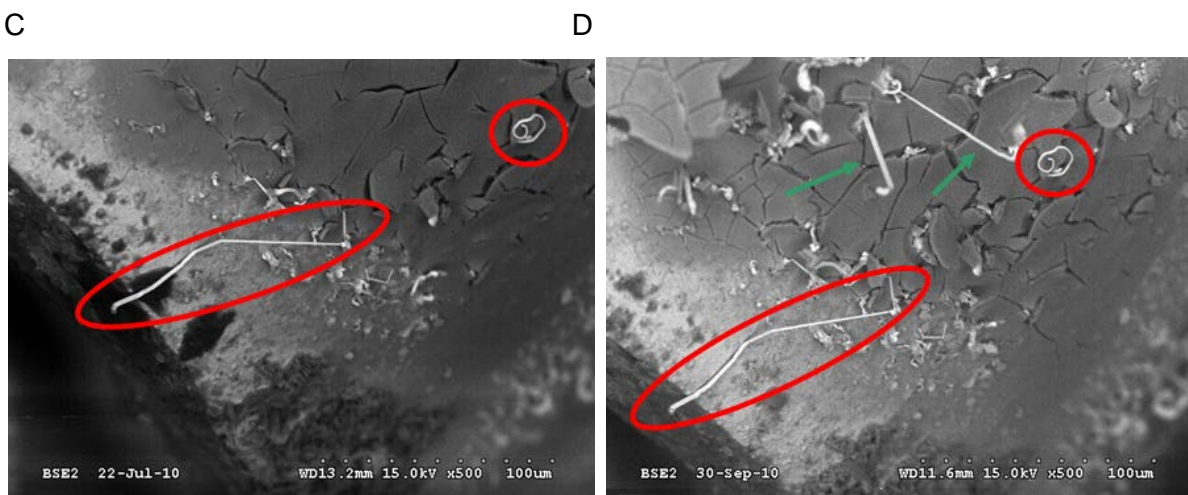
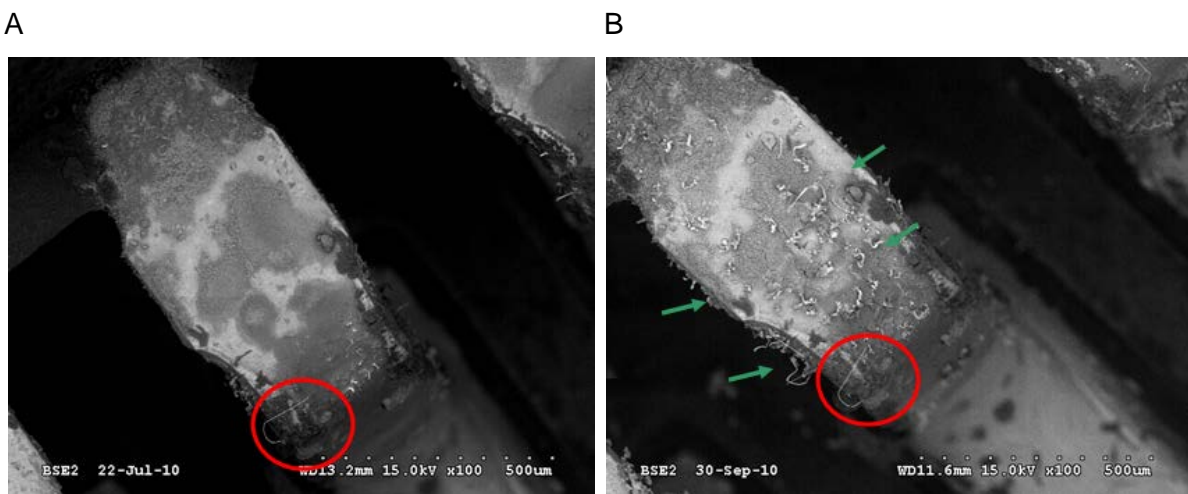


Figure 55: Assembly whisker images (A, C, E) after 500 h, and (B, D, F) 1,500 h at 85°C/85% RH. Circled whiskers appeared after 500 h and did not continue growing after additional 1,000 h. New whiskers formed during additional exposure are shown with arrows.

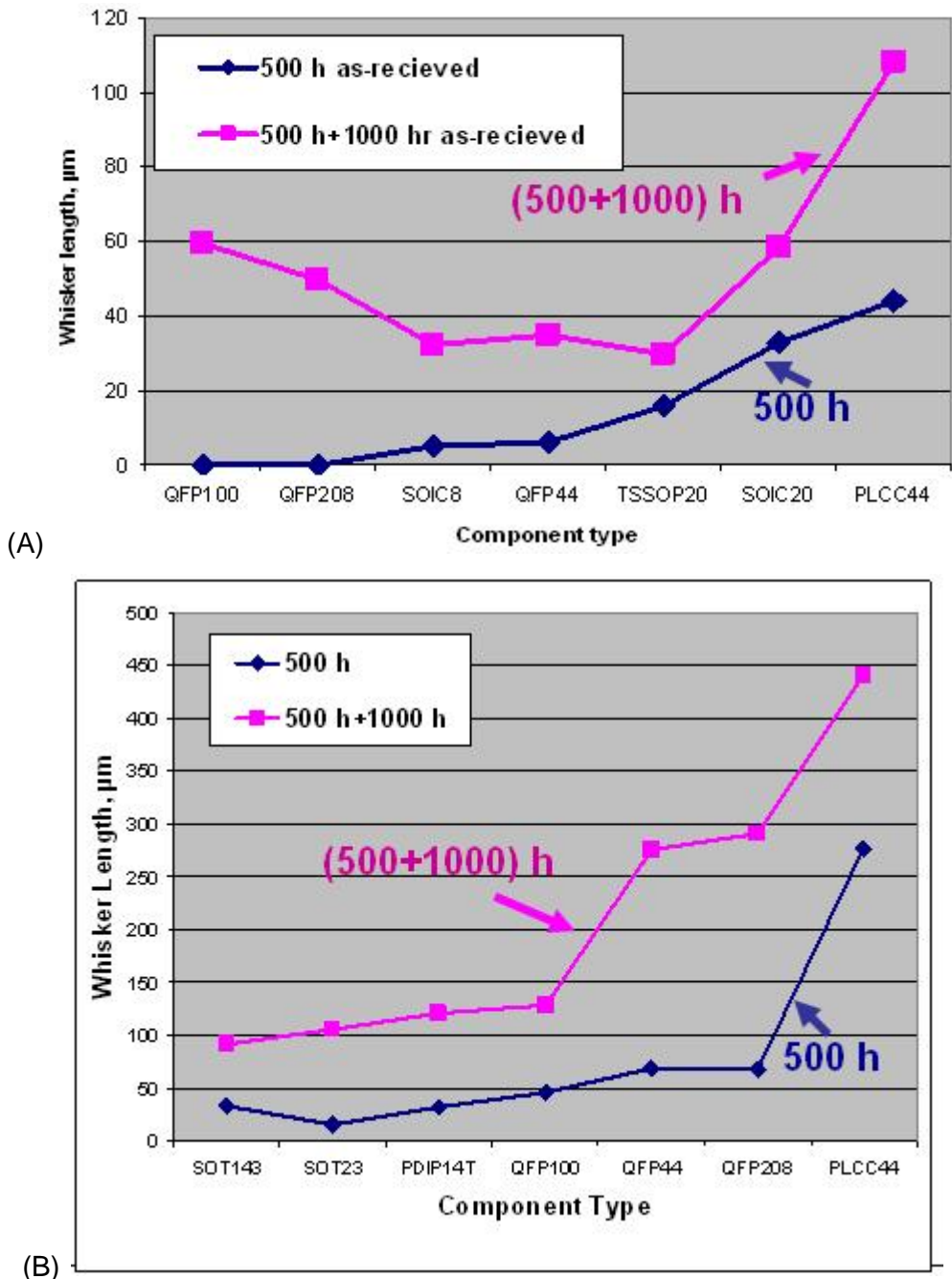


Figure 56: Maximum assembly whisker length comparison after 500 h and after additional 1,000 h at 85°C/85%RH for (A) as-received and (B) contaminated components in no-clean assemblies.

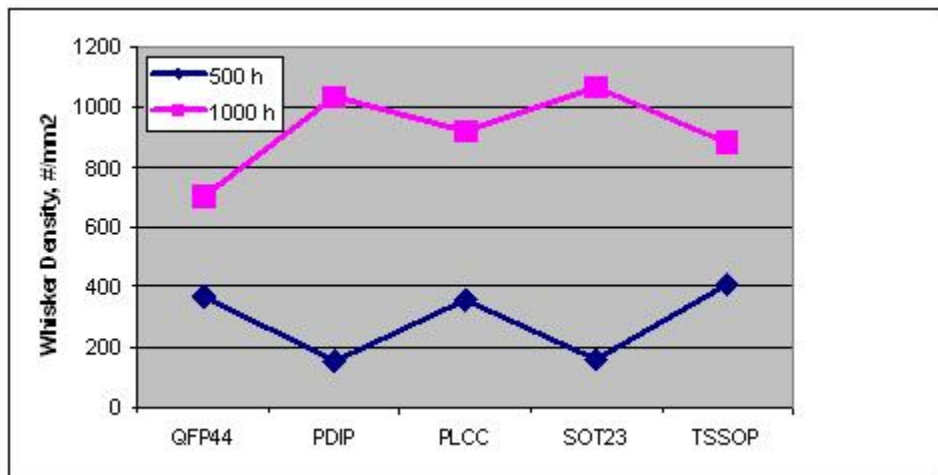


Figure 57: Whisker assembly density comparison after 500 h and additional 1,000 h at 85°C/85%RH

There were still no whiskers found on loose clean components after the additional 1,000 h (1,500 h total) in chamber, whereas whiskers longer than 10 microns and shorter than 40 microns were detected in cleaned assemblies. The only exception was a loose PIDP14T growing a 20 micron long whisker. In contrast, after soldering, the whisker length on the PIDP14T joint was more than 3x longer – 64.4 microns. The same comparison is valid for all type of components and level of contaminations – the whiskers on loose components with Cu alloy lead frame were shorter than those on assembled boards using SAC305 solder, which confirms the statement that lead-free soldering does not mitigate whisker formation. Actually, SAC305 soldering promotes whisker growth even if clean components are assembled on clean boards using post assembly cleaning process. For instance, the longest whisker on a loose QFP44 contaminated with Cl after 1,500 h at 85°C/85%RH was 23.6 microns. The same component assembled to PCB using SAC305 no-clean process grew a 105 micron whisker. Shorter whiskers after assembly than in the loose state were detected only on a SOT23 with alloy-42 lead frame material.

A typical example of whisker thickness distribution is shown in Figure 58. Three quarters (75%) of all whiskers were thinner than five microns. Among long whiskers, a typical thickness was in the range of 0.5 – 2.2 microns.

Similar to observations made after 500 h, there was no dependence on component type in the contamination influence on whisker length detected after additional 1,000 h at 85°C/85%RH (Figure 59). Surprisingly, no clean ROL0 resin rework flux promoted whisker formation as compared to ROL1 rosin rework flux residues (Figure 60). The trend to create more whiskers in no clean assembly compared to cleaned units was also observed by Oberndorff [37]. He cited the observation made in Japan that abietic acid promotes corrosion. Abietic acid is a main constituency of ROL0 flux used in this study to imitate a rework/hand soldering condition with partially activated flux residue (note the ROL0 flux residue is typically inert after the surface mount convection soldering thermal exposure).

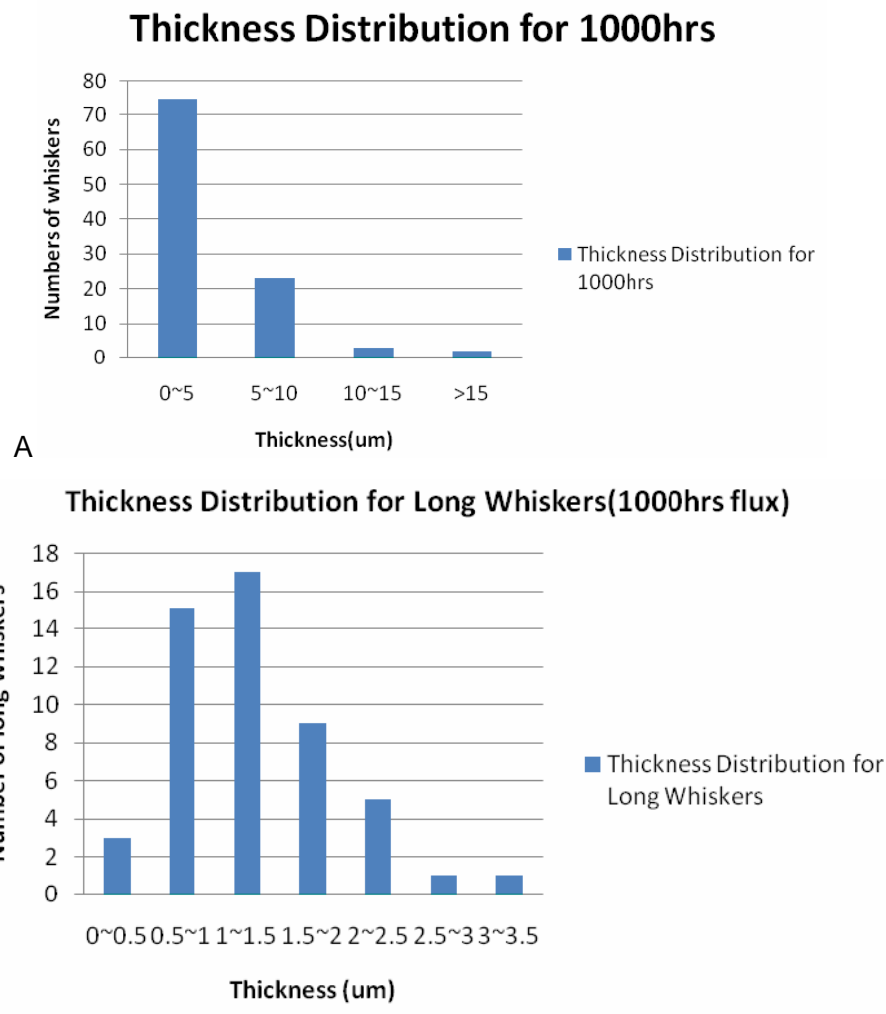


Figure 58: Assembly whisker thickness/diameter distribution; (A) thickness distribution after 1,000 h, and (B) thickness distribution for long whiskers (greater than 40 microns) after 1,000 h with flux.

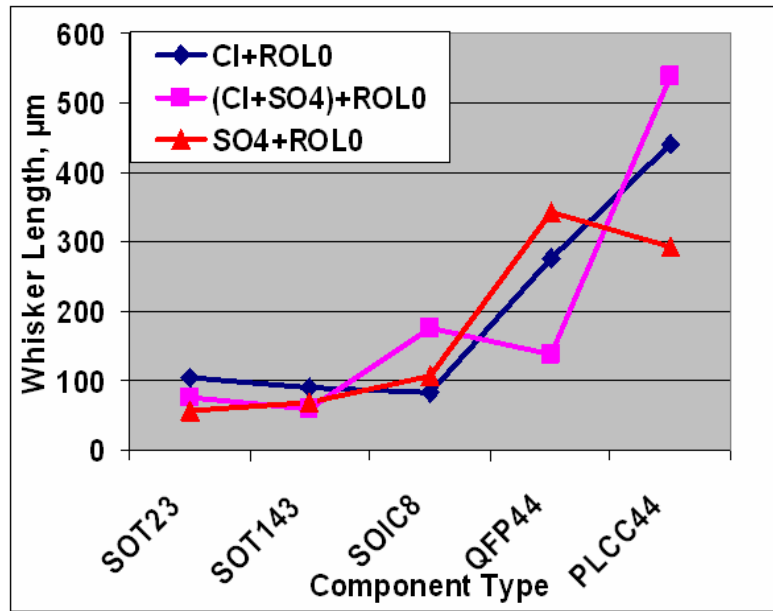


Figure 59: Maximum assembly whisker lengths after 1,500 h at 85°C/85%RH showing no significant difference in whisker length as a function of component contamination type.

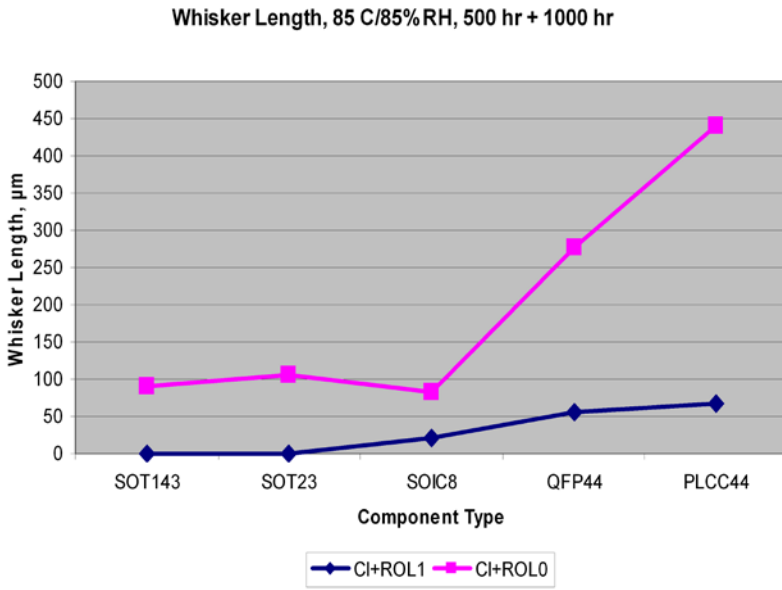


Figure 60: Maximum assembly whisker lengths after 1,500 h at 85°C/85%RH showing longer whiskers in assemblies with no-clean ROL0 resin flux residue compare to ROL1 rosin flux.

5.3.2.3 Metallographic examination

A typical solder joint of a leaded component is shown in Figure 61. Traditionally there are two zones in this type of joint: covered with thick solder and remaining thin Sn. In Sn-Pb solder joints, whiskers are associated with the thin Sn zone. In this study, a detailed analysis was performed on SAC305 solder joints. All 13 components were examined for solder coverage, ‘thin Sn’ microstructure, whisker locations, and the relationship between microstructure and whisker formation.

During component attachment to a printed circuit board (PCB) using SAC305 solder, solder melts and wets to the leads. Electroplated Sn also melts because the SAC soldering reflow temperature is above the Sn melting point (232°C). The resulting joint in comparison with a loose component is shown in Figure 61. The TTSOP20 loose and

assembled components after 500 h at 85°C/85%RH were used as an example. The thickness of the electroplated Sn on the loose TTSOP20 was 12 microns and was rather uniform across the lead (Figure 61A). After reflow the thickness of Sn and SAC solder coverage varies significantly. The solder wicked up the lead and mixed with the molten Sn. Surface tension dictated the thickness of the coverage, which was thin at the convex knee area and thicker at concave regions. The very top of the lead had solder coverage that extended to the component body that contained Ag₃Sn particles (Figure 61). The knee region was covered with an intermetallic layer about two microns thick with no Sn or small patches of the Sn (Figure 61). Although whiskers were found in all regions of solder joints including the solder fillet toe area (Figure 62), the longest whiskers grew from the top and sides of the leads (Figure 62B-D).

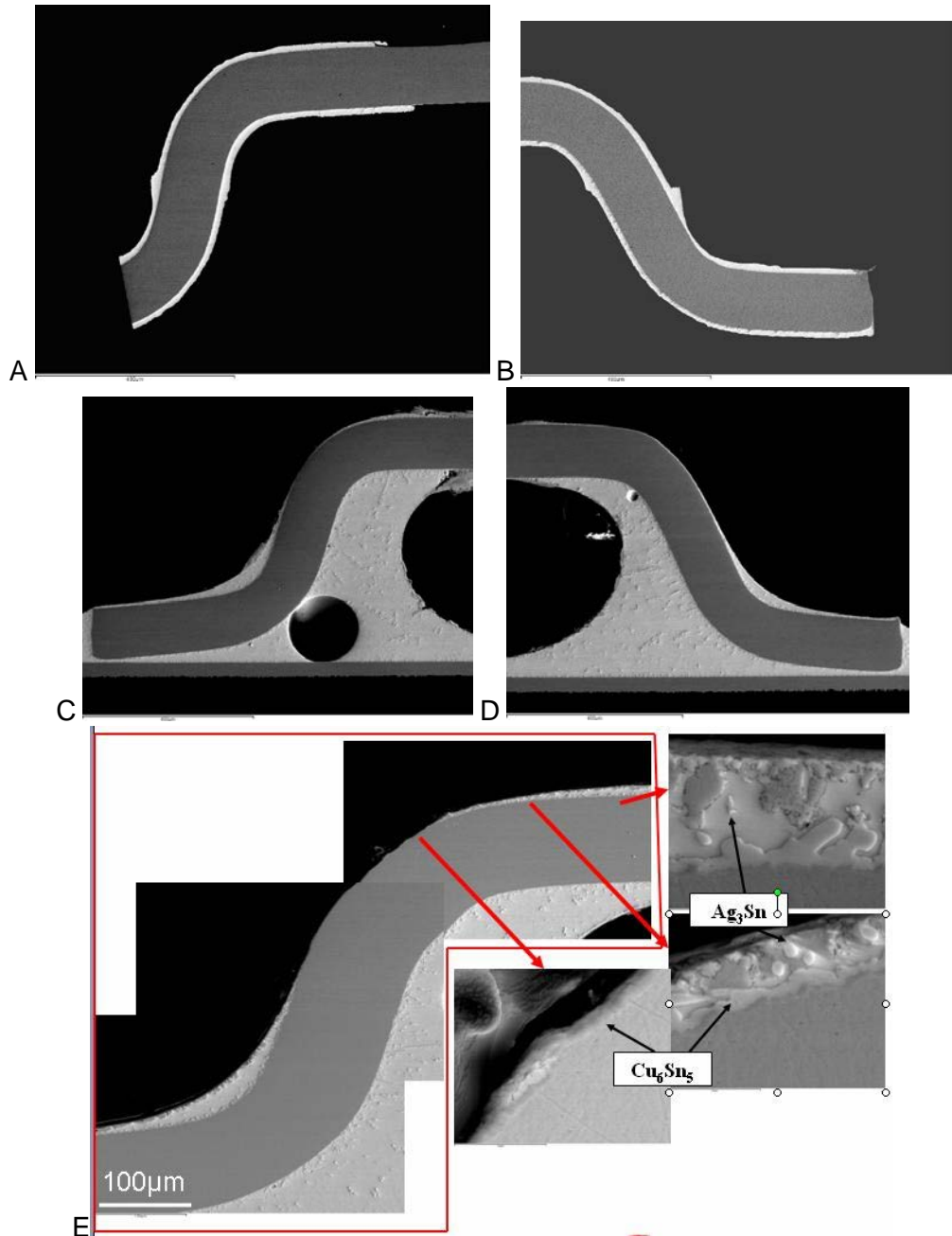


Figure 61: TTSOP20 (A, B) loose and (C, D, E) assembled component tin or solder coverage. Cross-sections after 500 at 85°C/85%RH were used as an example.

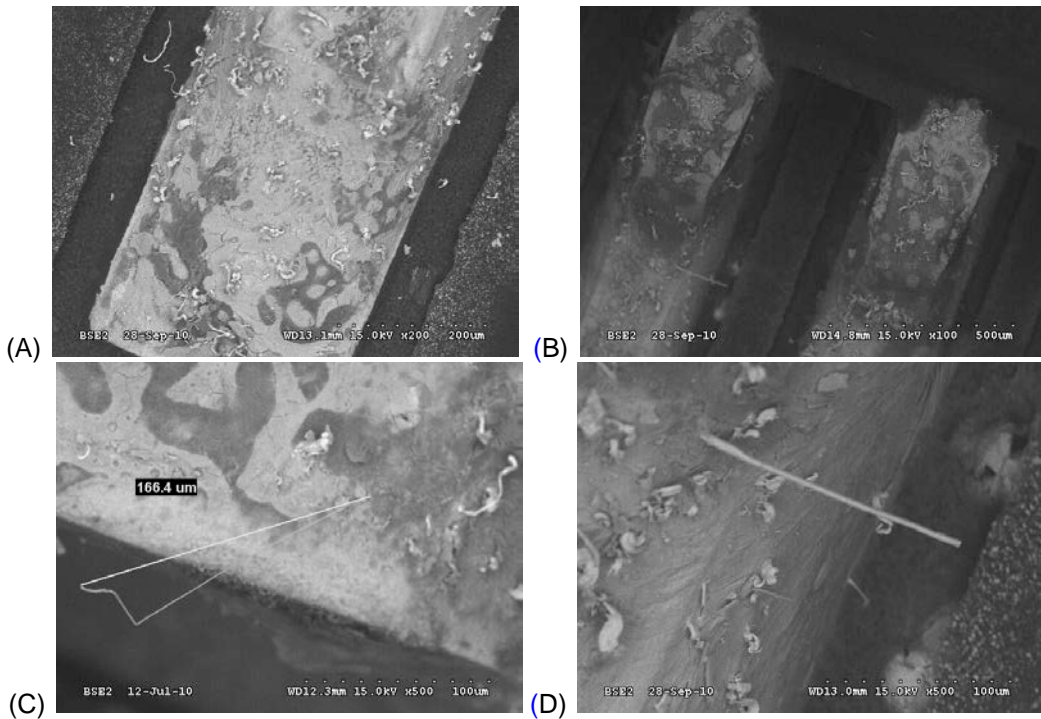


Figure 62: TTSOP20 assembly images illustrated whisker growth from solder fillet on (A) toe area and (B, C, D) from the top and sides of leads.

Figure 63 shows typical locations of long whiskers on low and high stand-off height components, PTH soldered leads, and discrete components. As a rule, the thickness of coverage in these locations is minimal and varies from 2.4 microns to 11.6 microns. In most joints, excluding only PDIP14T, the coverage contains some Ag_3Sn particles in the grain boundaries. The presence of the Ag_3Sn particles confirms that the Sn was melted and interacted with the SAC305 solder. The fraction of the particles varies significantly for different components and locations. Whiskers grow from the Sn grains surrounded by Ag_3Sn network.

The longest whiskers on PDIP14T were formed near the knee where the coverage looked like un-melted electroplated Sn. Because this component was attached to the PCB manually after reflow, it is possible the top part of leads in contact with the component body did not reach the Sn melting temperature (232°C). The intermetallic thickness in this layer was 1.0-micron, which was about two to three times thinner than in the rest of the components with Cu alloy lead frames.

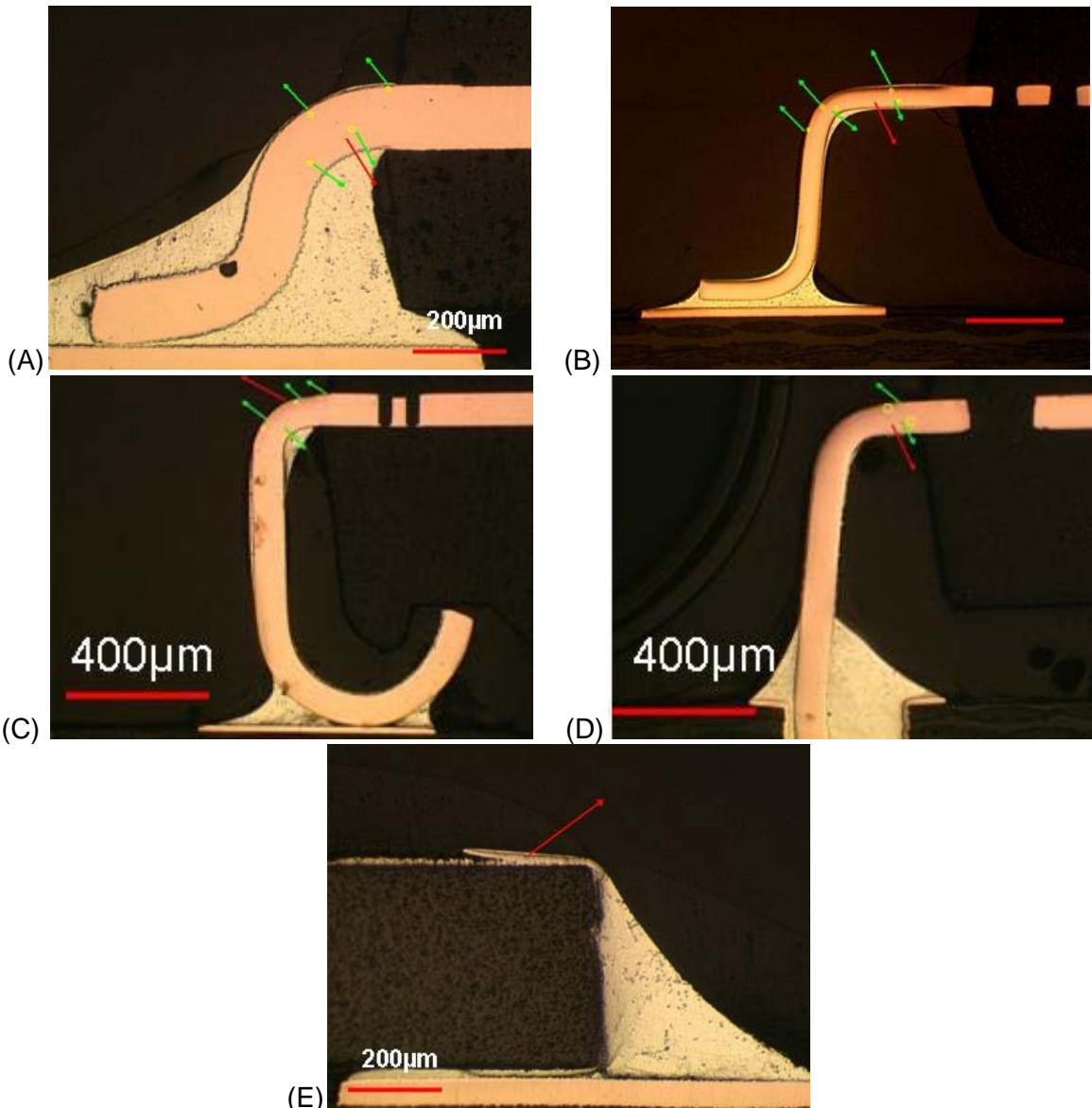


Figure 63: Typical locations of long whiskers on low and high stand-off height components, PTH soldered leads, and discrete components; red arrows – longest whiskers, green arrows – shorter whiskers, yellow circles – hillocks; (A) SOT, (B) QFP, (C) PLCC, (D) PDIP, and (E) chip resistor.

5.4 Summary

The experiment evaluated 72 SAC305 soldered assemblies and numerous unpopulated piece parts having various rework fluxes and ionic contamination types exposed to 85 °C/85 %RH. The following observations were made:

Results: Microstructural considerations

Factors increasing whisker propensity are:

- Thin regions of lead-free solder in the fillet regions
- Rough solder surface that tends to trap contamination
- Interdendritic corrosion sites between the primary tin grains of the lead-free solder
- Corrosion around Ag₃Sn intermetallic on the surface
- Non-uniform oxidation

Results: Part and cleanliness considerations

- As-received part lead defects were found that can result in increased whisker propensity in SAC soldered assemblies
 - Thin Sn plating; Sn plating thickness varied from 2 to 25 μm
 - Rough tin plating surface with deep grooves, voids, plating skips, exposed base metal especially near the lead-to-package interface, and protrusions of base metal into plating.
- Lead-free soldering **does not** mitigate whisker formation
 - The whiskers on loose, unassembled Cu alloy lead frame components were shorter than Cu alloy lead frame components on boards assembled using SAC305 solder
- Clean assemblies had significantly reduced whisker propensity
- Cl^- , SO_4^{2-} , NO_3^- , and Br^- are some of the ionic contaminants that promoted whisker growth
 - Evaluation included contamination consistent with real-world production components
 - High part contamination levels prior to soldering increased whisker propensity even if the assembly was cleaned after soldering
- Some rework flux contaminated components created very long whiskers in a short time
 - The tested low activity rework flux (ROL0) residues had a high whisker propensity
 - The tested mildly activated rosin fluxes (RMA) residues had low whisker propensity
- Cl^- is a good baseline to use for whisker growth testing

Results: Testing considerations

- Periodic sample removal and whisker SEM inspection results in under-reported whisker length as a function of time in 85°C/85%RH exposure
- Interval between successive examinations needs to be increased to report a proper length-time dependency

Outputs applied to the primary experiment:

- A NaCl salt solution was selected as intentional contamination material
- Progressively increasing inspection interval times were used during environmental exposure to ensure proper recording of whisker length versus time
- The PLCC20 was included in the QFP board design because it contained a high number of lead finish defects and the portion of the lead under the body is not typically conformal coated

In conclusion, lead-free solder does grow tin whiskers, particularly where it is less than 25 microns thick. Assembly contamination is an important consideration for whisker growth in harsh service environments. Sources of contamination that should be considered for high reliability systems in harsh service are: as-received part cleanliness, rework flux residues, ionic contamination in service (e.g. salt fog and sulfur compounds). In addition, the inherent roughness of lead-free solder joints tended to trap contamination. Interruption of high humidity conditions can interrupt whisker growth.

6. Screening experiment 2: Microstructure and whisker growth of SAC solder alloys with rare earth additions in different environments

6.1 Approach

It has been found that the addition of a small amount of a REE, such as Y, La, Ce, Er or Nd, to a lead-free solder such as SAC305 and SAC105 can improve its resistance to failure under shock loading. Unfortunately, the addition of a rare earth can also lead to tin whisker growth [19] [20].

The screening experiments were done to evaluate the addition of REE to SAC105 on the solder microstructure and Sn whisker growth. The rare earth elements chosen for this study were Y, La and Ce.

6.2 Methods and materials

Due to the relatively high melting points of the REE additions, the initial samples were prepared in a vacuum arc furnace. The samples each contained approximately one weight percent REE, which were subsequently diluted with SAC105 solder alloy to 0.5 and 0.15 weight percent REE. The resulting alloy samples were melted in an alumina crucible on a laboratory hot plate. From each melt, a portion was sucked into a length of 2 mm diameter Pyrex™ tubing, to obtain samples in the form of wires, from which small pieces could be cut for differential scanning calorimeter (DSC) studies and for reaction with a copper substrate to simulate a solder joint on copper.

Samples were made by placing a small piece of the alloy containing REE addition in a depression in a piece of copper substrate, along with some flux. This assembly was then heated to 240 °C and held at temperature so that the total time above the melting point was approximately one minute.

The resulting samples, as well as bulk samples of the solder alloys, were mounted in epoxy for metallographic examination. The samples were ground on a series of successively finer silicon carbide papers, then polished with six-micron diamond and finished with colloidal silica.

Polished samples were aged for various lengths of time under three different conditions. Some were aged in air under ambient conditions; some were aged in nitrogen; and some were aged under conditions of relatively high temperature and high humidity. All were examined for whisker formation.

6.3 Results and discussion

As shown by the binary phase diagrams with Sn (Figure 64), the REEs Y, La and Ce are all nearly insoluble in the solid state in Sn. As a result, the REEs form intermetallic compounds, such as CeSn₃, with Sn. The REEs also form ternary compound phases, of the form R₃Cu₄Sn₄, when other elements, such as copper, are present. Consequently, the REEs were present in the form of compound phases in samples of SAC solder to which the REEs were added. An example is shown in Figure 65A, in a sample that contained Ce. The phase shown was identified by EDX analysis to be CeSn₃.

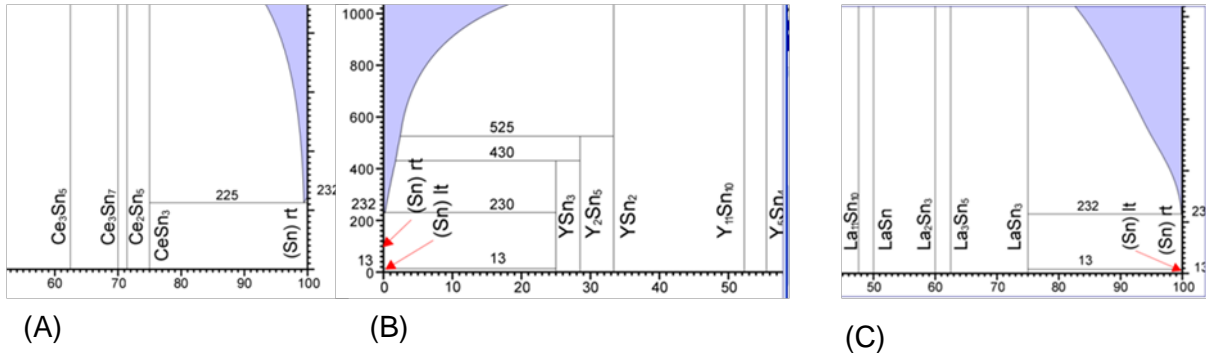


Figure 64: REE-Sn phase diagrams; (A) Ce-Sn, (B) Y-Sn and (C) La-Sn (Note: Sn rich side of the phase diagrams are shown.)

It is well known that the REEs are extremely reactive materials. Therefore, it is important to determine how the REEs might react when exposed to various atmospheres during aging of SAC+REE solder samples. An example of a sample that contained Ce is illustrated in Figure 65, after aging under ambient conditions for several days in air. Clearly, the original CeSn_3 compound phase has undergone a reaction. It was found that the original CeSn_3 phase had reacted with the atmosphere to form an oxide at the boundary between the CeSn_3 IMC and the primary Sn phase and tin nodules. A reaction of this type was observed for samples containing each of the rare earth elements tested, under all aging conditions. The result was the formation of Sn whiskers. The development of microstructure and its relationship to whisker formation is shown in detail in the following sections.

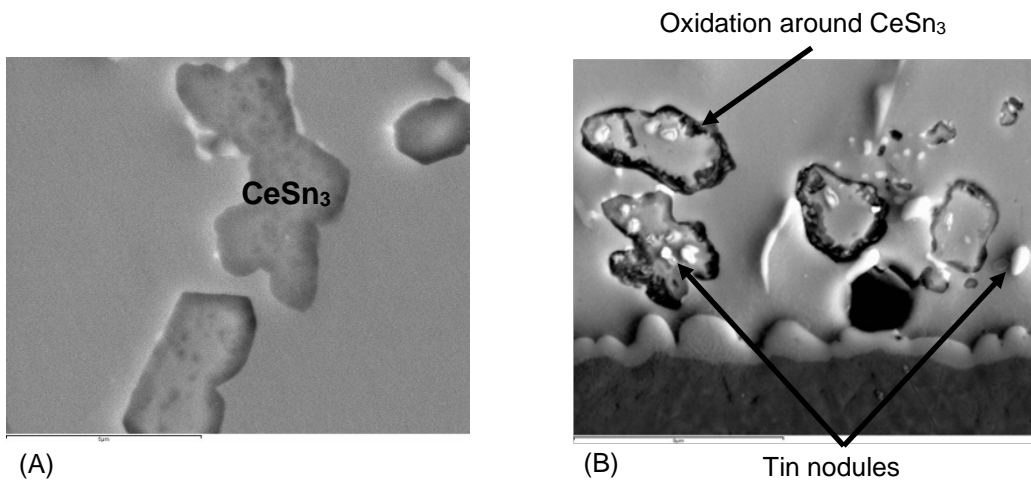


Figure 65: CeSn_3 particles in SAC105 solder; (A) fresh after polishing and (B) exposed to air for several days.

6.3.1 Microstructure formed during solidification

As noted earlier, the REEs are nearly insoluble in Sn so that, even when present in a small amount, REEs form an intermetallic compound with Sn. An example of the resulting microstructure, in this case formed by the addition of 0.5% Y to SAC 105 solder is shown in Figure 66. Note that a freshly polished sample is shown in this photomicrograph. It was seen that, in addition to the usual Cu_6Sn_5 and Ag_3Sn phases of this alloy, YSn_3 also appears. The YSn_3 tends to appear in the last liquid to freeze, as well as at the surface. Cross sections also showed a sample in which a ternary compound phase of the form $\text{Y}_x\text{Cu}_y\text{Sn}_z$ YSn_3 also appears. The nature of the eutectic Cu_6Sn_5 and Ag_3Sn phases in the solder alloy is illustrated in Figure 67. Ce and La additions to SAC 105 solder form compound phases similar to those produced by Y additions.

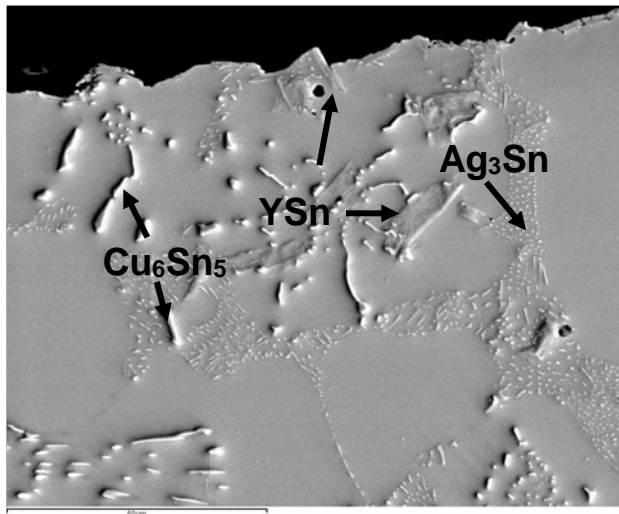


Figure 66: Microstructure of SAC105 + 0.5Y

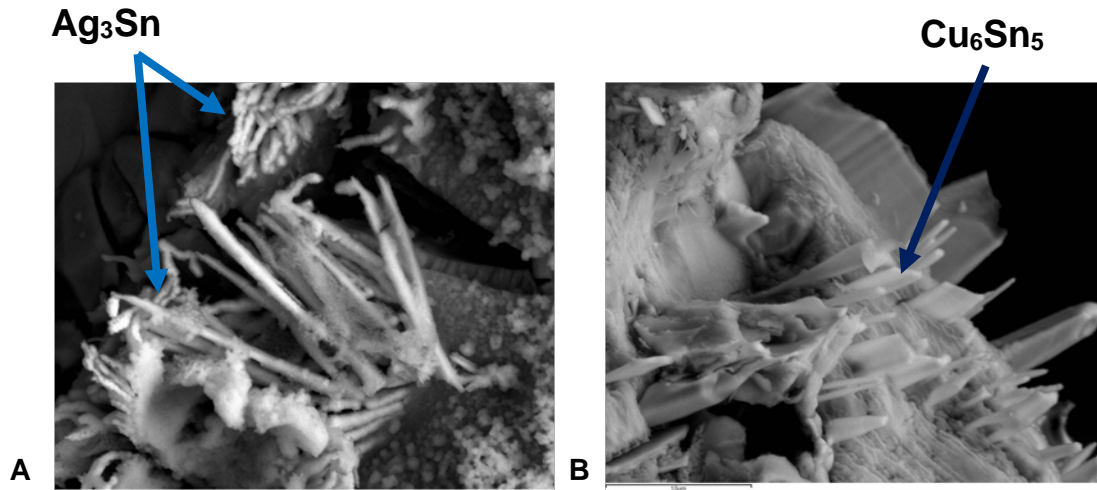


Figure 67: Examples of morphology of eutectic intermetallics; (A) Ag_3Sn and B Cu_6Sn_5 . Note that the IMC images were obtained by etching the Sn away.

6.3.2 Interaction of phases present with atmosphere

In general, the phases present in SAC105 solder alloy do not react with the atmosphere or with the fluxes to which they are normally exposed. However, the REEs are considerably more reactive than Ag, Cu, or Sn. Consequently, there exists the possibility that the REE may leave the intermetallic compound in which it was formed to produce a more stable compound. As illustrated in Figure 68, this occurs in the present case by interaction with the ambient atmosphere to form an oxide.

Interaction with an industrial flux can also occur, forming a compound with the REE. Since the oxides/chlorides formed in this way have a larger volume than the Sn-RE compound phase that was replaced, a compressive stress is introduced in the Sn region in which the REE oxides/chlorides have formed, thereby providing the essential factor required for whisker growth.

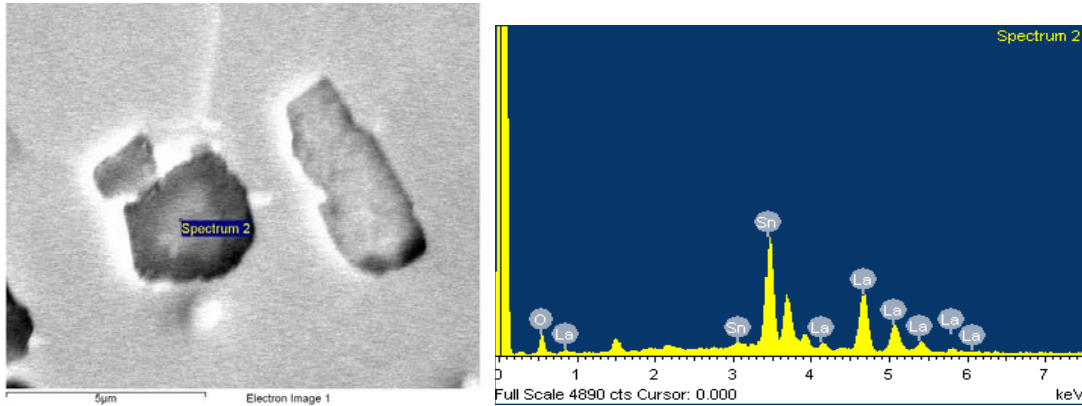


Figure 68: Microstructure and composition of LaSn_3 in SAC105 +0.5La after ambient atmosphere exposure.

6.3.3 Growth of whiskers

As noted in the preceding section, the formation of a REE oxide by reaction of a REE element, even in compound form with Sn, provides the essential factor, the presence of compressive stress, for the formation of Sn whiskers. It remained to be determined whether whisker growth would actually occur or not.

To investigate whisker growth, a series of samples were subjected to various atmospheres and then inspected for whisker growth. Table 8 presents results from the first sample set and Table 9 shows the results for a second sample set with shorter exposure times in all three atmospheres.

Whiskers were indeed found, growing from tin in the solder joints made using SAC 105 solder with added REE. Whiskers were also seen on solder joints growing from the RESn intermetallics.

Table 8: Experimental summary and results on first set of REE samples.

Samples	Ambient 8,400 h	Whisker Growth				Nitrogen Chamber after 85°C/85%RH	
		Nitrogen storage cabinet		85°C/85%RH			
		2,900 h	4,660 h	500 h	1,000 h		
SAC105+Ce, La, Y joints on Cu, ORH1				8μm	39μm	+	
SAC105+Ce, La, Y joints on Cu, INH1				None	20μm	+	
Directionally solidified SAC105+Y				+	+	244 μm	
Pieces of bulk SAC105+Ce, La, Y	20μm			+	+	+	
Cross-sections of SAC105+Ce, La, Y joints on Cu, ORH1		180μm	130μm				
Cross-sections of bulk SAC105+Ce, La, Y		271 μm(Ce)	250μm (La)				

Note: Blank cells indicates conditions that were not tested and + indicates there were some short (<10 microns) whiskers or hillocks. The nitrogen cross-section storage cabinet atmosphere oxygen concentration was 4.3 to 6.5% O_2 .

Table 9: Experimental results on second set of samples with shorter exposure time.

Samples	Whisker Growth										
	Ambient, h				Nitrogen storage cabinet, h				85°C/85%RH h		
	380	1130	1730	2210	380	1130	1730	2210	120	240	720
SAC105+Ce joints on Cu	None	None	95µm	95 µm	None	None	None	None	None	None	None
SAC105+ La, joints on Cu	None	None	None	+	None	None	None	None	None	None	None
HC, Cross-sections of SAC105+Ce, joints on Cu	None	None	None	+	None	None	None	None	None	None	11.5 µm
HC, Cross-sections of SAC105+La joints on Cu,	None	None	None	+	None	None	None	None	None	None	+
Cross-sections of bulk SAC105+Ce	None	None	None	+	None	None	None	97 µm	Not tested		
Cross-sections of bulk SAC105+ La	37µm	Not inspected			None	90µm	136µm	33.7 µm	Not tested		

Note: Cells with a + indicates there were some short (<10 microns) whiskers or hillocks. The nitrogen cross-section storage cabinet atmosphere oxygen concentration was 4.3 to 6.5% O₂.

As would be expected from the compressive stress requirement, the growth of whiskers depends on oxidation and/or corrosion of RESn IMCs that segregated to the sample surface (Figure 69), since the surface IMCs have access to oxygen and/or ions from the environment. From a practical perspective, during electronic assembly service environments of thermal cycling, shock and vibration solder fatigue cracks would eventually form, which would expose interior RESn IMC regions creating new whisker prone areas with time.



Figure 69: Segregation of RESn intermetallic particles on solder surface. Black arrows show the RESn IMC regions and the red arrow indicates a whisker.

Slow oxidation seems to promote longer straighter whiskers. Whiskers growing from solder joint cross sections after aging in nitrogen are shown in Figure 70. Note the amount of the darker LaSn₃ phase in this region. There is one whisker growing from the tin between the LaSn₃ and the Cu₆Sn₅ IMC near the copper substrate and one growing from the LaSn₃ IMC. Small diameter fine whiskers were observed growing from the RESn IMC (Figure 71). In addition, recrystallization of the primary tin and growth of an entire grain were observed (Figure 72).

For comparison, in the primary experiment, examination of SAC105 balls after PCTC +50 to +85°C cycling and HTHH 85°C/85%RH exposure showed that balls without REE additions did not grow whiskers, while those with REE did.

Overall, out of the 61 samples were tested, 29 of them grew whiskers (Figure 73). The longest whiskers were detected after slow oxidation in the nitrogen chamber. From the photomicrographs it is clear that the presence of REE in the SAC 105 solder results in the formation of whiskers during aging in a variety of environments. It is also clear that this is the result of the extreme reactivity of the REE. It may be concluded that the addition of REE to SAC solder presents the risk of device failure due to short circuiting by Sn whiskers.

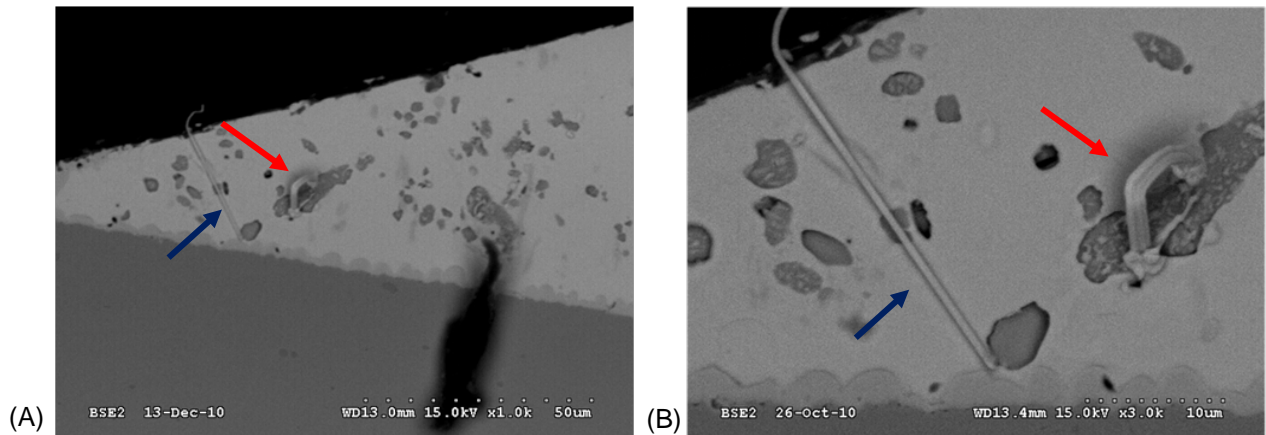


Figure 70: Whisker growing from cross-section of a solder joint of SAC105 +0.5La; (A) Overall and (B) high magnification SEM image. The blue arrow shows a whisker growing from the tin between the La_3Sn IMC above and the Cu_6Sn_5 on the substrate below. The red arrow shows a whisker growing from the LaSn_3 IMC. The dark material in (A) is debris on the section.

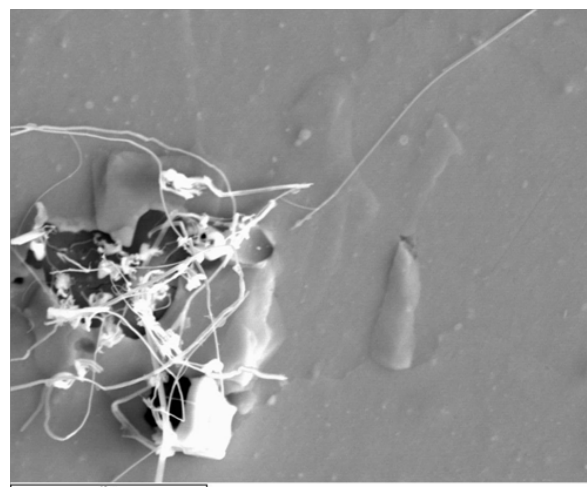


Figure 71: Thin whiskers growing from La_3Sn IMC in a bulk SAC105+0.5La cross-section held at room ambient conditions for 3,050 h.

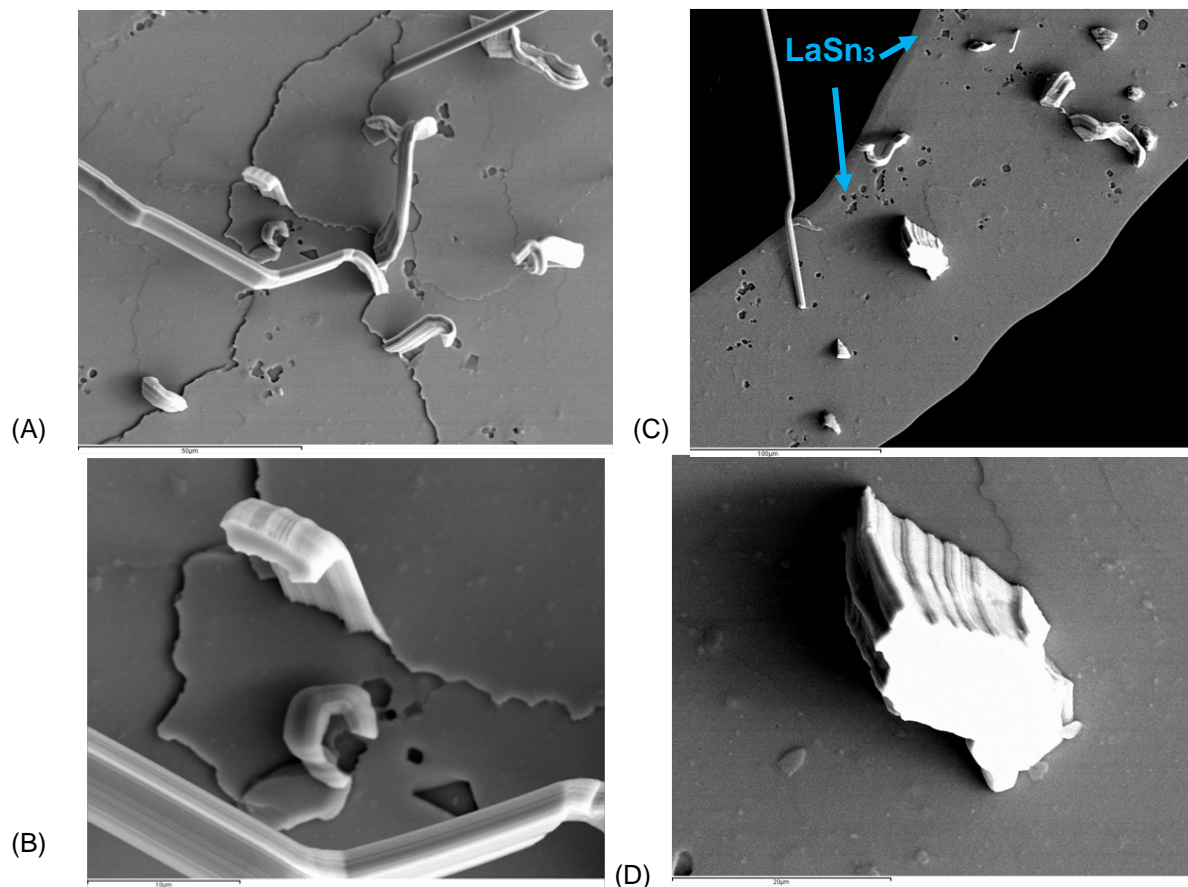


Figure 72: Whiskers growing from a cross-section of bulk SAC105+0.5La after 2,690 h of nitrogen cabinet storage; (A and B) Re-crystallization: Whisker growth from tin dendrite grain boundaries which indicates new grain nucleation (C and D) Entire grain growing: Typical hillock-whisker growth.

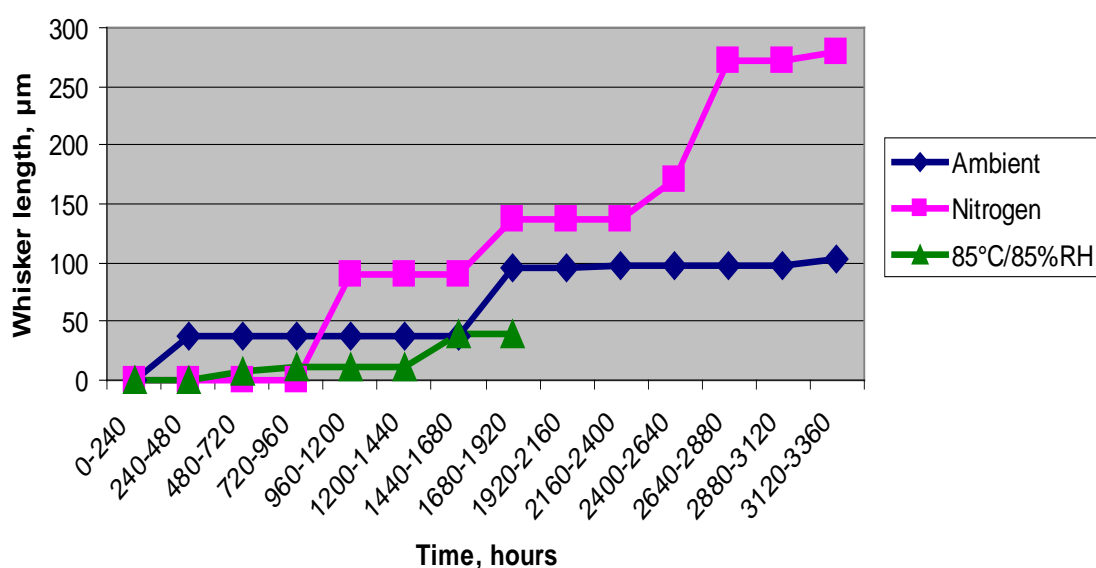


Figure 73: Whisker length after different environmental exposure.

6.3.4 REE in SAC whisker formation theory

It is theorized that tin whisker growth arising from solders doped with REEs are due to relatively rapid oxidation of the RESn intermetallic compounds. The manner in which RESn compound oxidation contributes to whisker growth is (1) liberation of Sn and (2) development of compressive stress by the RE oxide (Figure 74).

Since REEs are less noble than Sn, thus RE in RESn_3 is more prone to oxidation, which results in rapid oxidation of YSn_3 , LaSn_3 , and CeSn_3 . In addition, the surface active nature of REEs, results in a condition where RESn intermetallic tends to segregate to the surface giving it improved access to oxygen. The RESn IMC oxidation in the present work has been observed to start from the outer part RESn IMC adjacent to the solder and propagates inward. As the RE in the RESn intermetallic forms $\text{RE}_{\text{x}}\text{O}_{\text{y}}$ compounds, Sn is liberated, becoming available to form whiskers.

Also, contributing to compressive stress is the fact that REE oxidation product has greater volume than the original intermetallic. La_2O_3 (16.2%) and CeO_2 (12.3%) volumes are larger than the original intermetallic [87]. Thus with excess tin and compressive stress whiskers can readily form.

In addition, corrosion has also been observed in SAC+REE system with an industrial Zinc Chloride flux. In a similar process to the oxidation, the corrosion products of both RE and Sn have greater volume than the original intermetallic and it results in compressive stress promoting whisker growth.

The long whisker growth in nitrogen suggests the possibility that slower oxidation rate due to the lower oxygen concentration resulted in a slower strain rate that may be more favorable to whisker formation.

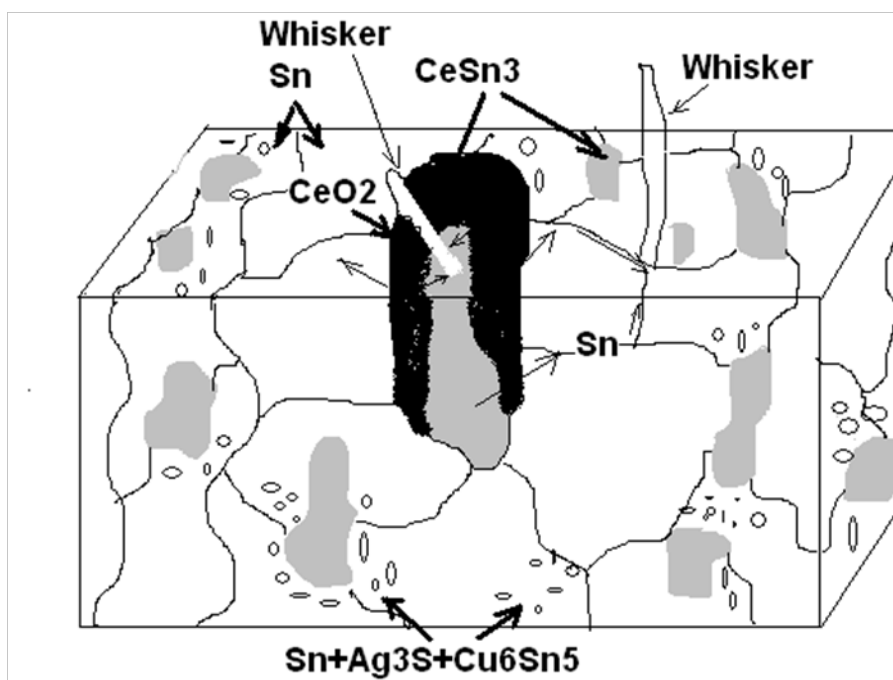


Figure 74: Schematic illustrating whisker growth of SAC with REE. For example, the oxidation of surface CeSn_3 IMC edges formed CeO_2 . The CeO_2 causes compressive stress due an increase in volume. In addition, Sn is liberated and becomes available for whisker growth. The whiskers can grow inside the CeSn_3 IMC and in the adjacent solder.

6.4 Summary

The following observations were made:

- Whiskers were observed on SAC105 doped with REE (Ce, La and Y), both on solder joints formed on copper and on free standing bulk solder samples
 - The whiskers formed after exposure to room temperature ambient conditions, 85°C/85%RH and in a room temperature nitrogen atmosphere (cross-section storage cabinet atmosphere (4.3 to 6.5% O₂))
 - The whisker growth was *not* limited to thin solder regions
- Tin whiskers were observed from RESn₃ intermetallic regions (CeSn₃, LaSn₃, and YSn₃) presumably during the early stages of oxidation and from solder some distance from oxidized RESn₃ intermetallic
- The accumulation of RESn₃ accumulation on the surface was independent of REE type or concentration
- The manner in which RESn compound oxidation contributes to whisker growth is (1) liberation of Sn and (2) development of compressive stress from the RE oxide
- Corrosion was also observed in SAC+REE system with an industrial Zinc Chloride flux; The corrosion product also had greater volume than the original intermetallic and would result in compressive stress that promotes whisker growth
- Ce doped SAC105 solder joints and bulk solder have shorter incubation period and longer whiskers than SAC105 with La
- Y doped SAC105 solder joints and bulk solder have a lower propensity of whisker formation than SAC105 with Ce or La which may be explained by ternary Y-Cu-Sn intermetallic formation having higher oxidation resistance
- The longest whiskers grow under slow oxidation conditions and from samples with additionally (mechanically) induced stress
- From a practical perspective, during electronic assembly service environments of thermal cycling, shock and vibration solder fatigue cracks would eventually form, which would expose interior RESn IMC regions creating new whisker prone areas with time

7. Primary experiments: Methods, materials, experiment design and assembly

7.1 Approach

Systematic tin whisker testing was performed to evaluate the key manufacturing and environmental variable combinations hypothesized to contribute to whisker growth. One of the challenges accompanying real electronic systems is understanding the details associated with the components, product design, manufacturing process, and service environments that contribute directly or conspire with one another to exacerbate whisker growth. In addition to executing relatively short duration whisker growth tests; this phase of testing included long term whisker growth to help quantify the overall long term DoD system risk. It is recognized that whiskers grow at a stress “sweet spot” which is a function of grain size, strain rate, and temperature [21][22]. The primary test utilizes a range of contamination, lead material, temperature cycling range and humidity levels in order to create a broad range of tin stress conditions.

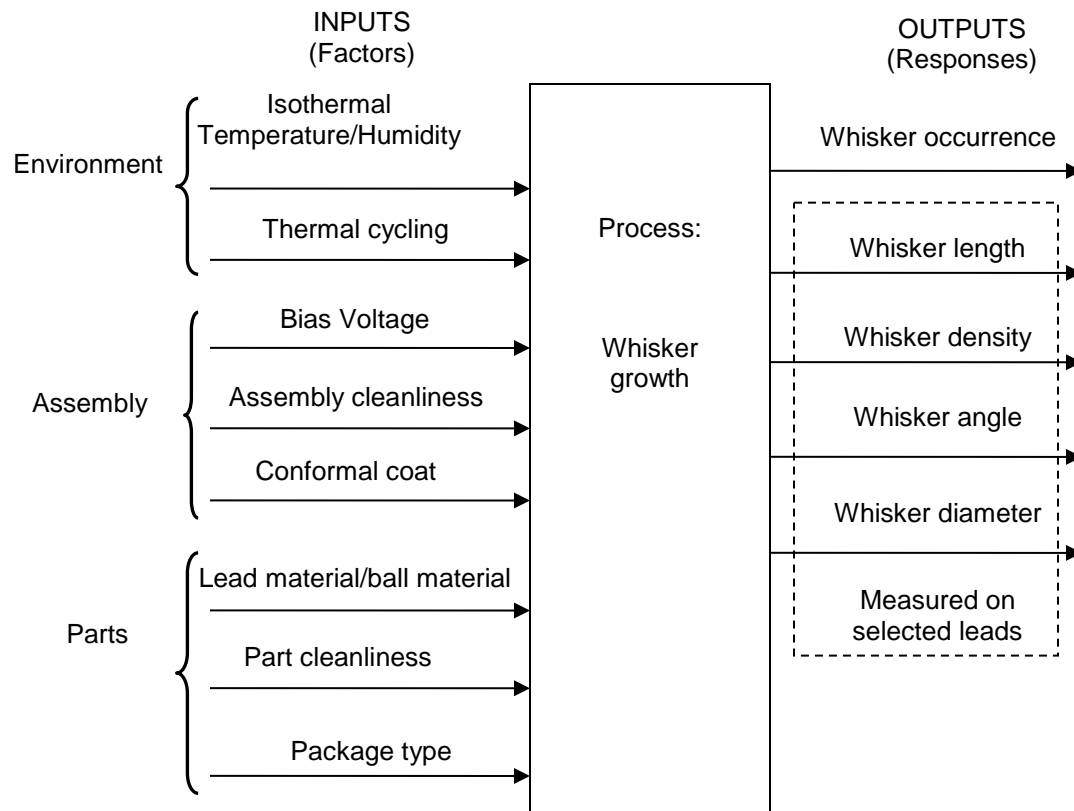
7.2 Design and environment variables

The experimental portion of this study was designed to study the role of selected material and manufacturing process variables in the growth of tin whiskers under certain isothermal and thermal cycling environments. Figure 75 lists the main variables included in the experiment, along with the outputs studied.

Several types of surface mount parts were selected for evaluation in four environments. The present study focused on surface mount parts because of the close lead-to-lead gap spacing and regions that are difficult to conformal coat. The environment selection provided a range of lead coefficient of thermal expansion (CTE), intermetallic growth (IMC) and corrosion stresses. The high humidity environment has low CTE and high corrosion stress, the large thermal cycle has high CTE and moderate to high corrosion stress, the power cycling simulation thermal cycle has low CTE and corrosion stress, and the long term high humidity test has low CTE, moderate corrosion, and high IMC stresses.

Three custom boards were designed to evaluate the key piece parts of interest. The small outline transistor (SOT) board has parts with both copper and alloy-42 leads, the quad-flat-pack (QFP) board has a range of high pin count leaded devices with very close spacing and the ball grid array (BGA) board contains lead-free ball alloys with a range of whisker propensity. A typical view of the samples in an environmental chamber is shown in Figure 76.

A summary of the test vehicle design, environmental variables, design of experiments and the inspection plan follows next.



Constant but controlled variables:

- Board laminate: High temperature glass epoxy
- Board metallization: Copper
- Board finish: Immersion tin
- Solder paste: 96.5Sn3Ag0.5Cu (SAC305), ROL1 flux cleanable no-clean solder paste
- Solder process: Surface mount convection reflow in an air atmosphere
- Assembly in accordance with J-STD-001 Class 3

Figure 75: Primary experiment factors.



Figure 76: Typical view of test vehicles installed in an environmental chamber.

7.2.1 SOT, QFP, and BGA board test vehicle design

The test vehicles for this study are small boards 6 cm x 6 cm in size. The board was found to be well suited for inspection by scanning electron microscopy (SEM), since the board fit easily into the SEM's sample chamber. The placement area was limited to 5 cm x 5 cm to ensure all leads of interest were contained in a region that could be viewed by the SEM.

The boards are 0.093" thick and are a double layer design on high temperature FR4 manufactured in accordance with IPC-6012 CLASS 3, TYPE 2. All boards have solder mask in accordance with IPC-SM-840 Class H, liquid photo-imageable over bare copper. The exposed traces, pads and plated through holes are immersion tin finished in accordance with IPC-6012, Type IT with solderability meeting the requirements of ANSI/J-STD-003, Class 3, Category 2.

Due to the small board size, the boards were laid out in 12-up panels with handling edges (Figure 77). The boards were separated after surface mount soldering, inspected, and then subjected to the environments.

The test vehicles contained two classes of components – the main class consists of the components in the tin whisker study, while the second consists of components required to complete the circuitry or make connections to test or monitoring equipment. The parts were allocated across three different board designs, designated as the SOT board, the QFP board and the BGA board.

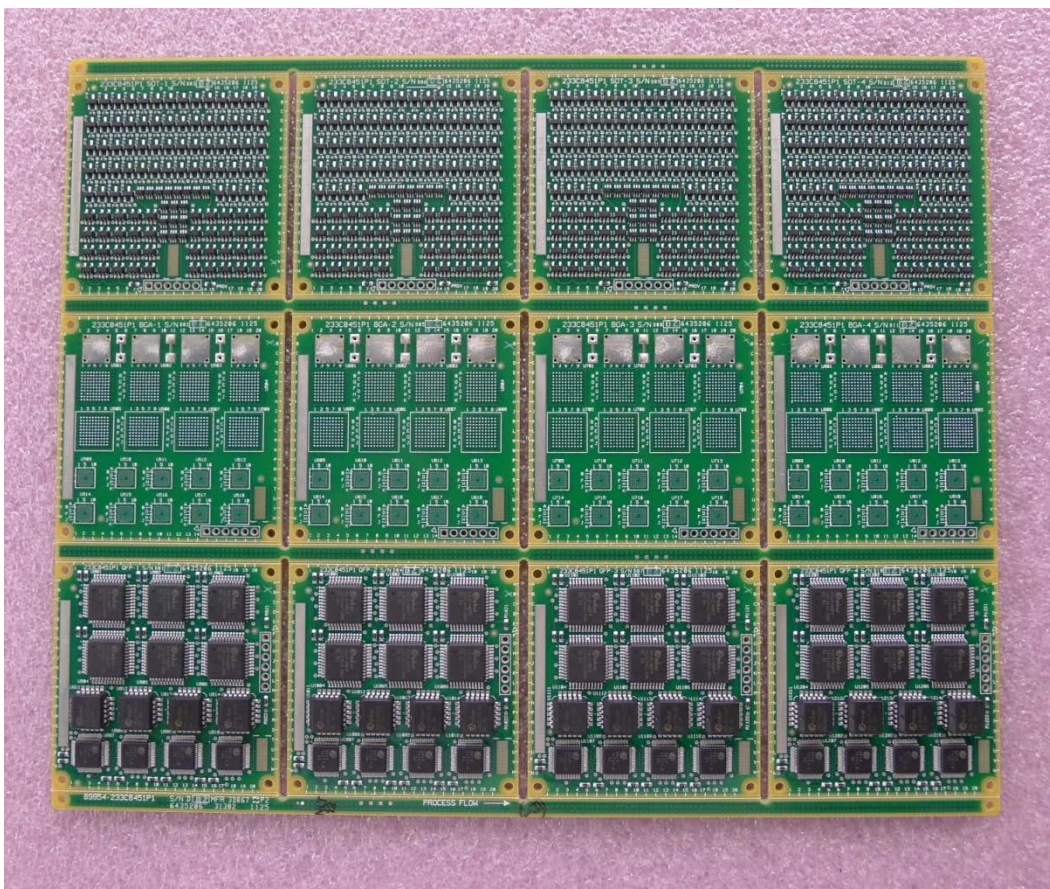


Figure 77: Test vehicle panel

7.2.1.1 Board features to facilitate testing

Each of the three boards was laid out with the test matrix in mind. Boards were laid out with all components on a single side of the assembly. This simplified the manufacturing process, and prevented any components from seeing additional reflow profiles as a consequence of being on the bottom side of the printed circuit board.

Efforts to simplify the inspection process were also made. Components were laid out in blocks of the same component type, which made the groupings easy to identify, and allowed the components to be laid out in straight rows. By placing the components in rows, the leads were aligned in a single plane, allowing the SEM operator to pan along the entire row without having to make excessive adjustments. In addition, silkscreen marks spaced every 0.254 cm on the perimeter of the board to improve area tracking on the board. In some cases, the same component type was used for more than one test condition on the same board – for instance, some SOT3s on the SOT board had a bias of 5 volts, while others were not biased. All of the components for the 5V bias condition were grouped together, and all of the unbiased components were in a second grouping, making it easy for the inspector to determine to which conditions a given component was exposed.

7.2.1.2 SOT board

The SOT board, shown in Figure 78, contained the three commercial component part numbers defined in Table 10 for the tin whisker assessment matrix. The lead compositions are given in Table 11. The SOT parts were selected because they were readily commercially available with both copper alloy and alloy-42 lead materials in similar packages from the same manufacturer and there was prior experience with tin whisker growth on alloy-42 SOT packages during power cycling when rework flux residues were present [10].

In addition to the components included specifically in the whisker study, the board included 0402 resistors which were used in completing the voltage bias circuitry for the SOT3 and SOT5 devices (Figure 79). In describing the data, the term bias1 refers to the part voltage bias. Even when a 5 volt bias is applied to the part, some of the leads are still at ground potential. The term bias2 refers to the actual pin voltage either ground (0 volts) or 5 volts. If the part bias1 is “0”, then all the leads bias, bias2, is also “0”. If the part bias1 = 5V, then SOT3 leads 1 and 3 have bias2 = 5, SOT5 leads 2 and 5 have bias2 = 5, and SOT3 lead 2, SOT5 leads 1, 3 and 4 have bias2 = 0.

A pin header for connection to a power supply and a small surface insulation resistance (SIR) comb pattern are also present. An exposed copper area to allow the boards to be scribed with a serial number was included on one edge of the board outside of the inspection area. The back side of the board included a large copper area that allows measurement of conformal coating thickness with an eddy current meter.

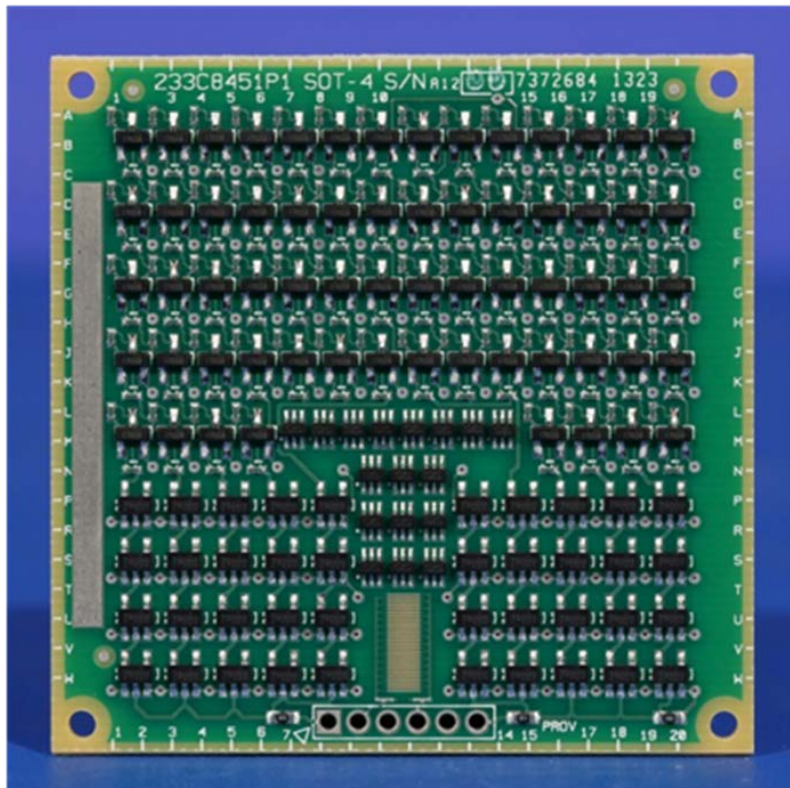


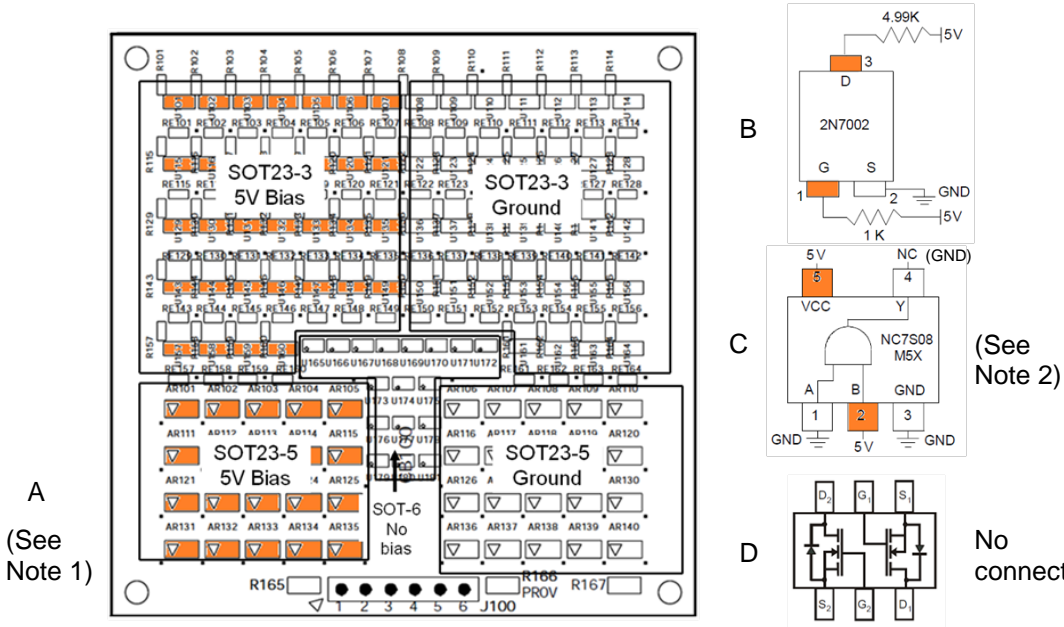
Figure 78: SOT Board

Table 10: SOT board parts under test

Designation Part No. Package	Vendor	Lead Frame Material	Plating Material	Leads per part	Total number of parts	Part voltage bias	Number of parts
SOT3 2N7002 SOT23-3	Fairchild	Alloy-42	Matte Sn	3	64	0 (GND)	32
						5 V	32
SOT5 NC7S08M5X SOT23-5	Fairchild	C194	Matte Sn	5	40	0 (GND)	20
						5 V	20
SOT6 2N7002DW- 7-F SOT363	Diodes Inc.	Alloy-42	Matte Sn	6	17	NC	17

Table 11: SOT board lead material composition

Lead material	Composition
Alloy-42	Fe-42Ni
C194	Cu2.1-2.6Fe-0.015-0.15P-0.05-0.2Zn



Note 1: 5V applied to Qty = 32 SOT23-3, and Qty = 20 SOT23-5

Note 2: The SOT5 pin 4 is at logic level 0 (ground) when pin 1 is ground and pin 2 is 5V.

Figure 79: SOT board voltage bias; (A) bias voltage on the overall board, with (B)(C) and (D) showing the device connections to the SOT3 (SOT23-2), SOT5(SOT23-5) and the SOT6 parts respectively.

7.2.1.3 QFP board

The QFP board, shown in Figure 80, is dominated by large leaded quad-flat-packs. The QFP board contains three component part numbers included in the experimental matrix, as shown in Table 12. The lead compositions are given in Table 13. The QFP board includes two pitches of QFPs as well as one plastic lead chip carrier (PLCC) package. The PLCC uses a copper alloy that exhibited high whisker propensity in the screening experiments and was found to have a high degree of tin finish defects. The PLCC is of additional interest because standard spray

conformal coating processes do not typically coat the portion of the lead under the package (Figure 81) leaving regions without coating whisker mitigation. The QFP board electrical schematic is shown in Figure 82. The combination of the part daisy chain and the board connections results in a voltage bias being established between various pairs of adjacent pins (e.g. on the QFP44 part, pin 2 is at 5V and pin 3 is grounded).

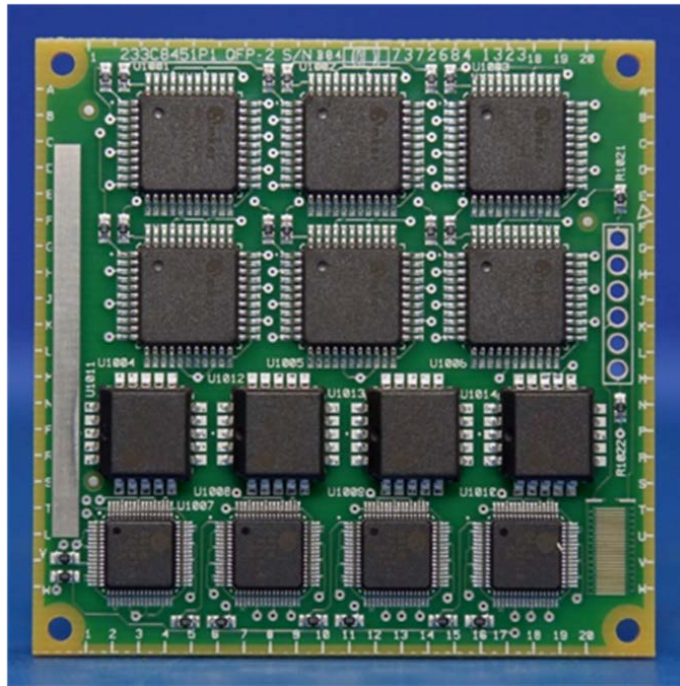


Figure 80: QFP Board.

Table 12: QFP board parts under test

Designation Part No. Package	Vendor	Lead Frame Material	Plating Material	Number of Leads
QFP44 A-QFP44-10mm-.8- 3.2-DC-Sn (0.8 mm pitch)	Practical components (Amkor)	C7025	Matte Sn	44/6
PLCC20 A-PLCC20T-DC-Sn (1.25 mm pitch)	Practical components (Amkor)	C151	Matte Sn	20/4
TQFP64 A-LQFP64-.7mm- .4mm-2.0-DC-Sn (0.4 mm pitch)	Practical components (Amkor)	C7025	Matte Sn	64/4

Table 13: QFP board lead material composition

Lead material	Composition
C7025	Cu2.2-4.2Ni0.25-1.2Si0.05-0.3Mg
C151	Cu0.1Zr

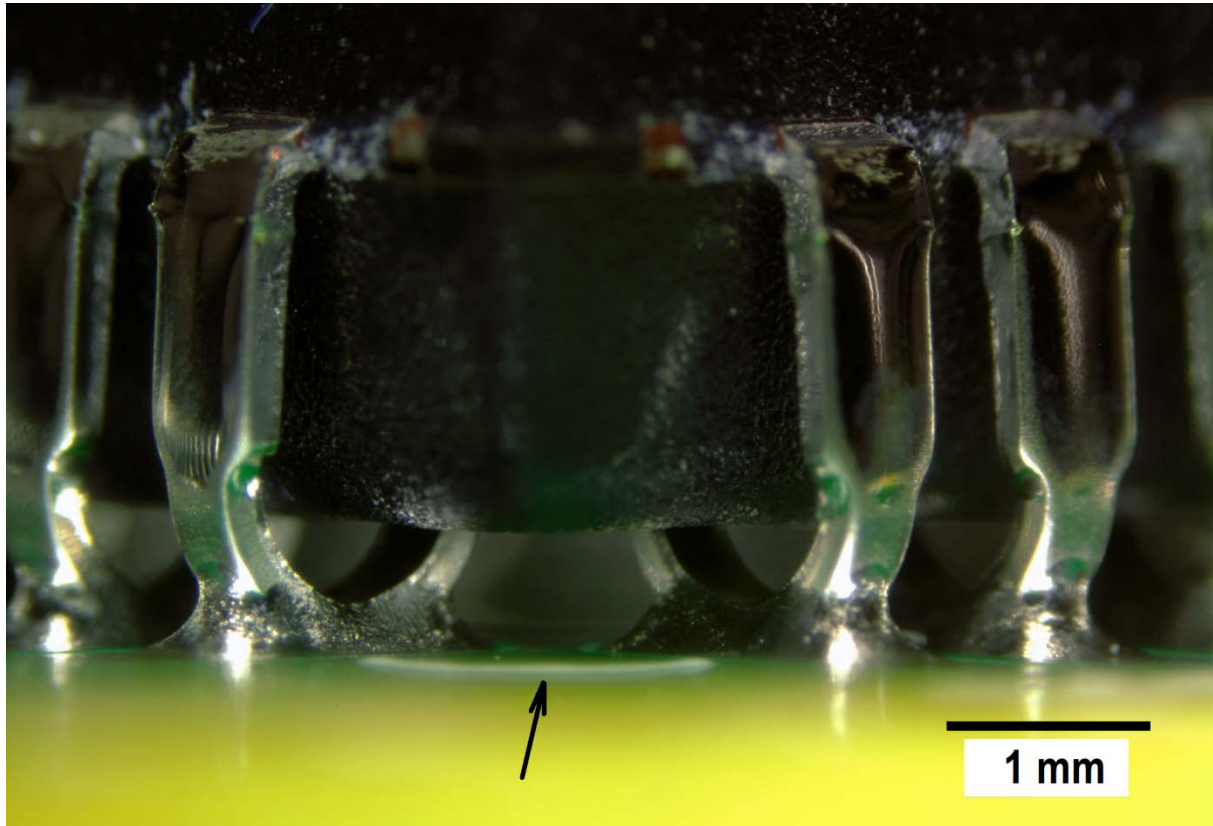


Figure 81: J-lead tin whisker conformal coating mitigation challenges. Underside of the part is difficult to conformal coat and the sheared lead tips enhance corrosion whisker stresses.

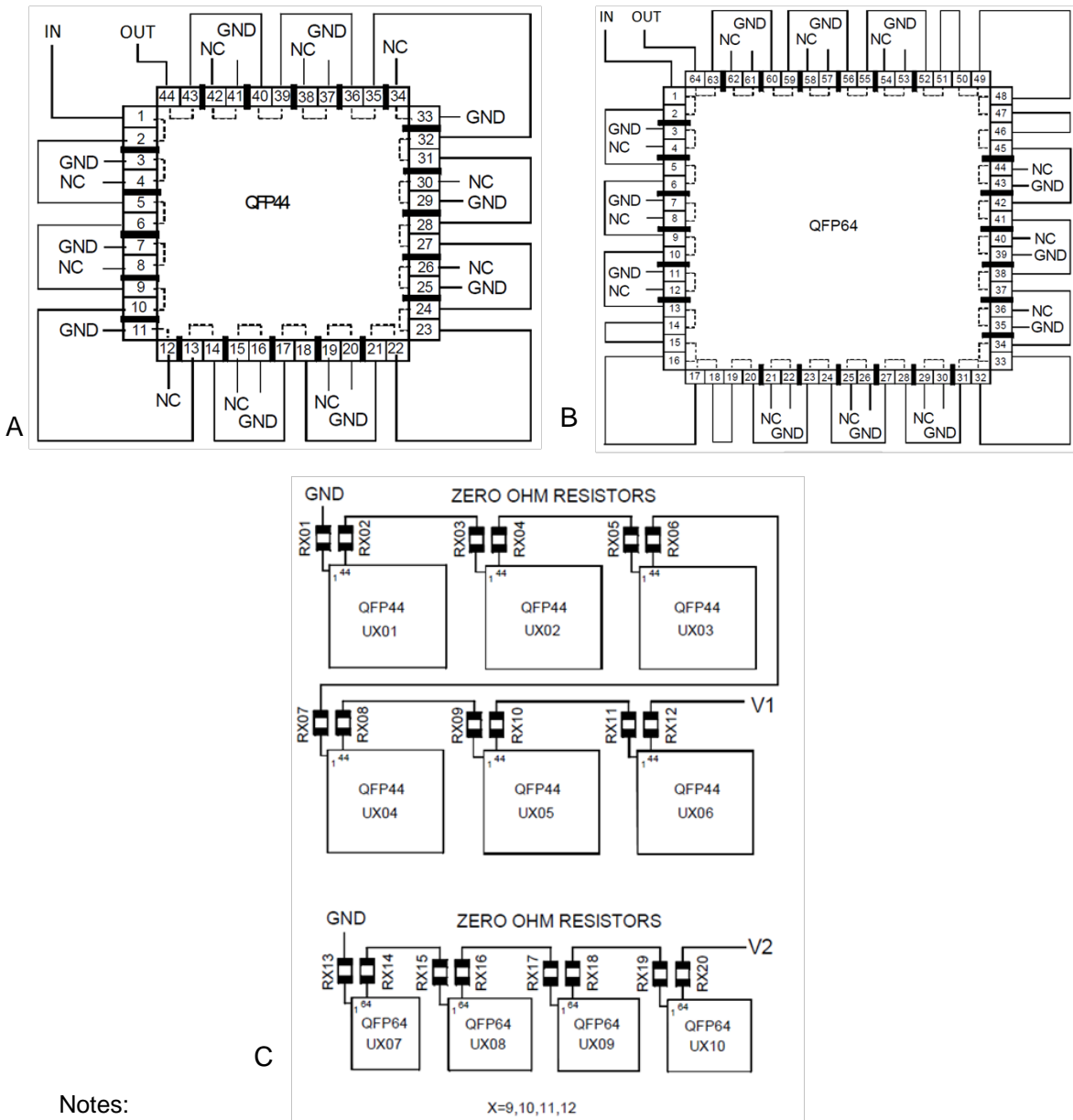


Figure 82: QFP board electrical schematic; (A) QFP44 (B) TQFP64 and (C) interconnects to 5V.

7.2.1.4 BGA board

The BGA board is shown in Figure 83. It contains two types of BGA component pad types (Table 14). Additional land patterns identical to those used for the 100 I/O 0.8mm pitch CABGA were also included in the design. These additional land patterns are used for applying solder spheres of the same diameter as would be found on the BGA component. The outside row of pins were tied together, but not connected to ground. (Note: no electrical connections were made to the BGA board from the outside of the chamber.)

In the present evaluation, BGA devices were not soldered to the boards because of the difficulty of inspecting for whiskers under the package; only balls were populated. Two different ball alloys were studied on the land pattern

area SAC105 and SAC105 with Ce rare earth element added. These were compared to pads printed with SAC305 paste. By using only the solder spheres and not a complete BGA device, inspection for whiskers is greatly simplified. The additional copper squares included in the design allows for whisker inspection of a larger mass of reflowed SAC305 paste without leads.

The SAC solder with REE was included in the test matrix because the REE have increased the propensity of SAC solders to generate tin whiskers. The screening experiments showed that Ce was chosen over La and Y because results have been published indicating that Ce has better oxidation resistance [87], which would be promising for incorporation in lead-free solder. The screening experiment in the present work (section 6) had a different result; Ce was at least as effective as Y and La in whisker formation. Therefore, to discourage industry from even considering Ce additions, the BGA board used Ce at a concentration much lower than the two percent being considered for improving drop shock performance. For the assembly, 0.4 mm (0.0157 inch) diameter spheres with a target REE concentration of 0.5% Ce were purchased, but the manufacturer had difficulty attaining this level. Then, after soldering to the board with SAC305 paste the Ce concentration was further reduced to <0.01%Ce.

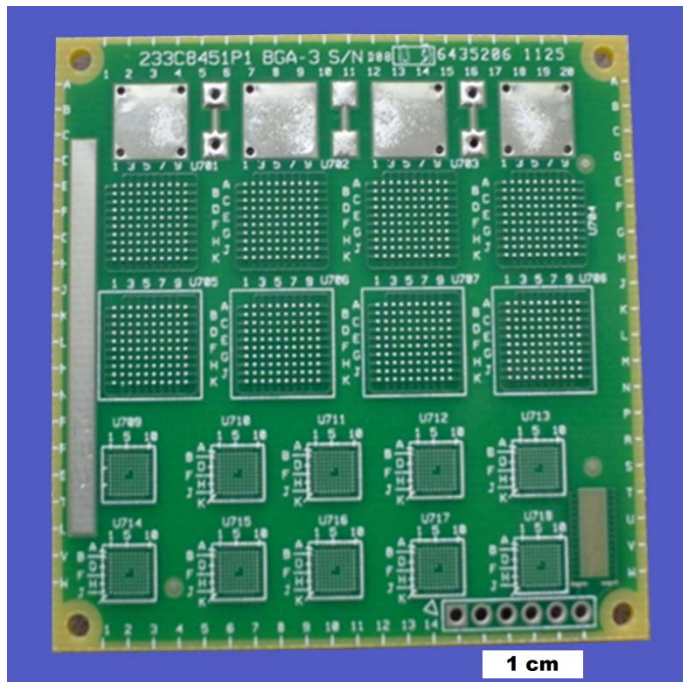


Figure 83: BGA board.

Table 14: BGA component solder pad patterns

Component	Number of Balls
0.8 mm pitch CABGA	100
0.4 mm pitch CVBGA	97

7.2.2 Environments

Four environments were selected to evaluate whisker growth as part of the effort to determine if certain combinations of factors are more conducive to whisker growth than others. Although recent work has suggested that it is not currently possible to predict future whisker growth based on short term whisker accelerated environmental tests [77], there are few alternatives. Isothermal high humidity and thermal cycling conditions were used to promote whisker growth and evaluate capability of the conformal coatings to provide tin whisker mitigation. The maximum temperature was selected to be 85°C for a number of reasons. First, it is the maximum temperature for the thermal cycling test in the JESD22-A121A [24]. Second, in high humidity conditions, 85 °C has been shown to promote whisker growth in lead-free solder alloys [27]. Third, under high humidity conditions, 85°C results in faster nucleation time than 50 or 70°C temperatures [34]. Finally, there was a concern that higher temperatures may induce other relaxation mechanisms other than whisker growth.

The two isothermal high humidity environments employed were 25°C/85%RH and 85°C/85%RH. Given that the humidity is constant, the lower temperature is expected to result in less whisker growth, but is representative of possible long term storage conditions in a humid location. The higher 85 °C temperature has been shown to grow whiskers in industry high humidity testing. Inspection intervals of 1,000 h and 4,000 h (1,000 + 3,000) were selected based on JESD201 industry standard test intervals [23].

The two thermal cycling environments used for testing were +50 to 85 °C and -55 to 85°C. The +50 °C lower limit represents a common base temperature for power on-off cycling testing and the -55 °C is the lower limit for many aerospace and defense applications. The two different lower limits result in a 4x increase in temperature differences from 35 to 140 °C. Since the temperature difference of the large cycle is four times greater than the smaller cycle, the larger cycle is expected to have four times the thermally induced stresses due to material thermal coefficient of expansion differences.

The +50 to 85 °C represents the conditions where whiskers grew during *power cycling* operation [10]. In this case, the boards were maintained at 50 °C and after power was applied, the power dissipated by the components caused the board to heat up. The part that exhibited whisker growth under those conditions had rework flux residue as well as a 5V DC bias between the leads [10]. The larger thermal cycle, -55 to +85°C is representative of some upper and lower limits encountered in service and is also included as one of the standard tests in JESD22-A121A. Condensing moisture events could occur during the transition from cold to hot in the -55 to +85°C cycle.

Table 15: Primary experiment environments

Temperature cycling					
Description	Temperature	Ramp and dwell	Temperature difference	Humidity	Duration
Simulated power cycling thermal cycling (PCTC)	+50 to +85 °C (1)	One hour cycle with 15 minute ramps and dwells	35 °C	Low (2)	1,750 cycles
Thermal shock cycling (TC)	-55 to +85 °C	Three cycles per hour with 10 minute dwells	140 °C	Low to high variation (3)	2,110 cycles
Isothermal high humidity					
High temperature/high humidity (HTHH)	85 °C	Isothermal	None	85 %RH	4,000 h
Long term low temperature/high humidity (LTHH)	25 °C	Isothermal	None	85 %RH	16,910 h over 3 years
Note 1: Actual measured chamber temperature was 48 to 88 °C. Note 2: Humidity was not controlled. It was measured to be between 25%RH at 88 °C to 10%RH at 48 °C. Note 3: Humidity was not controlled or measured					

7.3 Design of experiments (DOE)

The non-coated SOT board set (Table 16) was repeated for the coated boards. A set of non-coated and coated boards were subjected to each of the four environments. Separate test boards were fabricated for each contamination state in order to minimize contamination migration issues. Three board replicates were tested for each contamination state shown in Figure 84. Note that the piece part level of chlorine contamination was selected to be within the industry levels encountered (no standards exist) and that the assembly level of equivalent chlorine contamination was selected to be at the upper J-STD-001 Class 3 [17] industry limit for newly manufactured assemblies for DoD equipment.

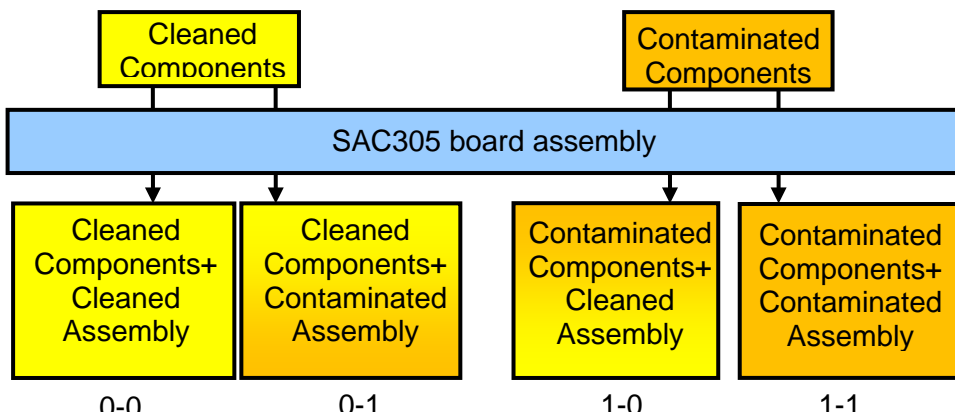
Table 16: Non-coated SOT board set

Run	Board SN (1)	Lead Alloy (2)	Package	Voltage (V) (3)	Part Contamination ($\mu\text{g/in}^2$)	Board Contamination ($\mu\text{g/in}^2$)
1	1, 2, 3	C194	SOT5	0	0	0
2				5		
3		A42	SOT3	0		
4				5		
5			SOT6	No Connect		
6	4, 5, 6	C194	SOT5	0	3	0
7				5		
8		A42	SOT3	0		
9				5		
10			SOT6	No Connect		
11	7, 8, 9	C194	SOT5	0	0	10
12				5		
13		A42	SOT3	0		
14				5		
15			SOT6	No Connect		
16	10, 11, 12	C194	SOT5	0	3	10
17				5		
18		A42	SOT3	0		
19				5		
20			SOT6	No Connect		

Notes: (1) SN = serial number, 3 board replicates per DOE run,

(2) C194 = Cu alloy leads and A42 = alloy-42 leads

(3) 0 and 5V bias levels built into the circuitry of each board



Board contamination nomenclature

0-0 No part contamination-No board contamination

0-1 No part contamination-Board contamination

1-0 Part contamination-No board contamination

1-1 Part contamination-Board contamination

Figure 84: Board contamination levels

7.3.1 Inspection plan

The collection of whisker length data has been constrained by inspection resources. In the present project utilized the following inspection plan:

Full statistical inspection “Priority 1” group:

- Non-conformal coated SOT boards
 - All environments
 - Lead alloy: Cu and alloy-42
 - DC Bias voltage: 0 and 5 V
 - All contamination levels

Limited inspection “Priority-2” group:

- Coated SOT boards
 - All environments
 - Some contamination levels
- QFP boards (non-coated and coated)
 - Some environments
 - Some contamination levels
 - Some coated assemblies
- BGA boards (non-coated and coated)
 - Some contamination levels

The inspections that have been completed to date are summarized in Table 17.

Table 17: Primary WP1753 experiment DOE samples

	Environment -->	+50C to +85C		85C/85%RH		-55 TO +85C		25C/85%RH	
Board	Part type (Lead Alloy) (1)	Non-coated (2)	Coated	Non-coated	Coated	Non-coated	Coated	Non-coated	Coated
SOT	SOT3 (A42)	Complete	Photo *	C	P*	C	P*	C	P*
	SOT5 (C194)	C	P*	C	P*	C	P*	C	P*
	SOT6 (A42)	C	P*	C	P*	C	P*	C	P*
QFP	QFP44 0.8mm Pitch (C7025)	H	H	C*	P*	H	H	P*	P*
	PLCC 1.25mm Pitch (C151)	H	H	C*	P*	H	H	P*	P*
	TQFP64 0.4mm Pitch (C7025)	H	H	C*	P*	H	H	P*	P*
BGA	SAC305 reflowed solder paste only	H	H	P*	P*	H	H	P*	P*
	SAC105 BGA Spheres only	H	H	P*	P*	H	H	P*	P*
	SAC105+REE BGA Spheres only	H	H	P*	P*	H	H	P*	P*

Notes:

(1) For SOT and QFP boards, each cell is comprised of 3 board replicates of 4 contamination levels each.

(2) C = Complete

C* = Completed partial inspection of QFP44, PLCC20, and TQFP64 at 1,000 h of the 1:1 contamination level

H = Hold samples built and exposed but not fully inspected because no significant whiskering is expected based on SOT results

P* = Limited photographs, no quantification of whisker growth or metallurgical analysis

7.4 Inspection methodology and measurement approach

7.4.1 Whisker inspection

The current assembly experiment whisker measurements have adapted applicable parts of the JESD22-A121A [24] industry part level whisker measurement method.

Sample size: The test vehicle and build matrix ensures that for the SOT experiments, 96 leads from at least six parts were available for inspection. The Priority-2 QFP board assemblies contained fewer parts because of their large size, and the design was constrained to 80 PLCC leads, but the leads were large having considerably more surface area than the other parts.

Initial inspection prior to environmental exposure: Optical inspection was in accordance with JESD22-A121A Para 6.3 except that only optical inspection was used to ensure that the samples do not have whiskers prior to environmental exposure. The scanning electron microscopic examination was not used because the vacuum and electron beam might alter the tin surfaces and the contamination.

Screening inspection: For selected configurations in the Priority-2 group, SEM photographs were obtained to determine if further inspection was necessary.

Detailed inspection: The detailed inspection was performed in accordance with JESD22-A121A 6.6.1 as modified herein using a scanning electron microscope. A scanning electron microscope was used at minimum magnification of 100x. Inspection intervals doubled in duration between successive inspections to ensure that SEM inspection process (nitrogen hold storage, vacuum in the microscope, and electron beam exposure) had minimal influence on whisker growth.

Statistical evaluations: It is unclear what distribution the various whisker attributes (length, diameter, density, or angle) would follow or how many leads would grow whiskers. In the present work, every effort was made to obtain sufficient whisker length (or other attribute) measurements to understand which factors are important and provide risk modeling inputs. At the final inspection points, additional leads were examined if needed. To provide a starting point for the number of replicate measurements and test samples, DOE design guidance by Schmidt [88] was used in combination with JESD22-A121A [24].

The minimum sample size can be determined for a given confidence level to determine the whisker length (or other attribute) standard deviation. In this case, an alpha value of 0.05 and power (e.g. 1-beta) value of 0.9 were used. An alpha of 0.05 corresponds to a 95 percent confidence that if the factors studied influence whisker measurements to a change, they would be included in the model. A power level of 0.90 would result in 90 percent confidence that if the factors did not influence the whisker measurements, they would be excluded from the model. The number of whisker measurement replicates required to capture changes to a level of one standard deviation is given in Table 18. The JESD22-A121A test sample size of 96 leads gives sufficient numbers of leads to detect low whisker propensity variable combinations.

Table 18: Number of experimental replicates planned.

Design of Experiment Type	Measured Parameter	alpha	Power level = (1-beta)	Replicates required (e.g. whisker lengths measured) (1)	Experimental replicates planned (e.g. whisker lengths measured)
4 factor 2 level Full factorial 16 run experiment	e.g. whisker length	0.05	0.90	4	30

Note: (1) replicates needed to detect a difference of one standard deviation in the mean

The SOT board inspections were performed on randomly selected parts. Typically, all the leads on two to four parts were selected on at least two boards to identify 24 to 48 leads for inspection. All the whiskers on a particular lead were measured. The goal was to obtain at least 30 whisker lengths for a particular variable combination. As was previously mentioned, the test included variable combinations that were expected to have low to high range of whisker growth. Sometimes more leads would need to be inspected, sometimes less, to obtain 30 whiskers. Note that based on the screening experiment results, leads with whiskers produced approximately 10 whiskers in an inspection area that was 500 microns by 200 microns in size (e.g. approximately 50 whiskers per mm²). Examination of 18 leads would result in 180 whiskers being available for assessment.

Whisker occurrence: The occurrence of a whisker was counted if it was observable at 100x magnification in the SEM. There was no differentiation between odd shaped eruptions and whiskers in the occurrence count.

Whisker length: The definition of whisker length was in accordance with JESD22-A121A as shown in Figure 85. For the whisker length measurements, a SEM magnification higher or lower than that used for inspection may be required, such that the whisker being measured approximately fills the field of view at the selected magnification.

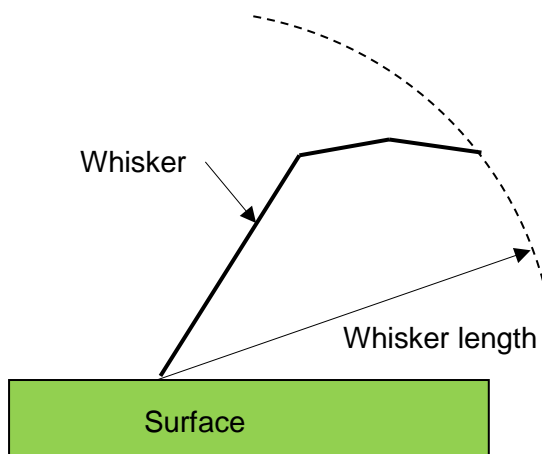


Figure 85: Whisker length definition.

A unique aspect of measuring whiskers on part solder joints is that nothing is planar and the sample must be continually rotated and tilted during the inspection. As the stage is tilted, the whisker length appears to increase until the SEM inspection azimuth angle is perpendicular to the whisker. Further tilting results in whisker beginning appear shorter. In the present work, the reported whisker length measurements were conservative. During the length measurement procedure, the SEM inspection azimuth axis was adjusted to be aligned to within ~30 degrees from perpendicular to the whisker. The SEM axis misalignment from the whisker normal resulted in a potential whisker length under-reporting of up to 15 percent as shown Figure 86.

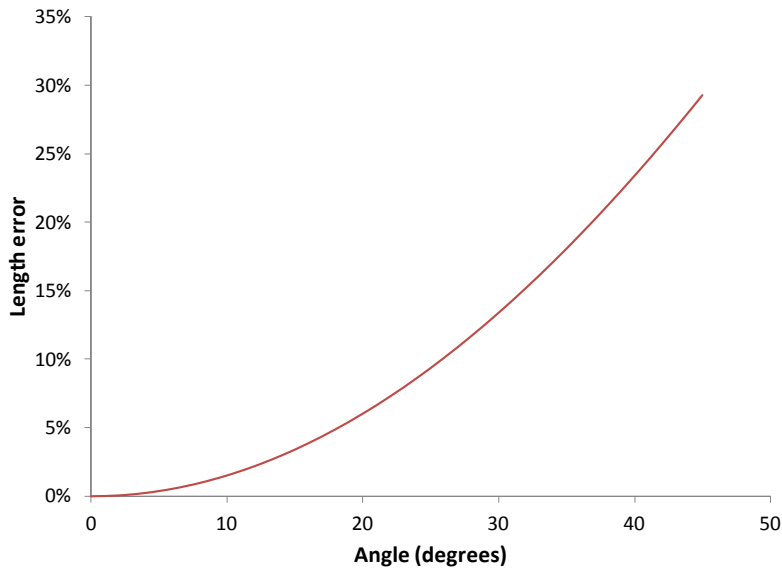


Figure 86: Whisker length error versus tilt angle.

Whisker density: Whiskers were measured and recorded in accordance with JESD22-A121A paragraph 6.7.3.2. The numbers of whiskers were recorded along with the region of the lead where the measurements were made. These were the same regions that were used to obtain the whisker length. Unlike JESD22-A121A, all whiskers were counted in the inspection region so that the appropriate whisker density can be determined.

Whisker location: The main motivation for tracking whisker location was to understand patterns related to the underlying metallurgy. The locations are defined in Figure 87.

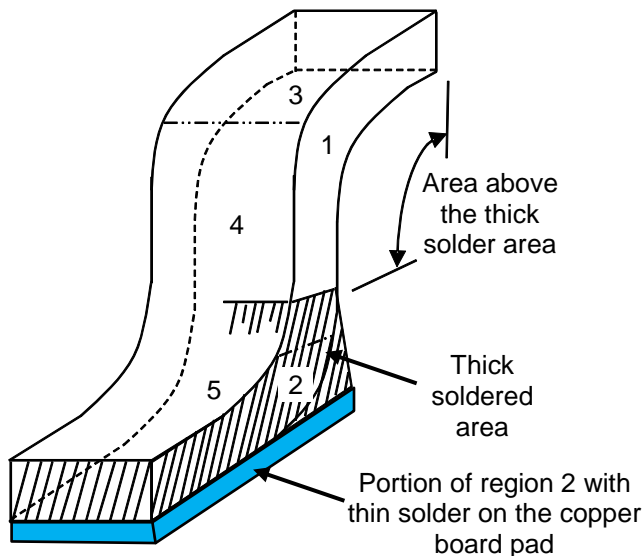


Figure 87: Whisker location definition. The hatched region 2 indicates the thick solder region on the lead and includes the thinner solder that wet onto the board pad. Areas 1, 3, 4 and 5 represent the thin solder or tin region above the thick solder area.

Whisker angle: For whiskers used for growth angle measurements, the whisker angle was approximately measured as shown in Figure 88.

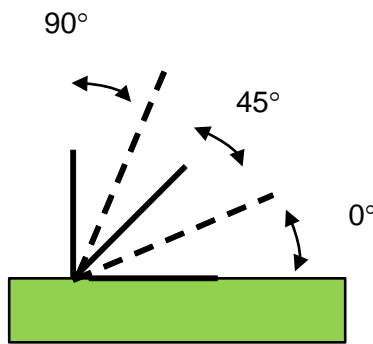


Figure 88: Whisker angle measurement definition

Whisker diameter or thickness: For selected whiskers, the whisker diameter or thickness was measured by drawing a line perpendicular to the whisker axis as shown in Figure 89 (Ref. [77]).

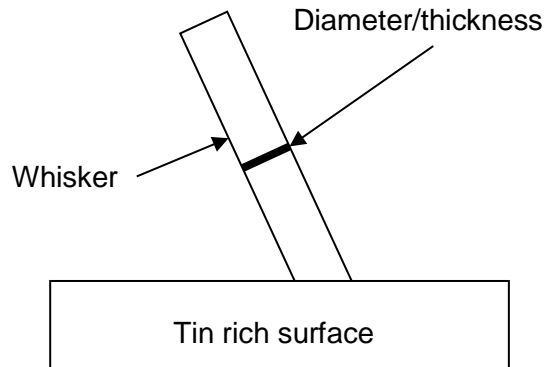


Figure 89: Whisker diameter or thickness measurement.

7.4.2 Metallurgical analysis

Sequential whisker cross-sectioning was performed on representative whiskers with SEM inspection at various slice depths (e.g. 5 whiskers sectioned with SEM at 5 slices per whisker). As required, a metallurgical evaluation was performed to determine the tin grain morphology, intermetallic layer thickness and morphology, and intermetallic particle distribution at the base of the whisker and in the whisker itself. Optical and SEM images and EDX elemental spectrum were used to record findings similar to the results published by Snugovsky in 2008 [10].

The whisker inspection was performed using a combination of optical and scanning electron microscopy. A key element of the present study was the use of high precision metallographic progressive polishing techniques to examine the sub-surface details of the whisker and nodule regions. The technique includes progressive polishing in the longitudinal and perpendicular directions and incorporates a special set of materials that allows removal of a

very thin layer in each step. The location from which whiskers or hillocks start growing was targeted. Sequential polishing permitted detailed analysis in order to understand the formation of the three-dimensional structure as well as reveal the whisker root features. Some of these features consist of intermetallic characteristics, tin grains, Ag_3Sn and Cu_6Sn_5 particle distribution and size, corrosion crevices and its relationship with lead-frame material, bulk solder microstructure and its defects such as flux related, shrinkage, and Kirkendall voids. Each polishing step was accompanied by SEM and EDX examinations. The detailed analysis of whisker formation was done on piece-parts with different surface finishes and lead-frame materials, with and without ionic contamination and from test vehicles assembled using different fluxes and cleaning chemicals. The data analysis techniques employed permit exploration of the key factors responsible for whisker formation and to formulate the mechanism of whisker nucleation and growth. The investigation focuses on solder regions with chemically modified microstructure and composition. It is expected that local very pure tin regions form due to diffusion associated with corrosion that propagates through the interdendritic eutectic structure.

7.4.3 Conformal coating inspection

SEM imaging is an effective means of evaluating coating coverage over the metal surfaces [52], coating cracking, and tin whiskers. With regard to coating coverage over metal, the SEM images can provide qualitative thickness information. The SEM image is dark when the coating is greater than approximately three microns thick and the electron beam cannot penetrate through the coating to the underlying metal. The SEM image becomes gray when the beam penetrates through the coating and interacts with the underlying metal. In this case, the coating is less than approximately three microns thick. The SEM image is brightest when directly imaging metal that either has no coating or very thin coating that the beam can easily penetrate. Note that some bright image regions on the leads evaluated with EDX (electron dispersive x-ray) were found to have a significant carbon peak suggesting that some coating was present. Also, in a particular image the darkness also increases due to the incident electron beam angle with respect to the coating surface. So even if the coating thickness has not changed, some regions of the lead could be darker or lighter depending upon the orientation of the lead surface. In addition, comparing different images can be problematic because incident electron beam energy and brightness/contrast settings change for each image.

A new process was developed to obtain high resolution coating thickness measurements in the SEM. Prior to cross-sectioning, the coated assemblies were sputtered with Au. The Au layer separated the coating from the epoxy mounting material and permitted coating thickness measurements down to 0.1 microns.

7.5 Part and assembly methods and materials

The overall assembly, test, and inspection sequence was:

- As-received part characterization
- Part cleaning and intentional part contamination
- Preparation for assembly/kitting
- Board assembly soldering
- Post soldering treatment
- Assembly characterization initial inspection
- Environmental exposure
- Storage of specimens in dry nitrogen while samples are in the inspection queue
- Screening inspection after environmental exposure for occurrence of whiskers
- Determine which combinations of factors would be examined in further detail
- Perform detailed measurements of whisker length, density, morphology, angle, and diameter for selected factor combinations (e.g. runs)
- Metallurgical evaluation of selected samples

Since whisker growth is a time dependent phenomena, careful records were maintained for component lot data, module soldering dates, process parameters, experiment start/stop times and inspection dates. The parts and assemblies were characterized with optical and SEM inspection and cross-sectioning.

The part characterization, contamination method, assembly soldering, initial assembly characterization and conformal coating details are provided next.

7.5.1 As-received part characterization

7.5.1.1 SOT and QFP boards

The typical results from the initial parts inspection of the SOT3, SOT5 and SOT6 is given in Figure 90. There were no significant anomalies in the plating pertaining to solderability. Some part defects important for whisker growth were detected that are not commonly reported such as exposed Cu and alloy-42 and deep surface grooves. The SOT3 part was also noted to have some silicon contamination present before cleaning.

The results from the initial parts inspection of the QFP44, TQFP64 and PLCC20 were similar to the SOT parts except that the PLCC in particular exhibited significant plating damage due to lead-forming process.

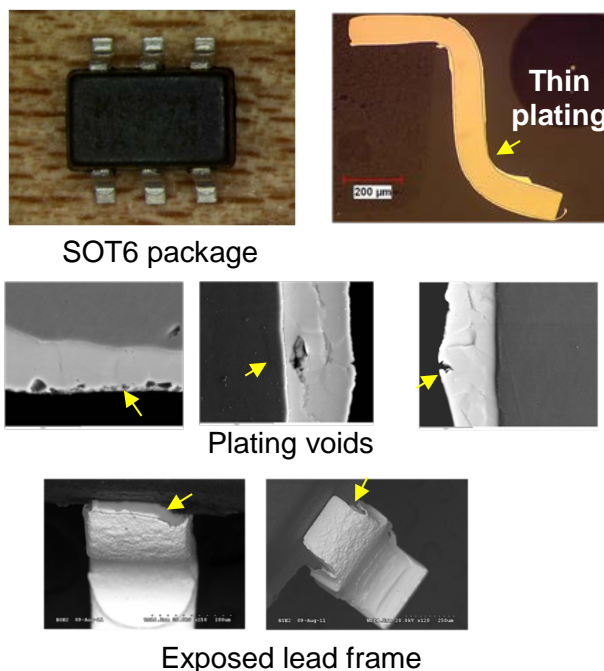


Figure 90: Cross-section, SEM and optical images of typical as-received part lead conditions that could contribute to whisker growth.

7.5.1.2 Industrial components quality summary

The RoHS Sn plated parts that meet plating criteria for solderability may have microstructural characteristics that may affect whisker formation:

- Uneven Sn plating
 - XRF measured thickness eight to 10 microns may vary from one micron to 38 microns as was found on the PLCC
 - Very thin Sn plating is more prone to whisker growth; An 8 micron tin plating minimum thickness is recommended for whisker mitigation [2] [89]
- Voids and cracks in plating
- Exposed lead material: Cu alloy and alloy-42
- Alloy-42 protrusions into the Sn plating
- Contamination
 - Cl, S, Si, Na, Br

- Main locations:
 - Surface roughness including voids and cracks
 - Grain boundaries
 - Gaps between the leads and plastic body
 - Edges and concave surfaces

7.5.2 Cleaning and contamination method

The cleaned part contamination levels are given in Table 19. For the cleaned parts, the intention was to have the level of contamination 10 times below typical acceptable industry levels. The contamination levels of the intentionally contaminated parts are shown in Table 20. For the intentionally contaminated parts, the goal was to have the part level contamination equal to $3.0 \mu\text{g/in}^2 \text{ Cl}^-$, but more contamination was trapped by SOT5, SOT6 TQFP64 and PLCC20 because they had rougher lead surfaces and greater numbers of gaps than the SOT3s. After intentional contamination, the contamination segregated on the tin surface to the rough regions, grain boundaries, and plating gaps as shown in Figure 91.

Table 19: Part contamination levels after cleaning.

(A) Total contamination levels

Part	Total Inorganic anions ($\mu\text{g/in}^2$)	Total Organic anions ($\mu\text{g/in}^2$)
SOT3	0.4	3.3
SOT5	0.3	0.0
SOT6	0.2	3.5
TQFP64	0.4	3.1
QFP44	0.2	2.4
PLCC20	3.7	0.0

(B) Concentrations of inorganic anions

Part	Fluoride ($\mu\text{g/in}^2$)	Chloride ($\mu\text{g/in}^2$)	Nitrite ($\mu\text{g/in}^2$)	Bromide ($\mu\text{g/in}^2$)	Nitrate ($\mu\text{g/in}^2$)	Sulphate ($\mu\text{g/in}^2$)	Total Inorganic anions ($\mu\text{g/in}^2$)
SOT3	0.0	0.0	0.0	0.0	0.2	0.2	0.4
SOT5	0.1	0.0	0.0	0.0	0.1	0.0	0.3
SOT6	0.1	0.0	0.0	0.0	0.1	0.0	0.2
TQFP64	0.1	0.0	0.0	0.0	0.2	0.1	0.4
QFP44	0.1	0.0	0.0	0.0	0.1	0.0	0.2
PLCC20	0.2	0.2	0.0	0.0	0.1	3.1	3.7

Table 20: Part contamination levels after intentional Cl contamination.

(A) Total contamination levels

Part	Total Inorganic anions ($\mu\text{g/in}^2$)	Total Organic anions ($\mu\text{g/in}^2$)
SOT3	1.9	0.0
SOT3 repeat	2.3	0.0
SOT5	8.7	0.0
SOT6	7.4	0.0
TQFP64	7.9	0.0
PLCC20	25	0.0

QFP 44	Not measured	Not measured
--------	--------------	--------------

(B) Concentrations of inorganic anions

Part	Fluoride ($\mu\text{g/in}^2$)	Chloride ($\mu\text{g/in}^2$)	Nitrite ($\mu\text{g/in}^2$)	Bromide ($\mu\text{g/in}^2$)	Nitrate ($\mu\text{g/in}^2$)	Sulphate ($\mu\text{g/in}^2$)	Total Inorganic anions ($\mu\text{g/in}^2$)
SOT3	0.1	1.7	0.0	1.0	0.0	0.1	1.9
SOT3 repeat	0.1	2.2	0.0	0.0	0.0	0.0	2.3
SOT5	0.3	6.7	0.0	0.0	0.0	0.7	8.7
SOT6	0.1	7.2	0.0	0.0	0.1	0.1	7.4
TQFP64	0.1	7.7	0.0	0.0	0.0	0.1	7.9
PLCC20	0.1	24.7	0.0	0.1	0.0	0.1	25.0

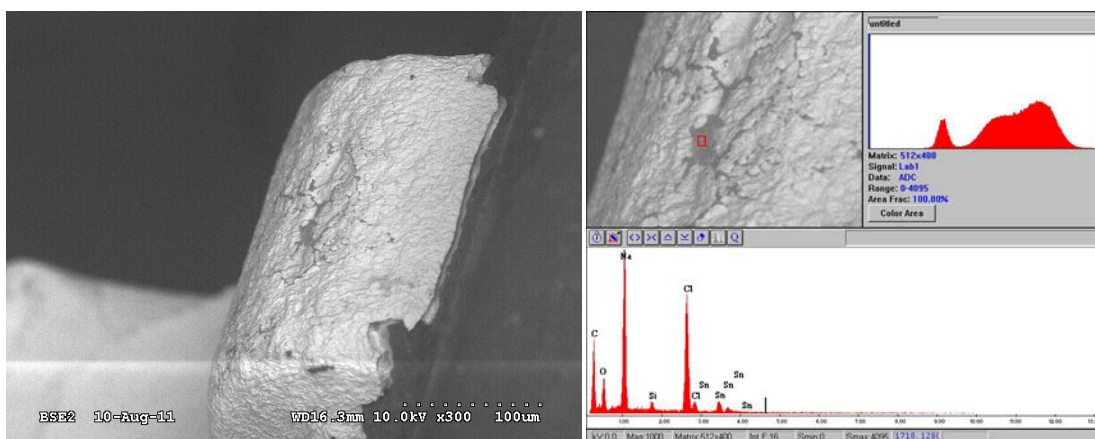


Figure 91: Typical contamination regions on intentionally contaminated (SOT6 shown).

7.5.3 Assembly soldering

Following the part cleaning/contamination processes, the SAC305 assembly soldering was performed. The boards on the panels were soldered in accordance with J-STD-001 Class 3, using SAC305 (Sn3Ag0.5Cu) alloy. Convection reflow in air was done with a 245 °C peak temperature using a paste with a ROL1 flux cleanable no-clean solder paste.

Each board was populated entirely either with clean parts or contaminated parts. After soldering and flux residue cleaning, selected boards were contaminated at the assembly level to 10 $\mu\text{g/in}^2$ Cl- (1.55 $\mu\text{g/cm}^2$ sodium chloride (NaCl) equivalent ionic or ionizable flux residue) to simulate the maximum level of contamination allowed by the J-STD-001 ionic residues test [17]. The assemblies were immersed in a solution of 160 +/- 10 ppm NaCl and then baked dry in an oven. The assembly contamination level of the intentionally contaminated assemblies was 5.2 ppm Cl- by ion chromatography with a total concentration of 12.5 $\mu\text{g/in}^2$ (1.94 $\mu\text{g/cm}^2$) equivalent Cl- as measured by resistivity of solvent extraction.

7.5.4 Conformal coating

The coating was an AR/UR blend (Humiseal UV40-250) qualified to both IPC-CC-830 and MIL-I-46058. The coating was applied with a machine spray process using multiple overlapping X-Y spray passes to achieve a thickness of 75 microns +/- 25 microns (3 mils +/- 1 mil) on a free and unencumbered surface.

7.5.5 Initial SOT, QFP, and BGA assembly characterization

7.5.5.1 SOT assembly metallurgical characterization

After soldering, the solder coverage and intermetallics were characterized using cross-sectioning. The SOT3 and SOT6 leads were fully covered in solder (Figure 92 and Figure 93), but the SOT5 leads were not (Figure 94). The Cu alloy lead terminations had SnCu interface IMC on the part leads and the board pads. However, the alloy-42 (Fe42Ni) lead terminations had SnCuFeNi interface IMC on the part leads and SnCuNi interface IMC on the board pads (Figure 95). The thinnest intermetallic was observed on the alloy-42 leads. One of the SOT3 parts was found to have Cl trapped at the thinnest part of the solder joint between the lead and Cu pad.

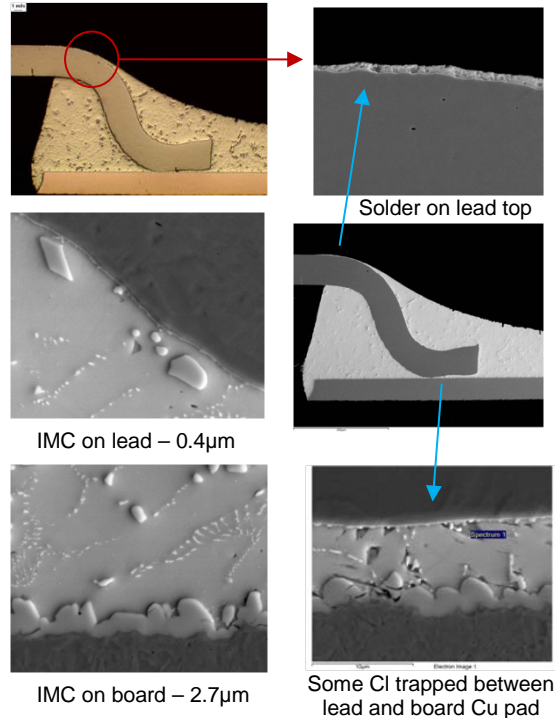


Figure 92: SOT3 soldered assembly cross-section.

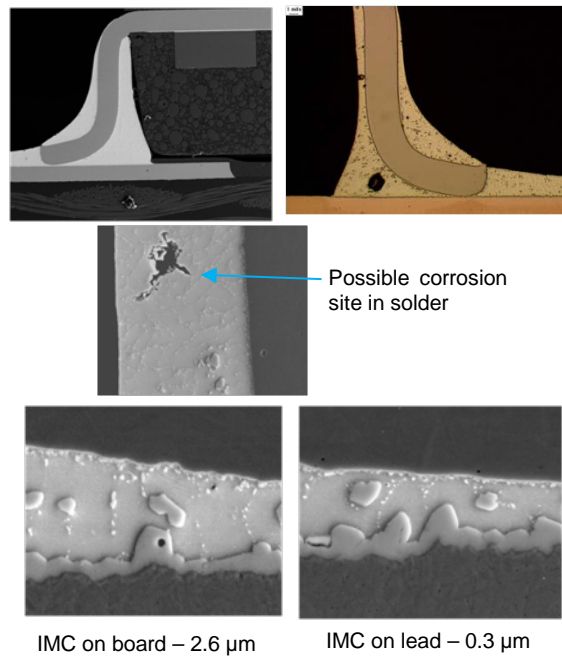


Figure 93: SOT6 soldered assembly cross-section.

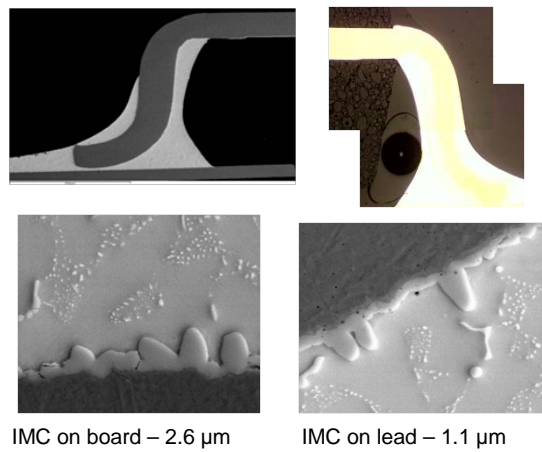


Figure 94: SOT5 soldered assembly cross-section.

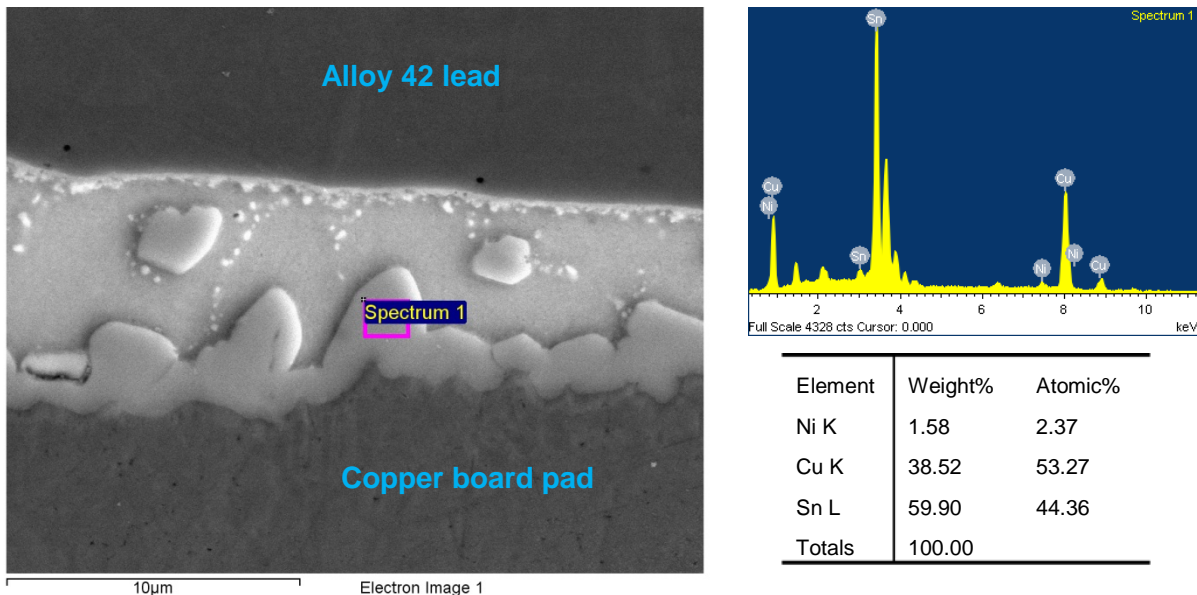


Figure 95: Board pad intermetallic on the alloy 42 SOT6 termination.

7.5.5.2 QFP board assembly characterization

No initial assembly cross-section characterization was performed.

7.5.5.3 BGA board assembly characterization

For the assembly, 0.4 mm (0.0157 inch) diameter spheres were ordered from a major solder manufacturer. The target concentration was 0.5 %Ce. The ball manufacturer had difficulty attaining this level and it was found to be <0.01%Ce. Then, after soldering to the board with SAC305 paste the Ce concentration was further reduced.

7.5.5.4 Conformal coating

The coated assemblies were examined optically and they met the requirements of J-STD-001 Class 3 for UR coatings. Cross-sections of the SOT3, SOT5 and SOT6 showed that the coating thickness was reduced to as little as 0.3 to 0.8 microns at the lead corners and on the lead bends (Figure 96). The coating also tended to pool up in large fillets between the SOT5 and SOT6 leads. These large fillets were on the order of 500 microns thick.

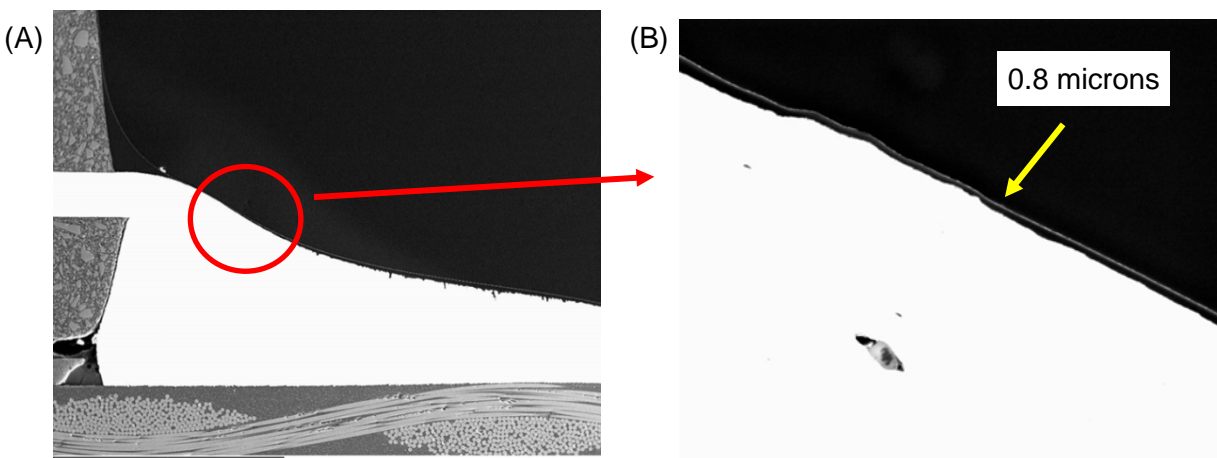


Figure 96: Cross-section of coated SOT3; (A) overall and (B) higher magnification view of the top of the lead showing thin coating.

7.6 Whisker density calculation areas

An area baseline was needed for whisker density (whiskers/mm^2) calculations. SEM photos and cross-sections were used to determine the areas associated with locations 1 through 5 for the SOT3, SOT5 and SOT6 parts. For the purposes of matching the whisker growth observations and the whisker risk modeling inputs, inspection region 2 was broken up into regions 2a (solder region above the board pad) and 2b (board pad region). In the high humidity testing, the whiskers grew from the thin solder on the board pad and not from the thick part of the solder joint. The area analysis photos consisted of a cross-section side view for regions 1, 2a and 2b, a cross-section front view for regions 4 and 2a, and two separate top views for regions 3 and 5 (Figure 97 through Figure 99). Note that the face areas used for regions 1, 2a and 2b needed to be counted twice because they were located on both sides of the lead. Also, the toe of the PWB pad was also included in region 2b, which results in a total of three surfaces needed make up region 2b.

Each photo was used in combination with a scaled spread-sheet plot to graphically locate points along the area perimeter. These points were then used to calculate the area using a matrix of triangular area elements (e.g. Figure 100 through Figure 102). Note that the subjective placement of the graph points results in some density variation. For instance, a previous analysis with a slightly different point placement determined area 2b to be 0.1953 mm^2 rather than 0.1798 mm^2 resulting in an eight percent difference in the calculated whisker density.

A summary of the area results are given in Figure 103 and Table 21 through Table 23.

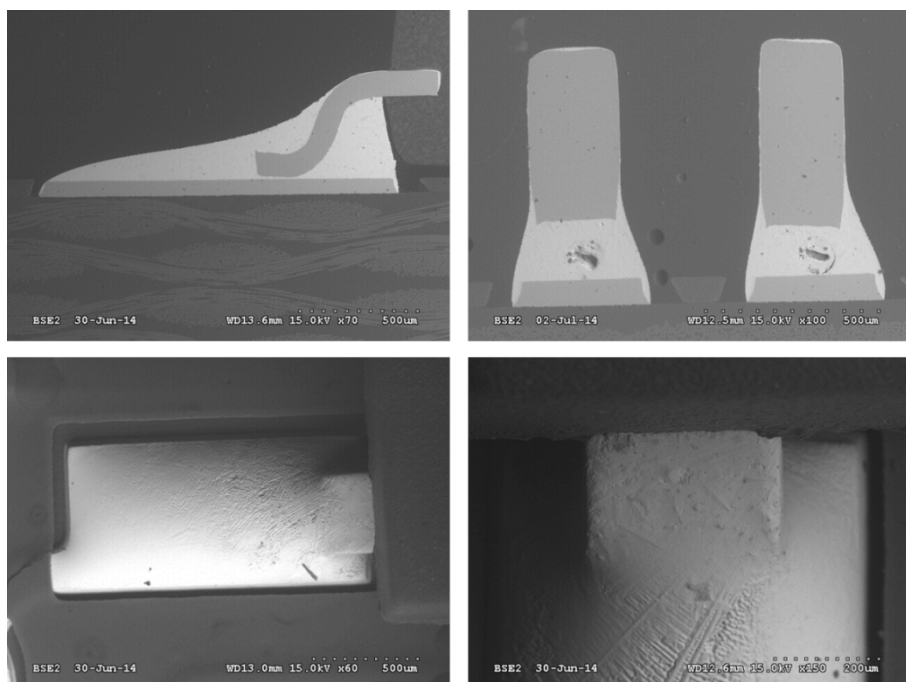


Figure 97: SEM images that were analyzed for the SOT 3. Top left: *Cross section side view for regions 1, 2a and 2b* Top Right: *Cross section front view for regions 4 and 2a* Bottom left: *Region 5* Bottom right: *Region 3*.

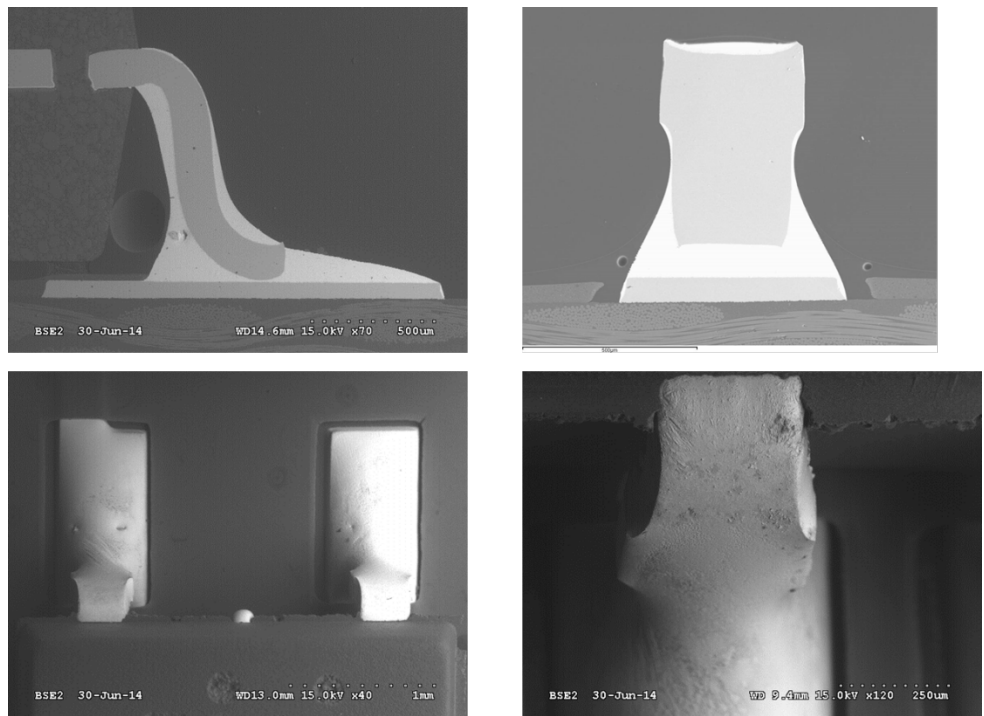


Figure 98: SEM images that were analyzed for the SOT 5. Top left: *Cross section side view for regions 1, 2a and 2b* Top Right: *Cross section front view for regions 4 and 2a* Bottom left: *Region 5* Bottom right: *Region 3*.

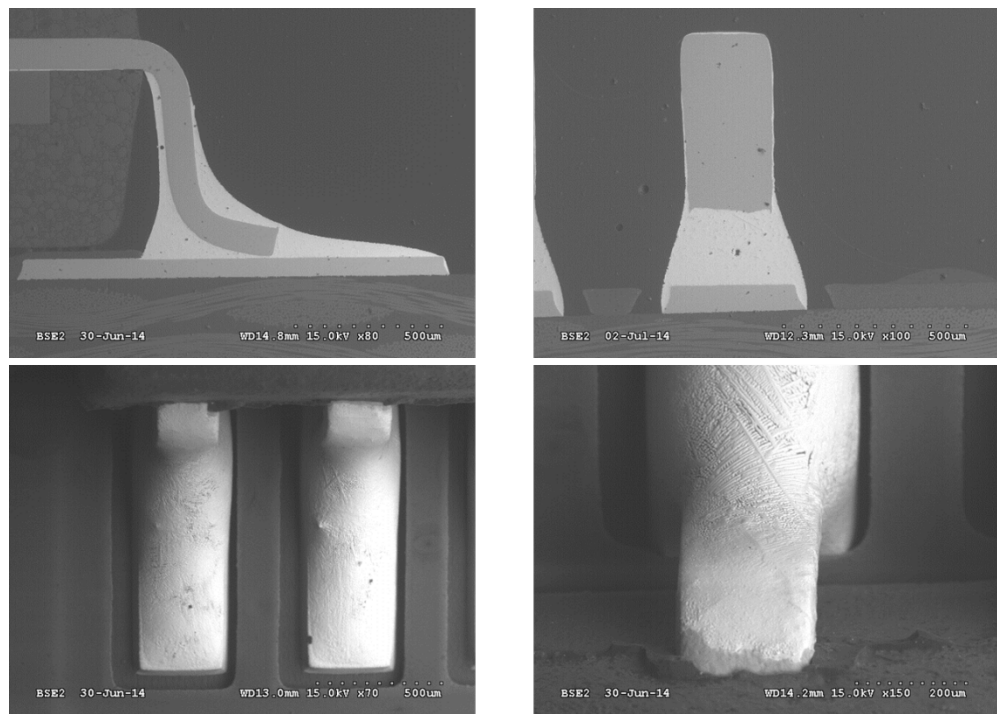


Figure 99: SEM images that were analyzed for the SOT 5. Top left: *Cross section side view for regions 1, 2a and 2b* Top Right: *Cross section front view for regions 4 and 2a* Bottom left: *Region 5* Bottom right: *Region 3*.

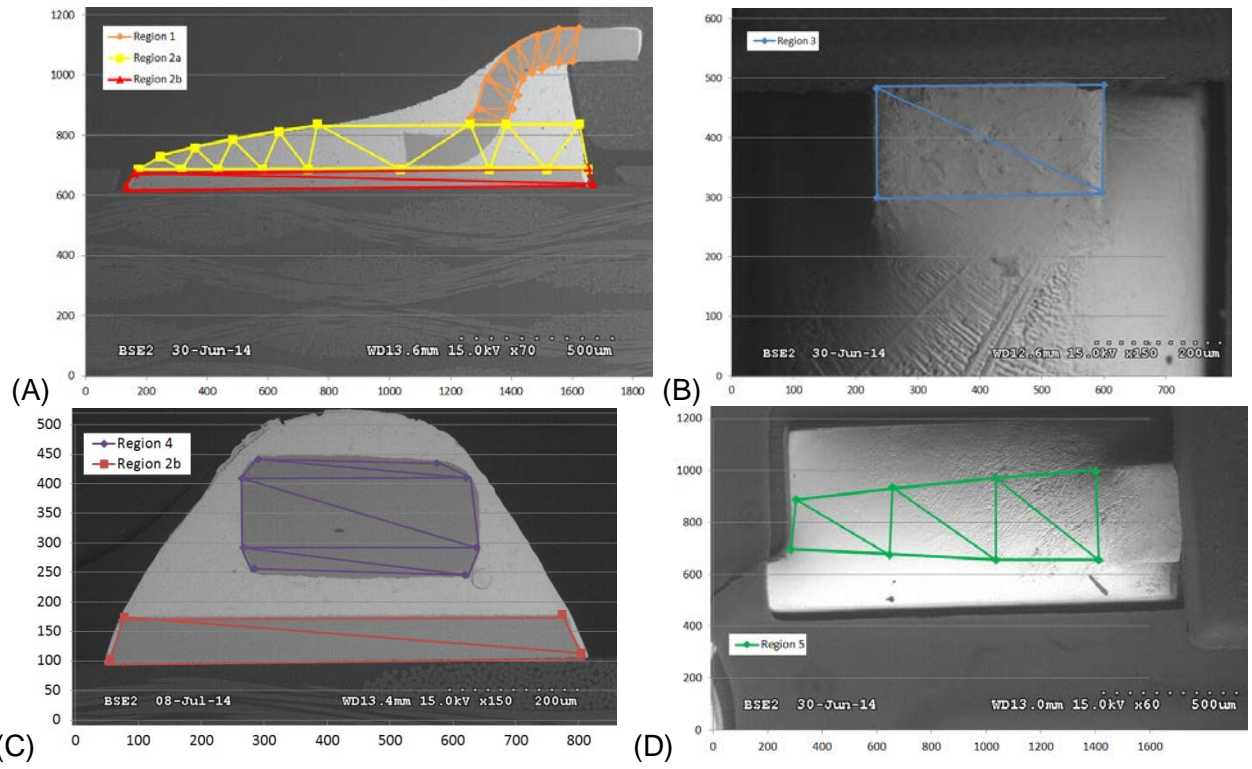


Figure 100: The SOT 3 coordinates graphed overtop the SEM image; (A) regions 1, 2a and 2b, (B) region 3, (C) region 4 and 2b, and (D) region 5.

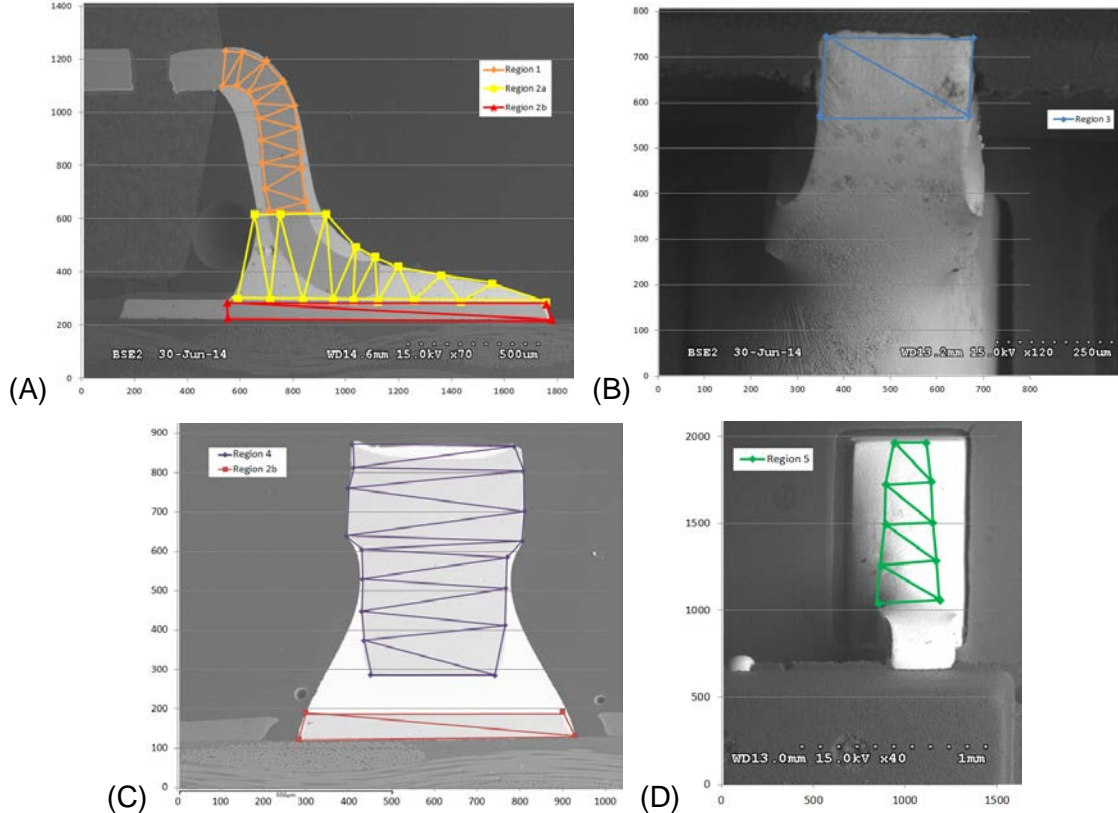


Figure 101: The SOT 5 coordinates graphed overtop the SEM image; (A) regions 1, 2a and 2b, (B) region 3, (C) region 4 and 2b, and (D) region 5.

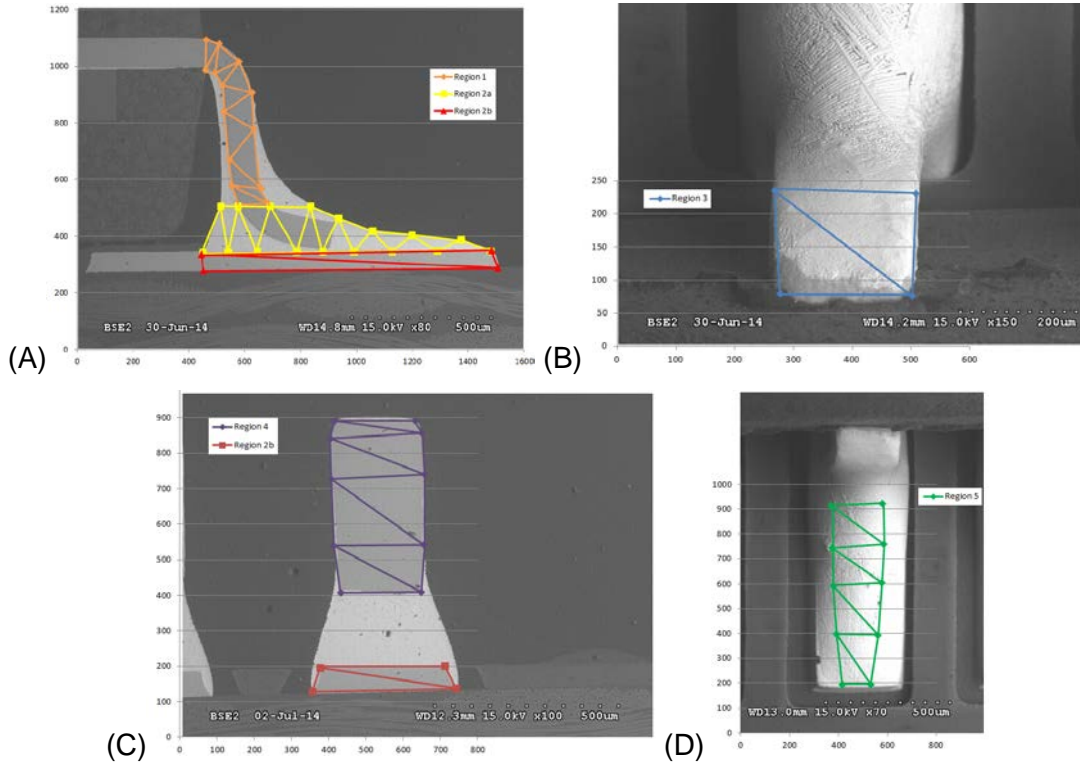


Figure 102: The SOT 6 coordinates graphed overtop the SEM image.

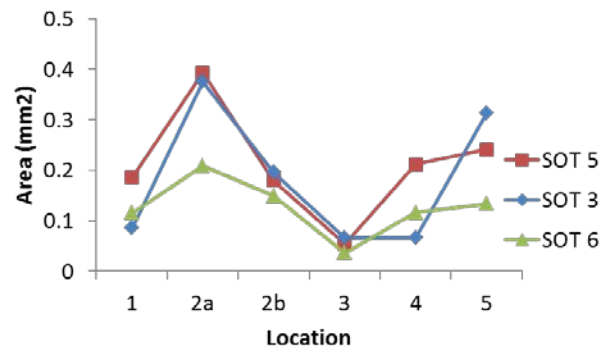


Figure 103: Summary of whisker growth location areas for the SOT3, SOT5 and SOT6 part terminations.

Table 21: Computed areas for the SOT3 whisker growth locations (mm^2).

SOT 3	
Loc 1 Area	0.0863
Loc 2a Area	0.3754
Loc 2b Area	0.1963
Loc 3 Area	0.0661
Loc 4 Area	0.0664
Loc 5 Area	0.3138
Total	1.1046

Table 22: Computed areas for the SOT5 whisker growth locations (mm²).

SOT 5	
Loc 1 Area	0.1867
Loc 2a Area	0.3930
Loc 2b Area	0.1798
Loc 3 Area	0.0544
Loc 4 Area	0.2115
Loc 5 Area	0.2413
TOTAL	1.2667

Table 23: Computed areas for the SOT6 whisker growth locations (mm²).

SOT 6	
Loc 1 Area	0.1160
Loc 2a Area	0.2084
Loc 2b Area	0.1493
Loc 3 Area	0.0364
Loc 4 Area	0.1166
Loc 5 Area	0.1334
Total	0.7601

8. Primary experiment 1 results and discussion: PCTC +50 to 85°C cycling

8.1 Experimental conditions

The environment simulates the condition where an electronic assembly is maintained at a high temperature and the power is turned on and off simulating high temperature operation [29]. The chamber shown in Figure 104 was used. The samples were oriented vertically during the testing. Typical temperature and humidity measurements are shown in Figure 105.

The following experimental conditions were maintained:

- Temperature:
 - Target +50 to 85°C cycling
 - Measured 48 to 88°C, $\Delta T = 40^\circ\text{C}$
 - One hour cycle with 15 minute ramps and dwells
- Humidity:
 - Recorded to be 10% RH at 88 °C to 25% RH at 48°C
- Inspection intervals:
 - Doubled cycle count between inspection intervals
 - Cycles 0 -250 from Sept-13-2011 to Sept-21-2011
 - First inspection (250 Cycles)
 - Cycles 251 -730 from Oct-4-2011 to Nov-1-2011
 - Second inspection (250 + 500 Cycles) (actual count: 250 + 480)
 - Cycles 731 – 1,797 from Dec-1-2011 to Jan-29-2012
 - Third inspection (250+500+1,000 Cycles) (actual count: 250 + 480 + 1067)

In the Cycles 731 - 1797 portion of the experiment, one board of the three board replicates had selected parts contaminated with a ROLO, no-clean flux used for rework. The flux was not cleaned off in order to simulate instances where flux would be trapped under parts during a typical rework [10].



Figure 104: Simulated power cycling temperature cycling chamber.

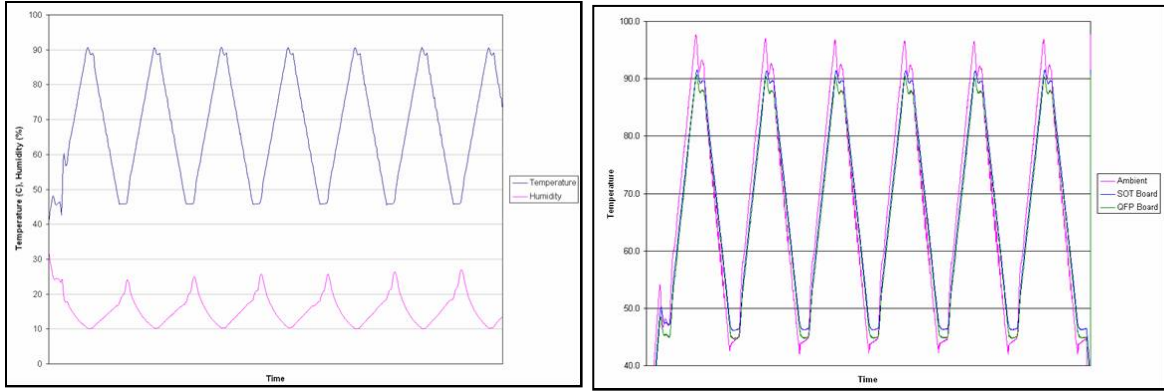


Figure 105: Temperature and humidity during simulated power cycling temperature cycling.

8.2 Whisker growth results

8.2.1 SOT board first inspection: 250 cycles

No hillocks or whiskers were observed during the first inspection.

8.2.2 SOT board second inspection: 730 (250+480) cycles

At the second inspection interval the alloy-42 SOT3 and SOT6 devices grew some whiskers. In contrast, the copper SOT5 did not grow whiskers; only small hillocks were found on the 1-1 board. A summary of the SOT3 and SOT6 alloy 42 whisker inspection results are given in Table 24 and Table 25. Typical whiskers observed during the second inspection are shown in Figure 106. The main factor for growth was the lead material. There was no difference between leads connected to 5V and those either connected to ground or not connected.

Table 24: Alloy-42 SOT3 results from second inspection after 730 PCTC cycles.

Cleanliness		Parts	Leads	# of Whiskers	Max length (microns)
0-0	# Measured	42	126		
	# With whiskers	26 (61.9%)	31 (24.6%)	57	7.1
0-1	# Measured	28	84		
	# With whiskers	12 (42.9%)	13 (15.5%)	29	7.5
1-0	# Measured	28	84		
	# With whiskers	12 (42.9%)	16 (19%)	30	9.4
1-1	# Measured	26	78		
	# With whiskers	14 (53.8%)	19 (24.4%)	44	9.4

Table 25: Alloy-42 SOT6 results from second inspection after 730 PCTC cycles.

Cleanliness		Parts	Leads	# of Whiskers	Max length (microns)
0-0	# Measured	8	48		
	# With whiskers	3 (37.5%)	4 (8.3%)	6	10
1-0	# Measured	8	48		
	# With whiskers	4 (50%)	4 (8.3%)	6	10.7
0-1	# Measured	8	48		
	# With whiskers	7 (87.5%)	13 (27.1%)	17	7.4
1-1	# Measured	8	48		
	# With whiskers	4 (50%)	4 (8.3%)	12	10.4

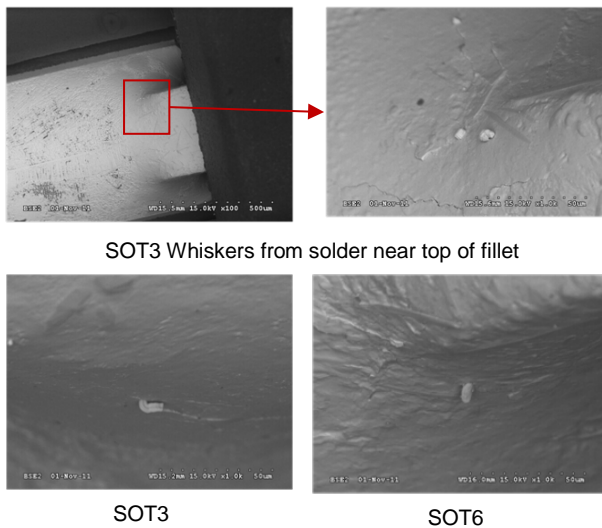


Figure 106: Whiskers observed after 730 PCTC cycles on alloy 42 parts with a 1-1 board (part contamination and assembly contamination).

8.2.3 SOT board third inspection: 1,797 (250 + 480 + 1067) cycles

As shown in Figure 107 and Figure 108, both the number of components that grew whiskers and the maximum whisker length increased from the second to the third inspection. Summaries of the alloy-42 part whisker inspection results are given in Table 26 to Table 29. The copper parts exhibited little whisker growth (Table 30). The box plot given in Figure 109 shows that the alloy-42 leads yielded the longest whiskers. Contamination had a moderate effect on the whisker growth on the alloy-42 leads. Note that the box and probability plots only include whiskers greater than one micron long.

As has been observed in other studies [77], the whisker lengths fit the lognormal distribution well. The alloy-42 probability plots shown in Figure 110 and Figure 111 indicate that there is a slight increase in whisker length with increased contamination. The whiskers on the SOT3 without flux were slightly shorter than those on the SOT6 and there was little difference between the two parts when flux was applied. Recalling that the contamination level of

the SOT3 was $2.2 \mu\text{g/in}^2$ while the SOT6 was $7.2 \mu\text{g/in}^2$, this data supports the trend that more contamination yields longer whisker growth. Part voltage bias was not a strong factor for whisker growth in this environment.

Recall that between the second and the third inspection some ROL0 flux was added to parts on board replicate three to simulate rework without cleaning. Examining all other factors combined, the flux contamination resulted in the longest whisker growth. The incomplete thermal activation of the flux contributed whisker growth even though the moisture levels were very low. The promotion of whisker growth from flux has also been observed by Ueshima [34] and Snugovsky [10] [18]. The copper lead whiskers were the short and very few were observed. As shown in the metallurgical assessment section, the whiskers on the alloy-42 part terminations grew from the lead region near the top of solder fillet.

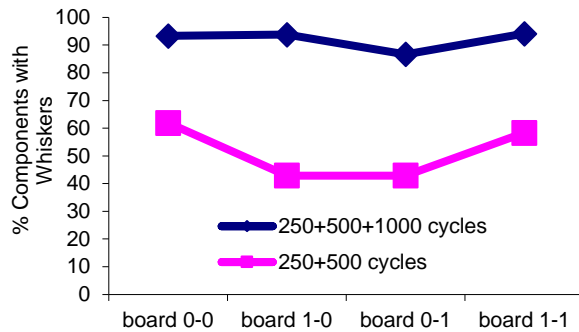


Figure 107: Percentages of SOT3 parts that grew whiskers between the second (730 cycles) and the third (1,797 cycles) PCTC inspection interval.

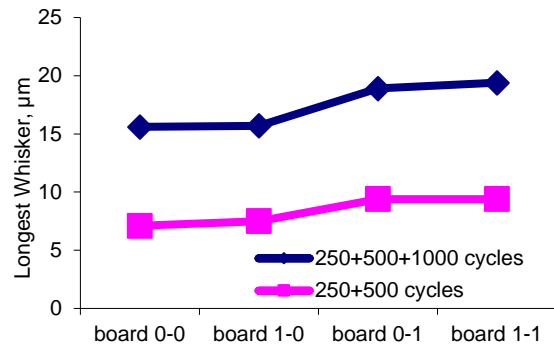


Figure 108: Maximum whisker lengths of SOT3 parts between the second (730 cycles) and the third (1,797 cycles) PCTC inspection interval.

Table 26: Alloy-42 SOT3 with no flux results from third inspection after 1,797 PCTC cycles.

Cleanliness		Parts	Leads	Total Whiskers	Max length (microns)	Average whisker per part
0-0	# Measured	15	45	45	15.6	3
	# With whiskers	14	27			
	Percent with whiskers	93.3	60			
1-0	# Measured	16	48	58	15.7	3.6
	# With whiskers	15	28			
	Percent with whiskers	93.8	58.3			
0-1	# Measured	15	45	43	18.9	2.9
	# With whiskers	13	18			
	Percent with whiskers	86.7	40			
1-1	# Measured	17	51	70	19.4	4.1
	# With whiskers	16	26			
	Percent with whiskers	94.1	51			

Table 27: Alloy-42 SOT3 with flux results from third inspection after 1,797 PCTC cycles.

Cleanliness		Parts	Leads	Total Whiskers	Max length (microns)	Average whisker per part
0-0	# Measured	10	30	28	15.4	2.8
	# With whiskers	9	18			
	Percent with whiskers	90	60			
1-0	# Measured	8	24	29	15.7	3.6
	# With whiskers	7	11			
	Percent with whiskers	87.5	45.8			
0-1	# Measured	8	24	25	18.9	3.1
	# With whiskers	6	9			
	Percent with whiskers	75	37.5			
1-1	# Measured	9	27	36	24.6	4
	# With whiskers	9	17			
	Percent with whiskers	100	63			

Table 28: Alloy-42 SOT6 with no flux results from third inspection after 1,797 PCTC cycles.

Cleanliness		Parts	Leads	# of Whiskers	Max length (microns)	Average whisker per part
0-0	# Measured	9	54	35	14.1	3.9
	# With whiskers	9	18			
	Percent with whiskers	100	33.3			
1-0	# Measured	13	78	76	19.5	5.8
	# With whiskers	13	38			
	Percent with whiskers	100	48.7			
0-1	# Measured	10	60	39	13.9	3.9
	# With whiskers	9	20			
	Percent with whiskers	90	33.3			
1-1	# Measured	10	60	29	17.3	2.9
	# With whiskers	7	15			
	Percent with whiskers	70	25			

Table 29: Alloy-42 SOT6 with flux results from third inspection after 1,797 PCTC cycles.

Cleanliness		Parts	Leads	# of Whiskers	Max length (microns)	Average whisker per part
0-0	# Measured	4	24	17	14.7	4.3
	# With whiskers	4	10			
	Percent with whiskers	100	41.7			
1-0	# Measured	5	30	40	20.7	8
	# With whiskers	5	20			
	Percent with whiskers	100	66.7			
0-1	# Measured	4	24	36	17.5	9
	# With whiskers	4	15			
	Percent with whiskers	100	62.5			
1-1	# Measured	4	24	38	21	9.5
	# With whiskers	4	15			

	Percent with whiskers	100	62.5			
--	-----------------------	-----	------	--	--	--

Table 30: Copper SOT5 results from third inspection after 1,797 PCTC cycles.

Cleanliness	Flux contamination	Lead	Location	Whisker Length (microns)
1-1	NO	3	5	2.7
1-1	NO	1	3	1.8
1-1	NO	1	3	0.5
0-0	NO	3	4	1.7
0-0	YES	4	4	0.5
0-1	YES	5	5	8.3
0-1	YES	5	5	6.5

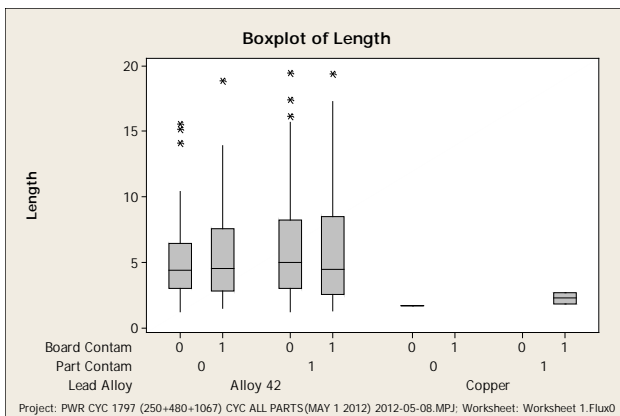


Figure 109: Box plot comparing whisker length (microns) for lead alloy, part contamination and board contamination combinations after 1,797 PCTC cycles where no flux was applied.

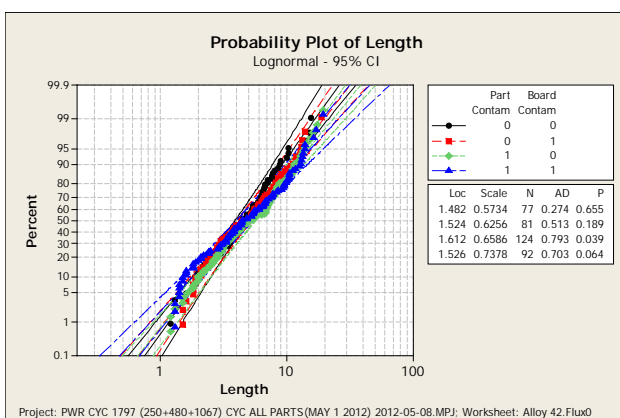


Figure 110: Whisker length (microns) probability plot for the alloy-42 leads with no flux after 1,797 PCTC cycles for various board contamination combinations.

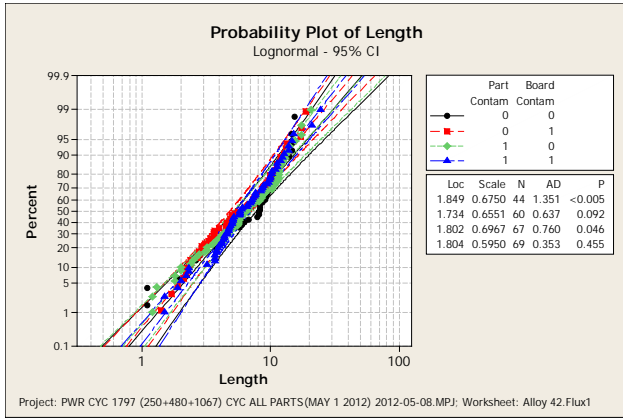


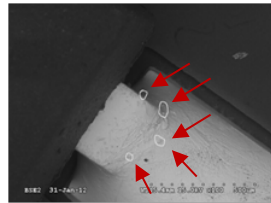
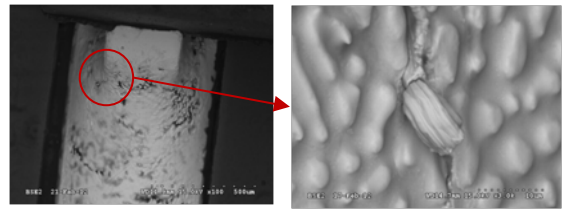
Figure 111: Whisker length (microns) probability plot from the alloy-42 lead set with flux applied after 1,797 PCTC cycles for various board contamination levels.

8.3 Metallographic evaluation

8.3.1 SOT metallographic observations

As is seen in Figure 112 and Figure 113, in some cases, the whiskers grew from between the tin dendrites. Figure 114 illustrates that there are several stress relaxation mechanisms occurring. In addition to whisker growth, there is grain boundary sliding, crack formation and grain recrystallization. The micro-cracks (Figure 115) that have formed to relieve the stresses often occur between the primary tin dendrites, around the Cu₆Sn₅ IMC, and in some cases through Ag₃Sn IMC after thermal cycling.

Cross-section images shown in Figure 116, Figure 117 and Figure 118 revealed the presence of corrosion, IMC nodules and thick IMC growth on the lead. The intermetallic is a Cu-Ni-Sn ternary intermetallic where the Ni source is the alloy-42 lead and the Cu source is the solder and the Cu board pad. The IMC on the board Cu pads before cycling was 2.6 microns and after cycling was 3.0 microns, but the IMC thickness on lead increased dramatically as is shown in Figure 118. Before cycling the IMC on the lead was 0.3 microns and after thermal cycling it was 1.6 microns, an increase of more than 5x. This significant intermetallic growth is expected to increase the compressive stresses that promote whisker growth.



Whiskers grow from solder where lead exits main fillet

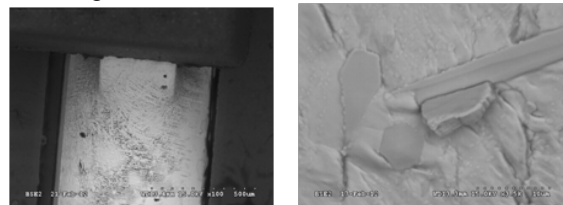


Figure 112: Whiskers observed on the SOT3 part with 1-1 contamination without flux after 1,797 PCTC cycles.

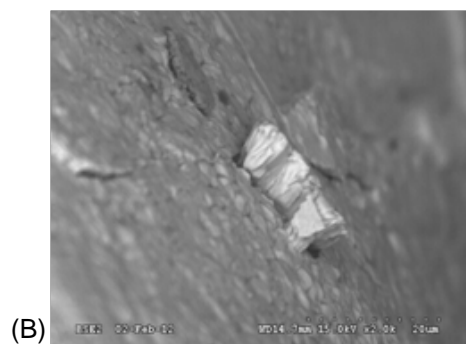
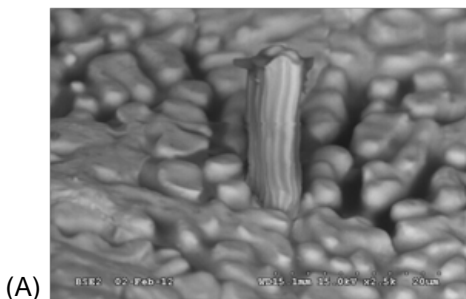


Figure 113: Whiskers observed on the SOT6 part with 1-1 contamination with flux applied after 1,797 PCTC cycles.

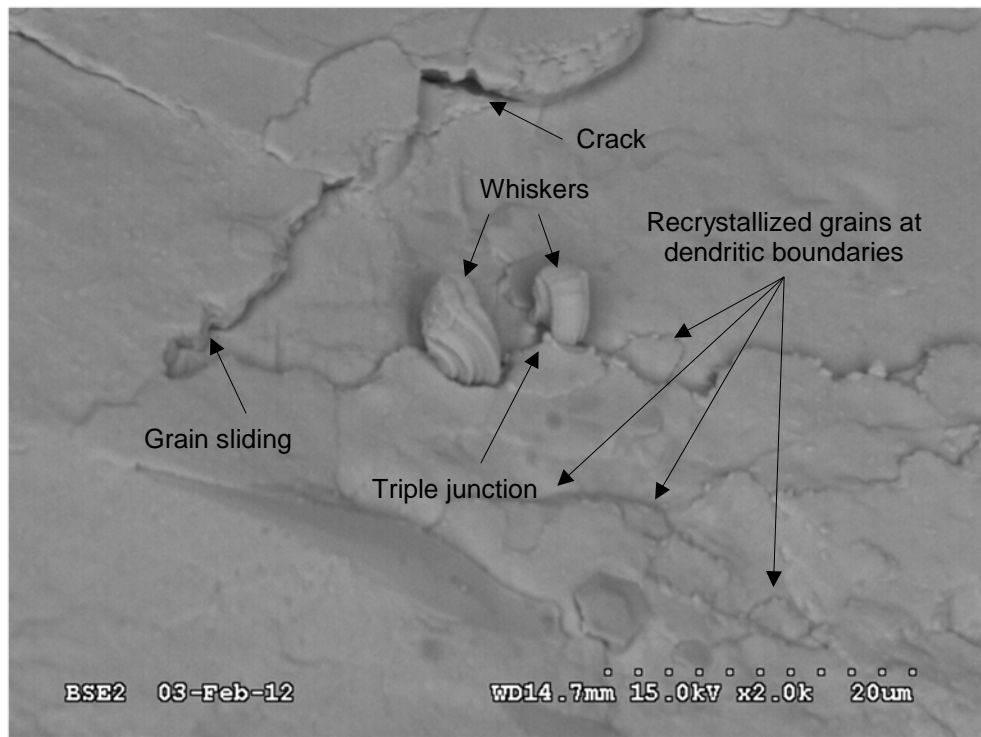


Figure 114: Competing mechanisms of stress relaxation (SOT3, 0-0 contamination level) after 1,797 PCTC cycles.

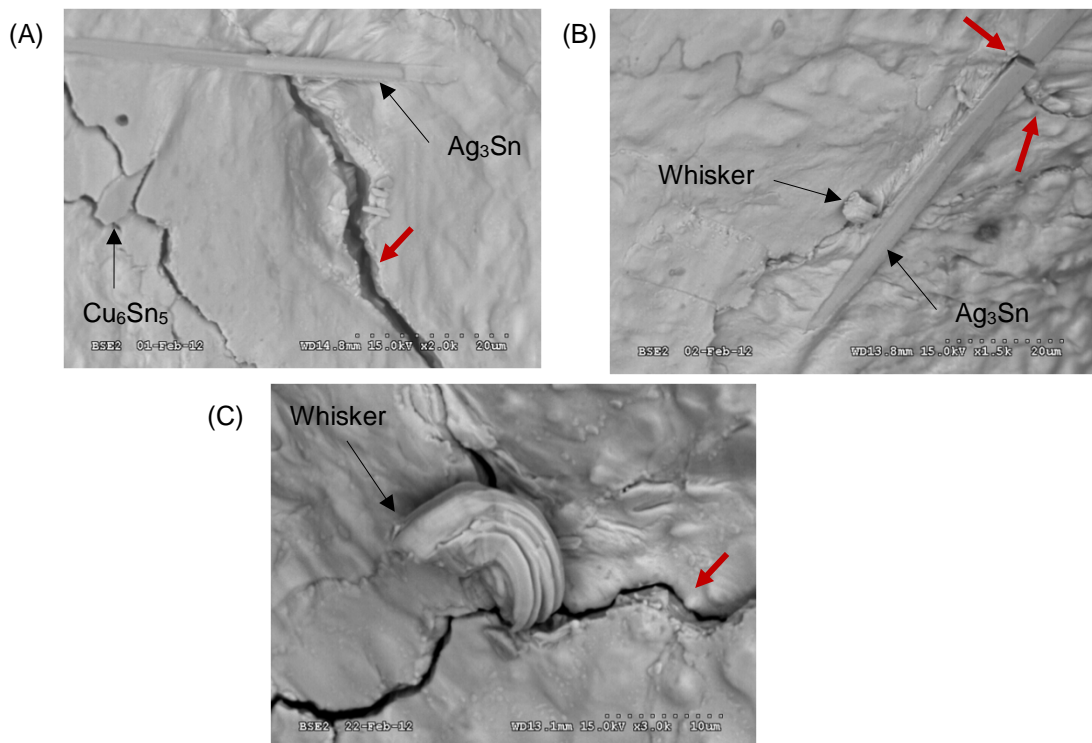


Figure 115: Micro-cracks (red arrows) in SAC305 fillets observed after 1,797 PCTC cycles; (A) SOT3 0-0 contamination level, (B) SOT3 1-1 contamination level with whisker adjacent to Ag_3Sn IMC and (C) SOT3 1-0 contamination level with whisker growing from primary tin dendrite triple junction Micro-cracks.

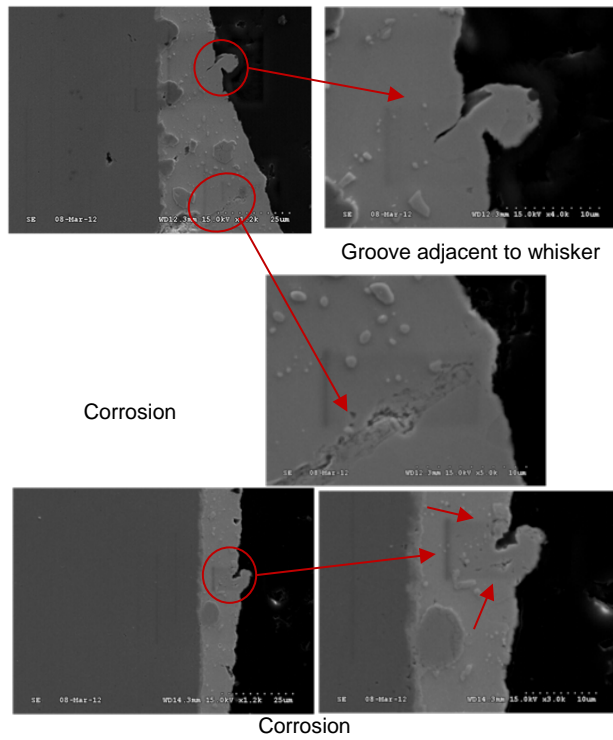


Figure 116: Cross-sections of a whisker growing from solder on a SOT6 alloy-42 lead with 1-1 contamination without flux showing evidence of corrosion after 1,797 PCTC cycles.

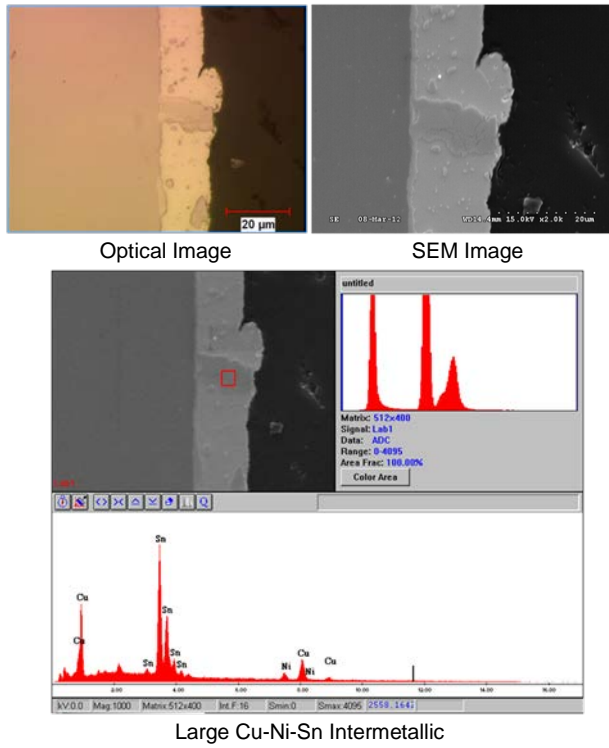


Figure 117: Cross-sections of a whisker growing from solder on a SOT6 alloy-42 lead with 1-1 contamination with flux applied after 1,797 PCTC cycles.

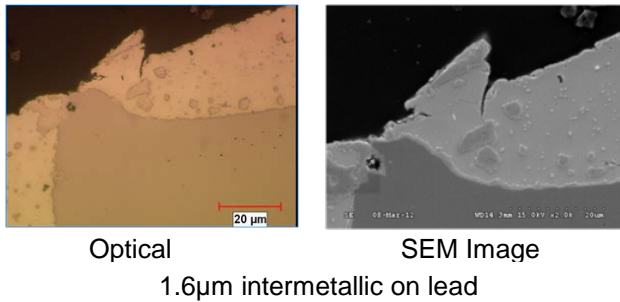


Figure 118: Cross-sections of a whisker growing from solder on a SOT6 alloy-42 lead with 1-1 contamination with flux applied after 1,797 PCTC cycles.

8.3.2 BGA ball whisker examination

The inspection for whisker growth on the SAC105 and SAC105+0.01Ce alloy balls soldered with SAC305 paste was performed at the second inspection point, 730 cycles. On a cleaned board with no contamination, the SAC105 balls did not form whiskers while the SAC105 with a very small amount of Ce had whisker growth (Figure 119). The whisker growth was not limited to a particular region of the ball surface.

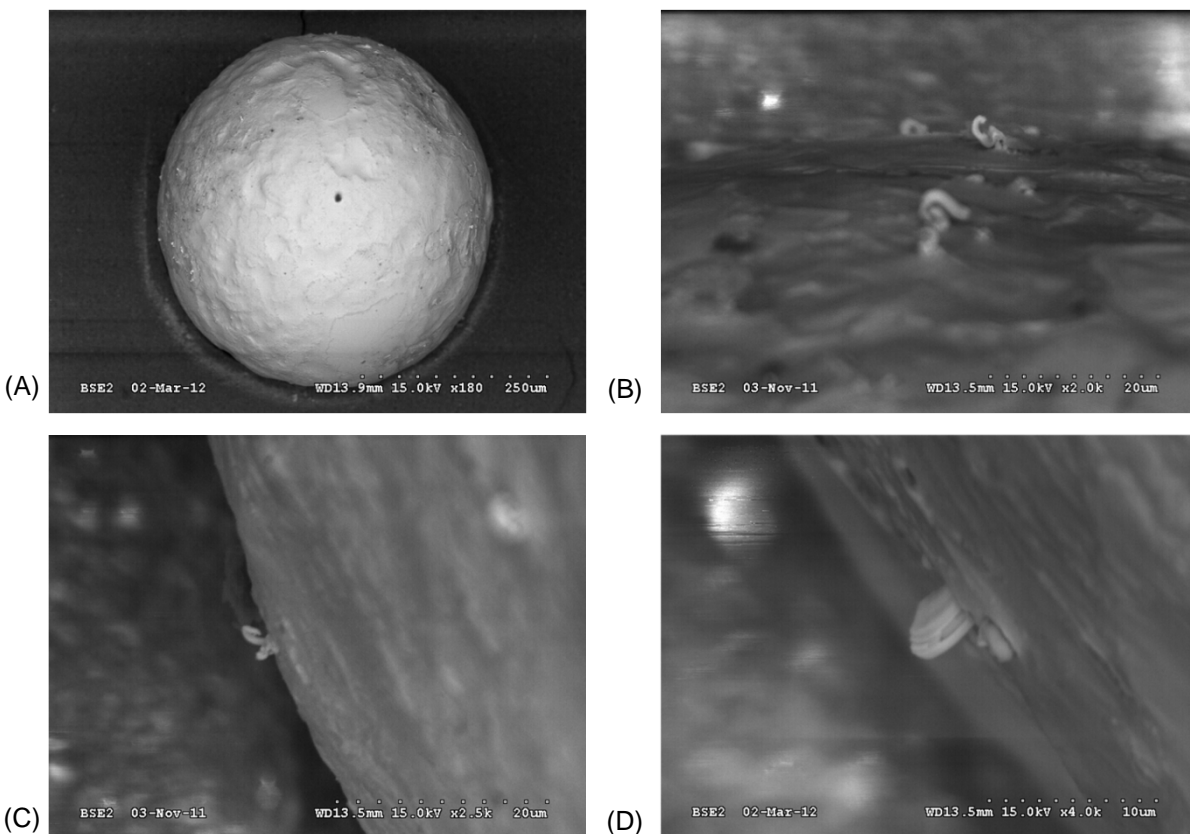


Figure 119: SEM images of tin whisker growth on SAC105+0.01Ce alloy balls soldered with SAC305 paste on a cleaned board with no contamination at the second simulated power cycling inspection point after 730 PCTC cycles; (A) overall ball, and (B-D) higher magnification images of whiskers.

8.4 Conformal coating

Conformal coating is a primary mitigation against the detrimental effects of whisker growth. No cracks were observed in the coating (Figure 120). One of the challenges with liquid coating spray application is obtaining uniform coating thickness. Surface tension causes coating thinning over corners and gravity forces result in coating thinning on vertical surfaces.

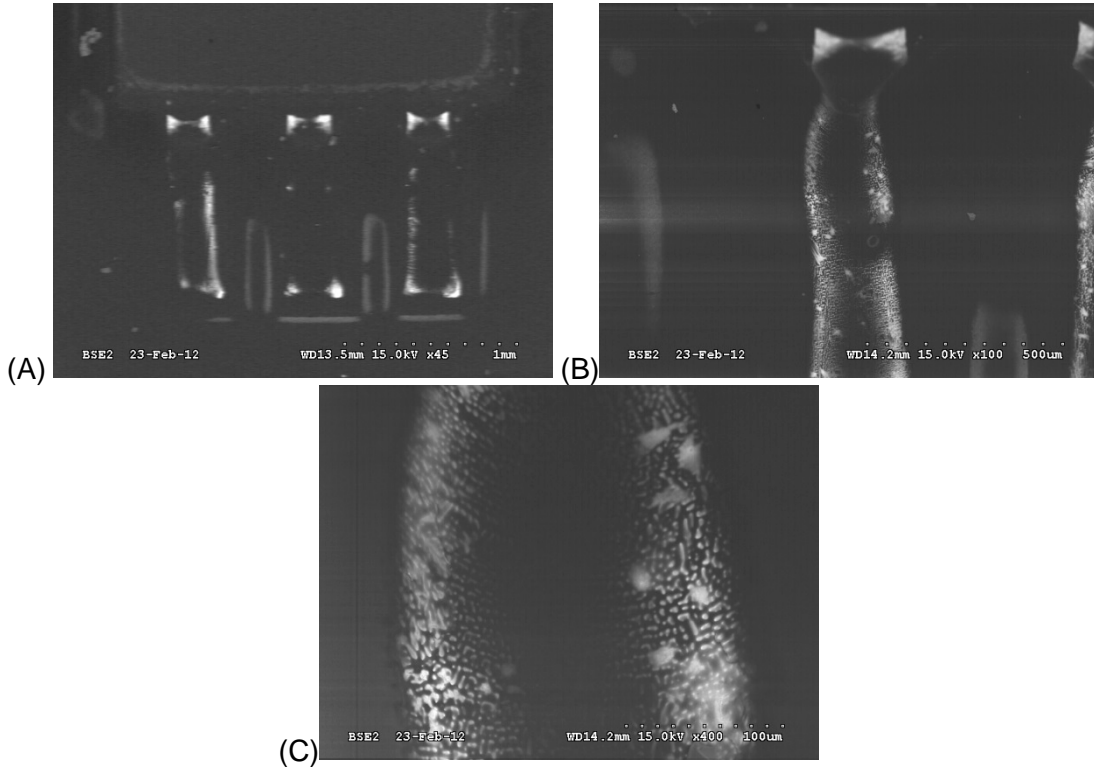


Figure 120: Conformal coating on SOT3 alloy-42 part after 1,797 PCTC cycles; (A) SOT6, 45x (B) SOT6, 100x, and (C) SOT6, 400X. No cracks observed.

8.5 Summary

The present experiment studied a combination of factors existing on representative production assemblies. The alloy-42 lead material is relatively common on small outline transistor and hermetic devices. Furthermore, the contamination levels used for the intentional contamination testing were consistent with production levels. Whisker growth from SAC305 was observed on all configurations except some of the copper lead configurations. In addition to whisker growth, grain boundary sliding, crack formation and grain recrystallization stress relaxation mechanisms were also observed. The most significant factor for whisker growth was the lead material and the next most significant factor was the contamination level. The alloy-42 leads with both the pre-soldering Cl contaminated parts and the post soldering contaminated assemblies grew the longest whiskers. The simulated power cycle thermal cycling temperature range in the present work was considerably lower than the industry piece part tests [23], but was sufficient to promote whisker incubation and growth. The difference in whisker growth between alloy-42 and copper indicates that the source of the whisker formation stress is due to the thermal expansion mismatch between the alloy-42 and the SAC305 solder. There was also a considerable increase in Cu-Ni-Sn intermetallic on the leads after the thermal cycling which could also promote whisker growth. The increase in whisker growth due to the presence of contamination was a little more surprising because the chamber air at the +50 °C low temperature cycling limit has low humidity. The inspection showed that the SAC105 balls did not form whiskers while the SAC105 with 0.01%Ce had whisker growth.

9. Primary experiment 2 results and discussion: TC -55 to +85°C cycling

9.1 Experimental conditions

Assemblies were tested using the JESD201 -55 to +85°C temperature profile [30] (10 minute dwells, three cycles per hour) in the chamber shown in Figure 121. A piston driven basket moved the samples between the hot and cold zones. During the test, select circuits had a five volt bias applied. The samples were mounted with the components facing down. The temperature was controlled using thermocouples in the chamber air stream. The humidity was not monitored or controlled. The whisker inspection was performed after 500 cycles. After the inspection, the samples were placed back in the chamber and re-examined after a total of 2,110 cycles (500+1,610).

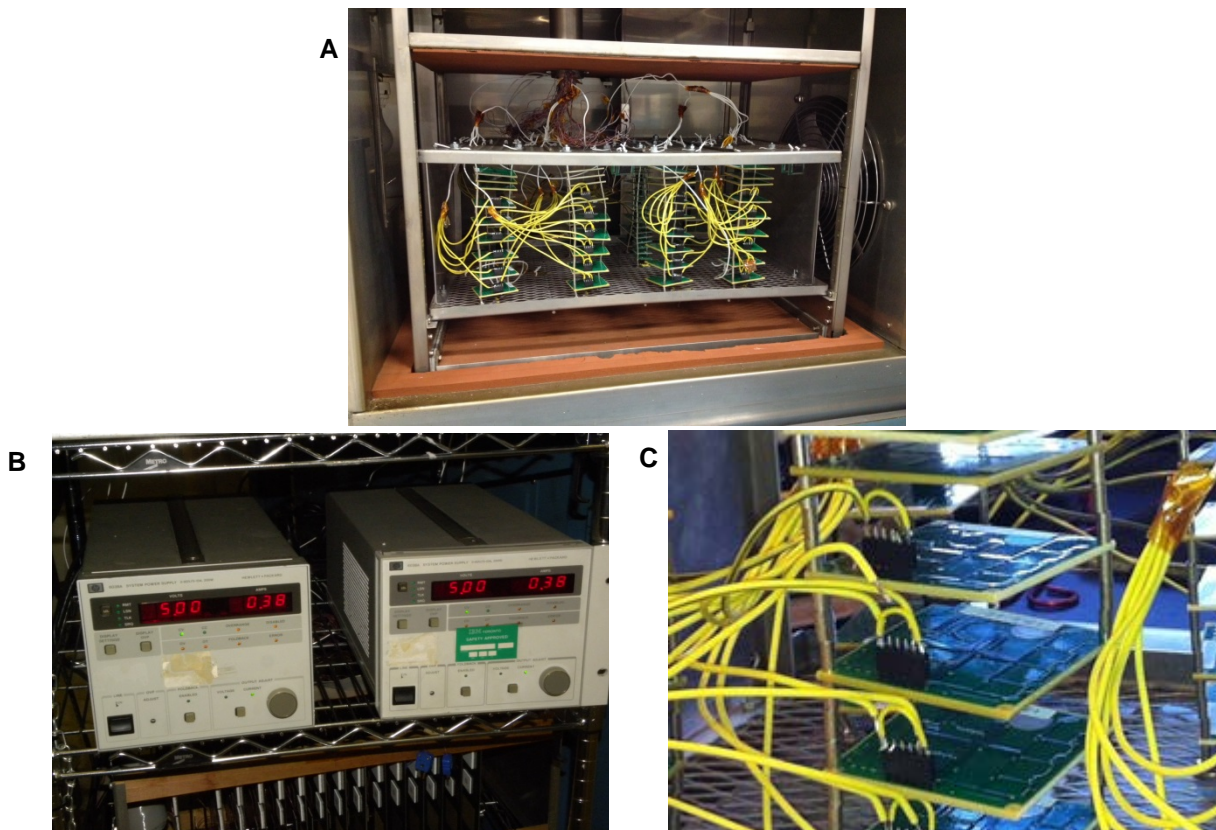


Figure 121: Sample set-up; (A) Thermal shock cycling chamber, (B) bias power supplies and (C) sample orientation in the chamber.

9.2 Whisker growth results

The greatest whisker nucleation and growth occurred from the alloy-42 leads. During thermal cycling, the whisker growth is driven by the CTE differences between the low CTE alloy-42 and the higher CTE solder. The longest whiskers were on the SOT6 termination; 32 microns after 500 cycles and 115 microns after 2,110 (500 + 1,610). The whiskers on the alloy-42 lead terminations predominantly grew from regions where the solder was thin near the top of the main solder fillet; however, there were also massive tin eruptions indicating a significant amount non whisker stress relaxation.

9.2.1 First inspection: 500 cycles

After 500 cycles of -55 to 85°C cycles (three cycles per hour), a total of 9,141 whiskers were counted and 207 were measured (Table 31). The majority of the whiskers grew on the alloy-42 lead terminations. The longest whiskers are: SOT6 – 32 microns, SOT3 – 21 microns and SOT5 – 16 microns. Contamination and voltage bias did not have a significant impact on whisker growth.

Table 31: Whisker measurement summary after 500 TC cycles.

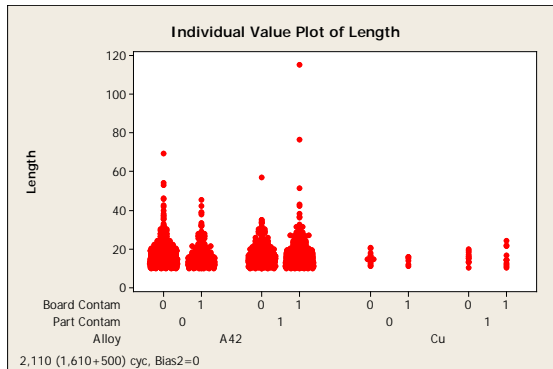
Component	Counted	Measured	Percent measured
SOT3	3474	40	1%
SOT6	5120	159	3%
SOT5	547	8	1%
Total	9141	207	2%

9.2.2 Second Inspection: 2,110 (500+1,610) Cycles

The samples were returned to the environmental chamber and an additional 1,610 cycles were accumulated. Then the exact same parts and leads previously examined at 500 cycles were re-inspected. After 2,110 (500+1,610) cycles, a total of 24,879 whiskers were counted and 2,360 whiskers were measured (Table 32). The whisker lengths are longer for alloy-42 than copper lead terminations (Figure 122 and Figure 123). The longest whiskers are: SOT6 – 115 microns, SOT3 – 64 microns and SOT5 – 24 microns. The whiskers on the alloy-42 lead terminations predominantly grew from regions where the solder was thin near the top of the main solder fillet (Figure 124). On the alloy-42 lead solder joints, several competing stress relaxation mechanisms in addition to whisker growth were found including excessive deformation, volume recrystallization with massive eruptions of the recrystallized grains (see bottom of Figure 124(B) and Figure 125). The copper alloy solder joints had very few whiskers and little evidence of solder recrystallization (Figure 126).

Table 32: Whisker measurement summary after 2,110 TC cycles.

Component	Counted	Measured	Percent measured
SOT3	9130	691	8%
SOT6	9866	1606	16%
SOT5	5883	63	1%
Total	24879	2360	9%

**Figure 122:** Individual value plot of whisker lengths (microns) after 2,110 TC cycles broken down by lead alloy, part contamination, and board contamination levels (Note: Bias2=0).

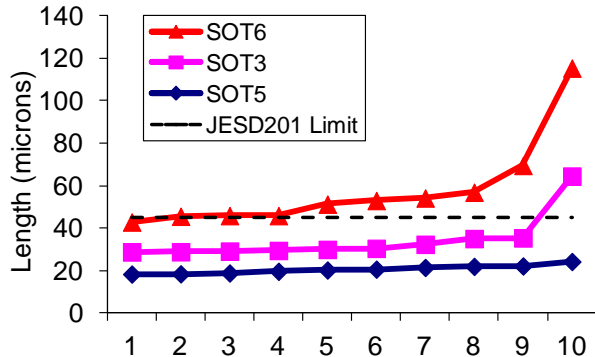


Figure 123: Ten longest whiskers after 2,110 TC cycles.

For the SOT6 and SOT3 alloy-42 leaded part solder joints, locations 1, 3 and 4 have the greatest numbers of whiskers (Figure 127). The SOT5 copper alloy leaded part solder joints had the many locations where no whisker growth occurred (Figure 128). The histogram of whisker location for measured whiskers longer than 10 microns shows similar results (Figure 129).

The lognormal curve fit seems to represent many of the whiskers length distributions reasonably well. Unfortunately some of the longest whiskers did not seem match the lognormal characteristic of the shorter whiskers (Figure 130, Figure 131 and Figure 132). Neither contamination (all parts) nor voltage bias (SOT3 and SOT5) devices had a significant impact on whisker growth.

Comparing whisker diameters for the various part types and lead location shows that the SOT3 and SOT6 parts had somewhat larger average diameters than the SOT5 (Figure 133). The average whisker diameter of the SOT6 part, which exhibited the greatest whisker growth, followed a lognormal distribution (Figure 134). Comparing whisker length with diameter showed that the longest whiskers were less than ten microns in diameter (Figure 135).

The whisker growth angle for the SOT6 parts is uniform (Figure 136).

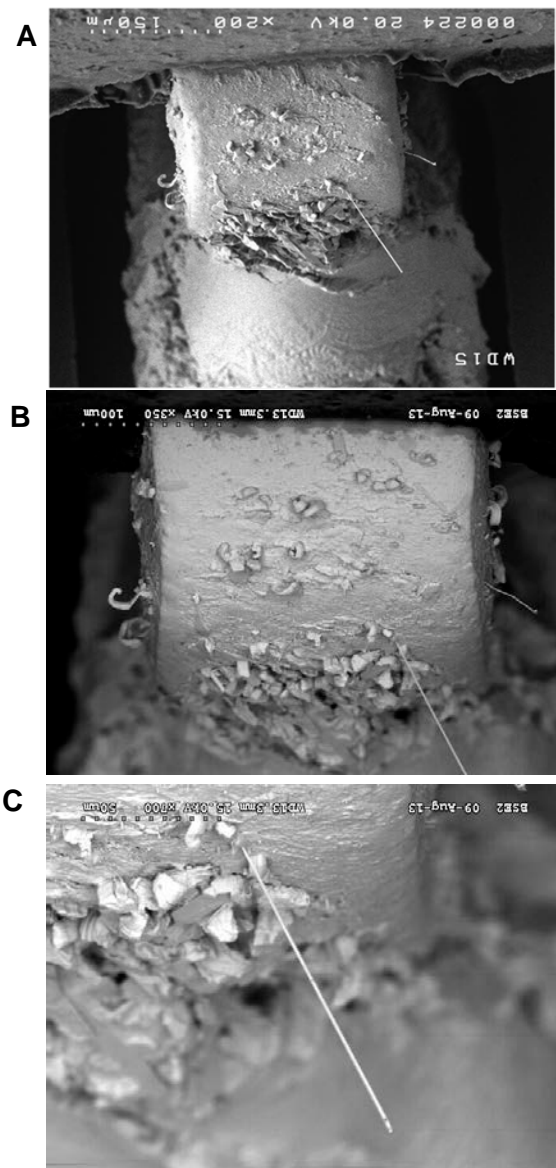


Figure 124: SEM images of whiskers on an alloy-42 lead frame SOT6 part termination with a 1-1 contamination level after 2,110 TC cycles; (A) Overall, (B) 350x close-up, and (C) 700x close-up.

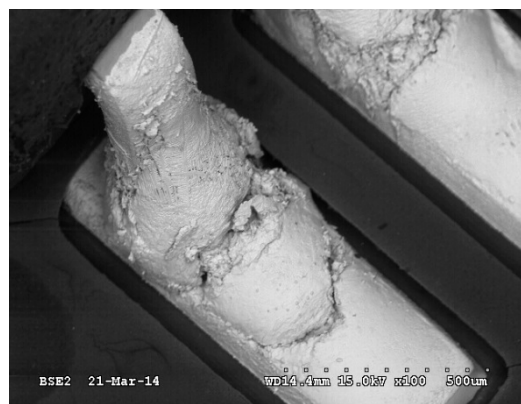


Figure 125: Massive recrystallization and solder fatigue cracks on a SOT6 after 2,110 TC cycles.

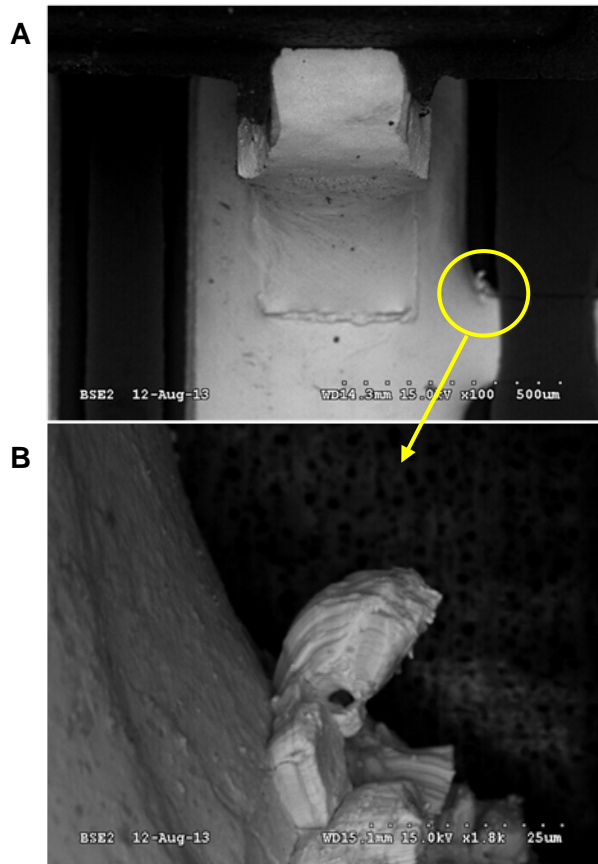


Figure 126: SEM images of whiskers on the board pad on a copper lead frame SOT5 part joint with a 1-1 contamination level after 2,110 TC cycles. (B) 1,800X close-up.

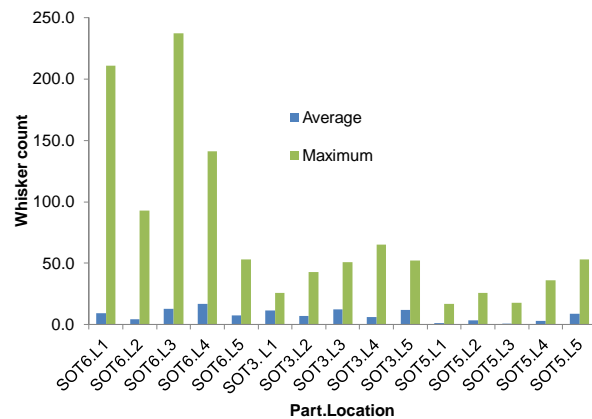


Figure 127: Average and maximum whisker count for the total whisker 24,879 count broken down by part and location after 2,110 TC cycles. Note: minimum whisker count is zero and is not plotted.

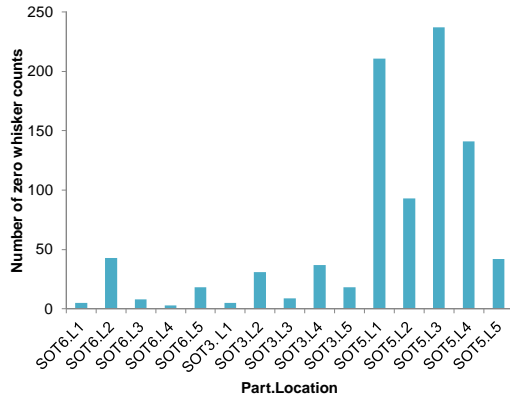


Figure 128: Number of instances where the lead location had no whiskers after 2,110 TC cycles. The SOT5 had many leads with no whiskers.

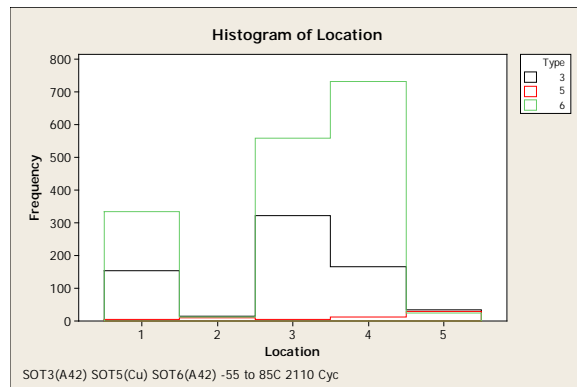


Figure 129: Whisker location histogram for SOT3, SOT5 and SOT6 termination whiskers longer than ten microns after 2,110 TC cycles.

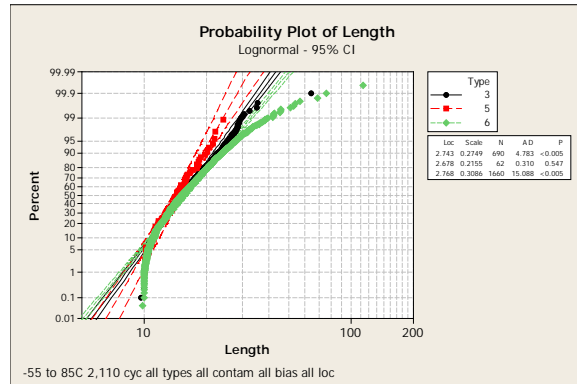


Figure 130: Probability plot of whisker length (microns) for SOT3, SOT5 and SOT6 part terminations with bias=0 after 2,110 TC cycles.

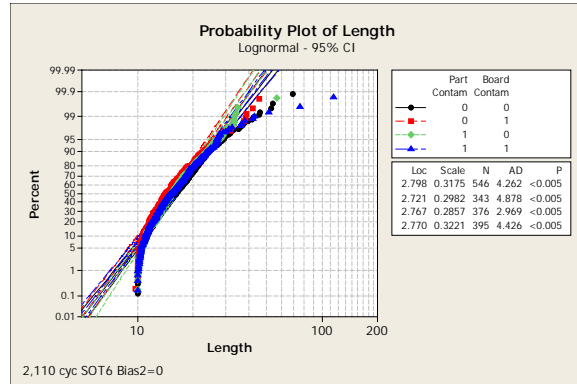


Figure 131: Probability plot of tin whisker lengths (microns) from SOT6 alloy-42 part lead terminations after 2,110 TC cycles.

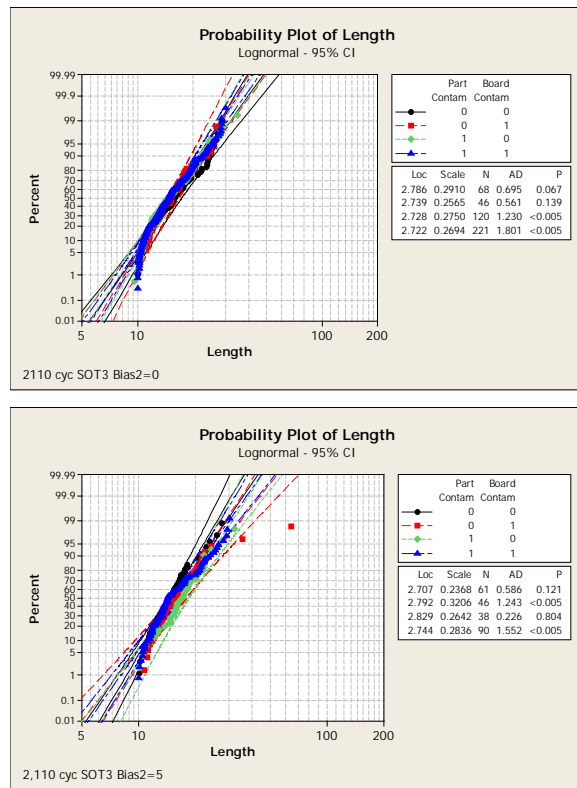


Figure 132: Probability plot of tin whisker lengths (microns) from SOT3 alloy-42 part lead terminations after 2,110 TC cycles with bias2=0 (top) and bias2=5 (bottom).

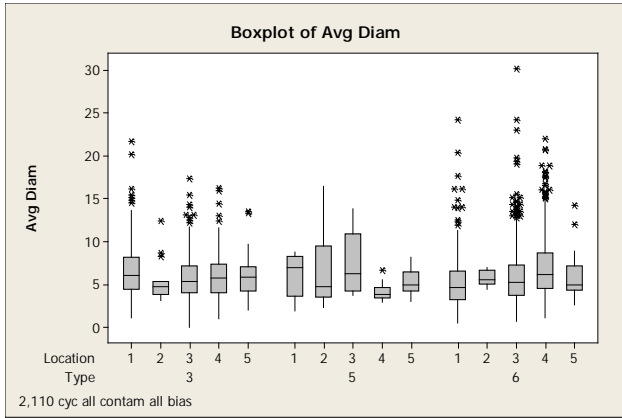


Figure 133: Box plot of average whisker diameter (microns) for the SOT6 part lead terminations after 2,110 TC cycles.

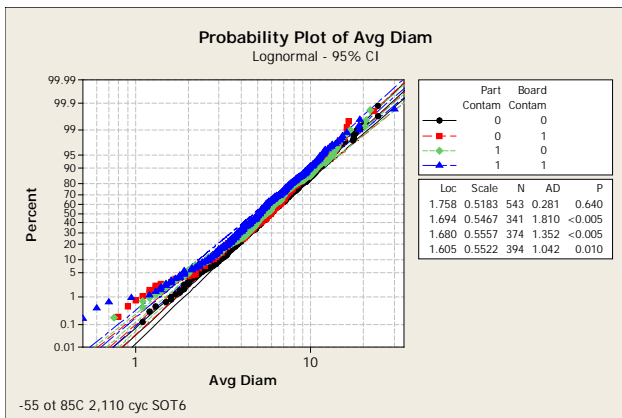


Figure 134: Probability plot of SOT6 average whisker diameter (microns) after 2,110 TC cycles.

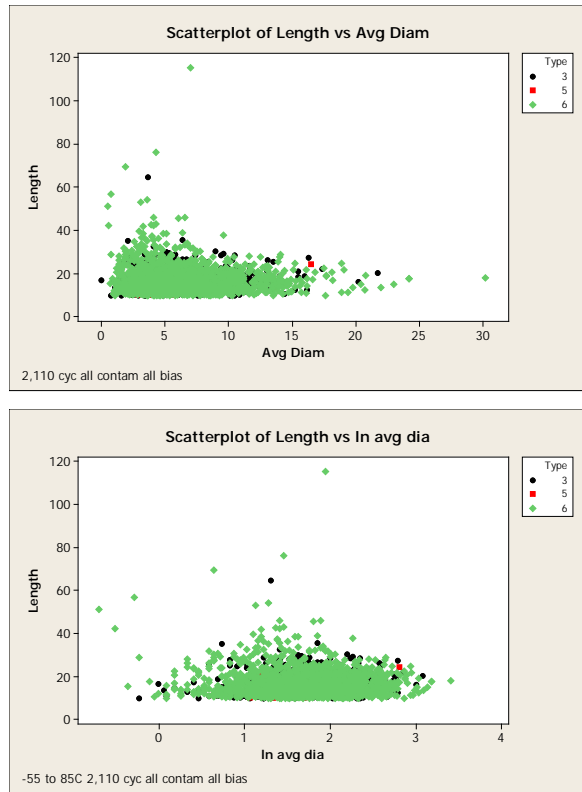


Figure 135: Scatter plot of whisker length (microns) versus diameter (microns) for copper and alloy-42 leads after 2,110 TC cycles; linear diameter (top) and natural log diameter (bottom).

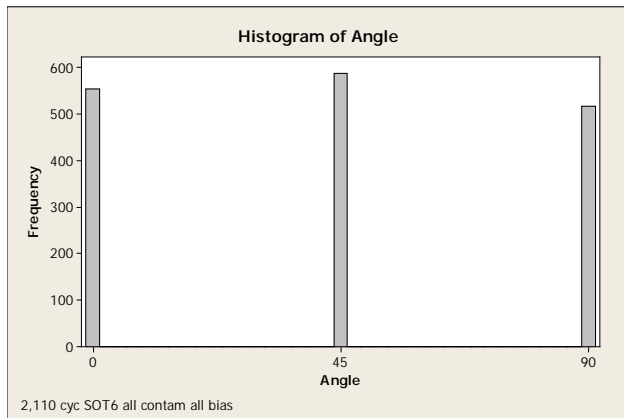


Figure 136: Histogram of whisker growth angle after 2,110 TC cycles.

9.3 Metallographic evaluation

The longest whisker observed in the present experiment grew from the SOT6 alloy-42 lead region above the solder fillet where the solder thickness is approximately 25 to 40 microns (Figure 137). The environments and termination materials result in the most significant solder whisker growth differences (Figure 138). The thermal cycling promotes whisker growth from terminations with alloy-42 lead materials toward the top of the lead while the high temperature high humidity environment has longer whisker growth on copper alloy lead terminations on the board copper pad.

An important consideration for whisker test design is whether or not the whisker growth is stopped by removal of the specimens from the test environment, inspected in the SEM and reintroduced into the test chamber again. The inspection interrupted the whisker growth during high temperature/high humidity whisker testing and could cause an under-reporting of whisker length. After the additional environmental exposure following the 500 cycle inspection, it was found that (1) whiskers can stop growing, (2) new whiskers can grow, (3) existing whiskers can resume growth, or (4) whiskers can retract (Figure 139).

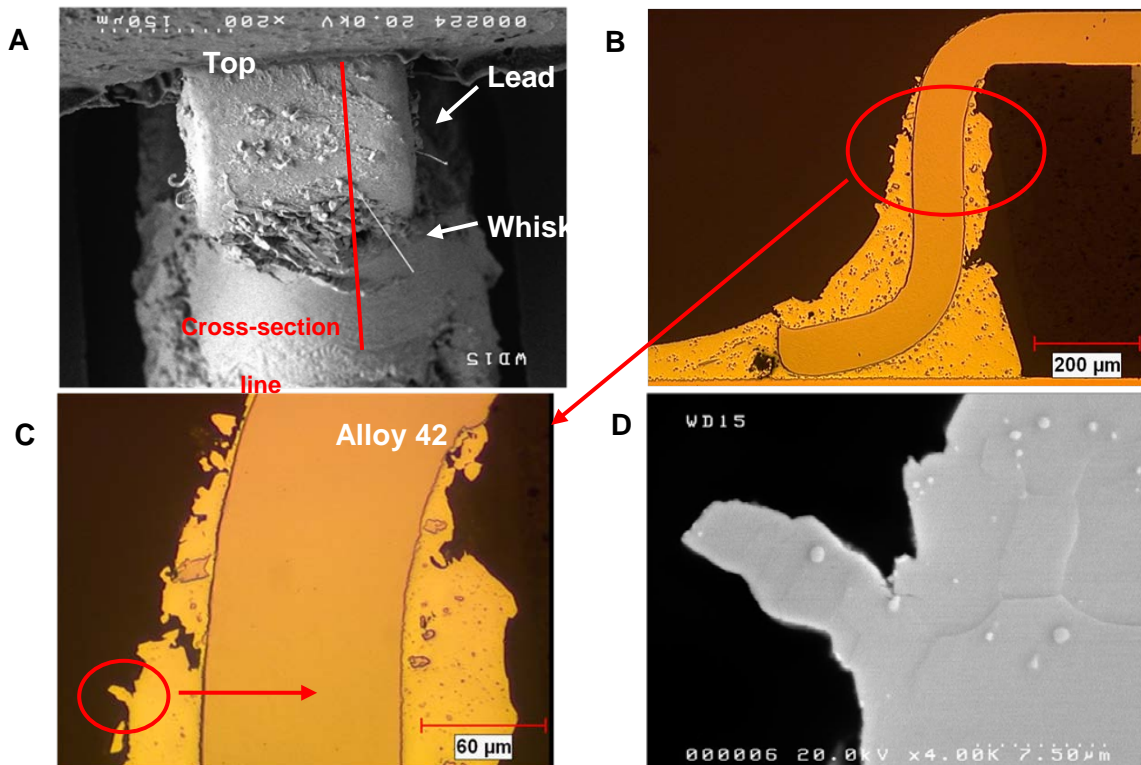


Figure 137: Cross-section of 115 micron long whisker on SOT6 alloy-42 lead with a 1-1 contamination level after 2,110 TC cycles; (A) Overall SEM, (B) overall cross-section optical image, (C) close-up optical image, and (D) SEM image of whisker base.

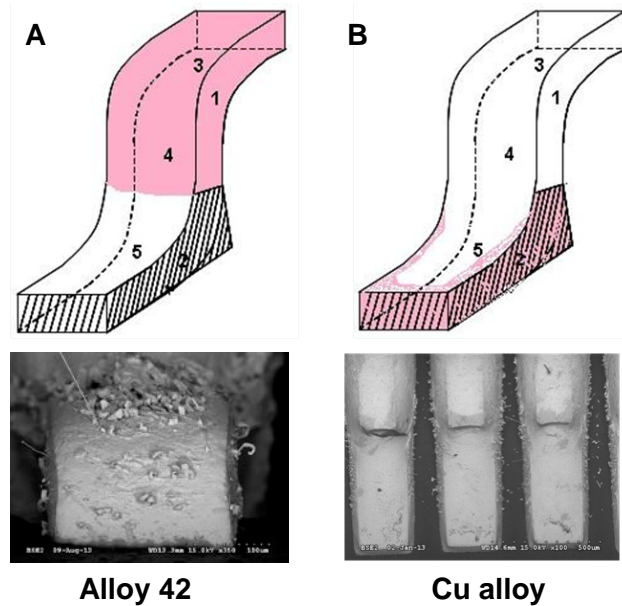


Figure 138: Comparison of whisker growth locations between (A) -55 to 85°C TC cycles and milder +50 to 85°C PCTC cycles with alloy-42 lead terminations dominating whisker growth and (B) 85°C/85% RH HTHH with copper lead terminations having the greatest whisker growth.

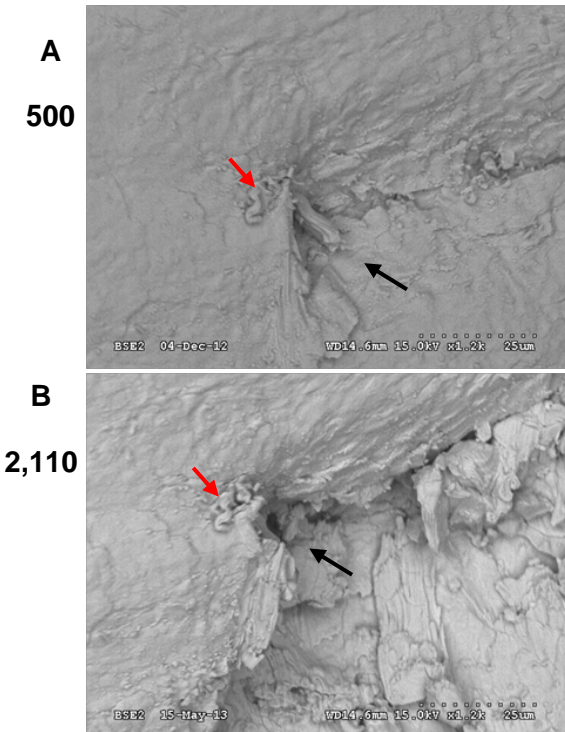


Figure 139: Whisker retraction (black arrow) and whisker growth termination (red arrows) between the (A) 500 and (B) 2,110 TC cycle inspections. SOT3, 0-1 contamination level, U36, lead 3 shown.

Another significant finding in the present work was that the whisker growth angle tended to change between inspection intervals (Figure 140). In some cases, the diameter also changed (Figure 140). In contrast to observations on thin tin [36], an increase in diameter does not correspond to arrested whisker growth.

The whisker nucleation sites are often recrystallized grains. The degree of SAC305 recrystallization is much more extensive in the thermal shock cycling (TC) than the simulated power cycling thermal cycling (PCTC) (Figure 141). There is a difference in both ramp rate and temperature difference between the two cycles. The TC exhibiting many recrystallized grains has a temperature difference of $\Delta T=140^{\circ}\text{C}$ while the PCTC with recrystallized grains at dendritic boundaries has a $\Delta T=35^{\circ}\text{C}$.

Recrystallized grains are not always visible. Sometimes whiskers growth starts from existing sub-grains (Figure 142).

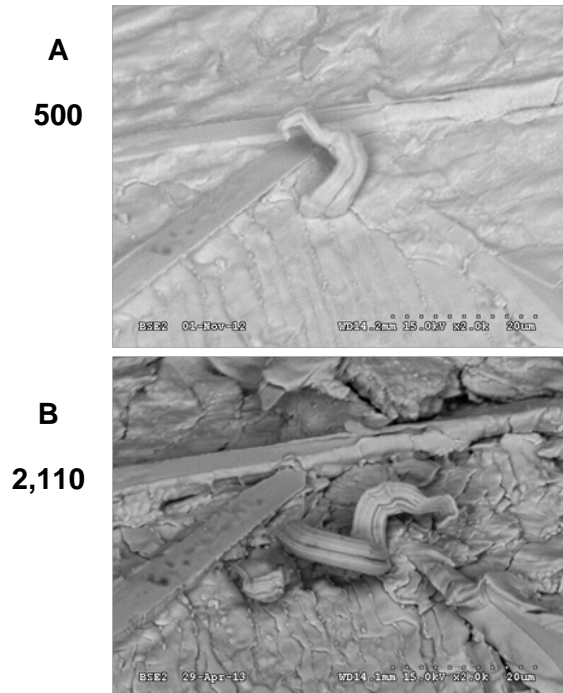


Figure 140: Whisker growth angle and diameter change on alloy-42 lead termination between the (A) 500 and (B) 2,110 TC cycle inspections. SOT3, 1-1 contamination level, U24, lead 1.

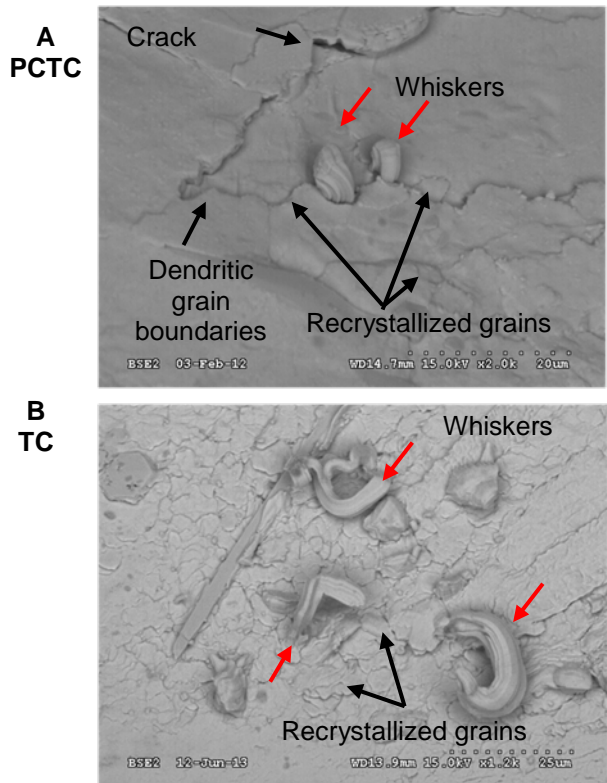


Figure 141: Comparison recrystallized grains after (A) +50 to 85°C PCTC, 1,797 cycles, one cycle per hour, 15 minute dwells, and (B) -55 to 85°C TC, 2,110 cycles, three cycles per hour, 10 minute dwells.

There are also other stress relaxation mechanisms competing with whisker growth. In some cases, significant non-whisker growth was observed between the 500 and 2,110 (500+1,610) cycle inspections. Large step like structures (Figure 143) and massive non-whisker eruptions (Figure 144) grew. Extensive recrystallization was also evident (Figure 145).

The lower stress PCTC cycling formed tin pyramid crystals while the thermal shock cycling in the present work resulted in massive eruptions (Figure 146).

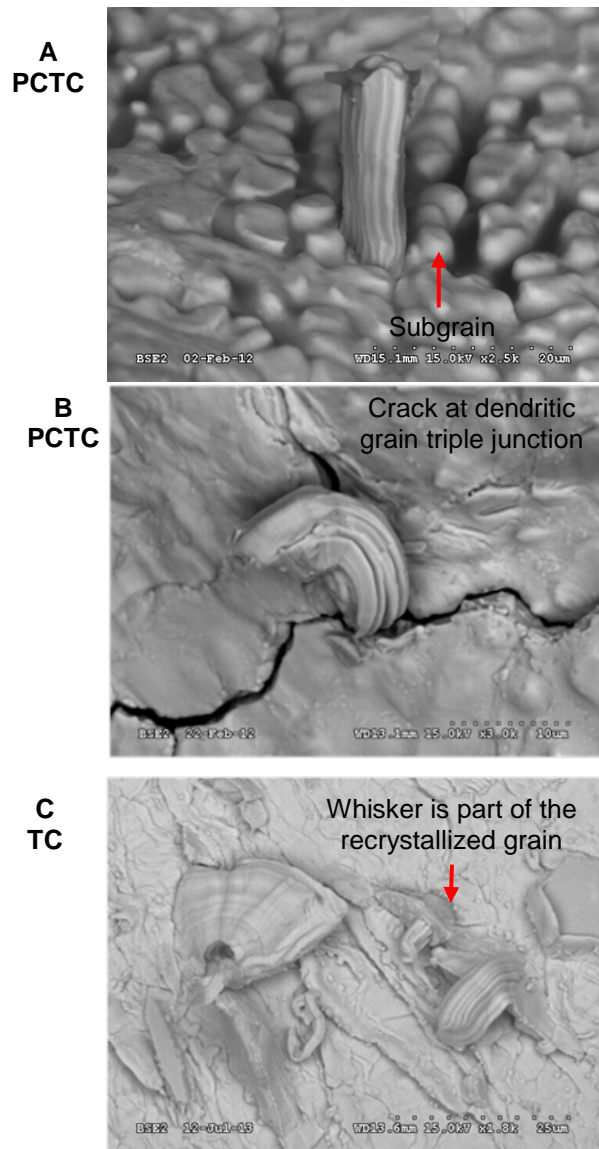


Figure 142: Recrystallized grains are not always visible; (A and B) +50 to 85°C PCTC, 1,797 cycles, one cycle per hour, 15 minute dwells, and (C) -55 to 85°C TC, 2,110 cycles, three cycles per hour, 10 minute dwells.

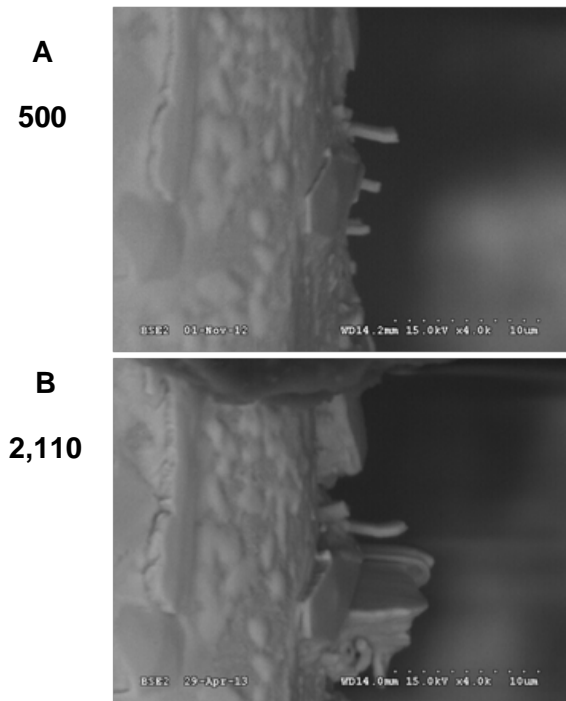


Figure 143: Large step like non-whisker growth between the (A) 500 and (B) 2,110 TC cycle inspections. SOT3, 1-1 contamination level, U24, lead two shown.

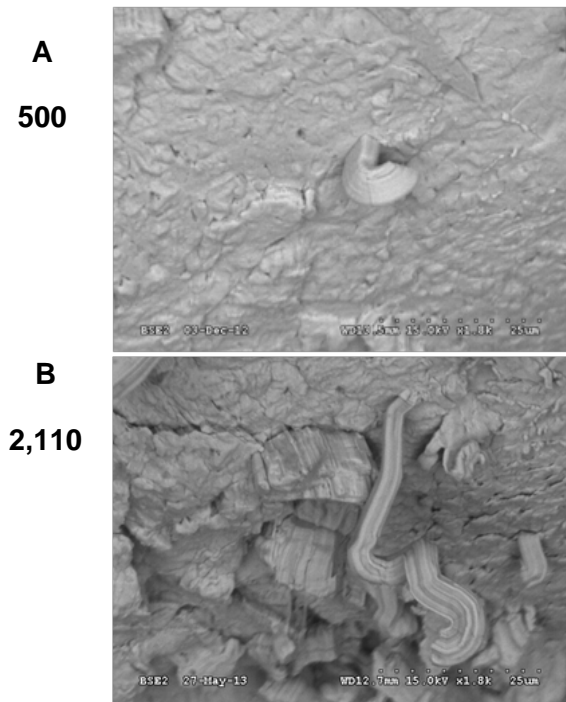


Figure 144: Massive eruptions of non-whisker growth and the resumption of whisker growth between the (A) 500 and (B) 2,110 TC cycle inspections. SOT6, 0-1 contamination level U73, lead six shown.

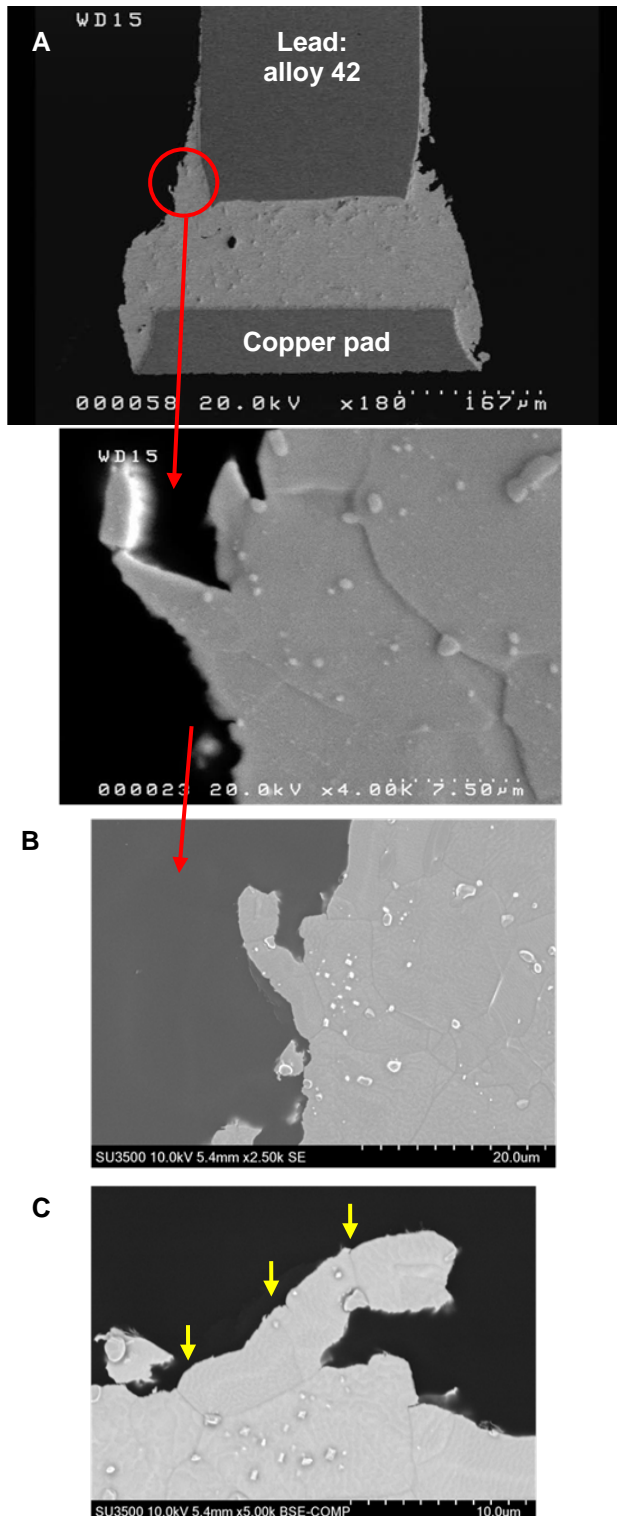


Figure 145: Extensive recrystallization on alloy-42 lead termination after 2,110 TC cycles; (A) First cross-section, (B) second cross-section with ion beam milling, and (C) close-up rotated image of (B). SOT6 at a 0-0 contamination level shown.

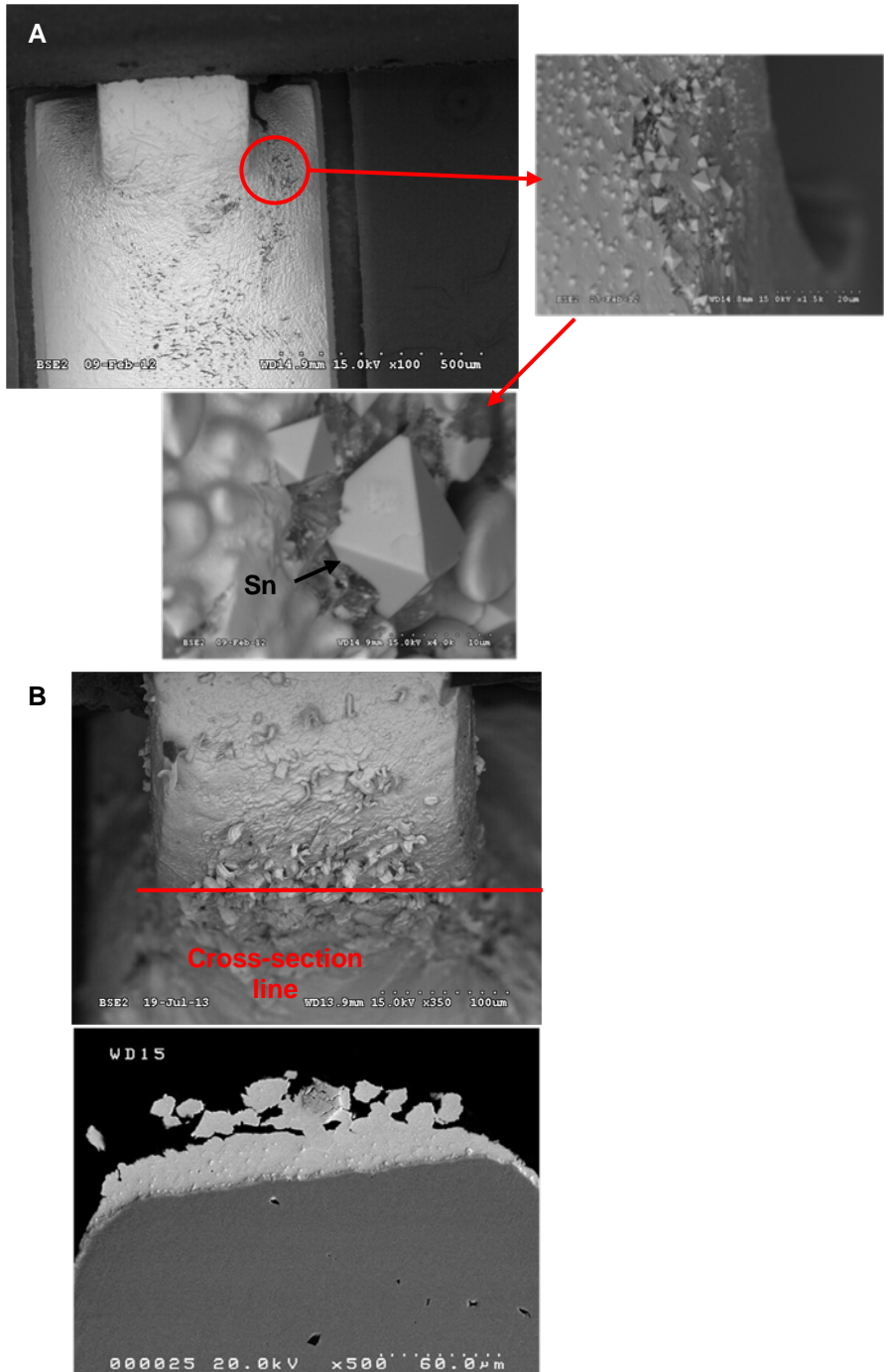


Figure 146: Whiskers compete with other relaxation mechanisms; (A) SOT3 with 1-1 contamination level in relatively mild +50 to 85°C PCTC, after 1,797 cycles, one cycle per hour, 15 minute dwells, and (B) SOT6 with 0-0 contamination level in -55 to 85°C TC, after 2,110 cycles, three cycles per hour, 10 minute dwells.

9.4 Conformal Coat Observations

A screening inspection was performed on selected conformal coated assemblies. SEM imaging of the coating after 2,110 thermal shock cycles revealed crack formation in the conformal coating. The cracks are most pronounced near the thicker coating regions of the fillets formed between the leads, the board, and the part body (Figure 147 and Figure 148). Often cracks started at a stress concentration near a lead edge and propagated into a thicker coating

region. Both the alloy-42 leaded terminations and the copper leaded terminations display similar conformal coating cracks. This suggests that coating expansion/contraction during the thermal shock cycling rapid thermal transitions is contributing to the fractures rather than the coefficient of expansion mismatches between the coating, part, lead, board, and solder. In locations where the coating was uniformly thin, there was no cracking.

Examining the parts that exhibited larger coating fillets, it was found that those with smaller lead-to-lead spacing and smaller gaps behind the lead exhibited greater coating fillet buildup (Figure 149). While the amount of applied coating is a key factor in the size of the coating fillets, the solder volume and the degree of solder wetting up the lead also play a key role. When the solder fills most of the gap behind the lead, a four sided structure is formed causing a capillary condition resulting in an increased fillet.

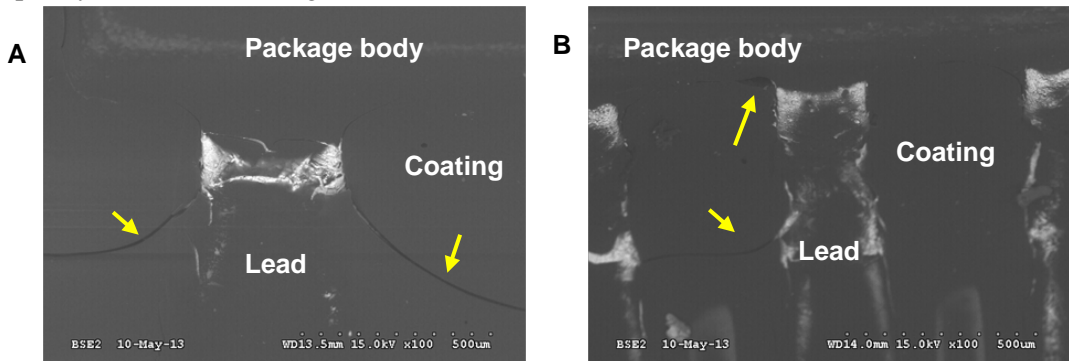


Figure 147: Conformal coated alloy-42 leads after 2,110 TC cycles (A) SOT3, 1-1 contamination level, 100X, and (B) SOT6, 0-0 contamination level, 100X. Arrows indicate coating crack locations.

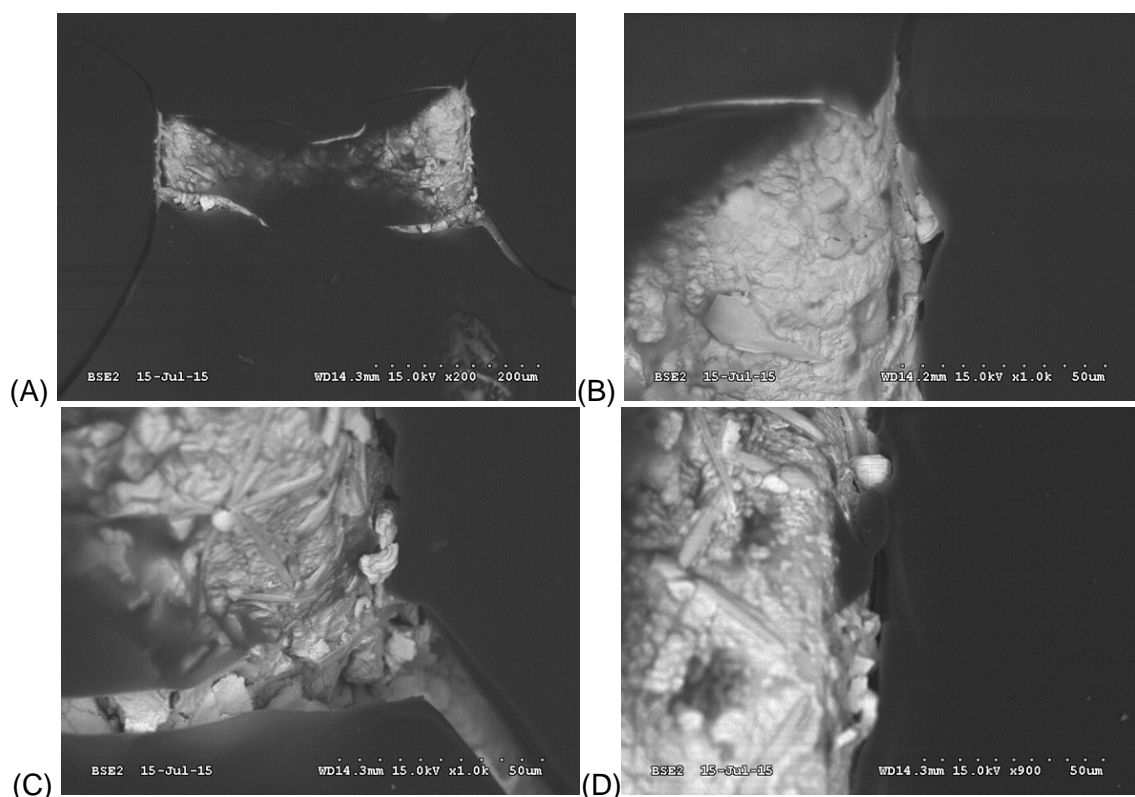


Figure 148: Conformal coated alloy-42 leads after 2,110 TC cycles (A) overall of the lead top, 200x, (B) whisker appears to be pushing the edge of the coating away from the lead, 1,000x, (C) whisker growth in a coating crack, 1,000x, and (D) whisker growth in a coating crack, 1,000x.

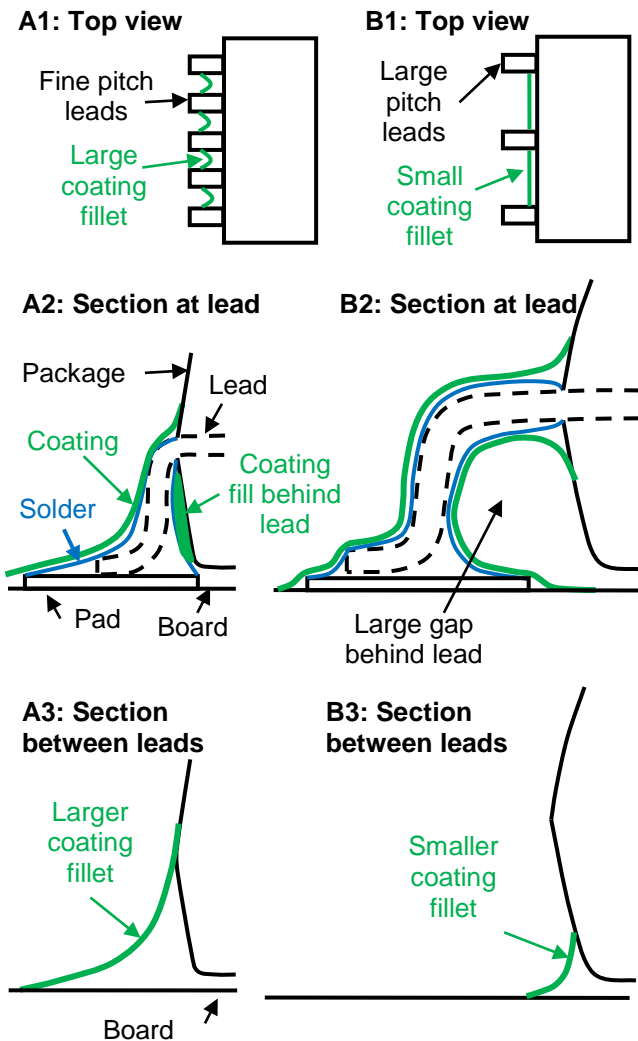


Figure 149: Part variables influencing coating fillets; (A) Large fillets on thinner finer lead pitch package: (A1) large fillet between leads, (A2) small gap behind the lead, and (A3) large coating fillet in section between leads. (B) Small fillets on thicker larger lead pitch package: (B1) small fillet between leads, (B2) coating does not fill large gap behind the lead, and (B3) small coating fillet in section between leads.

However, even with coating cracking, the samples with the coating showed improved whisker migration as compared to uncoated ones. Qualitatively the coated assemblies have short whiskers ($15\text{ }\mu\text{m}$ longest) and low density where the coating is thin, while the non-coated samples have longer whiskers ($\sim 30 - 40\text{ }\mu\text{m}$) and higher density (Figure 150).

With regard to coating cracking, the type of thermal cycling impacts conformal coating crack susceptibility. Reviewing the coated samples from the simulated power cycling thermal cycling test, no cracking was observed (Figure 120).

From the literature, coating cracking was not observed on thermal cycling performed by Han [52]. Han used a sequence of thermal cycles with three temperature ranges followed by high temperature/high humidity exposure given as: (1) 100 cycles from -55 to $+20^\circ\text{C}$, followed by (2) 100 cycles from -15 to 60°C , then by (3) 100 cycles from 20 to 95°C , and then (4) 200 h $50^\circ\text{C}/50\%$ RH. The AR1 material in the Han test is comparable to the AR/UR material in the present work and did not exhibit cracking after four loops through the environmental test sequence.

It is significant to note that the conformal coat cracking observed in the present work would not have been found using standard industry inspection methods. Magnifications on the order of 100 to 1,000X are used in the present coating examination. The current J-STD-001 [17] states that inspection of conformal coating may be performed without magnification and a magnification up to 4X may be used for referee purposes. Industry standard inspection methods in J-STD-001 need to be improved for conformal coating crack identification.

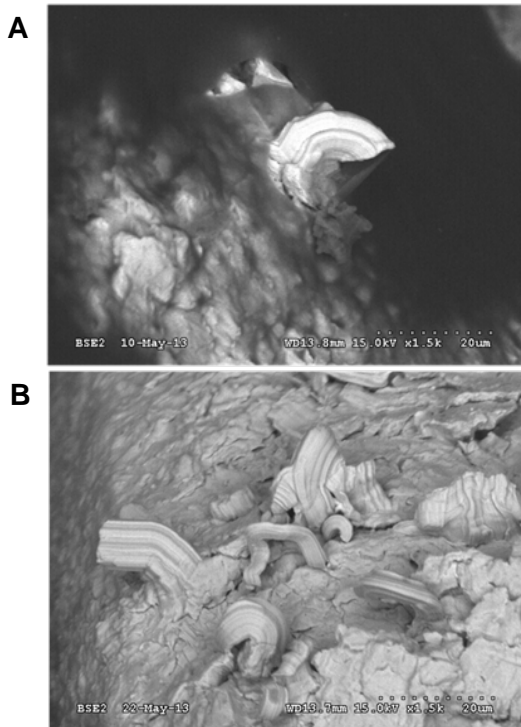


Figure 150: Coated and un-conformal coated alloy-42 SOT6 after 2,110 TC cycles; (A) Coated, 0-0 contamination level, 1,500x, and (B) no conformal coating, 0-1 contamination level, 1,500x.

9.5 Summary

9.5.1 Whisker length

Whisker growth was observed after exposure thermal shock cycling conditions after 500 and 2,110 (500+1,610) cycles. Lead material is the most significant factor contributing to whisker growth, while contamination and electrical bias had less influence. The following key points can be made:

- Alloy-42 lead terminations grew more and longer whiskers than copper lead terminations.
- Interruptions in thermal cycling followed by a SEM inspection can sometimes halt whisker growth, but the effect is not as pronounced as with high temperature/high humidity environments [16].
- There is a high risk of whisker growth in electronic assemblies if lead-free SAC305 solder is used unless mitigations are employed.
- Long whisker growth was observed from the SAC305 solder, particularly in the fillet and lead regions where the solder became thin. Whisker lengths exceeding the JESD201 length threshold for class-2 equipment were observed on the alloy-42 lead terminations after 2,110 cycles.
- Contamination and voltage bias did not have a significant impact on whisker growth under thermal shock cycling conditions.

9.5.2 Metallurgical observations

Optical microscopy, scanning electron microscopy in conjunction with cross-section examinations revealed that:

- The primary source of whisker growth stress was attributed to SAC305 and substrate coefficient of expansion mismatch during thermal cycling.
- Several competing stress relaxation mechanisms in addition to whisker growth were found on alloy-42 lead terminations including excessive deformation, volume recrystallization with massive eruptions of the recrystallized grains. This type of microstructure is not typical for most field conditions.
- Most of the whiskers were kinked.
- Changes in diameter occurred during whisker growth.
- Significant whisker angular rotation during growth occurred.

9.5.3 Conformal coating

Although inspection resources were limited, screening inspection of the conformal coated samples showed:

- The JESD201 -55 to +85°C three cycles per hour test causes cracking of harder conformal coatings not observed in service and may not allow whisker mitigation evaluation of certain conformal coatings.
- Industry standard inspection methods in J-STD-001 need to be improved for conformal coating crack identification during whisker mitigation assessments.
- Less severe PCTC thermal cycling does not crack the coating.
- Even with some coating cracks, the coating is mitigating whisker growth.

9.6 Conclusions

The alloy-42 lead terminations exhibited the longest whisker growth due to the CTE induced stresses on the solder and leads. The JESD201 -55 to +85°C three cycles per hour test is too harsh for optimal assembly whisker growth. In addition, it induced cracking of harder conformal coatings not observed under less severe conditions. Even with some coating cracks, the coating is mitigating whisker growth. Industry standard inspection methods in J-STD-001 are not sufficient for conformal coating crack identification during whisker mitigation assessments. Improvements in test and inspection methods for electronic assembly conformal coating tin whisker mitigation are needed.

10. Primary experiment 3 results and discussion: HTHH 85°C/85%RH

10.1 Environmental conditions

The experiment was performed in the temperature/humidity chamber shown in Figure 151 [31]. The temperature control was performed using thermocouples and humidity was controlled using both dry bulb temperature and wet bulb temperatures. A sheet metal shield was placed above the samples to ensure no condensation would collect on the samples. As shown in Figure 151B, the samples were hung in a vertical position. Inspections were performed at 1,000 h and 4,000 h. The test conditions were:

- Temperature:
 - 85°C Isothermal
- Humidity:
 - 85%RH constant
- Electrical bias:
 - Electrical bias continually applied



Figure 151: Temperature/humidity test set-up; (A) chamber and (B) sample orientation in the test chamber.

10.2 Whisker growth results

10.2.1 First inspection: 1,000 h SOT Board

A total of 15,564 whiskers were counted and 4,741 whiskers were measured (Table 33 to Table 36). The whisker lengths were longer for copper than alloy-42 lead materials (Figure 152). The longest whiskers were: SOT3 – 74 microns, SOT5 – 186 microns and SOT6 – 54 microns. As shown in Figure 153 and Figure 154, the majority of the whiskers grew from the thin solder fillet regions that were three to 25 microns thick near the printed circuit board copper pad and many were kinked.

Table 33: Whisker measurement summary after 1,000 h HTHH.

Component	Counted	Measured	Percent measured
SOT3	2438	867	35.6
SOT6	1106	486	43.9
SOT5	12020	3388	28.2
Total	15564	4741	30.5

Table 34: SOT5 (copper leads) whisker distribution after 1,000 h HTHH.

Cleanliness	Counted	Number of components	Whiskers per component
0-0	1566	11	142.4
1-0	4094	12	341.2
0-1	3531	12	294.3
1-1	2829	20	141.5

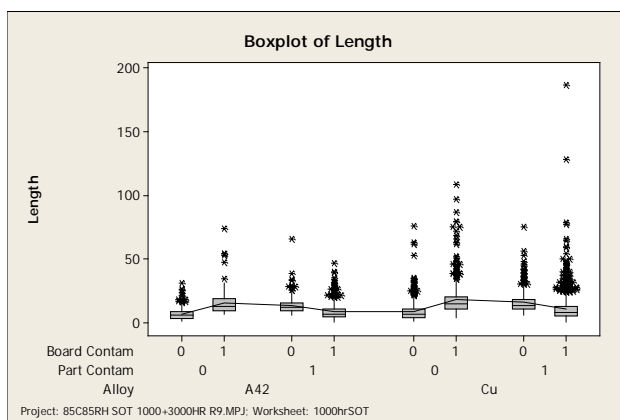
Table 35: SOT3 (alloy-42 leads) whisker distribution after 1,000 h HTHH.

Cleanliness	Counted	Number of components	Whiskers per component
0-0	407	16	25.4
1-0	998	16	62.4
0-1	684	16	42.8
1-1	349	24	14.5

(Note that more SOT3 parts were examined because it has fewer leads than the SOT5 and SOT6 parts)

Table 36: SOT6 (alloy-42 leads) whisker distribution after 1,000 h HTHH.

Cleanliness	Counted	Number of components	Whiskers per component
0-0	195	8	24.4
1-0	278	8	34.8
0-1	269	8	33.6
1-1	364	12	30.3

**Figure 152:** Box plot of whisker lengths after 1,000 h HTHH broken down by lead alloy, part contamination, and board contamination levels (Note: Bias2 = 0 e.g. leads tied to ground).

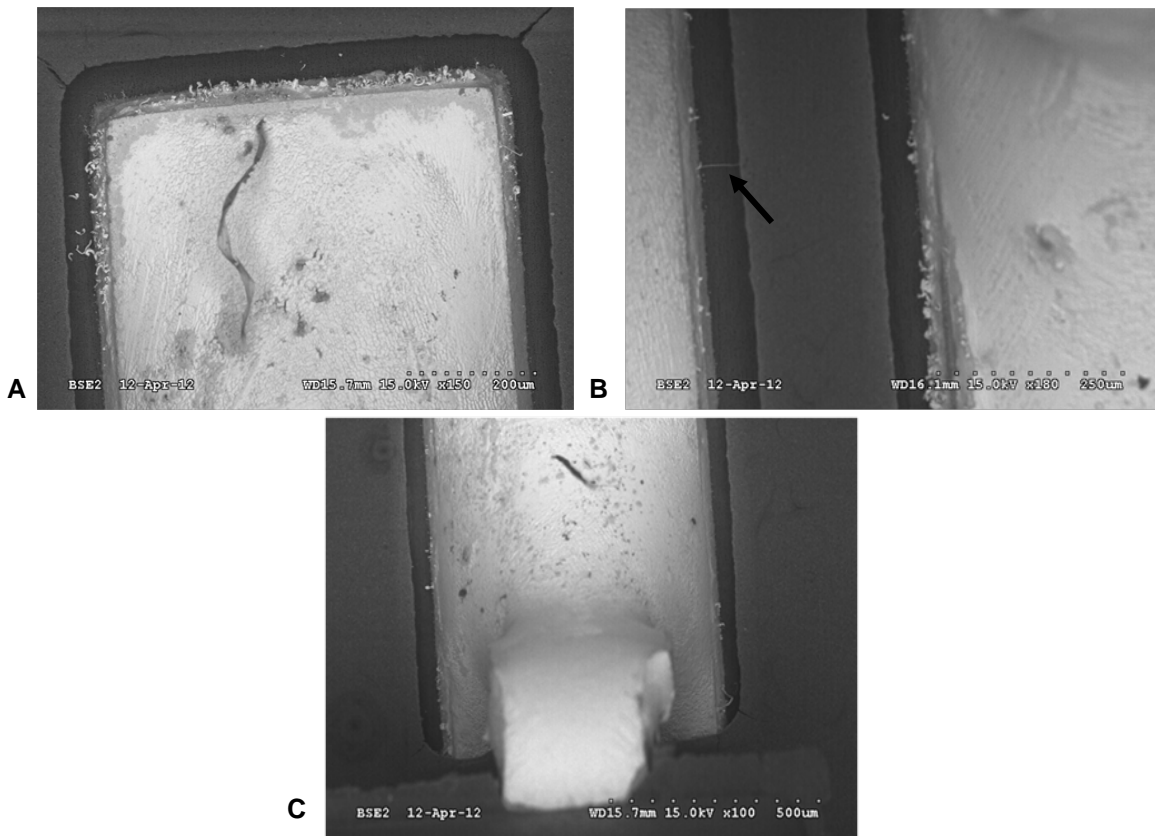


Figure 153: SEM images of copper lead frame SOT5 part with a 1-0 contamination level after 1,000 h HTHH; (A) toe, (B) side, and (C) heel region of a typical solder joint. In (B), an arrow indicates the location of a lone straight whisker along the edge. (Note that the large dark piece on the top of the joint in A and C are not whiskers.)

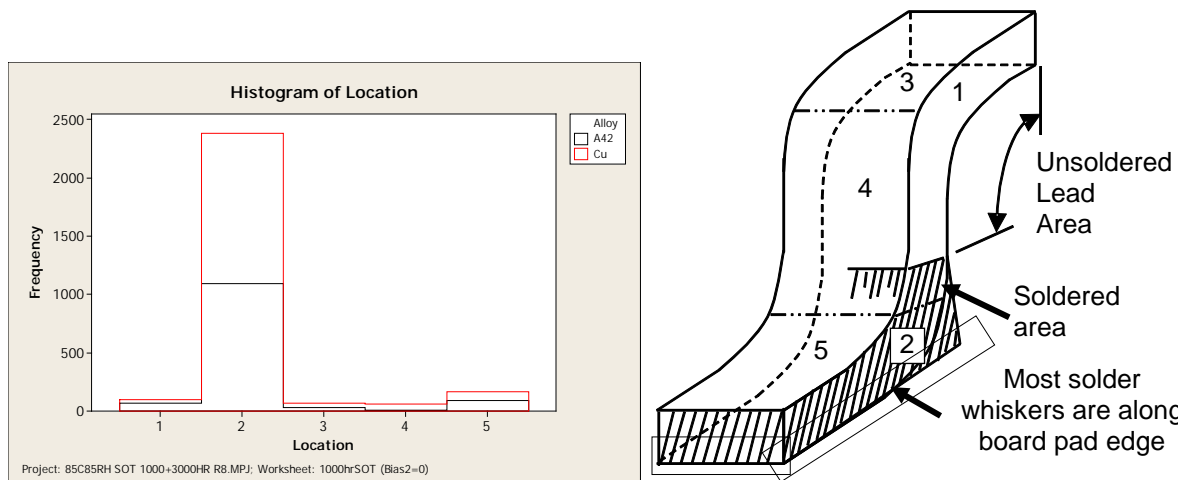


Figure 154: Whisker locations after 1,000 h HTHH with Bias2 = 0; histogram (left) and location definition (right). Note that for the 85°C/85%RH environment the majority of the whisker growth occurs along the very bottom of region 2 along the board pad edge.

Lead material and contamination had the most significant influence on whisker growth. The number of whiskers per lead termination was greater for the copper leads than for the alloy-42 leads for all contamination levels (Figure 155). For the Cu and alloy-42 leads, the intermediate contamination levels, 0-1 and 1-0 (part-board), exhibited the

greatest whisker density and longest 50th percentile whisker length (Figure 155, Figure 156 and Figure 157). However, for the copper leads, the longest whiskers were observed with the 1-1 contamination level.

The lognormal curve fit [77] [92][93] seemed to represent many of the whiskers length distributions reasonably well. Unfortunately, as has been observed by other researchers [94], some of the longest whiskers did not match the lognormal characteristic of the shorter whiskers.

Regarding bias voltage, there was no appreciable change in whisker length with applied bias (Figure 158 through Figure 161).

As far as whisker diameter is concerned, Figure 162 and Figure 163 show that the majority of whiskers were between one and five microns, regardless of alloy or contamination level. An inspection of the linear plot in Figure 163 indicates that the larger diameter whiskers were shorter than the smaller diameter whiskers. Examining the log length versus log diameter, the longest whiskers were less than approximately seven microns in diameter.

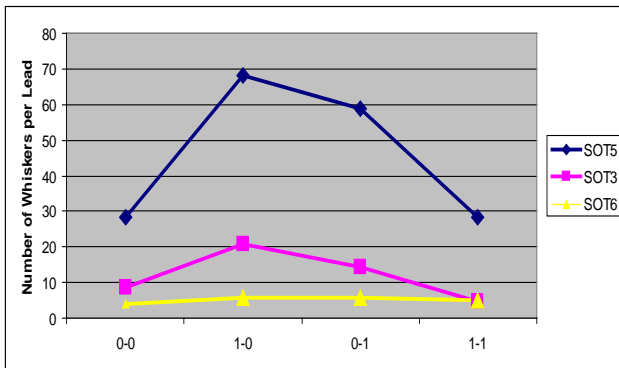


Figure 155: Whiskers per lead termination after 1,000 h HTHH for various contamination levels. The SOT5 device has copper leads and the SOT3 and SOT6 devices have alloy-42 leads.

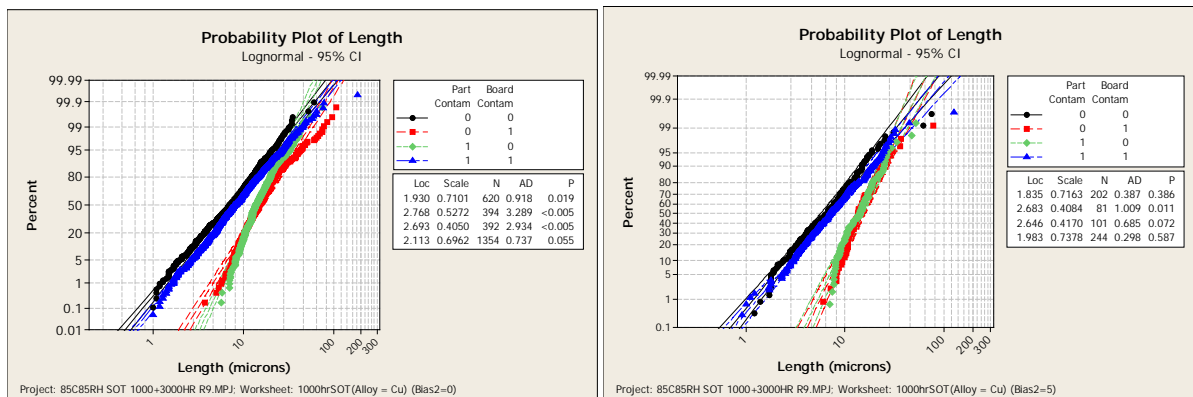


Figure 156: Probability plot of whisker lengths of terminations with copper leads after 1,000 h HTHH; bias2 = 0 (left) and bias2 = 5 (right) levels broken down by part contamination and board contamination level.

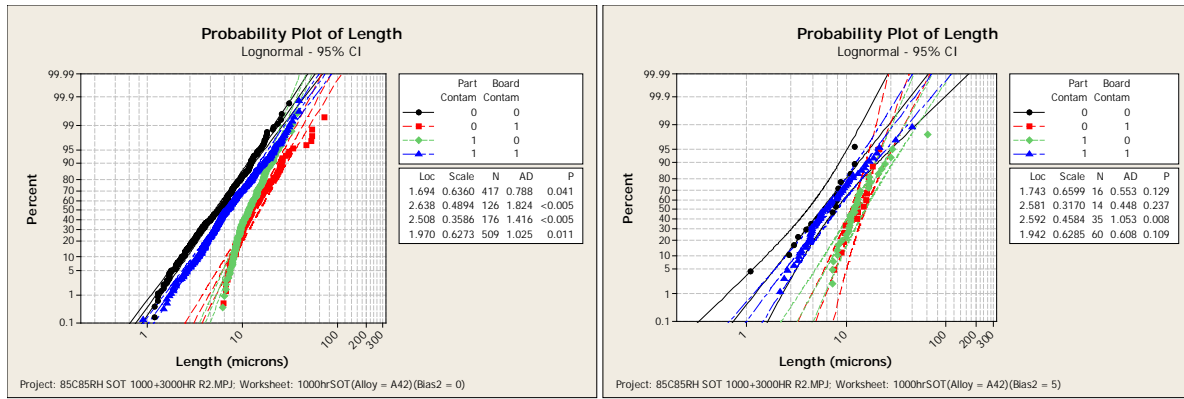


Figure 157: Probability plot of whisker lengths of terminations with alloy-42 leads after 1,000 h HTHH; lead bias2 = 0 (left) and lead bias2 = 5 (right) levels broken down by part contamination and board contamination level.

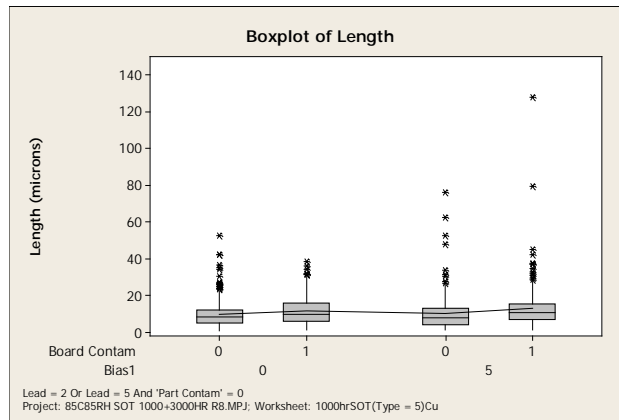


Figure 158: Box plot of whisker lengths of terminations with copper leads after 1,000 h HTHH showing the effect of board contamination and bias1 with no part contamination.

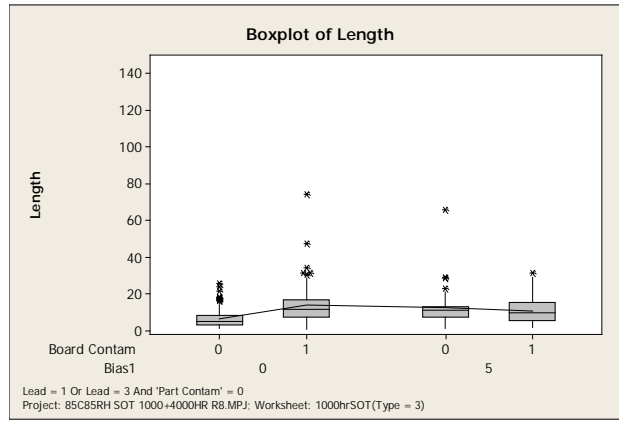


Figure 159: Box plot of whisker lengths of terminations with alloy-42 (SOT3 device) leads after 1,000 h HTHH showing the effect of board contamination and bias1 with no part contamination

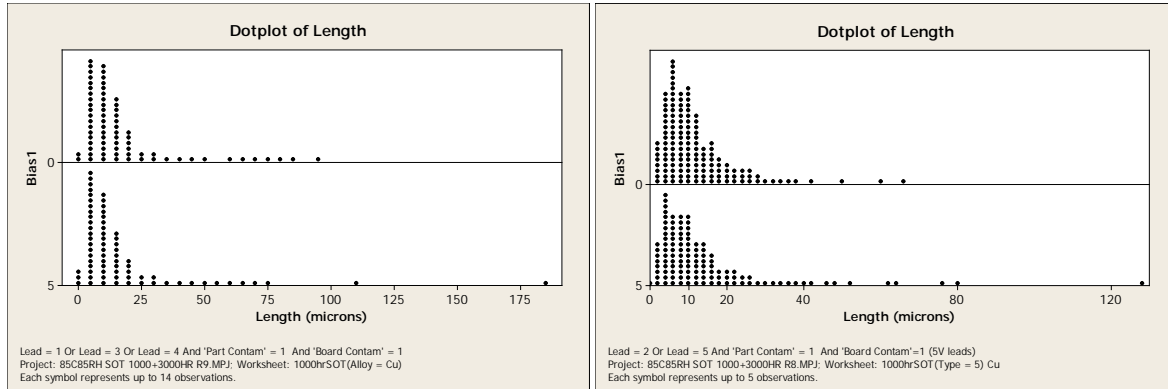


Figure 160: Dot plot of whisker length of terminations with copper (SOT5) leads at a 1-1 contamination level after 1,000 HTHH; ground leads (left) and 5V leads (right) with and without 5V part bias applied (e.g. bias1 = 0 and 5).

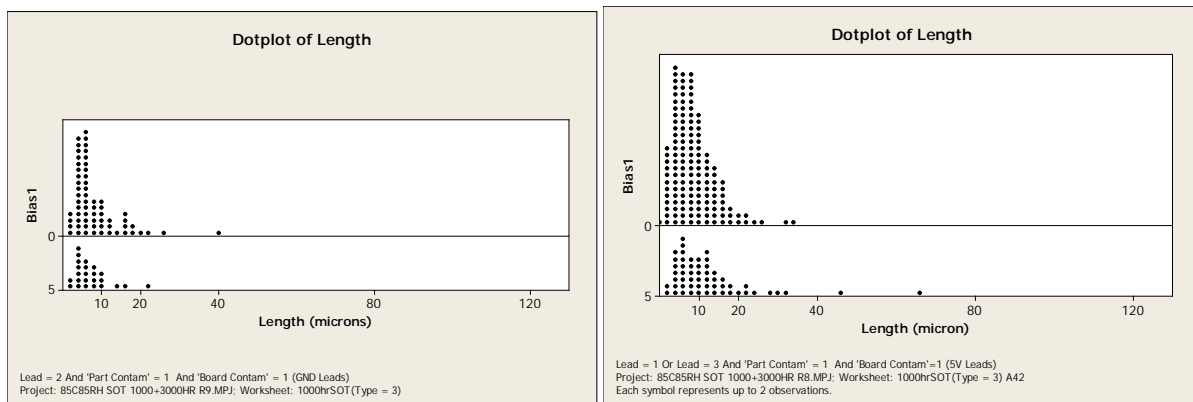


Figure 161: Dot plot of whisker length for terminations with alloy-42 (SOT3) leads at a 1-1 contamination level after 1,000 h HTHH; ground leads (left) and 5V leads (right) with and without 5V part bias applied (e.g. bias1 = 0 and 5).

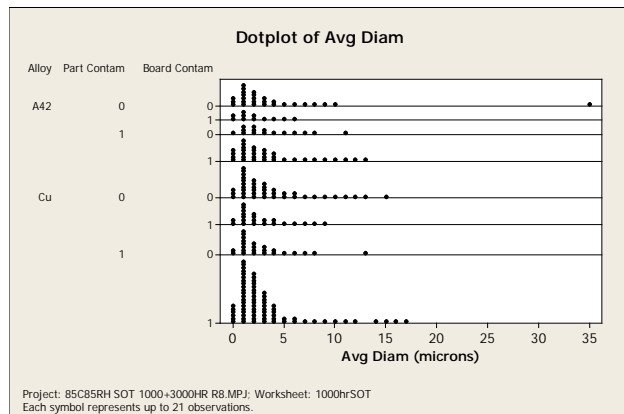


Figure 162: Dot plot of whisker diameter after 1,000 h HTHH broken down by lead material, part contamination, and board contamination.

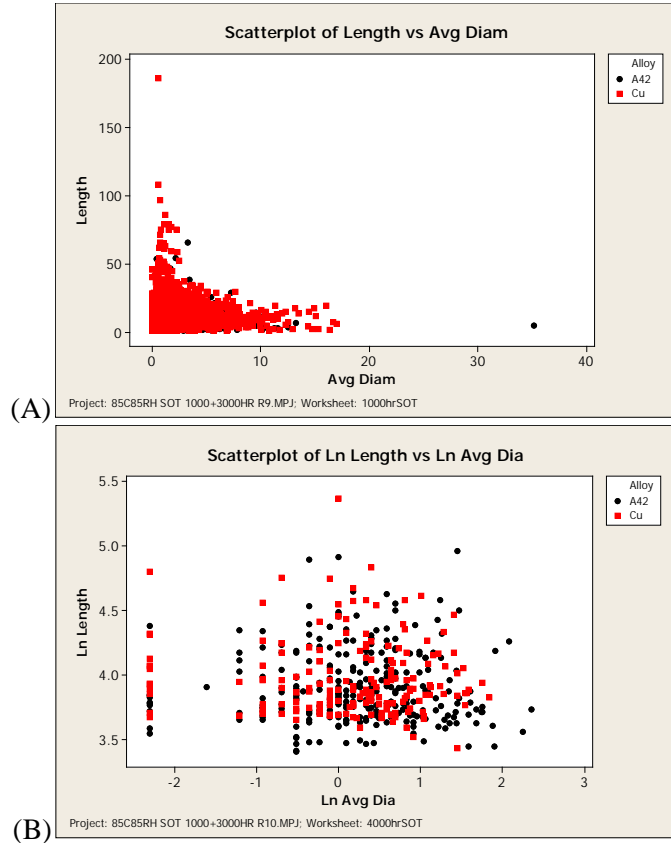


Figure 163: Scatterplot of (A) whisker length (microns) versus average diameter (microns) and (B) $\ln(\text{length})$ versus $\ln(\text{average diameter})$ for terminations with copper and alloy-42 leads after 1,000 HTHH.

10.2.2 Final inspection: 4,000 h SOT board

After the 1,000 h inspection was completed, the boards were placed back in the humidity chamber for an additional 3,000 h and then removed for inspection. Then the exact same parts and leads previously examined at 1,000 h were reevaluated. The numbers of whiskers counted and measured are summarized in Table 37.

After 4,000 h 75,386 whiskers were counted, 4.84 times more than were counted after 1,000 h. In an effort to manage the inspection time, only whiskers longer than about 40 microns were measured. Data on 489 whiskers were recorded. Lognormal length distributions were not reported because it was unclear how to best treat the whiskers population below 40 microns that were not measured.

As shown in Figure 164 and Table 38, the longest whiskers were: SOT3 – 142.5 microns, SOT6 – 153.2 microns, and SOT5 - 214.6 microns. Ten of the 14 longest whiskers were from parts or assemblies with some applied contamination. The individual value plot in Figure 165 shows that both “more whiskers longer than 40 microns” and “longer whiskers” were observed after 4,000 h as compared to 1,000 h. Note that by omitting whiskers shorter than 40 microns in the 4,000 hour plots, the arithmetic mean increases more than it would have if all the whisker lengths were measured. As with the 1,000 hour observation, copper leads grew longer whiskers than alloy-42 leads.

The box plot of whiskers per lead shown in Figure 166 indicates that the mean number of whiskers per lead termination was greater with the copper leads than with the alloy-42 leads.

Another consideration in the whisker growth process is whisker nucleation time. If a long time is required to nucleate the whiskers, then the fraction of time that they are growing is reduced. Figure 167 reveals that more than 1,000 h was needed for whisker nucleation with the alloy-42 lead in the 85 °C/85 %RH environment. The retarded whisker growth tendency is due to the fact that the Ni from the alloy-42 diffuses to the Cu board pad and a CuNiSn intermetallic is formed on the copper board pad. The CuNiSn intermetallic has a lower corrosion potential than SnCu and thus tends to have a lower whisker growth than the Cu lead configuration in high humidity. Note that an opposite trend was observed during simulated power cycling thermal cycling where thick CuNiSn intermetallic grew on the alloy-42 lead (Figure 118), which was postulated to increase whisker growth.

The lognormal probability plots comparing Cu and alloy-42 leads, various contamination levels, and whisker growth location are shown in Figure 168 to Figure 171. The longest whisker was from a Cu lead termination at location-5 (214.6 microns) and the next longest whisker was from an alloy-42 termination at the location-2 (145.2 microns). The whisker count for both the Cu and the alloy-42 lead terminations was dominated by whiskers growing on the board pad (location-2). The upper portion of the alloy-42 leads had few whiskers. The alloy-42 had more whiskers counted than the Cu leads because many of the Cu whiskers had broken off and were not counted.

Table 37: Whisker measurement summary after 4,000 h HTHH.

Component	Counted	Measured whiskers (1)	Percent Measured
SOT3	24639	197	0.8
SOT6	37641	185	0.5
SOT5	13106	107	0.8
Total	75386	489	0.6

Note 1: Measurements limited to whiskers longer than 40 microns

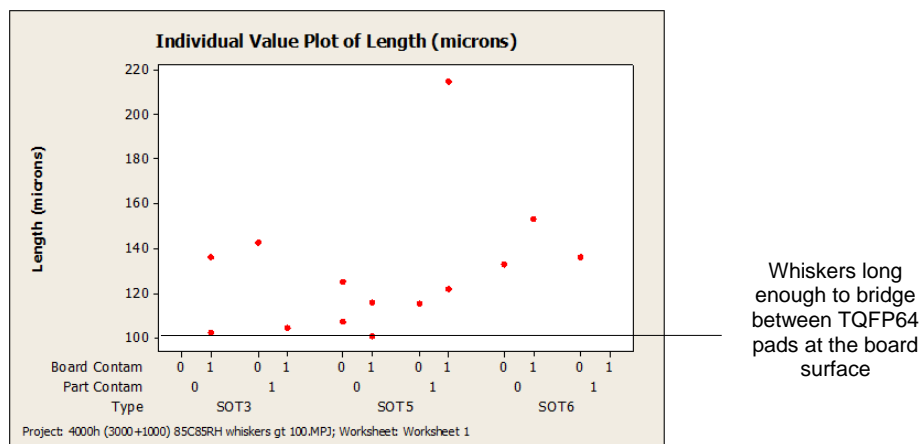


Figure 164: Whiskers longer than 100 microns after 4,000 h HTHH.

Table 38: Whiskers longer than 100 microns after 4,000 h HTHH.

Type	Comp #	Part Contamination	Board Contamination	Part Bias	Lead	Location	Length (microns)
SOT3	48	0	1	5	2	2	102.2
SOT3	42	0	1	0	3	2	136.1
SOT3	7	1	0	5	1	2	142.5
SOT3	45	1	1	5	2	2	104.4
SOT5	3	0	0	5	2	5	125.2
SOT5	36	0	0	0	5	2	107.3
SOT5	5	0	1	5	4	2	100.6
SOT5	14	0	1	5	1	2	115.7
SOT5	38	1	0	0	3	2	115.4
SOT5	14	1	1	5	4	2	121.7
SOT5	37	1	1	0	2	5	214.6
SOT6	74	0	0	U	3	2	133
SOT6	66	0	1	U	1	2	153.2
SOT6	73	1	0	U	1	2	136

Note: U = unpowered

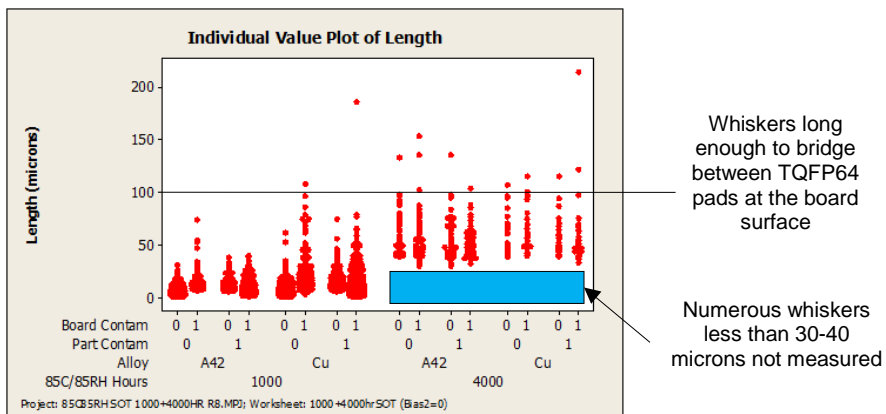


Figure 165: Dot plot of whisker length showing the difference between 1,000 and 4,000 h HTHH. Only whiskers longer than 30 to 40 microns were measured in the 4,000 hour data set.

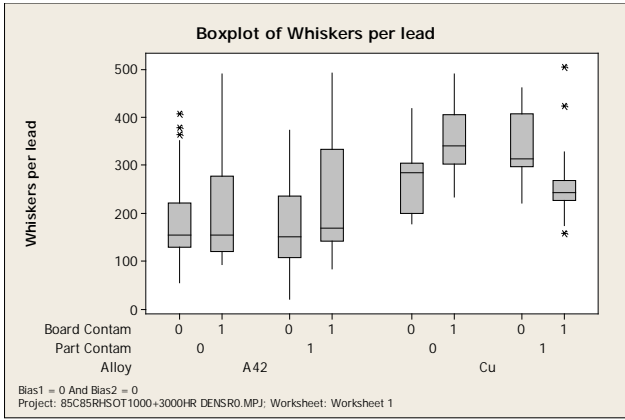


Figure 166: Box plot of whiskers per lead termination after 4,000 h HTHH broken down by lead alloy, part contamination, and board contamination (Bias1=0, Bias2 = 0).

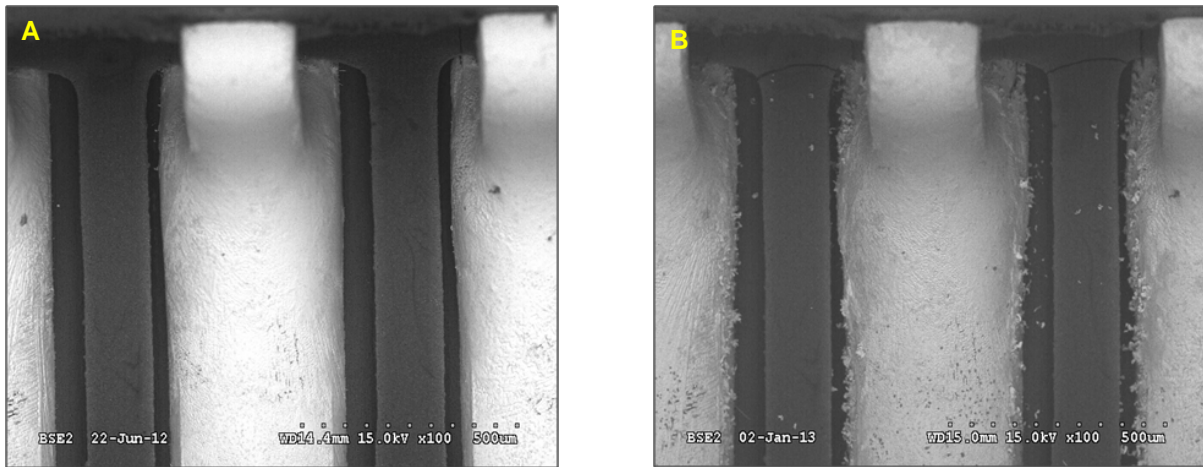


Figure 167: SEM images of an alloy-42 SOT6 at a 0-0 contamination level, part reference designator U65, lead 4 (A) 1,000 h and (B) 4,000 h HTHH. Whisker growth was shorter than the copper leaded SOT5.

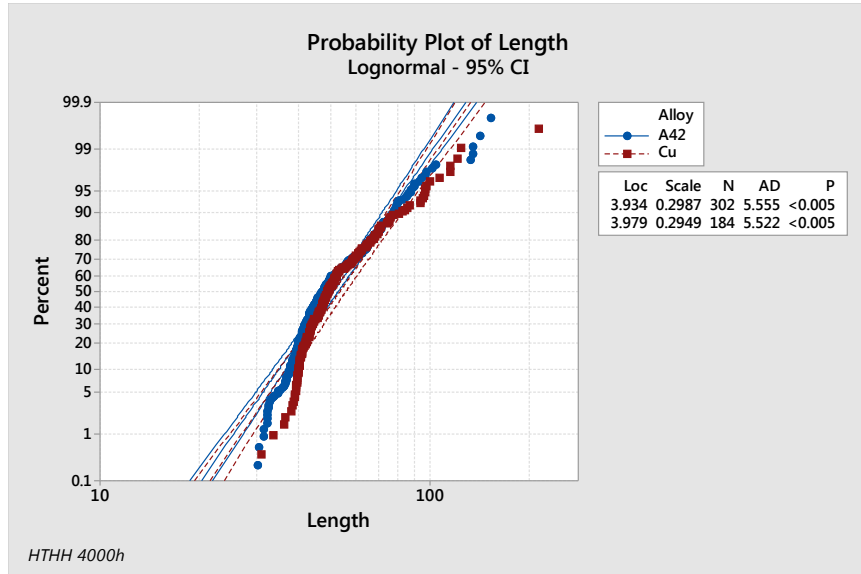


Figure 168: Probability plot of whisker lengths after 4,000 h HTHH; broken down by lead alloy for measured whiskers longer than 30 to 40 microns.

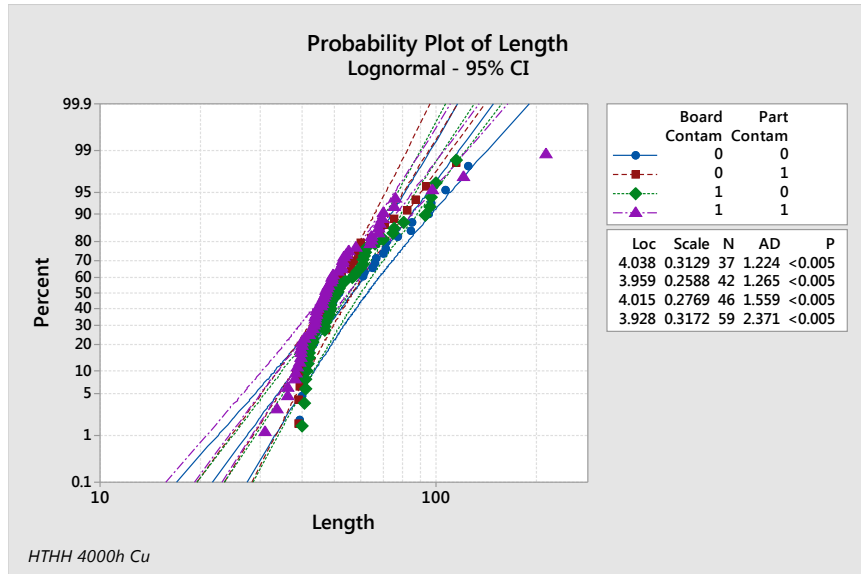


Figure 169: Probability plot of whisker lengths for Cu leads after 4,000 h HTHH; broken down by contamination level for measured whiskers longer than 30 to 40 microns.

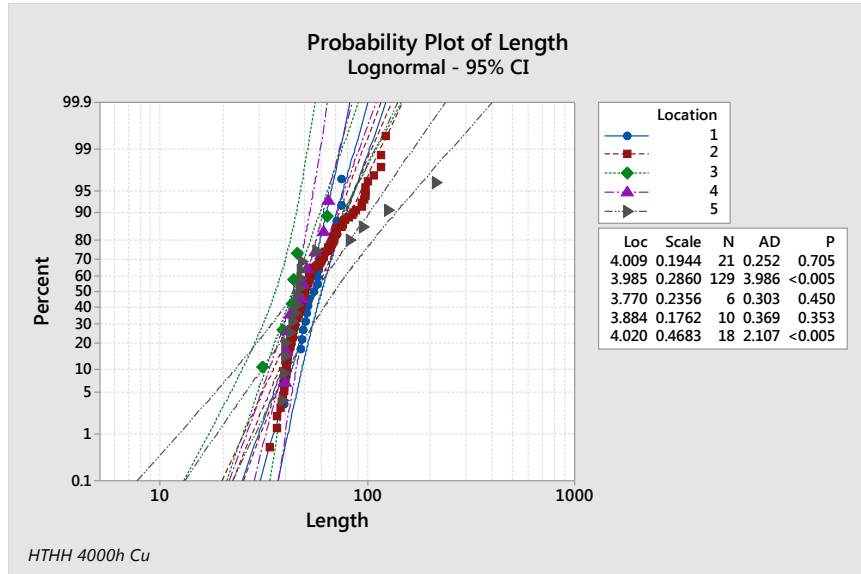


Figure 170: Probability plot of whisker lengths for Cu leads after 4,000 h HTHH; broken down by location for measured whiskers longer than 30 to 40 microns.

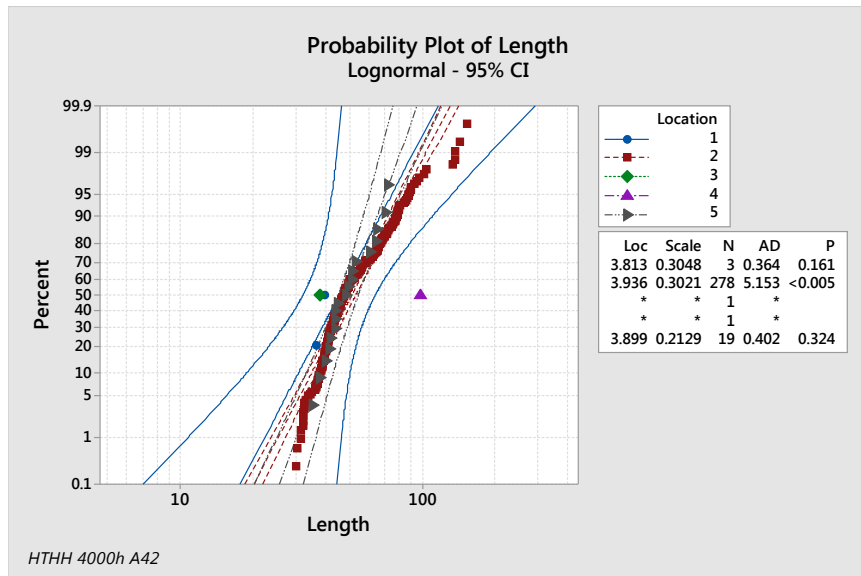


Figure 171: Probability plot of whisker lengths for alloy-42 leads after 4,000 h HTHH; broken down by contamination level for measured whiskers longer than 30 to 40 microns.

10.2.2.1 Whisker density details

The whiskers were counted on 385 leads. The resulting whisker density histogram from the five locations (Figure 172 to Figure 174) shows that some locations had many leads with no whisker growth and some locations where many leads had significant growth. The maximum whisker density of 2027 whiskers/mm² was growing from a board pad with an alloy-42 lead (Figure 175) was an order of magnitude larger than was observed on bright tin [92]. Of the ten highest whisker densities, eight were from boards that had board contamination (three alloy-42 with 1-1, three alloy-42 with 0-1, and one Cu with 0-1) and only two were clean (one alloy-42 and Cu with 0-0). The whisker density box plots comparing lead alloy and contamination (Figure 177 and Figure 177) show that there is a slight increase in whisker density with contamination level. Note that the whiskers growing from location-1 and -2 face the adjacent lead have a greater short circuit risk to the system operation as compared to locations-3, -4 and -5.

Examining the Cu lead termination 0-0 contamination level whisker density at the board pad edge (location-2) after 4,000h in further detail, the maximum whisker count for the SOT5 yielded a maximum whisker density of 1,580 whiskers/mm² (Table 39).

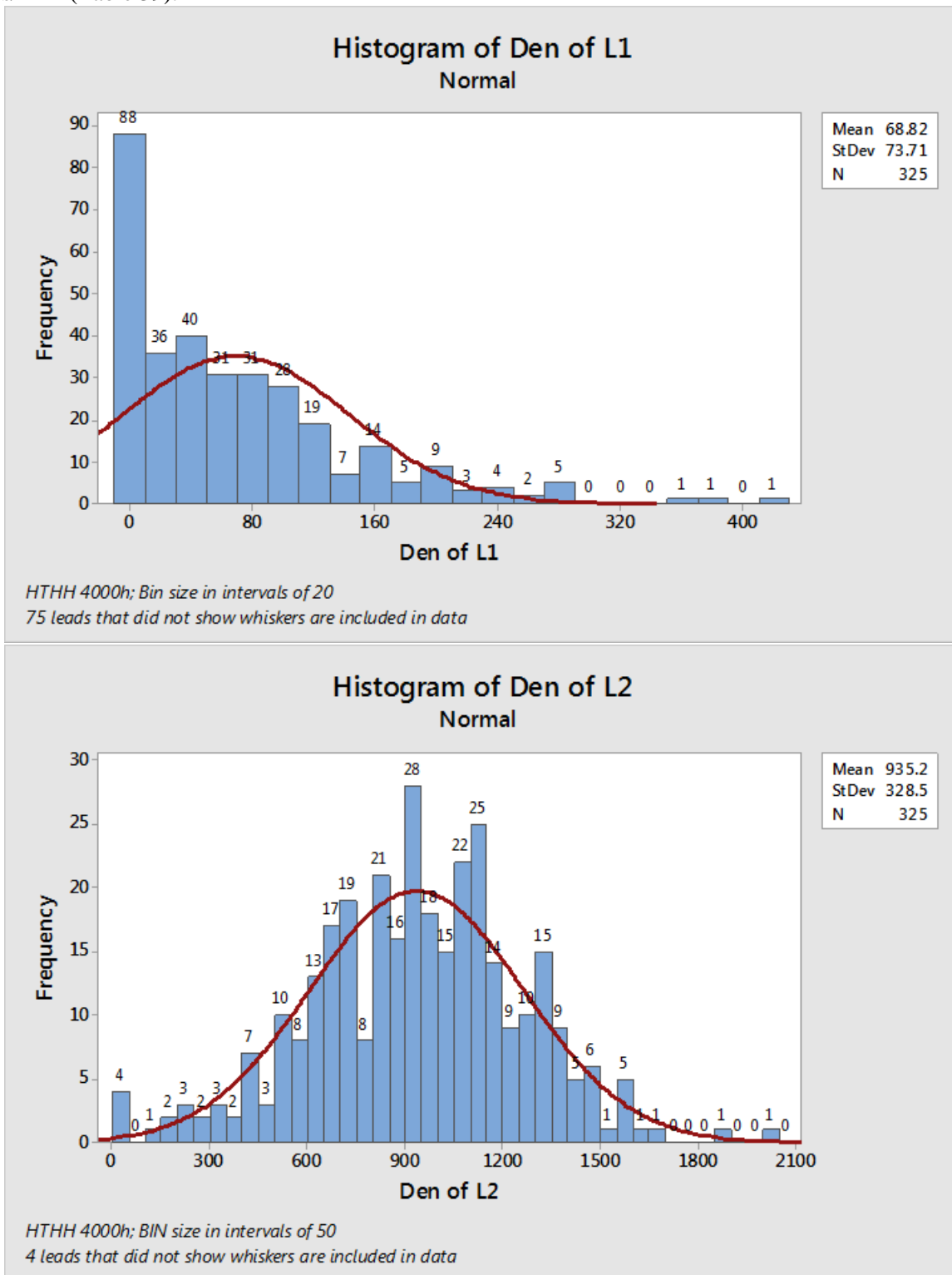


Figure 172: Histogram of whisker density (whiskers/mm²) at location-1 and -2 after 4,000 h HTHH for all contamination levels of Cu and alloy-42.

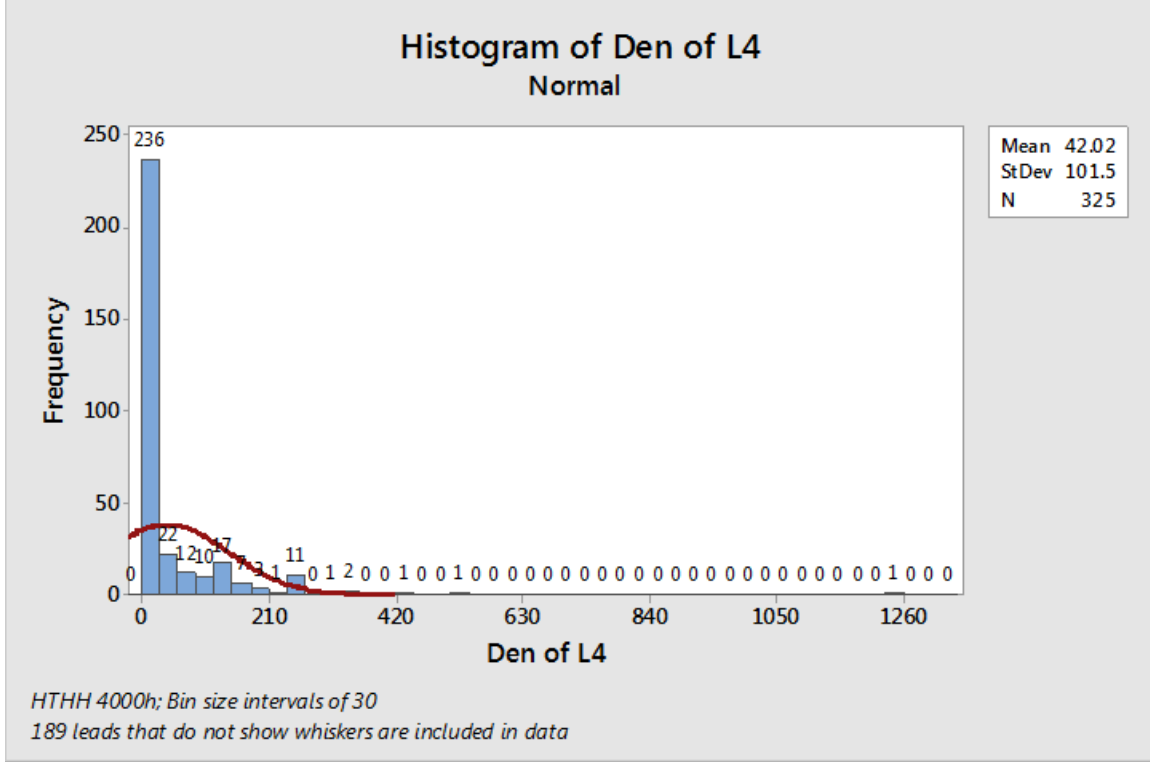
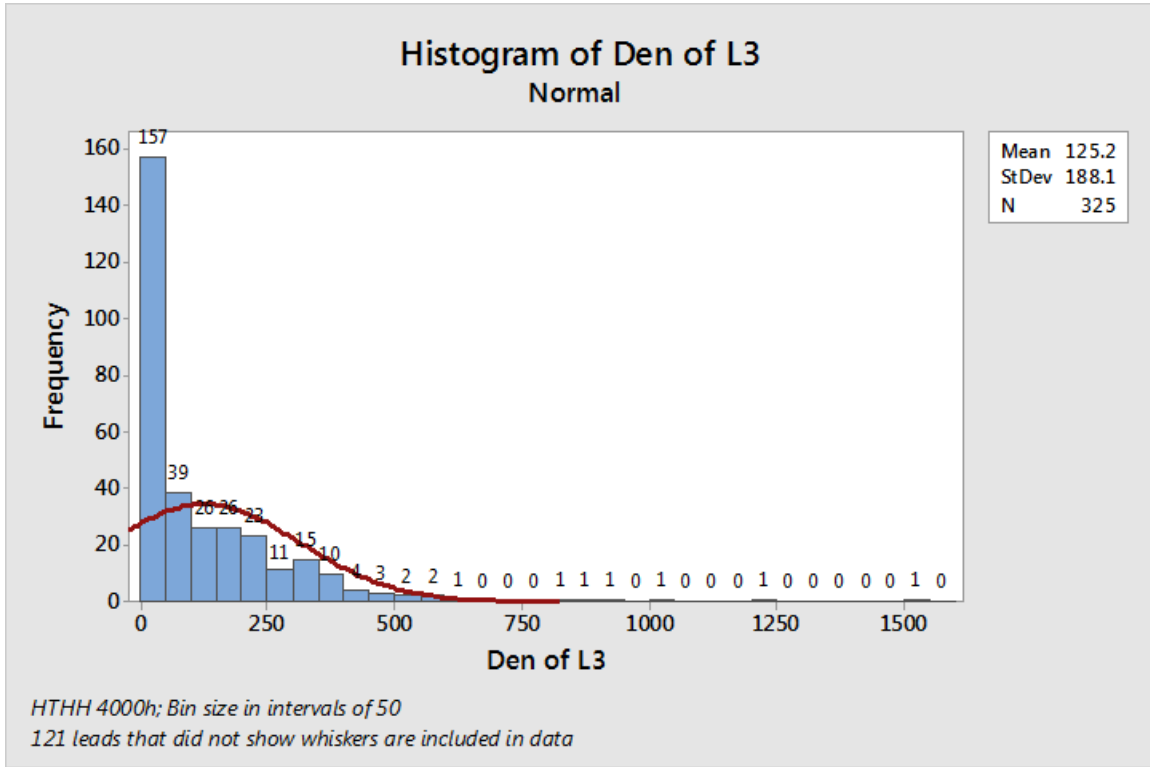


Figure 173: Histogram of whisker density (whiskers/mm²) at location-3 and -4 after 4,000 h HTHH for all contamination levels of Cu and alloy-42.

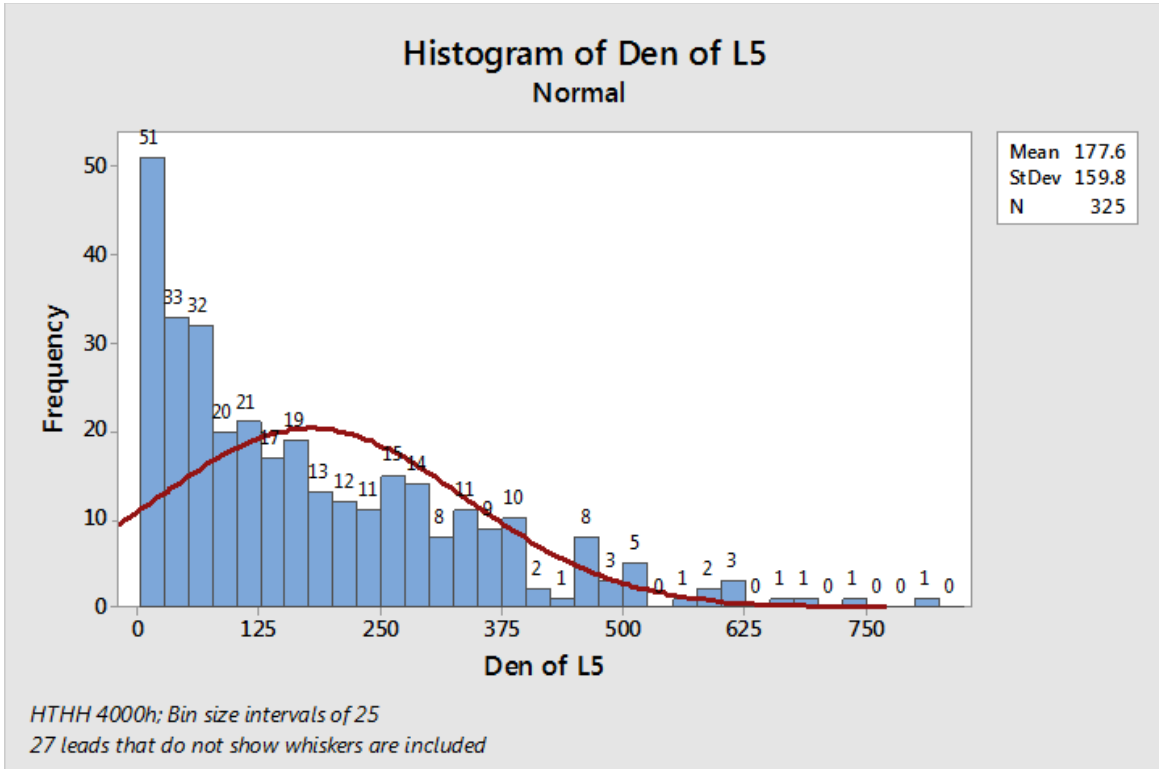


Figure 174: Histogram of whisker density (whiskers/mm²) at location-5 after 4,000 h HTHH for all contamination levels of Cu and alloy-42.

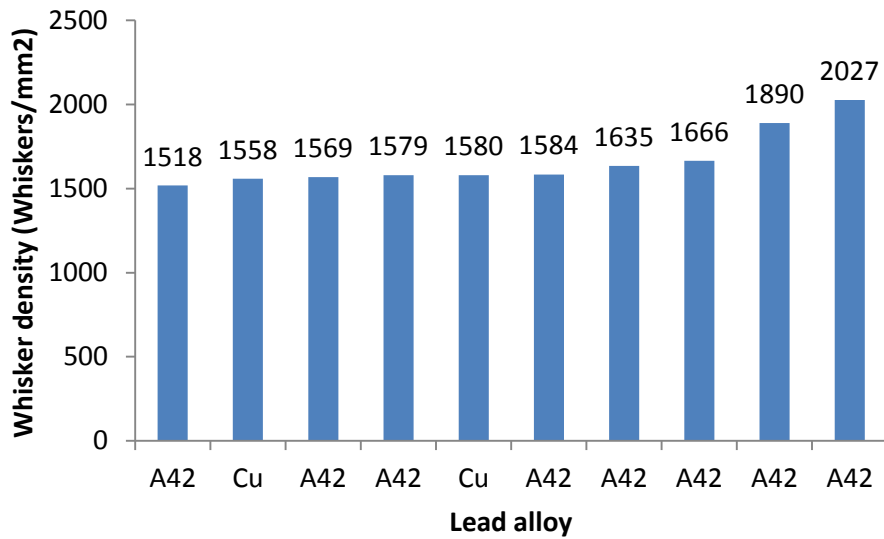


Figure 175: Top ten whisker densities at location-2 after 4000 h HTHH.

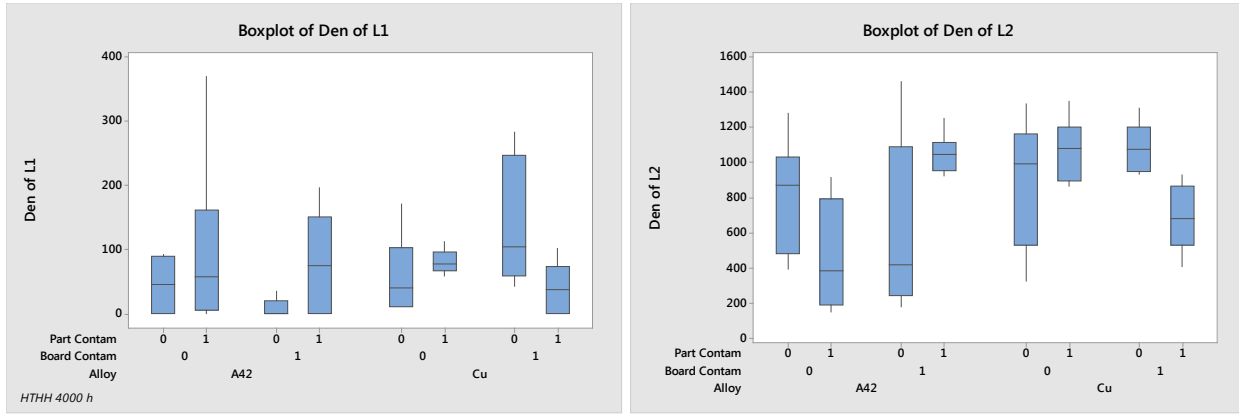


Figure 176: Box plots of whisker density (whiskers/mm²) comparing lead alloy and contamination after 4000 h HTHH for location-1, and -2, which grow directly toward the opposite lead.

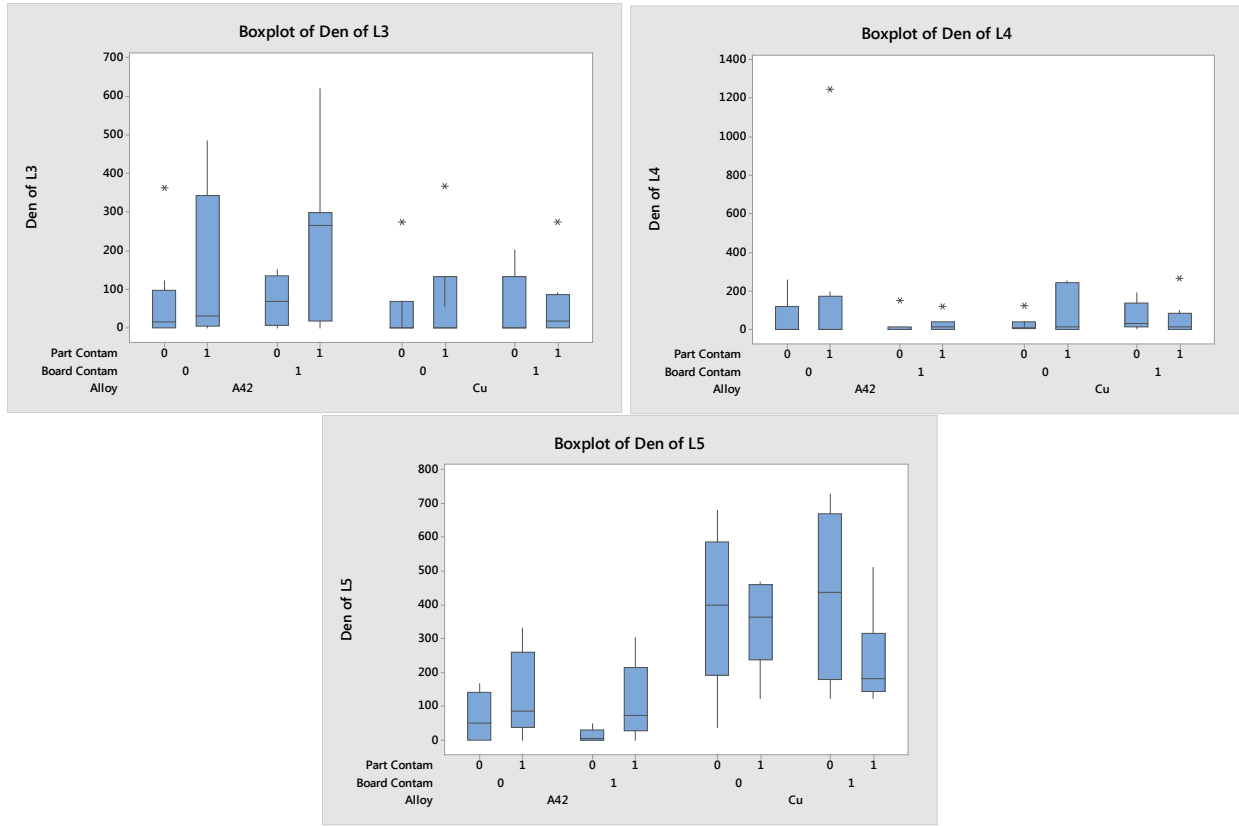


Figure 177: Box plots of whisker density (whiskers/mm²) comparing lead alloy and contamination after 4000 h HTHH for location-3, -4 and 5, growing from the front surfaces.

Table 39: Whisker density of whiskers growing from the solder at the board pad (location-2) for the SOT5 at a 0-0 cleanliness level after 4,000 h HTHH.

	Whiskers/pad	Pad side area (mm ²)	Whisker density (whiskers/mm ²)
Minimum	58	0.1798	323
Maximum	284	0.1798	1580
Average	182.8	0.1798	1017

10.3 Metallurgical observations

10.3.1 SOT board

The majority of the whiskers grew from SAC solder that has flowed around the board pad. The solder thickness in this region ranged from three to 25 microns thick. Figure 153 and Figure 178 show representative whisker growth from the board pad edge when a copper lead is present with a 1-0 and a 1-1 contamination level. These whiskers are similar to those formed when an alloy-42 lead is present (Figure 179).

The solder was partially oxidized (Figure 180). The compressive stress caused by the 29~34 percent volume increase of the Sn oxides as compared with the β Sn promotes whisker growth. These findings are consistent with other investigators assessing the role of humidity on tin whisker growth on electronic component leads [13] [37] [41] and on lead-free assemblies [79].

There are two possible explanations for the large number of broken whiskers. As shown in Figure 180, the thin regions of solder were completely oxidized and had no whiskers on the surface. This suggests that oxidation/corrosion propagating under a whisker can make the whisker attachment to the base more brittle. In another cross-section of a whisker through its base, voids and a crack were observed (Figure 181).

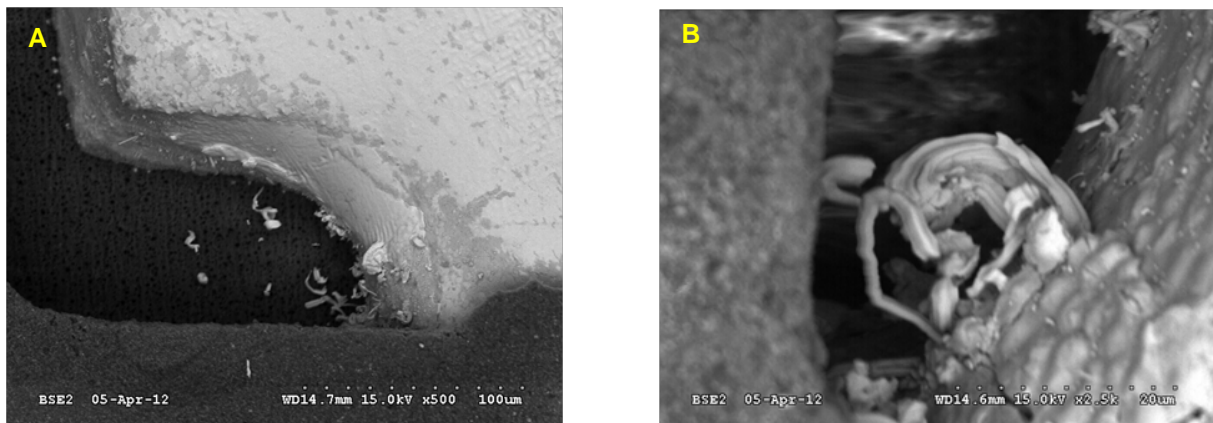


Figure 178: SEM images of a copper (SOT5) leaded part with a 1-1 contamination level after 1,000 h HTHH. Increasing magnification views shown from (A) to (B).

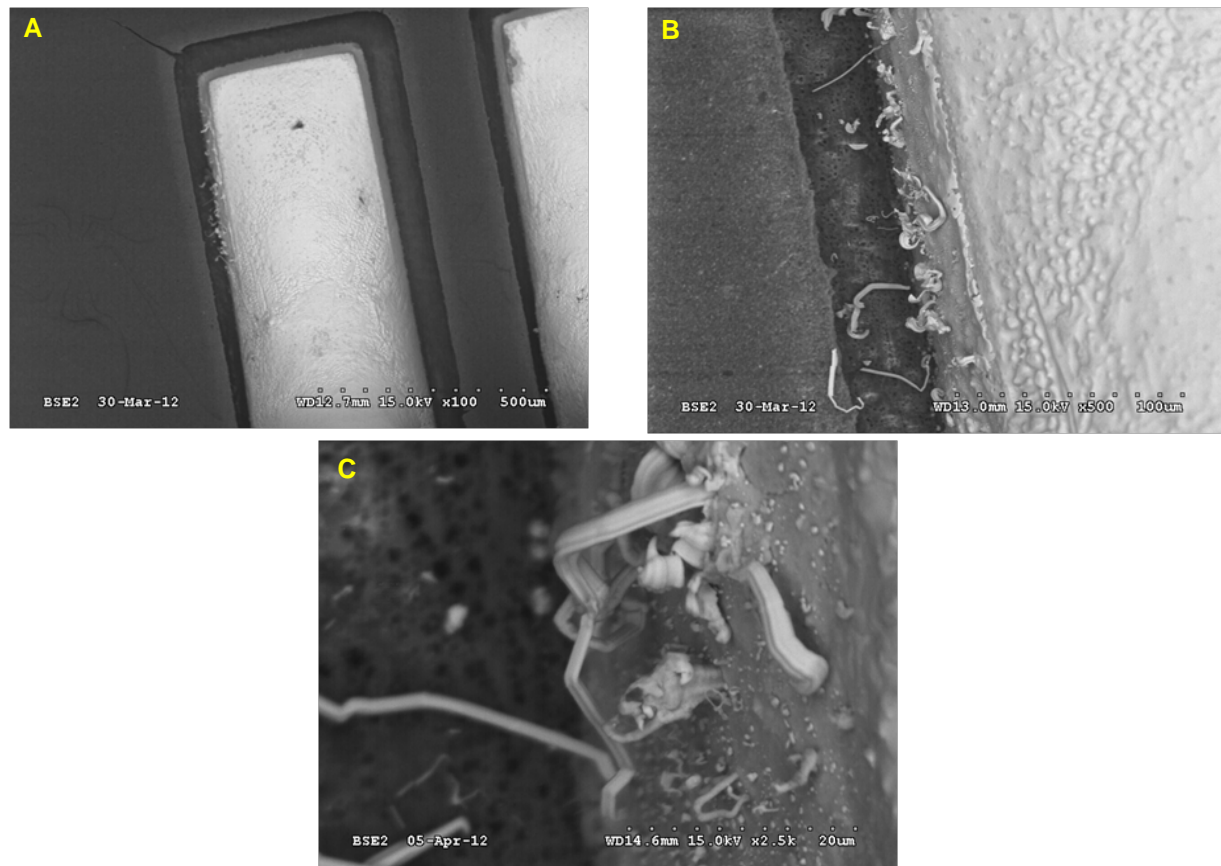


Figure 179: SEM images of an alloy-42 (SOT6) leaded part with a 1-1 contamination level after 1,000 h HTHH. Increasing magnification views shown from (A) to (C).

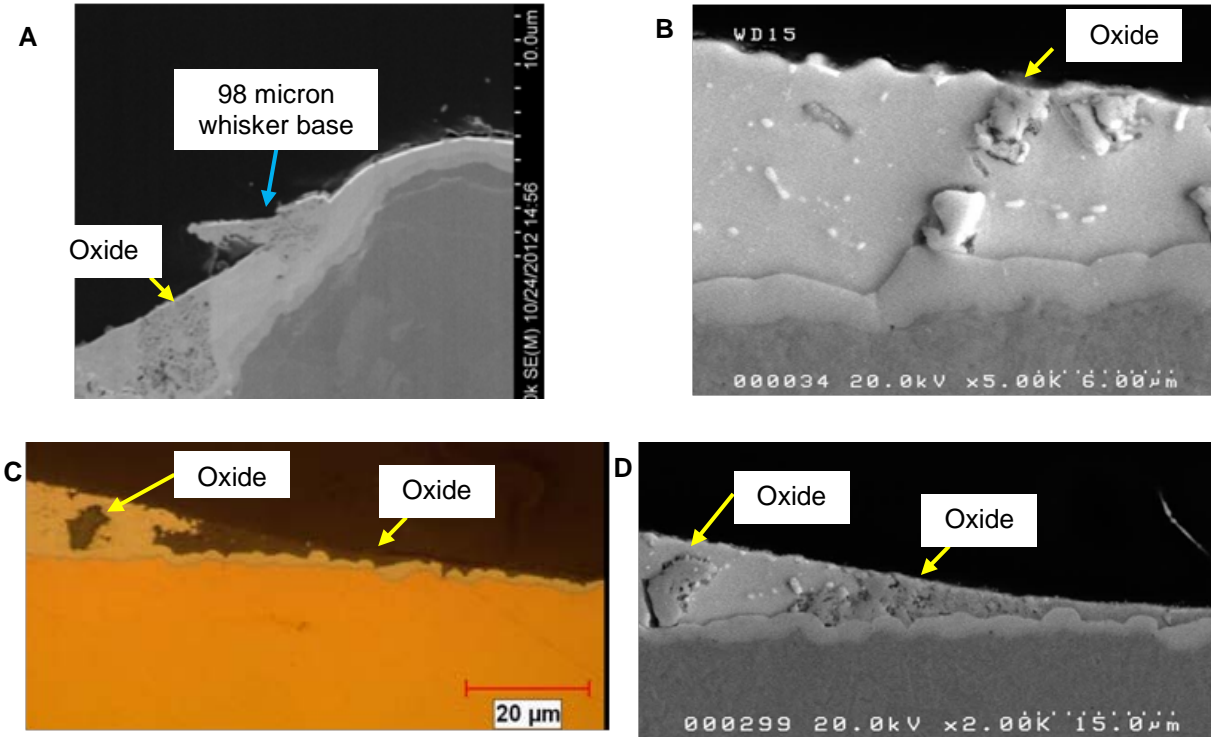


Figure 180: Partial oxidation of SAC solder with copper leaded part (SOT5) and 1-1 contamination; (A) SEM image of oxide near whisker, (B) SEM image of oxide in a thicker region of the SAC solder, (C) optical image of oxidation of solder near the base metal wetting line, and (D) SEM image of region shown in (C).

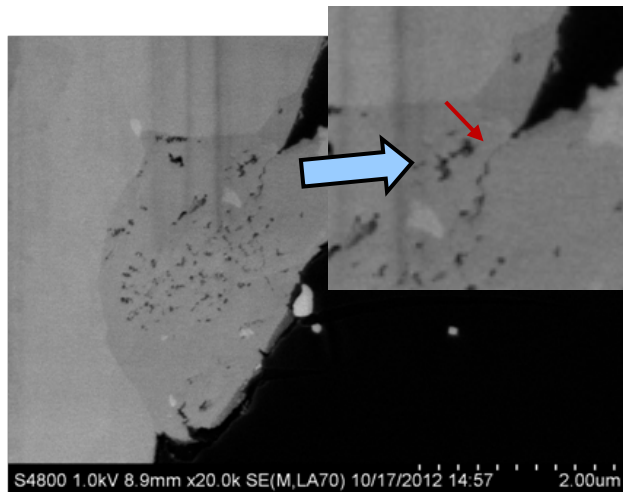


Figure 181: SEM image of voids and cracks observed in the whisker base. The crack is highlighted by an arrow. A large number of voids were observed in the root of the whisker.

Whisker striations were also observed similar to those found by other researchers [93]. Vertical striations were on smaller diameter whiskers (Figure 182) while both vertical and horizontal striations were observed on thicker whiskers (Figure 183).

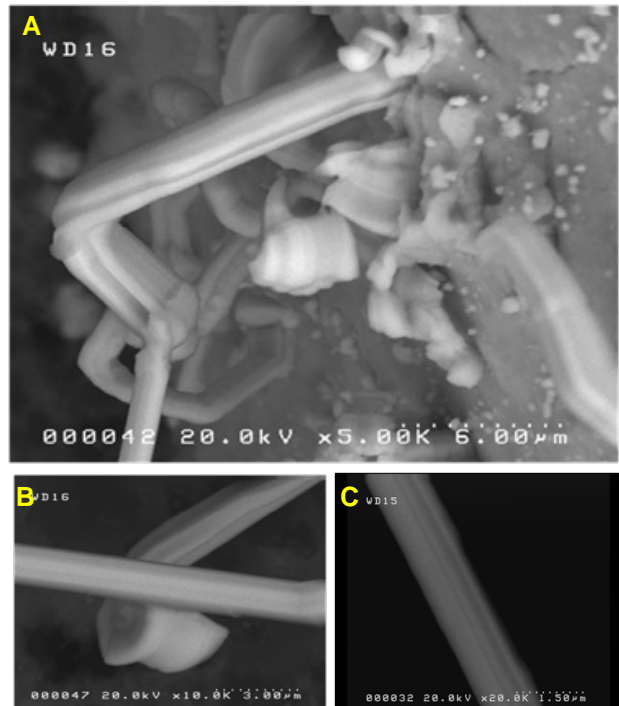


Figure 182: SEM images of vertical striations observed on smaller diameter whiskers. SEM images (A), (B) and (C) show increasing magnification views of typical striations.

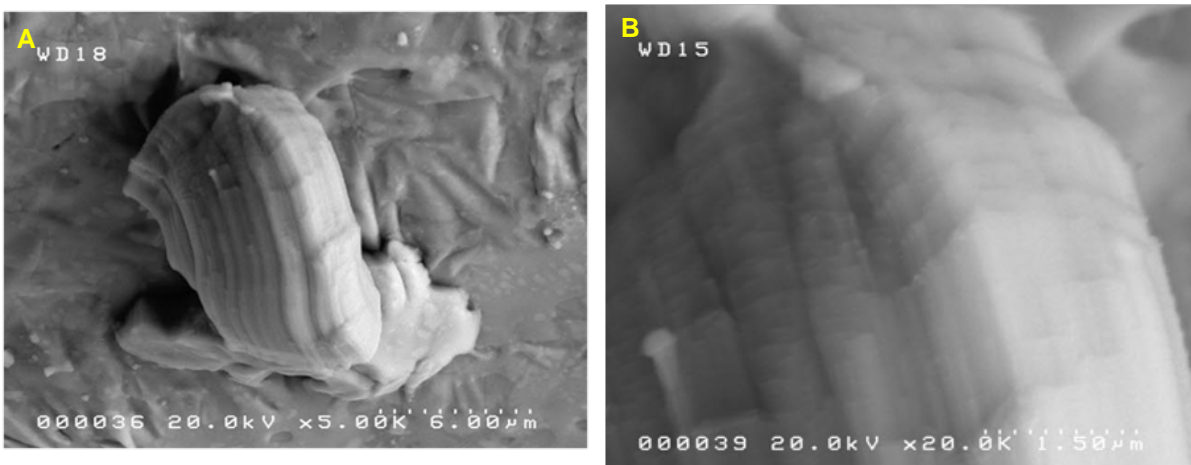


Figure 183: SEM images of vertical and horizontal striations observed on thicker whiskers. SEM images (A) and (B) show increasing magnification views of typical striations.

10.3.2 QFP board

Other copper leaded parts included in the humidity test also exhibited significant whisker growth at the 4,000 h inspection interval. While not part of the primary inspection set, the TQFP64 in Figure 184 exhibited a significant increase in whisker growth from 1,000 to 4,000 h. While small whiskers were generally observed at 1,000 h for the 0-0 contamination level, at 4,000 h there were many long enough to bridge between the board pads.

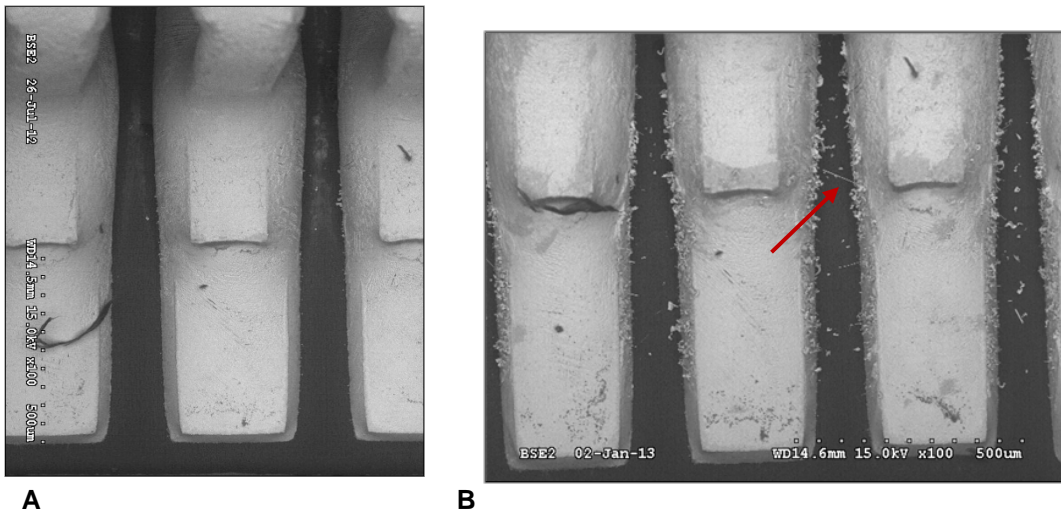


Figure 184: SEM images of a copper alloy lead 64 pin quad-flat-pack (QFP64 U08, lead 28) with a 0-0 contamination level after (A) 1,000 h and (B) 4,000 h HTHH. Arrow indicates a broken whisker that has nearly bridged between the printed wiring board pads. The TQFP lead alloy is C7025, which contains Ni, which is different from the SOT5 C194 alloy which does not.

10.3.3 BGA board

The inspection for whisker growth on the SAC105 and SAC105+0.01Ce alloy balls soldered with SAC305 paste was performed after 4,000 h (1,000+3,000 h). As was observed during power cycling, on a cleaned board with no contamination, the SAC105 balls did not form whiskers (Figure 185) while the SAC105 with a very small amount of Ce had whisker growth (Figure 186, Figure 187, and Figure 188). Unlike the tin whiskers that formed primarily at the board pad edges for the SOT and QFPs terminations, the whisker growth was not limited to a particular region of the ball surface.



Figure 185: No whisker growth was observed on SAC105 alloy balls soldered with SAC305 solder after 4,000 h of 85°C/85%RH.

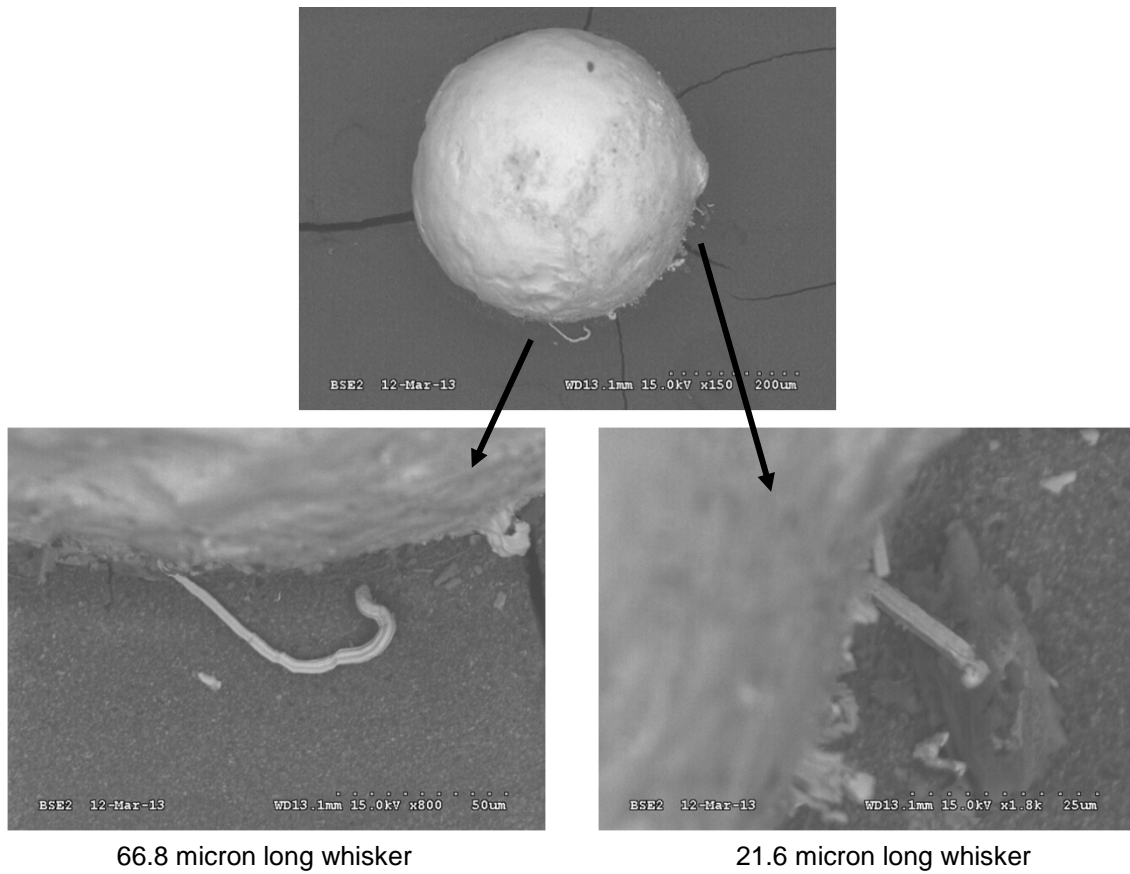


Figure 186: SEM images of tin whisker growth on a SAC105+0.01%Ce alloy ball soldered with SAC305 paste on a cleaned board with no contamination after 4,000 h of 85°C/85%RH.

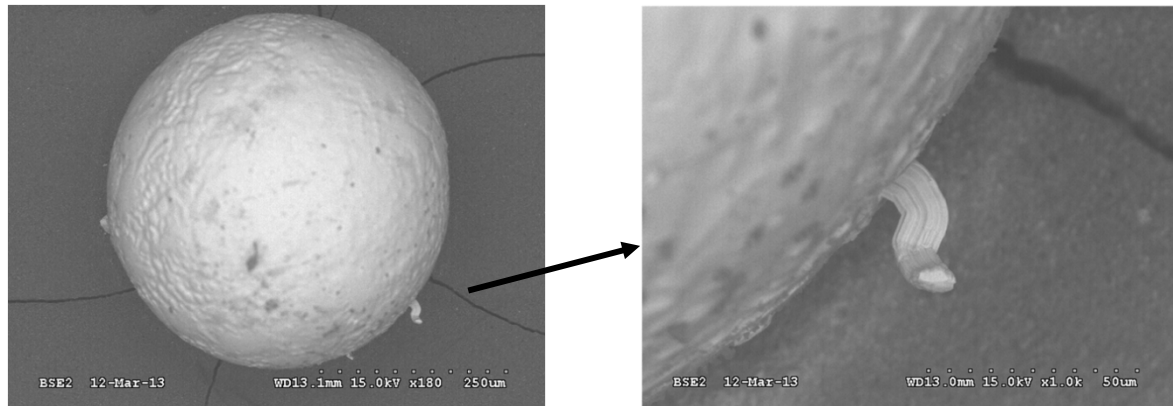


Figure 187: SEM images of a thicker whisker growing from a SAC105+0.01%Ce alloy ball soldered with SAC305 paste on a cleaned board with no contamination after 4,000 h of 85°C/85%RH.

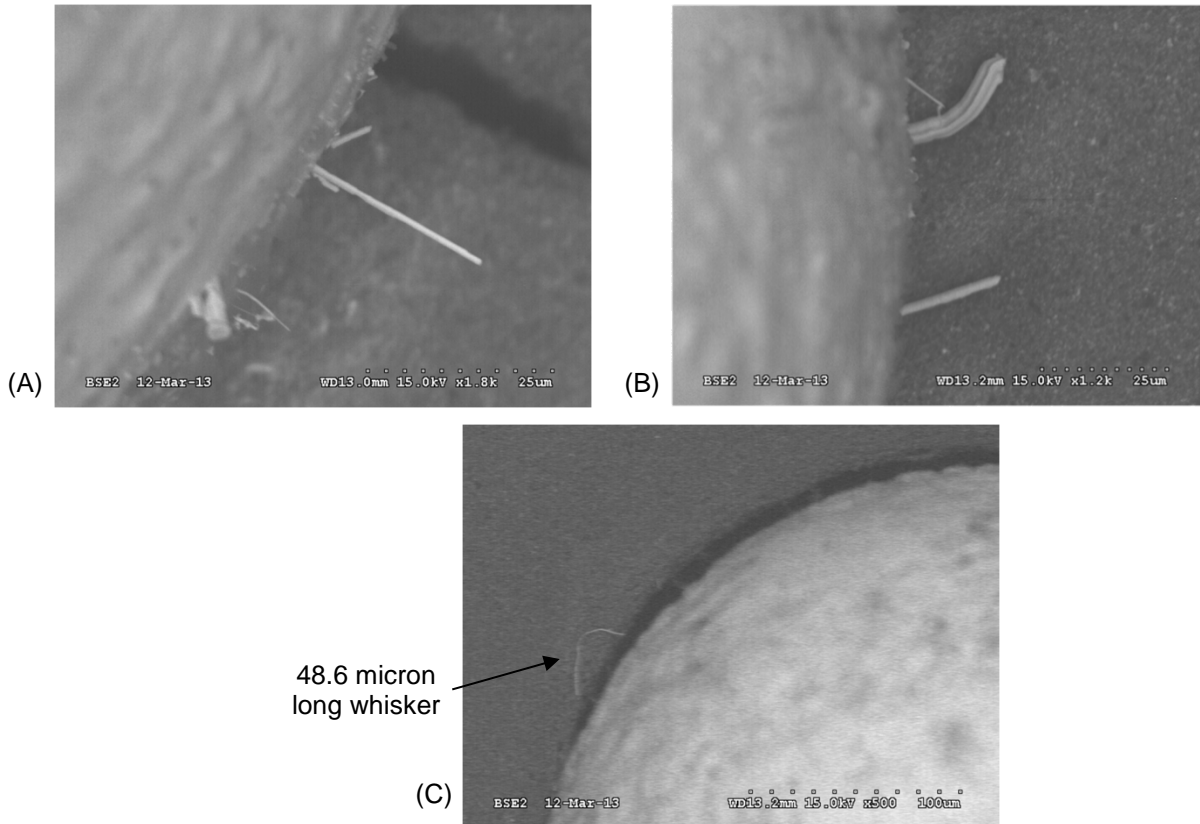


Figure 188: Additional SEM images showing varied density, morphology and length of tin whisker growth on SAC105+0.01%Ce alloy balls soldered with SAC305 paste on a cleaned board with no contamination after 4,000 h of 85°C/85%RH.

10.4 Conformal coating

After 4,000 h of HTHH exposure, the conformal coated SOT and QFP grew whiskers. The five volt biased pins exhibited greater corrosion on the coated SOT3 and SOT5 parts (Figure 189 and Figure 190). The coated SAC105+0.01%Ce (SAC+REE) solder balls had corrosion but no whiskers (Figure 191).

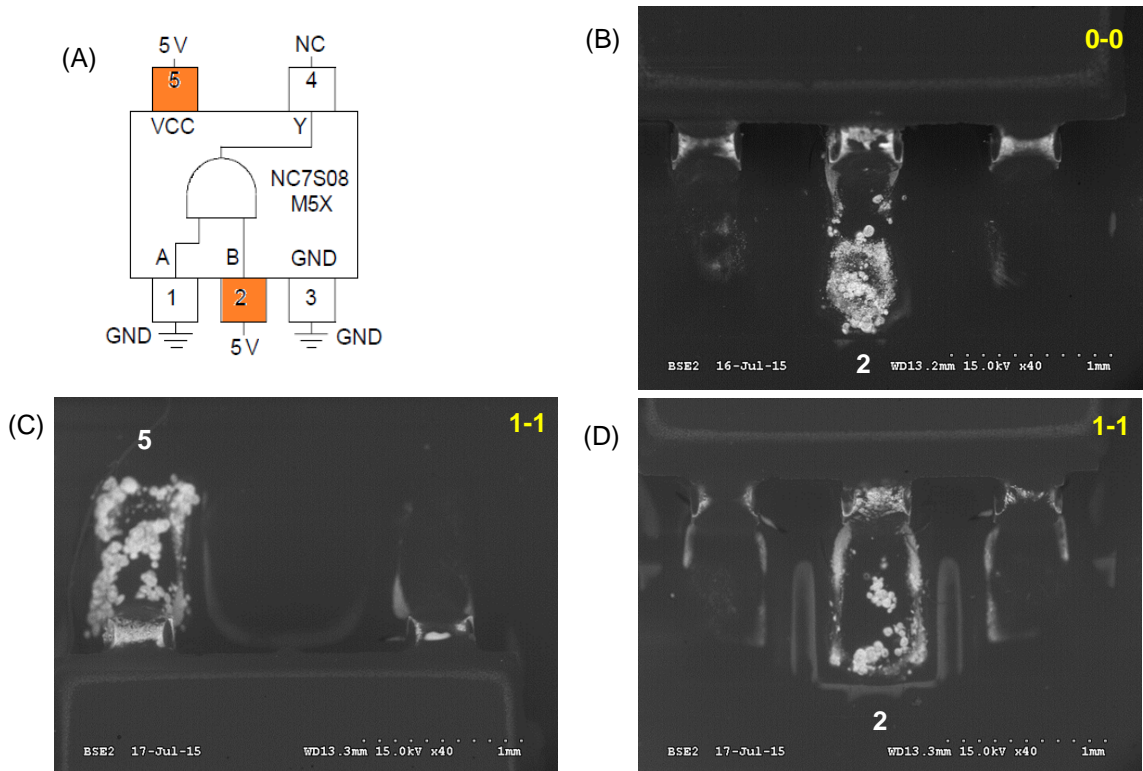


Figure 189: Influence of voltage bias on corrosion on coated SOT5 parts after 4,000 h HTHH; (A) electrical schematic, (B) 0-0 contamination level assembly, (C and D) 1-1 contamination level assembly.

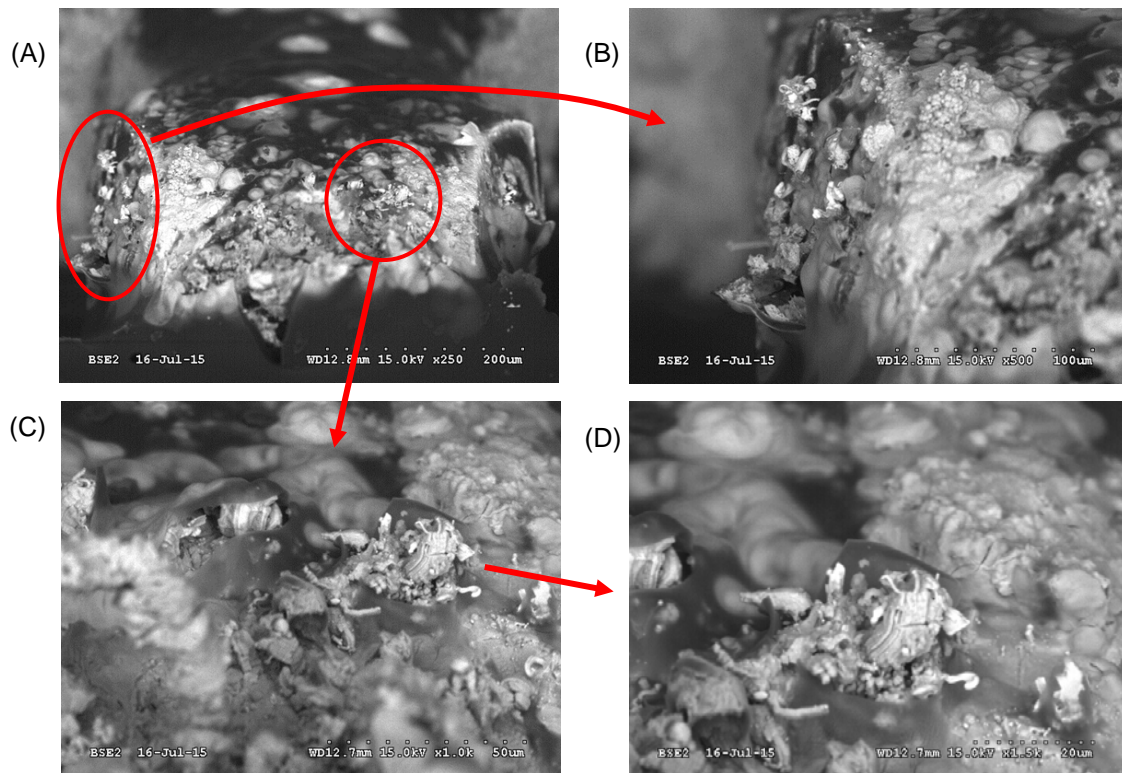


Figure 190: Detailed images of coated SOT5 lead 5 with a 0-0 contamination level after 4,000 h HTHH: (A) overall, 250x, (B) side of lead, 500x, (C) detailed image of nodule rupturing thin coating, 1,000x, (D) increasing magnification, 2,500x.

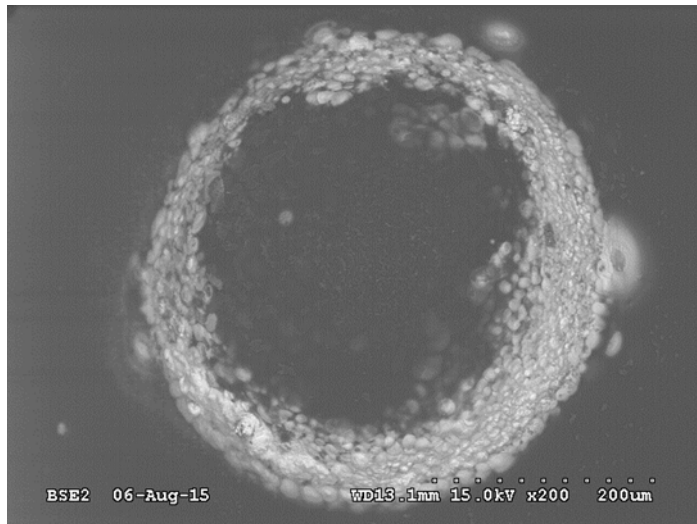


Figure 191: Corrosion on conformal coated SAC105+0.01%Ce (SAC+REE) solder balls after 4,000 h HTHH.

10.5 Summary

10.5.1 As-Received part factors

The lead-free Sn plated parts that meet the typical quality levels required to form a good solder joint can have microstructural characteristics that may increase whisker formation such as:

- Uneven Sn plating with very thin or skipped Sn plating in some locations
- Void and cracks
- Excessive contamination

10.5.2 Whisker length of SOT and QFP terminations

Large whisker growth was observed after 1,000 and 4,000 h of exposure to isothermal 85 °C/85 %RH conditions. Lead material and contamination level were the most significant factors contributing to whisker growth. Electrical bias had little influence even though there should be a difference in corrosion products on the anode and cathode. The following key points can be made:

- After 1,000 h there were 15,564 whiskers counted, and 4,741 whiskers measured
- After 4,000 h 75,386 whiskers were counted, 4.84 times more than were counted after 1,000 h; Data on 489 whiskers longer than 40 microns has been recorded
- There is a high risk of whisker growth in electronic assemblies if lead-free SAC305 solder is used without coating mitigation
- Long whisker growth was observed from the SAC305 solder, particularly in the regions where the solder became thin (three to 25 microns)
 - Whisker densities up to 2,027 whiskers per mm² were computed where the solder wicked onto the board pad edge after 4,000 h
 - Where the solder was thicker in the main part of the fillet, little or no whisker growth was observed
- Lead-free soldered assemblies exposed to 1,000 h of 85 °C/85 %RH grew whiskers with sufficient length to fail the JESD201 [23] piece part acceptance requirements for class 2

- Whisker growth occurred on SAC305 solder joints containing either the copper or the alloy-42 leaded components, but the alloy-42 leads exhibited a delay in long whisker growth
- Testing durations longer than 1,000 h were needed to ensure whisker nucleation and growth in 85 °C/85 %RH conditions
- Contaminated components in clean assemblies grow more long whiskers than clean components because of contamination entrapped in solder

10.5.3 Metallurgical observations

SOT and QFP optical microscopy, scanning electron microscopy in conjunction with cross-section examinations revealed that:

- The source of whisker growth stress was SAC305 solder oxidation and corrosion
- Many whiskers were broken from the joints forming debris between the leads
 - Oxidation of whiskers is believed to cause embrittlement making the whiskers susceptible to fracture under mechanical loading conditions
 - Once a whisker has fractured, the growth has terminated
- Whisker length
 - The longest whiskers are on terminations with the Cu alloy SOT5 lead frame
 - 186 microns (1,000 h) and 214 microns (4,000 h) on the 1-1 component/assembly contamination configuration
 - Slightly shorter whiskers were observed on terminations with the alloy-42 SOT3 and SOT6 lead frames
 - Whisker nucleation was delayed on the terminations with alloy-42 leads as compared to the terminations with copper leads
 - Particularly apparent on the board pads
 - The delay was attributed to the presence of the CuNiSn intermetallic on the copper board pads (the CuNiSn is more noble than the CuSn IMC).
 - Somewhat shorter whiskers were observed on clean assemblies
- Whisker locations:
 - Main - SAC305 on Cu board pad edge (location-2)
 - Some at locations 3, 4 and 5

SAC105+0.01%Ce alloy ball SEM inspection

- The SAC105 balls did not form whiskers while the SAC105 with 0.01%Ce had whisker growth on a cleaned assembly with no additional contamination.

11. Primary experiment 4 results and discussion: LTHH 25°C/85%RH

11.1 Experimental conditions

Assemblies were exposed to low temperature high humidity (LTHH) 25°C/85%RH simulated long term storage [32], with the inspection times indicated in Table 40. The samples were oriented vertically in the chamber and a drip shield was installed above the boards to prevent condensing drops from falling onto the boards.

Table 40: Long term high humidity exposure and inspection points over nearly three years.

Activity	Actual Start Date	Actual Finish Date	Inspection interval time (h)	Cumulative (h)
Testing 0-1,000 h	4-Oct-2011	16-Nov-2011	1,037	1,037
Inspection after 1,000 h	17-Nov-2011	7-Dec-2011	--	--
Testing 1,001-4,000 h	12-Dec-2011	30-Apr-2012	3,361	4,398
Inspection after 4,000 h	1-May-2012	25-May-2012	--	--
Testing 4,001-12,000 h	29-May-2012	4-Nov-2013	12,512	16,910
Inspection after 12,000 h	24-Jun-2014	20-Sep-2014	--	--

11.2 Whisker growth results

The whisker growth on cleaned assemblies with cleaned parts was less than on contaminated assemblies. The whisker count increased with increasing exposure time (Table 41).

Table 41: LTHH Whisker inspection summary

				Longest whisker (2)	
Inspection	Board	Counted	Measured	Part	Length (microns)
First inspection 1,037 h	SOT Board	No whiskers on clean assemblies (1). Some whiskers on contaminated assemblies (2).		SOT3	Less than 6
	QFP Board			PLCC20	49
				QFP44 (3)	132
Second inspection 4,398 h	SOT Board	369	47	SOT5	35
	QFP Board	102	102	PLCC20	145
Final inspection 16,910 h	SOT Board	4722	476	SOT5	92
(1) 0-0 contamination level					
(2) On assemblies with a 0-1 or 1-1 contamination level					
(3) Hollow whiskers on the 1-1 contamination level					

11.2.1 First inspection: 1,037 h SOT and QFP boards

At the first inspection after 1,037 h at 25°C/85%RH, some whisker growth observed was on the samples. Longer whiskers growth was observed when contamination levels were higher. No whiskers were observed on clean assemblies (Table 42).

Table 42: Whisker observations from the first inspection after 1,037 h LTHH.

Component	Contamination level (part-board)	Observations
SOT3	1-1	Short whiskers, not longer than 6 microns
SOT5	1-1	Almost no growth, maybe one small hillock
PLCC	1-1	Whiskers present. Longest is 49 microns
	0-1	Whiskers present. Longest is 33 microns
	1-0	No whiskers
	0-0	
QFP44	1-1	Hollow whiskers slightly longer than 10µm
	0-1	Hollow whiskers 15.9µm, 26.2µm, 33.4µm, and 132µm
	1-0	Short whiskers up to 4.6µm
	0-0	No hint of whisker growth

11.2.2 Second Whisker Inspection: 4,398 h SOT Boards

The samples were returned to the environmental chamber and an additional 3,361 h for a total of 4,398 h (1,037+3,361). On the SOT parts, a total of 369 whiskers were counted and 47 whiskers were measured (Table 43 to Table 49). The whiskers were longer for the Cu alloy SOT5 terminations than the alloy-42 terminations. Clean assemblies exhibited little or no whisker growth.

The top five longest whiskers and the corresponding average diameters are shown in Figure 192 and Figure 193. Even though the fit was not that good due to the limited number of data points, some probability plots are presented for reference. A comparison of whisker lengths for the various SOT part types is shown in Figure 194.

A comparison of SOT5 whisker lengths for the five whisker growth location is shown in Figure 195. The greatest whisker growth on the SOT5 part was observed in locations one and four.

Table 43: Whisker measurement summary from the SOT board second inspection after 4,398 h LTHH.

Component	Whiskers Counted	Whiskers Measured	Percent measured	Longest (micron)
SOT5	270	35	13%	35
SOT6	59	7	12%	27
SOT3	40	5	13%	28
Total	369	47		

Table 44: SOT5 component and lead whiskering summary from the second inspection after 4,398 h LTHH.

Cleanliness	Components/ Components w/ Whiskers	% of Components w/ Whiskers	Leads/ Leads with Whiskers	% of Leads w/ Whiskers
1-1	26	73	130	27.7
	19		36	
0-0	16	12.5	80	2.5
	2		2	
0-1	16	68.7	80	25
	11		20	
1-0	16	0	80	0
	0		0	
Overall	74	43.2	370	15.7
	32		58	

Table 45: SOT6 component and lead whiskering summary from the second inspection after 4,398 h LTHH.

Cleanliness	Components/ Components w/ Whiskers	% of Components w/ Whiskers	Leads/ Leads with Whiskers	% of Leads w/ Whiskers
1-1	10	50	60	13.3
	5		8	
0-0	8	0	48	0
	0		0	
0-1	8	62.5	48	14.6
	5		7	
1-0	8	0	48	0
	0		0	
Overall	34		204	
	10		15	

Table 46: SOT3 component and lead whiskering summary from the second inspection after 4,398 h LTHH.

Cleanliness	Components/ Components w/ Whiskers	% of Components w/ Whiskers	Leads/ Leads with Whiskers	% of Leads w/ Whiskers
1-1	39	10.2	117	2.6
	4		3	
0-0	16	0	48	0
	0		0	
0-1	16	25	48	8.3
	4		4	
1-0	16	0	48	0
	0		0	
Overall	87	9.2	261	2.7
	8		7	

Table 47: SOT5 whisker length summary from the second inspection after 4,398 h LTHH.

Cleanliness	Total Whiskers	Total Measured	Longest Whisker (μm)
1-1	160	17	28.3
0-0	7	0	0
0-1	103	18	35
1-0	0	0	0
Overall	270	35	35

Table 48: SOT6 whisker length summary from the second inspection after 4,398 h LTHH.

Cleanliness	Total Whiskers	Total Measured	Longest Whisker (μm)
1-1	51	1	12.2
0-0	0	0	0
0-1	8	6	26.7
1-0	0	0	0
Overall	59	7	26.7

Table 49: SOT3 whisker length summary from the second inspection after 4,398 h LTHH.

Cleanliness	Total Whiskers	Total Measured	Longest Whisker (μm)
1-1	9	1	17.7
0-0	0	0	0
0-1	31	4	28.3
1-0	0	0	0
Overall	40	5	28.3

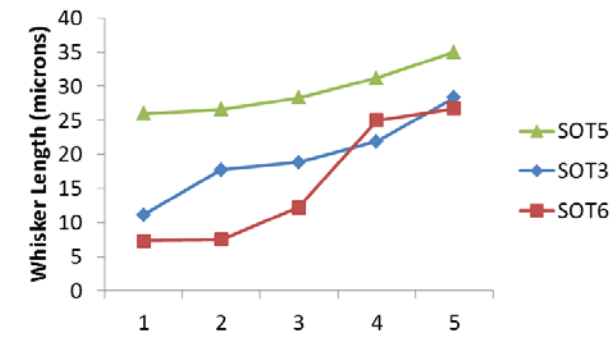


Figure 192: Five longest whiskers of the SOT parts from the second inspection after 4,398 h LTHH.

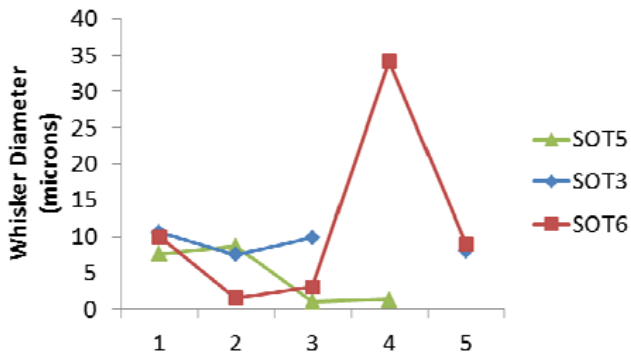


Figure 193: Corresponding average whisker diameters for SOT board from second inspection after 4,398 h LTHH (Note: some whisker diameters were not measured).

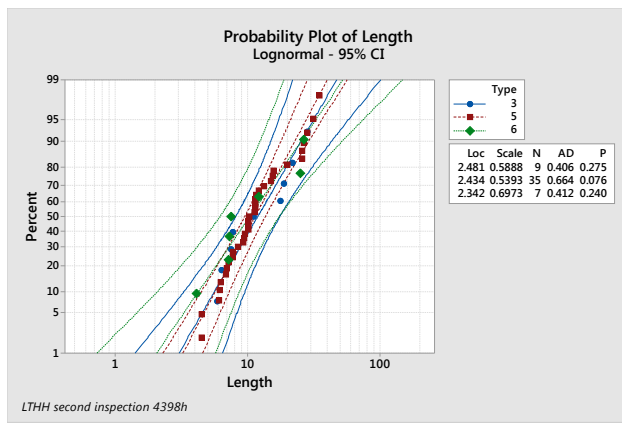


Figure 194: SOT board whisker length probability plot for the second inspection after 4,398 h LTHH.

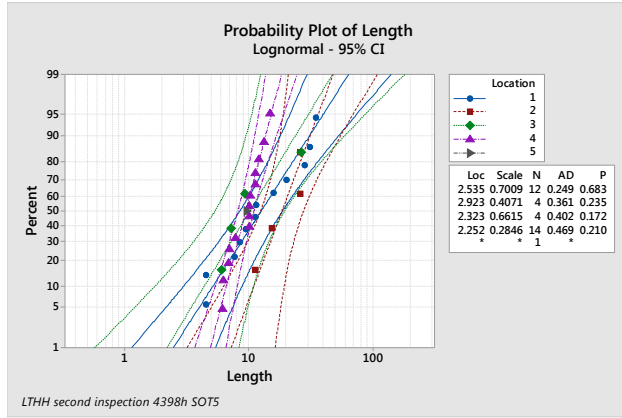


Figure 195: SOT5 whisker length probability plot by location for the second inspection after 4,398 h LTHH.

11.2.3 Second inspection: 4,398 h QFP Boards

During the second inspection after 4,398 h (1,037+3,361), a partial inspection of the QFP boards was performed. The QFP boards had longer whisker growth than the SOT boards. Only the samples with post assembly contamination (0-1 or 1-1) exhibited whisker growth. The whisker lengths for the PLCCs were longer than the

QFP44 which were longer than the TQFP64 (Figure 196 and Figure 197). The diameters of the top 10 whiskers ranged from below one micron to seven microns (Figure 198). The whisker location histograms (Figure 199 through Figure 201) for the PLCC, QFP44 and TQFP64 parts show that the majority of whisker grew from location four on the PLCC. The QFP44 had the most growth from locations one and four. The TQFP64 had the most growth from location one.

The tabular results summary of the PLCC, QFP44 and TQFP64 inspections are given in Table 50 through Table 53. Examining the whisker length distributions in further detail, the configurations with cleaned parts and contaminated boards had slightly more and longer whisker growth (Figure 202 through Figure 204). The lead bias voltage (Bias2) did not influence the whisker growth (Figure 205).

Locations 1, 3, and 4 on the lead exhibited the longest and the most whisker growth (Figure 205 through Figure 207).

There was no strong correlation between whisker diameter and whisker length (Figure 208). This is particularly evident when comparing \ln (diameter) and \ln (length). The whisker diameters ranged from below a micron to just under 12 microns. The diameters of the longest whiskers were between two microns and seven microns and the largest diameter whiskers tend to be the shortest in this sample set.

Table 50: Whisker measurement summary from the QFP board second inspection after 4,398 h LTHH.

Component	Whiskers Counted	Whiskers Measured	Percent measured	Longest whisker (micron)
PLCC20	69	69	100%	145
QFP44	18	18	100%	100
TQFP64	15	15	100%	22
Total	102	102		

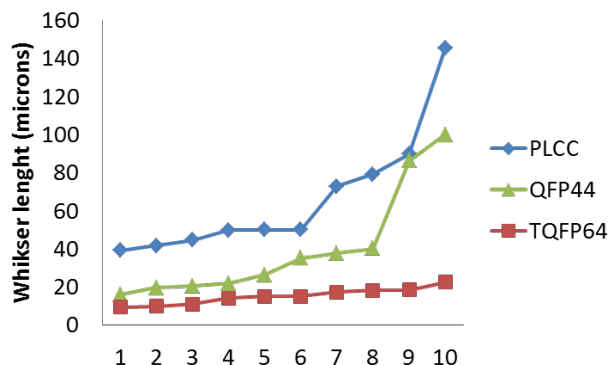


Figure 196: Ten longest whiskers of the QFP board parts from the second inspection after 4,398 h LTHH.

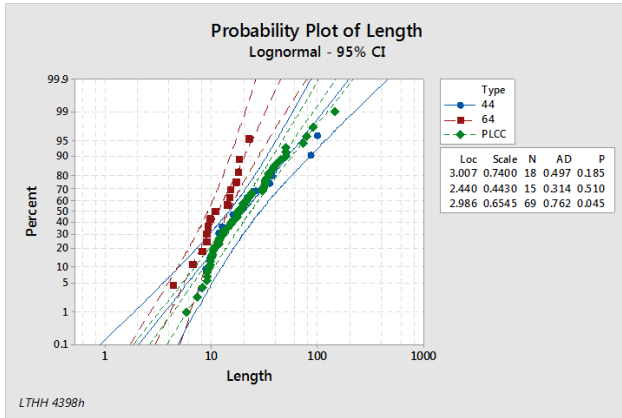


Figure 197: QFP board probability plot of whisker length for the PLCC, QFP44 and TQFP64 parts from the second inspection after 4,398 h LTHH.

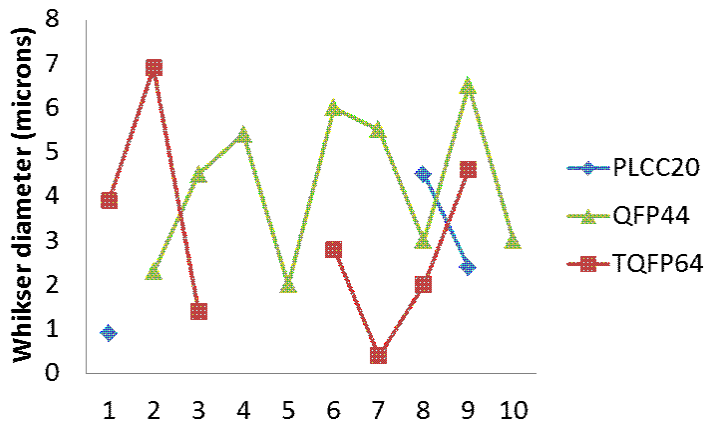


Figure 198: Corresponding average whisker diameters for the 10 longest whiskers of the QFP board parts from the second inspection after 4,398 h LTHH (Note: some whisker diameters were not measured).

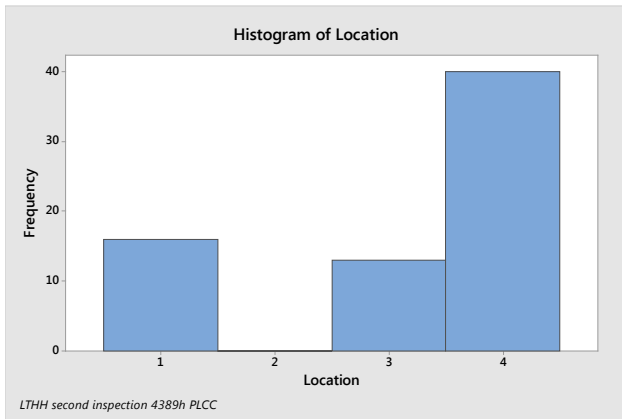


Figure 199: PLCC histogram of whisker location from the second inspection after 4,398 h LTHH.

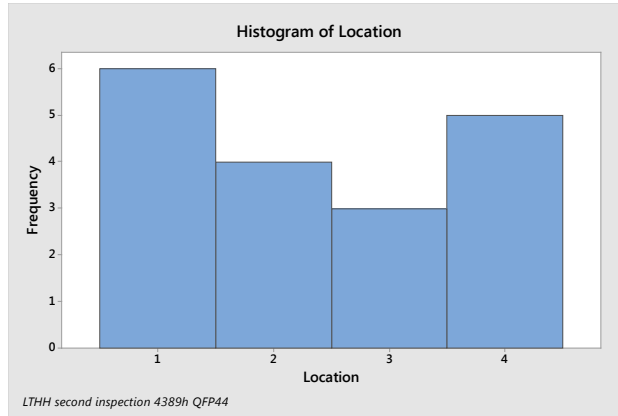


Figure 200: QFP44 histogram of whisker location from the second inspection after 4,398 h LTHH.

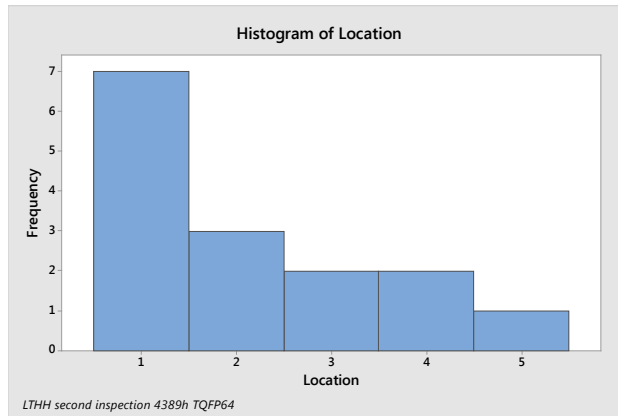


Figure 201: TQFP64 histogram of whisker location from the second inspection after 4,398 h LTHH.

Table 51: PLCC20 whisker summary from the second inspection after 4,398 h LTHH.

Cleanliness	Components/ Components w/ Whiskers	% of Components w/ Whiskers	Leads/ Leads with Whiskers	% of Leads w/ Whiskers
1-1	6	100%	40	48%
	6		19	
0-0	2	0%	25	0%
	0		0	
0-1	3	100%	18	100%
	3		18	
1-0	2	0%	30	0%
	0		0	
OVERALL	13		113	
	9		37	

Table 52: QFP44 whisker summary from the second inspection after 4,398 h LTHH.

Cleanliness	Components/ Components w/ Whiskers	% of Components w/ Whiskers	Leads/ Leads with Whiskers	% of Leads w/ Whiskers
1-1	4	75%	18	17%
	3		3	
0-0	2	0%	24	0%
	0		0	
0-1	2	100%	8	63%
	2		5	
1-0	2	0%	2	0%
	0		0	
OVERALL	10		52	
	5		8	

Table 53: TQFP64 whisker summary from the second inspection after 4,398 h LTHH.

Cleanliness	Components/ Components w/ Whiskers	% of Components w/ Whiskers	Leads/ Leads with Whiskers	% of Leads w/ Whiskers
1-1	3	67%	22	14%
	2		3	
0-0	2	0%	32	0%
	0		0	
0-1	2	100%	11	64%
	2		7	
1-0	2	0%	2	0%
	0		0	
OVERALL	9		67	
	4		10	

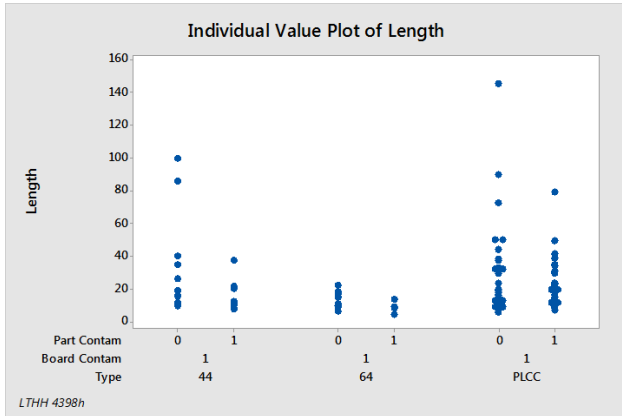


Figure 202: QFP individual value plot of whisker length for various contamination levels from the second inspection after 4,398 h LTHH.

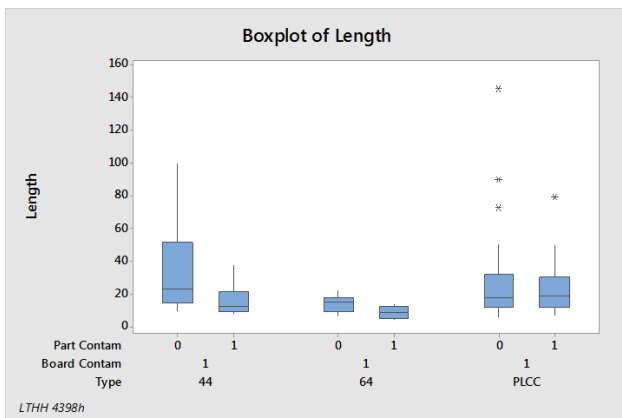


Figure 203: QFP box plot of whisker lengths for various contamination levels from the second inspection after 4,398 h LTHH.

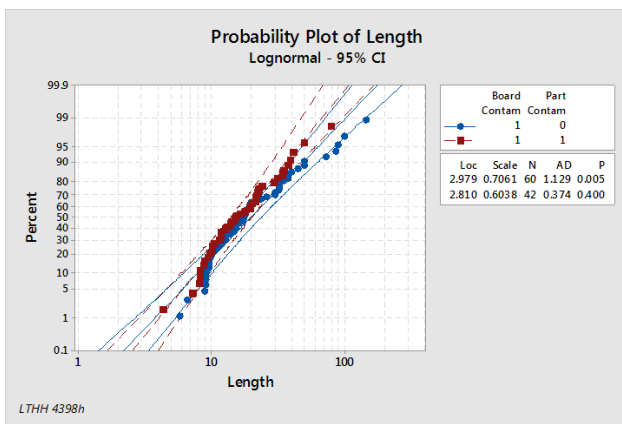


Figure 204: QFP board probability plot of whisker length for the PLCC, QFP44 and TQFP64 parts combined for various contamination levels from the second inspection after 4,398 h LTHH.

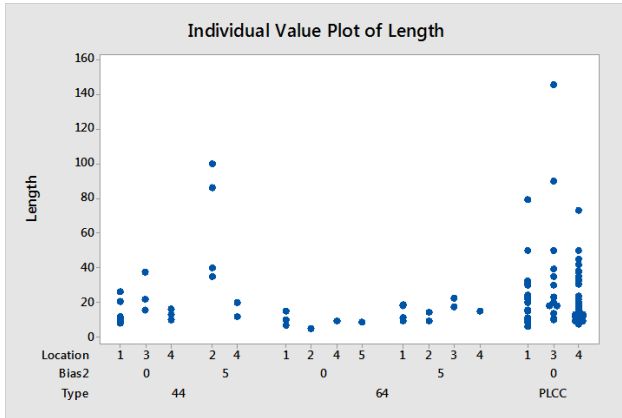


Figure 205: QFP board individual value plot of whisker length for Bias2, location and part type from the second inspection after 4,398 h LTHH.

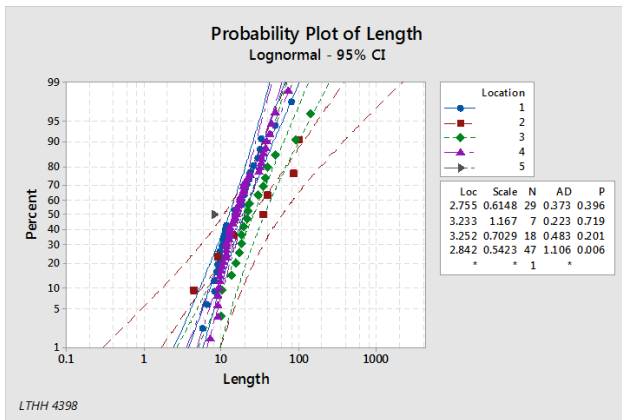


Figure 206: QFP board probability plot of whisker length for the PLCC, QFP44 and TQFP64 parts (combined) for various locations from the second inspection after 4,398 h LTHH.

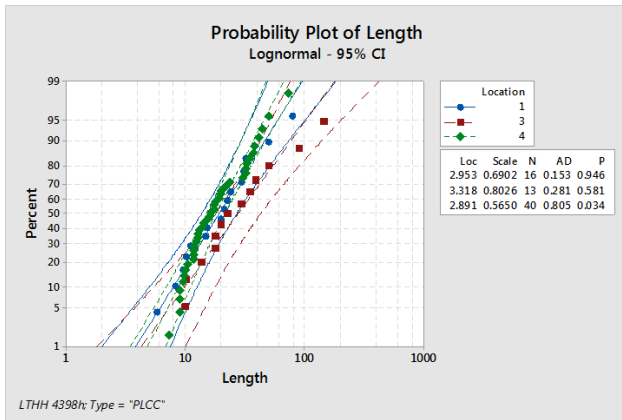


Figure 207: QFP board probability plot of whisker length for the PLCC part for various locations from the second inspection after 4,398 h LTHH.

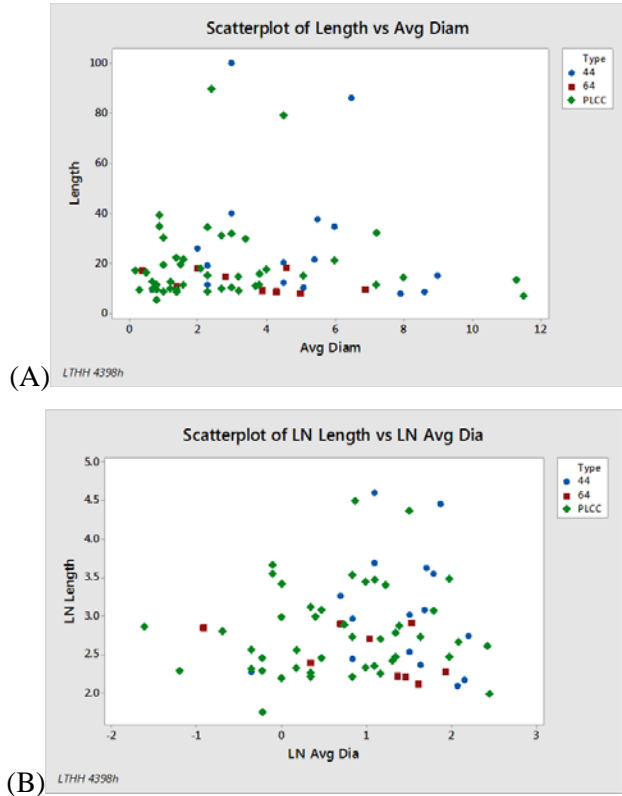


Figure 208: Whisker length versus diameter data from the second inspection after 4,398 h LTHH; (A) average diameter in microns and (B) ln (average diameter).

11.2.4 Final Inspection: 16,910 h SOT board

After the second inspection, the samples were returned to the environmental chamber for an additional 12,512 h for a total of 16,910 h ($1,037 + 3,361 + 12,512$). After nearly three years of storage, including inspection queue time, no whiskers longer than 10 microns were observed on clean assemblies. The long whiskers were only observed on NaCl contaminated assemblies. The copper alloy lead termination exhibited the most and the longest whisker growth with the alloy-42 having substantially reduced whisker growth (Table 54 through Table 60 and Figure 209). Note that low whisker growth on the alloy-42 lead terminations was also observed during the 85°C/85%RH high temperature high humidity (HTHH) experiments.

Many of the whiskers from the SOT5 termination had diameters that were very small (~0.1 micron) as compared to the SOT6 and SOT3 part terminations (Figure 210). Small diameter whisker growth was also observed on cross-sections of SAC solder containing rare earth elements after extended storage in nitrogen. Submicron whiskers were not evident in the HTHH or the TC.

The whisker count was reasonably consistent for the various leads (Table 61). The whisker count at locations one, three and four were the greatest (Table 62). Note that in the HTHH experiments, location-2 was the primary whisker growth location.

Table 54: Whisker measurement summary from the final inspection after 16,910 h LTHH.

Component	Whiskers Counted	Whiskers Measured	Percent measured	Longest (micron)
SOT5	4428	457	10%	92
SOT6	160	11	7%	64
SOT3	134	8	6%	83
Total	4722	476		

Table 55: SOT5 component lead whisker growth summary from the final inspection after 16,910 h LTHH.

Cleanliness	Components/ Components w/ Whiskers	% of Components w/ Whiskers	Leads/ Leads with Whiskers	% of Leads w/ Whiskers
1-1	16	100	80	98.8
	16		79	
0-0	16	6.2	80	1.2
	1		1	
0-1	16	100	80	91.2
	16		73	
1-0	16	31.2	80	6.2
	5		5	
Overall	64		320	
	38		158	

Table 56: SOT6 component lead whisker growth summary from the final inspection after 16,910 h LTHH.

Cleanliness	Components/ Components w/ Whiskers	% of Components w/ Whiskers	Leads/ Leads with Whiskers	% of Leads w/ Whiskers
1-1	8	100	48	47.9
	8		23	
0-0	8	12.5	48	2.1
	1		1	
0-1	8	100	48	41.7
	8		20	
1-0	0	0	0	0
	0		0	
Overall	24		144	
	17		44	

Table 57: SOT3 component lead whisker growth summary from the final inspection after 16,910 h LTHH.

Cleanliness	Components/ Components w/ Whiskers	% of Components w/ Whiskers	Leads/ Leads with Whiskers	% of Leads w/ Whiskers
1-1	48	14.6	144	6.9
	7		10	
0-0	48	0	144	0
	0		0	
0-1	48	25	144	12.5
	12		18	
1-0	48	2.1	144	1.7
	1		1	
Overall	192		576	
	20		29	

Table 58: SOT5 whisker growth summary from the final inspection after 16,910 h LTHH.

Cleanliness	Total Whiskers	Total Measured	Longest Whisker (µm)
1-1	2355	254	81
0-0	6	0	0
0-1	2040	203	92
1-0	27	0	0
Overall	4428	457	92

Table 59: SOT6 whisker growth summary from the final inspection after 16,910 h LTHH.

Cleanliness	Total Whiskers	Total Measured	Longest Whisker (µm)
1-1	126	4	23
0-0	1	0	0
0-1	33	7	64
1-0	0	0	0
Overall	160	11	64

Table 60: SOT3 whisker growth summary from the final inspection after 16,910 h LTHH.

Cleanliness	Total Whiskers	Total Measured	Longest Whisker (μm)
1-1	16	6	83
0-0	0	0	0
0-1	117	2	31
1-0	1	0	0
Overall	134	8	83

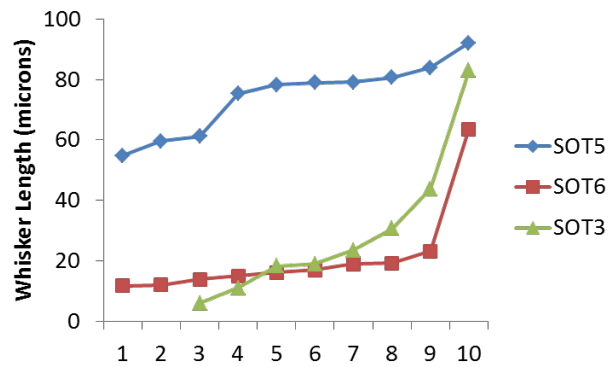


Figure 209: Ten longest whiskers on the SOT board parts from the final inspection after 16,910 h LTHH.

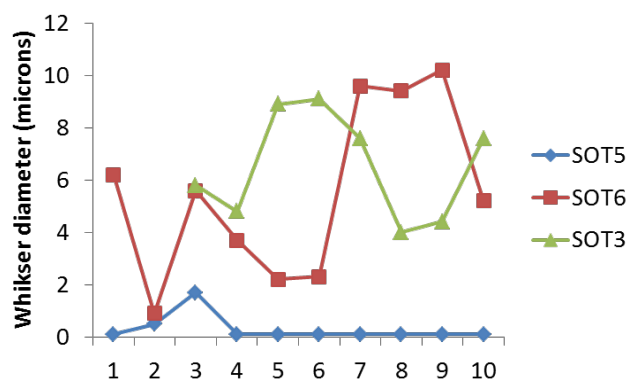


Figure 210: Corresponding average whisker diameters for the 10 longest whiskers of the SOT board parts from the final inspection after 16,910 h LTHH.

Table 61: SOT5 Total whisker count by lead for various contamination levels from the final inspection after 16,910 h LTHH.

Lead	Cleanliness (Part-Board)			
	1-1	0-0	0-1	1-0
Lead 1	417	6	381	3
Lead 2	540	0	364	18
Lead 3	266	0	418	5
Lead 4	482	0	320	1
Lead 5	650	0	557	0

Table 62: SOT5 Total whisker count by location for various contamination levels from the final inspection after 16,910 h LTHH.

	Cleanliness (Part-Board)			
	1-1	0-0	0-1	1-0
Length range (microns)				
Location	< 10µm	< 10µm	< 10µm	< 10µm
L1	487	0	757	2
L2	6	0	1	0
L3	552	0	271	9
L4	1052	6	806	16
L5	4	0	2	0
Length range (microns)				
Location	> 10µm	> 10µm	> 10µm	> 10µm
L1	48	0	78	0
L2	1	0	2	0
L3	72	0	34	0
L4	133	0	89	0
L5	0	0	0	0

11.2.4.1 Contamination and lead material

The individual value plot of whisker length for lead material and contamination level shown in Figure 211 illustrates the significantly higher whisker growth that occurred on the Cu alloy leads compared with the alloy-42. The whisker length lognormal probability plot by part type (Figure 212) again shows that the Cu alloy SOT5 with greater whisker growth but does not describe longest whiskers well.

Focusing on the SOT5, the whisker length lognormal probability plots for the for various contamination levels (Figure 213 and Figure 214) shows that when the board is contaminated, that the part level contamination has little impact on whisker length and that whisker length is not sensitive to lead bias.

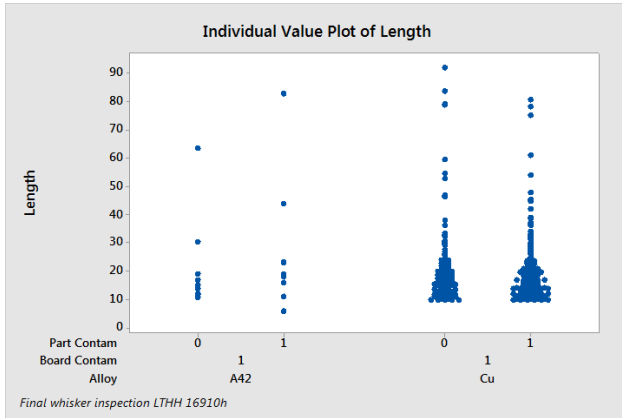


Figure 211: Final inspection whisker length individual value plot by part lead alloy and contamination level after 16,910 h LTHH. Note no whiskers longer than 10 microns were observed for the assemblies without board level contamination.

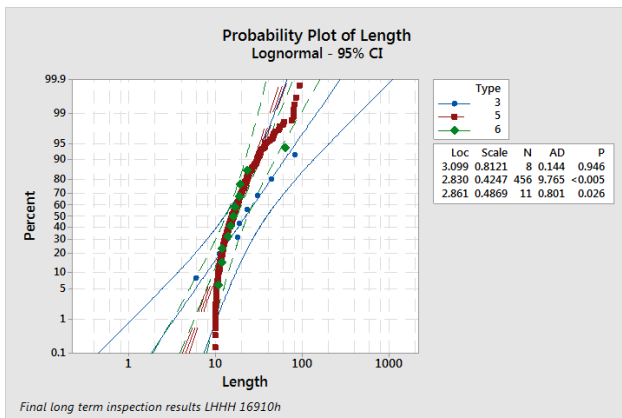


Figure 212: Final inspection whisker length probability plot for the SOT3, SOT5 and SOT6 part types after 16,910 h LTHH.

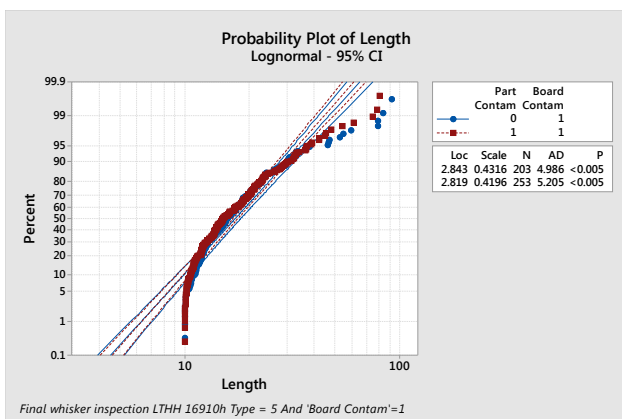


Figure 213: Final inspection whisker length probability plot for the SOT5 part leads for various contamination levels after 16,910 h LTHH (all bias levels combined).

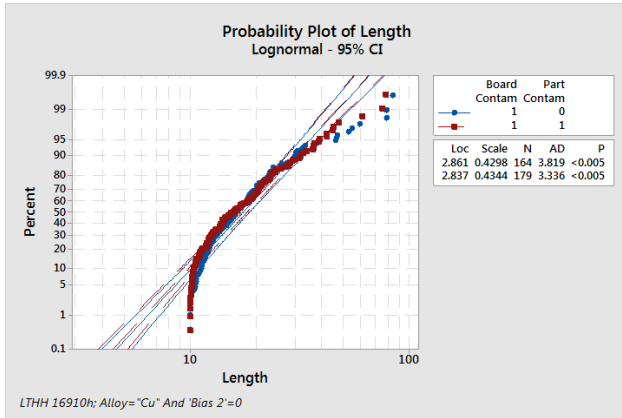


Figure 214: Final inspection whisker length probability plot for the SOT5 part leads with Bias2=0 for various contamination levels after 16,910 h LTHH.

11.2.4.2 Whisker diameter and angle

Whisker length versus diameter data from the second inspection is shown in Figure 215. Generally, the larger diameter whiskers tend to be shorter. In contrast to the earlier inspections and the high temperature/high humidity 85°C/85 percent RH short term test, there are many whiskers that are 0.1 to 0.3 microns in diameter.

The whisker growth angle distribution was relatively uniform (Figure 216).

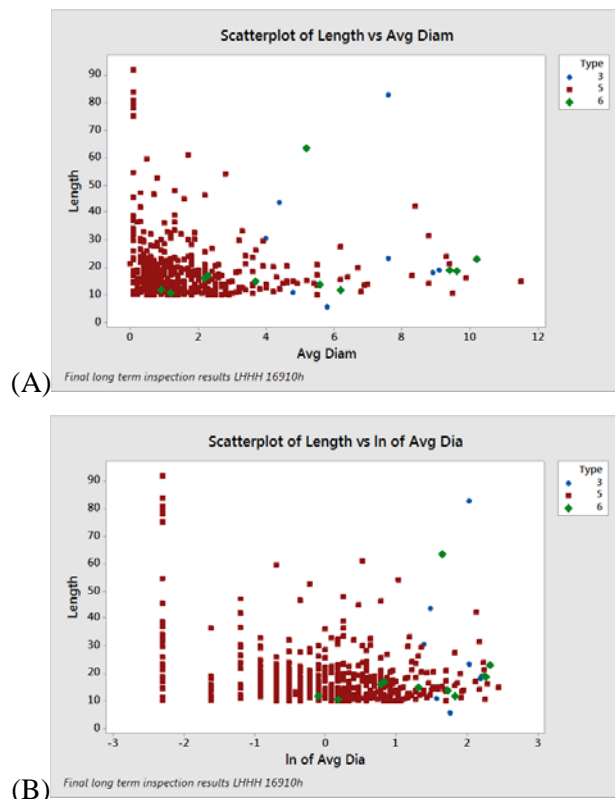


Figure 215: Whisker length versus diameter data from the final inspection after 16,910 h LTHH; (A) average diameter in microns and (B) ln (average diameter).

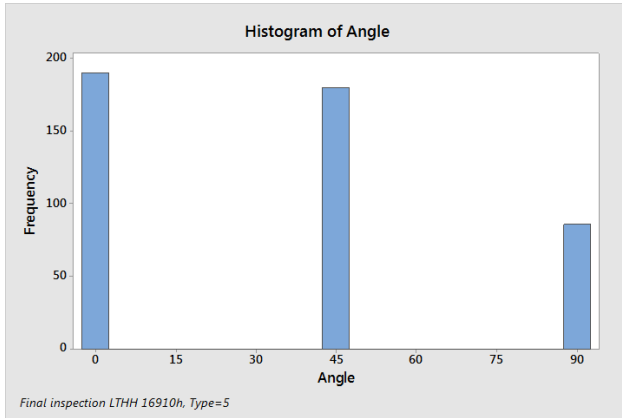


Figure 216: Final inspection whisker angle histogram for the SOT5 parts after 16,910 h LTHH.

11.2.4.3 Whisker growth location

The whiskers longer than 10 microns mainly grew from lead locations 1, 3 and 4 (Figure 217 and Figure 218). During the final inspection many more whiskers were counted than were measured (Table 54). As the whiskers were counted, the growth location was recorded so that whisker densities could be determined. The largest whisker density was observed for the SOT5 parts (Figure 219).

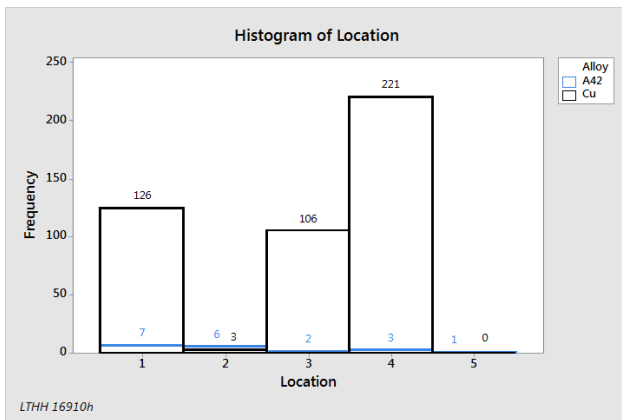


Figure 217: Location of whiskers longer than 10 microns from the final inspection after 16,910 h LTHH.

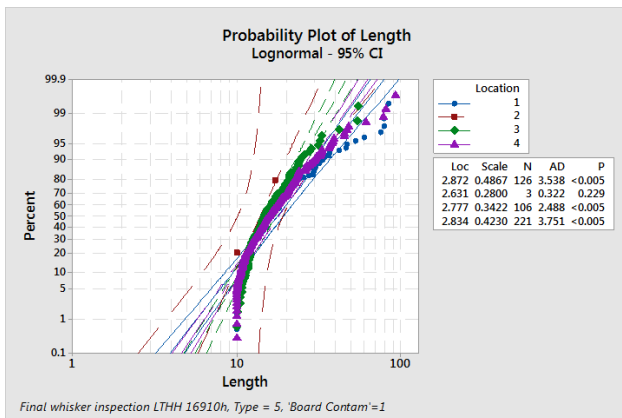


Figure 218: Final inspection whisker length probability plot for the SOT5 part lead terminations with board contamination level = 1 for various locations on the lead after 16,910 h LTHH.

11.2.4.4 Whisker density

A box plot showing whisker density by location and part type for the SOT board is shown in Figure 219. The SOT5 part termination whisker density at locations 1, 3, and 4 fit reasonably well to a lognormal probability distribution when sufficient data points were available (Figure 220 through Figure 222).

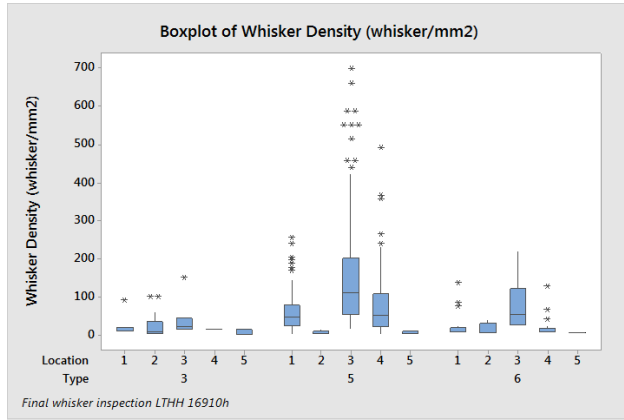


Figure 219: Final inspection whisker density box plot by part and location after 16,910 h LTHH.

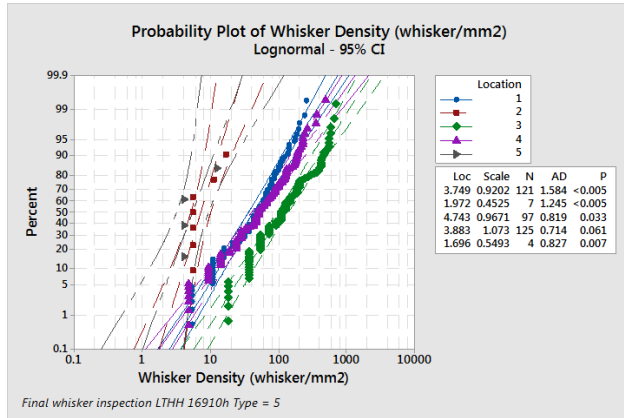


Figure 220: Final inspection whisker density probability plot for various locations on the SOT5 part termination after 16,910 h LTHH.

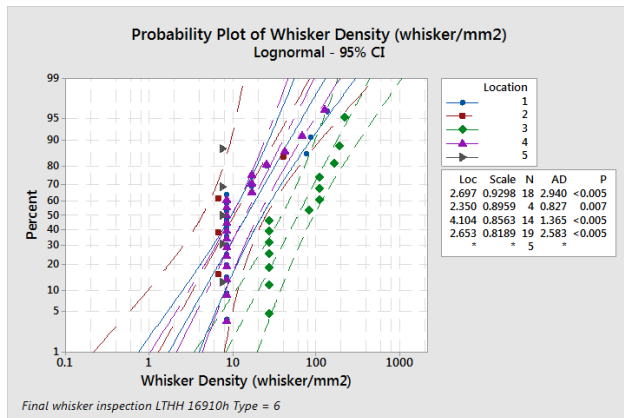


Figure 221: Final inspection whisker density probability plot for various locations on the SOT6 part termination after 16,910 h LTHH.

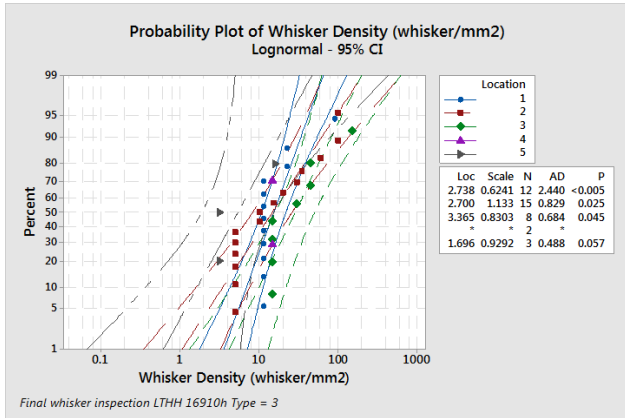


Figure 222: Final inspection whisker density probability plot for various locations on the SOT3 part termination after 16,910 h LTHH.

11.2.4.5 Electrical Bias

The application of electrical bias did not influence whisker length (Figure 223 through Figure 225) or density significantly (Figure 219 through Figure 228). It should also be noted that location-2 adjacent to the board surface, where electrical stress between leads is the greatest, had the fewest whiskers (Figure 218 curve for location-2), further re-enforcing the minor influence that bias voltage had on the whisker growth in this test.

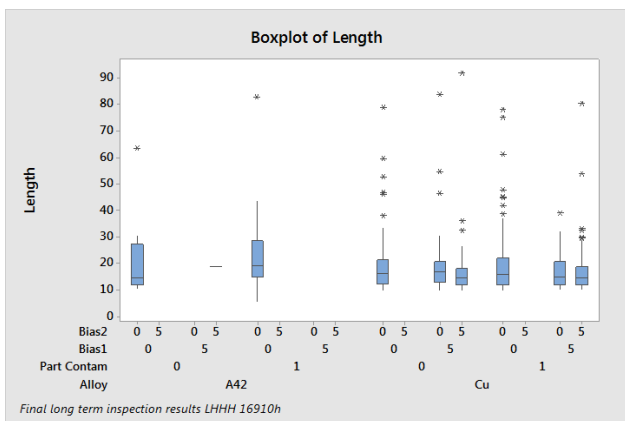


Figure 223: Final inspection whisker length box plot for various bias conditions, part contamination and lead alloy after 16,910 h LTHH.

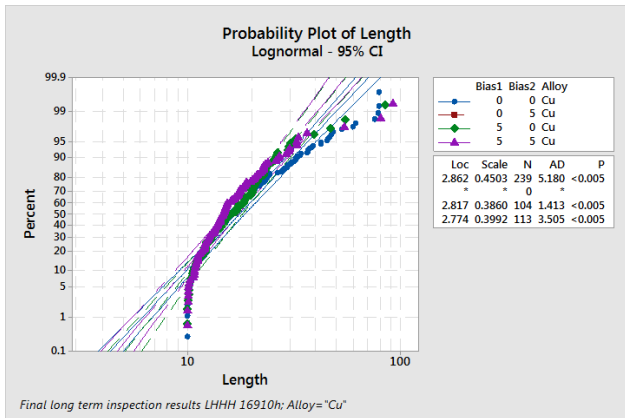


Figure 224: Final inspection whisker length probability plot for the SOT5 part lead terminations with board contamination level = 1 for various bias conditions after 16,910 h LTHH.

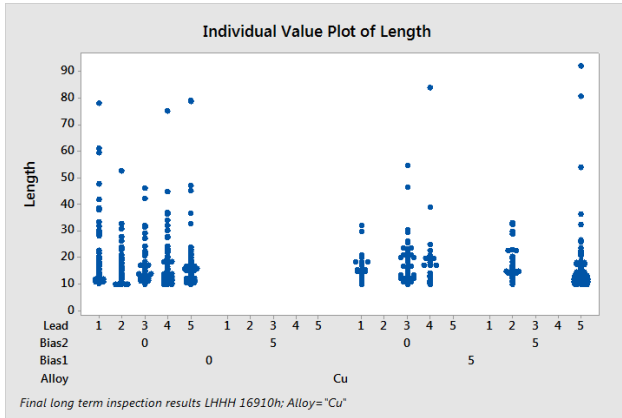


Figure 225: Final inspection whisker length box plot for copper lead terminations for various bias conditions and lead number. Under 5V Bias1 conditions, leads two and five have a 5V bias2 condition and leads one, three and four are grounded after 16,910 h LTHH.

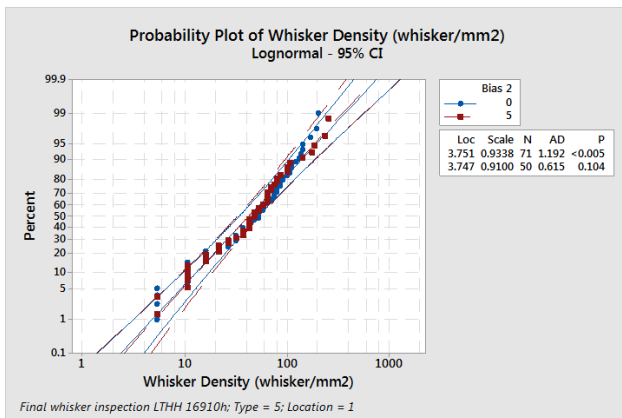


Figure 226: Final inspection whisker density probability plot comparing part bias for location-1 on the SOT5 part termination after 16,910 h LTHH.

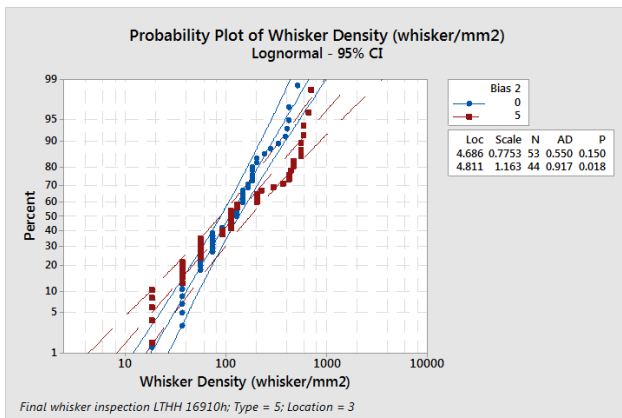


Figure 227: Final inspection whisker density probability plot comparing part bias for location-3 on the SOT5 part termination after 16,910 h LTHH.

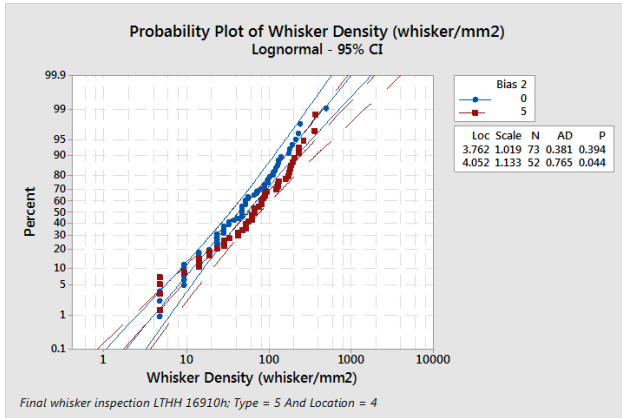


Figure 228: Final inspection whisker density probability plot comparing part bias for location-4 on the SOT5 part termination after 16,910 h LTHH.

11.2.5 Comparison between second (4,398 h) and final (16,910 h) LTHH inspection

The whisker lengths on the SOT parts increased from the 4,398 to the 16,910 h exposure times for both the copper and the alloy-42 lead terminations (Figure 229 and Figure 230). In addition, the diameter of the whiskers that grew over the long time interval was very small when compared to the whiskers observed during the second inspection (Figure 193, Figure 198 and Figure 127).

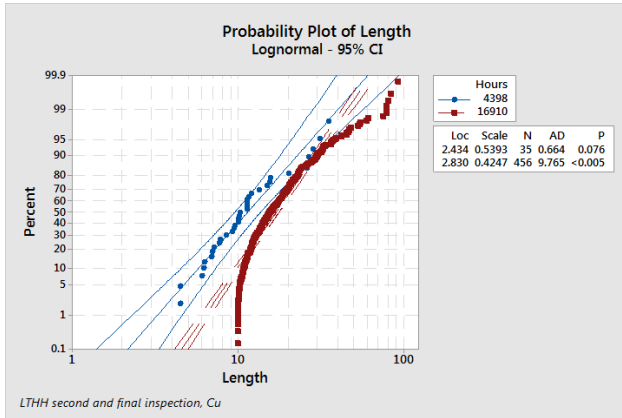


Figure 229: LTHH whisker length probability distribution comparison between the second (4,398 h) and the final inspection (16,910 h) of the SOT5 copper lead terminations.

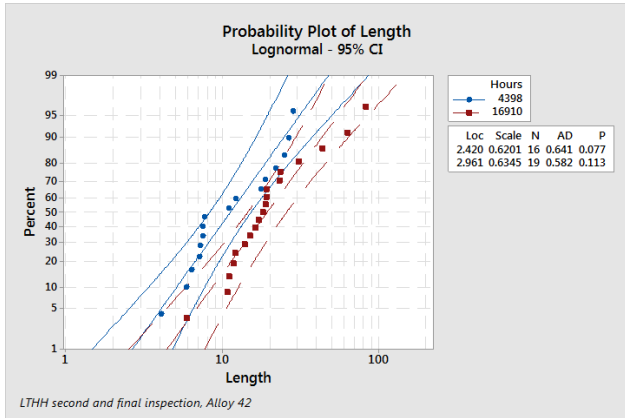


Figure 230: LTHH whisker length probability distribution comparison between the second (4,398 h) and the final (16,910 h) inspection of the SOT3 and SOT6 alloy-42 lead terminations.

11.3 Metallurgical Observations

11.3.1 First inspection metallurgy: 1,037 h LTHH

Some interesting hollow whiskers were observed as shown in Figure 231 and Figure 232. The hollow whiskers contained chlorine (Figure 233). There is evidence of hollow whiskers in the literature. Hollow tin/chromium whiskers have been observed on vapor deposited one micron thick tin on chromium annealed for one week at 180°C [43].



Figure 231: Hollow whiskers observed during the first inspection after 1,037 h LTHH on QFP44 termination board pad with a 0-1 contamination level observed.

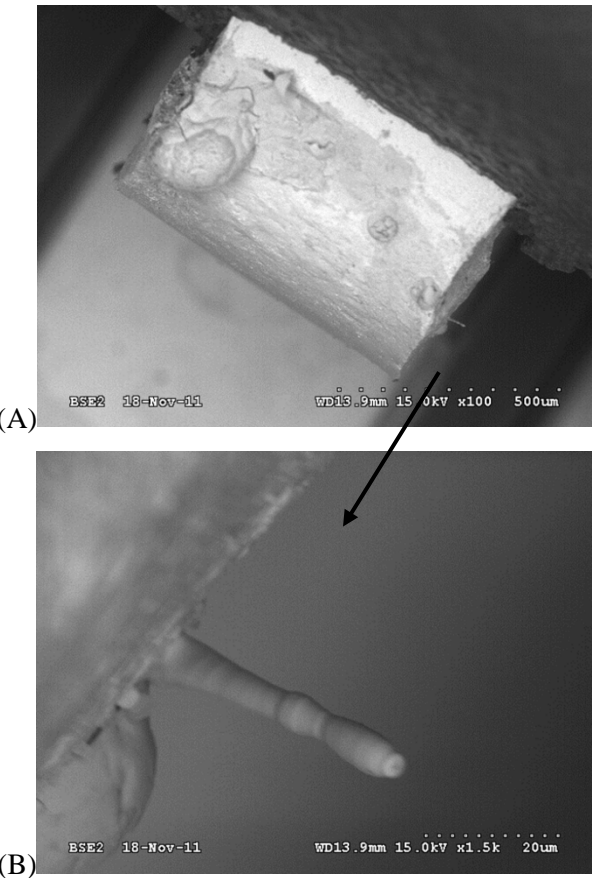


Figure 232: Hollow whisker observed during the first inspection after 1,037 h LTHH on QFP44 lead with a 1-1 contamination level during the first inspection; (A) overall image of lead and (B) close-up of whisker.

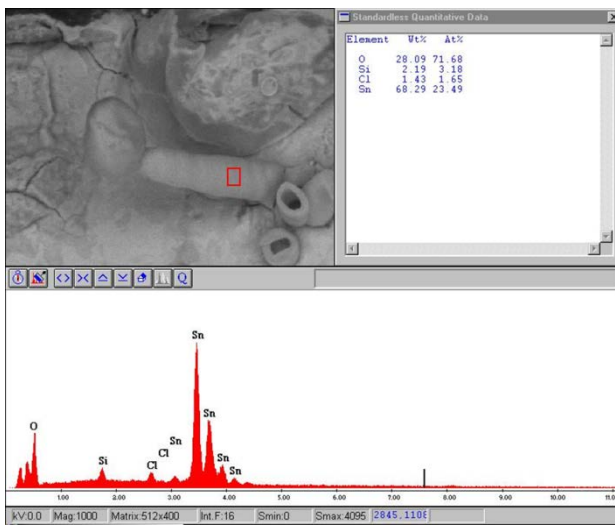


Figure 233: Elemental analysis of a hollow whisker.

11.3.2 Second inspection SOT metallurgical observations: 4,398 h LTHH

Conventional whiskers (Figure 234) and thin whiskers (Figure 235) were observed on the SOT board. The sub-micron diameter whiskers required scanning electron microscope magnifications of 500 to 1,000x or more to be detected. While thin whiskers were difficult to see, from an electrical perspective they have low fusing current

thresholds. In addition, the smaller diameter whiskers have higher electrical resistance which should result in a lower metal vapor arcing risk [95].

Similar to the first inspection, hollow whiskers were also observed during the second inspection (Figure 236).



Figure 234: Whisker observed on SOT5 termination during the second inspection after 4,398 h LTHH, U29, lead 2, 3,500x.



Figure 235: Thin whisker observed on SOT3 termination during second inspection after 4,398 h LTHH, U10, lead 3, 3,000x.

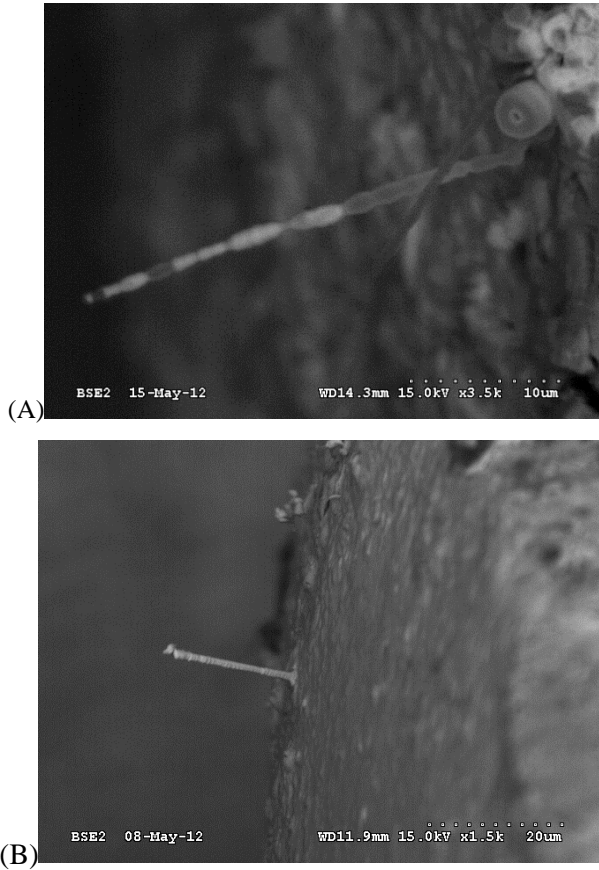


Figure 236: Hollow whiskers observed on SOT5 terminations during the second inspection after 4,398 h LTHH; (A) 0-1 contamination level U29, lead 5, 3,500x, and (B) 1-1 contamination level, U40, lead 2, 1,500x.

11.3.3 Second inspection QFP metallurgical observations: 4,398 h LTHH

A range of whisker morphologies and lengths were observed. PLCC whisker growth is shown in Figure 237 through Figure 239. Thin whiskers were beginning to form (Figure 238). The QFP44 whiskers are shown in Figure 240 through Figure 243 and the TQFP64 whiskers are shown in Figure 244. The greater lead-free solder thickness on much of the TQFP64 leads resulted in reduced whisker growth. Several instances of changing whisker diameter were observed; increasing whisker diameter (Figure 241 and Figure 243) and decreasing whisker diameter (Figure 239 and Figure 242). Of particular interest in Figure 242 was the presence of a diameter reduction and corrosion at the whisker base, halting further whisker growth.

As with the other inspections, hollow whiskers were also observed (Figure 244 and Figure 245) and in some cases were quite long.

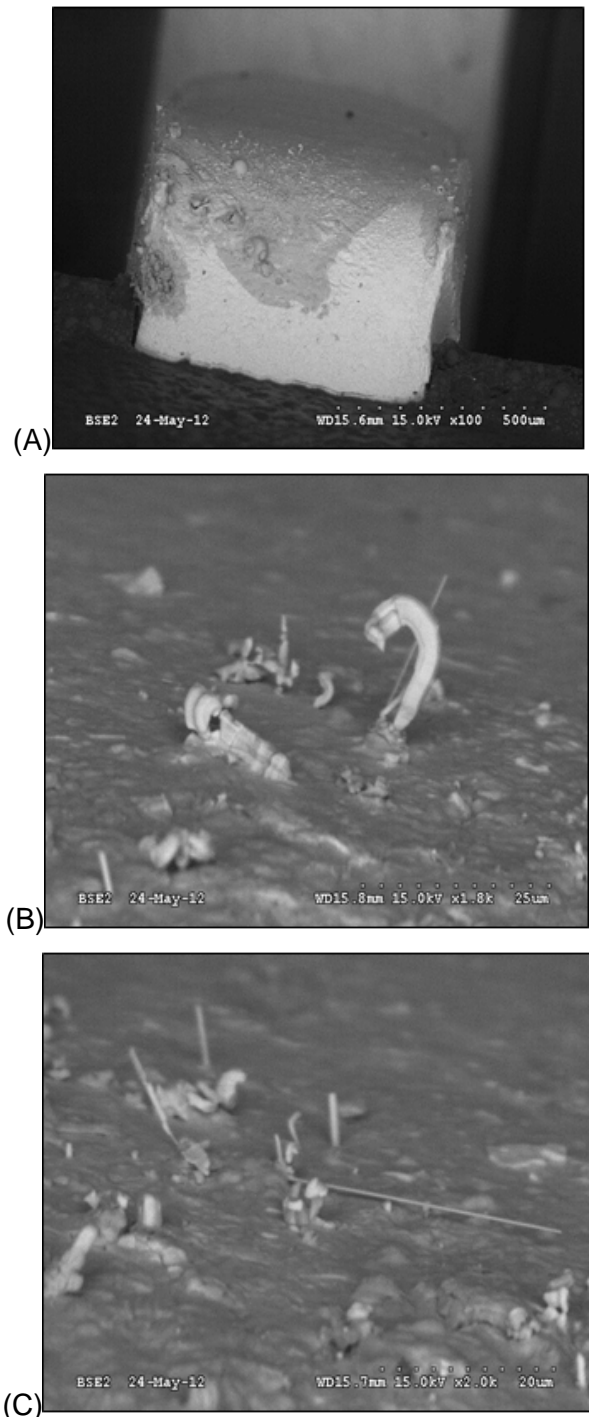


Figure 237: SEM images of whisker growth on a Cu lead frame PLCC part with a 0-1 contamination level from the second inspection after 4,398 h LTHH; (A) 100x, (B) 1800x, and (C) 2000x (A-QFP-LT-0-1-ncc-2, PLCC, U13, lead 13).

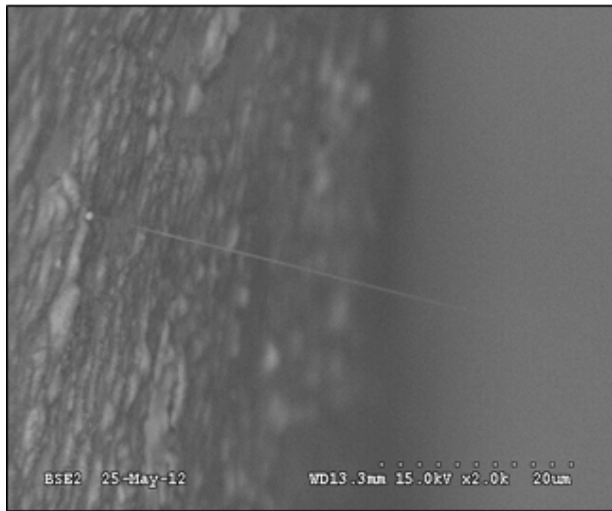


Figure 238: SEM images of thin whisker growth on a Cu lead frame PLCC part with a 1-1 contamination level from the second inspection after 4,398 h LTHH, 2000x (A-QFP-LT-1-1-ncc-3, PLCC, U12, lead 18).

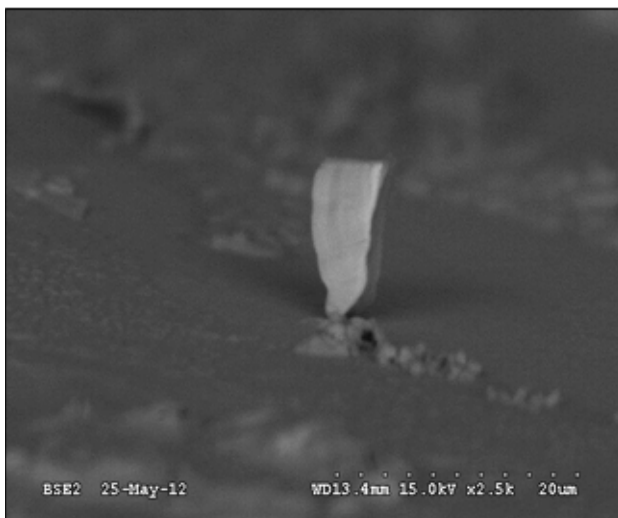


Figure 239: SEM images of decreasing diameter whisker on Cu lead frame PLCC part termination with a 1-1 contamination level from the second inspection after 4,398 h LTHH, 2500x (A-QFP-LT-1-1-ncc-3, PLCC, U12, lead 1).

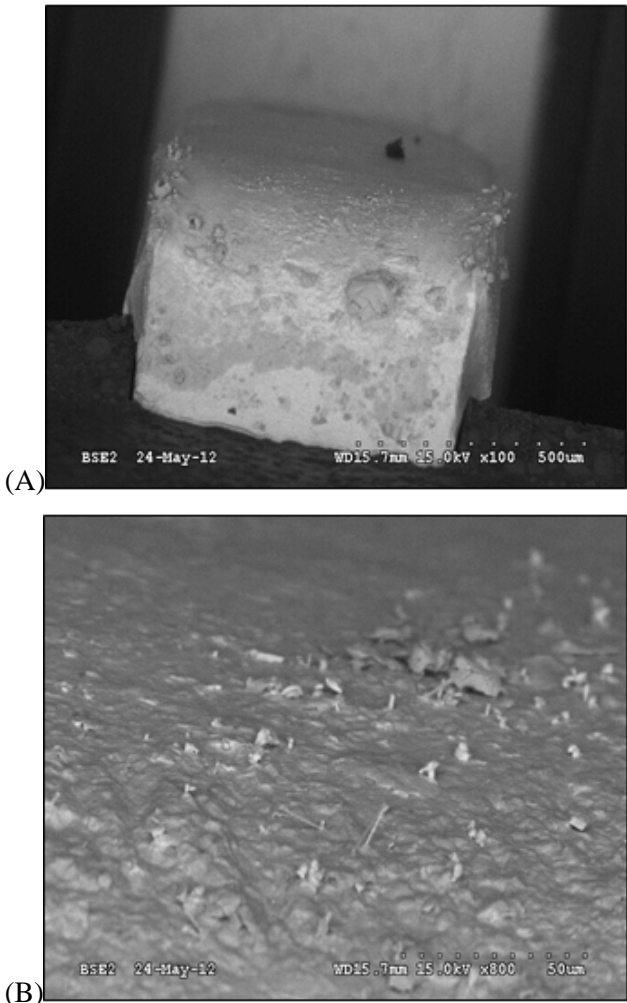


Figure 240: SEM images of nodule and whisker growth on a Cu lead frame QFP44 part termination with a 0-1 contamination level from the second inspection after 4,398 h LTHH; (A) 100x and (B) 800x (A-QFP-LT-0-1-ncc-2, PLCC, U13, lead 12).

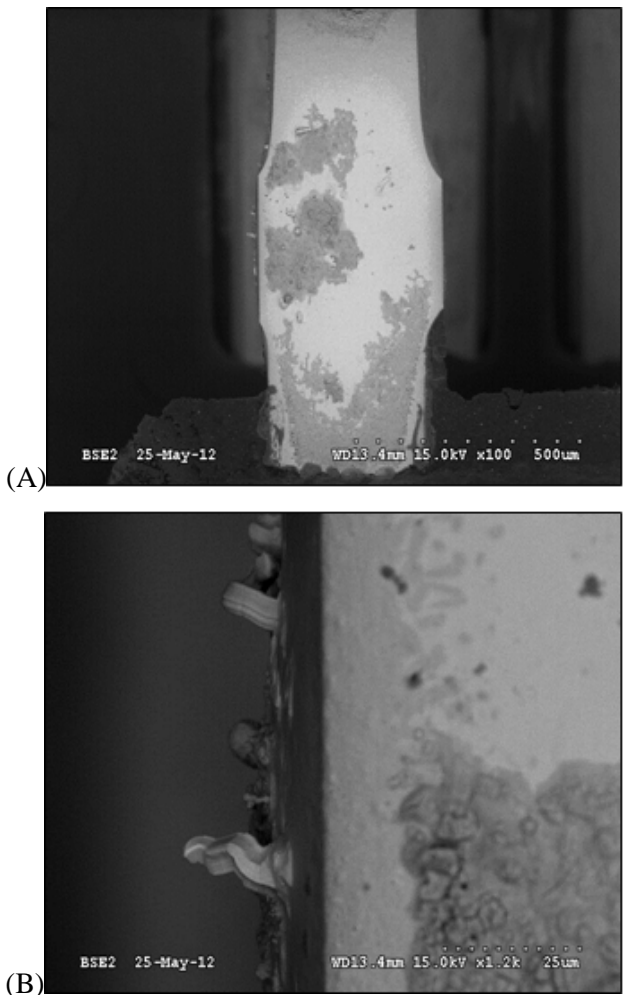


Figure 241: SEM images of whisker growth from the side of the lead on a Cu lead frame QFP44 part termination with a 1-1 contamination level from the second inspection after 4,398 h LTHH; (A)100x, (B) 1200x (A-QFP-LT-1-1-ncc-3, QFP44, U05, lead 11).

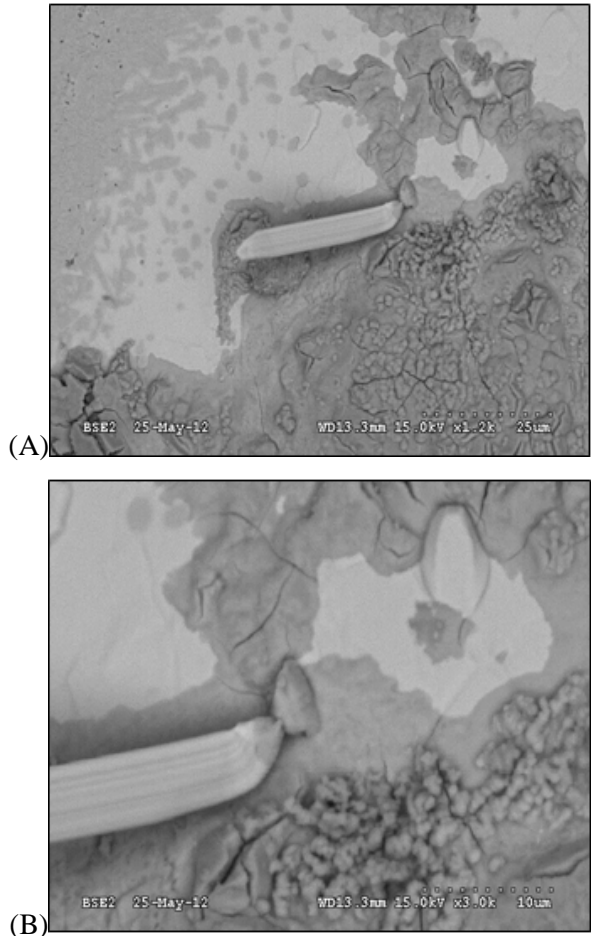


Figure 242: SEM images of decreasing diameter whisker with corrosion at whisker base terminating growth on Cu lead frame QFP44 part termination with a 1-1 contamination level from the second inspection after 4,398 h LTHH; (A) 1200x and (B) 3,000x (A-QFP-LT-1-1-ncc-3, QFP44, U05, lead 11).

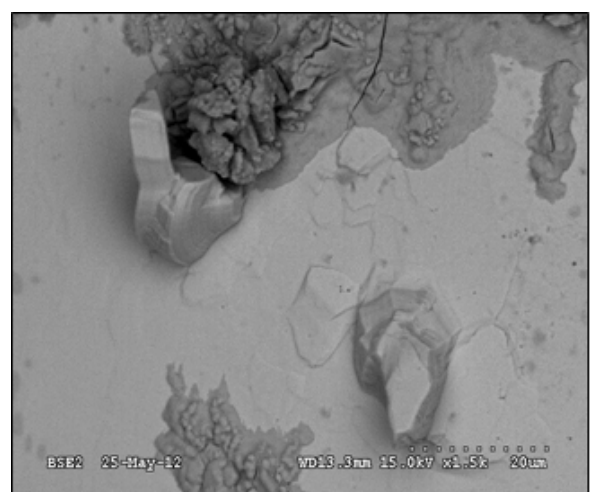


Figure 243: SEM images of increasing diameter whiskers/nodules on Cu lead frame QFP44 part termination with a 1-1 contamination level from the second inspection after 4,398 h LTHH, 1,500x (A-QFP-LT-1-1-ncc-3, QFP44, U05, lead 11).

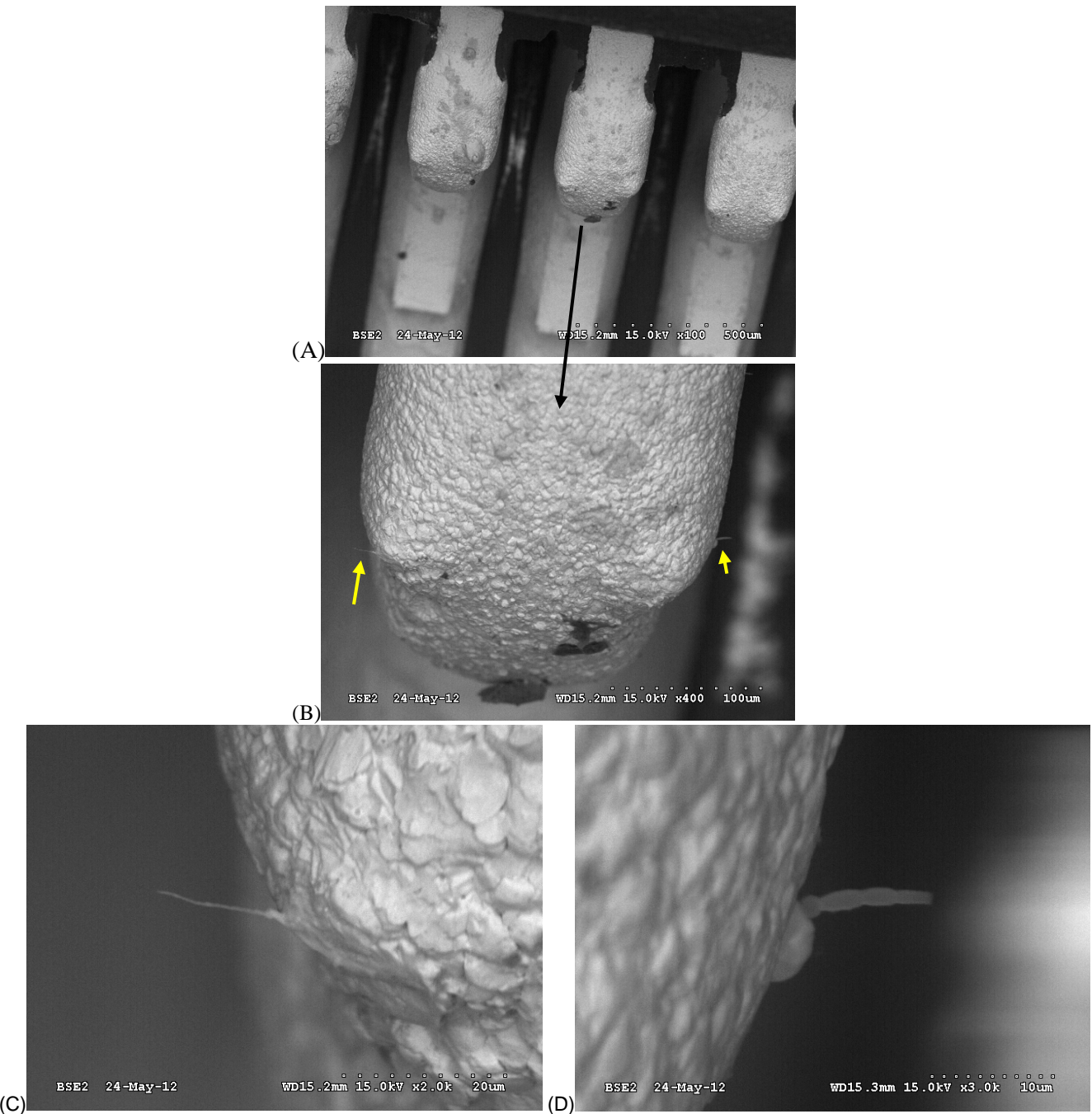


Figure 244: SEM images of whiskers observed during the second inspection on Cu lead frame TQFP64 part termination with a 0-1 contamination level from the second inspection after 4,398 h LTHH; (A) 100x, (B) 400x, (C) left whisker 2,000x, and (D) right whisker, 2,000x (A-QFP-LT-0-1-ncc-2, QFP64, U9, lead 10).

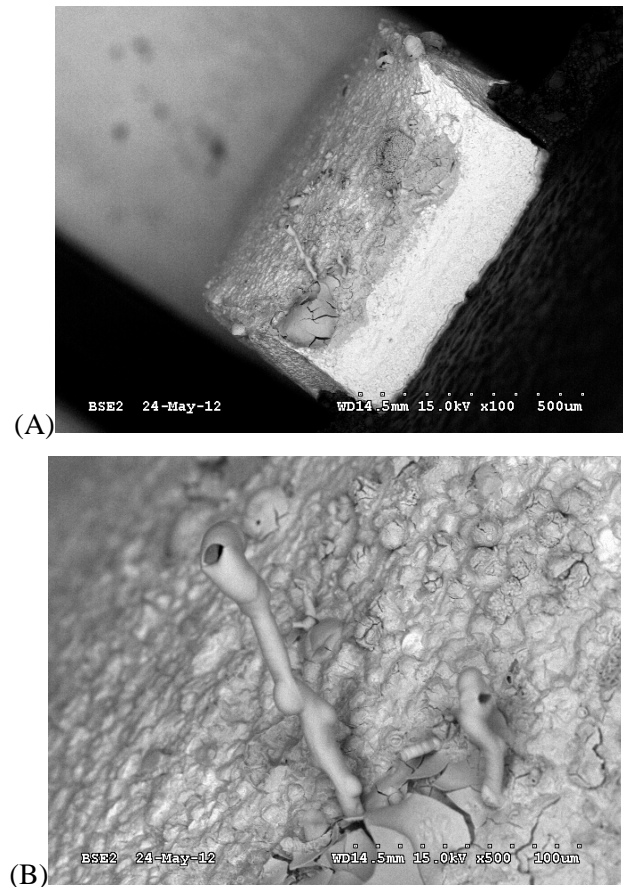


Figure 245: SEM images of hollow whisker on Cu lead frame PLCC part termination with a 0-1 contamination level from the second inspection after 4,398 h LTHH; (A) overall image of lead and (B) close up of long whisker, 100x (A-QFP-LT-0-1-ncc-2, PLCC, U12, lead 9).

11.3.4 Final Inspection Metallurgical Observations: 16,910 h

The longest whisker observed in the present experiment grew from the contaminated assemblies with copper alloy parts (SOT5, QFP44, TQFP64, and PLCC). The clean assemblies did not have appreciable whisker growth (Figure 246). When contamination was present, increased corrosion was observed between the second and the final inspection (Figure 247).

Similar to the HTHH experiments, in some cases original whisker growth was interrupted and additional whisker growth was observed between the second and final inspection (Figure 248). Numerous cases of thin submicron diameter and hollow whiskers were observed (Figure 249 – Figure 251).

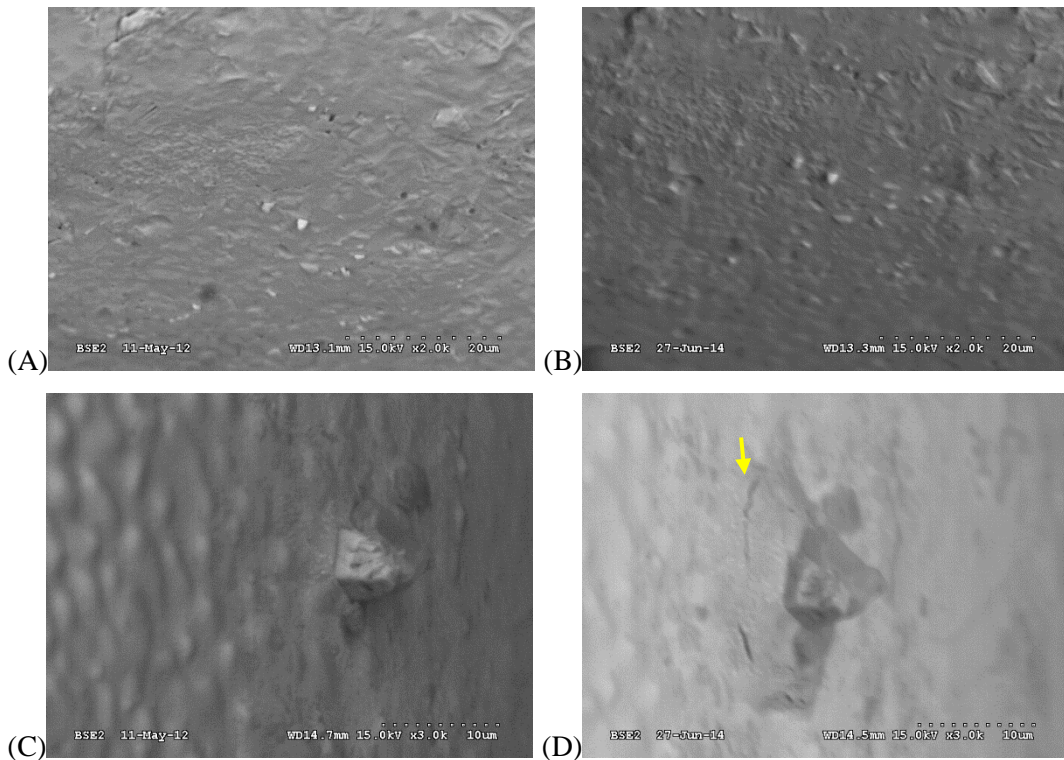


Figure 246: Comparison of clean Cu lead surfaces at a 0-0 contamination level at 4,398 h (A and C) and 16,910 h (B and D) LTHH. Images A and B show lead 3, 2000x (A-SOT-LT-0-0-ncc-1, SOT5, U23, lead 3). Images C and D show lead 2, 3,000x (A-SOT-LT-0-0-ncc-1 SOT5, U26, lead 2). Arrow in D highlights additional tin growth around the original whisker.

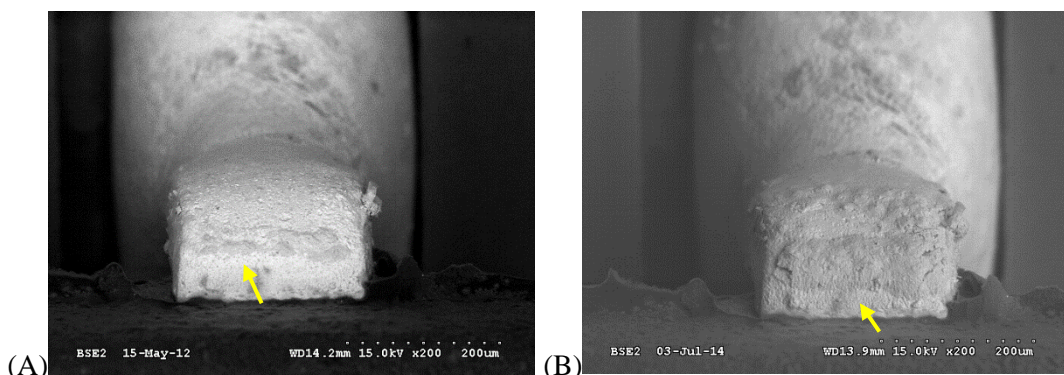


Figure 247: Comparison of corrosion/oxidation and whisker growth of SOT6 alloy-42 lead terminations at a 0-1 contamination level at (A) 4,398 h and (B) 16,910 h LTHH, 200x (A-SOT-LT-0-1-ncc-1, U75, lead 3.). Arrows in A and B indicate a typical corrosion/oxidation increase.

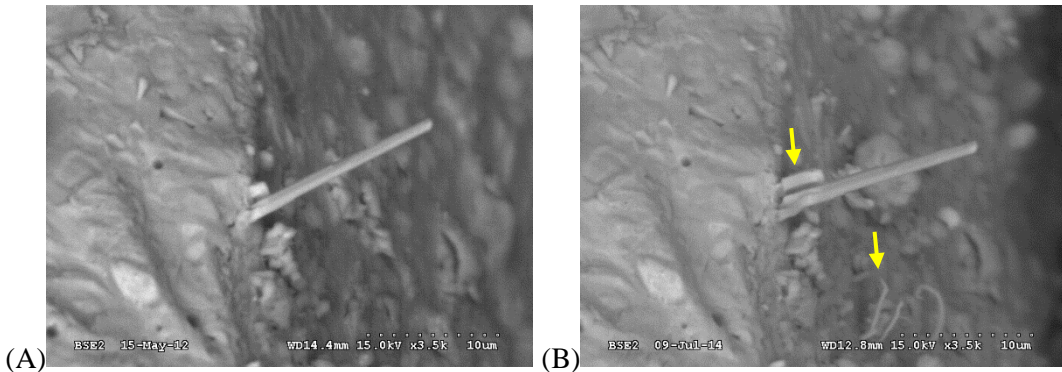


Figure 248: Comparison of corrosion/oxidation and whisker growth of SOT5 Cu lead terminations at a 0-1 contamination level at (A) 4,398 h and (B) 16,910 h LTHH, 3,500x (A-SOT-LT-0-1-ncc-1, U29, lead 2). Arrows show new whisker growth.

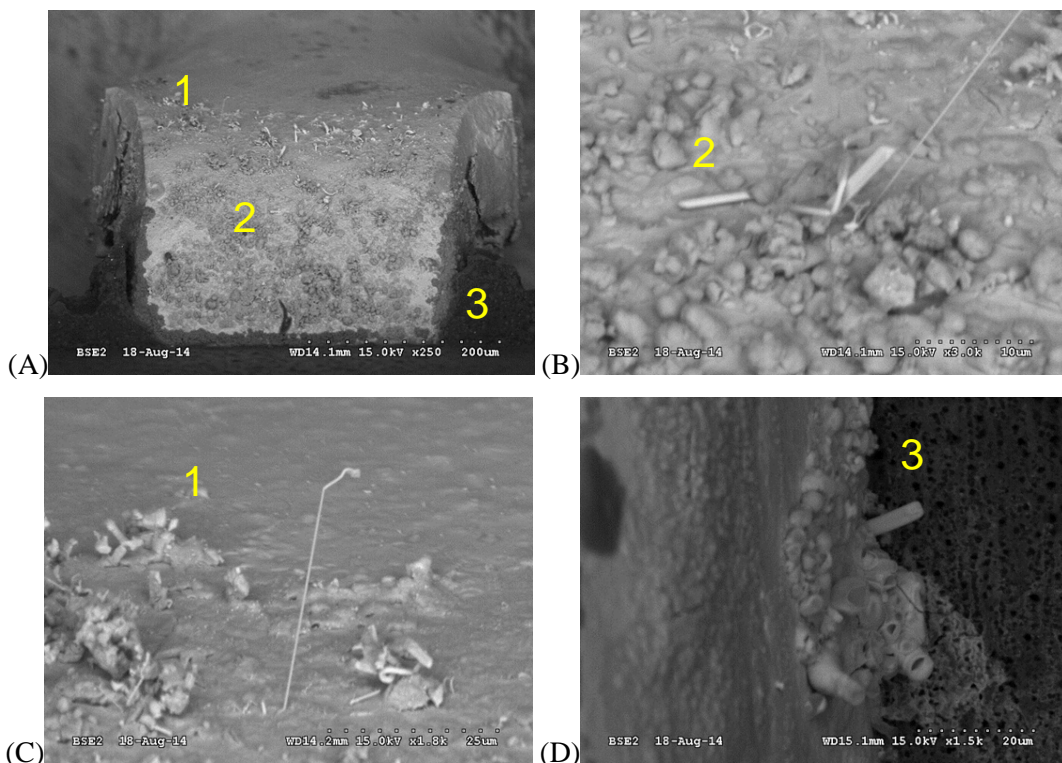


Figure 249: Thin and hollow whiskers observed on a SOT 5 lead with a 1-1 contamination level at 16,910 h LTHH (A-SOT5-LT-1-1-ncc3, SOT5, U30, lead 2); (A) overall 250x, (B) extremely thin whisker at location-2, 3,000x, (C) thin whisker at location-1, 1,800x, (D) hollow whiskers at location-3, 1,500x. Note that the thin whiskers were not visible at 250-300x magnification.

Thin whiskers were straight and kinked (Figure 250). Some of the extremely thin whiskers were shaped similarly to the larger hollow whiskers (Figure 251). The Cu leaded parts on boards that were not contaminated after assembly exhibited some recrystallization/whisker nucleation, small nodule formation and a small degree of oxidation (Figure 252 and Figure 253). The alloy-42 leads on clean assemblies exhibited the least oxidation and recrystallization (Figure 254).

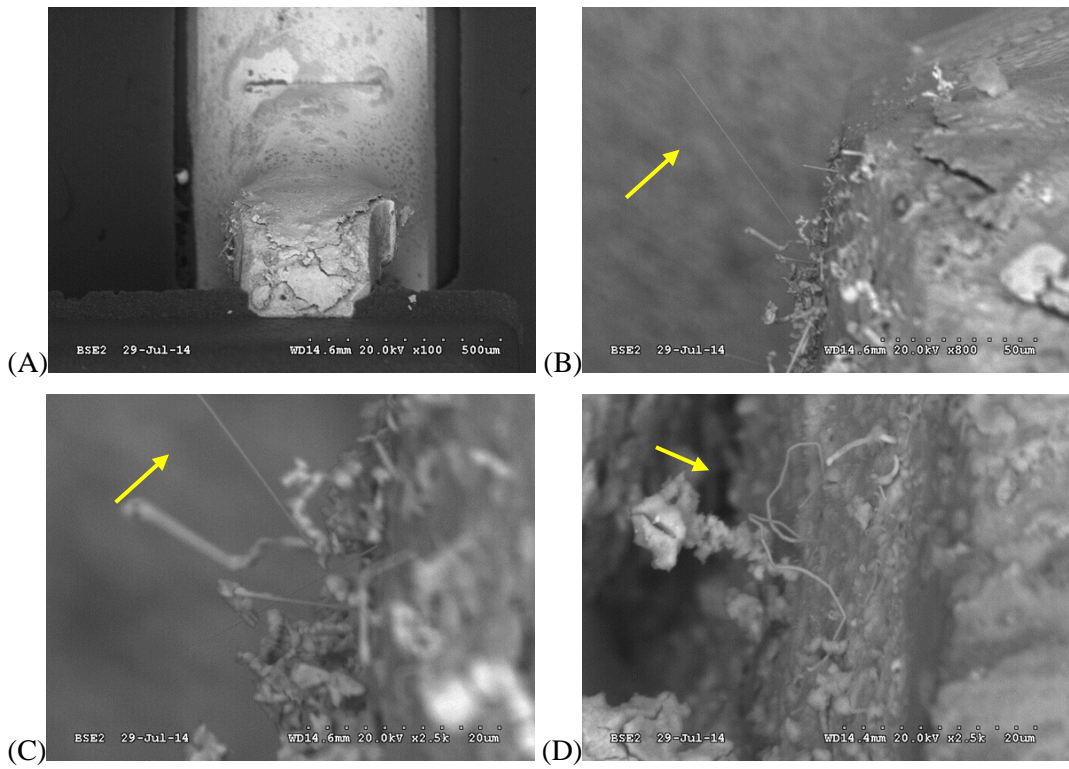


Figure 250: Thin whiskers straight and kinked whiskers observed on a SOT5 lead with a 1-1 contamination level at 16,910 h LTHH; (A) overall lead, 100x, (B) thin straight whisker, 800x, (C) close-up of B, 2500x, and (D) thin highly kinked whisker, 2500x (A-SOT5-LT-1-1-ncc3, SOT5, U40, lead 2).

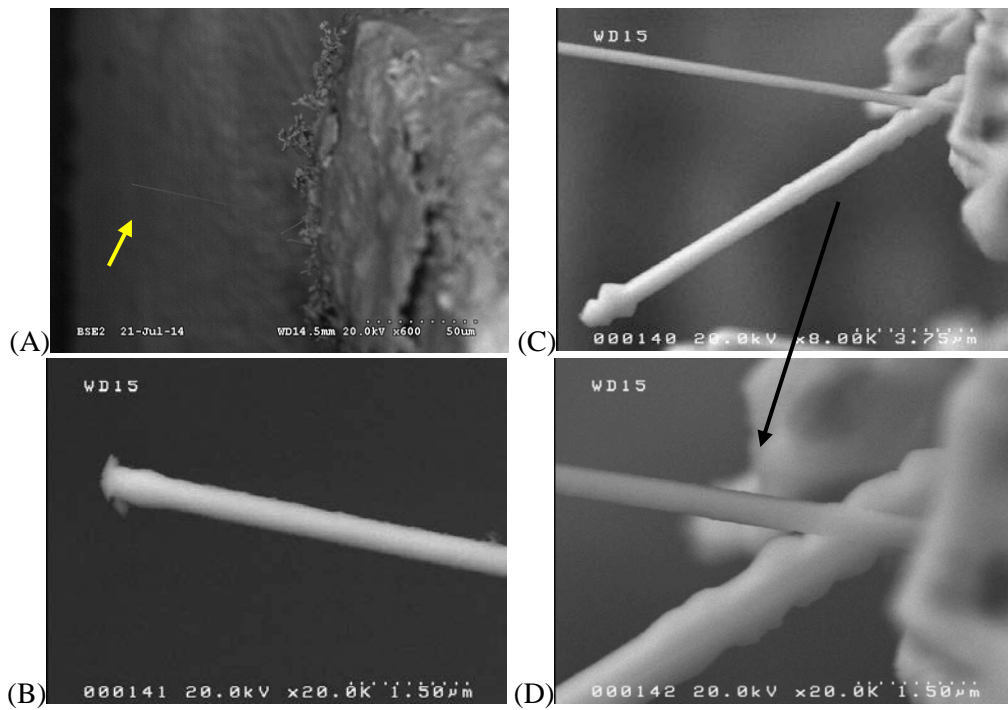


Figure 251: Extremely thin whiskers shaped similar to hollow whiskers observed at 16,910 h LTHH on a Cu alloy lead with a 0-1 contamination level (A-SOT-LT-0-1-ncc1, SOT5, U5, lead 2); (A) Overall SEM, 600x, (B) whisker tip, 20,000x, (C) whisker base, 8,000x, and (D) whisker base close-up 20,000x.

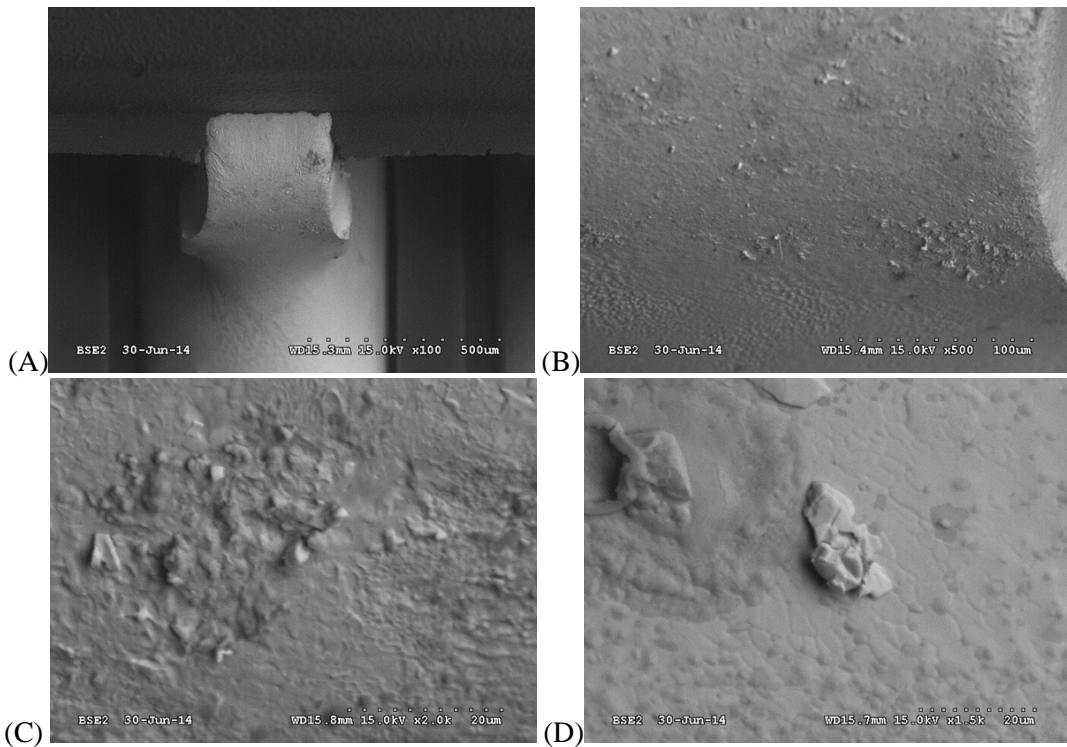


Figure 252: Recrystallized grains and oxidation (darker areas) around IMC particles observed at 16,910 h LTHH on a Cu alloy lead with a 1-0 contamination level (A-SOT5-LT-1-0-ncc1, SOT5, U7, lead 5 and 4); (A) Overall, 100x, (B) oxidation and whisker inception, 500x, (C) recrystallization, oxidation and whisker inception, 2,000x, and (D) oxidation and recrystallization, 1,500x.

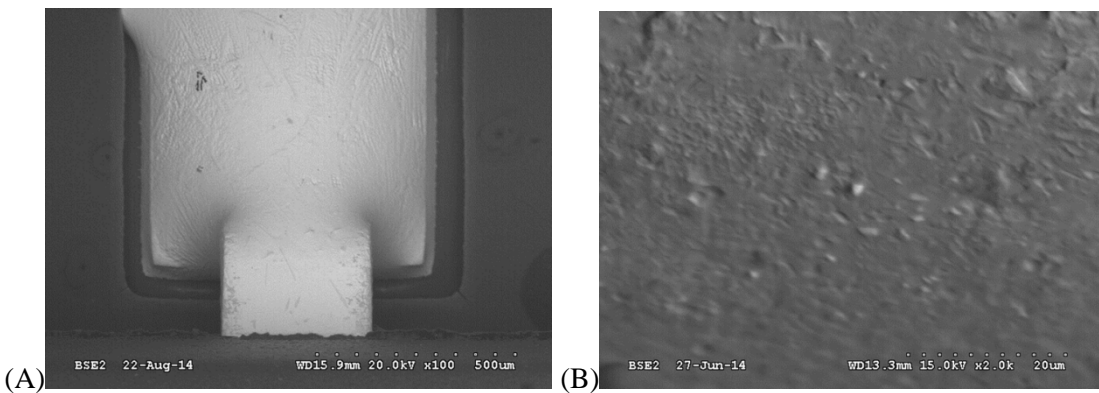


Figure 253: Almost no oxidation, some recrystallization but no whiskers were observed at 16,910 h LTHH on Cu alloy leads on clean parts and assemblies with a 0-0 contamination level (A-SOT5-LT-0-0-ncc1, SOT5, U23, lead 3); (A) overall SEM, 100x, and (B) close-up, 2,000x.

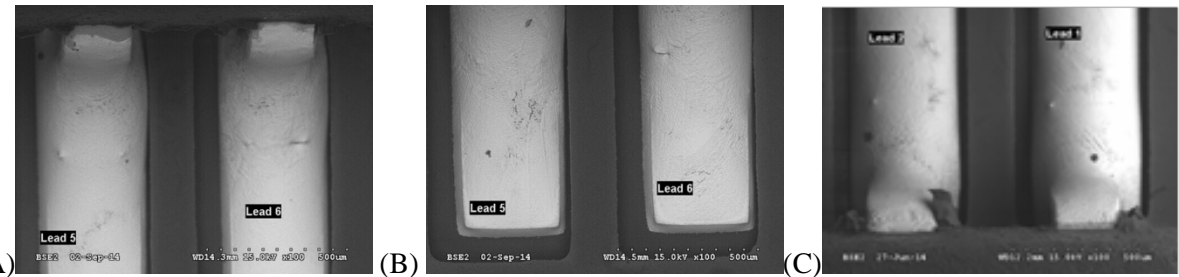


Figure 254: Very little oxidation and no whiskers observed at 16,910 h LTHH on SOT6 alloy-42 leads on clean assemblies, 100x; (A) 1-0 contamination (A-SOT-LT-1-0-ncc2, SOT6, U70), (B) 0-0 contamination level (A-SOT-LT-0-0-ncc1, SOT6, U69) (C) 1-0 contamination level (A-SOT-LT-1-0-ncc2, SOT6, U76).

Cross-sections of SOT5 leads on an assembly with a 1-1 contamination level showed oxidation/corrosion around the whisker and in the solder at the toe fillet (Figure 255). A SEM examination of the same section confirmed the extent of the oxidation/corrosion. It also revealed cracks near the whisker base. In addition, oxidation/corrosion of the whisker itself was observed (Figure 256). A cross-section through the heel fillet of a SOT5 lead with a 0-1 contamination level showed extensive solder roughness and oxidation/corrosion propagating along the solder's primary tin interdendritic spaces (Figure 257) similar to the HTHH experiments.

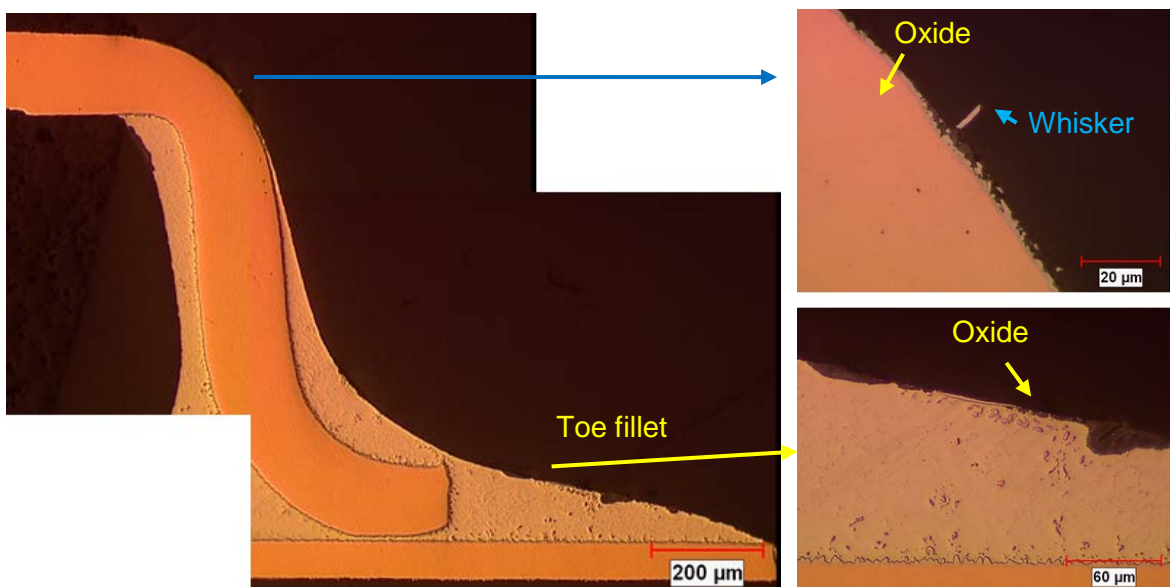


Figure 255: Optical image of a whisker cross-section showing oxidation around whisker after 16,910 h LTHH on a SOT5 Cu lead with a 1-1 contamination level (A-SOT-LT-1-1-ncc3, SOT5, U4, lead 1).

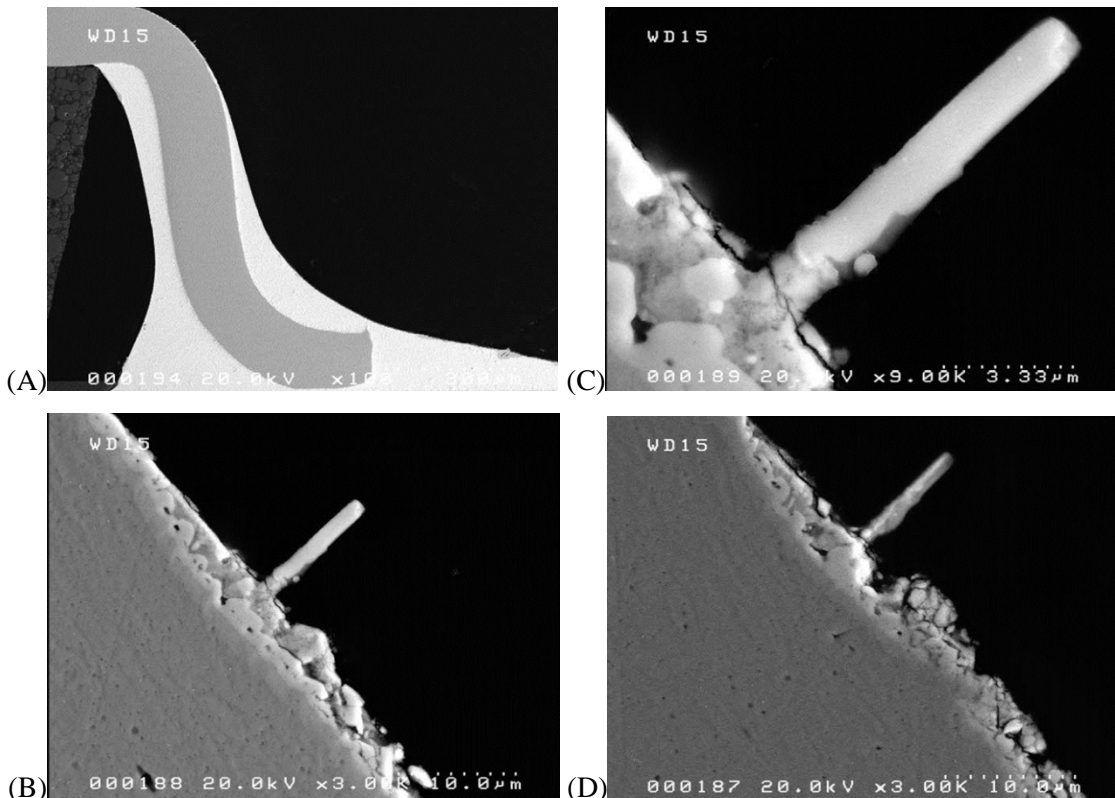


Figure 256: SEM image of a whisker cross-section showing oxidation (darker regions) around and on whisker after 16,910 h LTHH on a SOT5 Cu lead with a 1-1 contamination level (A-SOT-LT-1-1-ncc3, SOT5, U4, lead 1); (A) overall, 100x, (B) whisker, 3,000x, (C) whisker close-up showing a crack near the whisker base, 9,000x, and (D) second ion beam polish of whisker showing cracks in the oxide, 3,000x.

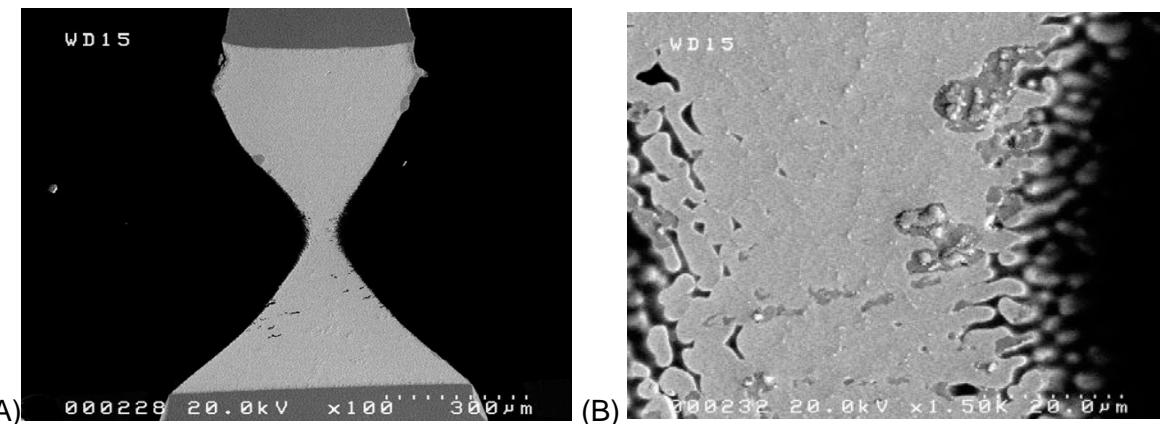


Figure 257: Heel fillet cross-section SEM image showing solder roughness and oxidation/corrosion after 16,910 h LTHH on a SOT5 Cu lead with a 0-1 contamination level (A-SOT-LT-0-1-ncc2, SOT5, U29, lead 4); (A) overall, 100x, (B) close-up showing oxidation (darker areas) propagation along the interdendritic boundaries, 1,500x.

11.4 Conformal coating

The conformal coated SOT and QFP parts did not exhibit physical degradation after 16,910 h of LTHH (Figure 258 and Figure 259). The coated SAC+REE ball did exhibit some small whisker growth (Figure 260). The coating thinned to less than a micron on the left and right sides of the ball above the solder fillet (Figure 261).

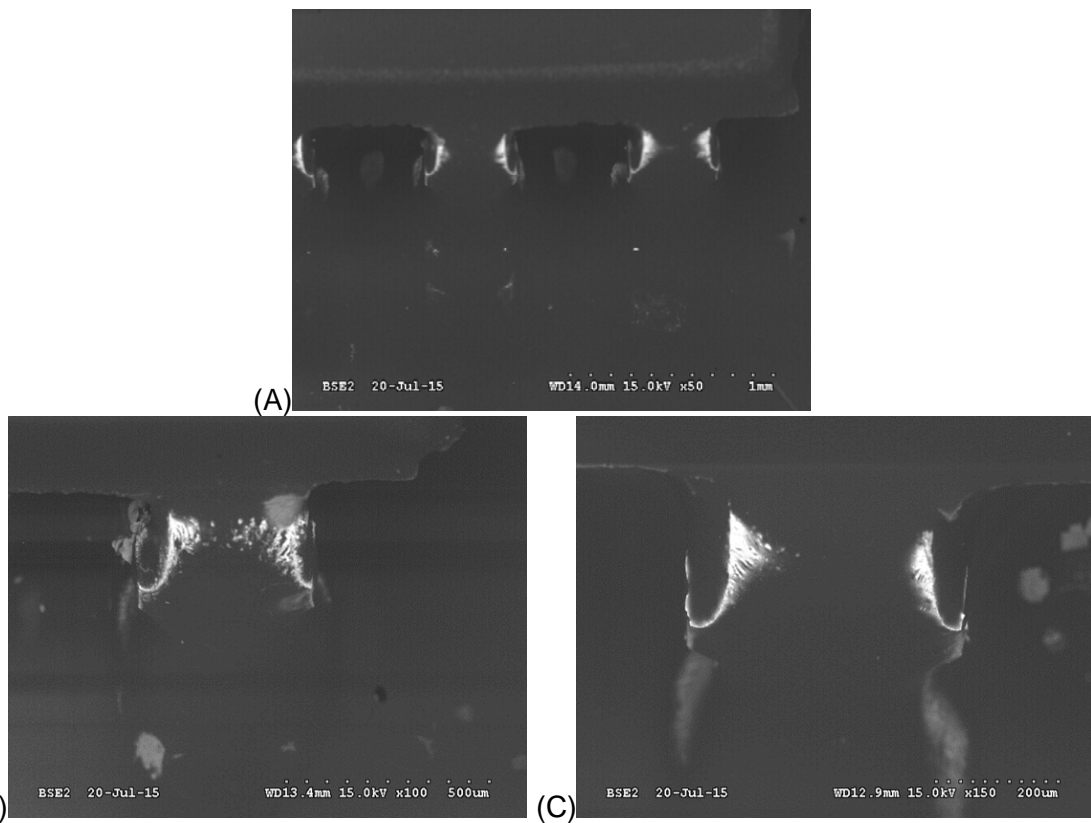


Figure 258: Conformal coating on SOT5, with 1-1 contamination level after 16,910 h LTHH; (A) overall, 50x, (B) top of lead, 100x, and (C) top of lead, 150x.

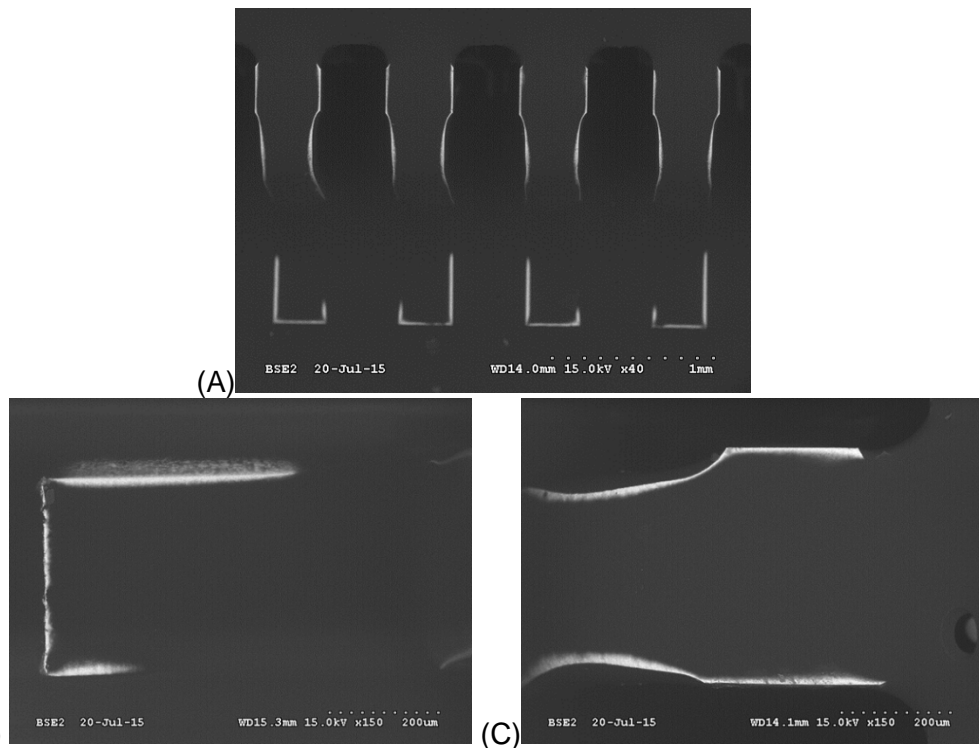


Figure 259: Conformal coating on QFP 44, with 1-1 contamination level after 16,910 h LTHH; (A) overall, 40x and (B) lead tip, 150x and (C) top of lead, 150x. No cracks or coating degradation observed.

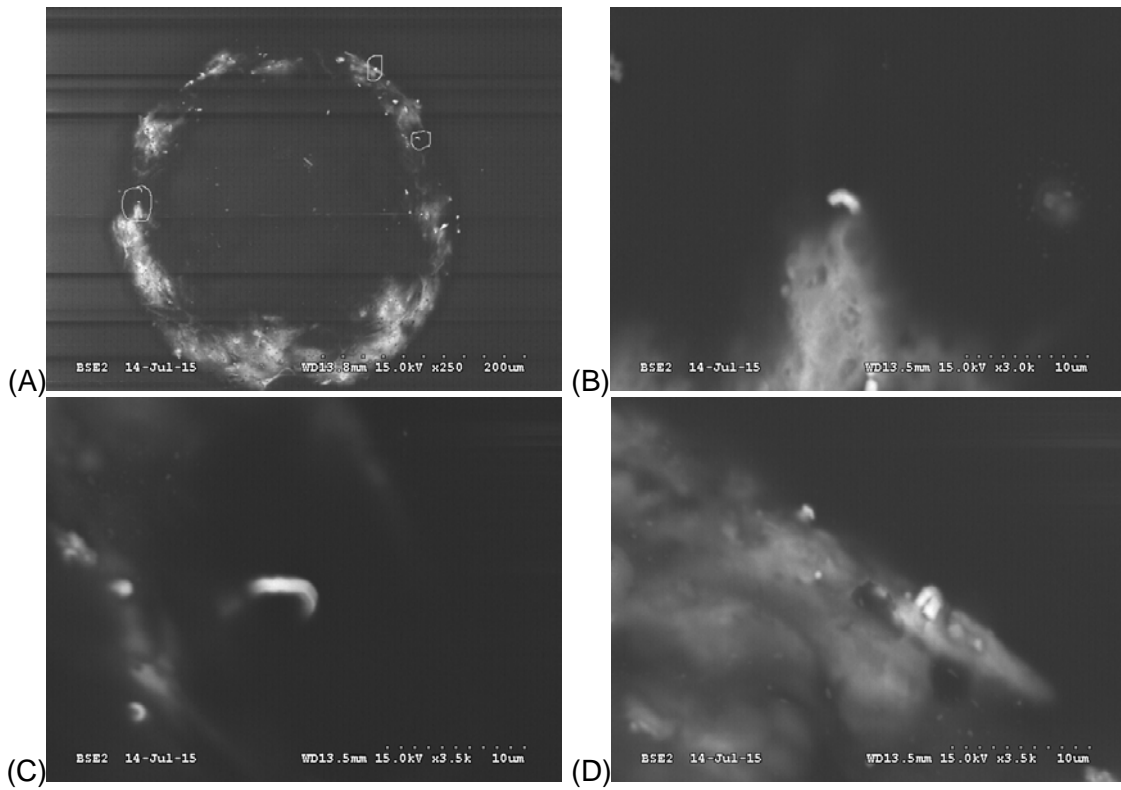


Figure 260: Conformal coating on SAC105+REE BGA ball after 16,910 h LTHH.

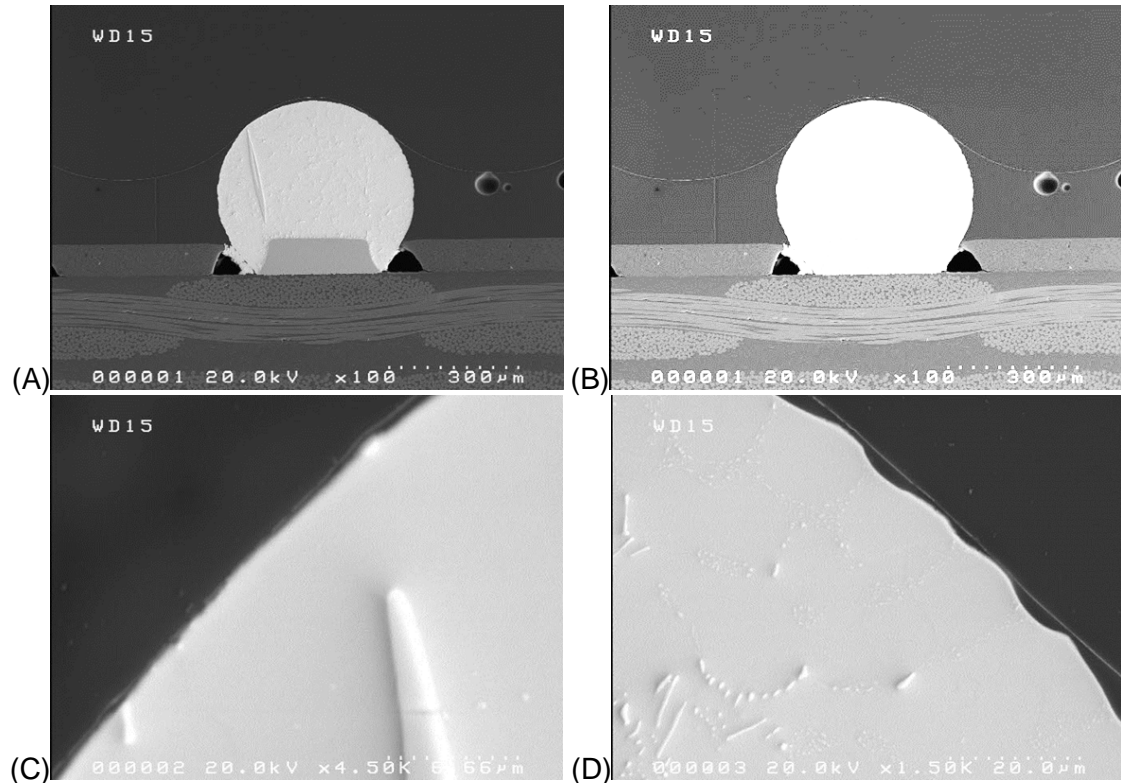


Figure 261: Cross-section of SAC105+REE BGA ball with conformal coating after 16,910 h LTHH; (A) overall ball, 100x, (B) overall ball with contrast enhanced to show coating, 100x, (C) close up of top left side, 4,500x, and (D) close-up of top right side, 4,500x. Light lines in the images is the gold sputtering applied to the top of the coating prior to cross-sectioning to enhance the demarcation between the coating and potting.

11.5 Summary

11.5.1 Whisker Length

The following points can be made from the whisker statistical analysis:

- Long whisker growth was observed from the SAC305 solder, particularly where the solder was five to 25 microns thick
- The 25°C/85%RH 16,910 h exposure (over three years) on SAC305 soldered SOT assemblies resulted in whiskers longer than the JESD201 piece part test limits for 4,000 h
- The 25°C/85%RH 1,000 and 4,398 h exposures on the QFP assemblies resulted in whiskers longer than the JESD201 piece part test limits for 4,000 h
- Lead material and contamination level were the most significant factors contributing to whisker growth
- Much greater whisker length and density was observed on Cu alloy lead terminations than the alloy-42 lead terminations (in contrast to thermal cycling environments)
- Whisker density for the SOT parts followed a lognormal distribution
- The primary growth location was from the front, sides and the top of the leads above the thick part of the solder joint (e.g. locations one, three and four)

11.5.2 Metallurgical Observations

Key metallurgical observations include:

- The source of whisker stress is SAC305 solder oxidation and corrosion
- Contaminated assemblies exhibited the greatest whisker growth
- Clean parts on cleaned assemblies had no whisker growth greater than 10 microns
- Contaminated parts on cleaned assemblies had a slight increase in whisker growth over the cleaned parts and cleaned assemblies
- Many submicron diameter whiskers were observed
 - Many thin submicron whiskers were observed during the final inspection which required SEM magnification levels of 500 to 1,000x or more to see. This highlights the need for improved whisker inspection methodologies in the industry standards.
 - While the thin whiskers were difficult to see, from an electrical perspective they have low fusing current thresholds. In addition, the smaller diameter whiskers have higher electrical resistance which should result in a lower metal vapor arcing risk.
- Corrosion was observed in the interdendritic regions during cross-section examination
- Whisker growth can terminate when the tin at the whisker base is completely transformed to corrosion/oxidation products
- The joint lead/board pad material couple is important
 - Whisker growth occurred on SAC305 solder joints containing either the copper or the alloy-42 lead components, but the alloy-42 leads exhibited a delay in whisker growth
 - Cu/Cu couples: Exhibited the greatest whisker density and growth

- Alloy-42/Cu couples: The alloy-42 leads soldered to Cu PWB pads tended to have reduced whisker density

The very low acceleration LTHH testing represents benign environments that are closer to real service conditions than the TC or HTHH testing. The resulting very small diameter long whiskers that were observed in the LTHH and the low stress SAC+REE element testing appear to be unique to low stress conditions. It should be noted that these fine whiskers were difficult to image and even higher magnifications are necessary for whisker inspection.

12. Whisker risk modeling

12.1 Approach

Analysis was conducted for gull-wing parts and some basic conductor geometries found with connectors and shields on assemblies (Figure 262). In order to form a tin whisker short circuit fault, a whisker must first grow and bridge from one conductor to an adjacent conductor (having a different electrical potential), then sufficient voltage needs to be present to cause disruptive electrical current flow, and the circuit function (hardware and software) must be sensitive to the unintended current flow.

The tin whisker short circuit risk modeling approach is outlined in Figure 263 [57] [58]. The first part of the analysis was to create a spacing distribution and a probabilistic bridging-risk model for various packages that is independent of time (e.g. only dependent upon the lead geometry). Once the bridging probability has been established, the short circuit probability can be determined for a particular whisker length distribution and circuit voltage. The current model uses whisker length, density and angle data from the current experimental investigation and industry in conjunction with whisker electrical conduction data from industry.

Whisker risk was analyzed by extending the rectangular parallel plate Monte Carlo models previously developed by McCormack and Meschter [96] and others [94][97] to capture the lead form, solder and the board pad details. The current approach used the lead geometry simplified with angled bends and utilized the efficiencies of Crystal Ball™ software specifically developed for Monte Carlo analysis.

Outputs from the Monte Carlo analysis were a whisker view factor and a lead-to-lead spacing distribution. Then, as is outlined in Figure 264, the calculation was repeated for different lead types, conformal coat coverage percentages and whisker growth angle distributions. The spacing distribution was then combined with the appropriate whisker length distribution to determine the probability of a whisker bridge. The various probabilities were then combined with the appropriate number of parts and lead spaces to determine the overall number of bridges. Finally, the number of bridges was multiplied by the Courey [98] shorting probability based on operating voltage in order to determine the expected number of shorts on the assembly.

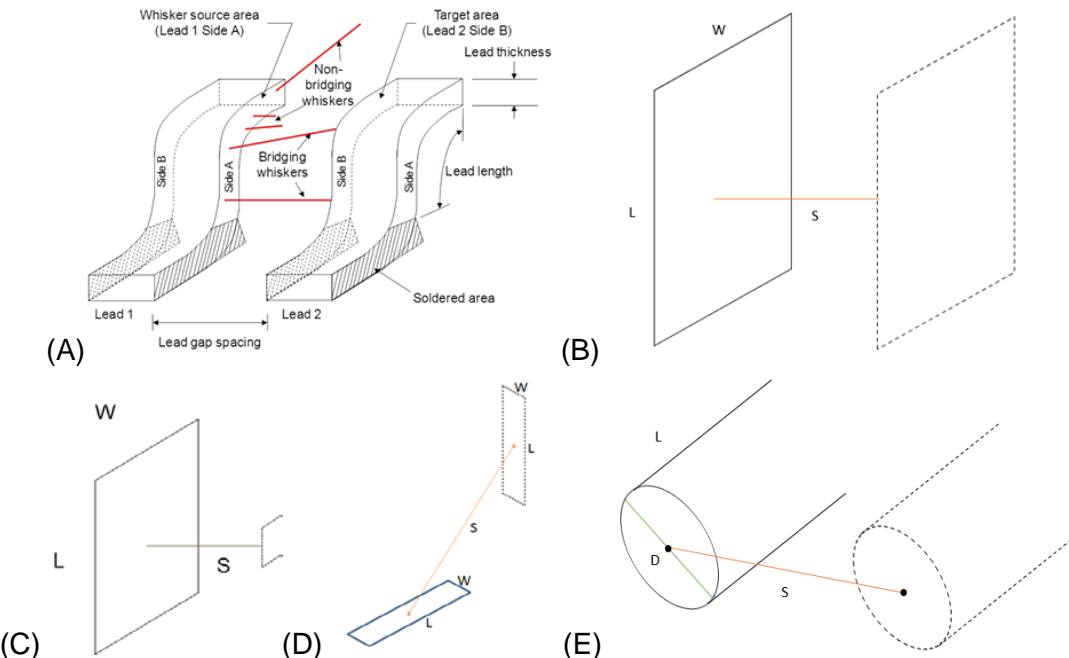


Figure 262: (A) schematic of gull wing leads with bridging and non-bridging whiskers (B) equal parallel plate, (C) unequal parallel plates, (D) equal perpendicular plates, and (E) parallel cylinders.

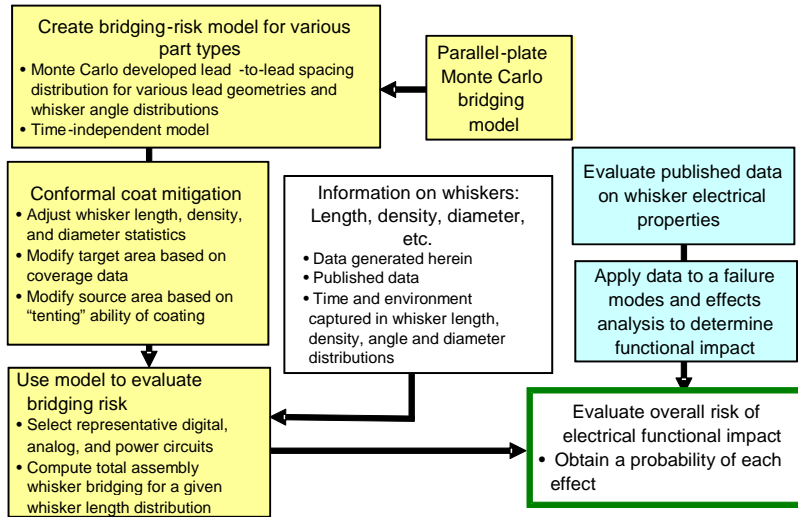


Figure 263: Overall whisker risk mitigation assessment approach.

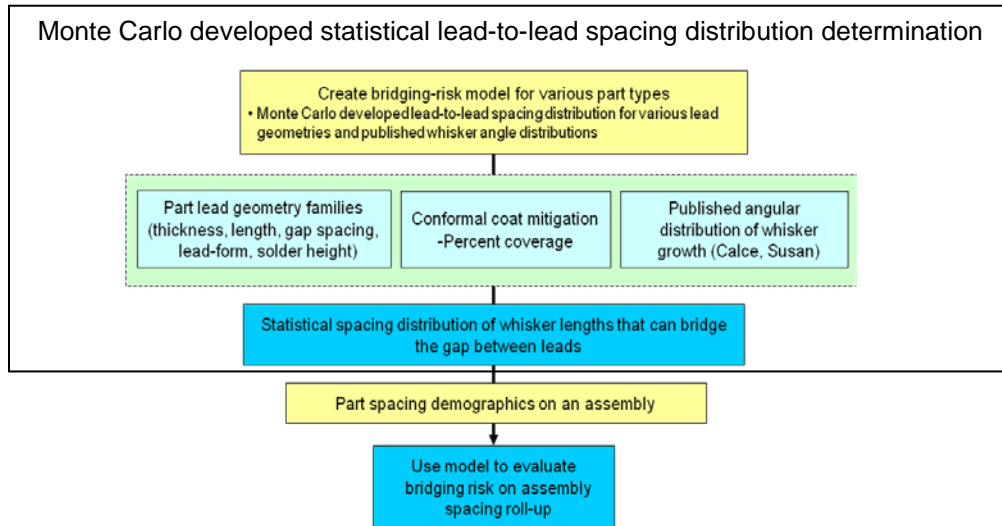


Figure 264: Computational approach to compute used to determine the overall bridging risk for an assembly.

12.2 Gull wing model development

The short circuit risk modeling analysis details for a given part at a particular operating voltage are given in Figure 265. This procedure was repeated for each part and the final short circuit risk was rolled up to an assembly level and then a box level. The geometric details required to perform the whisker short circuit analysis are similar to the information already collected to perform a solder joint fatigue analysis (e.g. lead stiffness is computed from the lead geometry). In addition, part voltage levels were already tabulated for electrical stress analysis and the printed circuit pad geometries were available from the design tools. While the largest unknown still remains to be the relationship between whisker length and service time and environment, the risk analysis was still useful in providing a quantitative whisker short circuit risk for a particular whisker distribution. It can be used to quantify whisker risk mitigations such as tin-lead soldering, tin-lead hot solder dipping or varying amounts of conformal coating coverage.

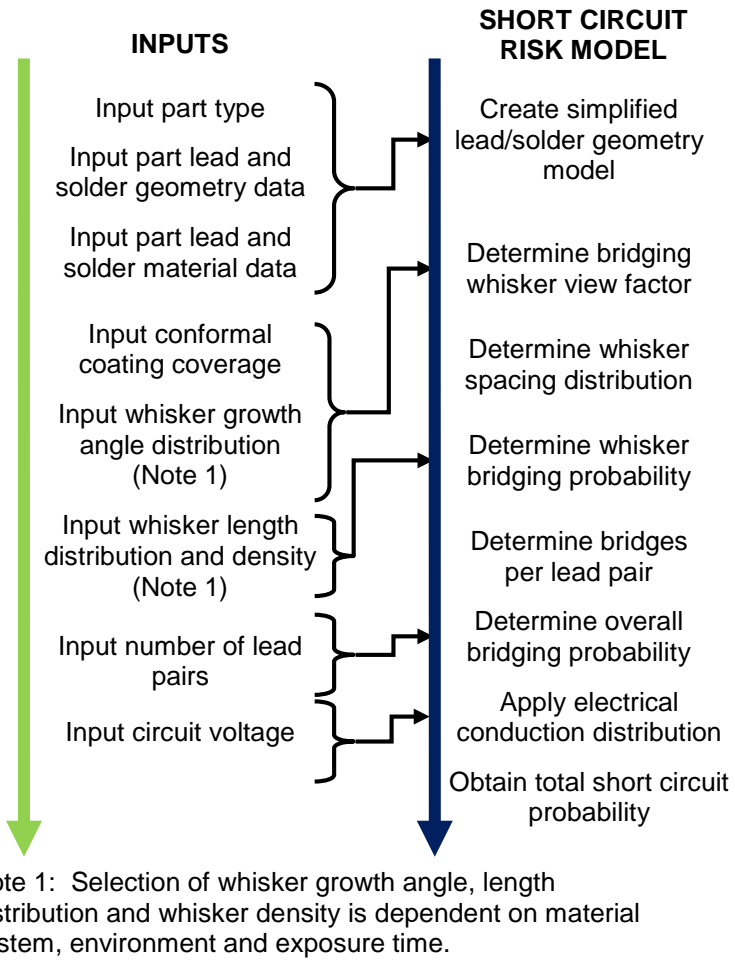


Figure 265: Short circuit risk model inputs and modeling analysis step details for a given part.

12.2.1 Motivating cases

12.2.1.1 Typical parts

In an effort to capture the needs of a top down systems level tin whisker short circuit analysis, a detailed assessment of part types and quantities in a typical flight control computer incorporating CPU, digital, analog, and power supply modules was used in the whisker bridging analysis. The number of lead gaps for the various modules is shown in Table 63. The CPU and digital boards had the greatest numbers of leads and the closest lead-to-lead spacing. A lead gap spacing distribution for a typical digital board is shown in Figure 266. In the present work, geometric bridging risk models have been completed for 10 component types and 85 specific parts with separate modeling of whiskers originating on the lead and solder surfaces.

Table 63: Number of lead gaps for various circuit boards from a control system

Description	# of leads	# of gaps
Analog 1	2009	1787
Power Supply	326	228
Digital 1	2573	2418
CPU	1144	1038
CPU-MEZZ	2512	2478

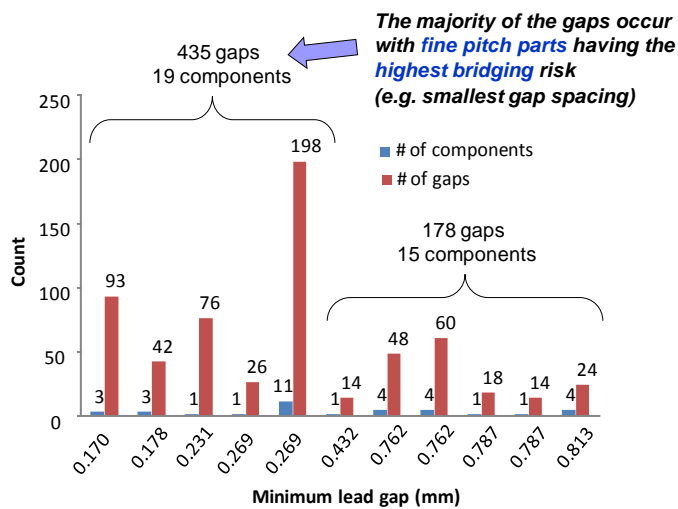


Figure 266: Part spacing demographic for a typical digital board.

12.2.1.2 Coating coverage

Conformal coating coverage measurements showed that coverage was dependent upon the coating type, the method of application, and lead geometry [52]. While vacuum deposited Parylene provides the best coverage, spray coating is the most common method used in industry because of its low cost, ease of application, and its reworkability. In the present work, conformal coating coverage was modeled for both the uncoated, fully coated and partially coated conditions. The partial coating was taken to have 90 percent coverage on the outside of the lead, 50 percent coverage on the sides, and no coverage on the back which is representative of a 100 percent solids low VOC urethane/acrylic spray coating (Figure 267). Note that in addition to coverage, satisfactory equipment humidity performance is dependent upon a combination of circuit impedance, material selection, and enclosure design. Both the AR/UR Manufacturer-1 and the UV40-250 shown in Figure 267 are qualified to IPC-CC-830 class 3 and have been successfully used for years in aerospace.

Spray coated assemblies of fine pitch parts can have very limited coverage of printed circuit board pads behind the leads (Figure 268). For the model, the “no coverage” on the back also includes the printed wiring board pads behind the leads. The reason for the low coverage was because the line of sight between the spray nozzle and the back of the pads was blocked by the leads.

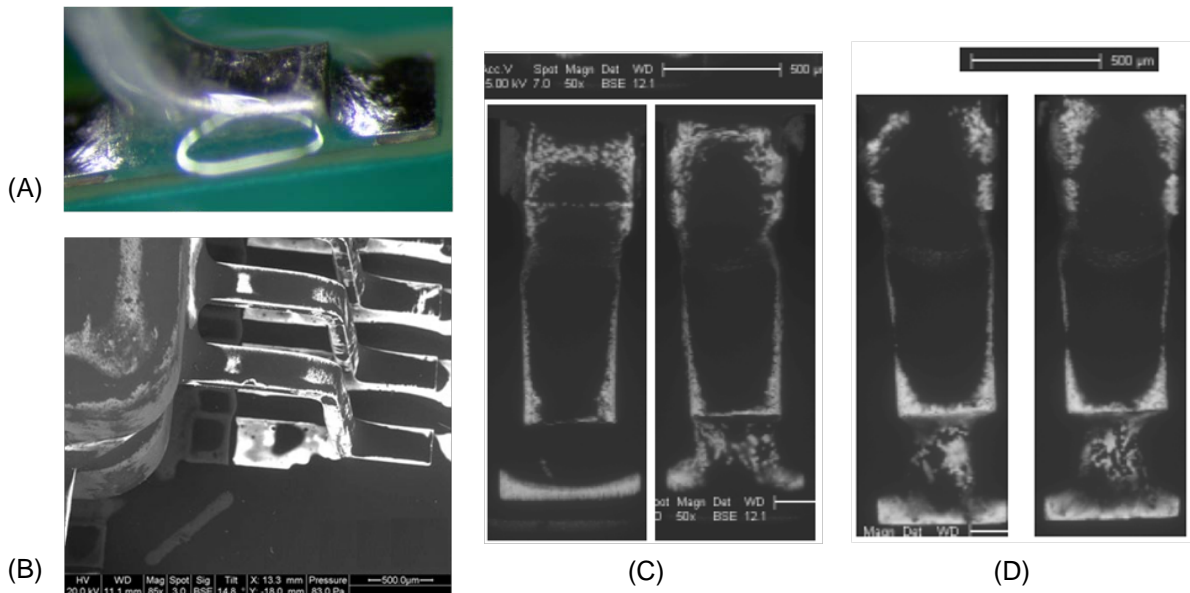


Figure 267: Conformal coating coverage assessment of low VOC 100 percent solids spray coatings; (A) Optical image, (B) isometric SEM [52], and (C) top SEM view of AR/UR Manufacturer-1 and (D) top SEM view of UV40-250 used in the present work. The light color in the SEM images indicates that the coating thickness was less than three microns.

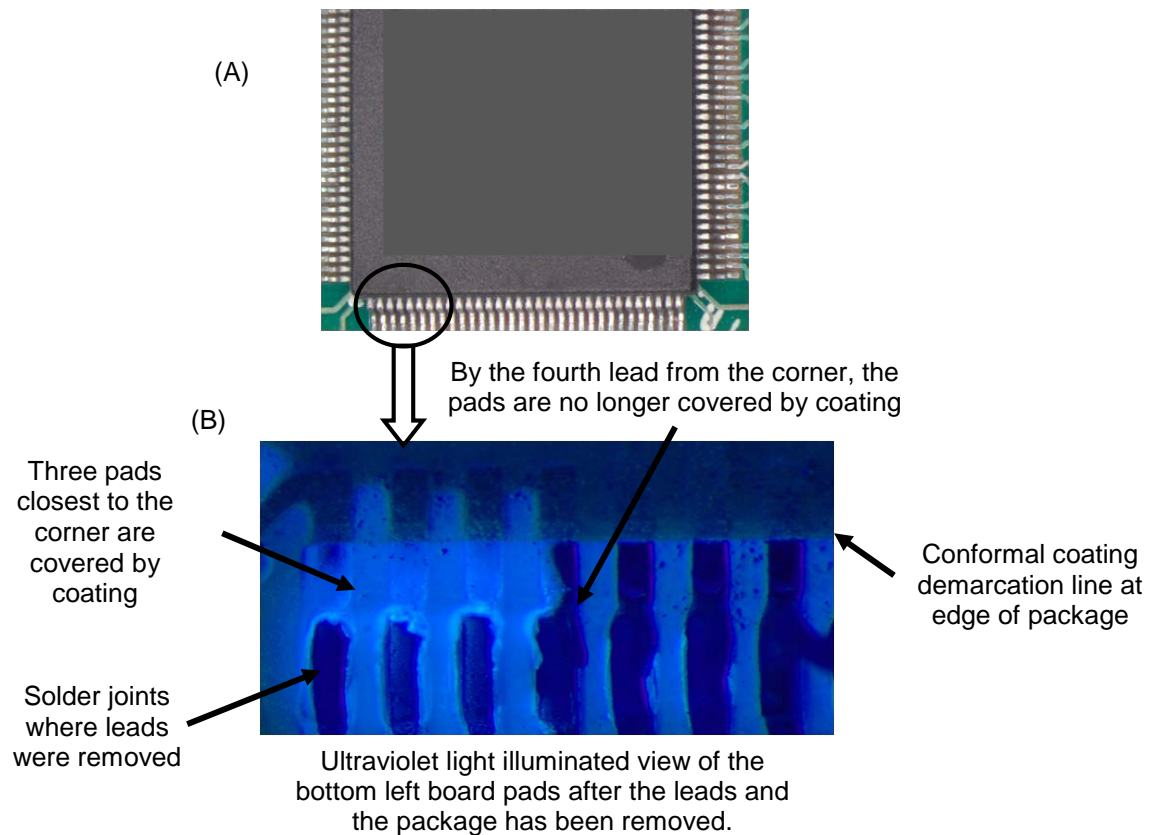


Figure 268: TQFP128 soldered to a board with tin-lead solder. The nominal lead-to-lead gap spacing is 220 microns. The coating was a 100 percent solids low VOC AR/UR coating [90]; (A) overall view and (B) higher magnification view with package removed and ultraviolet light illumination. The UV light causes the coating to fluoresce.

12.2.2 Bridging risk geometric modeling

The benefit of separating the geometric modeling from the whisker length distribution was that a reduced number of Monte Carlo simulations were needed. As shown in Figure 269, each lead configuration had a specific “distribution of spaces” that a hypothetical whisker could bridge across.

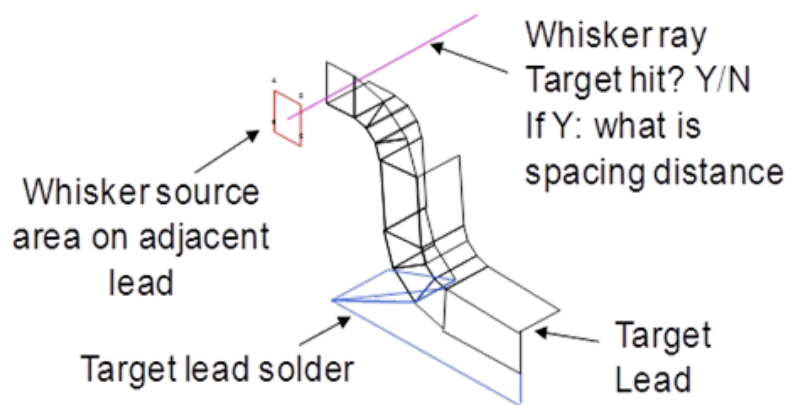


Figure 269: Determination of lead-to-lead spacing distance for a bridging whisker.

12.2.3 Lead geometry modeling

The geometric modeling used a simplified lead geometry to simulate the general lead form, but with sharp corner bends as shown in Figure 270. Datasheet dimensions for the gull-wing parts were reduced to the following part dimensions (Figure 270):

- Lead span length (L_L)
- First bend distance (A)
- First bend height (H)
- Lead foot length (f)
- Lead thickness (t)
- Lead width (W_L)

Also considered in the lead modeling were the lead width and spacing and the board pad dimensions:

- Pad width (W_P)
- Pad length (L_P)

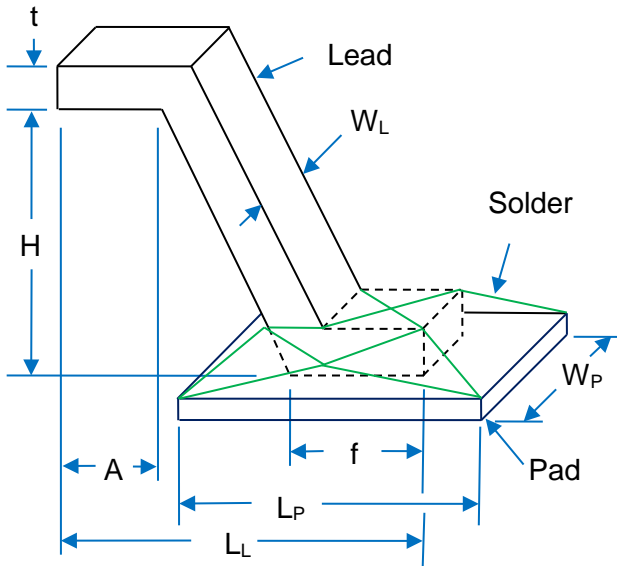


Figure 270: Simplified lead geometry

12.2.3.1 Board pad

Because testing identified significant whisker growth originating from the side of the board pad, the side of the board pad was added to the whisker risk model. In the present work, the printed wire board pad thickness was modeled to be 0.063 mm (e.g. two ounce plated copper), typical of complex assemblies with multiple via and surface plating operations, and was centered about the lead foot. This involved adding four triangles at the side and inside edges of the board pad. Because whiskers originating from the lead toe edge of the board pad have no capability to generate a bridge, these areas were not included.

The risk modeler should be aware that the bare board fabrication can result in differences between the nominal artwork design and the actual minimum board pad clearance. The surface copper pad clearances were challenging to maintain on this test board because the board surface copper was 63 microns thick (e.g. typical for a two ounce surface copper layer after plating). For example on the TQFP64 used in the present work (Figure 271), the nominal artwork pad design had a copper pad 228.6 microns wide with a space between pads of 171.4 microns on a pitch of 400 microns. The etching process resulted in a spacing reduction to 109 microns at the bottom of the pad adjacent to the board.

12.2.3.2 Solder bulge

The solder in the model went from the top of the board pad to the top of the lead foot and on top of the lead foot. The height of the solder heel fillet to be aligned with the top of the lead is a minimum heel fillet for a J-STD-001 Class 3 joint, which is conservative. However, the model is non-conservative because side and toe solder fillets are included in the model even though they are not required by J-STD-001. The solder joint can exhibit varying degrees of curvature near the lead, depending on solder volume, lead shape, and wetting. As shown in Figure 271, the solder flow around the edge of the pads reduced the pad-to-pad gap spacing from 109 microns to 60 microns near the lead. To accommodate this involved adding four triangles to represent the solder bulge. The maximum bulge location is modeled to be half way up the solder (Figure 270).

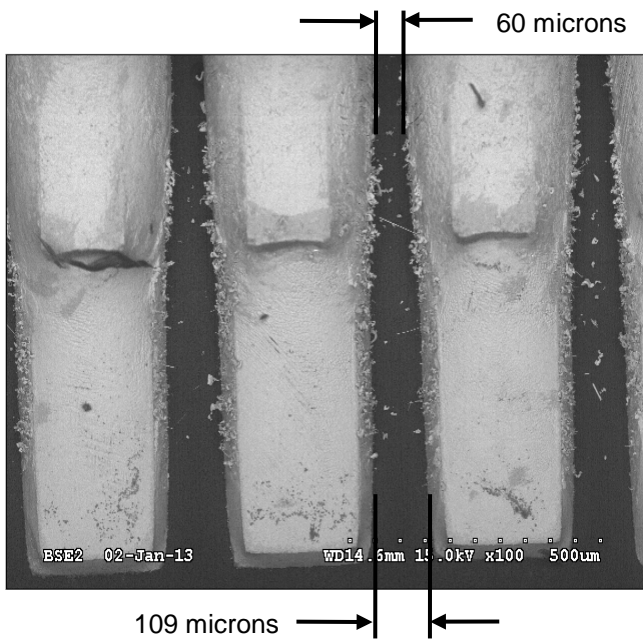


Figure 271: Gap spacing reduction at the board copper pad by board fabrication etch tolerances and a slightly bulbous solder joint at lead on the TQFP64 board pads (Note SEM image obtained after 4,000 h exposure at 85°C/85%RH).

12.2.3.3 Whisker mirror

The original version of the lead model generated the geometry for two separate leads based on the lead pitch. To simplify the addition of the solder and the pad, a whisker mirror (Figure 272) was used in between the lead locations to allow an identical lead to be represented without actually generating the geometries. The specific whisker vector was reflected by reversing the vector component perpendicular to the whisker mirror. Because an Excel lookup table was used to detect the contact between the reflected whisker and the lead/solder/pad, the Extreme Speed option was no longer functional with the Oracle Crystal Ball™ Monte Carlo software so the computation speed was somewhat slower. The performance of the whisker mirror was compared with the original model to verify the accuracy of the whisker mirror concept.

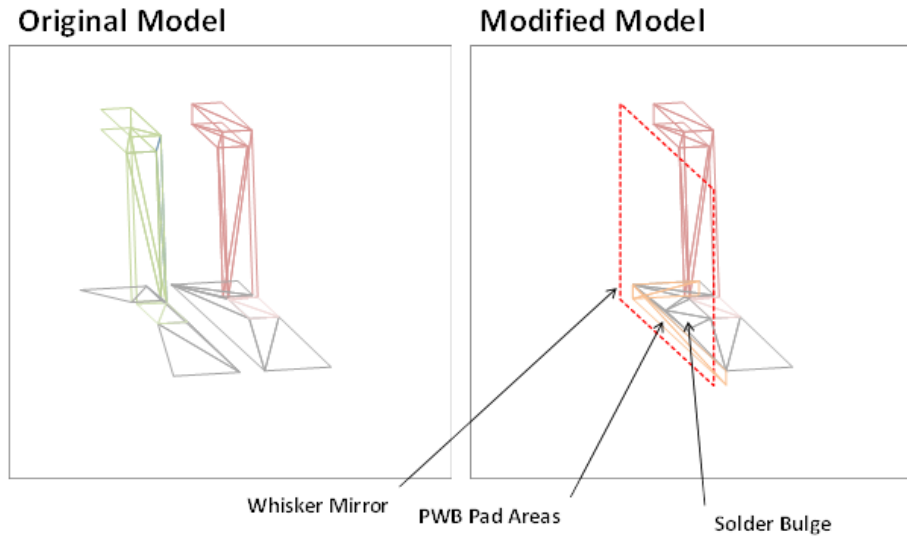


Figure 272: Modifications to the original whisker risk model.

12.2.4 Whisker risk data subset

The general approach for developing the simplified whisker risk model was to develop generic relationships based on factors and spacing distributions developed from a subset of lead geometries.

Specific lead geometries used were:

- SOIC (1.27-mm pitch)
- 0.65-mm pitch
- 0.5-mm pitch
- 0.4-mm pitch

For the 0.5-mm pitch geometry, thick and thin packages were considered with additional consideration given to long and nominal leads for thick packages. Typical dimensional tolerances (max., min., nominal) as provided in part drawings were also included. The specific list of packages and dimensions used is provided in Table 64.

Monte Carlo modeling was conducted for the listed parts/geometries for uncoated and partially coated leads. Partial coating is defined as follows:

- 90% effective on outside of lead
- 50% effective on sides of lead
- 0% effective on back/inside of lead

Separate calculations were performed for whiskers sourcing at the board pad, lead, and solder. A solder bulge based on a pad spacing reduction of 49 microns was considered to act at a height equal to 50 percent of the lead thickness.

Table 64: Parts and dimensions considered for risk modeling (dimensions in mm).

Part - variant	Packag e Height	Pkg. Seatin g Plane	Board Pad Length (L _P)	Boar d Pad Width (W _P)	Lead Span Length (L _L)	Lead Foot Length (f)	Lead Thick. (t)	Lead Widt h (W _L)	Lead Pitc h
SOIC-nominal	2.34	0.205	2.16	0.7	1.385	0.815	0.275	0.415	1.27
SOIC-max	2.35	0.29	2.16	0.7	1.495	1.02	0.32	0.48	1.27
SOIC-min	2.29	0.12	2.16	0.7	1.285	0.61	0.23	0.35	1.27
0.65mm-nominal	1.05	0.1	1.587	0.49	1	0.625	0.15	0.245	0.65
0.65mm-max	1.05	0.15	1.587	0.49	1.15	0.75	0.15	0.3	0.65
0.65mm-min	1.05	0.12	1.587	0.49	0.85	0.5	0.15	0.19	0.65
0.5mm-Long/Thick-nominal	3.4	0.375	1.762	0.37	1.3	0.6	0.145	0.22	0.5
0.5mm-Long/Thick-max	3.6	0.5	1.762	0.37	1.3	0.75	0.2	0.27	0.5
0.5mm-Long/Thick-min	3.2	0.25	1.762	0.37	1.3	0.5	0.09	0.17	0.5
0.5mm-Thick-nominal	1.4	0.1	1.64	0.37	1	0.6	0.145	0.22	0.5
0.5mm-Thick-max	1.45	0.15	1.64	0.37	1	0.75	0.2	0.27	0.5
0.5mm-Thick-min	1.35	0.05	1.64	0.37	1	0.45	0.09	0.17	0.5
0.5mm-Thin-nominal	0.8635	0.1015	1.589	0.37	0.95225	0.5465	0.145	0.235	0.5
0.5mm-Thin-max	0.965	0.152	1.589	0.37	1.13	0.699	0.2	0.27	0.5
0.5mm-Thin-min	0.888	0.051	1.589	0.37	0.7745	0.394	0.09	0.177	0.5
0.4mm-nominal	1.4	0.1	1.64	0.291	1	0.6	0.145	0.18	0.4
0.4mm-max	1.45	0.15	1.64	0.291	1	0.75	0.2	0.23	0.4
0.4mm-min	1.35	0.05	1.64	0.291	1	0.45	0.09	0.13	0.4

12.2.5 Simplified model development

Development of the simplified model was based on developing whisker view factor and spacing distribution using a range of lead and pad dimensions. All calculations were based on the use of dimensionless parameters to avoid complications in the simplified model due to selection of units.

12.2.5.1 Whisker view factor

The whisker view factor represents the probability that an infinite whisker will bridge between adjacent leads. All of the calculations were implemented in Microsoft Excel™ which is also the platform for the Crystal Ball™ software. Five probability distributions were used with random variables to generate the simulated whiskers as follows:

- Source area lookup – determines which source triangle is used to generate the whisker (scaled by area of triangle) – uniform distribution
- Triangle base fraction – determines position along the base of the source triangle – Uniform distribution
- Triangle side fraction – determines position from the triangle vertex (opposite the base) to point along the base – Triangular distribution
- Whisker angle from normal – Uniform distribution (see text)
- Whisker azimuth – Uniform distribution

An additional uniform random variable was used in conjunction with the conformal coating effectiveness on the applicable target surface to determine if a bridge occurred. A uniform distribution was selected for the whisker angle from the normal based on discussions among the investigators over the apparently conflicting results obtained by the present work, Susan [36] and Fang [92]. Each Monte Carlo calculation used one million simulated whisker trials with the results filtered for infinite whiskers resulting in a potential bridge. As shown in Figure 273, the ratio of potential bridges to the overall trials determined the whisker view factor for one lead to the other and a cumulative spacing distribution was developed for those whiskers indicating a bridge. A trial and error method in conjunction with the Excel solver was used to develop a metric that had the best correlation to whisker view factor based on dimensional calculations derived from part/pad data.

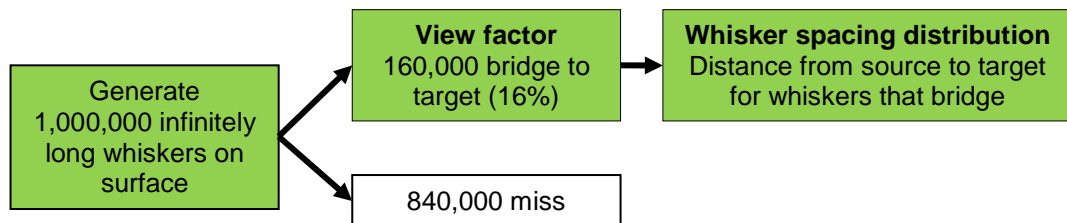


Figure 273: Example of a QFP lead view factor and whisker spacing distribution calculation flow.

12.2.5.1.1 Lead whisker uncoated view factor

The view factor for whiskers originating at the lead surface was based on the following metric (M_L):

s = Lead spacing

t = Lead thickness

A_w = Whiskerable area

A_s = Single sided area

$$M_L = \left(\frac{A_s}{A_w + s^2} \right)^{1.421215} \cdot \left(\frac{t}{s} \right)^{1.153123}$$

A plot providing the modeled view factor as a function of the above metric and the derived equation is provided in Figure 274.

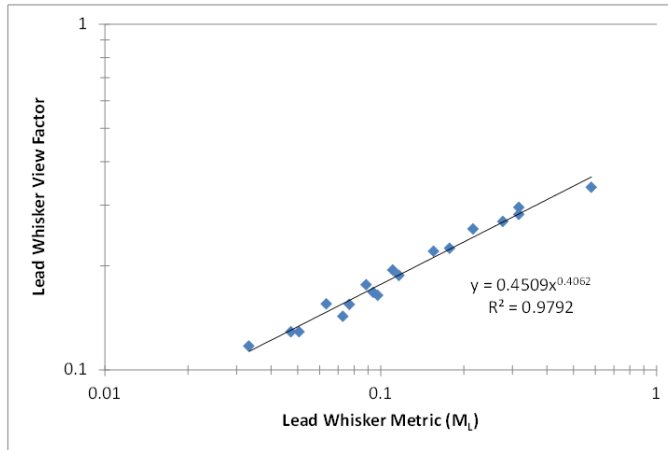


Figure 274: Lead whisker view factor correlation

12.2.5.1.2 Solder whisker uncoated view factor

The view factor for whiskers originating at the pad surface was based on the following metric (M_S):

s = Lead spacing

t = Lead thickness

A_W = Whiskerable area

$$M_S = \left(\frac{A_W}{s^2} \right)^{-0.50606} \cdot \left(\frac{t}{s} \right)^{1.97517}$$

A plot providing the modeled view factor as a function of the above metric and the derived equation is provided in Figure 275.

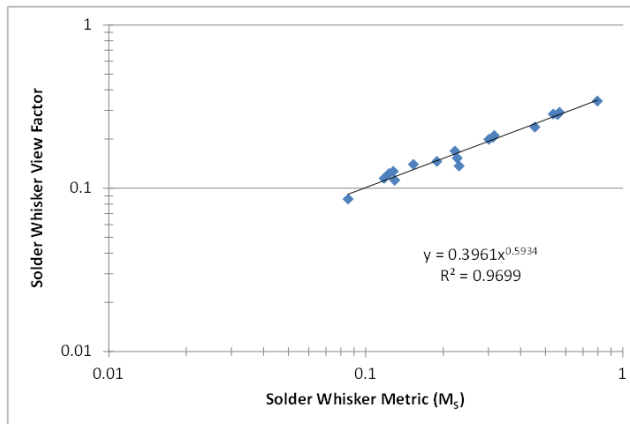


Figure 275: Solder whisker view factor correlation

12.2.5.1.3 Pad whisker uncoated view factor

The view factor for whiskers originating at the pad surface was based on the following metric (M_P):

s = Lead spacing

t = Lead thickness

$$M_P = \left(\frac{t}{s} \right)^{1.686625}$$

A plot providing the modeled view factor as a function of the above metric and the derived equation is provided in Figure 276.

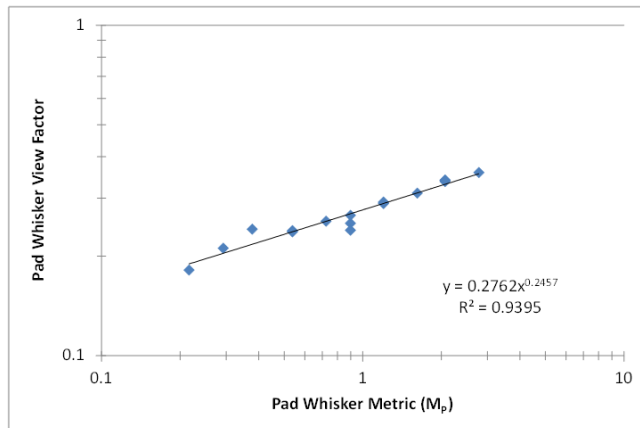


Figure 276: Pad whisker view factor correlation

12.2.5.1.4 Partially-coated whisker view factor

Although adjustment for uniformly conformal coated configurations can be globally applied to the appropriate overall uncoated view factor, partially coated configurations were more complex. Considering coating effectiveness of 90 percent on outside, 50 percent effective on sides, and 0 percent effective on back/inside (Figure 277), the view factor was plotted relative to the uncoated view factor (Figure 278) where it can be seen that the modeled view factor for the partially-coated configuration was 60 percent of the uncoated configuration (40 percent coating effectiveness).

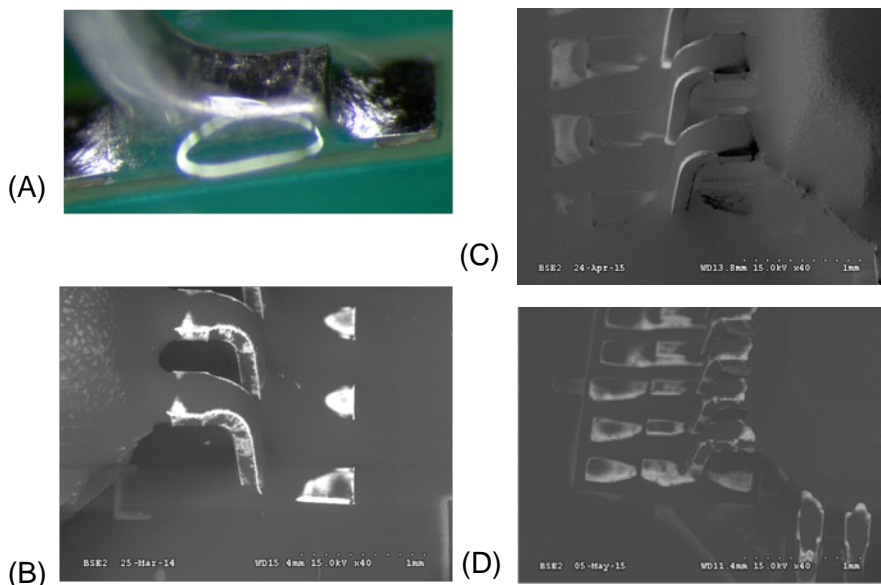


Figure 277: Conformal coating coverage assessment of low VOC 100 percent solids AR/UR UV cure spray coatings; (A) Typical optical image, and (B), (C) and (D) showing typical isometric SEM images of different packages and coating manufacturers. The light color in the SEM images indicates that the coating thickness was less than three microns.

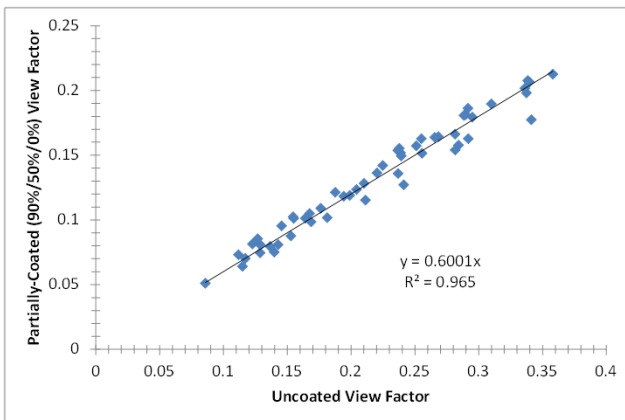


Figure 278: Partially-coated versus uncoated view factors

12.2.6 Whisker spacing distribution

The spacing distribution provides a cumulative fraction versus length between the minimum and maximum spacing starting at leads, solder, or pads and ending at any other feature as shown in Figure 279. Development of an appropriate distribution requires calculation of the minimum and maximum spacing and the appropriate intermediate fractions.

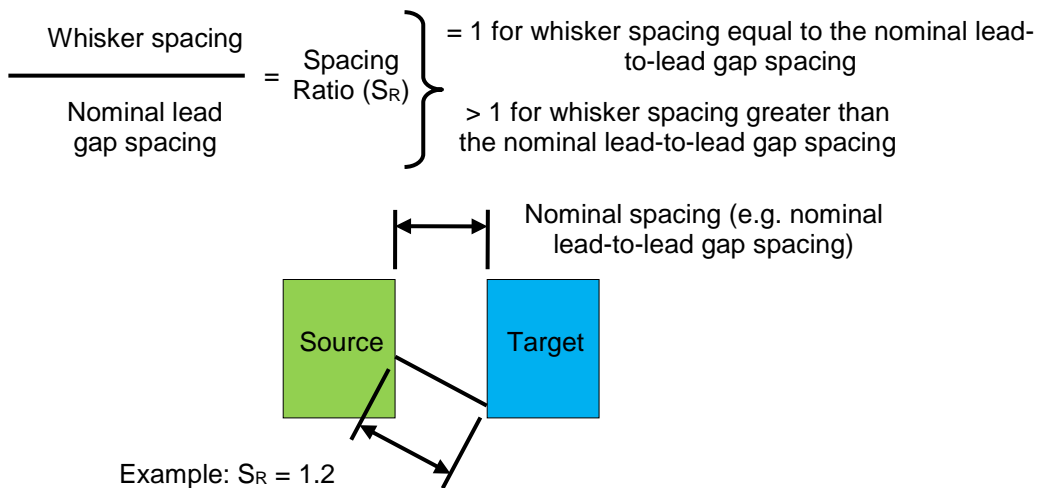


Figure 279: Description of whisker spacing to nominal spacing ratio (SR).

12.2.6.1 Minimum spacing

The minimum lead spacing was determined as a linear combination of board pad width, lead width, lead pitch, and spacing. The Excel solver was used to optimize the coefficients based on the minimum sum-squared error (SSE) between the predicted minimum spacing and that obtained from the model. Values of the coefficients to calculate the minimum spacing are provided in Table 65.

Table 65: Coefficients to calculate minimum spacing.

PWB Pad Width	Lead Width	Lead Pitch	Lead Spacing
Coeffs for Lead Spacing: -0.59941	-0.39821	1.014216	0
Coeffs for Solder Spacing: 0.002369	-0.00227	0	1.00259
Coeffs for Pad Spacing: -1.06902	0.054753	1.012726	0

12.2.6.2 Maximum spacing

The maximum lead spacing was determined as the diagonal of a rectangular prism with height defined in relationship to the first bend height. The width of the prism was defined as a linear combination of the lead width, lead pitch, and board pad width. The length of the prism was defined as a linear combination of the board pad length, lead span length, and first bend distance. The Excel solver was used to minimize the SSE between the predicted maximum spacing and that obtained from the model. Values of coefficients to calculate the maximum spacing are provided in Table 66.

Table 66: Coefficients to calculate maximum lead spacing

Length Direction			Width Direction		
PWB Pad Length	Lead Span Length	First Bend Dist.	First Bend Height	Lead Width	Lead Pitch
Coeffs for Lead Spacing: 0.569988	0.357226	0.395243	1.086483	0	1.151966
Coeffs for Solder Spacing: 0.514016	0.478274	0.407232	1.040679	0	1.30039
Coeffs for Pad Spacing: 0.662121	0.166851	0.433574	1.105011	0.792507	0.476286
					0.514922

12.2.6.3 Distribution development

The distributions were developed based on a non-dimensional distribution dividing the length values at each distribution point by the appropriate nominal spacing and then scaling the results linearly such that the maximum spacing produces a value of 10 while maintaining nominal spacing at one. Plotting the results as a function of cumulative spacing fraction produces reasonably consistent results as shown in Figure 280 through Figure 282.

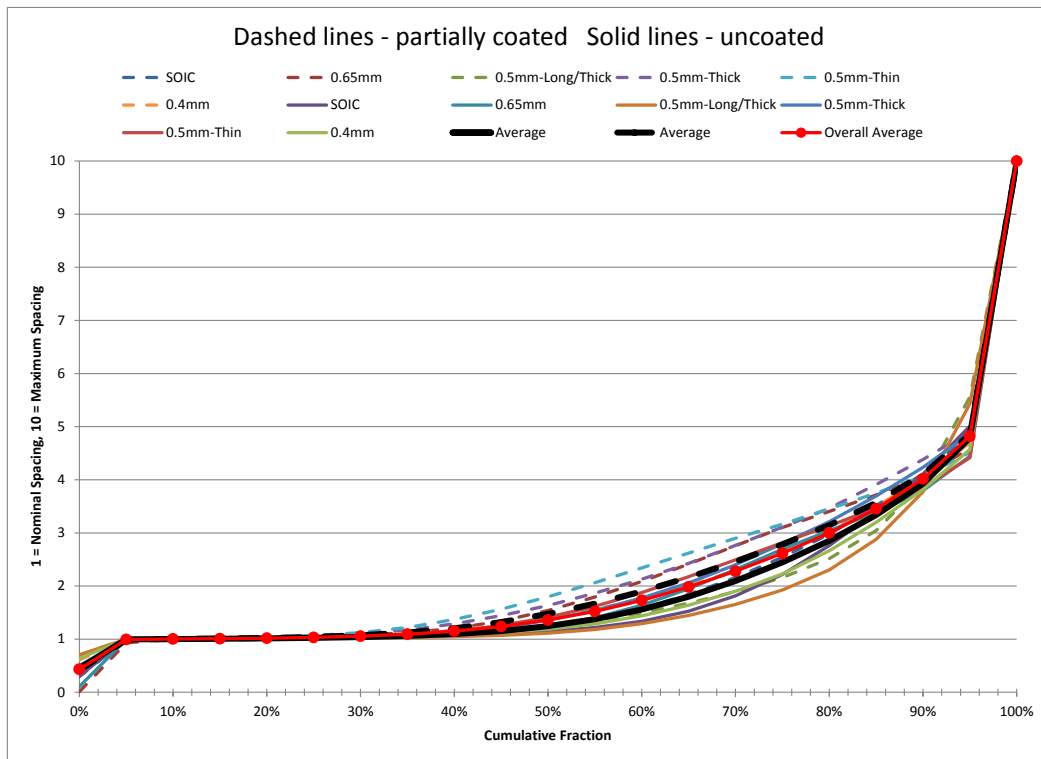


Figure 280: Non-dimensional spacing distribution for lead whiskers.

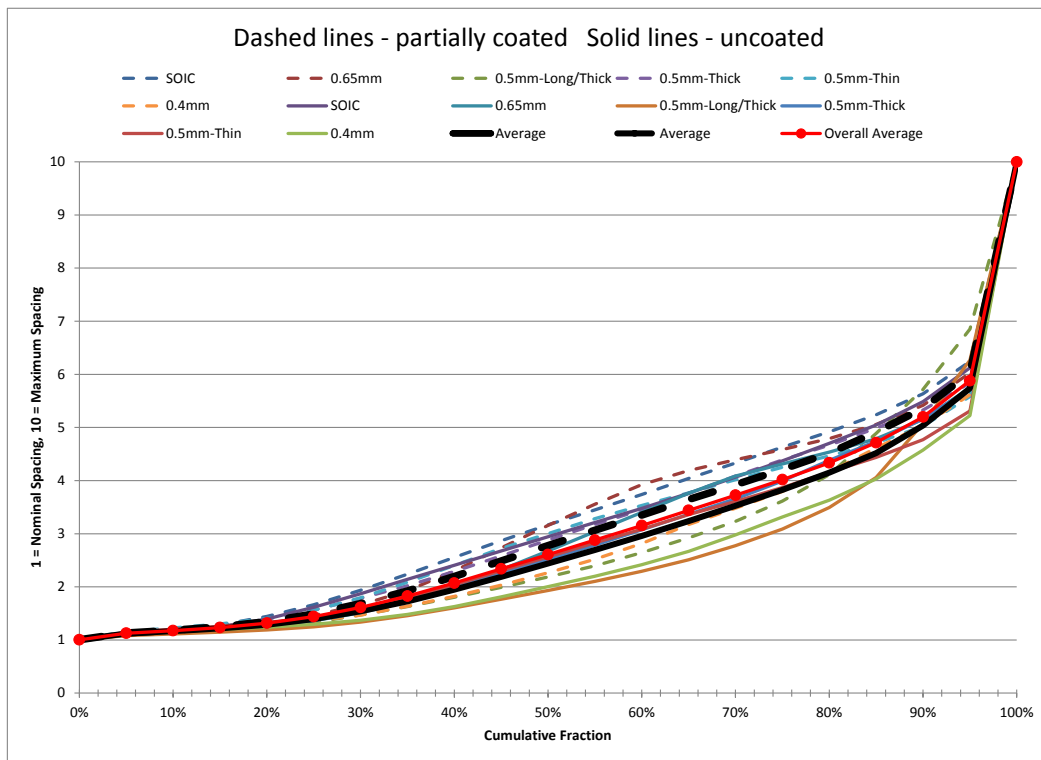


Figure 281: Non-dimensional spacing distribution for solder whiskers.

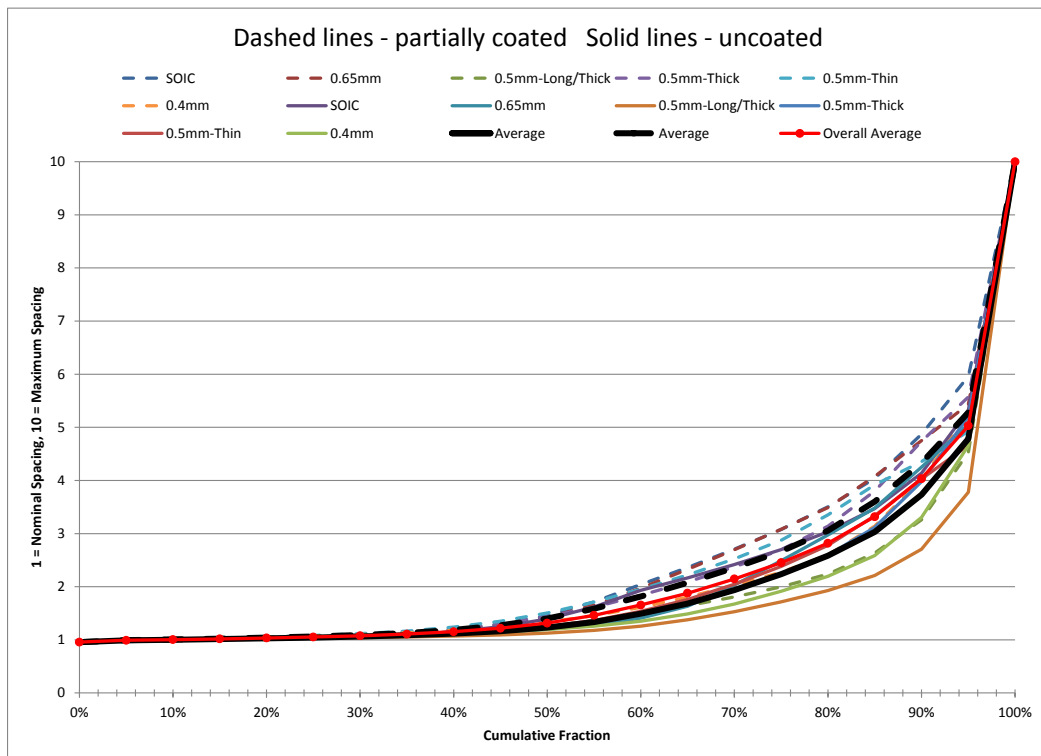


Figure 282: Non-dimensional spacing distribution for pad whiskers.

Specific non-dimensional distribution values for each type of whisker are summarized in Table 67. These values were used in conjunction with the appropriate nominal and maximum spacing to extract the length values for fractions greater than or equal to 5 percent. For whiskers originating at the solder or pad, the zero percent value is the minimum of the value extracted from the non-dimensional distribution and the minimum spacing value calculated in the *Minimum spacing* section. Because of the large variation in spacing with the non-dimensional distribution for the lead whisker at zero percent (Figure 280), the extracted lead whisker spacing distribution always uses the minimum calculated value (from *Minimum spacing* section).

Table 67: Non-dimensional whisker distribution

(1 = nominal spacing, 10 = maximum spacing)

Whisker Type			
Cumulative	Lead	Solder	Pad
0%	see text	1.0044	0.9578
5%	0.9942	1.1273	0.9913
10%	1.0030	1.1763	1.0043
15%	1.0087	1.2343	1.0179
20%	1.0183	1.3171	1.0341
25%	1.0331	1.4415	1.0534
30%	1.0564	1.6133	1.0768
35%	1.0935	1.8256	1.1080
40%	1.1513	2.0714	1.1527
45%	1.2376	2.3390	1.2185
50%	1.3597	2.6078	1.3157
55%	1.5228	2.8800	1.4609
60%	1.7293	3.1547	1.6554
65%	1.9823	3.4407	1.8783
70%	2.2778	3.7257	2.1462
75%	2.6158	4.0182	2.4525
80%	2.9996	4.3348	2.8195
85%	3.4536	4.7155	3.3169
90%	4.0182	5.1980	4.0333
95%	4.8218	5.8805	5.0295
100%	10.0000	10.0000	10.0000

12.2.7 Whisker length distributions

The risk model spreadsheet supports several different classic statistics distributions as well as a numerical distribution table.

12.2.7.1 Three-parameter lognormal distribution

The probability density function for the lognormal distribution is given by the following equation:

x_0 = Minimum

μ = Location parameter

σ = Scale parameter

$$f(x) = \frac{1}{(x - x_0) \cdot \sigma \cdot \sqrt{2\pi}} \cdot e^{-\frac{(\ln(x - x_0) - \mu)^2}{2\sigma^2}}$$

12.2.7.2 Three-parameter log-Cauchy

The probability density function for the log-Cauchy distribution is given by the following equation:

x_0 = Minimum

μ = Location parameter

σ = Scale parameter

$$f(x) = \frac{1}{(x - x_0) \cdot \pi} \cdot \left[\frac{\sigma}{(\ln(x - x_0) - \mu)^2 + \sigma^2} \right]$$

12.2.7.3 Cauchy distribution

The probability density function for the Cauchy distribution is given by the following equation:

x_0 = Location parameter

γ = Scale parameter

$$f(x) = \frac{1}{\pi \cdot \gamma \cdot \left[1 + \left(\frac{x - x_0}{\gamma} \right)^2 \right]}$$

12.2.7.4 Weibull distribution

The probability density function for the Weibull distribution is given by the following equation:

x_0 = Minimum

α = Characteristic Life

β = Shape parameter

$$f(x) = \frac{\beta}{\alpha} \left(\frac{x - x_0}{\alpha} \right)^{\beta-1} \cdot e^{-\left(\frac{x - x_0}{\alpha} \right)^\beta}$$

12.2.7.5 Numerical distribution

Because some measurements indicated a small but significant fraction of very long whiskers beyond those represented by some calculated distributions, the capability for a numerical distribution of whisker length was added. The numerical distribution is entered by providing a cumulative percentage and corresponding length. The cumulative numerical distribution is numerically differentiated to obtain a probability density function (PDF) with intermediate values linearly interpolated. The interpolated PDF is used in place of the calculated PDF in the whisker bridging probability calculation.

12.2.7.6 Location (third) parameter

The location parameter is a finite minimum length such that no whiskers are shorter than that length. Although there is some controversy over the use of a third location parameter in logarithmically based distributions and the third parameter is difficult to fit, a third parameter was added to provide additional flexibility to consider a minimum length whisker. The location parameter was added to the lognormal, log-Cauchy, and Weibull distributions.

12.2.7.7 Some lognormal distributions

Whisker length distributions derived from Barrie Dunn's data are shown Table 39. The lognormal parameters used to describe the distribution are given in terms of the 1.696 percentile and the 99.8 percentile whisker lengths. In the present experiments, the whiskers are considerably shorter than the 15 ½ year specimen 11 sample tested by Barrie Dunn [72]. Note that Dunn specimen 11 was tin over copper plated brass and did not exhibit the longest nor the shortest whisker growth amongst the samples tested; it was to be a "middle of the road" whisker length. For reference, lengths of other tin-over-copper underplated steel Dunn specimens are shown in Table 68.

Table 68: Lognormal parameters for the Dunn whisker measurements

Lognormal parameters	Derived data from 15 ½ year old Dunn specimen 11		
	0yr/3.5yr	8yr	15yr
1.696% length (micron)	0.010	0.010	0.010
99.8% length (micron)	0.400	0.525	0.733
Whisker μ (location, ln(mm))	-3.0401	-2.9247	-2.7831
Whisker σ (scale, nondim)	0.7379	0.7923	0.8591

Note: The 15 ½ year old sample data is from work by Dunn [72] used in a whisker bridging risk analysis by McCormack and Meschter [96].

Whisker length distribution for the HTTH testing is shown in Figure 283. Note that the lognormal mean, μ (Minitab™ Location parameter), in ln(microns) was converted to ln(millimeters) by subtracting ln(1,000) which is 6.9078. The lognormal shape is dimensionless and requires no conversion.

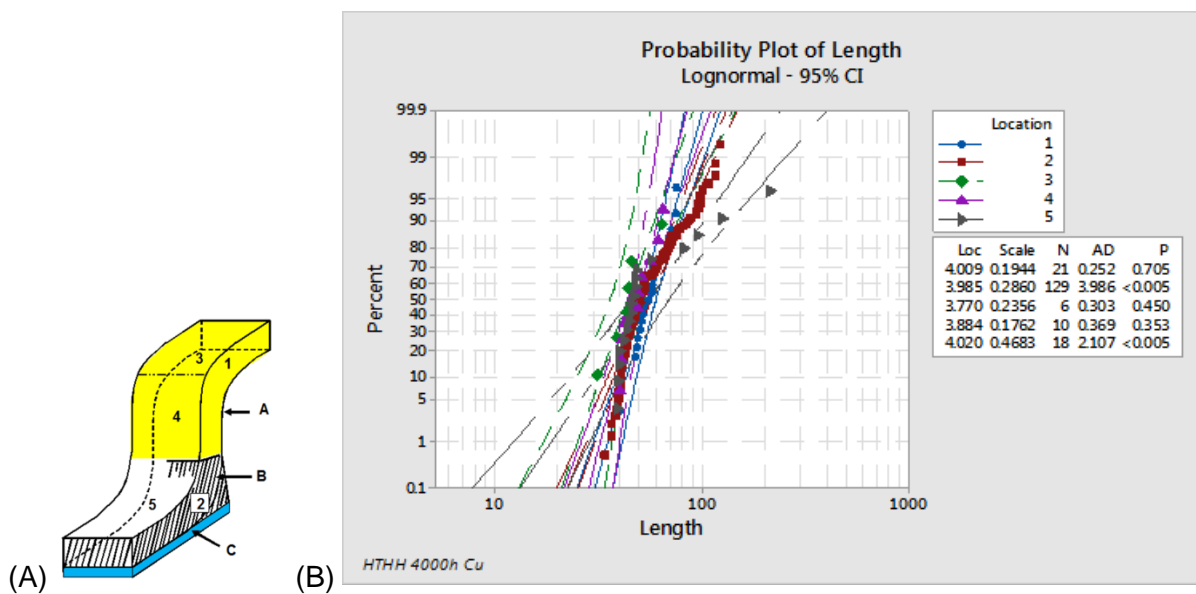


Figure 283: (A) Whisker growth locations, (B) Probability plot of whisker lengths (microns) from the HTHH testing for Cu leads after 4,000 h at 85°C/85%RH; broken down by location (from Figure 170) and (C) conversion of lognormal mean parameters from microns to mm.

12.2.8 Whisker density

Measurements of whisker growth by Fang [92] yielded a density 145 whiskers/mm² for bright tin, but much lower whisker density would be obtained with less whisker prone configurations. Whisker densities in the current work depend strongly on the test duration, location, materials, contamination, and environment. The densities varied from zero (no whiskers) on some of the termination areas/termination types during power cycling to 2,027 whiskers/mm² along the bottom edge of the board pad after 4,000 h at 85°C/85%RH HTHH (see whisker density box plots in Figure 176 and Figure 177). The 0-0 contamination level copper termination after 4,000 h whisker density along the pad edge ranged from 323 to 1,580 whiskers/mm² (Table 69).

Table 69: Whisker density of whiskers growing from the solder at the board pad (location-2) for the SOT5 at a 0-0 cleanliness level after 4,000 h at 85°C/85%RH HTHH (repeated from Table 39).

	Whiskers/ lead pad	Pad side area (mm ²)	Whisker density (whiskers/mm ²)
Minimum	58	0.1798	323
Maximum	284	0.1798	1580
Average	182.8	0.1798	1017

12.2.9 Whisker bridging probability

To determine the whisker bridging probability, let W represent the whisker length and S represent the spacing and B represents the bridging distance. The bridging distance is then given by:

$$B = W - S$$

$$W = B + S$$

The probability density function for bridging is given by:

$$f_B(b) = \int_{-\infty}^{\infty} f_{SW}(s, b + s) ds$$

Since whisker length and spacing are independent:

$$f_{SW}(s, w) = f_S(s) \cdot f_W(w)$$

Where $f_S(s)$ and $f_W(w)$ are whisker spacing and length distributions respectively, it follows that:

$$f_B(b) = \int_{-\infty}^{\infty} f_S(s) \cdot f_W(b + s) ds$$

The whisker bridging probability is given by:

$$P_B = \int_0^{\infty} \int_{-\infty}^{\infty} f_S(s) \cdot f_W(b + s) ds db$$

The above double integral was implemented numerically in Microsoft Excel™ based on the numerical whisker spacing distribution from the Monte Carlo analysis and a lognormal whisker length distribution. This value represents the probability that a whisker is of sufficient length to bridge between adjacent leads. The results of a hypothetical example calculation are given in Figure 284. The spacing distribution can quickly be compared to the whisker length distribution. The positive values of the bridge interference distribution are where the whisker is longer than the conductor-to-conductor space (note: the negative values, not plotted, occur when the whisker is shorter than the space).

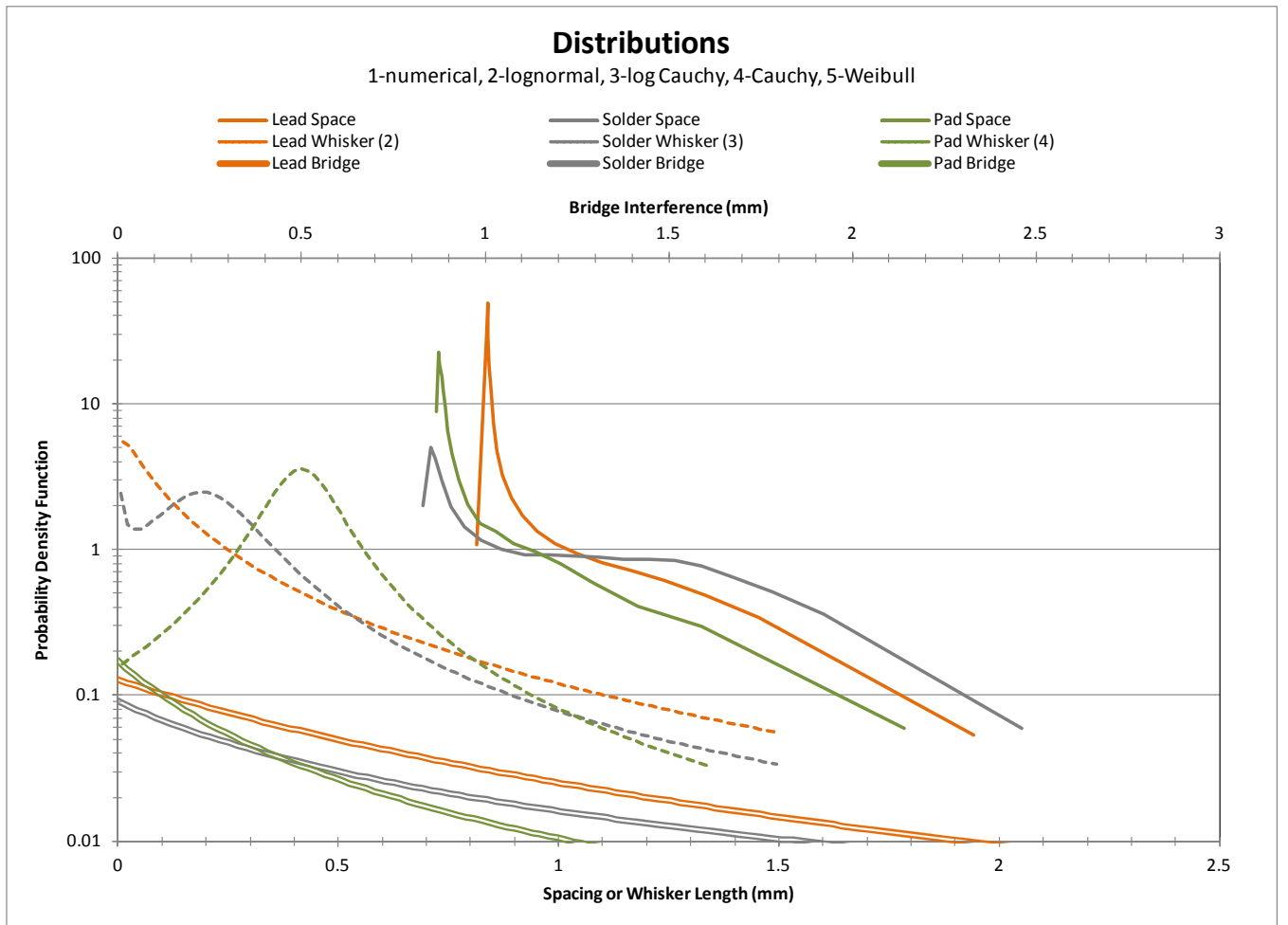


Figure 284: Hypothetical example of lead, solder and pad spacing/whisker length distribution and bridge interference plots.

12.2.10 Bridges per lead pair

Calculation of the overall number of bridges was determined on a part basis by multiplying the whiskerable area by the whisker density to determine the whiskers generated per lead. The whiskers-per-lead value was then multiplied by the whisker view factor and the whisker bridging probability to determine the bridges per lead pair.

12.2.11 Shorts per lead pair

As demonstrated by Courey [98], not all whisker bridges resulted in shorts, so the bridges calculated were multiplied by the shorting probability based on applied voltage from Figure 285. For a five volt bias, the shorting probability is 41.4%. So if 10 bridges are present, four would cause an electrical short circuit.

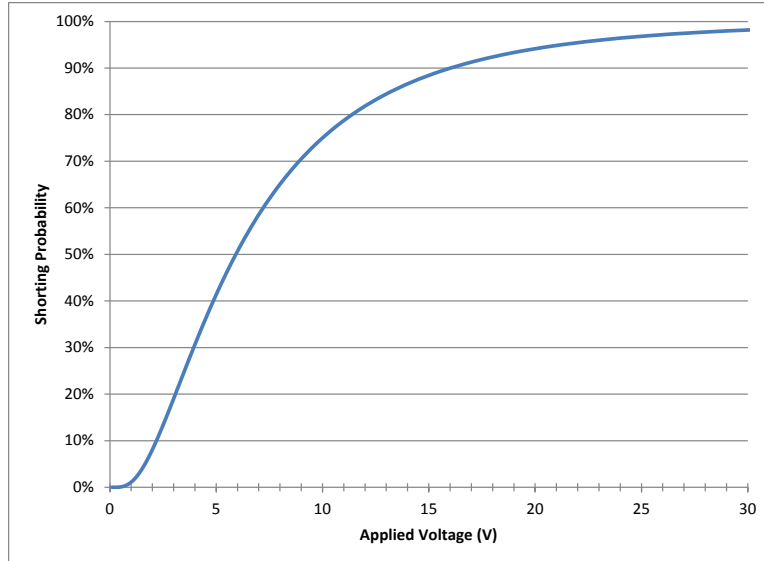


Figure 285: Probability of a bridge shorting (from Courey [98])

12.2.12 Overall roll-up

The shorts per part were determined by multiplying the shorts per lead pair by the number of spaces. The shorts per part was multiplied by the number of parts with the same lead configuration and number of leads and then summed for all of the parts in the assembly.

12.2.13 Whisker risk Spreadsheet

A Microsoft Excel™ spreadsheet has been developed that incorporates the aforementioned calculations, and will be made available at no charge to interested researchers on an as-is basis. This spreadsheet provides for user definition of the following:

- Multiple lead geometries for roll-up calculation (optional)
- Lead geometry
- Lead, solder, and pad whisker length distributions
- Lead, solder, and pad whisker density (whisker/mm²)
- Shorting probability distribution

12.2.14 Gull wing lead modeling

The risk model has been implemented in a spread-sheet to facilitate broad use. The package geometry typically available on the part manufacturers data sheet is inputted and the lead geometry was computed (Figure 286). Typically board pads are designed to be larger than the lead foot. The user inputs the pad creation rules and the pad geometry is determined. The user then can review the geometry computations and can adjust them.

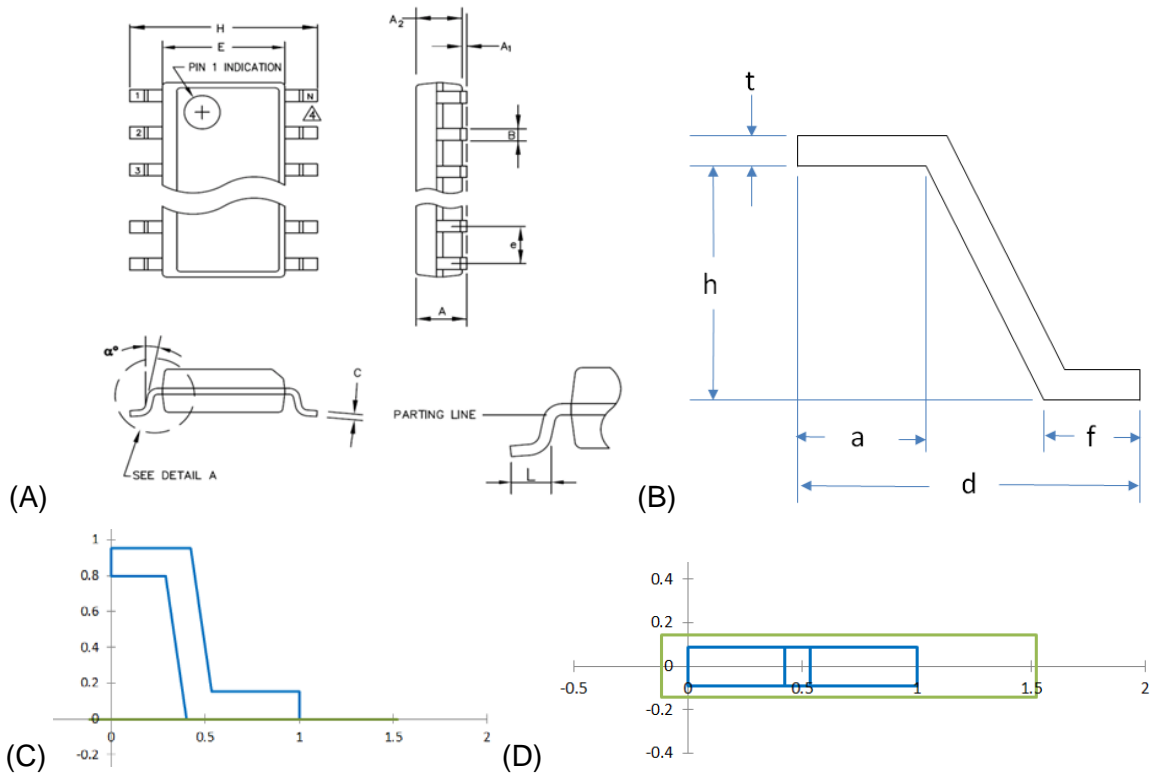


Figure 286: (A) Part drawing nomenclature, (B) lead dimension nomenclature, (C) side view of modeled lead and pad, and (D) top view of modeled lead and pad.

12.2.15 Gull wing lead risk calculation example

Problem statement: Determine the whisker short circuit risk using the HTHH 4,000 h data for a TQFP128 part with tin finished copper leads soldered with SAC305 to immersion tin copper board pads operating at 3.3 V.

Evaluate the following cases:

4. No coating
5. 40 percent effective conformal coating coverage (50 percent side lead coverage, 90 percent front lead coverage and no coating behind the leads or on the pads behind the leads)
6. 40 percent effective conformal coating coverage with added mitigation eliminating the board pad whiskers (e.g. tin-lead board plating with tin-lead solder or sufficiently thick and strong urethane coating coverage).

The TQFP128 is a 0.4 mm has leads on four sides and there are 124 spaces between adjacent leads. The default parameters used for the various geometry calculations and plotting are shown in Table 70. The “Lead Exit Fraction” defines where the lead exits the package. A value of 50% corresponds to a lead exiting the mid-point of package body. The part data sheet dimensions are given in Table 71 and the computed lead dimensions are in Table 72. The calculated distances and area parameters are given in Table 73.

The whisker length and density statistics entered into the spreadsheet for the lead, solder and pad were:

- HTHH 4,000 from Figure 283:
 - Lead: Location-1 $\mu = -2.8988 \ln(\text{mm})$ and $\sigma = 0.1944$, 400 whiskers/mm²
 - Pad: Location-2 (region C) $\mu = -2.9228 \ln(\text{mm})$ and $\sigma = 0.2860$, 400 whiskers/mm²
 - 400 whiskers/mm² was used to represent a moderately high whisker density

Solder: Estimated lognormal distribution for short whiskers: 1.7 percentile length = 1 micron, 99.8 percentile whisker = 25 microns, 10 whiskers/mm².

Note that the lognormal mean, μ (Minitab™ Location parameter), in ln(microns) was converted to ln(millimeters) by subtracting ln(1,000) which is 6.9078. The lognormal shape is dimensionless and requires no conversion. The lead, solder and pad materials spreadsheet inputs are summarized in Table 74 to Table 76.

Table 70: Model default parameters used to determine the simplified lead geometry

PWB = Printed wiring board

PWB Pad Length over Lead Foot Length (mm) =	1.04
PWB Pad Width over Lead Width (mm) =	0.111
Fraction for Minimum Whisker Length =	5.00%
Fraction for Maximum Whisker Length =	90.00%
Use Geometric Mean for Midpoints =	TRUE
Lead Exit Fraction*(%) =	50%
Minimum First Bend Distance* (mm) =	0.1
Pad Spacing Reduction from Solder Bulge (mm) =	0
Relative Height of Bulge (%) =	50%
Rounding Digits for Prompt Display =	4

Table 71: TQFP128 Part Drawing Dimensions (mm).

Part Description (optional, U9(TQFP)):	U9(TQFP)
Package Height (A ₂ , 1.4) =	1.4
Package Seating Plane (A ₁ , 0.1) =	0.1
Lead Span (H, 16) =	16
Body Width (E, 14) =	14
Lead Foot Length (L, 0.6) =	0.6
Lead Thickness (c, 0.1524) =	0.1524
Lead Width (B, 0.18) =	0.18
Lead Pitch (e, 0.4) =	0.4
Lead Angle from Vertical (α , 8) =	8
Number of Leads (128) =	128
Number of Sides with Leads (4) =	4

Table 72: TQFP128 manual over-ride option for lead and board pad dimensions (mm).

Lead Span Length (d, 1) =	
First Bend Distance (a, 0.2876) =	
First Bend Height (h, 0.8) =	
Lead Foot Length (f, 0.6) =	
Lead Thickness (t, 0.1524) =	
Lead Width (0.18) =	
Lead Pitch (0.4) =	
Total Lead Spaces (124) =	
PWB Pad Length (1.64) =	
PWB Pad Width (0.291) =	
PWB Pad Thickness =	0.063
Overall Coating Effectiveness =	0%

Table 73: TQFP128 Calculated parameters

Calculated Parameters:	
Lead Spacing =	0.22
Solder Spacing =	0.109
Pad Spacing =	0.109
Lead Thickness/Spacing (non-dim) =	0.6927
Lead Thickness/Solder Spacing (non-dim) =	1.3982
Lead Thickness/Pad Spacing (non-dim) =	1.3982
Lead View Factor Metric (non-dim) =	0.2971
Solder View Factor Metric (non-dim) =	0.2876
Pad View Factor Metric (non-dim) =	1.7600
Calculated Areas (dim²):	
Whiskerable Lead Area =	0.564815
Whiskerable Solder Area =	0.516046
Whiskerable Pad Area =	0.121653
Single Side Area =	0.351606

Table 74: Lead whisker input sheet

Lead Material/Finish (optional):	Tin over Cu194
Data Reference/Condition (optional):	Loc 1, 4,000 h 85C/85%RH, 400 whiskers/mm ²
Distribution =	2 (1-numerical, 2-lognormal, 3-log Cauchy, 4-Cauchy, 5-Weibull)
Whisker Density =	400
Whiskerable Area =	0.56481482
Total Whiskers Generated =	225.925929
Whisker Bridging Fraction =	0.00%
Whisker View Factor =	0.27539113
Coating Effectiveness =	0%
Total Whiskers Bridging =	8.6633E-10
Data can be entered as long/short whisker length/fraction or with specific distribution parameters	
3-Parameter Lognormal Distribution:	
Fraction for Short Whisker =	
Fraction for Long Whisker =	
Minimum Length =	
Whisker Minimum (0) =	
Whisker μ (location, ln(dim))=	-2.8988
Whisker σ (scale, nondim) =	0.1944

Table 75: Solder whisker input sheet

Solder Material (optional):	SAC305
Data Reference/Condition (optional):	Estimated 4,000 h 85C/85%RH, 1 to 25 microns, 10 whiskers/mm ²
Distribution =	2 (1-numerical, 2-lognormal, 3-log Cauchy, 4-Cauchy, 5-Weibull)
Whisker Density =	10
Whiskerable Area =	0.51604635
Total Whiskers Generated =	5.1604635
Whisker Bridging Fraction =	0.00%
Whisker View Factor =	0.18906768
Coating Effectiveness =	0%
Total Whiskers Bridging =	4.7194E-09
Data can be entered as long/short whisker length/fraction or with specific distribution parameters	
3-Parameter Lognormal Distribution:	
Fraction for Short Whisker =	1.700%
Fraction for Long Whisker =	99.80%
Minimum Length =	0
1.7% length =	0.001
99.8% length =	0.025
Whisker Minimum (0) =	
Whisker μ (location, ln(dim), -5.5424) =	
Whisker σ (scale, nondim, 0.644) =	

Table 76: Pad whisker input sheet

Pad Material/Finish (optional):	Immersion tin over copper
Data Reference/Condition (optional):	Loc 2-at pad, 4,000 h 85C/85%RH, 400 whiskers/mm ²
Distribution =	2
Whisker Density =	400
Whiskerable Area =	0.31735377
Total Whiskers Generated =	126.941507
Whisker Bridging Fraction =	0.21%
Whisker View Factor =	0.31735377
Coating Effectiveness =	0%
Total Whiskers Bridging =	0.08578387
Data can be entered as long/short whisker length/fraction or with specific distribution parameters	
3-Parameter Lognormal Distribution:	
Fraction for Short Whisker =	
Fraction for Long Whisker =	
Minimum Length =	
Whisker Minimum (0) =	
Whisker μ (location, ln(dim))=	-2.9228
Whisker σ (scale, nondim) =	0.286

A summary of the materials (Table 77) and the plot comparing the spacing, whisker length and bridging interference are provided (Figure 287) are obtained from the spread-sheet. The short circuit calculation results for each of the coating cases are given in Table 78 to Table 80 with graphical summary given in Figure 288. The added coating mitigation over the board pad significantly reduced the whisker short circuit risk.

Table 77: TQFP128 material summary.

Lead Material/Finish:	Tin over Cu194
Lead Data/Reference Condition:	Loc 1, 4,000 h 85C/85%RH, 400 whiskers/mm ²
Solder Material/Finish:	SAC305
Solder Data/Reference Condition:	Estimated 4,000 h 85C/85%RH, 1 to 25 microns, 10 whiskers/mm ²
Pad Material/Finish:	Immersion tin over copper
Pad Data/Reference Condition:	Loc 2-at pad, 4,000 h 85C/85%RH, 400 whiskers/mm ²

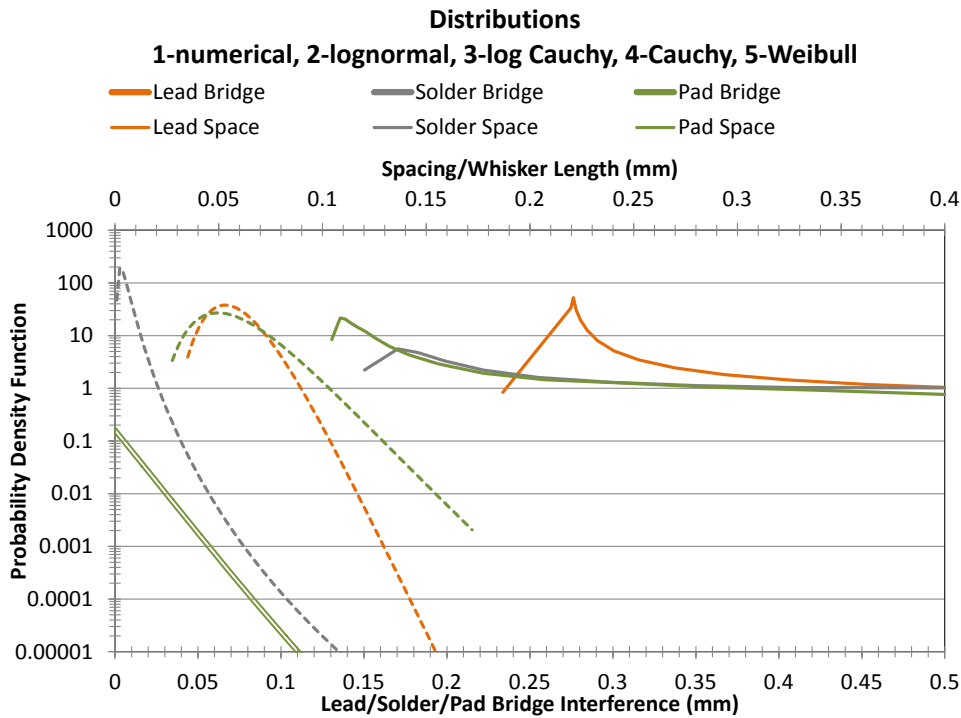


Figure 287: TQFP128 spacing, whisker length and bridging interference plots.

Table 78: Shorting results for TQFP128 with no coating.

WHISKER SHORTING RESULTS:		
Coating Effectiveness =	0	
Total lead spaces =	124	
Applied Voltage =	3.3	V
Shorting Probability =	0.225548	
Whisker Type:	Lead	Solder
Bridges per lead:	8.663E-10	4.719E-09
Bridges per part:	1.074E-07	5.852E-07
Shorts per part:	2.423E-08	1.320E-07
TOTAL SHORTS (this part only) =	2.399	

Table 79: Shorting results for TQFP128 with a 40 percent coating effectiveness.

WHISKER SHORTING RESULTS:		
Coating Effectiveness =	0.4	
Total lead spaces =	124	
Applied Voltage =	3.3	V
Shorting Probability =	0.225548	
Whisker Type:	Lead	Solder
Bridges per lead:	5.198E-10	2.832E-09
Bridges per part:	6.446E-08	3.511E-07
Shorts per part:	1.454E-08	7.920E-08
TOTAL SHORTS (this part only) =	0.864	

Table 80: Shorting results for the TQFP128 with added coating or tin-lead mitigation at the board (board pad whisker density set to zero).

WHISKER SHORTING RESULTS:			
Coating Effectiveness =	0.4		
Total lead spaces =	124		
Applied Voltage =	3.3	V	
Shorting Probability =	0.225548		
Whisker Type:	Lead	Solder	Pad
Bridges per lead:	5.198E-10	2.832E-09	0.0
Bridges per part:	6.446E-08	3.511E-07	0.0
Shorts per part:	1.454E-08	7.920E-08	0.0
TOTAL SHORTS (this part only) =	9.373E-08		

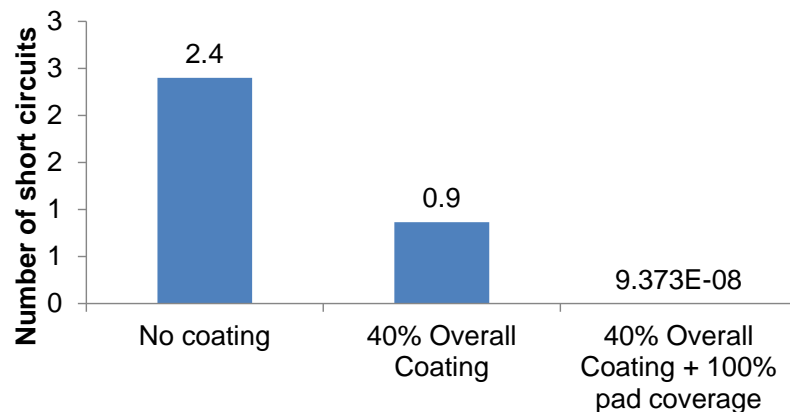


Figure 288: Summary of computed TQFP128 short circuits for three levels of coating mitigation.

12.3 Basic geometry risk modeling

The Monte Carlo whisker risk model was extended to incorporate the following:

- Parallel flat plates
- Parallel round pins
- Perpendicular flat plates

12.3.1 Whisker mirror

The model extensions used both the whisker mirror described in prior work and explicit modeling of the surfaces for the parallel configurations. The perpendicular flat plate model used explicit modeling of both surfaces and did not implement the whisker mirror.

12.3.2 Whisker risk data subset

The general Monte Carlo modeling approach used for developing the gull wing whisker risk model was used to develop generic view factor and relationships for the basic geometries. The generic view factors and spacing distributions used the specific geometries described in Table 81 through Table 83. The spacing and pitch dimension were defined to be:

- Parallel plate – spacing is the spacing between the plates
- Parallel round pins – pitch is distance between centerlines
- Perpendicular plate – spacing (S) is the spacing between the center of the plates (Figure 289)

Monte Carlo modeling was conducted for the listed geometries for uncoated leads only.

Table 81: Dimensions considered for the parallel flat plate model.

Length (mm)	Width (mm)	Spacing (mm)
0.3378	0.127	0.2
0.65	0.127	0.2
0.65	0.127	0.5
1	0.1	0.1
1	0.1	0.2
1	0.2	0.1
1	0.2	0.2
2	0.1	0.1
2	0.1	0.2
2	0.2	0.1
2	0.2	0.2
0.5	0.1	0.1
0.5	0.1	0.2
0.5	0.2	0.1
0.5	0.2	0.2
0.0635	0.14986	0.33
0.6812	0.14986	0.33
0.6812	0.14986	0.7366

Table 82: Dimensions considered for the parallel round lead model.

Length (mm)	Diam. (mm)	Pitch (mm)
0.3378	0.127	0.8
0.65	0.127	0.8
0.65	0.127	0.8
1	0.1	1
1	0.1	2
1	0.2	1
1	0.2	2
2	0.1	1
2	0.1	2
2	0.2	1
2	0.2	2
0.5	0.1	1
0.5	0.1	2
0.5	0.2	1
0.5	0.2	2
0.0635	0.14986	1.27
0.6812	0.14986	1.27
0.6812	0.14986	1.27

Table 83: Dimensions considered for the perpendicular flat plate model.

Length (L, mm)	Width (W, mm)	Spacing (S, mm)
0.3378	0.127	0.804546
0.65	0.127	1.025305
0.65	0.127	1.025305
1	0.1	1.414214
1	0.1	2.12132
1	0.2	1.414214
1	0.2	2.12132
2	0.1	2.12132
2	0.1	2.828427
2	0.2	2.12132
2	0.2	2.828427
0.5	0.1	1.06066
0.5	0.1	1.767767
0.5	0.2	1.06066
0.5	0.2	1.767767
0.0635	0.14986	0.942927
0.6812	0.14986	1.379707

Length (L, mm)	Width (W, mm)	Spacing (S, mm)
0.6812	0.14986	1.379707
0.3378	0.127	0.380282
0.65	0.127	0.601041
0.65	0.127	0.813173
1	0.1	0.777817
1	0.1	0.848528
1	0.2	0.777817
1	0.2	0.848528
2	0.1	1.484924
2	0.1	1.555635
2	0.2	1.484924
2	0.2	1.555635
0.5	0.1	0.424264
0.5	0.1	0.494975
0.5	0.2	0.424264
0.5	0.2	0.494975
0.0635	0.14986	0.278247
0.6812	0.14986	0.715026
0.6812	0.14986	1.002536

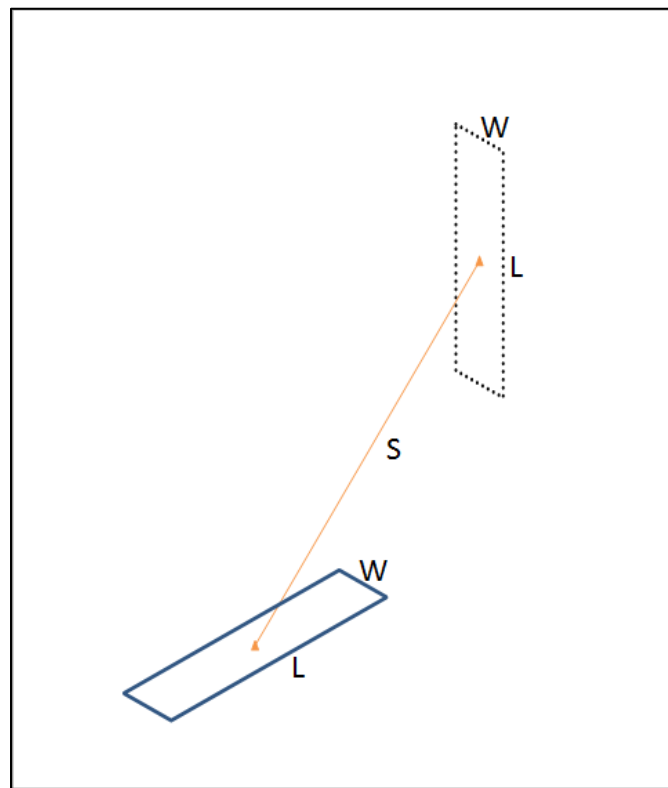


Figure 289: Perpendicular plate spacing.

12.3.3 Basic geometry model development

Development of the basic geometry model was based on developing whisker view factor and spacing distribution based on lead and pad dimensions. All calculations were based on the use of dimensionless parameters to avoid complications in the basic geometry model due to selection of units.

12.3.3.1 Whisker shape factor

The whisker shape factor represents the probability that an infinite whisker will bridge between adjacent leads. A trial and error method in conjunction with the Excel solver was used to develop a metric that has best correlation to whisker shape factor based on dimensional calculations easily derived from part/pad data.

12.3.3.1.1 Lead whisker parallel plates and pins

The shape factor for parallel plates and pins is based on the same metric (ML) as used in the prior work with the understanding that the single side area (A_s) is the projected area along the pitch axis (for plates $A_w=A_s$) and the lead thickness is the plate width or pin diameter:

s = Lead Spacing

t = Lead Thickness

A_w = Whiskerable Area

A_s = Single Side Area

$$M_L = \left(\frac{A_s}{A_w + s^2} \right)^{1.421215} \cdot \left(\frac{t}{s} \right)^{1.153123}$$

A plot providing the modeled shape factor as a function of the above metric and the derived equation is provided in Figure 290.

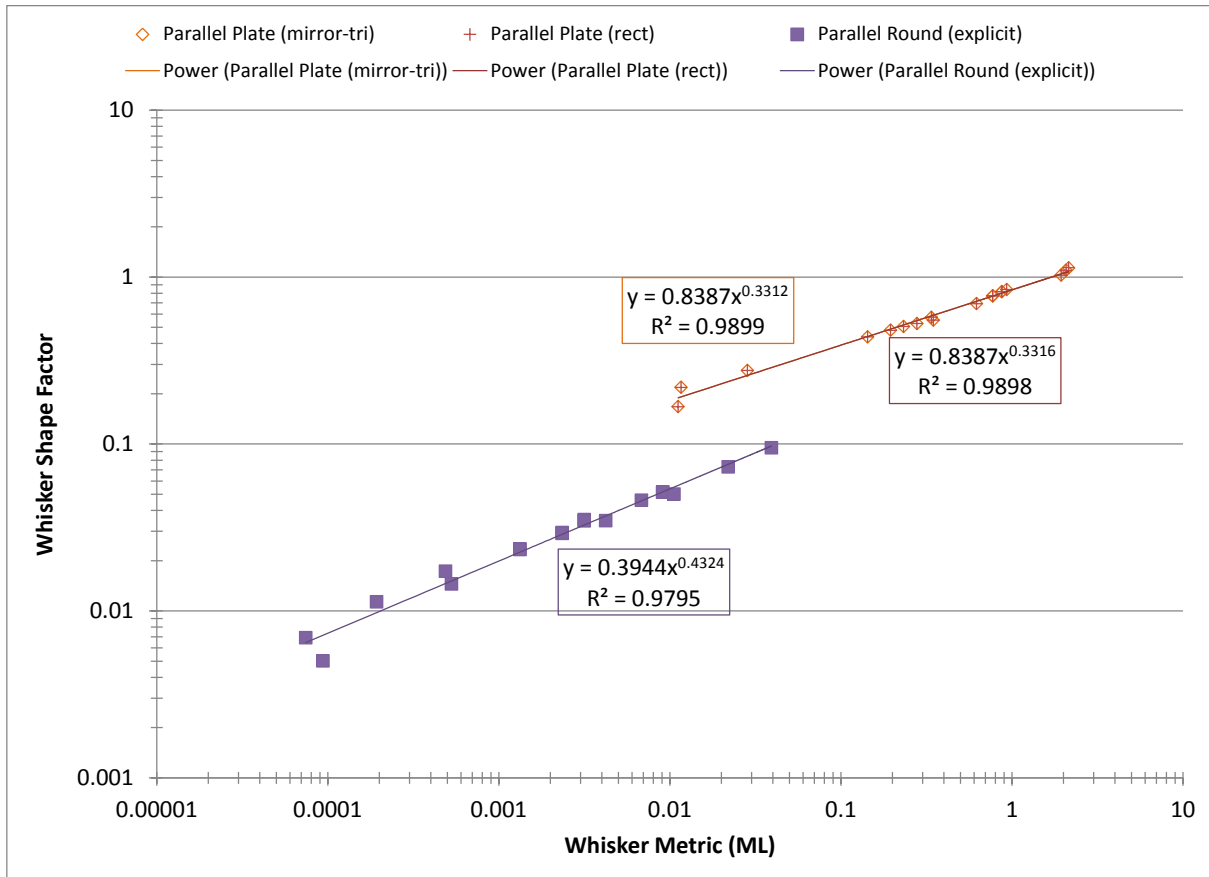


Figure 290: Parallel plate and round lead shape factor correlation.

12.3.3.2 Spacing distribution

The spacing distribution provides a cumulative fraction versus length between the minimum and maximum spacing. Development of an appropriate distribution requires calculation of the minimum and maximum spacing and the appropriate intermediate fractions.

12.3.3.2.1 Minimum spacing

The minimum spacing is determined by the specific geometry as follows:

- Parallel flat plates – the spacing between the plates
- Round leads – the pitch minus the lead diameter
- Perpendicular plates – the center spacing minus the lead length divided by the square root of 2

12.3.3.2.2 Maximum spacing

The maximum lead spacing is determined by the specific geometry as the extreme distance between the far corners of the geometry as follows:

- Parallel flat plates – square root of sum of squares of plate width, length, and spacing
- Round leads – square root of sum of squares of lead diameter, lead length, and pitch
- Perpendicular plates – use the following equation:

$$s_{\max} = \sqrt{\frac{l^2}{2} + \sqrt{2 \cdot l \cdot s + s^2 + w^2}}$$

l = Length
 w = Width
 s = Spacing

12.3.3.3 Distribution development

12.3.3.3.1 0%, 95%, and 100% Distribution points

Because of the controlled nature of the parallel and perpendicular geometries, the 0% distribution point is the minimum spacing and the 100% point is the maximum spacing. The intermediate points are based on the 95% point as calculated by a linear best fit based on the length, width, and minimum and maximum spacing. Specific coefficients for the 95% length prediction are shown in Table 84. Correlation between the Monte Carlo spacing and predicted are shown in Figure 291.

Table 84: Coefficients for Length, Width, and Max./Min. Spacing for 95% Spacing

	Length	Width	Spacing	
			Min.	Max.
Parallel Flat Plates	0.387985	0.457803	1.144546	-0.35014
Perpendicular Flat Plates	-0.33047	-0.202	0.034695	0.999461
Parallel Round Leads	0.017016	0.635506	0.037845	0.364181

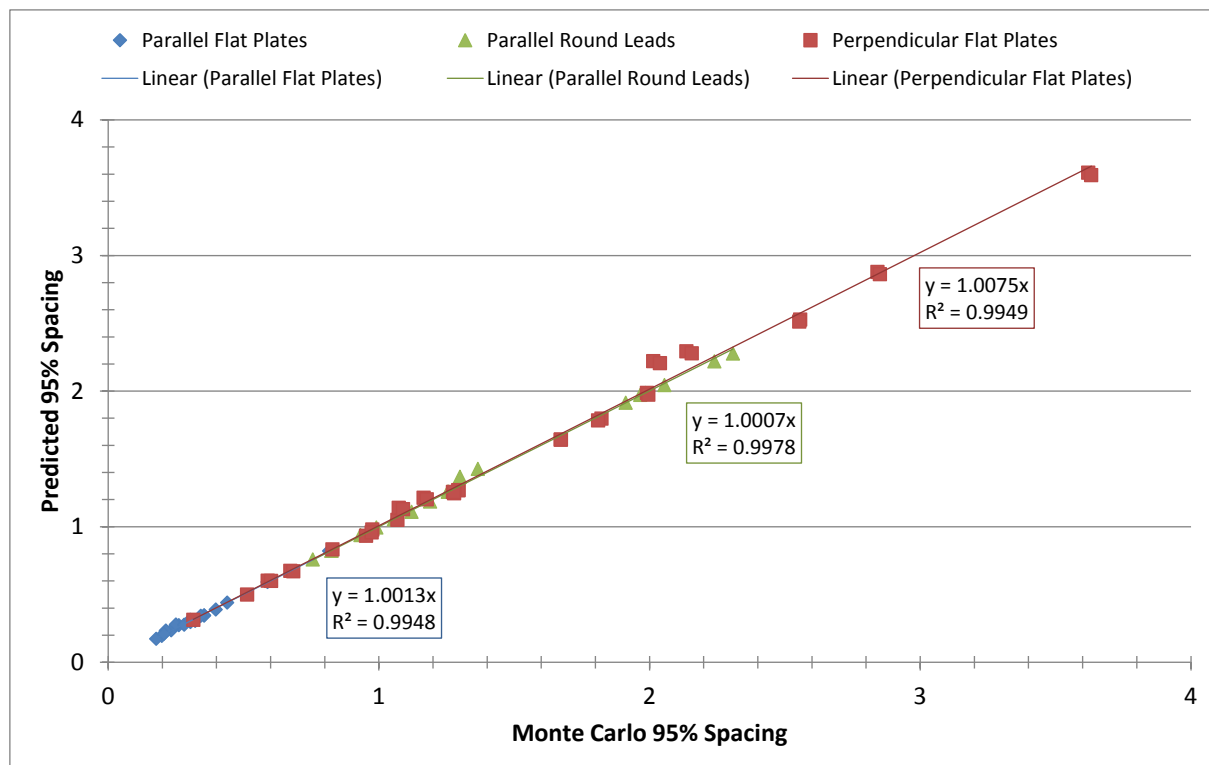


Figure 291: Correlation for 95% spacing prediction

12.3.3.3.2 Intermediate distribution points

The distributions were developed based on a non-dimensional distribution by subtracting the minimum spacing from the spacing values, dividing this value by the difference between 95% spacing point and the minimum spacing as follows (Note: this is a different approach from that used in the gull wing model.)

$$S = \frac{(s_i - s_{\min})}{(s_{95\%} - s_{\min})}$$

S = Non-Dimensional Spacing

s_i = Spacing of Point (from Monte Carlo)

$s_{95\%}$ = 95% Spacing (see text)

s_{\min} = Minimum Spacing

This produces a value of zero at 0% and nominally one at 95%. Plotting the results as a function of cumulative spacing fraction produces reasonably consistent results as shown in Figure 292 through Figure 294.

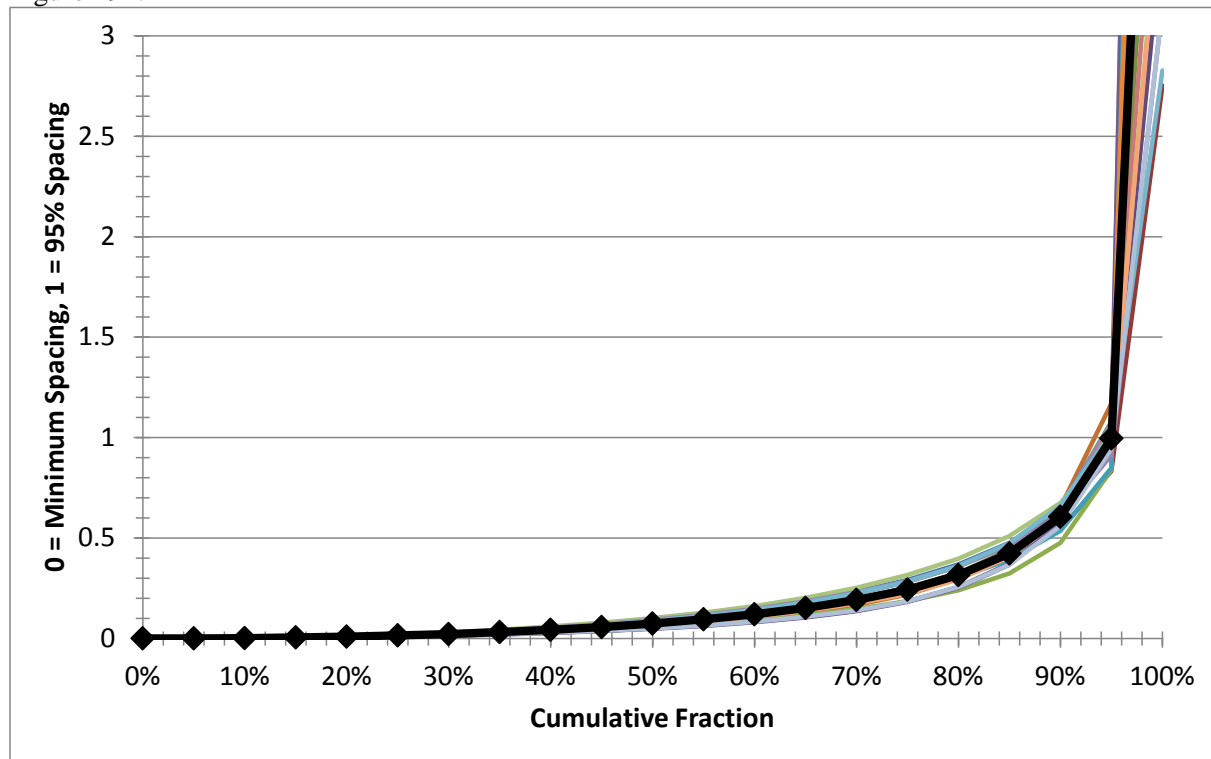


Figure 292: Non-dimensional spacing distribution for parallel flat plates.

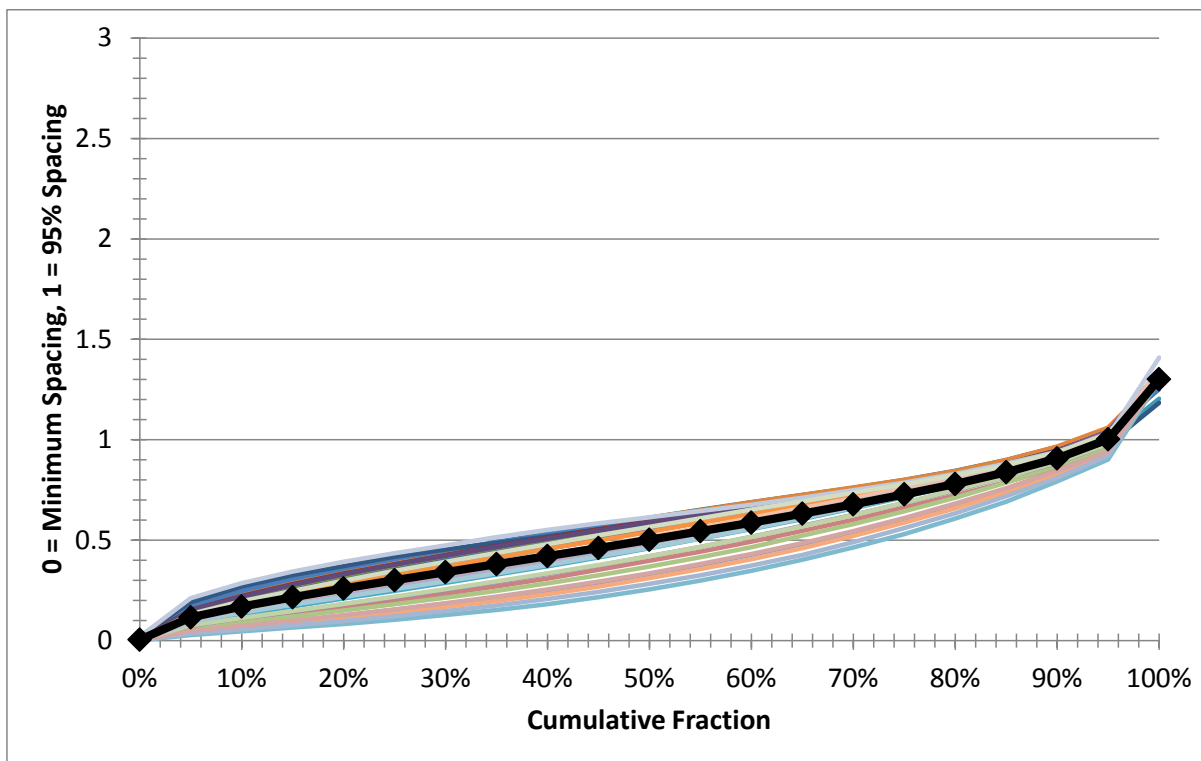


Figure 293: Non-dimensional spacing distribution for perpendicular flat plates.

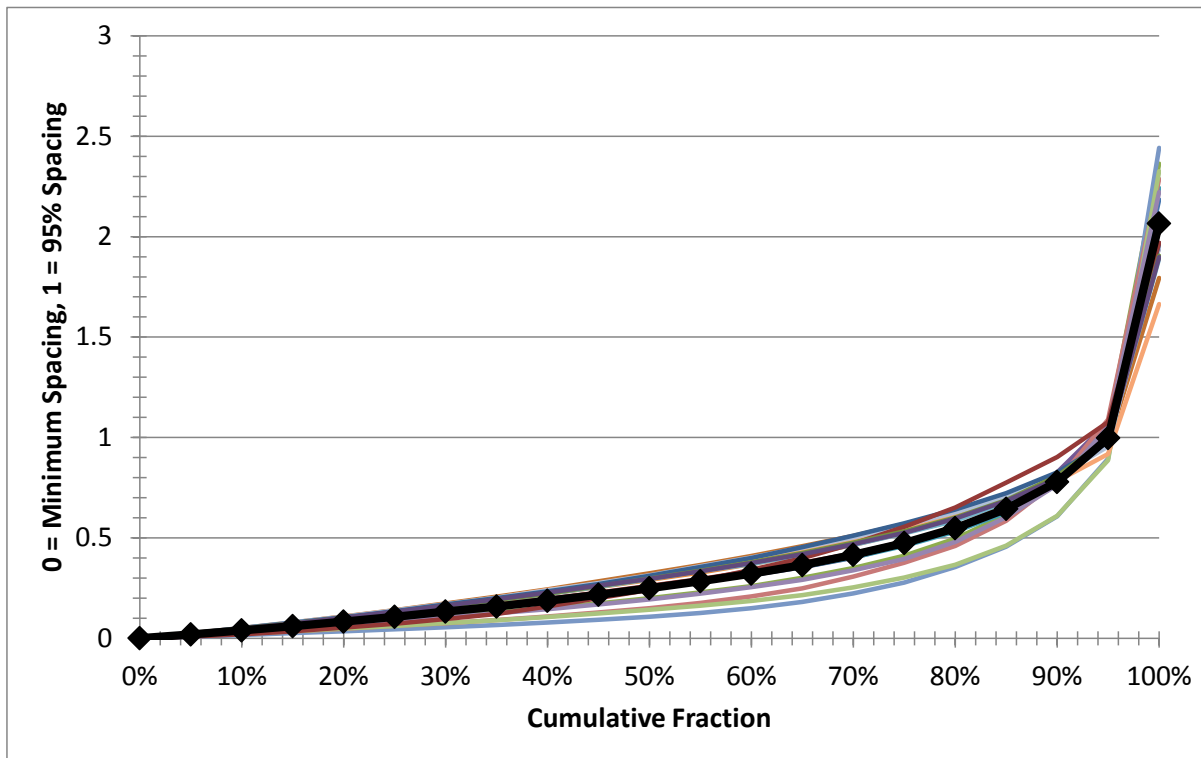


Figure 294: Non-dimensional spacing distribution for parallel round leads.

Specific non-dimensional distribution values for each type of scenario are summarized in Table 85. These values are used in conjunction with the appropriate minimum, 95%, and maximum spacings to extract the specific length as a function of cumulative fraction.

Table 85: Non-dimensional whisker distribution

(0 = minimum spacing, 1 = 95% spacing)

Cumulative	Parallel Plate	Perpendicular Plate	Parallel Round Lead
0%	0.0000	0.0000	0.0000
5%	0.0005	0.1151	0.0188
10%	0.0022	0.1694	0.0391
15%	0.0051	0.2162	0.0606
20%	0.0093	0.2593	0.0831
25%	0.0150	0.3006	0.1072
30%	0.0224	0.3410	0.1326
35%	0.0317	0.3807	0.1585
40%	0.0432	0.4206	0.1871
45%	0.0572	0.4610	0.2172
50%	0.0743	0.5024	0.2490
55%	0.0950	0.5444	0.2840
60%	0.1204	0.5876	0.3220
65%	0.1519	0.6324	0.3650
70%	0.1916	0.6789	0.4155
75%	0.2434	0.7279	0.4748
80%	0.3154	0.7800	0.5483
85%	0.4234	0.8385	0.6449
90%	0.6056	0.9078	0.7786
95%	1.0000	1.0000	1.0000
100%	Use maximum from text		

12.3.4 Special case of parallel large and small plates

A closed form solution for round plate with an infinitesimal source was used to develop an approximate view factor and distribution relationship for parallel large and small rectangular plates with only one plate generating whiskers. The radius for the large plate was approximated based on the same area as the rectangular target plate. Development of the analytical solution and inspection of Monte Carlo results leads to the preliminary hypothesis that whiskering between two unequal areas is reciprocal in that the number of whiskers making contact does not depend on which area generates the whiskers. It also follows that the distribution fractions will be identical for whiskers sourced from either plate. Using the geometry shown in Figure 295, the following view factor relationship was developed:

View Factor - Point to Large Circular Plate

$$F_V = \frac{s}{\pi^2} \cdot \int_0^r \left[\frac{2 \cdot \pi \cdot \rho}{(\rho^2 + s^2) \cdot \rho} \right] d\rho$$

r = Radius of Plate
 s = Spacing
 F_V = View Factor

$$F_V = \frac{2 \cdot \text{atan}\left(\frac{r}{s}\right)}{\pi}$$

Equating Areas

$$\pi \cdot r^2 = l_s \cdot w_s$$

$$r = \sqrt{\frac{l \cdot w}{\pi}}$$

l = Length of Target Plate
 w = Width of Target Plate

$$F_V = \frac{2 \cdot \text{atan}\left(\frac{\sqrt{l \cdot w}}{\sqrt{\pi \cdot s}}\right)}{\pi}$$

For Whiskers Sourced at the Large Plate and Hitting Small Plate:

$$F_{VL} = F_V \cdot \frac{A_S}{A_L}$$

A_S = Area of Small Plate
 A_L = Area of Large Plate
 F_{VL} = View Factor for Whiskers Originating
 at Large Plate

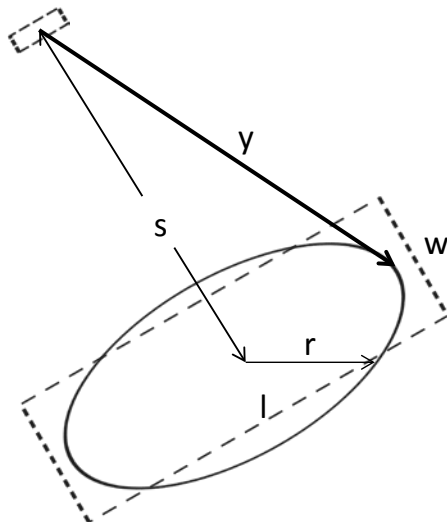


Figure 295: Small and large plate approximation.

Table 86: Comparison of approximate (closed-form) and Monte Carlo view factor

Configuration	Plate Length	Plate Width	Target Spacing	Target Length	Target Width	View Factor		
						Equation	Monte Carlo	Error
Plate to QFP lead + solder (0.5mm space)	9	7	0.5	1.6	1	0.0236	0.0236	-0.01%
Plate to 0603 lead + solder (0.5mm space)	9	7	0.5	1	0.75	0.0111	0.0110	0.15%
Plate to QFP lead + solder (1mm space)	9	7	1	1.6	1	0.0218	0.0217	0.76%
Plate to 0603 lead + solder (1mm space)	9	7	1	1	0.75	0.0102	0.0102	0.61%
Plate to QFP lead + solder (2mm space)	9	7	2	1.6	1	0.0186	0.0184	1.05%
Plate to 0603 lead + solder (2mm space)	9	7	2	1	0.75	0.0087	0.0086	1.51%
Plate to QFP lead + solder (4mm space)	9	7	4	1.6	1	0.0136	0.0133	2.25%
Plate to 0603 lead + solder (4mm space)	9	7	4	1	0.75	0.0064	0.0063	1.07%

The above relationships provide good agreement with the Monte Carlo results (Table 86). The view factor relationships can be used to develop the spacing distribution relationship, as follows:

Cumulative Spacing Distribution Fraction

$$F_S = \frac{F_r}{F_v}$$

$$r = \sqrt{y^2 - s^2}$$

$$F_S = \frac{\operatorname{atan}\left(\frac{\sqrt{y^2 - s^2}}{s}\right)}{\operatorname{atan}\left(\frac{\sqrt{1-w}}{\sqrt{\pi} \cdot s}\right)}$$

F_r = View Factor at Radius r

y = Whisker Length

F_S = Whisker Cumulative Fraction

Comparison of the approximate and Monte Carlo distribution factors are shown in Figure 296 and Figure 297. Divergence between the approximate and Monte Carlo models at 100% is due to the difference between the maximum from the use of the circle approximation and the actual maximum. Use of the approximate relationship is conservative since the 100% point represents a shorter length, a less conservative but valid approach would be to use the actual calculated maximum based on the geometry.

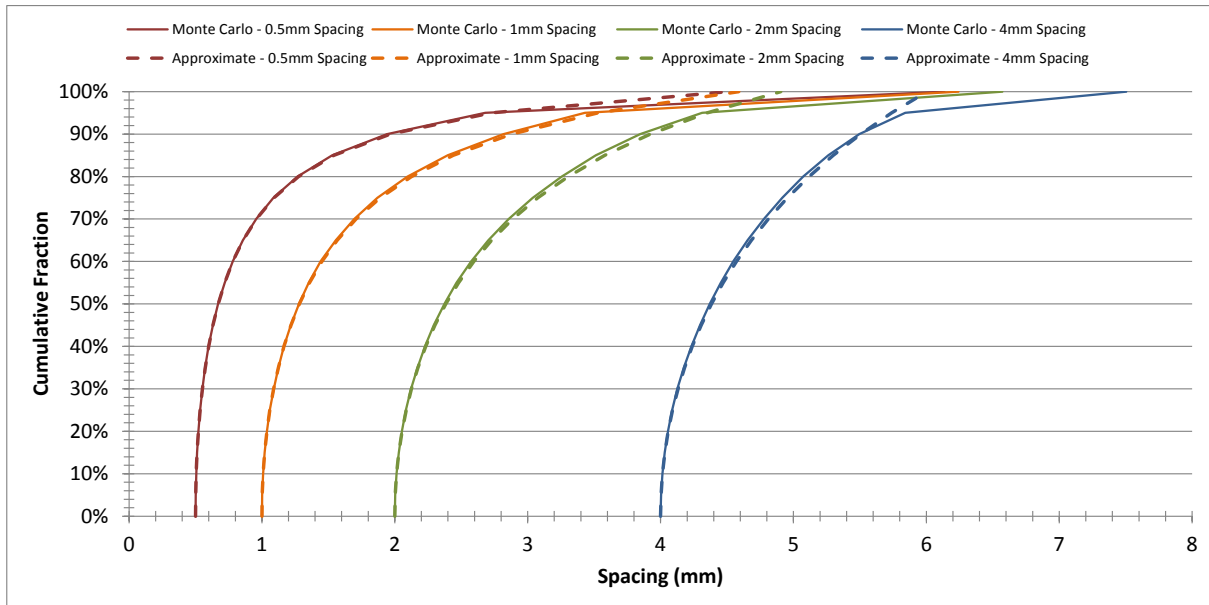


Figure 296: Comparison of whisker length distributions for plate to QFP lead and solder.

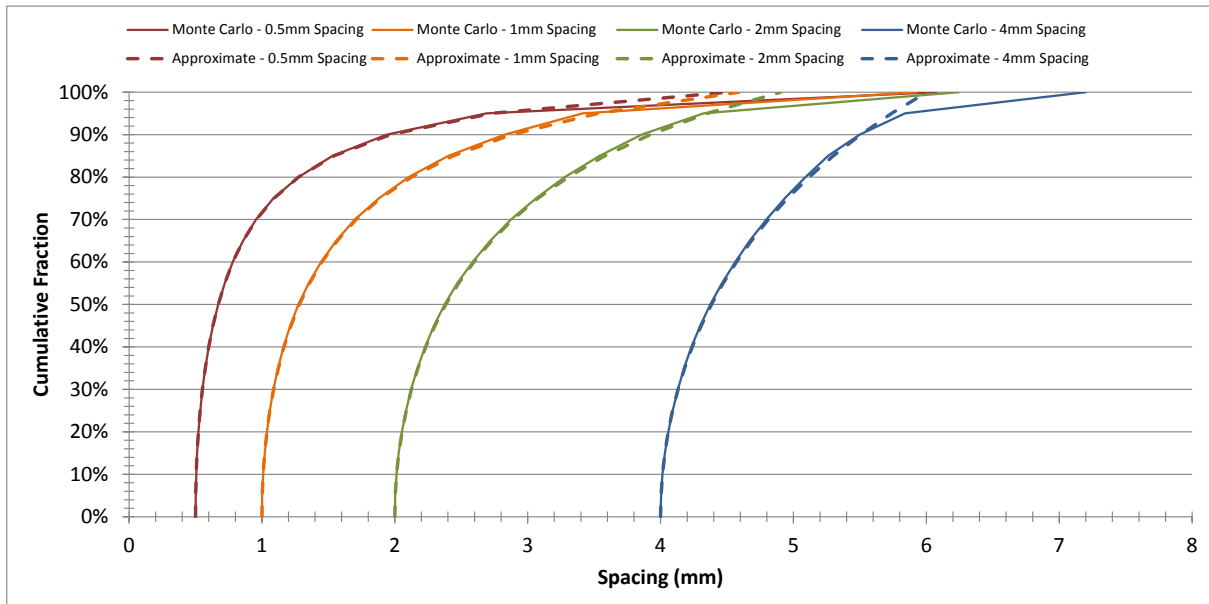


Figure 297: Comparison of whisker length distribution for plate to 0603 terminal and solder.

12.3.5 Basic geometry whisker risk model spreadsheet snapshot

The information that follows describes general operation of the spreadsheet.

12.3.5.1 General information

Green highlighted cells are for normal user input, blue highlighted cells are for default values that can but normally do not need to be changed. Values in red font are not recommended to change. There is no system of units but all units need to be consistent including part and pad dimensions and whisker

length distributions. Calculated values are shown in a blue font. Rows and columns not necessary for use of the spreadsheet are hidden. There are eight tabs included in the spreadsheet:

- User Notes
- Roll Up
- Model
- Whisker
- Distribution Plots
- Shorting Prob.
- Revision Info.
- Reference Data

12.3.5.2 User Notes tab

The *User Notes* tab provides a location to input general user notes. These notes are not used in the calculations.

12.3.5.3 Roll Up tab

The *Roll Up* tab (Figure 298) allows for input of varying dimensions and model cases and calculates the total number of shorts. To use the roll up capability, blank out cells with a red border on the Model tab, the first row of data (red border) is then used for calculations in the Model tab.

Description	Instances	Number of 2 perpendicular, 1 round, 4 large (mm)	Case Description	Length	Dia./Width	Pitch/Spacing	Shorts per Instance		Total Shorts
							Small Width (case 4 only)	Small length (case 4 only)	
Case 1	5	1	Equal Parallel Plates	9	7	1		0.000643	0.000642899
Case 2	1	2	Equal Perpendicular Plates	8	5	10		0.569932	0.56993227
Case 3	1	3	Parallel Round Leads	0.65	0.127	0.5		31.95309	30.9530688
Case 4	1	4	Large & Small Parallel Plates	9	7	0.5	1.6	1	
									OVERALL TOTAL SHORTS = 3,147

Figure 298: *Roll Up* tab

12.3.5.4 Model tab

The *Model* tab (Figure 299) provides the definition of the geometry, applied voltage, and the results.

12.3.5.5 Data entry

If dimensions have been entered roll up above, specific lead dimensions are calculated and provided with a default value (in parentheses). The specific data to be entered is as follows:

- Description (optional, Case 4)
- Case Code (4)
- Length (9)

- Width (7)
- Spacing (0.5)
- Smaller Length (1.6) – unequal plate model only (case 4)
- Smaller Width (1) – unequal plate model only (case 4)

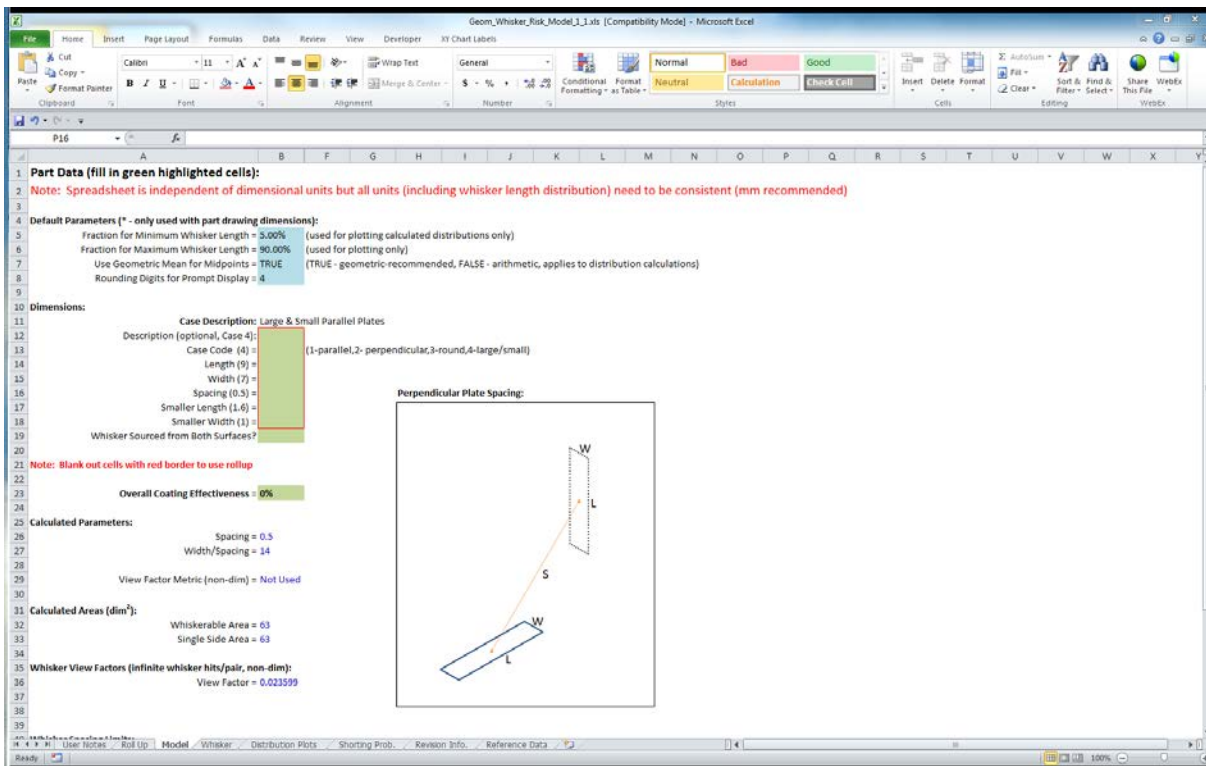


Figure 299: Upper portion of *Model* tab.

12.3.5.6 Other defining information

In addition to the dimensional information described above, an option that applies for only case 4 (unequal parallel plates) is provided that allows whiskers to be sourced from one or both surfaces. The default is TRUE indicating whiskers can originate at either of the unequal surfaces, change this to FALSE for whiskers originating at only one surface. For other cases, whiskers can always originate at both surfaces. The coating effectiveness represents the fraction of the target lead covered with conformal coating.

12.3.5.7 Applied voltage and final results

The applied voltage and results are located at the lower portion of the *Model* tab. The applied voltage is used in conjunction with the appropriate shorting probability to determine the number of bridges that result in shorts. The result, expressed as the total number of shorts for the part, is highlighted in light red (Figure 300).

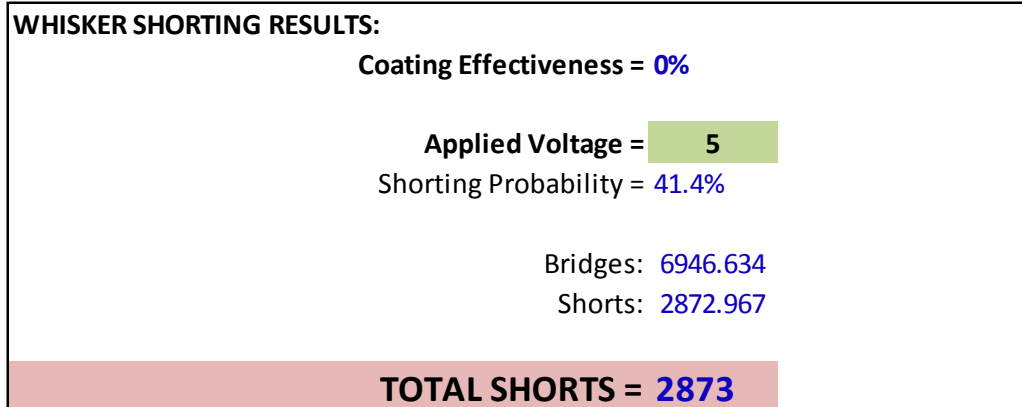


Figure 300: Lower portion of *Model* tab.

12.3.5.8 Default parameters

The default parameters are highlighted in blue (Figure 12) and may not need to be changed by the user except with a change in the system of units. Specific parameters that can be set are:

- Fraction for Minimum Whisker Length – this value is used for plotting calculated distributions
- Fraction for Maximum Whisker Length – this value is used to limit the numerical whisker length for plotting
- Use Geometric Mean for Midpoints – TRUE – use geometric mean for distribution calculations (recommended), FALSE – use arithmetic mean
- Rounding Digits for Prompt Display – sets how many digits are displayed in prompts with values

12.3.5.9 Whisker tab

The *Whisker* tab (Figure 301) defines the appropriate whisker length distribution and density to be applied to the appropriate spacing distributions. The whisker density is defined on this tab (cell B6) based on the number of whiskers generated per square unit (based on square of units used in the rest of the spreadsheet, so if mm used it is per mm^2). Cell B4 is a cell used to select the distribution type for each tab (1-numerical, 2-lognormal, 3-log Cauchy, 4-Cauchy, 5-Weibull).

12.3.5.9.1 Calculated distributions

The calculated distributions are selected by values of 2 through 5 in cell B4. The following parameters need to be supplied to define the distribution:

- Fraction for Short Whisker
- Fraction for Long Whisker
- Minimum Length (if applicable)
- Short% length
- Long% length

The distribution parameters are calculated based on lengths for user-defined short and long cumulative fractions. If the specific model parameters are known, they can be entered in cells B22 through B24 instead of calculating from the cumulative percentages.

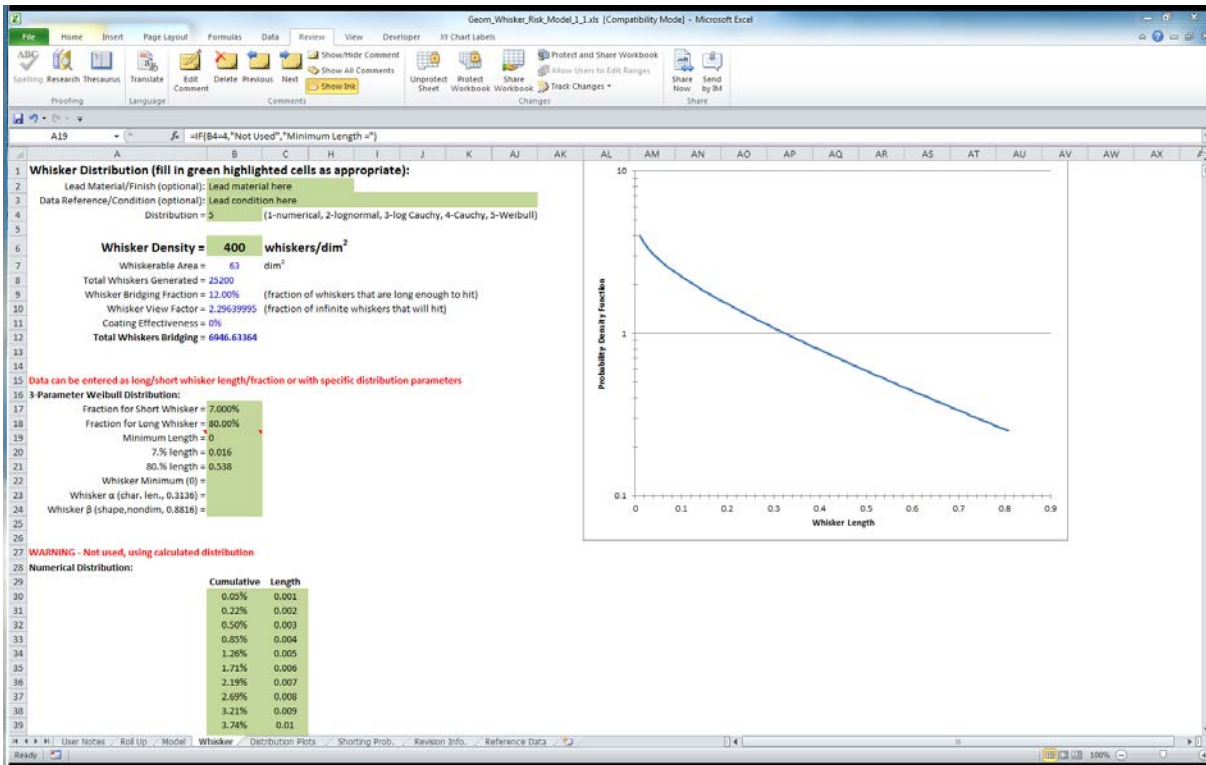


Figure 301: Whisker tab

12.3.5.9.2 Numerical distribution

The numerical distribution is selected by entering 1 in cell B4. The numerical distribution consists of an ordered list of cumulative percentages and corresponding whisker lengths (Figure 302) for up to 100 data points. Start data entry in cells B30 and C30 and fill in as many data points as needed, clear the remaining cells beyond those needed to define the distribution. Warnings will be generated if the minimum length is less than the minimum whisker spacing or if the maximum length is insufficient to calculate the bridging probability. It should be noted that the minimum/maximun lengths are the average of the first/last two lengths in the table. A warning will also be generated above the numerical distribution if a lognormal distribution is selected. Units for length column need to be in units consistent with the rest of the spreadsheet.

	A	B	C	H	I
26	Numerical Distribution:	Cumulative	Length		
27		1.70%	0.01		
28		19.99%	0.03		
29		40.23%	0.05		
30		55.73%	0.07		
31		66.88%	0.09		
32		74.87%	0.11		
33		80.64%	0.13		
34		88.04%	0.17		
35		92.26%	0.21		
36		94.80%	0.25		
37		96.40%	0.29		
38		97.44%	0.33		
39		98.13%	0.37		
40		98.62%	0.41		
41		98.96%	0.45		
42		99.20%	0.49		
43		99.38%	0.53		
44		99.51%	0.57		
45		99.61%	0.61		
46		99.69%	0.65		
47		99.75%	0.69		
48		99.80%	0.73		
49		99.93%	0.95		
50		99.97%	1.17		
51		99.99%	1.39		
52		99.99%	1.61		
53		100.00%	1.83		
54		100.00%	2.05		
55		100.00%	2.27		
56		100.00%	2.49		
57		100.00%	2.71		
58		100.00%	2.93		
59		100.00%	3.15		
60		100.00%	3.37		
61		100.00%	3.59		
62		100.00%	3.92		
63		100.00%	4.14		
64		100.00%	4.36		
65		100.00%	4.58		
66		100.00%	4.8		
67		100.00%	5.02		
68		100.00%	5.24		
69		100.00%	5.46		
70		100.00%	5.68		
71		100.00%	5.68		

Figure 302: Numerical whisker length distribution

12.3.5.10 *Distribution Plots* tab

The *Distribution Plots* tab (Figure 303) has no inputs but provides the following probability density plots:

- Spacing distributions as calculated by the spreadsheet (solid lines)
- Lead whisker length distributions as defined by the whisker length definition tab (dashed lines)
- Solder bridging probability density as calculated by the spreadsheet (double solid lines)

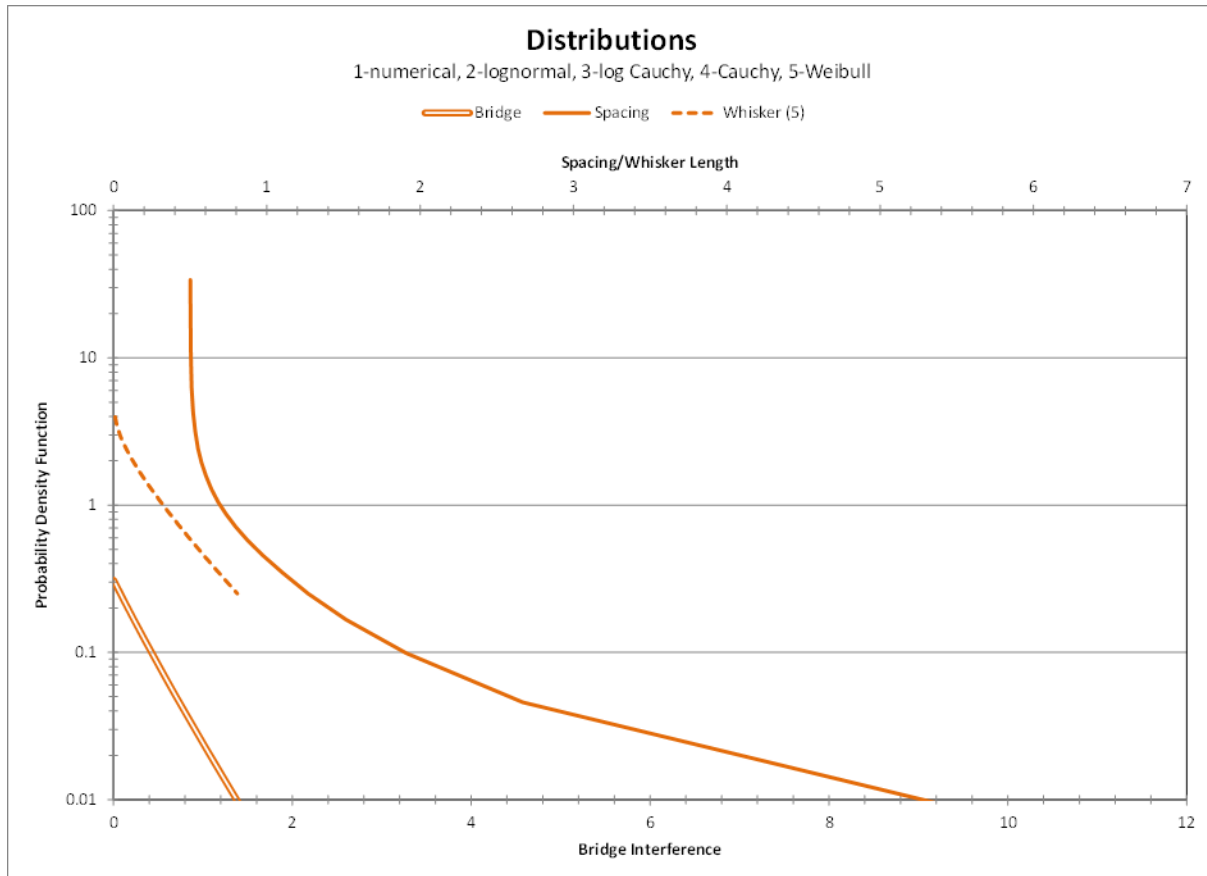


Figure 303: Distribution plots

12.3.5.11 Shorting Probability tab

The *Shorting Probability* tab (Figure 304) establishes the probability that a bridged whisker would result in a short at a given voltage using a lognormal distribution. The tab has inputs for the lognormal parameters to establish the shorting distribution with initial data based on published results from Courey [98].

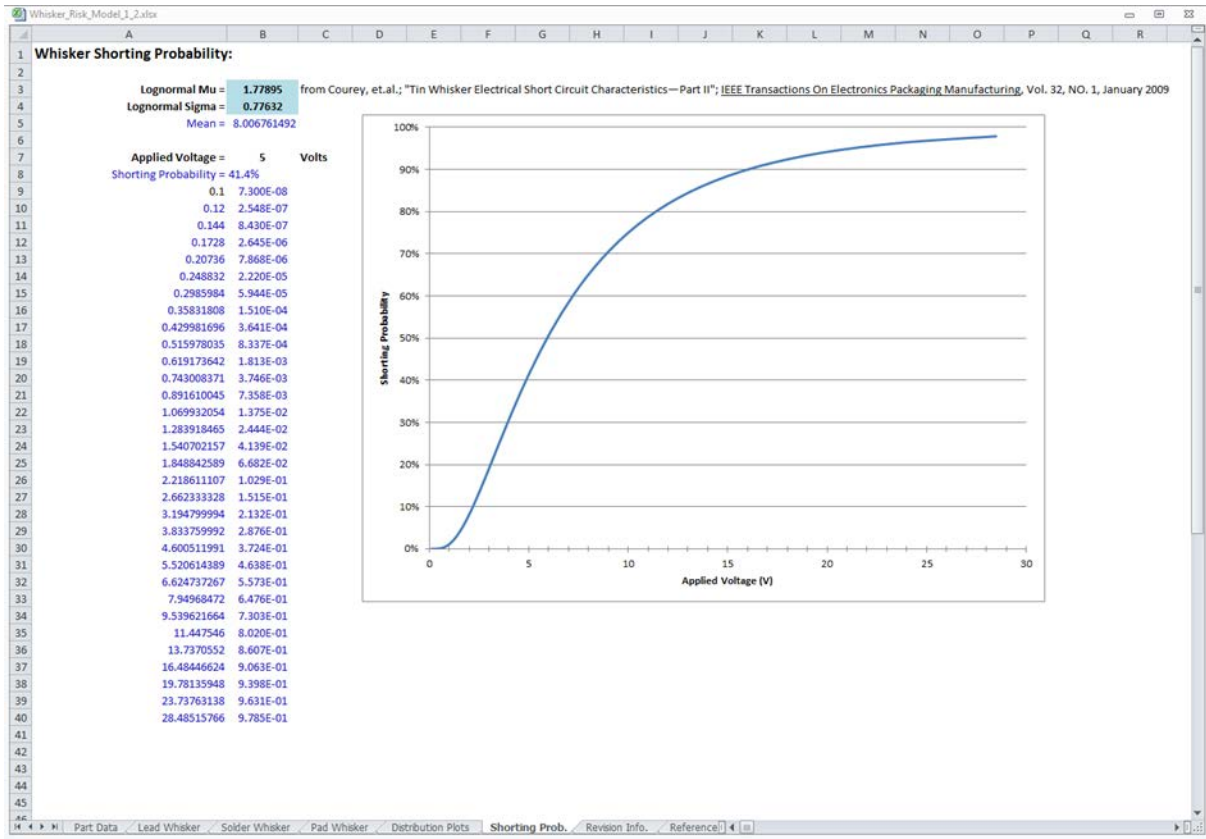


Figure 304: Shorting probability tab

12.3.5.12 Revision Info. tab

The *Revision Info.* tab provides a log of changes to the whisker risk spreadsheet with revision number and date.

12.3.5.13 Reference Data tab

The *Reference Data* tab provides a summary of the specific cases used to establish the whisker modeling correlations. Dimensions are as shown in Table 81 through Table 83 and are included in the spreadsheet for completeness. Caution should be used for cases that represent significant extrapolation from listed component types.

12.4 Whisker modeling assumptions

- Uniform whisker generation occurs over the entire lead, solder, or pad surface
- Lead geometry simplifications into multiple rectangular and triangular segments are valid
 - Solder wicks partially up the lead
- The distribution of the whisker angle from the vertical is uniform from perpendicular to parallel to the surface
- Whisker to whisker interaction from opposing surfaces would not result in a short circuit
- A partially conformal coated lead has 90 percent coverage on the outer surface of the lead/solder, 50 percent coverage on the side and zero percent coverage on the back
 - The conformal coating was assumed only to have an influence on the target area by limiting the area that the whisker can make electrical contact with

- A conservative assumption was made that the coating on the source side does not reduce the whisker generation
- Only short circuit conditions were considered
 - Degradation to high frequency circuits by antenna effects of whiskers were not evaluated
 - Whiskers greater than 40 microns long can impact circuits with frequencies above 6 GHz [99]
 - Fusing open of a whisker when the circuit current flow exceeds the whisker conduction capability was not considered
 - Metal vapor arcing was not considered

12.5 Discussion of assumptions

Uniform whisker generation on solder surface

The experimental results have shown that the whisker growth location on the solder was not uniform but is dependent upon lead material, environment and solder thickness. This requires a refinement in the model. In the case of alloy-42 leads during thermal cycling, the whiskers grew in the solder near the lead to solder interface (Figure 305). A whisker density of 1,580 whiskers/mm² was obtained for solder over the pad edge (Table 39) while the majority of the remaining solder fillet exhibited little or no whisker growth.

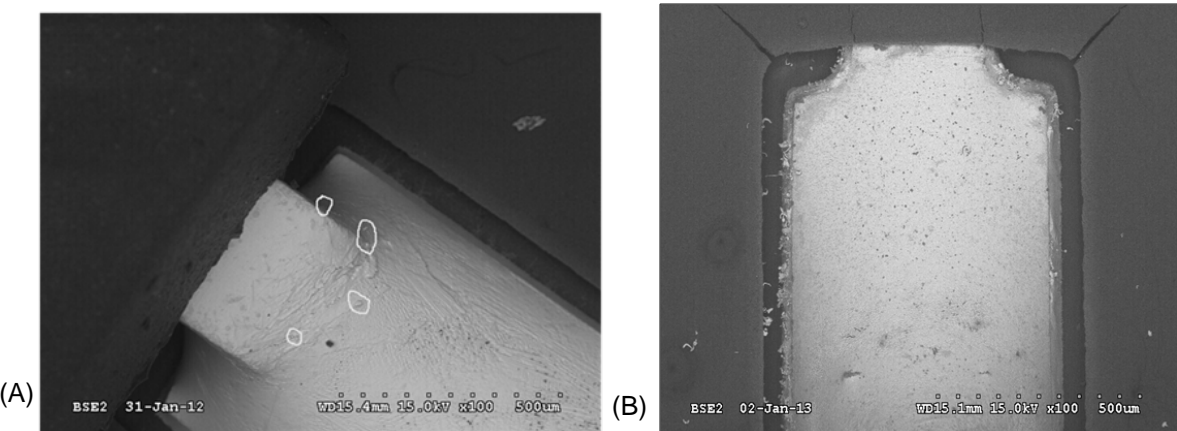


Figure 305: Location of whisker growth from SAC305 solder; (A) whiskers growing from the region where the lead exits the solder joint on a SOT alloy-42 lead after simulated power cycling thermal cycling from +50 to 85 °C and (B) whiskers growing from the edge of the board pad where solder has flowed around the edge on a SOT5 C194 lead at a 0-0 contamination level after 4,000 h of exposure to high temperature high humidity at 85°C/85%RH.

Lead geometry simplification: Solder and board fabrication variation decreasing gap spacing

In addition to the solder bulge factor included in the model, further reductions in gap spacing can occur. The J-STD-001 Class 3 manufacturing standards permit the leads to be able to shift off the pads 25 percent of the lead width. This is a heritage practical allowance to accommodate some of the part misalignment and bent leads without a substantial reduction in solder fatigue. However, the lead shift can result in a significant reduction in the gap spacing important for tin whisker risk analysis. The lead

width for the TQFP was measured to be 169 microns (Note: the part drawing permits 130 to 190 micron base metal width leads). Thus, a 25 percent overhang would potentially reduce the clearance by another 42 microns.

Given the fact that tin whisker risk assessment was dependent upon gap spacing, it is important that the assembly drawing design documentation defines the minimum acceptable clearances with whisker growth tolerance in mind.

Whisker angle

The main issue with the concept of whisker growth angle as it pertained to the whisker short circuit model was that it has recently been observed that whiskers can rotate as they grow and also move due to airflow. In-situ measurements by CALCE [100], Sandia [36] and others have revealed that changes in growth direction occur with time. In the presence of air currents, the whiskers can move as well. For example in air direct cooled equipment, the whiskers can move due to cooling air flow. Shorter whiskers are less prone to movement than longer whiskers. The whisker-to-whisker interaction likelihood will increase with whisker movement.

Whisker-to-whisker interaction

The present model does not include the possibility of whiskers from opposite surfaces making contact and shorting. This premise was supported in part by the insulating nature of the oxides on the whisker [101] and the relatively low whisker densities that have been observed in the past. In instances where the whisker density approaches the level observed on the edges of the board pads during the high temperature/high humidity exposure, this may no longer be a valid assumption. Whisker-to-whisker interaction would mean that the “effective” dielectric gap spacing between conductors was essentially reduced to half. The model could be updated to provide a first order assessment of this condition by assuming that whiskers that traverse half the distance to the adjacent conductor would have the potential to form a short circuit.

Conformal coat mitigation

Since it has been observed that whiskers can break through and penetrate most conformal coatings [80], the present model makes the conservative assumption that there is no difference in whisker generation (length and density) between coated and non-coated surfaces. A preliminary assessment of conformal coated SOTs in the present test showed that the coating did inhibit whisker growth but also underwent significant cracking. The whisker length inputs to the model can be updated to accommodate a change to the coated source whisker growth characteristics as data becomes available.

12.6 Summary

The modeling effort has highlighted some manufacturing parameters that influence the conductor-to-conductor spacing that are important for whisker risk management. Generally, the closer the gap spacing is, the greater the shorting risk between conductors. There are manufacturing processes both during bare board fabrication and soldering that influence effective gap spacing. Conformal coating and tin-lead solder dipping the parts with the smallest gap spacing significantly reduces shorting risk.

13. Transfer of knowledge

13.1 Presentations and papers

Since 2010, the principal investigators have published four journal articles and over 40 papers and presentations describing the tin whisker testing and modeling work. A key focus has been briefing the IPC Association Connecting Electronics Industries Association's Pb-free electronics risk management (IPC-PERM) council tasked with writing standards governing the use of lead-free electronic materials in aerospace and defense applications.

13.2 SAC solder whisker growth in IPC-PERM GEIA-STD-0005-2

Dr. Snugovsky wrote an appendix section titled "*Long Sn Whiskers in Pb-free Solder*", which was included in *GEIA-STD-0005-2 Rev A Standard for Mitigating the Effects of Tin Whiskers in Aerospace and High Performance Electronic Systems*, May 2012. This appendix included a discussion of the SERDP WP-1753 results on whisker growth on Sn-Ag-Cu solder with ionic contamination and on Sn-Ag-Cu alloys with additions of rare earth elements (REE) such as Ce, La, Er, and Y.

13.3 REE element specification in IPC J-STD-006

The SERDP WP-1753 testing has shown high tin whisker growth can occur when rare earth element (REE) is added to lead-free Sn1.0Ag0.5Cu (wt%) (SAC105) alloys. Even with concentrations as small as 0.01 wt% Ce, the SAC105 solder can grow whiskers. Dr. Snugovsky and Dr. Meschter are working with the leadership of the IPC-PERM council to modify *IPC/JEDEC J-STD-006 Requirements for Electronic Grade Solder Alloys and Fluxed and Non-Fluxed Solid Solders for Electronic Soldering Applications* to include a designation such that users know if rare earth element additions have been made to the solder.

14. Literature cited

Note bolded references are publications that resulted from the WP1753 research.

- [1] The Lead-free Electronics Manhattan Project Reports, Completed under U.S. Government Contract No. N00014-08-D-0758, The Benchmarking and Best Practices Center of Excellence at ACI Technologies, Inc., Philadelphia, PA, Phase 1: July, 30 2009 and Phase 2: February 10, 2010. Available for download at the Defense Acquisition University Lead-free Website (<https://acc.dau.mil/leadfree>).
- [2] GEIA-STD-0005-2, Standard for Mitigating the Effects of Tin Whiskers in Aerospace and High Performance Electronic Systems, ITAA, Washington DC, 2012.
- [3] G.T. Galyon, Annotated Tin Whisker Bibliography and Anthology, IEEE Trans. Packag. Manuf. Vol. 28, No. 1, January 2005, pp. 94-122.
- [4] G.T. Galyon and L. Palmer, An Integrated Theory of Whisker Formation: The Physical Metallurgy of Whisker Formation and the Role of Internal Stresses, IEEE Trans. Packag. Manuf. Vol 28, No. 1, January 2005, pp. 17-30.
- [5] M. Dittes, P. Oberndorff, and L. Petit, Proceedings of Electronic Components and Technology Conference, New Orleans, LA, 2003, p. 822.
- [6] R. Schetty, IEEE International Conference on the Business of Electronic Product Reliability and Liability, 2004.
- [7] M. Dittes, P. Oberndorff, P. Crema, and V. Schroeder, Proceedings of Electronic Packaging Technology Conference (Singapore, 2003), pp. 183.
- [8] J. Brusse, G. Ewell, and J. Siplon, Tin Whiskers: Attributes and Mitigation, Capacitor and Resistor Technology Symposium (CARTS), March 25-29, 2002, pp. 68-80.
- [9] J.W. Osenbach, R.L. Shook, B.T. Vaccaro, B.D. Potteiger, A.N. Amin, K.N. Hooghan, P. Suratkar, and P. Ruengsinsub, Sn Whiskers: Material, Design, Processing, and Post-Plate Reflow Effects and Development of an overall Phenomenological Theory, IEEE Trans. on Electronic Packag. Manuf. 28, 36, 2005.
- [10] P. Snugovsky, Z. Bagheri, M. Romansky, Whisker Growth on SAC Solder Joints: Microstructure Analysis, SMTA International Conference on Soldering and Reliability, Toronto, Ontario, Canada May 14-15, 2008.
- [11] Munson, T. "SAC Whiskers? Metal whiskers are not a new problem. But finding them in new places can be." Circuit Assembly, June 2007, pp. 58-59.
- [12] D. Hillman, The Role of Ionic Contamination as a Tin Whisker Initiator, IPC/SMTA Cleaning & Conformal Coating Conference, 2010.
- [13] J. W. Osenbach, J. M. DeLucca, B. D. Potteiger, A. Amin, R. L. Shook, and F. A. Baiocchi, Sn Corrosion and Its Influence on Whisker Growth, IEEE Trans. Electronics Packaging Manufacturing Vol. 30, 2007, pp. 23.
- [14] A. Baated, K.S. Kim, K. Suganuma, S. Huang, B. Jurcik, S. Nozawa, and M. Ueshima, The Effects of Reflow Atmosphere and Flux on Tin Whisker Growth of Sn-Ag-Cu Solder, Journal of Materials Science: Materials in Electronics; Oct 2010, Vol. 21 Issue 10, p1066.
- [15] O. Kurtz, J. Barthelmes, and K. Martin, Anti-Corrosion Solution for Reduction and Prevention of Corrosion Whiskers, Proceedings of the SMTA International Conference, 2008.

- [16] K. Sweatman, J. Masuda, T. Nozu, M. Koshi, and T. Nishimura, Proceedings of IPC Printed Circuits Expo, APEX Conference, Las Vegas, 2009.
- [17] J-STD-001 Requirements for Soldered Electrical and Electronic Assemblies, Joint JEDEC Solid State Technology Association/IPC Association Connecting Electronics Industries document, April 2010.
- [18] P. Snugovsky, S. Meschter, Z. Bagheri, E. Kosiba, M. Romansky, and J. Kennedy, Whisker Formation Induced by Component and Assembly Ionic Contamination, Journal of Electronic Materials, February 2012, Volume 41, Issue 2, pp 204-223 available for download at <http://link.springer.com/content/pdf/10.1007%2Fs11664-011-1808-5.pdf>**
- [19] D. Perovic, L. Snugovsky, J. Rutter, P. Snugovsky, Z. Bagheri, and S. Meschter, Microstructure and Whisker Growth of SAC Solder Alloys with Rear Earth Additions in Different Environments, SMTA International Conference on Soldering and Reliability, Toronto, Ontario, Canada May 2011.**
- [20] P. Snugovsky, Z. Bagheri, S. Meschter, D. Perovic, L. Snugovsky, and J. Rutter, Microstructure Formation and Whisker Growth in SAC105 Solder Joints with Rare Earth Elements, TMS 2011 Annual Meeting, San Diego, CA February 27 - March 03, 2011,**
- [21] P.T. Vianco, and J.A. Rejent, "Dynamic Recrystallization (DRX) as the Mechanism for Sn Whisker Development Part I: A Model", Journal of Electronic Materials, Volume 38, Number 9, pp. 1815-1825, September 2009.
- [22] P.T. Vianco, and J.A. Rejent, Dynamic Recrystallization (DRX) as the Mechanism for Sn Whisker Development. Part II: Experimental Study, Journal of Electronic Materials, Volume 38, Number 9, pp 1826-1837, September 2009.
- [23] JESD201A, Environmental Acceptance Requirements for Tin Whisker Susceptibility of Tin and Tin Alloy Surface Finishes, JEDEC Solid State Technology Association, Arlington, VA, September 2008.
- [24] JESD22-A121A, Test Method for Measuring Whisker Growth on Tin and Tin Alloy Surface Finishes, JEDEC Solid State Technology Association, Arlington, VA, July 2008.
- [25] A. Baate, K-S. Kim, K. Suganuma, S. Huang, B. Jurcik, S. Nozawa, and B. Stone, Effects of Reflow Atmosphere and Flux on Sn Whisker Growth of Sn-Ag-Cu Solders, Proc. SMTA International 2009.
- [26] M. Ueshima, The Influence of the Flux and Circumstance to Whisker Growth at the Solder Fillet, CALCE 3rd International Symposium on Tin Whiskers, University of Maryland Center for Advanced Life Cycle Engineering, 2009.
- [27] K. Sweatman, J. Masuda, T. Nozu, M. Koshi, and T. Nishimura, Corrosion Driven Whisker Growth in SAC305, SMTA Pan Pacific Symposium Conference Proceedings January 2010.
- [28] E. R. Crandall, G. T. Flowers, P. Lall, and M. J. Bozack, Whisker Growth Under Controlled Humidity Exposure, IEEE 57th Holm Conference on Electrical Contacts (Holm), 2011.
- [29] S. Meschter, P. Snugovsky, J. Kennedy, Z. Bagheri, and E. Kosiba, Tin Whisker Testing: Low Stress Conditions, International Conference on Solder Reliability, Toronto, Ontario, Canada, May 14-17, 2012.**
- [30] S. Meschter, P. Snugovsky, J. Kennedy, Z. Bagheri, and E. Kosiba, Strategic Environmental Research and Development Program (SERDP) Tin Whisker Testing and Modeling: Thermal Cycling Testing, International Conference on Solder Reliability, Toronto, Ontario, Canada ; May 13-15, 2014.**

- [31] S. Meschter, P. Snugovsky, J. Kennedy, Z. Bagheri, E. Kosiba, and A. Delhaise, SERDP Tin Whisker Testing and Modeling: High Temperature/High Humidity Conditions, SMTA International Conference on Soldering and Reliability Toronto, Ontario, Canada; May 14-17, 2013.
- [32] S. Meschter, P. Snugovsky, J. Kennedy, Z. Bagheri, and E. Kosiba, Strategic Environmental Research and Development Program (SERDP) Tin Whisker Testing and Modeling: Long Term Low Temperature High Humidity Testing, International Conference on Soldering and Reliability Toronto, Ontario, Canada, May 19-21, 2015.
- [33] S. Meschter, P. Snugovsky, Z. Bagheri, E. Kosiba, M. Romansky, J. Kennedy, L. Snugovsky, and D. Perovic, Whisker Formation on SAC305 Soldered Assemblies, *J. of Metals*, DOI: 10.1007/s11837-014-1183-9 available on line, Vol. 66, No. 11, November 2014, pp. 2320-2333.
- [34] M. Ueshima, The influence of the flux and circumstance to whisker growth at the solder fillet, CALCE 3rd International Symposium on Tin Whiskers, University of Maryland Center for Advanced Life Cycle Engineering, 2009.
- [35] P. Sarobol, J. E. Blendell, C. A. Handwerker, W.-H. Chen, J.P. Koppes, A. E. Pedigo, Y. Wang, and P. Su, Tin whisker and hillock growth via grain boundary sliding coupled with shear induced grain boundary migration, CALCE 6th International Symposium on Tin Whiskers, University of Maryland Center for Advanced Life Cycle Engineering, 2012.
- [36] D. F. Susan, J. R. Michael, W. G. Yelton, B. B. McKenzie, R. P. Grant, J. Pillars, and M. A. Rodriguez, Understanding and Predicting Metallic Whisker Growth and its Effects on Reliability: LDRD Final Report, SANDIA REPORT SAND2012-0519 Sandia National Laboratories Albuquerque, New Mexico, January 2012 <http://prod.sandia.gov/techlib/access-control.cgi/2012/120519.pdf>.
- [37] P. Oberndorff, M. Dittes, P. Crema, P. Su, and E. Yu, Humidity Effects on Sn Whisker Formation, *IEEE Trans. Electronics Packaging Manufacturing* Vol. 29, 2006, pp. 239.
- [38] V. G. Karpov, Electrostatic Theory of Metal Whiskers, *Physical Review Applied*, DOI: 10.1103/PhysRevApplied.1.044001, 2014
- [39] V. G. Karpov, 9th CALCE International Symposium on Tin Whiskers, IPC Europe Forum Innovation for Reliability, Essen Germany, October 13-15, 2015
- [40] E. Chason, F. Pei, N. Jadhav, Driving forces and mechanisms for Sn whisker nucleation and growth, *Prog. Surf. Sci.* 88 (2013) 103-131 presented at the 17th AIA-PERM meeting in Woburn, MA June 2013.
- [41] P. Su, J. Howell, and S. Chopin, A Statistical Study of Sn Whisker Population and Growth during Elevated Temperature and Humidity Tests, *IEEE Transactions on Electronics Packaging Manufacturing*, Vol. 29, No. 4, October 2006, pp. 246-251
- [42] C Handwerker, J. Blendell, Y. Wang, W-H. Chen, P. Sarobol, J. Koppes, Pedigo, B-Gil. Yoo, B. Phillipi, O. Kraft, G. Dehm, M. Williams, D. Chatain, and S. Curriotto, Stress Relaxation in Tin Films: Whisker Nucleation and Growth, High Density Packaging Users Group (HDPUG) Whisker Webinar, October 29, 2015.
- [43] J. Cheng, P. Vianco, and J.C.M. Li1, Hollow tin/chromium whiskers, *Applied Physics Letters* 96, 184102 doi: 10.1063/1.3419837, 2010.
- [44] T-H. Chuang and S.-F. Yen, Abnormal Growth of Tin Whiskers in a Sn₃Ag0.5Cu0.5Ce Solder Ball Grid Array Package, *Journal of Electronic Materials*, Vol. 35, No. 8, 2006, pp. 1621-1627.

- [45] Chuang, T-H et al., Oxidation-Induced Whisker Growth on the Surface of Sn-6.6(La, Ce) Alloy, Journal of Electronic Materials, Vol. 36, No. 12, 2007, pp.1697-1702.
- [46] Liu, M. and A. Ping, Sn Whisker Growth on the Surface of Sn-0.7Cu Pb-Free Solder with a Rare Earth (Nd) Addition, Journal of Electronic Materials, Vol. 38, No. 11, 2009.
- [47] Dudek, M.A. and N. Chawla, Oxidation Behavior of Rare-Earth-Containing Pb-Free Solders, of Electronic Materials, Vol. 38, No. 2, 2009, pp. 210-220.
- [48] IPC-JSTD-001E Subcommittee Task Team 5-22ARR, Conformal Coating Material and Application “State of the Industry” Assessment, 2015.
- [49] S. Meschter, J. Cho, S. Maganty, D. Starkey, M. Gomez, D. Edwards, A. Ekin, K. Elskens, J. Keeping, P. Snugovsky, E. Kosiba, Z. Bagheri, and J. Kennedy, Strategic Environmental Research and Development Program (SERDP) Nanoparticle Enhanced Conformal Coating for Whisker Mitigation, Proceedings of SMTA International, Rosemont, IL, September 28-October 2, 2014.
- [50] Project WP2213, Strategic Environmental Research and Development Programs (SERDP), US Department of Defense, Environmental Protection Agency and Department of Energy, 2012.
- [51] D. Hillman, R. Wilcoxon, N. Lower, and D. Grossman, Tin Whiskers Inorganic Coatings Evaluation (TWICE), SERDP Project WP-2212 Final Report, Strategic Environmental Research and Development Programs (SERDP), US Department of Defense, Environmental Protection Agency and Department of Energy, January 2015.
- [52] S. Han, M. Osterman, S. Meschter and M. Pecht, Evaluation of Effectiveness of Conformal Coatings as Tin Whisker Mitigation, Journal of Electronic Materials, DOI: 10.1007/s11664-012-2179-2, 6 July, 2012.
- [53] K.N. Tu, Interdiffusion and reaction in bimetallic Cu-Sn thin films, Acta Metallurgica, Volume 21, Issue 4, April 1973, Pages 347-354
- [54] N. Jadhav, E. Buchovecky, L. Reinbold, S. Kumar, A. Bower, and E. Chason, Understanding the Correlation Between Intermetallic Growth, Stress Evolution, and Sn Whisker Nucleation, IEEE Trans on Electronics Packaging Manufacturing, Volume: 33, Issue: 3, 2010, pp 183 – 192.
- [55] N. Jadhav, E. Buchovecky, E. Chason, and A. Bower, Real-time SEM/FIB Studies of Whisker Growth and Surface Modification, Journal of Metals, July 2010, pp. 30-37.
- [56] T. Woodrow, Tracer Diffusion in Whisker-Prone Tin Platings, Proceedings Surface Mount Technologies Association International Conference (SMTAI) Sept. 2006
- [57] S. Meschter, S. McKeown, P. Snugovsky, J. Kennedy, E. Kosiba, Tin Whisker Testing and Risk Modeling Project, SMTA Journal Vol. 24, Issue 3, 2011 pp. 23-31**
- [58] S. McKeown, S. Meschter, P. Snugovsky, J. Kennedy, SERDP Tin Whisker Testing and Modeling: Simplified Whisker Risk Model Development, International Conference on Soldering and Reliability Toronto, Ontario, Canada; May 13-15, 2014**
- [59] J. Brusse, Tin Whisker Observations on Pure Tin-Plated Ceramic Chip Capacitors, AESF SUR/FIN 2002, June 24 - 27, Electronics Finishing II Session sponsored by the American Electroplaters and Surface Finishers Society, Orlando, FL. 2002.
- [60] K. Suganama, Whisker Growth Behavior in High Vacuum with Thermal Cycling, Proceedings of TMS Annual Meeting San Diego, CA, Feb. 28 – March 3, 2011.
- [61] M. Dittes, P. Oberndorff, P. Crema, V. Schroeder, Tin Whisker Formation in Thermal Cycling Conditions, IEEE Electronics Packaging Technology Conference, 2003

- [62] T. Shibusaki, Q. Yu, M. Shiratori, M. Pecht, Pressure-induced tin whisker formation, *Microelectronics Reliability* Vol. 48, 2008, pp. 1033–1039
- [63] E. Chason, F. Pei, C. Briant, H. Kesari, A. Bower, Significance of nucleation kinetics in Sn whisker formation, *J. Electronic Materials*, Vol. 43, No. 12, 2014 pp. 4435-4441
- [64] W. J. Boettinger, M.E. Williams, K.-W. Mon, G.R. Stafford, NIST Sn Whisker Research, CALCE 1st International Symposium on Tin Whiskers, University of Maryland Center for Advanced Life Cycle Engineering, 2007.
- [65] W. J. Boettinger, C. E. Johnson, L. A. Bendersky, K.-W. Moon, M. E. Williams, and G. R. Stafford, Whisker and hillock formation on Sn, Sn–Cu and Sn–Pb electrodeposits, *Acta Mater.*, vol. 53, no. 19, pp. 5033–5050, Nov. 2005.
- [66] P. Oberndorff, M. Dittes, and L. Petit, Intermetallic formation in relation to tin whiskers, in Proc. IPC/Soldertec Int. Conf. Lead-Free Electronics, Towards Implementation of the RHS Directive, Brussels, Belgium, Jun. 11–12, 2003, pp. 170–178.
- [67] K. N. Tu, Irreversible processes of spontaneous whisker growth in bimetallic Cu–Sn thin film reactions, *Phys. Rev. B*, vol. 49, 1994, pp. 2030–2034.
- [68] E. R. Crandall, Factors Governing Tin Whisker Growth, Ph.D. Dissertation, Auburn University, Auburn, Alabama, August 4, 2012.
- [69] R. J. Fields, S. R. Low III, and G. K. Lucey Jr. In: M. J Cieslak, J. H. Perepezko, S. Kang, M. E. Glicksman, editors. *The Metal Science of Joining*, Warrendale, PA: The Minerals, Metals & Materials Society, 1992, pp. 165-173.
- [70] M. Sobiech, M. Wohlschlögel, U. Welzel, E. J. Mittemeijer, W. Hügel, A. Seekamp, W. Liu, and G. E. Ice, Local, submicron, strain gradients as the cause of Sn whisker growth, *Appl. Phys. Lett.*, vol. 94, pp. 221901-1–221901-3, 2009.
- [71] B. Dunn, A Laboratory Study of Tin Whisker Growth, ESA STR-223, European Space Research and Technology Centre Noordwijk, The Netherlands; September 1987.
- [72] B. Dunn, 15½ Years of Tin Whisker Growth – Results of SEM Inspections Made on Tin Electroplated C-Ring Specimens, ESTEC Materials Report 4562, European Space Research and Technology Centre Noordwijk, The Netherlands; March 22, 2006.
- [73] B. Dunn and M. Ashworth, An Investigation of Tin Whisker Growth over a 32 Year Period, 8th IPC/CALCE International Symposium on Tin Whiskers, Raleigh, NC, October 29, 2014.
- [74] K. Nishimi, Space Shuttle Program-Tin Whisker Mitigation, International Symposium on Tin Whiskers, University of Maryland Center for Advanced Life Cycle Engineering, 2007.
- [75] H. Leidecker and J. Brusse, Tin Whiskers: A history of Documented Electrical System Failures, A briefing prepared for the Space Shuttle Program Office, April 2006
http://nepg.nasa.gov/whisker/reference/tech_papers/2006-Leidecker-Tin-Whisker-Failures.pdf
- [76] L. Panashchenko, Long Term Investigation of Urethane Conformal Coating Against Tin Whisker Growth, IPC Tin Whisker Conference, Dec. 2010.
- [77] L. Panashchenko, Evaluation of Environmental Tests for Tin Whisker Assessment, Master's Thesis, University of Maryland ,College Park, Md.), 2009
<http://drum.lib.umd.edu/handle/1903/10021>.
- [78] I. Sakamoto, Whisker Test Methods of JEITA Whisker Growth Mechanism for Test Methods, *IEEE Transactions on Electronics Packaging Manufacturing*, Vol. 28, No. 1, January 2005.

- [79] Osenbach, J.W., Shook, R.L., Vaccaro, B.T, Potteiger, B.D., Amin, A.N., Hooghan, K.N., Suratkar, P., Ruengsinsub, P., Sn Whiskers: Material, Design, Processing, and Post-Plate Reflow Effects and Development of an Overall Phenomenological Theory, IEEE Trans. on Electronic Packaging Manufacturing, Vol. 28, No. 1, January 2005. pp. 36-62.
- [80] T.A. Woodrow and E. A. Ledbury, Evaluation of Conformal Coatings as a Tin Whisker Mitigation Strategy, Part II. The Proceedings of SMTA International Conference, Rosemont, IL; September 24-28, 2006.
- [81] NAVAIR Technical Manual, Cleaning and Corrosion Control, Volume III, Avionics and Electronics NAVAIR 01-1A-509-3, TM 1-1500-344-23-3, TO 1-1-689-3, July 15, 2008.
<http://www.robins.af.mil/shared/media/document/AFD-091006-033.pdf>
- [82] J.W. Osenbach, R.L. Shook, B.T. Vaccaro, B.D. Potteiger, A. Amin, Lead Free Packaging and Sn-Whiskers, Proceedings of the IEEE Electronic Components and Technology Conference, 2004.
- [83] B. Hilty, N. Corman, F. Herrmann, Electrostatic Fields and Current Flow Impact on Whisker Growth, IEEE Transactions on Electronic Packaging Manufacturing, 28(1), January 2005.
- [84] J. Arnold, G. Caswell, C. Hillman, and S. Binfield, WWW.dfrsolutions.com/.../HowDfRCanHelpYouControlIonicContami.White. Paper How DfR Can Help You Control Ionic Contamination.
- [85] J-STD-004 Requirements for Soldering Fluxes, Joint JEDEC Solid State Technology Association /IPC Association Connecting Electronics Industries document, January 2004
- [86] M. Huehne, Tin whisker test results for PCB test coupons with immersion tin surface finish, 4th International Symposium on Tin Whiskers, University of Maryland, June 23-24, 2010.
- [87] M. Dudek and N. Chawala, Oxidation behavior of rare-earth-containing Pb-free solders, J. Electronic Materials, Vol. 38, No. 2, 2009.
- [88] S. Schmidt and R. Launsby, Understanding Design of Experiments, Air Academy Press, Colorado Springs, CO 1994.
- [89] iNEMI Recommendations on Lead-Free Finishes for Components Used in High-Reliability Products Version 4, International Electronics Manufacturing Initiative, Herndon, Virginia, December 6, 2006.
- [90] S. Meschter, Tin Whisker Considerations and New Standards for Managing the Risks Associated with Lead-Free Solder Technology for the Aerospace and Military Industries, S.J. Meschter, IEEE/CPMT TC-7 Workshop on Accelerated Stress Testing & Reliability, Portland, Oregon, October 2008.
- [91] D. Susan, Joe Michael, Bonnie McKenzie, Graham Yelton; Crystallographic Analysis of Tin Whiskers with WEM/EBSD, 5th Annual Tin Whisker Conference, CALCE, September 14, 2011
- [92] T. Fang, M. Osterman, and M. Pecht, Statistical Analysis of Tin Whisker Growth, Microelectronics Reliability, Vol. 46, 2006, pp. 846-849
- [93] Y. Fukuda, M. Osterman, and M. Pecht, The Effect of Annealing on Tin Whisker Growth, IEEE Transactions on Electronics Packaging Manufacturing, Vol.29, No.4, October 2006, pp. 252-258.
- [94] R. Hilty and N. Corman, Tin Whisker Reliability Assessment by Monte Carlo Simulation, IPC/JEDEC Lead-free Symposium, San Jose, CA, April 2005
- [95] S. Han, M. Osterman, M. Pecht, Likelihood of Metal Vapor Arc by Tin Whiskers, IMAPS Advanced Technology Workshop on High Reliability Microelectronics for Military Applications, Linthicum Heights, MD, May 17-19, 2011.

- [96] S. McCormack, and S. Meschter, Probabilistic assessment of component lead-to-lead tin whisker bridging, SMTA International Conference on Solder Reliability, Toronto, Ontario, Canada, May 20-22, 2009.
- [97] T. Fang, Tin Whisker Risk Assessment Studies, Dissertation for Doctor of Philosophy, University of Maryland Mechanical Engineering Department, 2005
- [98] K. Courey, et.al., Tin Whisker Electrical Short Circuit Characteristics—Part II, IEEE Trans. Elec. Packaging Manufacturing, Vol. 32, No. 1, 2004.
- [99] G. Galyon, and R. Gedney, Avoiding Tin Whisker Reliability Problems, Circuits Assembly AUGUST 2004, pp. 26-31.
- [100] CALCE Whisker Growth Videos, Center for Advanced Life Cycle Engineering, University of Maryland, http://www.calce.umd.edu/tin-whiskers/whisker_movie_19min.html .
- [101] T. Fang, S. Mathew, M. Osterman, M. Pecht; Assessment of risk resulting from unattached tin whisker bridging, Circuit World, 2007

Appendix A – List of Scientific/Technical Publications

Journal Articles

- Title: Whisker Formation on SAC305 Soldered Assemblies
- Author(s): S. Meschter, P. Snugovsky, Z. Bagheri, E. Kosiba, M. Romansky, J. Kennedy, L. Snugovsky, and D. Perovic
- Journal Name: Journal of Metals
- Vol Number: Vol. 66 No. 11
- Pages: 2320-2333
- Pub Date: 2014-11-15
- Title: SERDP Tin Whisker Testing and Modeling Project
- Author(s): Stephan Meschter, Polina Snugovsky, Jeff Kennedy, Steve McKeown and Eva Kosiba
- Journal Name: SMTA Journal
- Vol Number: Volume 24 Issue 3
- Pages: 23-31
- Pub Date: 2011-07-01
- Title: Whisker Formation Induced by Component and Assembly Ionic Contamination
- Author(s): Polina Snugovsky, Stephan Meschter, Zohreh Bagheri, Eva Kosiba, Marianne Romansky and Jeffrey Kennedy
- Journal Name: Journal of Electronic Materials
- Vol Number: Volume 41, Issue 2
- Pages: 204-223
- Pub Date: 2012-02-01
- Title: Whisker Formation on SAC305 Soldered Assemblies
- Author(s): S. Meschter, P. Snugovsky, Z. Bagheri, E. Kosiba, M. Romansky, J. Kennedy, L. Snugovsky, and D. Perovic
- Journal Name: J. of Metals
- Vol Number: vol. 66 no. 11
- Pages: 2320-2333
- Pub Date: 2014-11-01

Conference Proceedings

- Title: SERDP Project Review
Author(s): S. Meschter
Conference Name: AIA-Pb-Free Electronics Risk Management (PERM) Consortium Meeting
Date: 2012-01-31
- Title: SERDP Tin Whisker Screening Experiment Results
Author(s): Heather McCormick, Jimmy Chow, Stephan Meschter, Polina Snugovsky, and Eva Kosiba
Conference Name: 5th International Symposium on Tin Whiskers, Univ. of Maryland
Date: 2011-09-14
- Title: SERDP Tin Whisker Testing and Modeling Project
Author(s): Stephan Meschter, Polina Snugovsky, Jeff Kennedy, Steve McKeown and Eva Kosiba
Conference Name: 5th International Symposium on Tin Whiskers, Univ. of Maryland, College Park, MD
Date: 2011-09-14
- Title: SERDP Tin Whisker Testing and Modeling Project
Author(s): Stephan Meschter, Polina Snugovsky, Jeff Kennedy, Steve McKeown and Eva Kosiba
Conference Name: October Universal Instruments AREA Consortium Meeting, Binghamton University, Binghamton, NY
Date: 2011-10-12
- Title: Project WP-1753 Tin Whisker Testing and Modeling Project
Author(s): Polina Snugovsky and Stephan Meschter
Conference Name: AIA-PERM (Pb-free Electronics Risk Management) Consortium Meeting #9, Oak Ridge, Tennessee
Date: 2011-06-14
- Title: Lead-free Electronics: The Tin Whisker Challenge
Author(s): Polina Snugovsky
Conference Name: Phillips Health Care Lead-free Conference, Andover, MA

Date: 2011-08-18

Title: WP-1753 Whisker testing and modeling poster

Author(s): Stephan Meschter and Polina Snugovsky

Conference Name: SERDP-ESTCP Partners in Partners in Environmental Technology Technical Symposium & Workshop, Washington, D.C.

Date: 2011-11-29

Title: SERDP Tin Whisker Testing and Modeling: Low Stress Conditions

Author(s): S. Meschter and P. Snugovsky

Conference Name: AIA-Pb-Free Electronics Risk Management (PERM) Consortium Meeting

Date: 2012-07-31

Title: SERDP Tin Whisker Testing and Modeling: High Temperature/High Humidity Conditions

Author(s): Stephan Meschter, Polina Snugovsky, Jeff Kennedy, Zohreh Bagheri, Eva Kosiba, and Andre Delhaise

Conference Name: IPC/CALCE Tin Whisker Symposium 2013

Date: 2013-11-13

Title: SERDP Tin Whisker Testing and Modeling: Low Stress Conditions

Author(s): S. Meschter, P. Snugovsky, J. Kennedy, Z. Bagheri and E. Kosiba

Conference Name: 2012 International Conference on Solder Reliability (ICSR2012)

Date: 2012-05-15

Title: Tin Whisker Mitigation in Assembly

Author(s): P. Snugovsky, S. Meschter, Z. Bagheri, E. Kosiba, M. Romansky, J. Kennedy

Conference Name: IPC Tin Whiskers Conference

Date: 2012-04-17

Title: Whisker Growth in Low and High Stress Environments: Metallurgical Assessment and Statistical Analysis: Part 2. Statistical Analysis

Author(s): P. Snugovsky, S. Meschter, E. Kosiba, Z. Bagheri

Conference Name: 6th International Symposium on Tin Whiskers, CALCE University of Maryland

Date: 2012-11-27

Title: Whisker Growth in Low and High Stress Environments: Metallurgical Assessment and Statistical Analysis

Author(s): S. Meschter, P. Snugovsky

Conference Name: Whisker Growth in Low and High Stress Environments: Metallurgical Assessment and Statistical Analysis, IEEE International Reliability Innovations Conference (IRIC)

Date: 2013-03-07

Title: SERDP tin whisker testing and modeling: thermal cycling testing

Author(s): S. Meschter, P. Snugovsky, E. Kosiba, Z. Bagheri and J. Kennedy

Conference Name: SMTA International Conference on Soldering and Reliability (ICSR)

Date: 2014-05-13

Title: SERDP tin whisker testing and modeling: short circuit risk analysis

Author(s): S.A. McKeown, S.J. Meschter, P. Snugovsky, and J. Kennedy

Conference Name: SMTA International Conference on Soldering and Reliability (ICSR)

Date: 2014-05-13

Title: SERDP tin whisker testing and modeling: thermal cycling testing

Author(s): S. Meschter, P. Snugovsky, E. Kosiba, Z. Bagheri and J. Kennedy

Conference Name: 21st IPC Lead-free Electronics Risk Management (PERM) meeting

Date: 2014-07-22

Title: SERDP tin whisker testing and modeling: short circuit risk analysis

Author(s): S.A. McKeown, S.J. Meschter, P. Snugovsky, and J. Kennedy

Conference Name: 21st IPC Lead-free Electronics Risk Management (PERM) meeting

Date: 2014-07-22

Title: Tin whisker testing and modeling

Author(s): S. Meschter, P. Snugovsky, J. Kennedy, Z. Bagheri, and E. Kosiba

Conference Name: SMTA International 2014

Date: 2014-09-28

Title:	SERDP Tin Whisker Testing and Modeling: High Temperature/High Humidity Conditions
Author(s):	S. Meschter, P. Snugovsky, J. Kennedy, S. McKeown, Z. Bagheri and E. Kosiba
Conference Name:	Proceedings of the 2013 International Conference on Solder Reliability (ICSR2013)
Date:	2013-05-14
 Title:	Influence of Ionic Contamination on Tin Whiskers
Author(s):	S. Meschter and P. Snugovsky
Conference Name:	SMTA/IPC Cleaning and Coating Conference
Date:	2012-11-13
 Title:	SERDP Tin Whisker Testing Presentation
Author(s):	S. Meschter and P. Snugovsky
Conference Name:	18th Lead(Pb)-free Electronics Working Group Meeting (PERM)
Date:	2013-09-24
 Title:	SERDP Tin Whisker Testing and Modeling: High Temperature/High Humidity (HTHH) Conditions
Author(s):	Stephan Meschter, Polina Snugovsky, Jeff Kennedy, Zohreh Bagheri, and Eva Kosiba,
Conference Name:	Defense Manufacturers Conference (DMC)
Date:	2013-12-02
 Title:	Whisker Growth in Low and High Stress Environments: Part 2 Statistical Analysis
Author(s):	S. Meschter and P. Snugovsky
Conference Name:	CALCE Tin whisker conference
Date:	2012 11-27
 Title:	Assembly Considerations to Minimize Whisker Growth
Author(s):	P. Snugovsky and S. Meschter,
Conference Name:	IEEE ASTR Conference
Date:	2012 Oct

Title:	SERDP WP1753 Tin Whisker Testing and SERDP WP2213 Nanoparticle Enhanced Conformal Coating Update
Author(s):	S. Meschter and P. Snugovsky
Conference Name:	19th Lead-free Electronics Risk Management (PERM) Meeting
Date:	2014-02-11
Title:	SERDP Tin Whisker Testing and Modeling: Thermal Cycling Testing
Author(s):	P. Snugovsky, S. Meschter, E. Kosiba, Z. Bagheri and J. Kennedy
Conference Name:	8th Annual CALCE/IPC Tin Whisker Symposium
Date:	2014-10-29
Title:	SERDP Tin Whisker Testing and Modeling: Simplified Whisker Geometric Short Circuit Risk Model Development
Author(s):	S. Meschter, P. Snugovsky, E. Kosiba, Z. Bagheri and J. Kennedy
Conference Name:	8th Annual CALCE/IPC Tin Whisker Symposium
Date:	2014-10-28
Title:	SERDP WP1753 Tin Whisker Testing and Modeling: Low Temperature High Humidity Test Results
Author(s):	S. Meschter, P. Snugovsky, Z. Bagheri, E. Kosiba, M. Romansky, and J. Kennedy
Conference Name:	SMTA International Conference on Soldering and Reliability (ICSR)
Date:	2015-05-19
Title:	Electronic Assembly and Whisker Formation: Effect of Cleanliness
Author(s):	P. Snugovsky, S. Meschter, Z. Bagheri, E. Kosiba, J. Kennedy, L. Snugovsky, D. Perovic
Conference Name:	TMS2015 Lead-Free Solder Workshop
Date:	2015-03-15
Title:	Assembly: Cleanliness and Whisker Formation
Author(s):	P. Snugovsky, E. Kosiba, S. Meschter, Z. Bagheri, J. Kennedy
Conference Name:	Proceedings IPC 2015 APEX Conference
Date:	2015-02-22

Title:	SERDP WP1753 Lead-free soldered assembly whisker test results after extended 25C/85%RH testing
Author(s):	S. Meschter, P. Snugovsky, J. Kennedy, Z. Bagheri
Conference Name:	23rd IPC PERM Council Meeting
Date:	2015-02-3
 Title:	Development of a Test Vehicle for the Study of Tin Whiskers
Author(s):	Heather McCormick, Jimmy Chow, Stephan Meschter, Polina Snugovsky, and Eva Kosiba
Conference Name:	2011 International Conference on Solder Reliability (ICSR2011), Toronto, Ontario, Canada
Date:	2011-05-04
 Title:	Whiskers in SAC105+REE
Author(s):	Polina Snugovsky
Conference Name:	9th Aerospace Industries Association Lead-free Electronics Risk Management (AIA-PERM) Meeting
Date:	2011-06-14
 Title:	Tin Whisker Testing and Modeling
Author(s):	Stephan Meschter, Polina Snugovsky, Jeff Kennedy, Steve McKeown and Eva Kosiba
Conference Name:	2011 International Conference on Solder Reliability (ICSR2011), Toronto, Ontario, Canada
Date:	2011-05-04
 Title:	Influence of Board and Component Cleanliness on Whisker Formation
Author(s):	P. Snugovsky, S. Meschter, P. Kapadia, M. Romansky, J. Kennedy and E. Kosiba
Conference Name:	IPC/SMTA High Performance Cleaning & Coating Conference
Date:	2010-11-16
 Title:	Tin whiskers on solder joints
Author(s):	P. Snugovsky and S. Meschter
Conference Name:	Aerospace Industries Association Lead(Pb)-Free Electronics Risk Management (AIA_PERM) Consortium Meeting Number 7
Date:	2010-01-11

Title:	Influence of Board and Component Cleanliness on Whisker Formation
Author(s):	P. Snugovsky, S. Meschter, P. Kapadia, M. Romansky, J. Kennedy and E. Kosiba
Conference Name:	Aerospace Industries Association Lead(Pb)-Free Electronics Risk Management (AIA_PERM) Consortium Meeting Number 7
Date:	2010-01-11
Title:	Tin-Whisker Testing and Modeling (SERDP WP-1753) Overview
Author(s):	S. Meschter and P. Snugovsky
Conference Name:	Aerospace Industries Association Lead(Pb)-Free Electronics Risk Management (AIA_PERM) Consortium Meeting Number 7
Date:	2010-01-11
Title:	Whisker Formation Induced by Component and Assembly Ionic Contamination
Author(s):	P. Snugovsky, S. Meschter, Z. Bagheri, E. Kosiba, M. Romansky, and J. Kennedy
Conference Name:	TMS2011 Annual Meeting
Date:	2011-02-27
Title:	Whisker Growth in Low and High Stress Environments: Metallurgical Assessment and Statistical Analysis: Part 1. Metallurgical Assessment
Author(s):	P. Snugovsky, S. Meschter, E. Kosiba, Z. Bagheri
Conference Name:	6th International Symposium on Tin Whiskers, CALCE University of Maryland
Date:	2012-11-27
Title:	Tin whisker testing
Author(s):	Polina Snugovsky
Conference Name	9th Aerospace Industries Association Lead-free Electronics Risk Management (AIA-PERM) Meeting
Date:	2011-06-14
Pub Location:	Oak Ridge, Tennessee
Title:	Influence of Ionic Contamination on Tin Whiskers
Author(s):	S. Meschter, P. Snugovsky

Conference Name SMTA/IPC Cleaning and Coating Conference
Date: 2012-11-13
Pub Location: Chicago, Illinois

Title: Microstructure Formation and Whisker Growth in SAC105 Solder Joints with Rare Earth Elements
Author(s): P. Snugovsky, Z. Bagheri, S. Meschter, D. Perovic, L. Snugovsky, and J. Rutter

Conference Name TMS 2011 Annual Meeting
Date: 2011-02-27
Pub Location: San Diego, CA

Other

Title: Strategic Environmental Research and Development Program (SERDP) Tin Whisker Testing And Modeling: Tin Whisker Growth on SAC305 Assemblies and Risk Modeling
Pub Type: Industry Webinar
Pub Name: Bill Rollins Weekly Tin Whisker Telecon
Author(s): S. Meschter, P. Snugovsky, J. Kennedy, Z. Bagheri, E. Kosiba
Pub Date: 2014-11-12
Pub Location: Webinar

Appendix B – Initial test vehicle characterization